Structures Research Report 2021/ P0034538-P0034539

University of Florida
Civil and Coastal Engineering

UF

Gator Engineering
University of Florida
Civil and Coastal Engineering

Final Report June 2021

Fiber-Reinforced Concrete Traffic Railings for Impact Loading

Principal investigator:
Gary R. Consolazio, Ph.D.

Co-Principal investigator:
H.R. Trey Hamilton, Ph.D., P.E.

Graduate research assistant:
Jeffrey M. Honig

Department of Civil and Coastal Engineering
University of Florida
P.O. Box 116580
Gainesville, Florida 32611

Sponsor:
Florida Department of Transportation (FDOT)
David Wagner, P.E. – Project manager

Contract:
UF Project No. P0034538-P0034539
FDOT Contract No. BDV31-977-72

DISCLAIMER

The opinions, findings, and conclusions expressed in this publication are those of the authors and not necessarily those of the State of Florida Department of Transportation.

SI (MODERN METRIC) CONVERSION FACTORS

*APPROXIMATE CONVERSIONS **TO** SI UNITS*

SYMBOL	WHEN YOU KNOW	MULTIPLY BY	TO FIND	SYMBOL
LENGTH				
in	inches	25.4	millimeters	mm
ft	feet	0.305	meters	m
yd	yards	0.914	meters	m
mi	miles	1.61	kilometers	km
AREA				
in^2	square inches	645.2	square millimeters	mm^2
ft^2	square feet	0.093	square meters	m^2
yd^2	square yard	0.836	square meters	m^2
ac	acres	0.405	hectares	ha
mi^2	square miles	2.59	square kilometers	km^2
VOLUME				
fl oz	fluid ounces	29.57	milliliters	mL
gal	gallons	3.785	liters	L
ft^3	cubic feet	0.028	cubic meters	m^3
yd^3	cubic yards	0.765	cubic meters	m^3
NOTE: volumes greater than 1000 L shall be shown in m^3				
MASS				
oz	ounces	28.35	grams	g
lb	pounds	0.454	kilograms	kg
T	short tons (2,000 lb)	0.907	Megagrams	Mg (or "t")
TEMPERATURE (exact degrees)				
°F	Fahrenheit	5(F-32)/9 or (F-32)/1.8	Celsius	°C
FORCE and PRESSURE or STRESS				
kip	1,000 pound force	4.45	kilonewtons	kN
lbf	pound force	4.45	newtons	N
lbf/in^2	pound force per square inch	6.89	kilopascals	kPa
ksi	kips force per square inch	6.89	Megapascals	MPa

TECHNICAL REPORT DOCUMENTATION PAGE

1. Report No.	2. Government Accession No.	3. Recipient's Catalog No.
4. Title and Subtitle Fiber-Reinforced Concrete Traffic Railings for Impact Loading		5. Report Date June 2021 6. Performing Organization Code 8. Performing Organization Report No.
7. Author(s) Gary R. Consolazio, H.R. Trey Hamilton, Jeffrey M. Honig		2021/P0034538-P0034539
9. Performing Organization Name and Address University of Florida Department of Civil and Coastal Engineering 365 Weil Hall, P.O. Box 116580 Gainesville, FL 32611-6580		10. Work Unit No. (TRAIS) 11. Contract or Grant No. BDV31-977-72
12. Sponsoring Agency Name and Address Florida Department of Transportation Research Management Center 605 Suwannee Street, MS 30 Tallahassee, FL 32399-0450		13. Type of Report and Period Covered Final Report 14. Sponsoring Agency Code
15. Supplementary Notes		

16. Abstract

Fiber-reinforced concrete (FRC) utilizes a large number of small, discontinuous fibers, typically made of steel, synthetic, glass, or natural materials, mixed within the concrete. Adding distributed, discrete fibers has been found to improve hardened mechanical properties, relative to typical concrete, such as tensile strength, ductility, toughness, and impact resistance. In highway bridge construction, concrete traffic railings are commonly employed as a highway safety device. The purpose of a traffic railing is to keep errant vehicles within the roadway and prevent vehicles from colliding with more dangerous obstacles or prevent more serious accidents from occurring. In the present study, FRC was investigated as a possible means of eliminating the need for installation of a rebar cage (consisting of flexural and shear steel reinforcing bars), instead using steel fiber as an alternative form of reinforcement within a concrete traffic railing.

Primary objectives of this study consisted of: (1) developing an FRC mixture suitable for use in the proposed traffic railing and (2) conducting experimental pendulum impact tests to evaluate whether the proposed FRC railing possesses impact resistance equivalent to (or greater than) that of a traditional rebar reinforced concrete (R/C) railing. Consequently, a number of multiple potential trial FRC mixtures were developed and produced on a small (laboratory) scale. These mixtures consisted of various fiber types and volumes. Fresh and hardened mechanical properties of the produced trial mixtures were evaluated, and an FRC mixture employing 2-in.-long, hooked-end steel fibers with a 1% fiber volume was subsequently selected for use in the proposed FRC railing. Following small-scale mechanical testing, the selected FRC mixture was produced on a larger scale and used to form two 13-ft long FRC traffic railing impact test specimens consisting of a traffic railing integrated with a partial bridge deck.

To facilitate direct comparisons between the proposed FRC railing and the standard R/C railing, test specimens of both types (3 FRC and 3 R/C) were pendulum impact tested. Pendulum impact test protocols were developed from vehicle impact conditions prescribed in AASHTO MASH. Equivalent impact energy (155 kip-ft) from a single-unit truck test level 4 (TL-4) impact test was delivered to each impact test specimen using a 10,300-lb pendulum impactor dropped from 15 ft. Peak impact forces conservatively exceeded the 54-kip design force specified in AASHTO LRFD Bridge Design. From the conducted tests, it was shown that the proposed FRC railing performed adequately, withstanding the designed impact test with minimal damage and matching the maximum deflection levels of the standard R/C railing specimens.

17. Key Words	18. Distribution Statement
Fiber-reinforced concrete, FRC, traffic railings, guardrails, vehicle impact loads, pendulum impact testing,	No restrictions.

19. Security Classif. (of this report)	20. Security Classif. (of this page)	21. No. of Pages	22. Price
Unclassified	Unclassified	465	

Form DOT F 1700.7 (8-72). Reproduction of completed page authorized

ACKNOWLEDGEMENTS

The authors thank the Florida Department of Transportation (FDOT) for providing the funding that made this research possible. Additionally, the authors would like to recognize that, without the contributions made by the staff of the FDOT Marcus H. Ansley Structures Research Center, this project would not have been successfully completed. David Wagner, Christina Freeman, Sam Adeniji, William Potter, Stephen Eudy, Justin Robertson, Paul Tighe, Ben Allen, Miguel Ramirez, Michael Waters were all exceptional participants in this research. Their expertise in fabrication, construction, testing, and instrumentation allowed the project to progress effectively.

EXECUTIVE SUMMARY

Fiber-reinforced concrete (FRC) utilizes a large number of small, discontinuous fibers, typically made of steel, synthetic, glass, or natural materials, mixed within the concrete. Adding distributed, discrete fibers has been found to improve hardened mechanical properties, relative to typical concrete, such as tensile strength, ductility, toughness, and impact resistance. In highway bridge construction, concrete traffic railings are commonly employed as a highway safety device. The purpose of a traffic railing is to keep errant vehicles within the roadway and prevent vehicles from colliding with more dangerous obstacles or prevent more serious accidents from occurring. In the present study, FRC was investigated as a possible means of eliminating the need for installation of a rebar cage (consisting of flexural and shear steel reinforcing bars), instead using steel fiber as an alternative form of reinforcement within a concrete traffic railing.

Primary objectives of this study consisted of: (1) developing an FRC mixture suitable for use in the proposed traffic railing and (2) conducting experimental pendulum impact tests to evaluate whether the proposed FRC railing possesses impact resistance equivalent to (or greater than) that of a traditional rebar reinforced concrete (R/C) railing. Consequently, a number of multiple potential trial FRC mixtures were developed and produced on a small (laboratory) scale. These mixtures consisted of various fiber types and volumes. Fresh and hardened mechanical properties of the produced trial mixtures were evaluated, and an FRC mixture employing 2-in.-long, hooked-end steel fibers with a 1% fiber volume was subsequently selected for use in the proposed FRC railing. Following small-scale mechanical testing, the selected FRC mixture was produced on a larger scale and used to form two 13-ft long FRC traffic railing impact test specimens consisting of a traffic railing integrated with a partial bridge deck.

To facilitate direct comparisons between the proposed FRC railing and the standard R/C railing, test specimens of both types (3 FRC and 3 R/C) were pendulum impact tested. Pendulum impact test protocols were developed from vehicle impact conditions prescribed in AASHTO MASH. Equivalent impact energy (155 kip-ft) from a single-unit truck test level 4 (TL-4) impact test was delivered to each impact test specimen using a 10,300-lb pendulum impactor dropped from 15 ft. Peak impact forces conservatively exceeded the 54-kip design force specified in AASHTO LRFD Bridge Design. From the conducted tests, it was shown that the proposed FRC railing performed adequately, withstanding the designed impact test with minimal damage and matching the maximum deflection levels of the standard R/C railing specimens.

TABLE OF CONTENTS

DISCLAIMER ii

SI (MODERN METRIC) CONVERSION FACTORS iii

TECHNICAL REPORT DOCUMENTATION PAGE iv

ACKNOWLEDGEMENTS v

EXECUTIVE SUMMARY vi

LIST OF FIGURES x

LIST OF TABLES xxii

CHAPTER 1 INTRODUCTION 1

1.1 Background 1
1.2 Objectives 4
1.3 Scope of work 4

CHAPTER 2 BACKGROUND AND LITERATURE REVIEW 6

2.1 Introduction 6
2.2 FRC fiber options 6
2.2.1 Fiber mechanical behavior 6
2.2.2 Steel fibers 8
2.2.3 Synthetic fibers 8
2.2.4 Other fiber types and hybrid fibers 9
2.3 Previous (related) FRC studies 9
2.4 Slip-form railing construction and freshly mixed property requirements 11
2.5 Concrete traffic railing design 12
2.5.1 AASHTO *LRFD* Bridge Design Specifications 12
2.5.2 MASH specifications 13
2.5.3 Texas DOT single slope traffic railing (SSTR) 14
2.5.4 Railing selection for the present study : FDOT 36-in. SSTR 15

CHAPTER 3 FRC MIXTURE DEVELOPMENT AND LABORATORY-SCALE TESTING 17

3.1 FRC mixture development 17
3.1.1 Selected fibers for evaluation 17
3.1.2 Trial FRC mixtures overview 21
3.2 Static laboratory-scale testing 24
3.3 Dynamic laboratory-scale testing 30
3.3.1 Dynamic (laboratory-scale) pendulum impact testing overview 30
3.3.2 Dynamic (laboratory-scale pendulum impact) test results 33

3.4 Preliminary FRC railing design strength based on laboratory-scale testing....................37
3.4.1 Implementation of FRC....................37
3.4.2 FRC 36-in. SSTR design....................38
3.5 Scaled-up FRC production at the ready-mix batch plant level....................39
3.5.1 Preliminary FRC mixture design....................39
3.5.2 FRC production approach using a concrete batch plant....................39
3.5.3 Production trial attempt #1: Unsuccessful trial....................41
3.5.4 Production trial attempt #2: Successful trial....................44

CHAPTER 4 DESIGN AND FABRICATION OF A FULL-SCALE PENDULUM IMPACTOR....................49

4.1 Vehicle impact test equivalency and initial impactor test protocols....................49
4.2 Pendulum impactor design....................54
4.3 Pendulum impactor fabrication....................59

CHAPTER 5 FULL-SCALE RAILING PENDULUM IMPACT TEST PROGRAM....................65

5.1 Overview....................65
5.1.1 Full-scale railing specimen design with integrated bridge deck....................65
5.1.2 Construction of test specimens....................68
5.1.3 Installation of test specimens....................71
5.2 Instrumentation plan....................77
5.2.1 Contact tape switches....................78
5.2.2 Optical break beams....................79
5.2.3 Accelerometers....................80
5.2.4 High speed cameras....................82
5.2.5 Laser displacement sensors....................83
5.2.6 Concrete strain gages....................84
5.2.7 Rebar strain gages....................84

CHAPTER 6 FULL-SCALE CENTER OF RAILING (COR) IMPACT TEST RESULTS....................86

6.1 Introduction....................86
6.2 FRC railing....................86
6.2.1 Impact testing of FRC COR specimen 1....................86
6.2.2 Impact testing of FRC COR specimen 2....................94
6.3 Standard (R/C) railing....................105
6.3.1 Impact testing of R/C COR specimen 1....................105
6.3.2 Impact testing of R/C COR specimen 2....................116
6.4 Comparison of FRC and R/C COR test specimen results....................126
6.4.1 Overview....................127
6.4.2 Comparison of COR acceleration data and pendulum impact forces....................127
6.4.3 Comparison of COR laser displacement data....................127
6.4.4 Comparison of COR external concrete strain gage data....................128
6.4.5 Comparison of COR internal steel rebar strain gage data....................129

CHAPTER 7 FULL-SCALE END OF RAILING (EOR) IMPACT TEST RESULTS 131

7.1 Introduction...131
7.2 FRC railing 133
7.2.1 Impact testing of FRC EOR specimen 1 (FRC test specimen 3) 133
7.3 Standard (R/C) railing..145
7.3.1 Impact testing of R/C EOR specimen 1 (R/C test specimen 3)............................145
7.4 Comparison of FRC and R/C EOR test specimen results.....................................158
7.4.1 Overview 158
7.4.2 Comparison of EOR acceleration data and pendulum impact forces...................158
7.4.3 Comparison of EOR laser displacement data...158
7.4.4 Comparison of EOR external concrete strain gage data and cracking patterns ...159
7.4.5 Comparison of EOR internal steel rebar strain gage data 161

CHAPTER 8 SUMMARY, CONCLUSIONS, RECOMMENDATIONS, AND FUTURE DIRECTIONS..163

8.1 Summary and conclusions 163
8.2 Recommendations...164
8.2.1 Ability to slip-form...164
8.2.2 FRC flexural strength tests 164
8.3 Future implementation..165

REFERENCES 166

APPENDIX A *LRFD* DESIGN STRENGTH CALCULATIONS FOR FDOT 36-IN. SINGLE-SLOPE TRAFFIC RAILING (INDEX NO. 521-427) 170

APPENDIX B *LRFD* DESIGN STRENGTH CALCULATIONS FOR FRC 36-IN. SINGLE-SLOPE TRAFFIC RAILING...178

APPENDIX C SPECIMEN FORMWORK AND TRIAL PRODUCTION DRAWINGS 186

APPENDIX D LARGE-SCALE TRIAL MIXTURE PRODUCTION DETAILS AND BATCH-PLANT MIXTURES FOR SPECIMEN PRODUCTION 237

APPENDIX E HARDENED MECHANICAL PROPERTIES OF RAILING CONCRETE MIXTURES 264

APPENDIX F PENDULUM IMPACTOR FABRICATION DRAWINGS 266

APPENDIX G IMPACT TEST SPECIMEN (DECK AND RAILING) CONSTRUCTION DRAWINGS..315

APPENDIX H IMPACT TEST SPECIMEN ANCHORING SEQUENCE DRAWINGS 388

APPENDIX I IMPACT TEST SPECIMEN INSTRUMENTATION PLANS 406

LIST OF FIGURES

Figure | Page

Figure 1.1 Slip-formed concrete traffic railing (Photo credit: Gomaco) 1

Figure 1.2 Slip-formed construction of conventionally rebar-reinforced traffic railings (Photo Credit: Gomaco) 2

Figure 1.3 Florida DOT traffic railing: (a) Current reinforcement design (after FDOT, 2020a); (b) Proposed FRC railing without secondary steel rebar cage 2

Figure 1.4 Variation of load-deformation curves for unreinforced concrete and FRC (after ACI Committee 544, 2002)...3

Figure 2.1 Various types of commercially available fibers: (a) Steel hooked-end fiber; (b) Helix steel fiber; (c) Forta-Ferro synthetic fiber; (d) BASF polypropylene fiber 6

Figure 2.2 Pullout failure mechanism of a straight steel fiber (Markovic 2006)............................7

Figure 2.3 Pullout failure mechanism of a hooked-end steel fiber (Markovic 2006).....................7

Figure 2.4 Fiber failure mechanisms (Zollo 1997) 7

Figure 2.5 Steel fiber configurations: (a) Straight silt sheet or wire; (b) Deformed silt sheet or wire; (c) Hooked-end wire; (d) Flattened-end silt sheet or wire; (e) Machined chip; (f) Melt extract; (after ACI Committee 544, 2002) 8

Figure 2.6 Failure patterns for slabs containing 2% fiber volumes: (a) Polyolefin fibers (top and bottom surfaces); (b) Steel fibers (top and bottom surfaces); (Photo credit: Ong et al. 1999) 10

Figure 2.7 Precast parapet with: (a) High-performance concrete (7250 psi, 0% fiber volume); (b) Steel FRC (14.4 ksi, 4% fiber volume); (Charron et al., 2011) 11

Figure 2.8 Retained railing shape after slip-forming (Photo credit: Gomaco) 12

Figure 2.9 Railing construction formwork: (a) Railing formwork components; (b) Railing formwork cross-section with internal vibrators located within the hopper for compaction (Figure credit: Wirtgen Group) 12

Figure 2.10 Texas DOT single slope traffic railing (SSTR) standard details...............................15

Figure 2.11 FDOT 36-in. single-slope traffic railing (FDOT 2020a)...16

Figure 3.1 Slump tests for trial FRC production: (a) Standard (hand rodded) slump (measured 0.25-in. slump); (b) Slump with vibration (measured 0.0-in. slump) 24

Figure 3.2 Production of FRC flexural beams during trial batching for future testing: (a) Prior to vibrating the specimen molds; (b) After vibrating the molds 25

Figure 3.3 Preparation of an FRC flexural beam for EN 14651 testing: (a) Prior to saw cutting; (b) After saw cutting to create the 'notch' at the mid-span 25

Figure 3.4 EN 14651 FRC flexural test setup: (a) Side view; (b) Corner view; (c) CMOD clip gage during evaluation; (d) Close-up view of the CMOD during specimen evaluation 26

Figure 3.5 Sika hooked-end steel fibers: (a) Fiber photograph; (b) CMOD flexural test results using Sika hooked-end steel fibers at 1.0% and 0.5% fiber volumes (trial mixtures 2 and 4) 27

Figure 3.6 Hooked-end steel FRC flexural specimen after completion of CMOD test: (a) Crack formation after completion; (b) Fiber distribution across crack interface with additional loading..27

Figure 3.7 Helix 5-25 steel fibers: (a) Fiber photograph; (b) CMOD flexural test results using Helix 5-25 steel fibers at 1.0% and 0.5% fiber volumes (trial mixtures 3 and 5)....28

Figure 3.8 Forta-Ferro synthetic fibers: (a) Fiber photograph; (b) CMOD flexural test results using Forta-Ferro synthetic fibers at 1.0% and 0.5% fiber volumes (trial mixtures 6 and 7) 28

Figure 3.9 BASF synthetic fibers: (a) Fiber photograph; (b) CMOD flexural test results using BASF synthetic fibers at 1.0% and 0.5% fiber volumes (trial mixtures 8 and 9)....29

Figure 3.10 Typical load-CMOD (displacement) curve with specified $CMOD_{1,2,3,4}$ values (after EN 14651) 29

Figure 3.11 CMOD flexural test results using Sika hooked-end steel fibers at 1.0% fiber volumes (comparison of mixtures 2 and 11)..30

Figure 3.12 Specimen configuration and support conditions for pendulum impact testing: (a) Specimen dimensions; (b) Specimen support conditions..32

Figure 3.13 Pendulum impact test overview...32

Figure 3.14 Aluminum honeycomb cartridge configuration: (a) Cartridges attached to front of pendulum impactor; (b) Side view of tapered cartridge 33

Figure 3.15 Acceleration of the 1100-kg block versus time data: (a) FRC (1.0% Sika hooked-end steel fiber) slab specimens; (b) Plain (unreinforced) concrete slab specimens 34

Figure 3.16 Force versus time data (per acceleration data shown in Figure 3.15) 34

Figure 3.17 Force versus computed midspan displacement (from laser displacement sensor data)..35

Figure 3.18 Final (preserved) state of FRC specimen-2 36

Figure 3.19 Stress distributions for an FRC flexural member: (a) FRC beam section; (b) Actual distribution; (c) Simplified nonlinear distribution (after ACI 544.4R-18)....37

Figure 3.20 Simplified FRC design approach compared to R/C design: (a) FRC cross-section and stress distribution; (b) Conventional R/C cross-section and stress distribution; (after ACI Committee 544, 2018)....38

Figure 3.21 FDOT UHPC mixer used to introduce fibers into the concrete delivery truck mixture....40

Figure 3.22 Excessively stiff mixture prior to introduction of fiber: (a) Stiffness of mixture out of the truck; (b) 1.0-in. standard slump after adding 36 additional gallons of water....43

Figure 3.23 Scaled-up FRC production: (a) Standard (7-in.) slump after adding additional water to the truck delivery mixture; (b) UHPC mixer grate (where fibers were discharged); (c) Mixture after adding fiber; (d) Inside railing formwork with first lift placed; (e) Standard (2.5-in.) slump after second FRC lift; (f) Vibration slump after second FRC lift (1.75-in. slump) 47

Figure 3.24 Filled FRC railing formwork after trial FRC production 48

Figure 3.25 Additional trial FRC production specimens (4-in. x. 4-in. x 14-in. flexural beams and 4-in. x 8-in. cylinders)....48

Figure 4.1 Pendulum at FDOT Structures Research Center (Tallahassee, FL) 49

Figure 4.2 Test conditions for: (a) *MASH* TL-4 impact (after Sheikh et al. 2011); (b) Proposed pendulum impact test 50

Figure 4.3 FEA impact force-time curves for single-slope traffic railings for various railing heights (after Sheikh et al. 2011) 51

Figure 4.4 Aluminum honeycomb: (a) Cell structure and crush sequence of rectangular cartridge; (b) Force-deformation curve for an individual rectangular aluminum honeycomb cartridge (after Groetaers et al. 2016) 52

Figure 4.5 Anticipated force-time curve from the developed crushable nose design....54

Figure 4.6 FEA impact simulation (side elevation view) at start of pull-back process 56

Figure 4.7 FEA impact simulation (side elevation view): (a) At drop height; (b) Before impact; (c) At end of impact 56

Figure 4.8 FEA front nose telescoping sequence: (a) At start of impact; (b)–(e) Intermediate states of impact; (f) At end of impact and peak impact force 57

Figure 4.9 FEA impact simulation: (a) Side elevation view at end of impact; (b) Force-time results from FEA impact simulation compared to the (anticipated) force-time curve design 58

Figure 4.10 FEA impact simulation (isometric view) at end of impact with preliminary impact test specimen design....58

Figure 4.11 Overall design and major components of the pendulum impactor....59

Figure 4.12 Repurposed steel hanger frame 59

Figure 4.13 Steel hanger frame suspended above the concrete block formwork with embedded steel components correctly positioned....60

Figure 4.14 Embedded steel components within the concrete block formwork....60

Figure 4.15 Embedded steel positioned inside the concrete block formwork 61

Figure 4.16 Steel hanger frame and concrete formwork ready for concrete placement....61

Figure 4.17 Formed concrete block connected to the steel hanger frame 62

Figure 4.18 Teflon strips positioned within the steel guide tubes with magnets to hold them in place while the adhesive sets 63

Figure 4.19 Teflon strips adhered within the steel guide tube....63

Figure 4.20 Complete pendulum impactor: Fabricated aluminum front nose placed inside the concrete block 64

Figure 4.21 Complete pendulum impactor: Aluminum front nose placed inside the concrete block and the front nose tubes protruding out the back of the block....64

Figure 5.1 Main components of the pendulum impact test specimen....66

Figure 5.2 Preliminary FEA model of deck-railing impact test specimen: (a) Back isometric view; (b) Isometric view underneath—to show how the central deck portion of the specimen is elevated, similar to a typical bridge deck overhang....66

Figure 5.3 Approach for selecting cross-sectional deck dimensions: (a) Typical bridge cross-section; (b) Exterior girder and railing; (c) Selected geometry for test specimen....67

Figure 5.4 Standard 36-in. single-slope traffic railing (after FDOT 2020a)....67

Figure 5.5 FRC 36-in. single-slope traffic railing....68

Figure 5.6 Reinforcing bars positioned inside deck formwork....68

Figure 5.7 Deck-to-railing connection bars and end-support buttress reinforcement positioned inside deck formwork 69

Figure 5.8 Deck concrete placement 69

Figure 5.9 Construction of railing portion of R/C test specimen: (a) Railing reinforcement positioned inside railing formwork; (b) Railing concrete placed and formed 70

Figure 5.10 Construction of FRC test specimen: (a) Deck concrete cast with railing formwork in position; (b) Railing reinforcement positioned inside railing formwork 71

Figure 5.11 Completed (FRC) test specimen 71

Figure 5.12 Test specimen lifted out of the formwork by crane 72

Figure 5.13 Test specimen being moved into position on the pendulum foundation 72

Figure 5.14 Impact test specimen in position on pendulum foundation 73

Figure 5.15 Backside of impact specimen after being positioned onto the pendulum foundation (with temporary HSS lifting element still connected) 73

Figure 5.16 Diagram of impact test specimen with additional anchoring elements placed: (a) Front isometric view; (b) Back isometric view 74

Figure 5.17 Post-tensioning fourth (front right) threaded bar for anchoring test specimen to pendulum foundation with the FDOT loading assembly 75

Figure 5.18 Anchored test specimen 75

Figure 5.19 Placing grout between test specimen and small reaction element (steel slide stopper) as a secondary reaction system to prevent specimen from sliding during impact testing 76

Figure 5.20 Aluminum loading wedge adhered to front face of railing 76

Figure 5.21 Pendulum impactor and impact test specimen prepared and ready for testing (with instrumentation in place) 76

Figure 5.22 Instrumentation plan used in pendulum impact testing 77

Figure 5.23 External instrumentation: (a) Front concrete strain gage and tape switch sensor locations; (b) Back concrete strain gage and laser displacement sensor locations 78

Figure 5.24 Tape switches adhered to the impact face of the aluminum loading wedge 79

Figure 5.25 Optical break beam sensors: (a) Close up of an individual sensor; (b) Break beam sensors positioned for testing 80

Figure 5.26 Accelerometers installed on pendulum impactor (top view)....................................81

Figure 5.27 Accelerometers installed on the pendulum impactor: (a) AC-1 mounted to the top of the concrete back block; (b) AC-2 mounted to the bottom of the concrete back block; (c) AC-3 mounted to the left mounting plate on the aluminum front nose; (d) AC-4 mounted to the right mounting plate on the aluminum front nose..........................82

Figure 5.28 High-speed digital video camera..83

Figure 5.29 Laser displacement sensor mounted behind a test specimen....................................83

Figure 5.30 Concrete strain gages (3 and 4) adhered to concrete railing surface..........................84

Figure 5.31 Strain gage attached to deck reinforcing bar and protected with waterproof tape 85

Figure 6.1 Impactor pulled back to 15-ft drop height (prior to release) 87

Figure 6.2 High-speed video frames from HSC-1 (FRC COR test 1) showing crush deformation of aluminum honeycomb: (a) At initial impact; (b) – (e) Intermediate frames; (f) At peak impact force..88

Figure 6.3 High-speed video frames from HSC-2 (FRC COR test 1): (a) At start of impact; (b) – (c) Intermediate frames; (d) At peak impact force...89

Figure 6.4 FRC COR test 1 specimen after completion of impact test..89

Figure 6.5 Break beam data for FRC COR test 1 90

Figure 6.6 Tape switch data for FRC COR test 1 90

Figure 6.7 Raw concrete back block acceleration data (AC-1 & AC-2) for FRC COR test 1 (in the impact direction, local Y direction of accelerometer)..91

Figure 6.8 Raw front nose acceleration data (AC-3 & AC-4) for FRC COR test 1 (in the impact direction, local Y direction of accelerometer) 92

Figure 6.9 Computed impact forces from back block for FRC COR test 1..................................92

Figure 6.10 Computed impact forces from front nose for FRC COR test 1.................................93

Figure 6.11 Raw and filtered total computed impact force for FRC COR test 1 93

Figure 6.12 Filtered total experimental impact force for FRC COR test 1 compared to FEA prediction 94

Figure 6.13 High-speed video frames from HSC-1 (FRC COR test 2) showing crush deformation of aluminum honeycomb: (a) At initial impact; (b) – (e) Intermediate frames; (f) At peak impact force..95

Figure 6.14 High-speed video frames from HSC-2 (FRC COR test 2): (a) At start of impact; (b) – (c) Intermediate frames; (d) At peak impact force 96

Figure 6.15 FRC COR test 2 specimen after completion of impact test.......................................96

Figure 6.16 Break beam data for FRC COR test 2 97

Figure 6.17 Tape switch data for FRC COR test 2 97

Figure 6.18 Raw concrete back block acceleration data (AC-1 & AC-2) for FRC COR test 2 (in the impact direction, local Y direction of accelerometer) 98

Figure 6.19 Raw front nose acceleration data (AC-3 & AC-4) for FRC COR test 2 (in the impact direction, local Y direction of accelerometer) 98

Figure 6.20 Computed impact forces from back block for FRC COR test 2.................................99

Figure 6.21 Computed impact forces from front nose for FRC COR test 2 99

Figure 6.22 Raw and filtered total computed impact force for FRC COR test 2 100

Figure 6.23 Filtered total experimental impact force for FRC COR test 2 compared to FEA prediction 100

Figure 6.24 Laser displacement sensor data from FRC test 2 101

Figure 6.25 External concrete strain gage data for locations on the top front face of the railing during FRC COR test 2 102

Figure 6.26 External concrete strain gage data for locations on the lower front face of the railing during FRC COR test 2 102

Figure 6.27 External concrete strain gage data for locations at the toe of the railing and deck during FRC COR test 2...103

Figure 6.28 External concrete strain gage data for locations on the back face of the railing during FRC COR test 2...103

Figure 6.29 Internal rebar strain gage data during FRC COR test 2: (a) Deck rebar; (b) Railing rebar...104

Figure 6.30 Impactor pulled back to 15-ft drop height (prior to release) 105

Figure 6.31 High-speed video frames from HSC-1 (R/C COR test 1) showing crush deformation of aluminum honeycomb: (a) At initial impact; (b) – (e) Intermediate frames; (f) At peak impact force; (g) – (h) Sliding and separation of loading wedge.....106

Figure 6.32 High-speed video frames from HSC-2 (R/C COR test 1): (a) At start of impact; (b) – (c) Intermediate frames; (d) At peak impact force 107

Figure 6.33 R/C COR 1 test specimen after completion of impact test....................................107

Figure 6.34 Break beam data for R/C COR test 1 108

Figure 6.35 Tape switch data for R/C COR test 1 108

Figure 6.36 Raw concrete back block acceleration data (AC-1 & AC-2) for R/C COR test 1 (in the impact direction, local Y direction of accelerometer)...110

Figure 6.37 Raw front nose acceleration data (AC-3 & AC-4) for R/C COR test 1 (in the impact direction, local Y direction of accelerometer) 110

Figure 6.38 Computed impact forces from back block for R/C COR test 1...............................111

Figure 6.39 Computed impact forces from front nose for R/C COR test 1................................111

Figure 6.40 Raw and filtered total computed impact force for R/C COR test 1.........................112

Figure 6.41 Filtered total experimental impact force for R/C COR test 1 compared to FEA prediction 112

Figure 6.42 Laser displacement sensor data for R/C COR test 1 113

Figure 6.43 External concrete strain gage data for locations on the top front face of the railing during R/C COR test 1 114

Figure 6.44 External concrete strain gage data for locations on the lower front face of the railing during R/C COR test 1 114

Figure 6.45 External concrete strain gage data for locations at the toe of the railing and deck during R/C COR test 1 115

Figure 6.46 External concrete strain gage data for locations on the back face of the railing during R/C COR test 1 115

Figure 6.47 Internal rebar strain gage data during R/C COR test 1: (a) Deck rebar; (b) Railing rebar...116

Figure 6.48 High-speed video frames from HSC-1 (R/C COR test 2) showing crush deformation of aluminum honeycomb: (a) At initial impact; (b) – (e) Intermediate frames; (f) At peak impact force...117

Figure 6.49 High-speed video frames from HSC-2 (R/C COR test 2): (a) At start of impact; (b) – (c) Intermediate frames; (d) At peak impact force..118

Figure 6.50 R/C COR test 2 specimen after completion of impact test.....................................118

Figure 6.51 Break beam data for R/C COR test 2 119

Figure 6.52 Tape switch data for R/C COR test 2 119

Figure 6.53 Raw concrete back block acceleration data (AC-1 & AC-2) for R/C COR test 2 (in the impact direction, local Y direction of accelerometer) 120

Figure 6.54 Raw front nose acceleration data (AC-3 & AC-4) for R/C COR test 2 (in the impact direction, local Y direction of accelerometer) 120

Figure 6.55 Computed impact forces from back block for R/C COR test 2..............................121

Figure 6.56 Computed impact forces from front nose for R/C COR test 2................................121

Figure 6.57 Raw and filtered total computed impact force for R/C COR test 2.........................122

Figure 6.58 Filtered total experimental impact force for R/C COR test 2 compared to FEA prediction 122

Figure 6.59 Laser displacement sensor data from R/C COR test 2 123

Figure 6.60 External concrete strain gage data for locations on the top front face of the railing during R/C COR test 2 123

Figure 6.61 External concrete strain gage data for locations on the lower front face of the railing during R/C COR test 2 124

Figure 6.62 External concrete strain gage data for locations at the toe of the railing and deck during R/C COR test 2..124

Figure 6.63 External concrete strain gage data for locations on the back face of the railing during R/C COR test 2..125

Figure 6.64 Internal rebar strain gage data during R/C COR test 2: (a) Deck rebar; (b) Railing rebar...126

Figure 6.65 Total impact force for each traffic railing impact test..127

Figure 6.66 Comparison of captured displacements...128

Figure 6.67 Comparison of external concrete strain gages on the deck near the railing toe (on the front side of the impact specimen)...129

Figure 6.68 Comparison of external concrete strain gages located at the center of the specimen (on back side of the impact specimen)...129

Figure 6.69 Comparison of internal strain gages located on the top deck rebar.........................130

Figure 6.70 Comparison of internal strain gages located on the railing connection rebar 130

Figure 7.1 Main components of EOR specimen...131

Figure 7.2 External EOR instrumentation: (a) Front concrete strain gage and tape switch sensor locations; (b) Back concrete strain gage and laser displacement sensor locations 132

Figure 7.3 FRC EOR specimen prepared and ready for pendulum impact testing (with instrumentation in place)....133

Figure 7.4 High-speed video frames from HSC-1 (FRC EOR test 1) showing crush deformation of aluminum honeycomb: (a) At initial impact; (b) – (e) Intermediate frames; (f) At peak impact force....134

Figure 7.5 High-speed video frames from HSC-2 (FRC EOR test 1): (a) At start of impact; (b) – (c) Intermediate frames; (d) At peak impact force....135

Figure 7.6 FRC EOR test 1 specimen after completion of impact test....135

Figure 7.7 Cracking found on FRC EOR test 1 specimen: (a) On front railing face; (b) On back railing face....136

Figure 7.8 Break beam data for FRC EOR test 1 137

Figure 7.9 Tape switch data for FRC EOR test 1 137

Figure 7.10 Raw concrete back block acceleration data (AC-1 & AC-2) for FRC EOR test 1 (in the impact direction, local Y direction of accelerometer) 138

Figure 7.11 Raw front nose acceleration data (AC-3 & AC-4) for FRC EOR test 1 (in the impact direction, local Y direction of accelerometer) 138

Figure 7.12 Computed impact forces from back block for FRC EOR test 1....139

Figure 7.13 Computed impact forces from front nose for FRC EOR test 1 139

Figure 7.14 Raw and filtered total computed impact force for FRC EOR test 1....140

Figure 7.15 Filtered total experimental impact force for FRC EOR test 1 compared to FEA prediction 140

Figure 7.16 Laser displacement sensor data from FRC EOR test 1 141

Figure 7.17 Concrete strain gage data for locations with out of range readings on the front face of the railing (due to cracking) for FRC EOR test 1 142

Figure 7.18 Concrete strain gage data for locations with in range readings on the front face of the railing for FRC EOR test 1 142

Figure 7.19 Concrete strain gage data for locations on the back (non-impact) face of the railing during FRC EOR test 1....143

Figure 7.20 Internal rebar strain gage data during FRC EOR test 1: (a) Deck rebar; (b) Railing rebar....144

Figure 7.21 Poor concrete consolidation of R/C EOR specimen 1 prior to testing: (a) Front face of railing; (b) Bottom of the (cross-sectional) railing face at free end....145

Figure 7.22 High-speed video frames from HSC-1 (R/C EOR test 1) showing crush deformation of aluminum honeycomb: (a) At initial impact; (b) – (e) Intermediate frames; (f) At peak impact force....147

Figure 7.23 High-speed video frames from HSC-2 (R/C EOR test 1): (a) At start of impact; (b) – (c) Intermediate frames; (d) At peak impact force....148

Figure 7.24 R/C EOR test 1 specimen after completion of impact test....148

Figure 7.25 Cracking found on R/C EOR test 1 specimen: (a) On front railing face; (b) On back railing face....149

Figure 7.26 Break beam data for R/C EOR test 1....150

Figure 7.27 Tape switch data for R/C EOR test 1....150

Figure 7.28 Raw concrete back block acceleration data (AC-1 & AC-2) for R/C EOR test 1 (in the impact direction, local Y direction of accelerometer)....151

Figure 7.29 Raw front nose acceleration data (AC-3 & AC-4) for R/C COR test 1 (in the impact direction, local Y direction of accelerometer)....151

Figure 7.30 Computed impact forces from back block for R/C EOR test 1....152

Figure 7.31 Computed impact forces from front nose for R/C EOR test 1....152

Figure 7.32 Raw and filtered total computed impact force for R/C EOR test 1....153

Figure 7.33 Filtered total experimental impact force for R/C EOR test 1 compared to FEA prediction....153

Figure 7.34 Laser displacement sensor data from R/C EOR test 1....154

Figure 7.35 Concrete strain gage data for locations with out of range readings on the front face of the railing (due to cracking) for R/C EOR test 1....155

Figure 7.36 Concrete strain gage data for locations with in range readings on the front face of the railing for R/C EOR test 1....155

Figure 7.37 External concrete strain gage data for locations on the back face of the railing during R/C EOR test 1....156

Figure 7.38 Internal rebar strain gage data during R/C EOR test 1: (a) Deck rebar; (b) Railing rebar....157

Figure 7.39 Total impact force for each traffic railing impact test....158

Figure 7.40 Comparison of displacements....159

Figure 7.41 Comparison of external concrete strain gages on the deck near the railing toe....160

Figure 7.42 Comparison of crack pattern on the front (impact) face of EOR railing specimens: (a) FRC EOR specimen; (b) R/C EOR specimen....160

Figure 7.43 Comparison of crack pattern on the back (non-impact) face of EOR railing specimens: (a) FRC EOR specimen; (b) R/C EOR specimen....161

Figure 7.44 Comparison of internal strain gages located on the top deck rebar....162

Figure 7.45 Comparison of internal strain gages located on the railing connection rebar....162

Figure 8.1 Final (investigated) FRC 36-in. single-slope traffic railing....163

Figure E.1 ASTM C1609 flexural test results for FRC EOR mixture samples (using Sika hooked-end steel fibers at 1.0% fiber volume, mixture no. 13)....265

LIST OF TABLES

Table | Page

Table 2.1 Design forces and vertical height requirements for traffic railings (after Table A13.2-1 in AASHTO *LRFD Bridge Design Specifications,* 2017) 13

Table 2.2 Change in test vehicles from *NCHRP Report 350* (1993) to MASH (AASHTO, 2016) 14

Table 2.3 Change in test level conditions from *NCHRP Report 350* (NCHRP, 1993) to MASH (AASHTO, 2016) 14

Table 3.1 Commercially available steel fibers 19

Table 3.2 Commercially available synthetic fibers 20

Table 3.3 Mixture proportioning requirements (FDOT, 2020b) 21

Table 3.4 Mixture constituents and proportions for the slip-formed concrete traffic railing mixture design provided by Argos (control mixture design) 21

Table 3.5 Selected fiber types and fiber volumes for evaluation 23

Table 3.6 Preliminary trial FRC mixture test matrix 23

Table 3.7 Mixture constituents and proportions for mixture design no. 2 (1.0% fiber volume) 23

Table 3.8 Comparison of computed residual tensile strengths 37

Table 3.9 Mixture constituents and proportions for mixture design no. 11 (1.0% fiber volume) 39

Table 3.10 Mixture constituents and proportions for mixture design no. 12 (1.0% fiber volume) 41

Table 3.11 Comparison between truck delivery and mixture design no. 12 44

Table 3.12 Mixture constituents and proportions for mixture design no. 13 (1.0% fiber volume) with revised admixture quantities due to supplier change 45

Table 3.13 Comparison between truck delivery and mixture design no. 13 (see Appendix D) 46

Table 4.1 Comparison between *MASH* TL-4 impact and proposed pendulum impact test 50

Table 4.2 Aluminum honeycomb cartridge characteristics 54

Table 5.1 Specifications for pressure sensitive tape switches 79

Table 5.2 Specifications for optical break beams 80

Table 5.3 Specifications for accelerometers 82

Table 5.4 Specifications for high-speed cameras 83

Table 5.5 Specifications for laser displacement sensors..84

Table 5.6 Specifications for concrete strain gages..84

Table 5.7 Specifications for rebar strain gages 85

Table 6.1 Full-scale COR impact test summary 86

Table 7.1 Full-scale EOR impact test summary 133

Table 8.1 Mixture constituents and proportions for the final (developed) FRC mixture design.164

Table E.1 Average compressive strength of concrete deck samples at 28 days 264

Table E.2 Average compressive strength of concrete deck samples near day of impact testing 264

Table E.3 Average compressive strength of concrete or FRC railing samples at 28 days 264

Table E.4 Average compressive strength of concrete or FRC railing samples near day of testing 265

CHAPTER 1
INTRODUCTION

1.1 Background

In highway bridge construction, concrete traffic railings, which are longitudinal safety devices intended to redirect errant vehicles, are commonly constructed using a slip-forming process (shown in Figure 1.1). Concrete slip-forming is an on-site construction technique in which fresh concrete is placed, formed, and finished in a single continuous motion. The use of slip-forming results in a continuous (jointless) structural element, and typically leads to an overall reduction in construction time relative to alternative concrete forming techniques. When applied to the construction of concrete traffic railings, however, conventional steel reinforcing bars contained within the final railing cross-section must be securely installed prior to the start of slip-forming (as shown in Figure 1.2). Expending time, labor, and cost on rebar installation diminishes the efficiency of slip-formed traffic railing construction. In the present study, fiber reinforced concrete (FRC) was investigated in order to replace rebar cage (consisting of flexural and shear reinforcing bars) in railings with fibers while retaining the typical railing connection bars (Figure 1.3). This investigation was performed using full-scale pendulum impact testing and complementary high-resolution finite element analysis (FEA).

Figure 1.1 Slip-formed concrete traffic railing (Photo credit: Gomaco)

(a) (b)

Figure 1.2 Slip-formed construction of conventionally rebar-reinforced traffic railings
(Photo Credit: Gomaco)

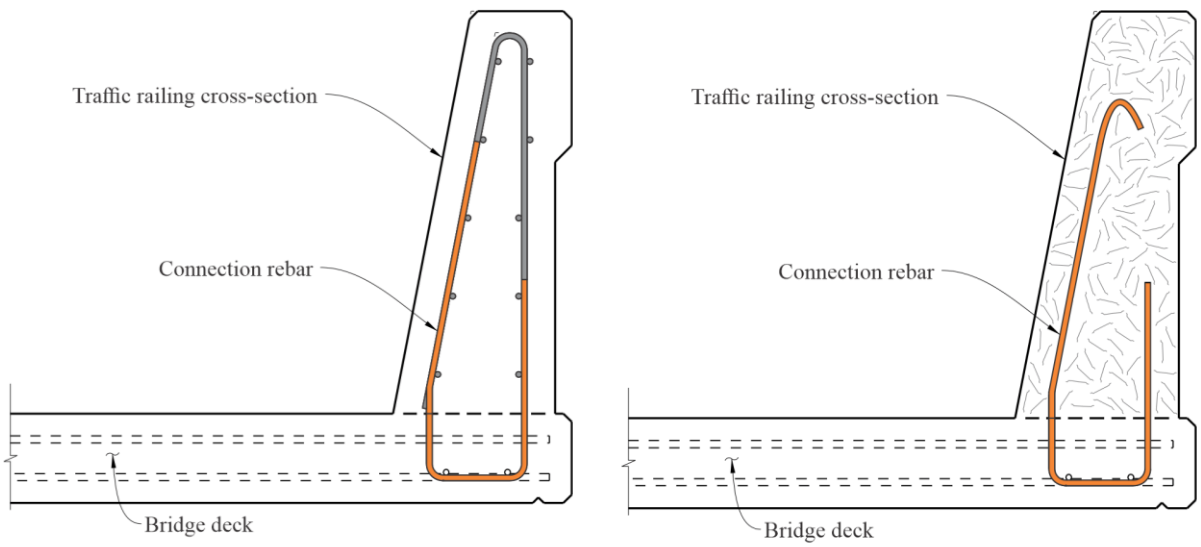

(a) (b)

Figure 1.3 Florida DOT traffic railing: (a) Current reinforcement design (after FDOT, 2020a); (b) Proposed FRC railing without secondary steel rebar cage

Conventional (plain, unreinforced) concrete is a quasi-brittle composite material that is strong in compression, relatively weak in tension, and exhibits a low strain capacity. When plain concrete is subjected to tensile load, cracks initially form in the weakest area of the concrete matrix—the transition zone, i.e. the aggregate-paste interface. As tensile load is increased, cracks within the transition zone remain stable but continue to grow in length, width, and in number, until a point of instability is reached. At this point, cracks propagate rapidly and a brittle failure is observed.

Therefore, in traditional rebar-reinforced concrete (rebar-R/C), a relatively small number of continuous steel reinforcing bars are strategically embedded within the concrete to carry tensile stresses and to prevent sudden (brittle) failure. In contrast, FRC employs a large number of small discontinuous fibers—typically made of steel, synthetic, glass, or natural materials—to provide improved tensile strength—relative to plain concrete. Adding small, discrete fibers to plain concrete has been found to improve hardened mechanical properties such as tensile strength, ductility, toughness, and impact resistance (ACI Committee 544, 2002). In FRC production, the fibers are added during the mixing process. As a result, the fibers become distributed in randomly oriented directions within the FRC matrix. Consequently, when the hardened FRC cracks under the application of tensile load, a subset of the embedded fibers bridge the cracks, thereby improving ductility and toughness, as compared to plain concrete (see Figure 1.4). Enhancements in the mechanical properties of FRC generally depend upon the geometric and mechanical properties of the fibers, the distribution and concentration of fibers, fiber-concrete bond properties, and the characteristics of the concrete. In many structural applications, fibers are added to concrete only to supplement the conventional steel reinforcing bars, by providing crack control (and thus improved durability), but are not typically used to serve as primary reinforcement.

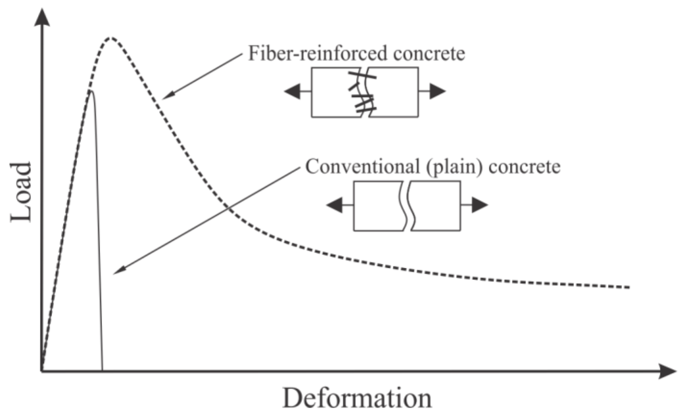

Figure 1.4 Variation of load-deformation curves for unreinforced concrete and FRC (after ACI Committee 544, 2002)

In the present research, FRC is used so that the longitudinal bars and a portion of the vertical bars used in the current barrier reinforcing cage can be eliminated. It is anticipated that the reduction in bar reinforcement will improve the overall efficiency of slip-forming by reducing both construction time and/or cost. The distributed nature of fibers in FRC could also yield additional performance benefits. To form the structural connection between a bridge deck and traffic railing, steel reinforcing bars extending vertically from the deck up into the body of the proposed FRC traffic railing must be retained (as shown in Figure 1.3b). Under lateral vehicle impact loading, the redirectional capacity (i.e., overturning strength) of the traffic railing is at least partially a function of the pull-out capacity of the vertical steel reinforcing bars. Providing highly distributed crack resistance—using distributed fibers in the concrete railing—will hypothetically increase the rebar pull-out capacity, and increase lateral resistance to vehicle impact loading. Additionally, while FRC does not eliminate cracking, it does promote better distribution and smaller widths of cracks when the concrete is stressed beyond its cracking strength. It is anticipated that this behavior will result in post-impact damage that is more repairable than damage in a corresponding barrier with conventional concrete and reinforcement. Another beneficial characteristic of FRC is the resistance to spalling provided locally by the fibers. For overpass bridges, which span over active traffic lanes, motorist safety would be improved by reducing the potential for impact-induced spalling—which could lead to the danger of falling concrete rubble. Finally, since the FRC traffic railing will use minimal steel reinforcing bars (only vertical bars to connect the railing and deck), the aesthetic appearance will be improved by reducing crack sizes and accordingly reducing (or eliminating) staining associated with rebar corrosion.

To ensure adequate motorist safety, traffic railings on the national highway system (NHS) are required to satisfy nationally adopted design criteria for vehicle impact loading [e.g., AASHTO

Manual for Assessing Safety Hardware (AASHTO, 2016)]. Consequently, the FRC traffic railing concept developed in this study was designed with consideration of MASH-specified vehicle impact loading conditions. Additionally, slip-formed traffic railing construction requires the use of a non-segregating, low-slump concrete mixture—so that the plastic concrete retains its shape after forming. Therefore, fiber selection in this study focused on both fresh concrete properties (slump, etc.) as well as hardened mechanical properties (strength, toughness, etc.).

1.2 Objectives

Primary objectives of this study were: (1) to develop a fiber-reinforced concrete (FRC) mixture that has fresh concrete characteristics that are suitable for use in slip-forming, and (2) to evaluate, using experimental pendulum impact testing and complementary numerical simulation, whether the proposed FRC railing possesses impact resistance equivalent to (or greater than) that of a traditional rebar-reinforced (rebar-R/C) concrete traffic railing.

Relative to rebar-R/C, FRC has the potential to exhibit improvements in characteristics such as tensile strength, crack control, durability, ductility, toughness, and impact resistance. The constituent material (glass, carbon, steel, etc.), geometry, volume, and distribution of the embedded fibers all affect FRC performance. For example, past studies have demonstrated that inclusion of synthetic- or steel-fibers yields increases in toughness and impact resistance which vary in proportion to volume of fiber introduced. However, adding fibers to concrete also affects the workability characteristics of fresh concrete (e.g., slump). Achieving fresh concrete characteristics that are suitable for use in slip-forming, yet simultaneously achieving adequate mixing and distribution of fibers within the concrete, can be a particular challenge. Consequently, key components of this study involved the investigation of different fiber materials, geometries, etc., as well as the investigation of additives (e.g., superplasticizers), so as to produce an FRC mixture that is viable for use in slip-form construction.

It must also be noted that tensile failure mechanisms in FRC can be associated with fiber pullout (from the surrounding concrete matrix), or with fiber rupture (sudden failure), depending on the fiber material characteristics, fiber geometry, and loading rate. Physical tests conducted for the purpose of evaluating vehicle impact resistance of an FRC traffic railing should therefore be dynamic in nature. In the present study, a suitable impact testing protocol was developed, and FRC traffic railing impact tests were performed using the FDOT pendulum impact test facility. Pendulum impact results were used to demonstrate that the proposed FRC traffic rail system is structurally equivalent to an existing FDOT traffic railing.

1.3 Scope of work

The scope of work included in this study was organized into the following key phases:

- <u>Laboratory-scale production of trial FRC mixtures</u>: Trial FRC mixture designs were developed and produced (i.e., batched) on a limited 'laboratory-scale' employing various commercially-available fiber options at multiple fiber content volumes. Focus was given to assessing the workability characteristics (e.g., slump) and to assessing the suitability of the freshly mixed FRC for potential use in a slip-formed concrete traffic railing. During trial mixture production, small-scale test specimens (e.g., cylinders and flexural beams) were formed, which were subsequently used to evaluate the hardened mechanical properties of each trial mixture. Based on the quantified mechanical properties (specifically those deemed most critical for the proposed application), the most suitable FRC mixture was selected for use in full-scale pendulum impact test specimens.

- Design of FRC traffic railing: The FDOT 36-in. single-slope traffic railing (SSTR) was selected as the standard traffic railing for investigation in the present study. Therefore, an FRC 36-in. SSTR was designed to be structurally equivalent to the existing FDOT 36-in. SSTR, by following yield line analysis concepts prescribed in AASHTO *LRFD Bridge Design Specifications* with adaptations to account for the mechanical properties of FRC.

- Develop procedures for pendulum impact testing of traffic railing specimens: Vehicle impact test conditions prescribed in *AASHTO MASH* (AASHTO, 2016) were used to develop pendulum impact test protocols. Equivalent impact energy from a single-unit truck (SUT) test level 4 (TL-4) impact test (56 mph at 15 deg.) was used to develop initial pendulum impactor conditions. To produce 155 kip-ft of impact energy, a 10,000-lb impactor was selected with an estimated initial drop height of 15.5 ft. Additionally, a force-time curve presented in literature from FEA vehicle impact simulations was used to develop a crushable nose configuration on the pendulum impactor, designed to deliver similar vehicle impact forces presented in the literature.

- Pendulum impact testing of FRC and R/C traffic railings: Traffic railing test specimens were designed for pendulum impact testing. To facilitate direct comparisons between a traditionally reinforced concrete (R/C) traffic railing and the proposed FRC traffic railing, test specimens of both types (R/C and FRC) were designed. Each test specimen consisted of a segment of traffic railing cast on top of a portion of bridge deck—using formwork. The partial-deck beneath the railing portion of the test specimen was designed to attach to the rigid universal foundation that is located in the south 'bay' of the FDOT impact pendulum. To assess the structural performance and adequacy of the proposed FRC traffic railing, 3 FRC and 3 standard R/C traffic railing test specimens (with an integrated partial-deck) were pendulum impact tested. Following the completion of impact testing, detailed analysis/interpretation of data collected from each test type was completed to establish whether the proposed FRC traffic railing was shown to be structurally equivalent to the traditional (standard FDOT) R/C system.

CHAPTER 2
BACKGROUND AND LITERATURE REVIEW

2.1 Introduction

The following section summarizes a review of related literature for the present study. The literature review was conducted with a focus on fiber options for FRC mixture design, FRC properties (specifically dynamic mechanical properties), slip-form construction, and current design standards for concrete traffic railings.

2.2 FRC fiber options

Generally, wide ranging types of fiber are commercially available (Figure 2.1) and an equally wide range of applications exist for such fibers in the construction of structures. Fibers in FRC are primarily categorized based on the type of fiber material utilized (steel, glass, synthetic, or natural), but may also be further sub-categorized based on geometric characteristics such as length and end geometry (e.g. hooked-end, etc.).

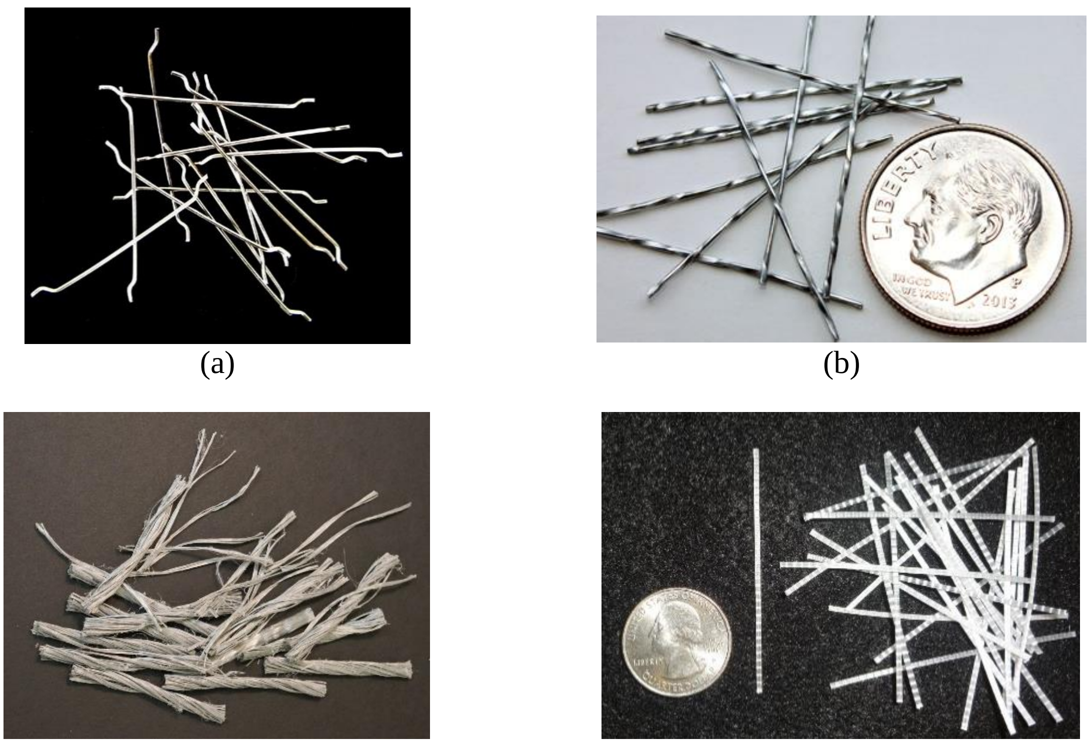

(a) (b)

(c) (d)

Figure 2.1 Various types of commercially available fibers: (a) Steel hooked-end fiber; (b) Helix steel fiber; (c) Forta-Ferro synthetic fiber; (d) BASF polypropylene fiber

2.2.1 Fiber mechanical behavior

Relative to the total unit volume of FRC produced in a single batch, the volume of reinforcing fibers can range from low to high. Fiber concentration—which is typically expressed as a volume percentage—significantly affects the hardened concrete performance as well as mixing and placing properties. Fiber content is considered 'low' for volume percentages ranging from 0.1% to 1.0%, 'moderate' for the range 1% to 3%, and 'high' for the range 3% to 12% (Zollo, 1997). When fibers are used as reinforcement in FRC, they are intended to mitigate cracks at both the micro- and macro-levels (Banthia and Sappakittipakorn, 2007). Initially, at the smaller micro-level, fibers help prevent crack initiation and also help to slow the growth of small cracks. As cracks continue to grow in size and coalesce into larger macro-cracks, reinforcing fibers provide a mechanism to again slow the macro-crack propagation—through 'bridging'—which results in additional concrete strength, toughness, and ductility (Banthia and Sappakittipakorn, 2007).

The ability of fibers to bridge macro-cracks and slow concrete rupture is dependent on the path of the crack through and around fibers. Moreover, crack bridging is highly dependent on the number of fibers encountered as a crack propagates, as well as the surface area and strength of the fibers themselves (Zollo, 1997). Fiber 'failure' may involve either fiber pullout or fiber rupture. Fiber pullout is the preferred failure mechanism since the alternative, fiber rupture, results in a more brittle FRC failure mode (Banthia and Trottier, 1994). In general, the fiber pullout mechanism is primarily responsible for the enhanced strength and ductility of FRC.

After initial cracking, the matrix-fiber bond is broken and subsequent concrete element deformation can be attributed to fiber extension (Markovic, 2006; Zollo, 1997). Fibers with higher aspect ratios (i.e., ratio of length to diameter) and with deformed shapes tend to exhibit increased toughness (Figures 2.2–2.3) because more energy is required to debond and finally pullout the fiber, relative to shorter and straighter fiber types. However, fibers with aspect ratios of greater than 100 have been found to cause workability and fiber distribution difficulties (ACI Committee 544, 2002).

Fiber rupture—sometimes referred to as fiber failure—occurs when the fiber-matrix bond is stronger than the fiber rupture strength. As a result, fibers rupture without fully debonding and the observed ductility becomes dependent upon the mechanical properties (e.g., rupture strength) of the fiber and may lead to a more brittle failure mode (as shown in Figure 2.4).

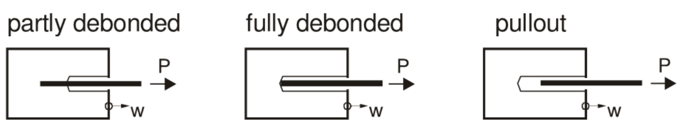

Figure 2.2 Pullout failure mechanism of a straight steel fiber (Markovic 2006)

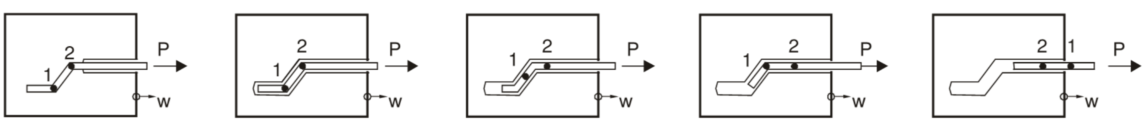

Figure 2.3 Pullout failure mechanism of a hooked-end steel fiber (Markovic 2006)

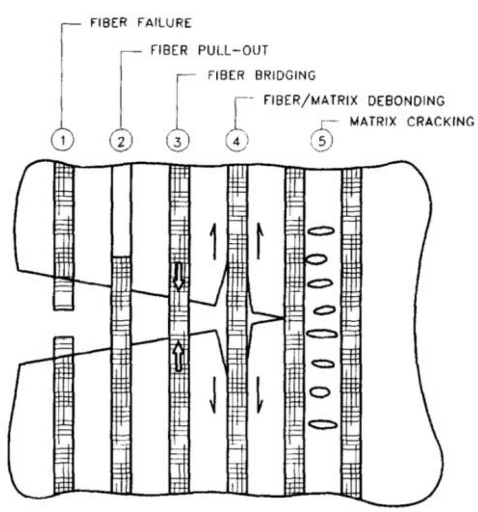

Figure 2.4 Fiber failure mechanisms (Zollo 1997)

2.2.2 Steel fibers

Steel fibers are short, discrete lengths of steel (typically ranging from 0.25 to 3 in. in length)—which also vary in shape (Figure 2.5)—with an aspect ratio (length to diameter ratio) ranging from 20 to 100 (ACI Committee 544, 2002). Each geometric shape—which is partly defined by the production process of the steel fibers—has a different impact on both the freshly mixed FRC properties and hardened FRC properties. For example, hooked ends improve resistance to pullout (Kosmatka et al., 2003) but can also adversely influence the fresh concrete mixture workability. In contrast, straight fibers have less pullout resistance, but also have less adverse influence on workability.

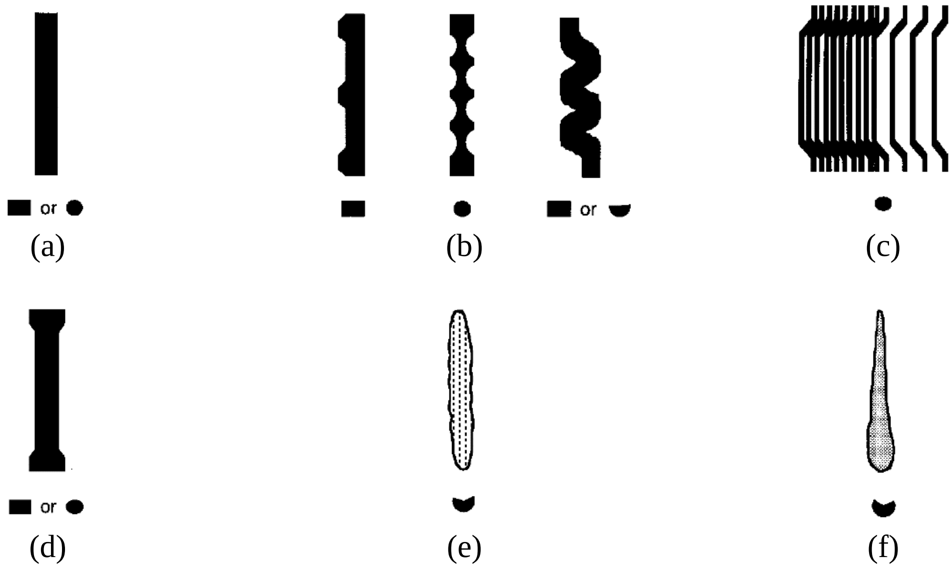

Figure 2.5 Steel fiber configurations: (a) Straight silt sheet or wire; (b) Deformed silt sheet or wire; (c) Hooked-end wire; (d) Flattened-end silt sheet or wire; (e) Machined chip; (f) Melt extract; (after ACI Committee 544, 2002)

According to Bencardino et al. (2010), steel fibers are usually used to improve mechanical properties while lower modulus (i.e., more flexible) fibers are used to improve crack control. However a common concern with steel fibers is potential for corrosion. In a structural FRC element (e.g., a traffic railing) within which steel fibers are approximately uniformly distributed, a certain portion of the fibers will be located at or near the surface—with effectively zero cover—and will therefore be susceptible to corrosion. Fiber corrosion will be limited to surface zones since the fibers are discontinuous and therefore do not provide a means of propagating corrosion to the internal element core. However, corrosion-induced surface color changes (in varying shades of brown) have been observed in FRC mixtures employing steel fibers, particularly in aggressive environments (Kosa and Naaman, 1990; ACI Committee 544, 2002). Therefore, when considering the use of steel fibers, aesthetics (e.g., color change) must also be considered (and investigated).

2.2.3 Synthetic fibers

A wide range of man-made materials—developed in the petrochemical and textile industries (ACI Committee 544, 2002)—have been utilized in synthetic FRC mixtures. Some of the more commonly used synthetic fibers are nylon and polypropylene. Synthetic fibers can be further subdivided into microsynthetic or macrosynthetic fibers, which are differentiated by a fiber length of 1.5 in.; microsynthetic fibers are shorter than 1.5 in. and macrosynthetic fibers are longer than 1.5 in. (ACI Committee 544, 2008). More generally, synthetic fibers are available in lengths from 0.2 in. to around 2.5 in. (ACI Committee 544, 2002). Macrosynthetic fibers are also sometimes referred to as 'structural fibers' while microsynthetic fibers may be considered 'non-structural fibers'. The use of synthetic fibers has been shown to improve crack distribution, reduce crack size, and improve other properties (e.g., synthetic fibers are not alkali reactive) (ACI Committee 544, 2002).

2.2.4 Other fiber types and hybrid fibers

Due to its relatively light weight characteristic, glass FRC has been extensively used in architectural cladding applications, reducing overall self-weight of the structure, and therefore reducing structural member sizes as wells as cost (Kosmatka et al., 2003). However, when glass fibers were first adopted for use in FRC, conventional types of glass (E-glass and A-glass) were found to be highly alkali reactive. Moreover, glass fibers were found to react with the cement paste during hydration, degrading the mechanical properties of the fiber reinforcement (ACI Committee 544, 2002). Although alkali-resistant (AR) glass fibers have since been developed to improve long-term durability, most commercially available glass fibers have been found to exhibit a reduction in tensile strength when used in concrete exposed to normal outdoor environments (ACI Committee 544, 2002).

Natural fibers, made from naturally occurring materials such as coconut, bamboo, sisal, jute, and wood, can be obtained at a relatively low cost and vary in length from 0.1 in. to over 17 in. (ACI Committee 544, 2002). Although such fibers have historically been used to reinforce cement composites (and other brittle materials), little research has been focused on the use of natural fibers as a form of concrete reinforcement. Additionally, deficiencies in long term durability are a concern for natural fibers (ACI Committee 544, 2002).

2.3 Previous (related) FRC studies

For steel FRC, ACI 544.1R-96 (ACI Committee 544, 2002) reported that dynamic strength may be 40% larger than that of corresponding plain concrete matrix. Peak dynamic loads at failure have been found to be 2 to 3 times the corresponding peak static load (ACI Committee 544, 2002). For polypropylene FRC, it has been reported that first-crack strength and failure strength are both increased with the addition of polypropylene fibers. In both steel and polypropylene FRC, impact strength has been found to increase as fiber content is increased (ACI Committee 544, 2002).

Ong et al. (1999) conducted low velocity drop-weight tests on steel and synthetic FRC slabs with fiber volumes ranging from 0% to 2%. Hooked-end steel fibers (with a length of 1.2 in. and an aspect ratio of 60), straight polyolefin fibers (with a length of 2 in. and an aspect ratio of 80), and straight polyvinyl alcohol fibers (with a length of 0.47 in. and an aspect ratio of 60) were compared. The study revealed that steel fibers performed better than the two polymeric fibers based on cracking characteristics, energy absorption, and slab integrity after impact. Additionally, it was observed that as fiber volume increased, the flexural capacity and fracture energy also increased, for all fiber types considered.

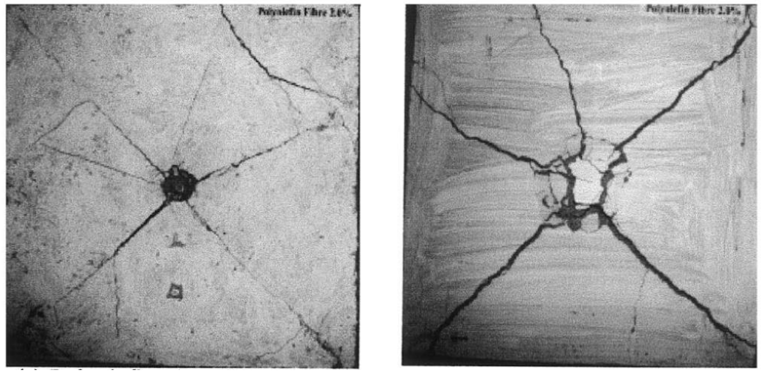

(a)

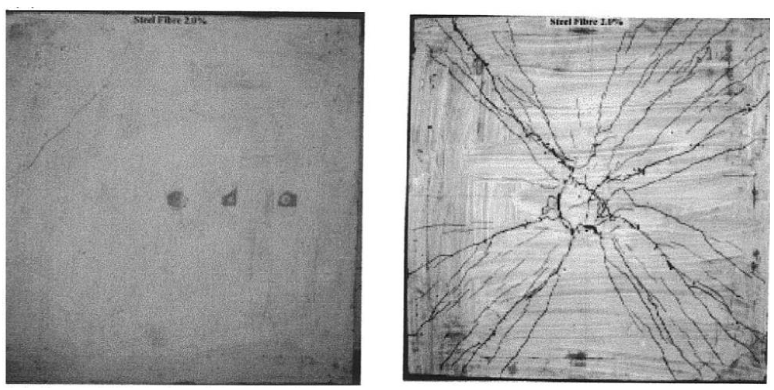

(b)

Figure 2.6 Failure patterns for slabs containing 2% fiber volumes: (a) Polyolefin fibers (top and bottom surfaces); (b) Steel fibers (top and bottom surfaces); (Photo credit: Ong et al. 1999)

Hrynyk and Vecchio (2014) also investigated the impact performance of concrete slabs using drop-weight impact tests. Slabs in this study contained a combination of longitudinal steel reinforcing bars (in two directions) and hooked-end steel fibers. Hooked-end steel fibers (with a length of 1.18 in. and aspect ratio of 80) were added with volume ratios that ranged from 0% to 1.5%. The target compressive strength of the FRC was 7250 psi. Two parameters were varied in the study: 1) steel fiber volume, and 2) steel reinforcement ratio. Based on the results of multiple drop-weight impact tests, it was concluded that the addition of hooked-end steel fibers reduced crack spacings and widths; mitigated localized damage due to the drop-weight (e.g., less spalling and scabbing at the point of impact); and increased slab stiffness and capacity. Additionally, a fiber volume of 1.5% (the highest volume considered) was found to be the only case for which the slab failure mode was not controlled by punching shear.

In Charron et al. (2011), four precast bridge parapets (i.e., 6.6-ft long railing specimens) were designed and tested to study the influence of fiber reinforcement. Three of the tested parapets were constructed using steel FRC (with different fiber volumes and different concrete compressive strengths) while the fourth made use of high performance concrete. For one of the parapets, Charron et al. (2011) reduced the cross-sectional dimensions by increasing the concrete compressive strength (from 7250 psi to 17.4 ksi) and the steel fiber reinforcement volume (from 0% to 4%). Additionally, all traditional bar reinforcement was removed, relying only on straight steel fibers with a length of 0.4 in. and an aspect ratio of 50 (Figure 2.7). Although it was noted that removal of all traditional rebar was not the most cost effective design, the authors demonstrated that traditional steel bar reinforcement could be effectively replaced with FRC.

Combinations of quasi-static and dynamic tests on 2-meter (6.6-ft) long specimens were used to demonstrate structural adequacy of the FRC systems.

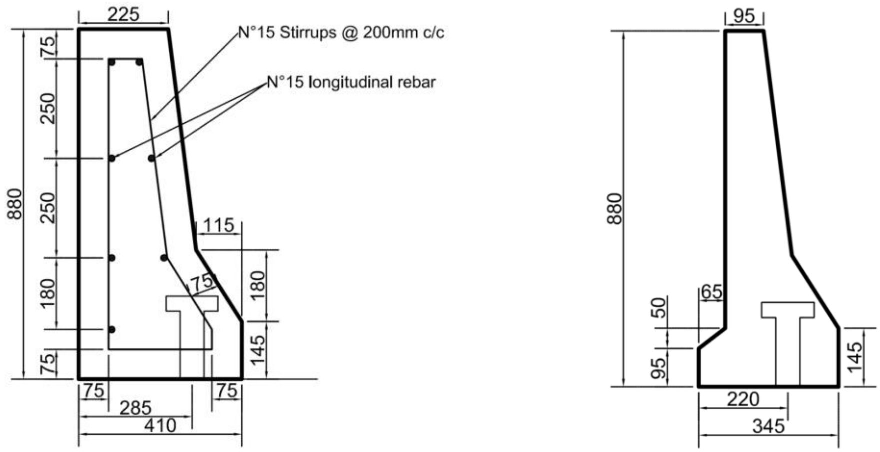

(a) (b)

Figure 2.7 Precast parapet with: (a) High-performance concrete (7250 psi, 0% fiber volume); (b) Steel FRC (14.4 ksi, 4% fiber volume); (Charron et al., 2011)

2.4 Slip-form railing construction and freshly mixed property requirements

In slip-form construction, a low-slump concrete mixture is required such that at the end of the slip-forming process, the freshly formed concrete will retain its shape without any (edge) support, as shown in Figure 2.8 (Pekmezci et al., 2007). Typically, slip-form construction requires the use of a concrete mixture with a slump less than 2.0 in., ensuring that the mixture will retain its shape (Pekmezci et al., 2007; Voigt et al., 2010; Wang et al. 2008). To consolidate and form the stiff (low-slump) concrete mixture, the slip-form 'paving' machine uses extensive vibration energy, which is provided by internal vibrators, as shown in Figure 2.9b (Pekmezci et al., 2007).

During slip-form construction, a continuous supply of (adequately) uniform concrete is necessary. Variation in mixtures between supply trucks can contribute to finishing difficulties (Green, 1997). Therefore, allowable slump ranges are typically specified to remain within a narrow margin. For conventional traffic railing designs, steel reinforcement is required. As a consequence, steel reinforcement must be placed (and firmly secured) before the slip-forming construction process may begin. With the presence of steel reinforcement during the slip-forming process, the conventional steel rebar reinforcement will provide support to the shape of the freshly formed concrete (i.e., the rebar 'cage' assists the concrete in retaining its shape after forming). Conversely, if steel reinforcement is removed from a traffic railing design (e.g., if fiber reinforcement is used to replace conventional steel rebar reinforcement, as proposed in the present study), the fresh concrete mixture must maintain an even smaller range of allowable slump, because support aid from the rebar reinforcement has been removed. For scenarios where 'free-standing' railings (i.e., railings without conventional rebar reinforcement) are used, the slump is typically specified to range from 0.75 in. to 1.0 in. (Green, 1997).

Figure 2.8 Retained railing shape after slip-forming (Photo credit: Gomaco)

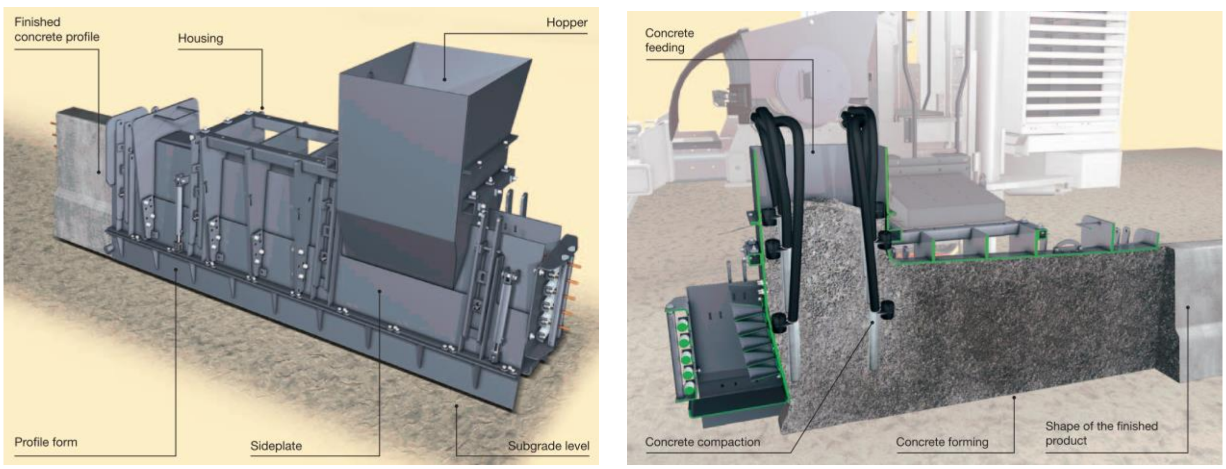

(a) (b)

Figure 2.9 Railing construction formwork: (a) Railing formwork components; (b) Railing formwork cross-section with internal vibrators located within the hopper for compaction (Figure credit: Wirtgen Group)

2.5 Concrete traffic railing design

To ensure the safety of motorists, the Federal Highway Administration (FHWA) has provided national policies that must be met for highways and bridges throughout the U.S. Additionally, the American Association of State Highway and Transportation Officials (AASHTO) and the National Cooperative Highway Research Program (NCHRP) have provided design guidelines and policies regarding concrete traffic railing safety. The following section catalogs concrete traffic railing design guidelines. Since the Florida Department of Transportation (FDOT) is a primary sponsor of the present study, guidelines specific to the FDOT were also reviewed.

2.5.1 AASHTO *LRFD* Bridge Design Specifications

Section 13 and Appendix A13 of AASHTO *LRFD Bridge Design Specifications* contain specifications related to the design of traffic railings (i.e., cover design specifications for bridge traffic barrier systems, which are also referred to as railings). As specified in AASHTO *LRFD*, newly designed railings must be shown to be 'structurally' and 'geometrically' crashworthy (AASHTO, 2017).

The purpose of a traffic railing is to keep errant vehicles within the roadway and prevent vehicles from colliding with more dangerous obstacles (or prevent more serious accidents from occurring). In order to design a railing such that it is able to provide 'structural' strength during an impact, AASHTO *LRFD* provides a series of design guidelines and strength prediction equations (based on yield line theory), to compute the ultimate strength of a railing during impact. The required strength of a railing depends on typical vehicle speeds and common vehicle sizes used on the roadway. In AASHTO *LRFD*, the ultimate strength of a concrete traffic railing is determined by selecting a specified design impact test level. AASHTO *LRFD* specifies six different impact test levels—with Test Level 1 (TL-1) the lowest level of impact and Test Level 6 (TL-6) the highest (i.e., TL-6 pertains to the largest required design forces).

Along with 'structural' adequacy, a railing must also be 'geometrically' crashworthy, such that during an impact, the railing is able to sufficiently prevent an errant vehicle from escaping the roadway (i.e., prevent a vehicle from rolling over the railing). Therefore, AASHTO *LRFD* specifies minimum design height requirements for each impact test level. Specified design forces and minimum railing height requirements provided by AASHTO *LRFD* are reproduced in Table 2.1.

Table 2.1 Design forces and vertical height requirements for traffic railings
(after Table A13.2-1 in AASHTO *LRFD Bridge Design Specifications,* 2017)

	Railing Test Levels					
Design requirement	TL-1	TL-2	TL-3	TL-4	TL-5	TL-6
Transverse design force (kips)	13.5	27.0	54.0	54.0	124.0	175.0
Minimum railing height (in.)	27.0	27.0	27.0	32.0	42.0	90.0

2.5.2 MASH specifications

To determine whether or not a railing design is crashworthy, impact testing is generally required, as determined by the FHWA. *NCHRP Report 230* (NCHRP, 1981) *and NCHRP Report 350* (NCHRP, 1993) were both developed to provide uniformity in impact testing procedures of railings (and other safety hardware). *NCHRP Report 350* includes definitions of crash test levels with specified vehicle, vehicle speed, and impact angle for each impact test level. AASHTO *LRFD* test levels coincide with those reported in *NCHRP Report 350*.

NCHRP Report 350 was published in 1993 and was formally implemented as the national standard by FHWA in 1998 (Silvestri-Dobrovolny et al., 2017). However, since that time, the vehicle fleet found on roadways has changed (e.g., vehicle sizes have generally increased). Therefore, to provide crash criteria that is more representative of current roadway conditions in regards to vehicle sizes and typical speeds, *NCHRP Report 350* was superseded by the AASHTO Manual for Assessing Safety Hardware (MASH). MASH contains revised impact testing criteria to better represent the current fleet of vehicles and place greater safety-performance demands on many roadside safety devices (Silvestri-Dobrovolny et al., 2017). For example, the small car impact test vehicle specified in *NCHRP 350* was increased in mass from 820 kg (referred to as the 820C test vehicle) to 1100 kg in MASH (referred to as the 1100C test vehicle). A comparison of the test vehicle fleet requirements between *NCHRP 350* and MASH is provided in Table 2.2. Similarly, a comparison of specific test level impact criteria from *NCHRP 350* and MASH is provided in Table 2.3.

Table 2.2 Change in test vehicles from *NCHRP Report 350* (1993) to MASH (AASHTO, 2016)

Test vehicle type	NCHRP 350 test vehicle designation	MASH test vehicle designation
Passenger car	820C (1809 lb)	1100C (2420 lb)
Pickup truck	2000P (4409 lb)	2270P (5000 lb)
Single-unit truck	8000S (17,636 lb)	10000S (22,000 lb)
Tractor-van trailer	36000V (79,366 lb)	36000V (79,300 lb)

Table 2.3 Change in test level conditions from *NCHRP Report 350* (NCHRP, 1993) to MASH (AASHTO, 2016)

Test level	Test vehicle type	*NCHRP 350* (NCHRP, 1993)	*MASH* (AASHTO, 2016)
TL-3	Passenger car	Impact speed: 62 mph Impact angle: 20 deg.	Impact speed: 62 mph Impact angle: **25 deg.**
TL-3	Pickup truck	Impact speed: 62 mph Impact angle: 25 deg.	Impact speed: 62 mph Impact angle: 25 deg.
TL-4	Single-unit truck	Impact speed: 50 mph Impact angle: 15 deg.	Impact speed: **56 mph** Impact angle: 15 deg.
TL-5	Tractor-van trailer	Impact speed: 50 mph Impact angle: 15 deg.	Impact speed: 50 mph Impact angle: 15 deg.

In 2016, the second edition of MASH was published by AASHTO. After its release, FHWA and AASHTO adopted a joint implementation agreement that established dates for implementing MASH compliant safety hardware (Silvestri-Dobrovolny et al., 2017). In summary, FHWA policy is that all new or replacement railings on the NHS must be evaluated using the 2016 edition of MASH. Furthermore, all new or replacement railings must meet TL-3 crash test criteria at a minimum (Silvestri-Dobrovolny et al., 2017). This newly accepted policy took effect on December 31, 2019.

2.5.3 Texas DOT single slope traffic railing (SSTR)

Due to the increase in vehicle mass and impact speed in TL-4 of MASH, the impact kinetic energy for TL-4 has increased by 56 percent compared to *NCHRP Report 350* impact criteria. Additionally, in AASHTO *LRFD*, for TL-4 railing design, the minimum railing height is 32 in. and must be designed to provide a 54-kip (transverse) impact load. However, these specifications were based on TL-4 impact conditions prescribed in *NCHRP Report 350*, and as a result must be updated to account for the increase in impact severity from *NCHRP 350* to MASH (Sheikh et al., 2011).

In Sheikh et al. (2011), it was reported that previous testing was conducted on a 32-in. New Jersey profile concrete traffic railing, to evaluate impact performance differences related to the changes in impact severity under MASH criteria. The previously successful 32-in. railing under *NCHRP Report 350* impact criteria was found to be unsuccessful when impact-tested under MASH criteria. During the failed impact test, the TL-4 single-unit vehicle rolled over the top of the barrier, indicating the need to consider taller railing requirements for MASH TL-4 railings. As a result, Sheikh et al. (2011) used FEA impact simulations of MASH TL-4 impact conditions to determine a more suitable minimum railing height, using a single slope barrier profile.

Based on the findings of Sheikh et al. (2011), a minimum railing height of 36 in. was recommended for MASH TL-4 railings. Additionally, considering the increase in railing height, Sheikh et al. (2011) recommended that TL-4 (transverse) design impact loads specified in AASHTO *LRFD* be increased from 54 kips to 80 kips, based on results of FEA impact simulations.

To compare and validate FEA impact simulation results, Sheikh et al. (2011) conducted a TL-4 impact test on a standard Texas DOT 36-in. single slope traffic railing (SSTR), following MASH impact criteria. The 36-in. SSTR (Figure 2.10) was selected for testing since it was a standard railing in Texas that met the recommended minimum railing height and was determined to provide an impact resistance of 80 kips, as determined by using the AASHTO *LRFD* yield line equations. Based on the MASH TL-4 impact test conducted by Sheikh et al. (2011), the 36-in. Texas DOT SSTR was considered to be suitable for MASH TL-4 implementation on Texas highways.

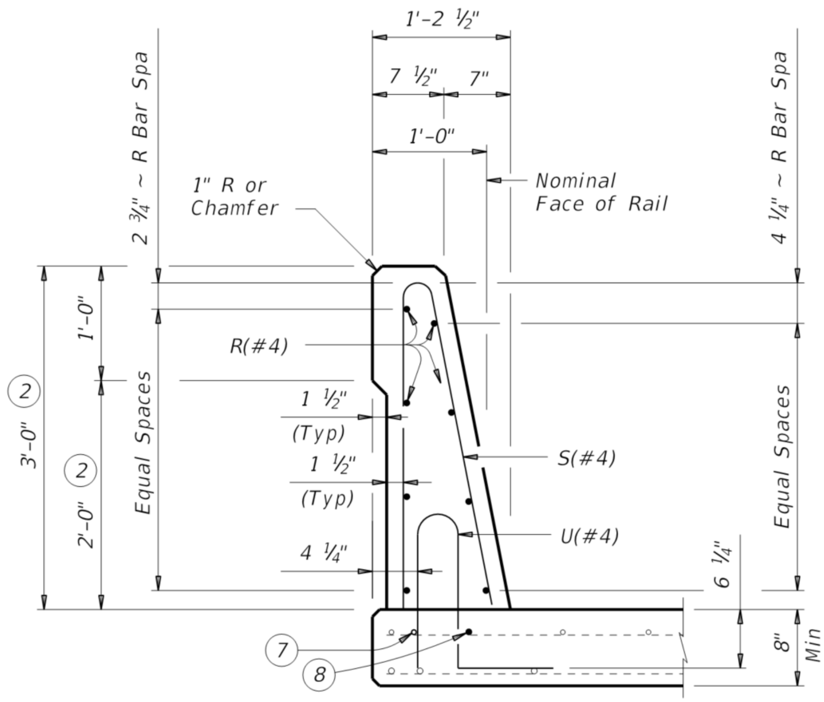

Figure 2.10 Texas DOT single slope traffic railing (SSTR) standard details

2.5.4 Railing selection for the present study : FDOT 36-in. SSTR

Due to future MASH implementation requirements, as specified by FHWA, a new MASH TL-4 compliant traffic railing was needed for the FDOT—the primary sponsor of the present study. Since an existing MASH crash-tested railing was available, provided by the Texas DOT in the form of the 36-in. SSTR, a modified version of the Texas DOT SSTR was adopted by FDOT.

The 36-in. 'single-slope' traffic railing, shown in Figure 2.11, is the new basic default traffic railing for use on FDOT bridges and retaining walls. Furthermore, the TL-4 36-in. railing was selected for incorporation into FDOT design standards due to its simple forming ability (i.e., the single-slope profile provides a simple geometry to form during construction). Although the shape of the FDOT single-slope railing is similar to that of the Texas DOT railing, minor adjustments in the design (e.g., width dimensions) were made by FDOT to provide an increase in concrete cover. Selected reinforcement details were also modified in the FDOT railing.

Although the FDOT railing was not directly impact tested, the 36-in. railing design adopted by FDOT was evaluated to have the required design strength (FDOT, 2020a). Additionally, since the FDOT railing has the same single-slope geometry as the Texas DOT 36-in. railing, which has been crash tested to MASH TL-4 criteria, the FDOT 36-in. single-slope traffic railing was determined to meet MASH crashworthiness requirements.

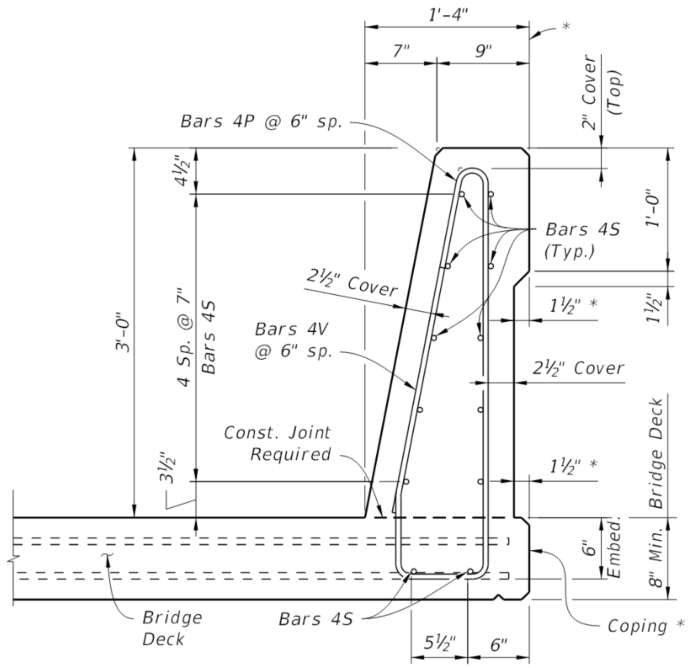

Figure 2.11 FDOT 36-in. single-slope traffic railing (FDOT 2020a)

Due to the need for a MASH compliant traffic railing, a modified version of the Texas DOT single slope traffic railing was adopted by FDOT. The primary objective of the present study was to determine the viability of a fiber-reinforced traffic railing. Therefore, the FDOT 36-in. single-slope traffic railing was used as the standard traffic railing (with additional adjustments to include the use of FRC) for investigation in the present study. To determine the design strength of the current FDOT 36-in. single-slope traffic railing, an ultimate strength yield line analysis worksheet was developed following AASHTO *LRFD Bridge Design Specifications*, and is provided in Appendix A.

CHAPTER 3
FRC MIXTURE DEVELOPMENT AND LABORATORY-SCALE TESTING

3.1 FRC mixture development

3.1.1 Selected fibers for evaluation

A wide variety of fibers are commercially available for use in FRC. Improved mechanical properties of FRC (relative to plain concrete), which have been demonstrated through prior studies, can be advantageous for use in FRC traffic railings. A major component of the present study involves the development of an FRC mixture that balances low slump and workability while also providing mechanical properties that meet impact performance requirements for traffic railings. Since the proposed FRC traffic railing will use minimal steel reinforcing bars (recall Figure 1.3b), it will be imperative that the railing remains structurally adequate through use of fiber reinforcement. Based on information collected during the literature review, various types of commercially available fibers were identified and considered as possible candidates for use in FRC traffic railing design. Consideration was given to mechanical characteristics, economics, and commercial availability within the U.S. An overview of the FRC related literature review findings include:

- For fresh concrete, the addition of fibers will reduce slump, which is beneficial for the present study—specifically for slip-formed concrete.
- The addition of fibers to plain concrete greatly improves residual tensile strength (i.e., the tensile strength after cracking has initiated).
- For applications involving impact loading, researchers have primarily focused on the use of steel fibers (hooked-end and straight) due to the higher tensile strength and modulus of elasticity that can be achieved by the use of such fibers.
- Studies related to the impact performance of FRC have indicated that steel fibers perform better than synthetic material types (i.e., show improved cracking behavior and increased impact capacity).
- It has also been demonstrated that, with the proper concrete mixture design, steel fibers in FRC can be used to replace traditional rebar reinforcement in precast concrete barriers.
- Corrosion is a potential risk associated with the use of steel fibers, but is likely to be limited to surface aesthetics since fibers are discontinuous and therefore do not allow for system wide corrosion propagation. Investigation of potential issues related to surface corrosion and aesthetics will be limited, in this study, to making observations based on preparation and testing of FRC specimens.

FRC mixing and testing was conducted to definitively identify an appropriate fiber type for use in the present study. In the following section, a variety of commercially available fibers are listed. Both steel and synthetic fibers were considered; steel fibers were included as the primary focus for impact resistance, but synthetic fibers were also included due to potential concerns regarding corrosion.

A primary focus of the present study was to identify a fiber type that would provide the necessary pullout strength and resistance required for vehicle impact loading. Commercially available steel fibers that were reviewed are listed in Table 3.1, along with corresponding properties. Commercially available fibers made of synthetic materials are listed in Table 3.2. In each table, mechanical and geometric properties are listed, based on information obtained either from data sheets provided by the distributor, or through conversation with the distributor directly.

Not all distributors provide the same types of information in their respective data sheets (e.g., some do not include tensile strength of the fiber). Additionally, fiber dosages (percent fiber by volume) are based on recommendations provided by the distributor, but are typically applicable to situations in which fiber is used as secondary reinforcement and shrinkage control, but not as a total replacement for reinforcing bars. Therefore, the dosages (fiber percentages by volume) considered in the present study are higher than those typically recommended by distributors. Nevertheless, it was still informative to compare typical dosage ranges for each type of fiber reviewed. Cost data was available for only a few of the fibers listed. Typically, fibers are sold to a concrete batch plant, and final mixture cost is determined based on a number of factors including fiber material costs, shipping costs, the costs of additional mixture chemicals used in the final mixture design (e.g., high range water reducing admixture), and costs associated with additional mixing time (many fiber producers recommend additional mixing time to ensure uniform fiber distribution).

Table 3.1 Commercially available steel fibers

Producer	Commercial product name	Material	Shape/Sample photo	Properties and notes
Sika	SikaFiber Force 1050	Steel		• Tensile strength = 152 ksi • Length = 2 in. • Aspect ratio = 50 • Dosage guideline = 0.2%–0.6% by volume of concrete • Cost estimate = $1.10 per lb
Euclid	PSI Steel Fiber C6560	Steel	Hooked-end (Similar to Sika fiber shown)	• Tensile strength = 160 ksi • Length = 2.375 in. • Aspect ratio = 65 • Dosage guideline = 0.2%–0.75%
Propex	Novocon HE1050	Steel	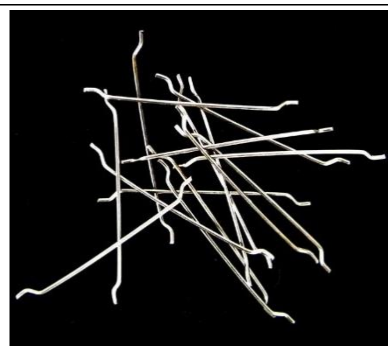 (Similar to Sika fiber shown above)	• Tensile strength = 159 ksi • Length = 2 in. • Aspect ratio = 50 • Dosage guideline ≥ 0.2%
Bekaert	Dramix 3D	Steel	Hooked-end (Similar to Sika fiber shown)	• Tensile strength = 246 ksi • Length = 2 in. • Aspect ratio = 66 • Dosage guideline = 0.2%–0.4% • Cost estimate = $0.80 per lb
Helix	Helix 5-25	Steel	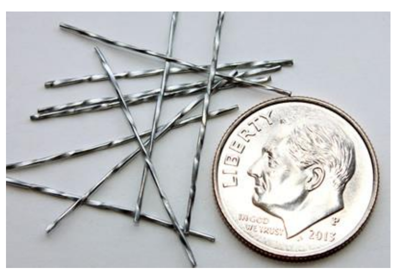	• Tensile strength = 246 ksi • Length = 1 in. • Aspect ratio = 50 • Dosage guideline = calculated on a case by case basis (designed) • Zinc coated for improved corrosion resistance • Cost estimate = $2.50 per lb

Table 3.2 Commercially available synthetic fibers

Producer	Commercial product name	Material	Shape/Sample photo	Properties and notes
Forta	Forta-Ferro	Copolymer/ Polypropylene blend		• In twisted bundles • Tensile strength = 83–96 ksi • Length = 2.25 in. • Dosage guideline = 0.2%–2.0% • Cost estimate = $5.50 per lb • Note: cost is based on weight, which is much lighter than steel
Sika	SikaFiber Force 950m	Copolymer/ Polypropylene blend	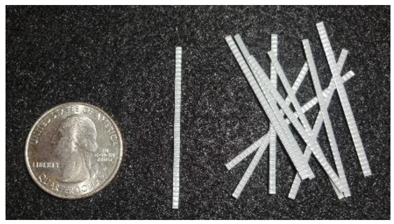 (Note: fine-micro-fiber not shown)	• Blended with fine-micro-fiber • Tensile strength = 75 ksi • Length = 2 in. • Dosage guideline = 0.3% • Provided in pre-measured 5-lb bags
BASF	MasterFiber MAC 2200 CB	Polypropylene	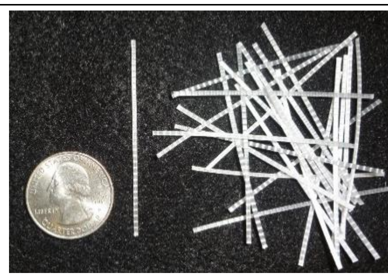	• Chemically enhanced to improve bond • Tensile strength = 85 ksi • Length = 2.1 in. • Aspect ratio = 83 • Dosage guideline = 0.2%–0.8%
BASF	MasterFiber MAC Matrix	Polypropylene	Straight, 'embossed' (Similar to BASF Mac 2200 CB)	• Tensile strength = 85 ksi • Length = 2.1 in. • Aspect ratio = 70 • Dosage guideline = 0.2%–0.8%
Euclid	Tuf-Strand SF	Polypropylene/ Polyethylene blend		• Tensile strength = 87–94 ksi • Length = 2 in. • Aspect ratio = 74 • Dosage guideline = 0.2%–1.3%

Based on the fiber properties listed in Table 3.1 and Table 3.2, multiple fiber types were selected and used in early stage laboratory testing to determine a final (suitable) fiber candidate. For initial laboratory FRC fresh mixture preparation and hardened concrete mechanical testing, two steel fiber types (Sika hooked-end steel fibers; Helix steel fibers) and two synthetic fibers (Forta-Ferro synthetic fibers; BASF MasterFiber MAC 2200 CB fibers) were obtained and investigated. The set of four fibers were reduced at a later stage of the present study, based on results from laboratory-scale mixing and testing. All fibers selected for testing are currently made in the U.S., so as to ensure that if they are selected and recommended for use in FRC traffic railing construction, the fibers meet FDOT construction requirements.

3.1.2 Trial FRC mixtures overview

The four selected fibers types (Sika hooked-end steel fibers; Helix steel fibers; Forta-Ferro synthetic fibers; BASF MasterFiber MAC 2200 CB fibers) were used in trial mixture design and (small, laboratory-scale) FRC production at various selected fiber content volumes. The mixture designs were developed for use in slip-formed concrete traffic railings. During the production of each trial mixture, fresh concrete properties were tested, and small-scale specimens (i.e., 4-in. x 8-in. cylinders and 4-in. x 4-in. x 14-in. flexural beams) were produced.

To develop an FRC mixture design specific to slip-form construction of concrete bridge railings, a concrete batch plant was contacted for mixture design guidance. Argos, a batch plant located in Tallahassee, FL, was accommodating and provided an FDOT-approved concrete mixture design used for slip-form concrete traffic railing construction. The FDOT-approved mixture design provided by Argos was then used as a baseline design and adjusted to account for the addition of reinforcing fibers. Laboratory-scale FRC mixture designs were then developed and produced for the selected fiber types at selected fiber content volumes.

Concrete mixture design requirements for FDOT construction projects are provided in *Standard Specifications for Road and Bridge Construction* (FDOT, 2020b). Standards specific to the concrete mixture used in constructing 36-in. single-slope concrete traffic railings (FDOT, 2020b) are shown in Table 3.3 (as specified for Class II concrete). Since slip-form construction requires a relatively stiff mixture, FDOT standards state that the required target slump of 3 in. (which is specified for typical Class II concrete) may be reduced for slip-form operations. The slip-formed concrete mixture design provided by Argos, shown in Table 3.4, is designed to achieve an adjusted target slump ranging from 0.5 in. to 1.5 in.

Table 3.3 Mixture proportioning requirements (FDOT, 2020b)

Description	Requirement
Class of concrete for concrete traffic railings	Class II
28-day compressive strength (psi)	3400
Maximum water to cementitious materials ratio	0.53
Minimum total cementitious materials content (lb/yd^3)	470

Table 3.4 Mixture constituents and proportions for the slip-formed concrete traffic railing mixture design provided by Argos (control mixture design)

Product	Quantity	Units
Cement – Type I/II	434	lb/yd^3
Fly Ash – Class F	108	lb/yd^3
No. 57 Stone – Coarse aggregate	1740	lb/yd^3
Silica Sand – Fine aggregate	1218	lb/yd^3
Water	287	lb/yd^3
	[34.5]	[gallons/yd^3]
Darex AEA – Air-entraining admixture	4	fl oz/yd^3
WRDA 64 – Water-reducing admixture	32.5	fl oz/yd^3

Selected fibers along with the selected fiber content volumes for trial FRC production are shown in Table 3.5. Fiber content volumes of 0.5% and 1.0% were selected based on initial mixture testing and based on recommendations from fiber suppliers. Completed laboratory-scale trial FRC mixtures productions are shown in Table 3.6.

Trial FRC mixtures listed in Table 3.6 are numbered in chronological order of testing. Due to the objective of the present study, initial trial FRC mixtures were developed to provide the highest achievable residual flexural strength (which is a function of tensile residual strength). FRC residual strength can be considered as a property analogous to ductility. Higher residual strength is achieved (in part) by increasing the fiber content volume in a mixture design. As a result, for the trial FRC mixtures, a 1.0% fiber volume was selected as a starting point for fresh and mechanical property testing. Although 1.0% fiber volume may produce desirable mechanical properties for the present study, it is also considered an elevated value of volume content, and has the potential to cause difficulties in surface finishing and in other fresh properties. This elevated value of 1.0% fiber volume was selected as an upper limit on probable volume ratios to determine whether difficulties in production might arise. Furthermore, for the synthetic fiber types, it was determined in early stage trial mixtures that a 1.0% fiber volume may not be achievable (i.e., 1.0% synthetic fiber content may produce fiber balling and other impractical fresh mixture issues). As a result, for the selected synthetic fiber types a 0.5% fiber volume was tested first, before moving to the 1.0% fiber volume. For brevity of this report, only mixture design no. 2—1.0% hooked-end steel fiber—is shown (Table 3.7). The remaining FRC mixture designs are similar to mixture no. 2 and were also derived from the Argos baseline mixture.

For the design of each trial FRC mixture (Table 3.6), fiber content was added to the baseline mixture design provided by Argos. Based on an absolute volume mixture design method, fiber proportions were determined using the selected fiber content volume and the known fiber specific gravity. Coarse and fine aggregate proportions were then adjusted to account for the addition of fiber so as to maintain the design volume.

Initially, it was intended to maintain coarse to fine aggregate ratios similar to the baseline mixture design in the FRC mixtures (i.e., coarse to fine aggregate ratio=1.4). However, after completion of the first two FRC trial mixtures, it was determined that coarse aggregate content was too high, producing mixtures that were difficult to finish and form. Based on recommendations provided by fiber distributors, a reduced coarse to fine aggregate ratio of 1.0 was selected. For the remainder of the FRC trial mixtures (i.e., in trial mixture numbers 4 through 9), coarse aggregate content was reduced to maintain a coarse to fine aggregate ratio of 1.0.

Table 3.5 Selected fiber types and fiber volumes for evaluation

Producer	Commercial product name	Material	Selected fiber content volumes for evaluation
Sika	SikaFiber Force 1050	Steel	• 0.5% fiber volume • 1.0% fiber volume
Helix	Helix 5-25	Steel	• 0.5% fiber volume • 1.0% fiber volume
Forta	Forta-Ferro	Copolymer/ Polypropylene blend (synthetic)	• 0.5% fiber volume • 1.0% fiber volume
BASF	MasterFiber MAC 2200 CB	Polypropylene (synthetic)	• 0.5% fiber volume • 1.0% fiber volume

Table 3.6 Preliminary trial FRC mixture test matrix

Mixture number	Fiber type	Material	Fiber content	Coarse to fine aggregate ratio
(Control) 1	None	NA	NA	1.4
2	Sika hooked-end	Steel	1.0% volume	1.4
3	Helix	Steel	1.0% volume	1.4
4	Sika hooked-end	Steel	0.5% volume	1.0
5	Helix	Steel	0.5% volume	1.0
6	Forta	Synthetic	0.5% volume	1.0
7	Forta	Synthetic	1.0% volume	1.0
8	BASF	Synthetic	0.5% volume	1.0
9	BASF	Synthetic	1.0% volume	1.0

Table 3.7 Mixture constituents and proportions for mixture design no. 2 (1.0% fiber volume)

Product	Quantity	Units
Cement – Type I/II	434	lb/yd^3
Fly Ash – Class F	108	lb/yd^3
No. 57 Stone – Coarse aggregate	1700	lb/yd^3
Silica Sand – Fine aggregate	1210	lb/yd^3
Water	287	lb/yd^3
	[34.5]	[gallons/yd^3]
Sika hooked-end steel fiber (1.0% fiber volume)	132.3	lb/yd^3
Darex AEA – Air-entraining admixture	4	fl oz/yd^3
WRDA 64 – Water-reducing admixture	32.5	fl oz/yd^3

During the production of trial FRC mixtures, standard slump cone tests in accordance with ASTM C143 were conducted to determine whether or not the 0.5 in. to 1.5 in. target slump range could be achieved (as shown in Figure 3.1a). Additionally, after completion of preliminary trial mixtures, a (modified) 'vibration slump test' was introduced for the production of subsequent trial FRC mixtures. Since the trial mixtures are intended for use in concrete slip-form machines, which employ high-energy vibration to consolidate and form concrete in the slip-form construction process, the 'vibration slump test' was introduced to gain insight into how the fresh trial FRC mixtures would consolidate and form in a slip-form construction setting (see Figure 3.1b).

The vibration slump test was conducted by implementing the standard slump test on a vibration table. In the standard slump cone test, the cone mold is sequentially filled in three equal depth layers. Rodding is used to consolidate the mixture within the mold after the addition of each layer. A similar procedure was used in the modified vibration slump cone test. However, after each layer of fresh FRC was added to the slump cone mold, the vibration table was turned on for 30 seconds after rodding. After rodding and vibrating all three layers in the slump cone, the cone mold was removed and the slump was measured.

The 30 second vibration time in the modified vibration slump cone test was selected based on ASTM C31, which specifies how to make concrete cylinder test specimens. According to ASTM C31, the use of vibration for consolidation should last around 10 seconds for low slump concretes. However, in slip-form construction, the concrete may typically be vibrated for a longer period of time, hence the selection of 30 seconds.

(a) (b)

Figure 3.1 Slump tests for trial FRC production: (a) Standard (hand rodded) slump (measured 0.25-in. slump); (b) Slump with vibration (measured 0.0-in. slump)

3.2 Static laboratory-scale testing

To evaluate the (hardened) mechanical properties of the trial FRC mixtures, static (laboratory-scale) standard compressive strength and FRC flexural tests were completed. Standard concrete compressive strength tests in accordance with ASTM C39 were completed for each trial FRC mixture, using 4-in. x 8-in. cylinders. Although mechanical testing was primarily focused on the flexural (i.e., indirect tensile) behavior of the trial FRC mixtures, compressive strength tests were conducted to ensure that the required 3400 psi compressive strength was achieved for each trial mixture.

Three commonly used flexural tests used to characterize improved tensile properties of FRC (relative to plain concrete) are: 1) ASTM C1399, 2) ASTM C1609, and 3) EN 14651. For the ASTM C1399 test, a beam specimen is loaded twice. For the first loading stage, the beam specimen is supported on a steel plate and loaded until an initial crack is produced. Then, the beam is unloaded, the underlying steel plate is removed, and the beam is reloaded to measure the FRC residual strength. For ASTM C1609, the flexural beam specimen is loaded only once, without the use of a steel plate (i.e., initial 'first-peak' loads, residual loads, and corresponding stresses are captured with one displacement-controlled loading sequence).

For the European EN 14651 test, the flexural beam specimen is loaded only once. However, after the beam specimen has been molded (Figure 3.2), it is cut with a saw, creating a 'notch' in the bottom surface at midspan (Figure 3.3). The 'notch' is used to force initiation of cracking at midspan in a three-point flexural bending test. As load is increased during the flexural test, the crack mouth opening displacement (CMOD)—which is the displacement across the 'notch'—is measured using a clip gage (Figure 3.4). Furthermore, linear variable differential transformers (LVDTs) may be used to measure vertical displacement of the specimen as it is loaded.

 

(a) (b)

Figure 3.2 Production of FRC flexural beams during trial batching for future testing: (a) Prior to vibrating the specimen molds; (b) After vibrating the molds

(a)

(b)

Figure 3.3 Preparation of an FRC flexural beam for EN 14651 testing: (a) Prior to saw cutting; (b) After saw cutting to create the ‘notch’ at the mid-span

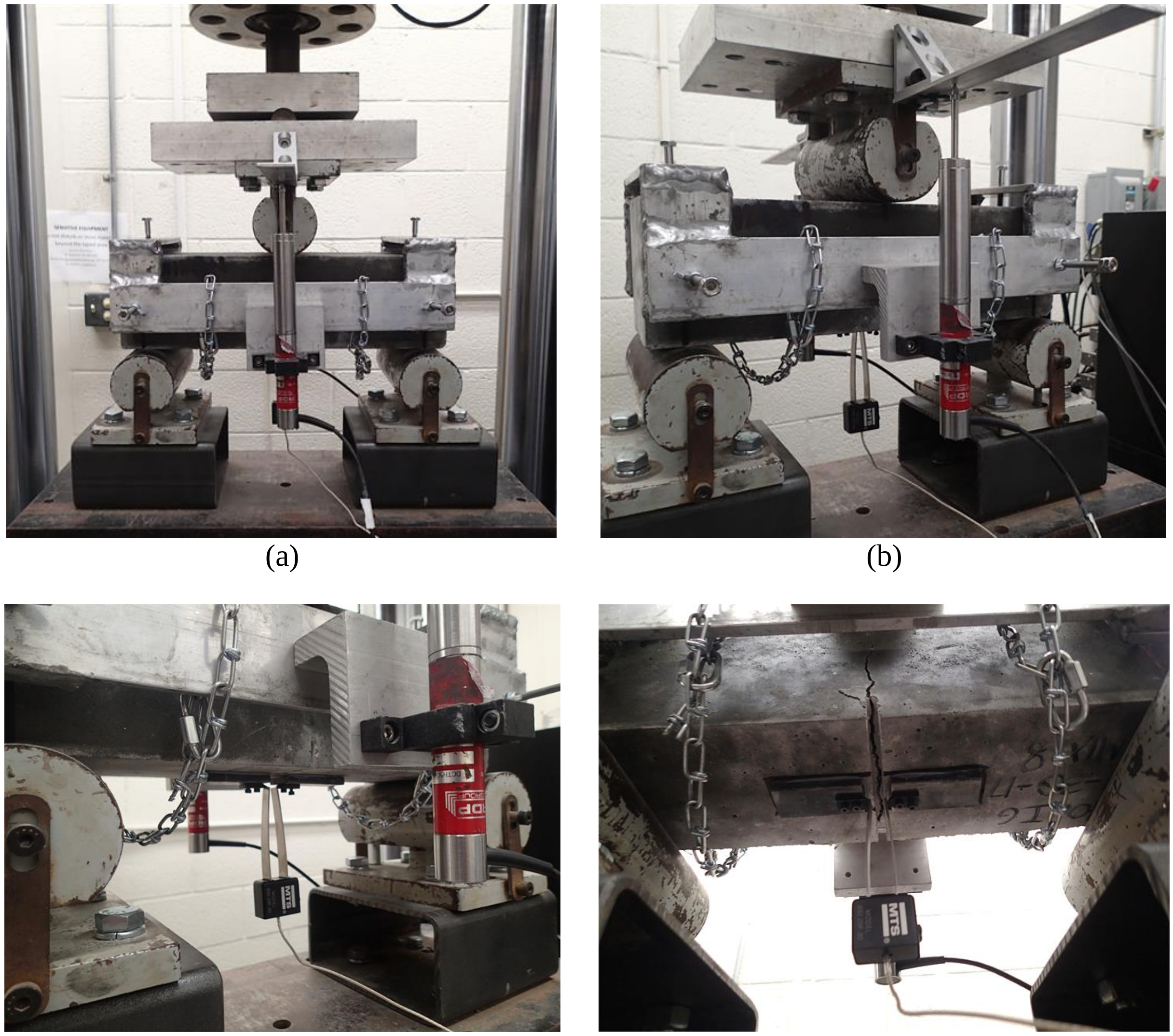

Figure 3.4 EN 14651 FRC flexural test setup: (a) Side view; (b) Corner view; (c) CMOD clip gage during evaluation; (d) Close-up view of the CMOD during specimen evaluation

All three test methods were considered for use in the present study, however the European EN 14651 test (which may be referred to as the 'CMOD' test) was selected for use in preliminary mechanical FRC testing. Selection of the CMOD test was based, in part, on the consideration that FEA models developed later in this study will require calibration and/or validation against experimental data. Simulating the CMOD experimental test conditions—for model calibration/validation purposes—was deemed to be preferable to simulating the ASTM test conditions for several reasons. First, in the CMOD test, introduction of a midspan notch effectively guarantees that cracking will initiate at a known location and in a repeatable manner, as opposed to the more varied crack initiation locations that occur in the ASTM C1399 and ASTM C1609 tests. Next, the CMOD test involves a single stage of monotonic loading, whereas the ASTM C1399 test involves multiple stages of loading (initial loading with a steel plate present, crack initiation, unloading, removal of the steel plate, and then reloading to characterize residual tensile strength). Finally, the CMOD test includes measurement of several key displacements—which will prove useful in model calibration—that are not measured in the ASTM tests.

For each trial FRC mixture, two flexural beam specimens were used in the CMOD flexural test (at 28 days), to determine which trial mixture exhibited suitable mechanical properties for use in slip-formed FRC traffic railings. Load-displacement curves obtained while conducting the CMOD test—which is a displacement (i.e., CMOD) controlled test—using Sika hooked-end steel fibers are provided in Figure 3.5. Representative photographs of an FRC beam specimen (with Sika hooked-end steel fibers) after completion of the CMOD test are provided in Figure 3.6. CMOD flexural test results with Helix 5-25 steel fibers, Forta-Ferro synthetic fibers, and BASF synthetic fibers are shown in Figures 3.7–3.9.

(a)

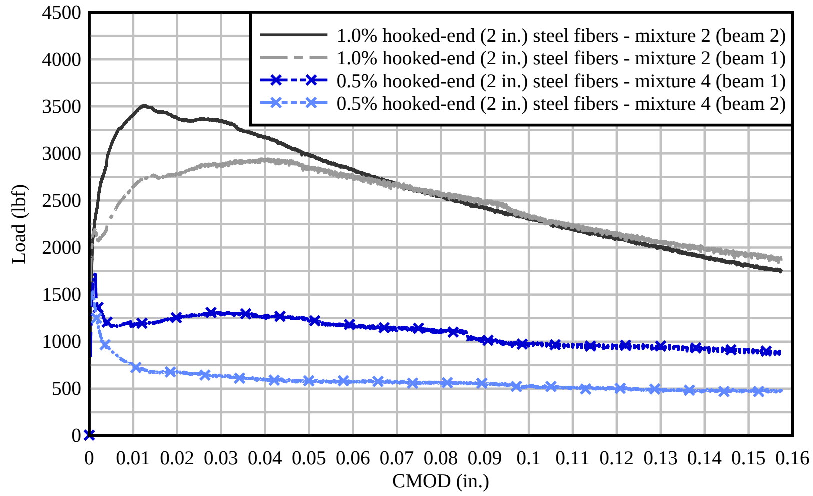

(b)

Figure 3.5 Sika hooked-end steel fibers: (a) Fiber photograph; (b) CMOD flexural test results using Sika hooked-end steel fibers at 1.0% and 0.5% fiber volumes (trial mixtures 2 and 4)

(a)

(b)

Figure 3.6 Hooked-end steel FRC flexural specimen after completion of CMOD test: (a) Crack formation after completion; (b) Fiber distribution across crack interface with additional loading

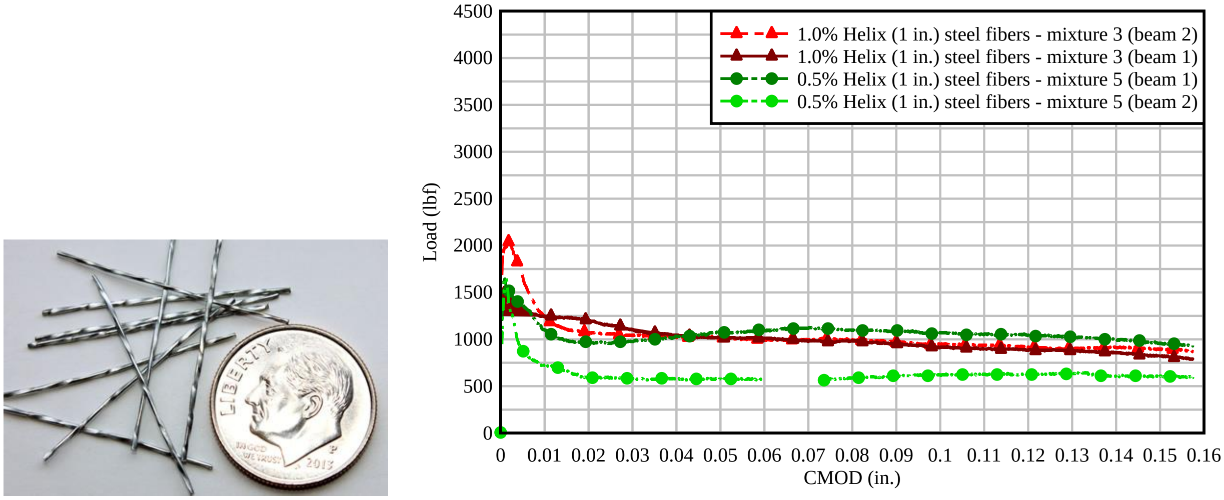

(a) (b)

Figure 3.7 Helix 5-25 steel fibers: (a) Fiber photograph; (b) CMOD flexural test results using Helix 5-25 steel fibers at 1.0% and 0.5% fiber volumes (trial mixtures 3 and 5)

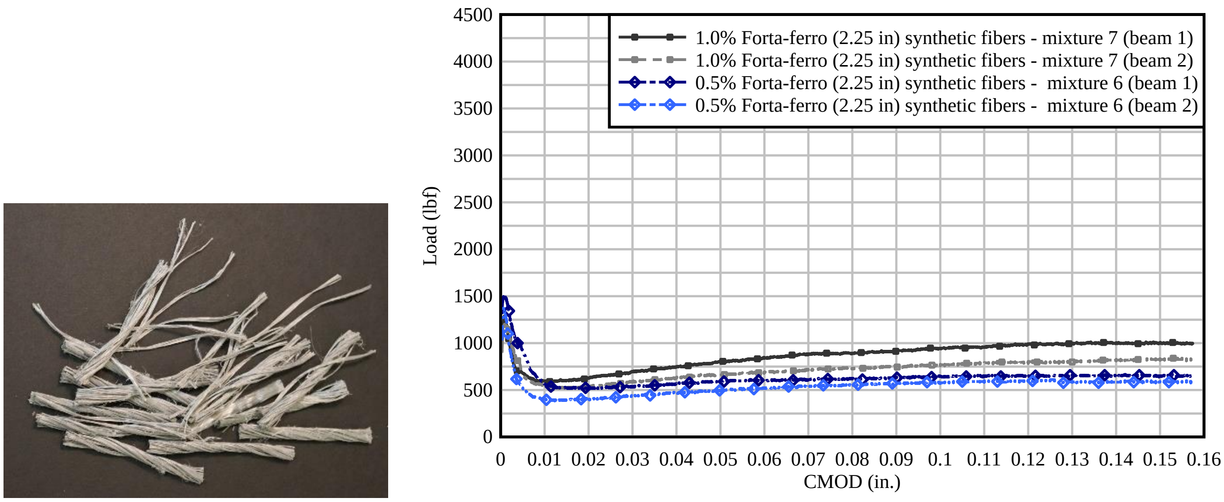

(a) (b)

Figure 3.8 Forta-Ferro synthetic fibers: (a) Fiber photograph; (b) CMOD flexural test results using Forta-Ferro synthetic fibers at 1.0% and 0.5% fiber volumes (trial mixtures 6 and 7)

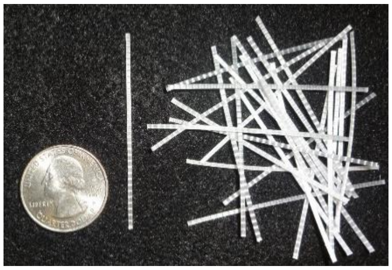

(a)

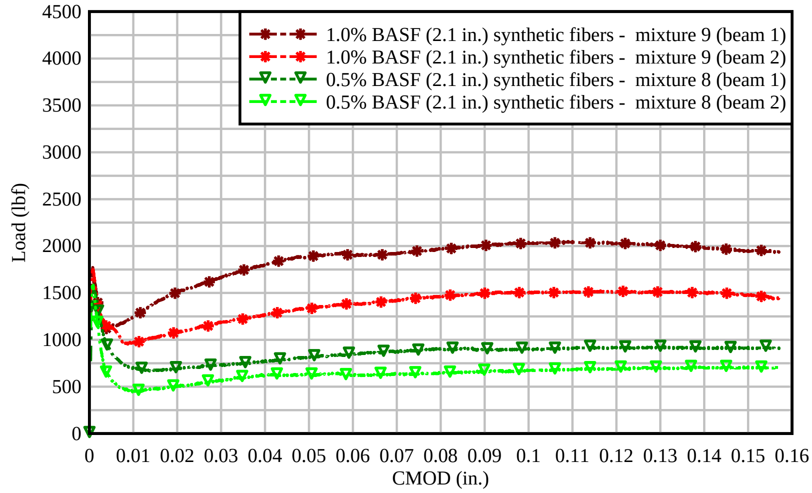

(b)

Figure 3.9 BASF synthetic fibers: (a) Fiber photograph; (b) CMOD flexural test results using BASF synthetic fibers at 1.0% and 0.5% fiber volumes (trial mixtures 8 and 9)

For the EN 14651 standard flexural FRC test, CMOD is measured using a clip gage as load is increased. Tensile behavior of FRC is then characterized in terms of residual flexural tensile strength values determined from the load-CMOD curve. As opposed to allowing for the determination of FRC residual tensile strength at arbitrary CMOD values, the EN 14651 standard specifies the computation of residual tensile strength at four different values of CMOD ($CMOD_1$, $CMOD_2$, $CMOD_3$, $CMOD_4$), as shown in Figure 3.10. These four CMOD values pertain to different levels of deformation, and provide a standard for computing FRC residual tensile strength. Since vehicle impact conditions for traffic railings may produce relatively large deformations, $CMOD_4$ values were judged most applicable to the design of an FRC railing. Additionally, due to the (typically) gradual decrease in load as CMOD is increased (Figure 3.10), $CMOD_4$ will produce lower (i.e., more conservative) values of FRC residual tensile strength relative to the other three CMOD values ($CMOD_1$, $CMOD_2$, $CMOD_3$).

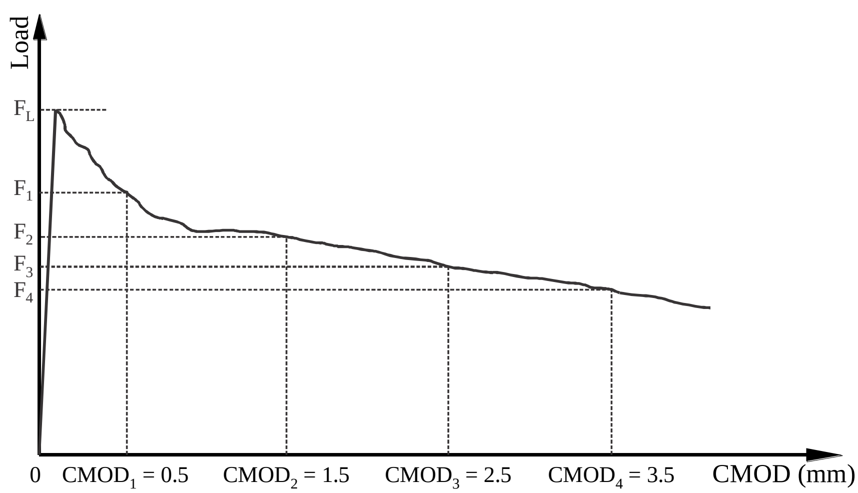

Figure 3.10 Typical load-CMOD (displacement) curve with specified $CMOD_{1,2,3,4}$ values (after EN 14651)

Based on preliminary CMOD flexural test results, trial mixture number 2 (Sika hooked-end steel fibers at 1.0% fiber volume) produced the largest FRC residual tensile strength (i.e., largest load in the latter half of the load-displacement curve), and therefore the most promising mechanical properties for use in an FRC traffic railing. As a result, additional hardened mechanical properties were evaluated (under static and dynamic loading conditions) using an FRC mixture with Sika hooked-end steel fibers at 1.0% fiber content volume. However, trial FRC mixture number 2 was determined to have excess coarse aggregate content, based on evaluation of fresh properties. Therefore, intermediate tests (i.e., additional small-scale tests) for evaluation of hardened mechanical properties were conducted using an adjusted mixture design (mixture design no. 11)—with a reduced coarse-to-fine aggregate ratio of 1.0, but retaining the 1.0% fiber volume.

For the additional FRC mixture (mixture design no. 11), four flexural beam specimens were evaluated using the CMOD test. Load-displacement curves obtained while conducting the CMOD test using the additional trial mixture no. 11 specimens are provided in Figure 3.11, and are compared with trial mixture no. 2 results (which contained the same Sika hooked-end steel fibers at 1.0% fiber volume). As shown in Figure 3.11, loads corresponding to $CMOD_4$ (0.138 in.)—which were judged most applicable to the design of an FRC railing—for mixture no. 11 are similar to those obtained with mixture no. 2. Furthermore, the average load corresponding to $CMOD_4$ produces a residual flexural tensile strength of 887 psi for mixture no. 11, following the standard bending stress equation (as prescribed in EN 14651):

$$\sigma = \frac{Mc}{I} \quad (3.1)$$

where σ is the flexural stress, M is the applied moment, c is the distance from the neutral axis, and I is the gross moment of inertia of the specimen.

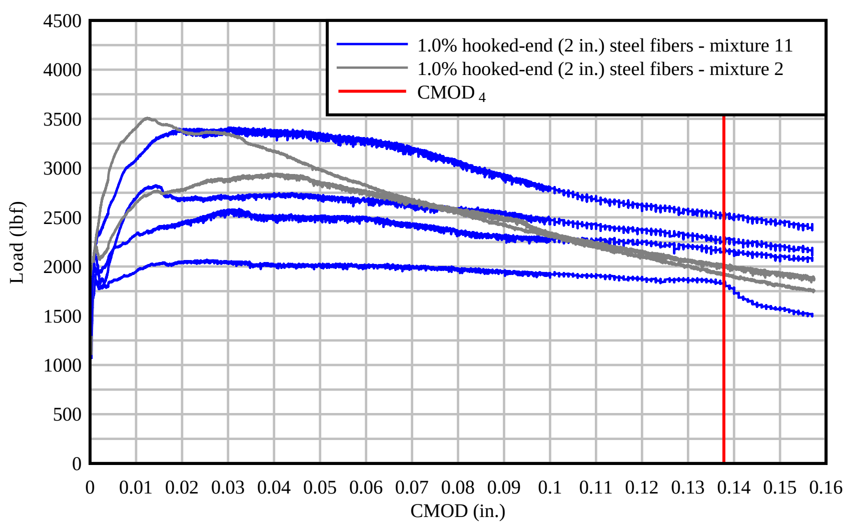

Figure 3.11 CMOD flexural test results using Sika hooked-end steel fibers at 1.0% fiber volumes (comparison of mixtures 2 and 11)

3.3 Dynamic laboratory-scale testing

3.3.1 Dynamic (laboratory-scale) pendulum impact testing overview

The following section provides a summary of the dynamic test setup and procedures that were used to evaluate the mechanical properties of FRC under impact loading. Since a three-point loading configuration is used in the static CMOD test, the design of the pendulum impact test also consisted of a three-point loading configuration as shown in Figure 3.12. The pendulum impact test setup was designed to apply load at the midspan of the 4-in. x 12-in. x 36-in. ‘slab’ specimen using an 1100-kg impactor. Dimensions of the slab specimen were selected to assure one-way bending, when loaded at the midspan. Each specimen was oriented vertically (i.e., the 36-in. span length of the specimen was vertical) to provide the ability to capture (i.e., observe with a high-speed camera) flexural displacements and subsequent failure of the specimen during the dynamic impact.

An overview photograph of the pendulum impact test setup is provided in Figure 3.13. A reaction frame from a previous FDOT funded project was modified with additional steel elements (e.g., steel plates and angles) to provide support conditions for the specimen, as shown in Figure 3.12b. Heavy duty chains were attached to the back of the 1100-kg impactor, providing the ability to abruptly stop the impactor. Additionally, a timber 'backstop' was placed behind the impact slab specimen to stop any remaining momentum of the specimen once the impactor was stopped. Stopping the impactor (with chains) and stopping the impact specimen (with the timber 'backstop') provided the ability to preserve the final state of the impact after a desired specimen displacement was achieved. Preserving each FRC specimen in its final state provided the ability to assess whether fiber pullout or fiber rupture occurred during impact loading.

To apply a dynamic impact load to each slab specimen, two aluminum honeycomb cartridges were placed at the front of the impactor, as shown in Figure 3.14. Use of the aluminum cartridges provided the ability to control (i.e., prescribe) the approximate magnitude of force applied to the specimen. Because the compressive crush strength of the aluminum material is known (278 psi), the cross-sectional dimensions of the two cartridges were selected such that the applied impact force was equivalent to the expected failure of the FRC slab specimen (which was computed to be approximately 6.0 kips). The shape of the cartridge was tapered such that as the aluminum crushed during impact, the magnitude of the impact force would linearly increase (until reaching failure of the specimen). Based on the designed geometry of the two aluminum cartridges, the impact force was expected to start at approximately 4.3 kips, and linearly increase to a maximum force of 7.1 kips.

During the duration of the impact, force was indirectly measured through the use of accelerometers, which were placed on the 1100-kg impactor. Impact force was (therefore indirectly) computed by multiplying acceleration data by the known mass of the impactor. Since dynamic impact forces were not measured directly, use of a high-speed camera positioned to the side of each impact specimen (as shown in Figure 3.14b) provided a second, independent method of estimating the impact force. By reviewing high-speed video of each impact, impact force was computed by visually approximating the crush depth of the aluminum honeycomb cartridges, and was subsequently used to confirm (or compare) force data determined from accelerometer data. The impact test setup was designed so that after approximately 2.5-in. of midspan slab displacement was achieved, the impact would be abruptly halted. The impactor drop height of 19 in. was selected to produce an impact speed of approximately 120 in./sec.

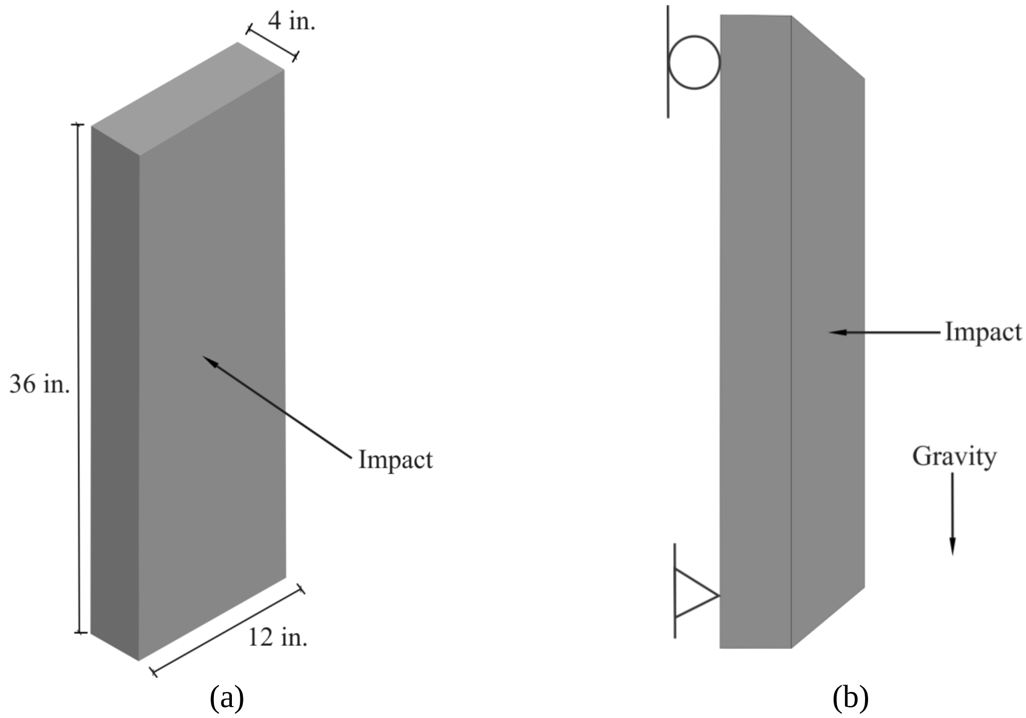

Figure 3.12 Specimen configuration and support conditions for pendulum impact testing: (a) Specimen dimensions; (b) Specimen support conditions

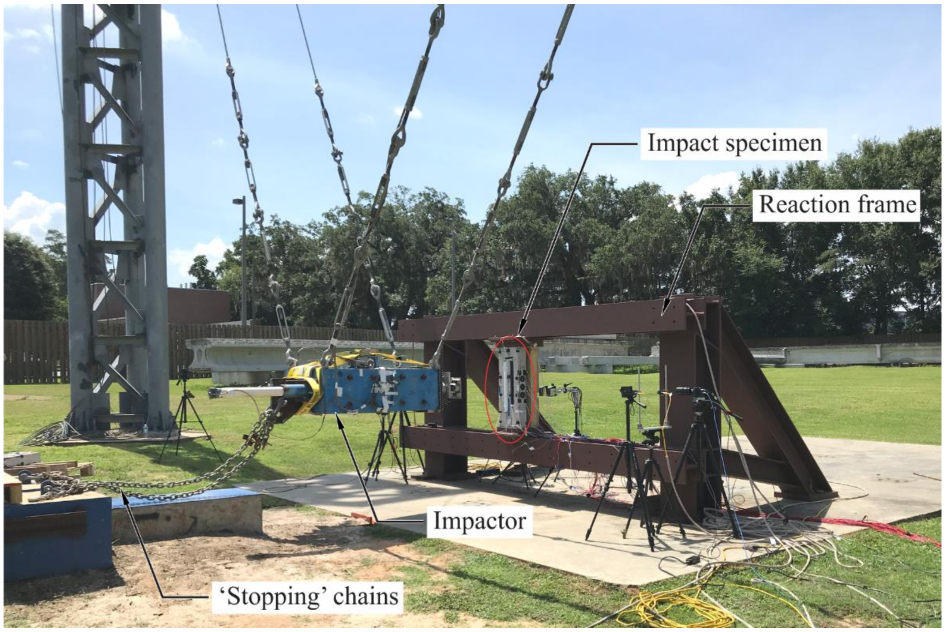

Figure 3.13 Pendulum impact test overview

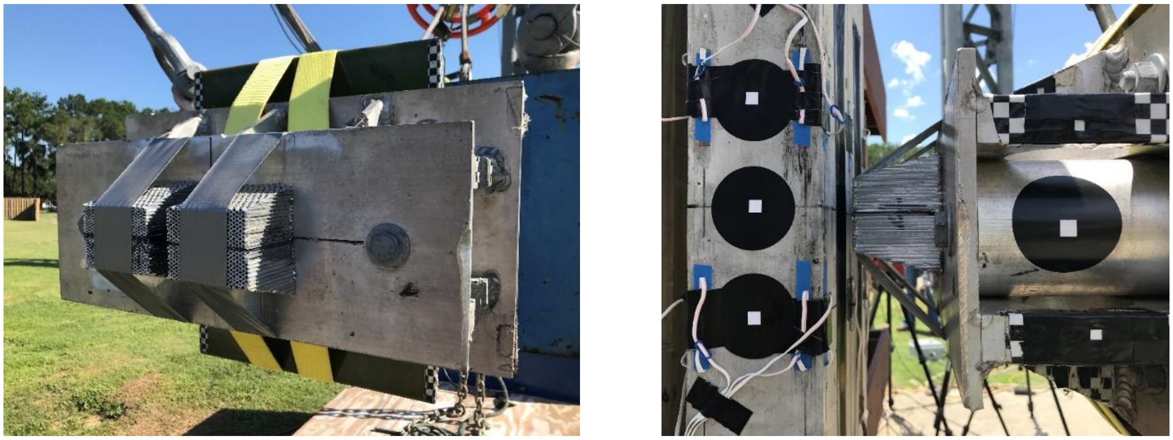

(a) (b)

Figure 3.14 Aluminum honeycomb cartridge configuration: (a) Cartridges attached to front of pendulum impactor; (b) Side view of tapered cartridge

3.3.2 Dynamic (laboratory-scale pendulum impact) test results

For the dynamic pendulum impact test, four different specimens—two plain, unreinforced concrete and two FRC—were used to evaluate (and compare) the dynamic mechanical properties of FRC (relative to the plain specimens). One slab specimen of each type (i.e., one plain and one FRC) was evaluated with pendulum impact testing after 28 days of curing. The two remaining specimens (one plain, one FRC) were impact tested at 49 days.

Acceleration of the 1100-kg impactor block versus time data for the four pendulum impact tests are shown in Figure 3.15, with the initial time of impact and final time of interest (i.e., 'impact end time') included. Impact start time was determined from tape switch data—i.e., pressure sensors placed on the front (impact area) of the slab specimen. As a consequence, a minor delay is shown between the marked start time—when contact between the cartridge and tape switch was triggered—and when acceleration deviates from zero, since additional time is required to collapse the tape switch before the start of the slab impact. Impact end time was determined after reviewing high-speed video of each impact and determining the time at which the slab specimen had failed and come into contact with the timber 'backstop'. Because acceleration data correspond with acceleration of the impactor, negative values were measured, since the impactor mass decelerates as the impact occurs. As shown in Figure 3.15, results from the impact tests showed good repeatability for each specimen type (FRC or plain).

Acceleration data were then used to compute impact forces, as shown in Figure 3.16, by multiplying accelerations by the 1100-kg mass of the impactor (1103-kg mass to be more precise, based on measured weights). Subsequently, negative block acceleration corresponds with a positive impact force acting on the slab. Computed force data were expected to produce a force that varied linearly with increasing deformation, due to the tapered shape of the aluminum cartridges. As shown in Figure 3.16, the computed impact forces from acceleration data followed the intended (theoretical) linear trend before failure of the specimen was reached.

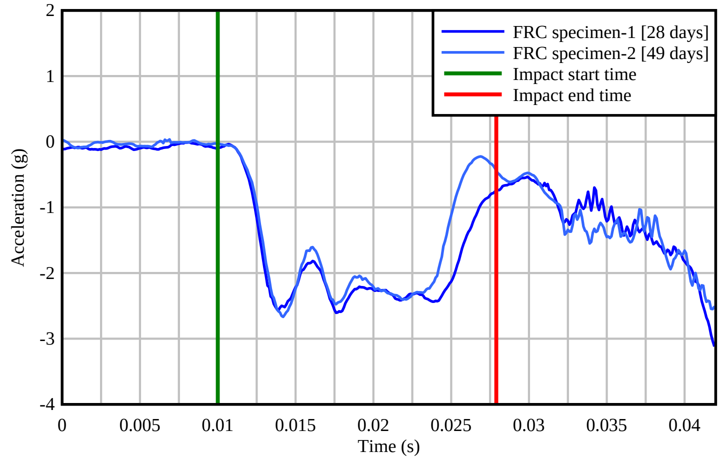

(a)

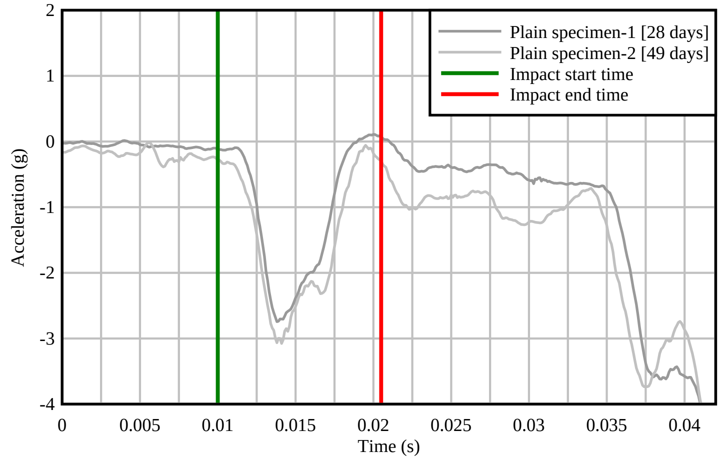

(b)

Figure 3.15 Acceleration of the 1100-kg block versus time data: (a) FRC (1.0% Sika hooked-end steel fiber) slab specimens; (b) Plain (unreinforced) concrete slab specimens

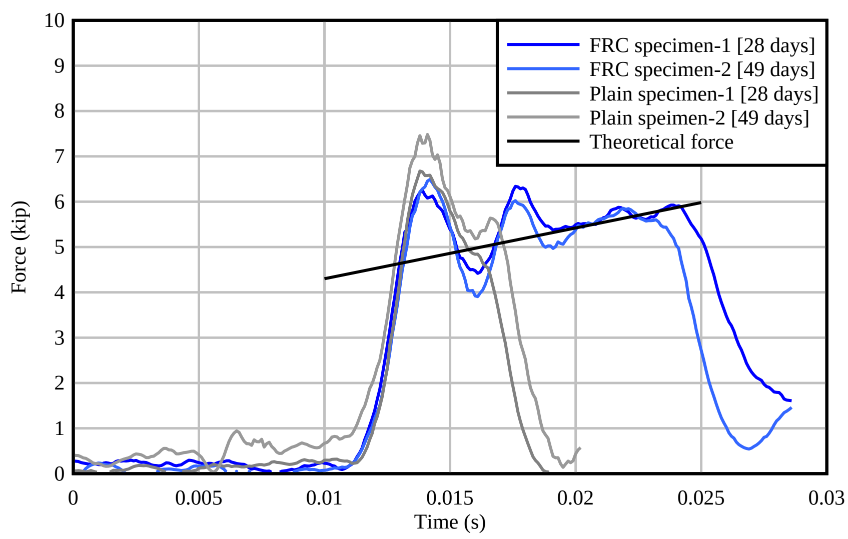

Figure 3.16 Force versus time data (per acceleration data shown in Figure 3.15)

To evaluate the amount of energy absorbed by each specimen, an additional load-displacement curve was generated from impact test data (Figure 3.17). Displacement data shown in Figure 3.17 are computed midspan displacements. During each pendulum impact test, laser displacement sensors were positioned behind the slab—between the timber 'backstop'—at a 14.75-in. height from the bottom of the specimen. Because cracking was expected to occur near the midspan of the specimen, laser displacement sensors were instead positioned below the midspan (at the 14.75-in. height), so that cracking would not interfere with laser displacement sensor data. Consequently, deflections at midspan were computed assuming kinematic rotations of the specimen. Since there was no elastic rebound in either of the failed concrete slabs, absorbed energy (or dissipated energy) is defined as the area under the force-displacement curve. Based on the results presented in Figure 3.17, the FRC specimens dissipated approximately twice the energy that the plain concrete specimens dissipated.

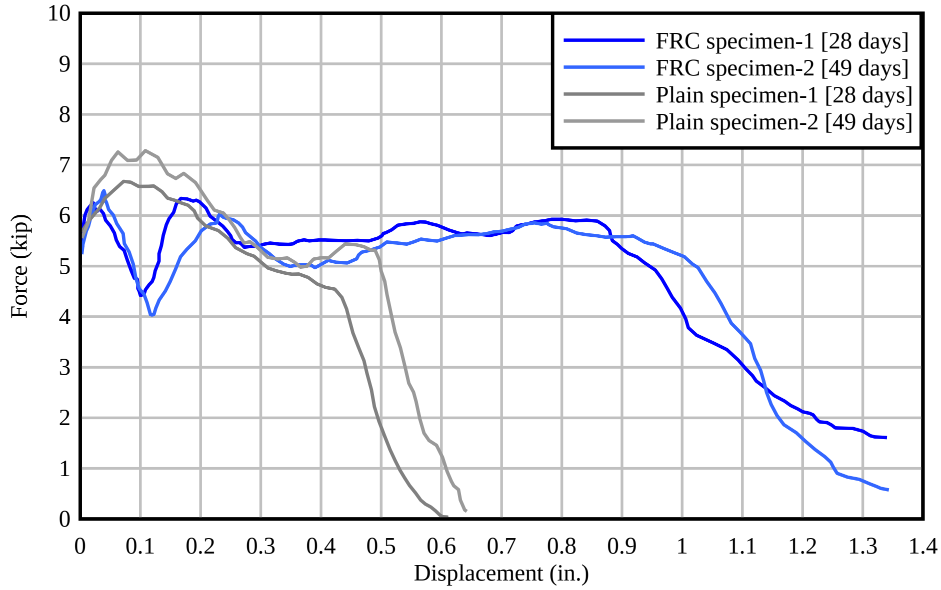

Figure 3.17 Force versus computed midspan displacement (from laser displacement sensor data)

After completing the pendulum impact tests, the FRC specimens were inspected to determine whether the steel fibers pulled out of the concrete, or ruptured. Fiber pullout is the preferred failure mechanism of FRC, since fiber rupture dissipates less energy and could lead to a less ductile response. After inspecting the failure surfaces of the FRC specimens (Figure 3.18) for signs of fiber rupture, it was determined that fiber pullout was the dominant failure mechanism for both of the FRC specimens. In both FRC specimens, previously hooked-end fibers with straightened ends were found throughout the crack region—clear evidence that fiber pullout occurred.

Figure 3.18 Final (preserved) state of FRC specimen-2

For static loading conditions (i.e., from CMOD test results), residual flexural tensile strength was computed using load corresponding to $CMOD_4$ (0.138 in.) in Equation 3.1. To correlate pendulum impact test results with EN 14651 (CMOD) test results (i.e., to determine equivalent residual strength values from FRC pendulum impact tests), a similar approach using a 0.138-in. crack opening (as prescribed in EN 14651) was taken. High-speed video of the two FRC specimen impact tests was reviewed to determine an approximate time at which a crack of 0.138 in. was formed in each FRC slab specimen. With an approximate 0.138-in. crack time determined, average pendulum impact force corresponding to the 0.138-in. crack time was then used in Equation 3.1 to compute an approximate FRC dynamic residual flexural tensile strength value. For the static loading condition (i.e., from CMOD test results), FRC trial mixture no. 11 produced a flexural tensile strength of 887 psi. In comparison, for the dynamic loading condition (i.e., from pendulum impact test results), for the same trial FRC mixture no. 11, a residual flexural tensile strength of 1368 psi was produced (more than a 50% increase). However, expressions presented in EN 14651 (and in ASTM C1399) used to compute residual flexural tensile strength assume a linear stress distribution, so that in flexure, the stress at the extreme fiber can be computed using the standard bending stress equation (Equation 3.1). In general, these assumptions are typically limited to the elastic range, and are not applicable for large (plastic) deformations (i.e., although these assumptions and equations are employed in the standardized test methods, they may be considered an oversimplification when applied to FRC).

Therefore, an additional approach was also used to quantify the FRC residual tensile strengths from both the CMOD test data and the dynamic pendulum impact test data. In this latter approach, a nonlinear stress distribution (per ACI 544.4R-18) was used (Figure 3.19c). Using load corresponding with inelastic deformation of the specimen determined from static and dynamic testing (i.e., the load corresponding to an equivalent $CMOD_4$ for the static and dynamic conditions), the residual tensile strength was computed. Specifically, the value of residual tensile strength (f_{ctd}) shown in Figure 3.19c was iterated until the computed flexural capacity was equivalent to that of the tested specimen. Comparison of the two approaches for calculating the residual tensile strength are shown in Table 3.8. For future testing, both approaches will be employed, as appropriate (e.g., yield line analyses of traffic railings, per AASHTO recommendations, would make use of the residual strength determined per nonlinear stress distribution of Figure 3.19c).

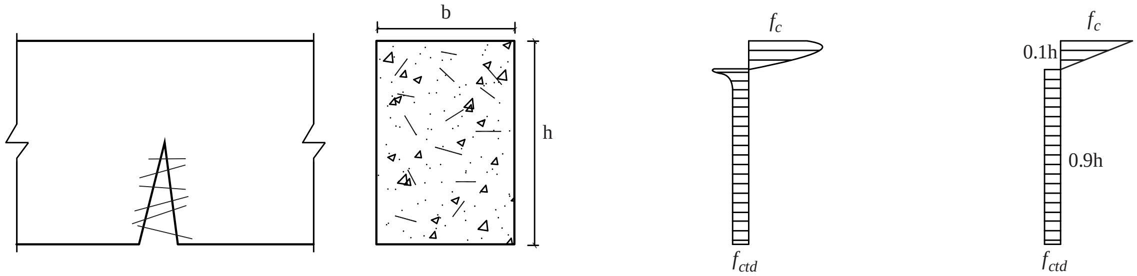

Figure 3.19 Stress distributions for an FRC flexural member: (a) FRC beam section; (b) Actual distribution; (c) Simplified nonlinear distribution (after ACI 544.4R-18)

Table 3.8 Comparison of computed residual tensile strengths

Stress distribution used to compute residual tensile strength	Static (EN 14651) test	Dynamic (pendulum impact) test
Linear (per EN 14651)	887 psi	1368 psi
Nonlinear (per ACI 544.4R-18)	317 psi	490 psi

3.4 Preliminary FRC railing design strength based on laboratory-scale testing

3.4.1 Implementation of FRC

The objective of the present study was to remove the majority of steel reinforcing bars (i.e., flexural and shear steel) contained within the traffic railing cross-section and replace them with the use of FRC. Therefore, the FRC mixture used to replace conventional steel reinforcement must provide at least equivalent tensile strength. To account for the tensile strength of FRC in the design of a 36-in. FDOT FRC SSTR, a simplified tensile stress block was assumed for FRC in tension, following the approach described in ACI (ACI Committee 544, 2018). As shown in Figure 3.20, simplifying the actual tensile stress distribution of FRC to a uniform tensile stress block provides the ability to easily compute the moment strength of an FRC cross-section, similar to standard moment strength calculation methods used for conventional R/C design. For the tensile zone of FRC, the magnitude of the simplified tensile stress (f_{ctd}) can be determined from standard FRC flexural tests, such as the EN 14651 (CMOD) test. This simplified approach was then implemented in design strength calculations of a 36-in. FDOT FRC SSTR.

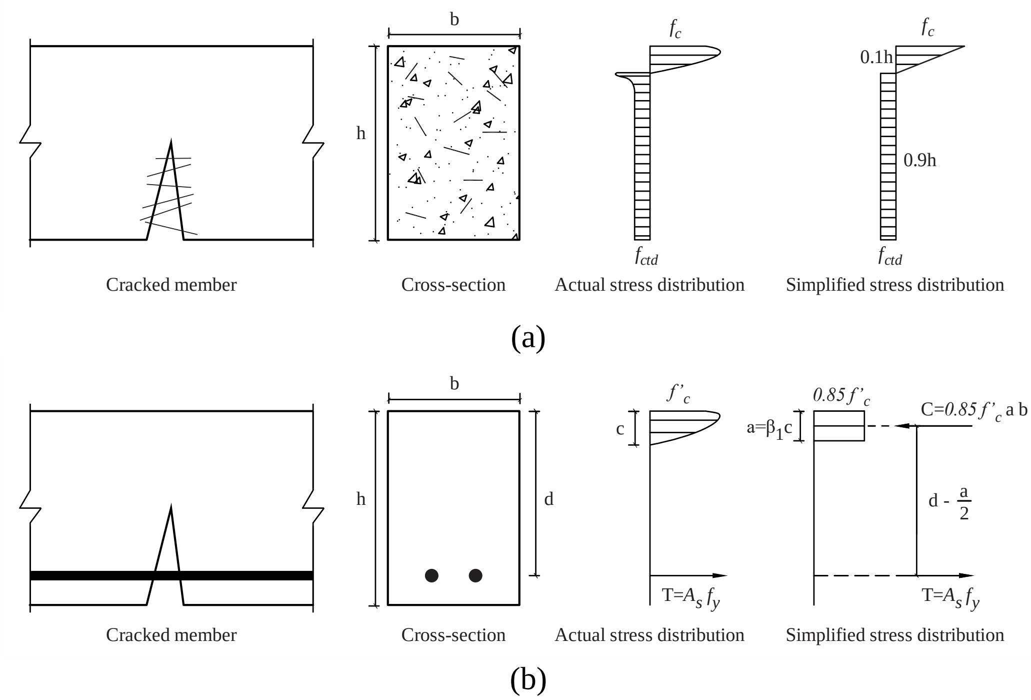

Figure 3.20 Simplified FRC design approach compared to R/C design: (a) FRC cross-section and stress distribution; (b) Conventional R/C cross-section and stress distribution; (after ACI Committee 544, 2018)

3.4.2 FRC 36-in. SSTR design

Design strength calculations for the 36-in. FRC SSTR are provided in Appendix B. To compute the design strength of the FRC railing under 'equivalent lateral impact' load, the design calculations for a standard 36-in. FDOT SSTR were modified by removing reinforcing (flexural and shear) steel within the railing cross-section, and instead assuming a simplified tensile stress block for FRC (as shown in Figure 3.20). The required FRC tensile design strength (f_{ctd}) was then iteratively revised until the FRC railing design strength was found to be equivalent to the previously computed standard FDOT SSTR design strength (i.e., values of f_{ctd} were iterated until the 36-in. FRC SSTR design strength was found to be equivalent to the 105.5-kip railing resistance load computed for the current FDOT 36-in. SSTR, detailed in Appendix A).

As shown in Appendix B, the *design* tensile strength (f_{ctd}) required for the FDOT FRC SSTR was determined to be approximately 250 psi. In comparison, for trial FRC mixture no. 11 (1.0% hooked-end steel fiber), the load corresponding to $CMOD_4$ (0.138 in.) was found to produce an average residual flexural tensile strength of 887 psi (per EN 14651). Following the design approach in ACI (ACI Committee 544, 2018), to correlate experimental flexural (residual) tensile strength to (uniform) design tensile strength, the average experimental strength is divided by 3. Following this design approach, the computed design strength for this mixture is 295 psi (i.e., 887/3=295). Since the design strength of the developed FRC mixture is greater than the required 250 psi value assumed in the FRC railing design worksheet, it was assumed that using FRC mixture no. 11 (1.0% hooked-end steel fibers) would produce FRC material strength properties that are sufficient for a 36-in. FRC SSTR. However, additional full-scale dynamic tests (using an FRC traffic railing) were needed to confirm this assumption.

3.5 Scaled-up FRC production at the ready-mix batch plant level

In previous tasks of the present study, FRC mixtures were produced at a small, laboratory scale—at a maximum volume of 0.130 cubic yards (3.5 ft^3). However, to form (subsequent) FRC railing impact test specimens, FRC production at a larger (batch-plant level) scale was required—at a volume of approximately 1.85 cubic yards (50 ft^3) per impact test specimen. Consequently, a successful FRC mixture was produced in coordination with a concrete batch plant (in Tallahassee) at a volume of 1.5 cubic yards (40.5 ft^3).

Batch-plant level FRC production facilitated the ability to evaluate scaled-up FRC production techniques and the ability to determine any unforeseen challenges associated with the scaling-up process. The following section provides a summary of scaled-up FRC production to the ready-mix batch-plant level. FRC mixture design no. 11 (provided in Table 3.9)—which was previously produced to form the small-scale dynamic impact test specimens—was also used for the scaled-up production phase of this study.

3.5.1 Preliminary FRC mixture design

To produce FRC at a larger scale (batch-plant level), a previously produced FRC mixture—mixture design no. 11 presented in Deliverable 2.3 (repeated in Table 3.9)—was to be scaled-up for the present task. Mixture design no. 11 was previously produced to form small-scale dynamic impact test specimens presented in Deliverable 2.3.

Table 3.9 Mixture constituents and proportions for mixture design no. 11 (1.0% fiber volume)

Product	Quantity	Units
Cement – Type I/II	434	lb/cy
Fly Ash – Class F	108	lb/cy
#57 Stone – Coarse aggregate	1440	lb/cy
Silica Sand – Fine aggregate	1440	lb/cy
Water	287 [34.5]	lb/cy [gallons/cy]
Sika hooked-end steel fiber (1.0% fiber volume)	132.3	lb/cy
Darex AEA – Air-entraining admixture	4	fl oz/cy
WRDA 64 – Water-reducing admixture	23.8	fl oz/cy

3.5.2 FRC production approach using a concrete batch plant

The primary objective for scaling-up FRC production was to determine an effective approach for introducing fiber into a large-scale FRC mixture. Additionally, the scaling-up process would be used to identify any necessary mixture design adjustments associated with the increase in production volume. During the small-scale production process, fiber was introduced by adding the fibers by hand—to prevent fiber balling—during the mixing process. Consequently, by using a concrete batch plant to produce FRC, two possible fiber introduction techniques were considered:

1. To have the batch plant introduce the fiber before or upon delivery of the concrete mixture. This technique is the standard approach for batch-plant level production of FRC. With this technique, fibers may be introduced either with the aggregate (i.e., during the batching process) or may be introduced into the concrete delivery truck at the delivery site. Asking the batch plant to introduce the fibers relies on cooperation from the batch plant and assumes the plant operators are sufficiently familiar with FRC production techniques.

2. To introduce fibers using the FDOT ultra-high performance concrete (UHPC) mixer. With this technique, all constituents of the mixture excluding the fiber would be mixed and delivered by the concrete batch plant. Upon delivery of the mixture, the wet concrete—without fiber—would be transferred to the FDOT UHPC mixer. Once a known volume of concrete is added to the UHPC mixer, fibers would then be efficiently introduced/added to the mixture with additional mixing time. The UHPC mixer contains a steel grate at the top that is intended for the addition of fiber—since typical UHPC mixes include fiber. Using the UHPC mixer as an additional FRC (large-scale) production step, provides more control over the introduction of fibers and allows for fine-tuning water and admixture quantities if necessary.

Relying on the batch plant to introduce fiber is the easier approach of the two techniques considered. However, introduction of fiber by the batch plant also relies heavily on the cooperation of the plant and reduces control of the FRC production process by the research team. Therefore, the approach of using the FDOT UHPC concrete mixer (Figure 3.21) was instead selected.

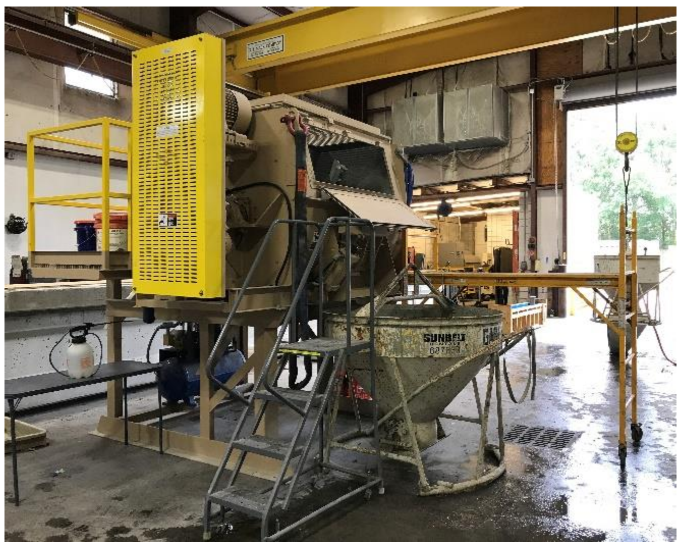

Figure 3.21 FDOT UHPC mixer used to introduce fibers into the concrete delivery truck mixture

Additionally, it was decided that the scaled-up FRC production should be used to form a trial FRC railing (i.e., instead of only evaluating the FRC production process and discarding the produced FRC mixture, the opportunity would be used to form a trial railing, enabling the ability to evaluate the designed/constructed formwork [shown in Appendix C] and the ability to evaluate FRC consolidation within the railing formwork). Consequently, 'trial FRC railing production' drawings (Appendix C) including no. 4 bar reinforcement—which are included in the FRC railing impact specimen—were developed and were used to form a trial FRC railing specimen. Including no. 4 reinforcing bars—with geometry similar to the geometry that will be used in future impact specimens—in a portion of the trial FRC railing specimen enabled evaluation of FRC consolidation near and around the reinforcement. Under impact loading conditions, a critical area in the railing is near the toe and bottom surface of the rail—i.e., near the connection joint between the railing and the bridge deck. Consequently, it was of interest to evaluate the consolidation (including fiber distribution and orientation) of the trial FRC railing specimen in that critical area (with inclusion of reinforcement). It should be noted that the 4V bar geometry for the trial FRC railing specimen (Appendix C) does not match the current FDOT Standard Plans Index 521-427 (FDOT, 2020a). A contractor's optional 45-deg. bend in the 4V bar was included in the trial specimen reinforcement. Furthermore, the 4V geometry was extended to provide adequate space between the 45-deg. bend and the back vertical portion of the 4V bar (also part of the reinforcing detail)—i.e., the elevation of the bend was raised to create a similar distance between the front 4V bend and the back (vertical) portion of the 4V bar, as detailed in FDOT Standard Plans Index 521-427 (FDOT, 2020a). The purpose of considering the bend was to evaluate FRC consolidation near and around the bend.

3.5.3 Production trial attempt #1: Unsuccessful trial

To order a delivery of the partial mixture (i.e., mixture design no. 11 without fiber) for FRC production trial attempt #1, the previously developed mixture design (shown in Table 3.9) was submitted to SRM. At that point in time, SRM notified UF that the #57 limestone (coarse aggregate) included in the mixture design—and all previous trial FRC mixtures produced in the present study—was unavailable in the Tallahassee and surrounding areas because the limestone from nearby quarries did not meet FDOT standards. As an alternative, SRM had been using #67 stone (coarse aggregate), which is slightly smaller in size (0.75 in. to No. 4 sieve versus 1.0 in. to No. 4 sieve). Consequently, a new mixture design was required, to replace the #57 coarse aggregate with the smaller #67 coarse aggregate. Since the two coarse aggregates have different specific gravity values, the mixture design constituents and proportions were adjusted to develop a new trial FRC mixture design: mixture design no. 12. The new mixture design no. 12 (Table 3.10) was then submitted to SRM for up-scaled FRC production trial attempt #1.

The approach for developing mixture design no. 12 was to adjust the coarse and fine aggregate proportions from mixture design no. 11 to achieve a 27-ft^3 theoretical yield, including fiber (to be added using the UHPC mixer) and based on the aggregate specific gravity values provided by SRM. Furthermore, a coarse-to-fine aggregate ratio of 1.0 was to be maintained, based on previous trial FRC mixtures. Although the newly developed mixture design no. 12 was not (previously) produced at a small, laboratory scale, the mixture design proportions were adjusted to be as close as possible to the previously successful FRC mixture, but with materials that were available from SRM.

It should also be noted that in order to meet *FDOT Standard Specifications for Road and Bridge Construction Section 346-4* (FDOT, 2020b), the water and cementitious material contents were not adjusted from the previous mixture design no. 11, maintaining the maximum allowable water to cementitious material ratio of 0.53. Consequently, the coarse and fine aggregate contents were increased from 1440 lb/cy (in design no. 11) to 1556 lb/cy (in design no. 12), an 8% increase to reach theoretical yield of 27 ft^3 and to maintain a 1:1 ratio of coarse to fine aggregate.

Table 3.10 Mixture constituents and proportions for mixture design no. 12 (1.0% fiber volume)

Product	Quantity	Units
Cement – Type I/II	434	lb/cy
Fly Ash – Class F	108	lb/cy
#67 Stone – Coarse aggregate	1556	lb/cy
Silica Sand – Fine aggregate	1556	lb/cy
Water	287	lb/cy
	[34.5]	[gallons/cy]
Sika hooked-end steel fiber (1.0% fiber volume)	132.3	lb/cy
Darex AEA – Air-entraining admixture	4	fl oz/cy
WRDA 64 – Water-reducing admixture	23.8	fl oz/cy

Although only 1.5 cubic yards (40.5 ft^3) of concrete was required for trial FRC production to conservatively fill all trial production forms, it was recommended (by FDOT) to order a minimum of 3.0 cubic yards (81.0 ft^3). Such a minimum order is also a requirement for FDOT mixes per the quality control plan of the concrete plant. The intent of the minimum order size was to ensure adequate consistency of the delivery mixture and to provide additional concrete for FRC production if necessary.

On June 6, 2019, 3.0 cubic yards of concrete mixture design no. 12—without fiber—were delivered to the FDOT research facility for trial FRC production attempt #1. Typically, concrete batch plants provide a 'ticket' with the concrete delivery truck, which details the proportions of the mixture that were added to the truck. Furthermore, concrete delivery mixtures are commonly batched with less water than specified in the mixture design, so that water may be added to the mixture upon delivery (if necessary). Knowing the batched proportions of the delivery mixture enables additional water to be added on-site to achieve a desired consistency. As part of the FRC mixture production process, it was planned that upon delivery of the batch plant mixture (prior to the introduction of fiber), a (standard) slump test would be conducted to gauge the consistency of the mixture in the truck and determine how much water (if any) should be added to the mixture. To adequately introduce fibers into the mixture with the UHPC mixer, it was desired to achieve a minimum (initial) slump of approximately 3.0 in. (based on previous trial FRC production).

Unfortunately, for trial FRC production attempt #1, the delivery ticket was not provided. Without the ticket, mixture proportions that were added to the truck by the batch plant were unknown, making it difficult to determine how much water could be added before exceeding the design. Furthermore, the consistency of the mixture out of the truck was excessively stiff—i.e., based on the characteristics of the mixture out of the truck, it was clear that a large amount of water was required to achieve a desirable consistency for introduction of fiber (Figure 3.22a). Consequently, additional water was added to the truck in an attempt to reduce the stiffness (i.e., increase the slump). However, without the batch plant quantities know, it was impossible to know how much water was needed to match the intended mixture design. In summary, additional water was added five separate times in an attempt to reduce the stiffness—each time evaluating how the additional water influenced the stiffness, and each time finding that additional water was required. In total, approximately 36 gallons of water was added to the 3.0-cubic yard mixture. After additional water was added for the fifth time, a slump test was conducted (see Figure 3.22b) and approximately one hour of time had passed since the arrival of the truck. At that point in time, it was determined that the mixture was too stiff for fiber introduction and too much time had passed—little time remained before the mixture would begin to set. As a result, trial FRC production attempt #1 was aborted and ruled an unsuccessful attempt.

(a) (b)

Figure 3.22 Excessively stiff mixture prior to introduction of fiber: (a) Stiffness of mixture out of the truck; (b) 1.0-in. standard slump after adding 36 additional gallons of water

After the unsuccessful trial FRC production attempt #1, SRM was contacted to determine the mixture quantities that were added to the delivery truck, so that a possible cause of the failure could be determined. In Table 3.11, the mixture quantities that were added to the truck—reported by SRM to UF over the phone—are summarized, and are compared to mixture design no. 12. In summary, a major cause of the failed mixture was likely due to water in the delivered mixture being ~22% less than the design (i.e., more than the expected amount of water was held from the delivery—typically, 10% of the mixture water is held, but it was determined that ~22% of the water was withheld).

In Table 3.11, the first column of quantities summarizes the total quantities added to the truck. Dividing the total quantities by 3 (since it was a 3.0-cubic yard mixture) produces approximate quantities per cubic yard, which are shown in the second column. It should be noted that the quantities per cubic yard are approximate because additional aggregate moisture content adjustments were unknown. The last column of quantities summarizes mixture design no. 12 for comparison. Additionally, the approximate quantities of water (in gallons) that were added to the truck after delivery—the five separate instances—are shown separately.

Once delivered, 3 gallons of water were added to the truck mixture—after recognizing how stiff/dry the mixture was. Then, 6 more gallons of water were added, to reach what was assumed to be the 10% held quantity. Since the mixture was still too stiff/dry, 9 more gallons of water were added to the truck three separate times—bringing the total volume of water in the truck mixture up to ~117 gallons. Excluding the unknown (minor) adjustments for aggregate moisture content, the total water quantity added to the truck was only approximately 13.5 gallons beyond the original mixture design (i.e., only 4.5 gallons/cy beyond the 34.5 gallons/cy called for in the design). As a result, the failure of the mixture was attributed to the large portion of water that was withheld from the delivery truck.

Table 3.11 Comparison between truck delivery and mixture design no. 12

Product	Total truck quantity	Truck quantity (per cy quantities)	Design no. 12 (per cy quantities)
Cement – Type I/II	1240 lb	413 lb/cy	434 lb/cy
Fly Ash – Class F	330 lb	110 lb/cy	108 lb/cy
#67 Stone – Coarse aggregate	4780 lb	1593 lb/cy	1556 lb/cy
Silica Sand – Fine aggregate	4660 lb	1553 lb/cy	1556 lb/cy
Water	675 lb [81 gallons]	225 lb/cy [27 gallons/cy]	287 lb/cy [34.5 gallons/cy]
Additional water added to the truck (after initial delivery)	3+6+9+9+9=36 gallons (total=117 gallons)	1+2+3+3+3=12 gallons/cy (total=39 gallons/cy)	-
Sika hooked-end steel fiber	-	-	132.3 lb/cy
Darex AEA – Air-entraining admixture	12 fl oz	4 fl oz/cy	4 fl oz/cy
WRDA 64 – Water-reducing admixture	72 fl oz	24 fl oz/cy	24 fl oz/cy

3.5.4 Production trial attempt #2: Successful trial

Since the trial FRC production attempt #1 was unsuccessful, SRM was contacted to develop a new mixture design for trial FRC production attempt #2. At that point in time, UF was notified by SRM that SRM had chosen to switch admixture suppliers from Grace (GCP) to BASF. Consequently, a new mixture design was required, to account for the admixture change. After discussion with SRM, a new (revised) mixture design—mixture design no. 13—was used in the (successful) trial FRC production attempt #2, and is shown in Table 3.12.

It should be noted that there were two major changes associated with the development of mixture design no. 13—specifically related to the admixture supplier change by SRM. First, the BASF MasterGlenium 7920 water-reducing admixture is a high-range water-reducer—whereas the previously used GCP WRDA 64 admixture is a standard water-reducer. Second, a retarding admixture was recently added to the standard FDOT railing mixture design used by SRM. Therefore, the retarding admixture was also added to the trial FRC mixture design no. 13—providing more time for the FRC production process. Due—in part—to these two admixture changes, the trial FRC production attempt #2 was a success—where fibers were added to the delivery mixture using the FDOT UHPC mixer, and a trial FRC railing was formed, along with 11 (4-in. x 4-in. x 14-in.) flexural beams and 9 (4-in. x 8-in.) cylinders.

Table 3.12 Mixture constituents and proportions for mixture design no. 13 (1.0% fiber volume) with revised admixture quantities due to supplier change

Product	Quantity	Units
Cement – Type IL	424	lb/cy
Fly Ash – Class F	133	lb/cy
#67 Stone – Coarse aggregate	1535	lb/cy
Silica Sand – Fine aggregate	1608	lb/cy
Water	267	lb/cy
	[32.0]	[gallons/cy]
Sika hooked-end steel fiber (1.0% fiber volume)	132.3	lb/cy
Darex AEA – Air-entraining admixture	4	fl oz/cy
MasterSet DELVO – Retarding admixture	28	fl oz/cy
MasterGlenium 7920 – High-range Water-reducing admixture	12	fl oz/cy

On June 20, 2019, 3.0 cubic yards of concrete mixture design no. 13—without fiber—was delivered to the FDOT research facility for trial FRC production attempt #2—with a ticket containing the mixture quantities, as requested by UF. For trial FRC production attempt #2, the FRC production and forming procedure (i.e., the process used for fiber introduction) consisted of the following steps:

1. Upon delivery of the truck mixture, batch quantities added to the truck (from the included delivery ticket, shown in Appendix D) were input into a mixture design spreadsheet—which was developed beforehand. By having a spreadsheet readily available, any required/possible water content adjustments could be quickly determined. Additionally, the delivery truck mixture proportions could be compared to FRC mixture design no. 13.

2. After entering the truck mixture quantities into the mixture design spreadsheet, it was determined that additional water should be added to the truck mixture to improve the consistency for the addition of fiber. In total, 44 gallons of water were used (i.e., the mixture was delivered with 29 gallons, and 15 more gallons were added upon arrival). A comparison of the delivered truck mixture and mixture design no. 13 is provided in Table 3.13 (and is further detailed in a printout of the mixture design spreadsheet included in Appendix D).

3. After adding 15 additional gallons of water, a slump test was conducted, where a 7-in. standard slump—prior to the addition of fiber—was measured, as shown in Figure 3.23a. The high measured slump measurement was attributed to the introduction of high-range water-reducing admixture. Furthermore, the high slump indicated that the consistency of the mixture was more than adequate for the addition of fiber using the UHPC mixer.

4. The truck mixture was then transferred to the UHPC mixer—which has a maximum capacity of 1.11 cubic yards (30 ft^3)—for fiber introduction. In order to produce 1.5 cubic yards (40.5 ft^3) of FRC (the volume needed to fill all trial production forms), two separate 'lifts' of FRC production were required—since the total FRC volume exceeded the capacity of the UHPC mixer. For each 'lift', 0.75 cubic yards (20.25 ft^3) of the truck mixture—without fiber—was transferred to the UHPC mixer. Once placed into the mixer, the mixer was turned on and fibers were introduced (through the steel grate at the top of the mixer, shown in Figure 3.23b). Approximately 2 minutes were required to fully discharge all fibers through the grate and into the mixer. With the fiber introduced into the mixture, 2 additional minutes were used for mixing, to allow the fibers to distribute evenly throughout the entire mixture.

5. Once the first 0.75-cubic yard (20.25-ft^3) 'lift' of FRC was produced (Figure 3.23c), the FRC was transferred to the railing formwork (where the form was partially filled, as shown in Figure 3.23d) and internally vibrated.

6. To produce the second 'lift' of FRC, the process was then repeated—where an additional 0.75 cubic yards (20.25 ft^3) of the truck mixture was transferred to the UHPC mixer, the fibers were introduced, and the remaining forms were filled.

7. After the production of the second FRC lift, standard slump and vibration slump tests were conducted on the FRC mixture. By that time, approximately one hour of time had passed since the arrival of the delivery truck. As a result, the high-range water-reducing admixture began to lose effect. Consequently, the standard slump and vibration slump of the FRC mixture were measured as 2.5 in. and 1.75 in., respectively (shown in Figure 3.23e and Figure 3.23f)—a relatively large reduction in slump compared to the initial 7-in. slump of the delivery mixture (without fiber). It should be noted that standard slump tests and vibration slump tests of the first FRC lift were not conducted—to ensure adequate time was available for the production and placement of the second FRC lift.

8. In addition to filling the railing formwork (Figure 3.24), 11 flexural beam specimens and 9 cylinder specimens were formed (Figure 3.25). 5 of the flexural beams and 4 of the cylinders were formed with the first FRC lift. The remaining 6 flexural beams and 5 cylinders were formed with the second FRC lift.

Table 3.13 Comparison between truck delivery and mixture design no. 13 (see Appendix D)

Product	Total truck quantity	Truck quantity (per cy quantities)	Design no. 13 (per cy quantities)
Cement – Type IL	1270 lb	423.3 lb/cy	424 lb/cy
Fly Ash – Class F	400 lb	133.3 lb/cy	133 lb/cy
#67 Stone – Coarse aggregate	4700 lb	1535.5 lb/cy	1535 lb/cy
Silica Sand – Fine aggregate	5020 lb	1608.1 lb/cy	1608 lb/cy
Water	241.7 lb [29 gallons]	155.9 lb/cy [18.7 gallons/cy]	267 lb/cy [32.0 gallons/cy]
Additional water added to the truck (after initial delivery)	15 gallons (total=44 gallons)	5 gallons/cy (total=23.9 gallons/cy)	-
Sika hooked-end steel fiber	-	-	132.3 lb/cy
Darex AEA – Air-entraining admixture	11 fl oz	3.7 fl oz/cy	4 fl oz/cy
MasterSet DELVO – Retarding admixture	20 fl oz	6.7 fl oz/cy	28 fl oz/cy
MasterGlenium 7920 – High-range water-reducing admixture	30 fl oz	10 fl oz/cy	12 fl oz/cy

(a)

(b)

(c)

(d)

(e)

(f)

Figure 3.23 Scaled-up FRC production: (a) Standard (7-in.) slump after adding additional water to the truck delivery mixture; (b) UHPC mixer grate (where fibers were discharged); (c) Mixture after adding fiber; (d) Inside railing formwork with first lift placed; (e) Standard (2.5-in.) slump after second FRC lift; (f) Vibration slump after second FRC lift (1.75-in. slump)

Figure 3.24 Filled FRC railing formwork after trial FRC production

Figure 3.25 Additional trial FRC production specimens
(4-in. x. 4-in. x 14-in. flexural beams and 4-in. x 8-in. cylinders)

As shown in Table 3.13 (and Appendix D), the intended mixture design was achieved with the concrete delivered by SRM. Due to the use of the high-range water-reducing admixture, less water than what was specified in the design was used for the FRC production.

In trial production attempt #1, the batch-plant delivery mixture was excessively stiff—partly due to the unknown quantity of water that was present in the mixture. As a result, fiber could not be introduced and the FRC production attempt was aborted and determined to be an unsuccessful attempt. For trial FRC production attempt #2, the FRC mixture design was revised—consisting of a change to a high-range water-reducing admixture and the addition of a retarding admixture. As a result of the mixture design modifications, the second trial FRC production was a success, where fibers were introduced using the FDOT UHPC mixer, and a trial FRC railing was formed (along with other laboratory-scale specimens). The procedures used during this phase of the study were planned to be used for subsequent large-scale FRC production (i.e., to produce FRC railing impact specimens).

CHAPTER 4
DESIGN AND FABRICATION OF A FULL-SCALE PENDULUM IMPACTOR

4.1 Vehicle impact test equivalency and initial impactor test protocols

As opposed to employing vehicle impact testing as prescribed in AASHTO *MASH* (AASHTO, 2016) (which is an expensive endeavor that is outside the scope of the present study), pendulum impact testing utilizing the FDOT pendulum facility (Figure 4.1) was conducted. Correspondingly, a new pendulum impactor was designed and fabricated for the present study to replicate (similar) vehicle impact test conditions. Using a pendulum impactor is a more cost-effective approach when compared to vehicle crash testing, while still providing an adequate tool to evaluate the structural strength of the proposed railing. However, it should be noted that pendulum impact testing is not a replacement for vehicle crash testing, which may be required to sufficiently ensure the crashworthiness of the proposed FRC railing.

Figure 4.1 Pendulum at FDOT Structures Research Center (Tallahassee, FL)

Since the railing under investigation is specified by FDOT (2020a) as TL-4, vehicle impact test conditions prescribed in AASHTO *MASH* (AASHTO, 2016) were used to develop pendulum impact test protocols. Specifically, the most severe TL-4 vehicle impact test was selected: a 56-mph, '10000S' (22,000-lb [10,000-kg]) single-unit truck (SUT) impact at a 15-deg. impact angle (recall Tables 2.2–2.3). For the initial pendulum impact testing conditions, a 10,000-lb impactor was assumed with an initial drop height of 15.5 ft. These two conditions—which are within the maximum capacity and maximum drop height of the FDOT pendulum facility towers—produce an impact velocity of 21.5 mph (31.5 ft/sec) and the same impact energy as the transverse (perpendicular to barrier) component of a TL-4 SUT impact (i.e., the pendulum impact will produce the same kinetic energy as the transverse/perpendicular component of a 56-mph SUT impact at 15 deg.). A comparison of the *MASH* TL-4 impact and the pendulum impact test conditions are provided in Figure 4.2 and Table 4.1.

(a)

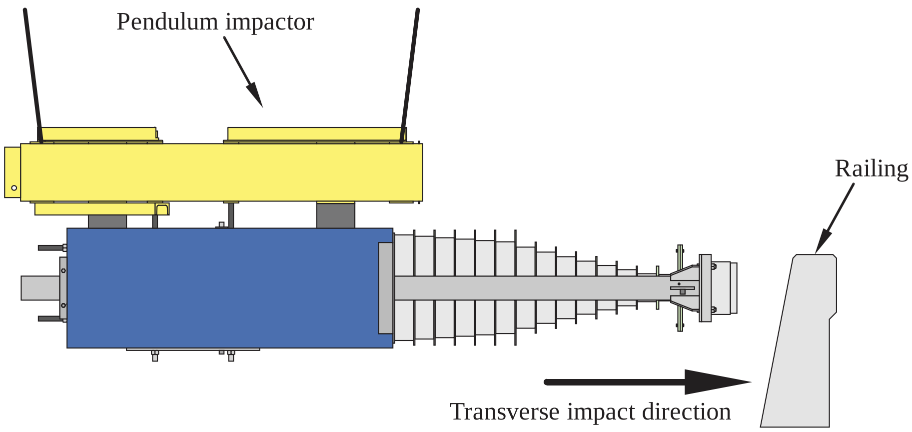

(b)

Figure 4.2 Test conditions for: (a) *MASH* TL-4 impact (after Sheikh et al. 2011);
(b) Proposed pendulum impact test

Table 4.1 Comparison between *MASH* TL-4 impact and proposed pendulum impact test

	MASH TL-4 SUT impact	Pendulum impact
Kinetic impact energy (kip-ft)	155	155
Impact mass (lb)	22,046	10,000
Transverse velocity (mph)	14.5	21.5
Drop height (ft)	N/A	15.5

In the case of the AASHTO *MASH* 56-mph SUT impact, the impact is oblique (i.e., the vehicle strikes the barrier at 15-deg. and is then redirected). Only the transverse (i.e., perpendicular) component of the impact was considered for pendulum impact test protocol calculations, since the longitudinal component is considered to have minimal influence on the redirectional capacity of the railing. Additionally, an oblique impact with the pendulum impactor is not feasible because such an impact would produce uncontrollable twisting of the impactor—a situation that is considered dangerous with regard to the integrity of the tower hanger cables and the safety of nearby observers. Therefore, pendulum impact test protocols were designed for a direct (i.e., 'head on', *non*-oblique) pendulum impact test. The velocity of the 10,000-lb pendulum impactor was computed such that test impact energy will match the transverse component of impact energy (155 kip-ft) of the AASHTO *MASH* TL-4 SUT test.

In addition to selecting pendulum impact test conditions, a conceptual crushable nose configuration was developed (i.e., force-deformation characteristics of the impactor were determined). The geometric design of the 36-in. SSTR originates from research conducted by Texas Transportation Institute (TTI). In Sheikh et al. (2011), FEA impact simulations and a subsequent 10000S (SUT) crash test were used to determine the crashworthiness of the 36-in. SSTR. Additionally, impact force versus time curves—determined from FEA impact simulations—for TL-4 SUT impacts with various single-slope railing heights were determined and is shown in Figure 4.3. The 36-in. force-time curve presented by TTI (shown in purple) was used to develop preliminary force-deformation characteristics of the pendulum impact test (i.e., the preliminary crushable nose configuration was developed in an attempt to reproduce a similar force-time curve presented by TTI).

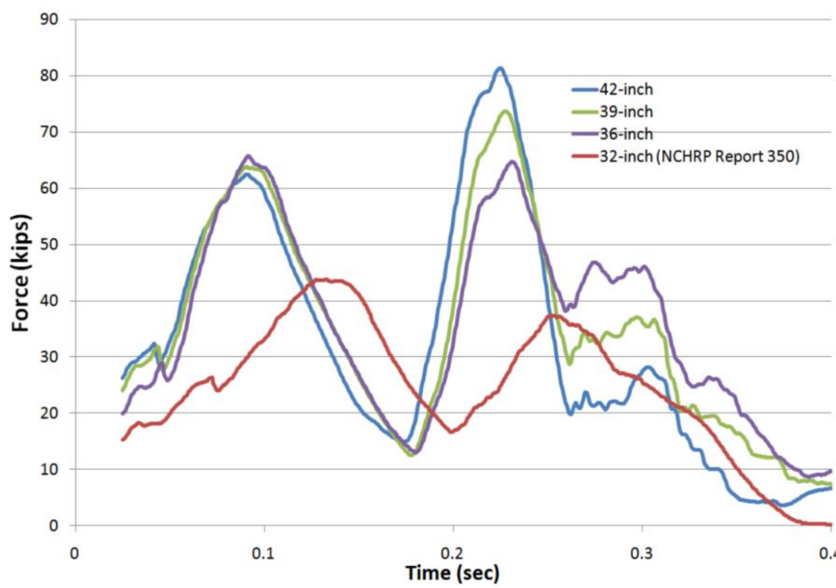

Figure 4.3 FEA impact force-time curves for single-slope traffic railings for various railing heights (after Sheikh et al. 2011)

To achieve a force-time curve similar to that of the 36-in. SUT impact condition, aluminum honeycomb material was selected for use in the crushable nose of the pendulum impactor. Force-deformation characteristics of the aluminum honeycomb material—which have been documented in previous FDOT projects (e.g., Consolazio et al. 2016)—provide the ability to achieve a designed force-deformation curve by using a series of aluminum honeycomb cartridges of varying dimensions. Typically, the compressive strength of the material is first measured (or known) and the cross-sectional area (length and width dimensions) of each cartridge is selected, thereby achieving a desired force—and a designed force-time curve by stacking multiple honeycomb cartridges together in series.

As shown in Figure 4.4, for an individual rectangular cartridge, a (nearly) constant force is applied until approximately 75% to 80% of the total cartridge thickness has crushed under compression. For the design purposes of the new pendulum impactor, the full force-deformation curve of each honeycomb cartridge was considered, but only the constant portion of the curve was relied upon (i.e., the additional energy dissipation beyond the 75% deformation point was effectively ignored). By only relying on the constant force region of the curve, a stepwise linear force-time curve is produced.

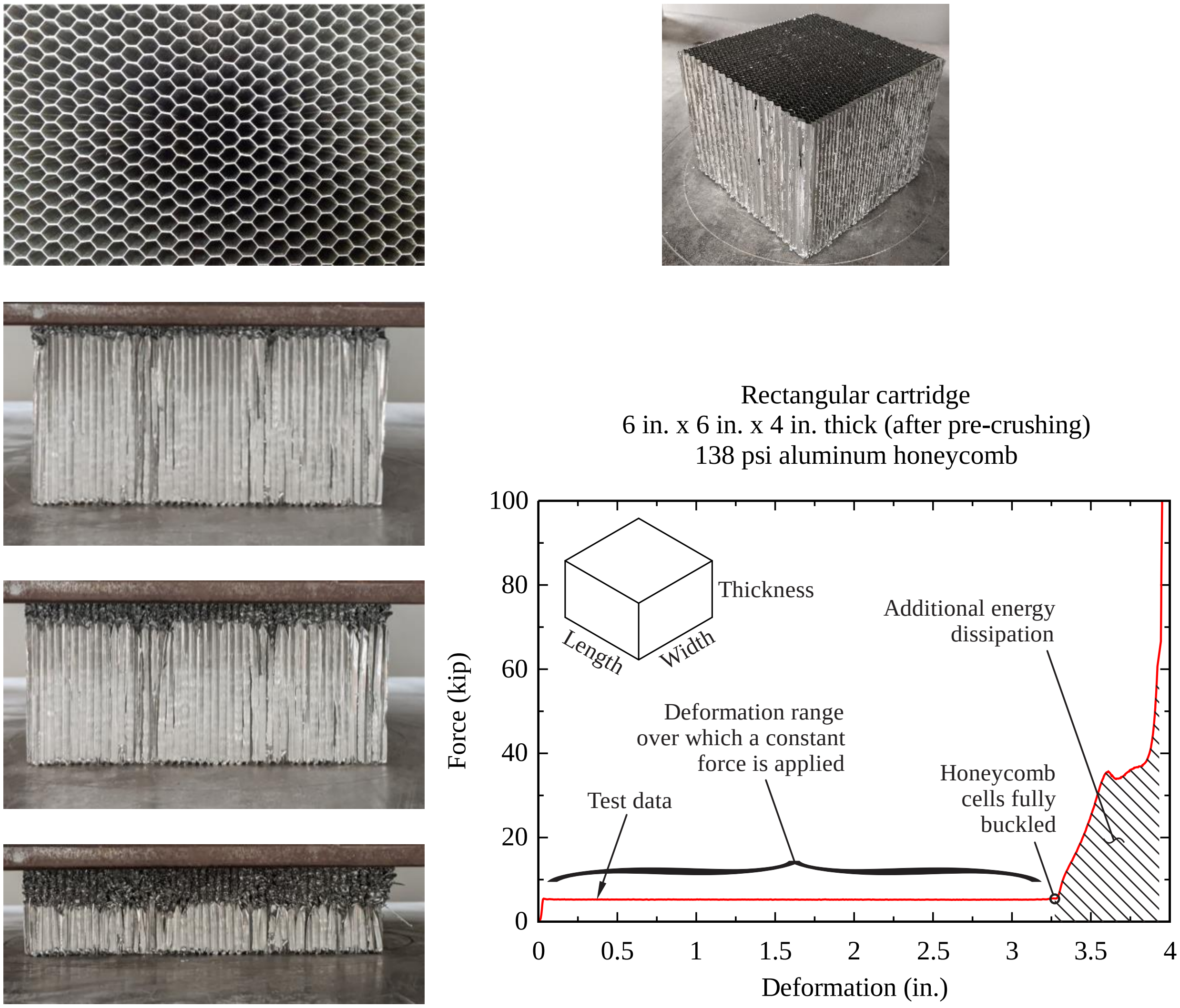

(a) (b)

Figure 4.4 Aluminum honeycomb: (a) Cell structure and crush sequence of rectangular cartridge; (b) Force-deformation curve for an individual rectangular aluminum honeycomb cartridge (after Groetaers et al. 2016)

In terms of the overall design of the crushable nose and the pendulum impactor, the 15.5-ft drop height produces a pendulum impact velocity of 21.5 mph. The kinetic energy of the impactor (155 kip-ft) is then dissipated and delivered to the railing test specimen through the force-deformation of the crushable nose (i.e., the kinetic energy of the 10,000-lb mass is consumed through the crushing sequence of aluminum honeycomb cartridges). The crushable nose is an additional component of the pendulum impactor and was designed to attach to the front of the impactor, with a series of honeycomb cartridges in position and with the ability to telescope (i.e., slide through) the impactor as each honeycomb cartridge crushes in sequence. Each cartridge is designed to consume the kinetic energy of the impactor—which is converted to a force-deformation (with the force being applied to the railing test specimen). Consequently, the design of the front cartridge (i.e., the first cartridge) required the consideration of the front nose mass and its corresponding kinetic energy. In other words, the front cartridge was designed to consume the kinetic energy of the telescoping front nose and the subsequent cartridges are designed to consume the kinetic energy of the remaining impactor mass.

Based on a pendulum impact velocity of 21.5 mph, one 6-in. thick front cartridge and fifteen 4-in. thick aluminum honeycomb cartridges of increasing cross-sectional area were required to dissipate the kinetic energy (155 kip-ft) of the pendulum impact test. Of the 16 total, the first 12 cartridges are required to produce the first peak of the force-time curve—i.e., from zero until reaching the first 65-kip peak of the TTI force-time curve. Additionally, design of the 4 subsequent (i.e., remaining) cartridges produces a force-time curve that conservatively deviates from the TTI curve in Figure 4.3. A force-time curve that more 'realistically' follows the curves in Figure 4.3—where force increases to 65-kips, subsequently decreases, and then increases again due to vehicle redirection and 'backslap' of the rear SUT tandem—is nearly impossible to safely reproduce with an impact pendulum. (Difficulty in reproducing the TTI curve arises due to the increase and subsequent decrease in force. When using a crushable nose, lower strength cartridges will crush first—even if placed behind higher strength cartridges—and will not produce the desired curve). Instead, a conservative impact condition was designed in which, once the peak 65-kip force is reached, a nearly constant 65-kip force is maintained until all remaining kinetic energy is consumed.

However, it is noted that if multiple cartridges of exactly the same size and material strength are used in sequence, it is not guaranteed that the cartridges will crush in sequential order (due to minor imperfections, etc.), potentially leading to unpredictable impactor response. To avoid this situation, a slight linear increase in force (from 59.5 kips to 68.8 kips) for the final 6 cartridges was used to produce an *average* 65-kip force in the design of the impactor force-time curve (see black line in Figure 4.5). The final (stepwise linear) force-time curve produced with the designed cartridge sizes is shown in red in Figure 4.5.

Based on the kinetic energy used during impact testing, it was determined that the force-time curve produced from the proposed crushable nose design reaches the second 65-kip peak in the force-time curve presented by TTI (as shown in Figure 4.5). Additionally, by ensuring that the impact force does not decrease below the 65-kip initial peak force, the designed pendulum impact test is considered more severe (i.e., more conservative) than a TL-4 SUT impact. Test protocol calculations demonstrate that the proposed pendulum impact test imparts the same kinetic energy and peak force levels as the TL-4 SUT impact test, while also producing approximately a load impulse (area under the force-time diagram) that is 80% of the value obtained from the simplified TTI force-time history. Furthermore, the peak impact force (more than 65 kips) exceeds the 54-kip (transverse) design force specified in *AASHTO LRFD Bridge Design* (2017, recall Table 2.1)—which is consistent with recommendations that have been published subsequent to the release of AASHTO *MASH* (AASHTO, 2016). The final stepwise linear curve (the red curve in Figure 4.5) is achieved using the cartridge characteristics provided in Table 4.2, starting with a small cartridge (cartridge 1) at the front of the impactor and gradually increasing in size and corresponding force to the final cartridge (cartridge 16). Note that the front cartridge (cartridge 1), which was determined to require a 6-in. thickness due to the kinetic energy of the front nose, is made up of two combined cartridges (1A and 1B) with 2-in. and 4-in. thicknesses, correspondingly.

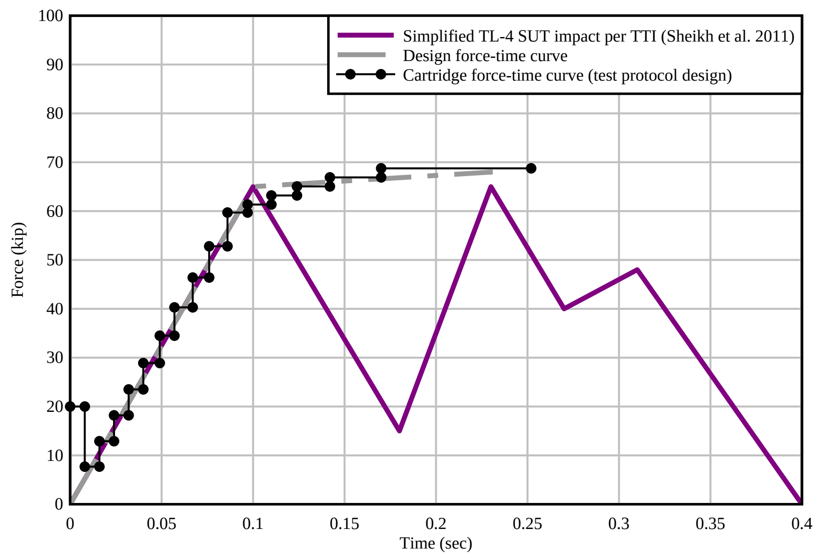

Figure 4.5 Anticipated force-time curve from the developed crushable nose design

Table 4.2 Aluminum honeycomb cartridge characteristics

Cartridge #	Compressive strength (psi)	Length (in.)	Width (in.)	Thickness (in.)*	Design force (kip)
1A	138	11.00	12.75	2.00	19.5
1B	138	11.14	13.00	4.00	20.0
2	138	5.07	11.00	4.00	7.7
3	138	5.20	18.00	4.00	12.9
4	138	5.50	24.00	4.00	18.2
5	138	7.10	24.00	4.00	23.5
6	138	8.73	24.00	4.00	28.9
7	138	10.42	24.00	4.00	34.5
8	138	12.17	24.00	4.00	40.3
9	138	14.00	24.00	4.00	46.4
10	138	15.94	24.00	4.00	52.8
11	138	18.02	24.00	4.00	59.7
12	138	18.53	24.00	4.00	61.4
13	138	19.08	24.00	4.00	63.2
14	138	19.65	24.00	4.00	65.1
15	138	20.20	24.00	4.00	66.9
16	138	20.75	24.00	4.00	68.8

* Maximum thickness after cartridge pre-crushing

4.2 Pendulum impactor design

The following pendulum impact test conditions were then used to develop a full-scale pendulum impactor design:

- 10,000-lb impactor
- 15.5-ft drop height
- 21.5-mph impact speed
- 155-kip-ft kinetic impact energy

Fabrication drawings for the pendulum impactor design are provided in Appendix F. FEA models—developed iteratively—incorporating approximate front nose aluminum honeycomb cartridge designs were used to confirm that the designed force-time curve for the pendulum impact test can be achieved. Additionally, finite element analysis (FEA) impact simulation models analyzed in LS-DYNA (Livermore Software Technology, 2020) (see Figures 4.6 through 4.10) were used to develop the design of the pendulum impactor, which is detailed in Figure 4.11. The following bullet points summarize FEA results/findings used to develop the design of the pendulum impactor:

- Some FEA models include the entire pull-back process (i.e., pulling the impactor from the bottom-hang position to the correct 15.5-ft drop height). By modeling the pull-back process, the correct pull-back location (i.e., location to attach the pull-back cable) could be determined with more confidence. Modeling the pull-back process also provided the ability to determine the correct swing path of the impactor and computation of axial forces in the pendulum hanger cables.
- FEA models were used to determine the required sizes of plates and tubes in the aluminum front nose. For example, the diameter of the aluminum telescoping tubes was determined based on stress results from multiple model iterations. Due to the swing path of the impactor (and relatively long length of the front nose), the impact will not occur in a purely horizontal manner. Instead, the test was designed such that the impact initiates as the pendulum impactor is still swinging downwards. As the honeycomb cartridges on the front nose continue to crush, the impactor reaches the bottom of the swing. Then, the impactor continues to swing upwards before coming to a stop. By designing the swing to occur with the first half of the impact during the downswing and the second half of the impact during the upswing, stresses in the aluminum front nose tubes were found to be minimized.
- FEA impact simulations incorporated the geometry of the FDOT 36-in. single-slope railing (the railing under investigation for the present study). By incorporating the railing geometry, it was determined that the slope of the railing causes the front nose to be redirected upwards during impact. As a result, bending stresses in the front nose tubes were found to be in excess of 25 ksi (near yield strength of high-strength aluminum). Therefore, a loading wedge was placed between the railing and the aluminum front nose, to prevent redirection of the front nose and reduce stresses in the aluminum tubes.
- In early FEA model iterations, the front nose ‘keeper plates’ (to be welded to each telescoping tube) showed signs of permanent deformation in cases of accidental eccentric loading during pendulum impact simulations. Although the current design of the front nose does not show signs of an eccentric loading condition, aluminum stiffener plates were added to the front nose as a safety precaution.
- Once the front nose components were designed, impact force data from FEA simulations showed an undesirable spike in force during the crushing phase of the front cartridge (i.e., the impact force spiked to 75 kip, well beyond the 17-kip design force of the first cartridge). The cause of the spike was attributed to an under-designed front aluminum honeycomb cartridge—the front cartridge is intended to fully consume (dissipate) the kinetic energy of the aluminum front nose. An under-designed front cartridge means that the front nose did not come to a stop (i.e., kinetic energy of the front nose was not fully consumed) until after the crushing of the front cartridge. After multiple model iterations and revisions, the total thickness of the front cartridge was increased from 4.0 in. to 6.0 in.—requiring two stacked aluminum honeycomb cartridges to produce a 6.0-in.

thickness (as detailed in Table 4.2). Additionally, the overall cartridge design force was increased from 17 kip to 20 kip to produce a force-time curve without any excessive force spikes. Once a force-time curve without any excessive force-spikes was achieved, acceleration data from the front nose and back block were used to determine accelerometer (instrumentation) requirements for the impact test.

- Selected FEA models also incorporated the geometry and reinforcement of a concrete deck-railing impact test specimen (see Figure 4.10). The impact test specimen was modeled with `MAT_CSCM` (continuous surface cap model), a commonly used material model for modeling the behavior of concrete in LS-DYNA. By simulating the impact test with an impact test specimen and `MAT_CSCM` material, FEA results provide the ability to predict the anticipated outcomes of experimental impact tests.

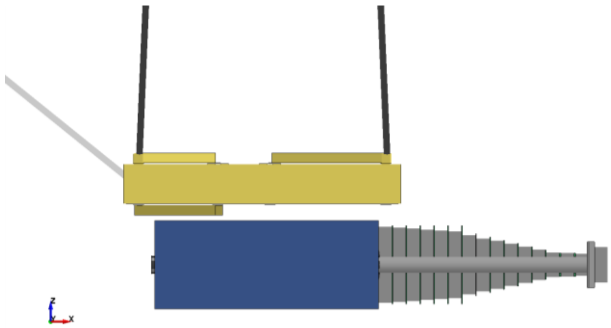

Figure 4.6 FEA impact simulation (side elevation view) at start of pull-back process

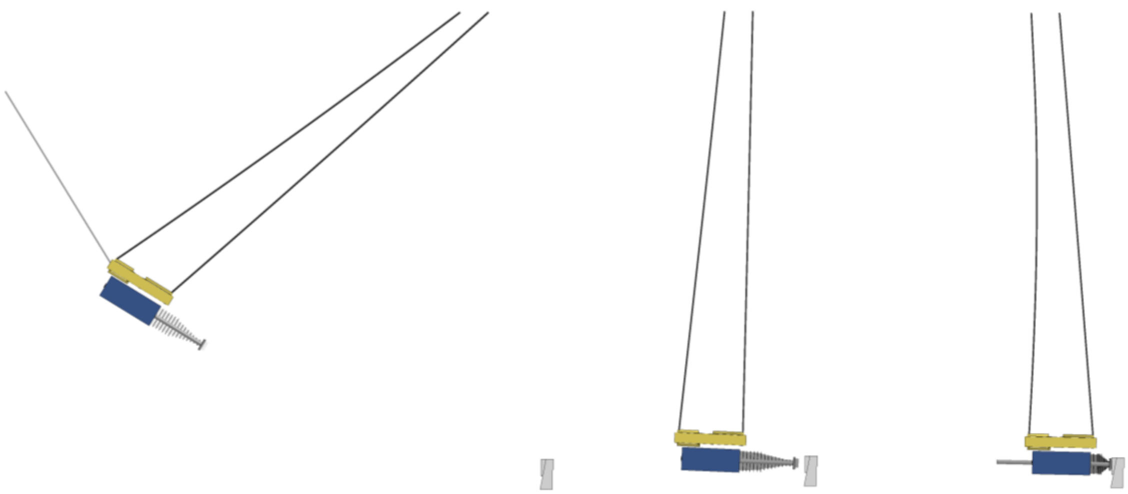

(a) (b) (c)

Figure 4.7 FEA impact simulation (side elevation view): (a) At drop height; (b) Before impact; (c) At end of impact

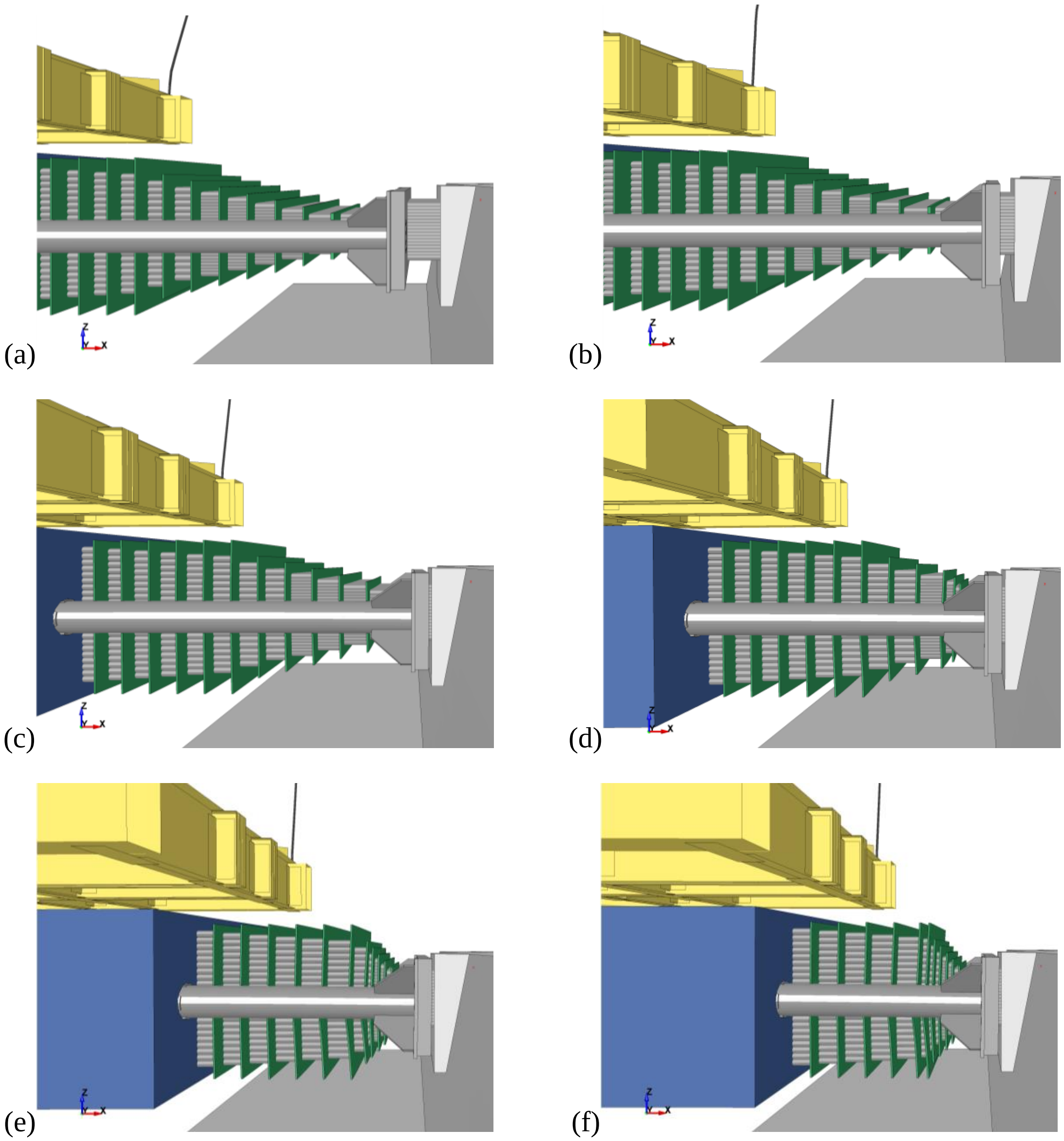

Figure 4.8 FEA front nose telescoping sequence: (a) At start of impact;
(b)–(e) Intermediate states of impact; (f) At end of impact and peak impact force

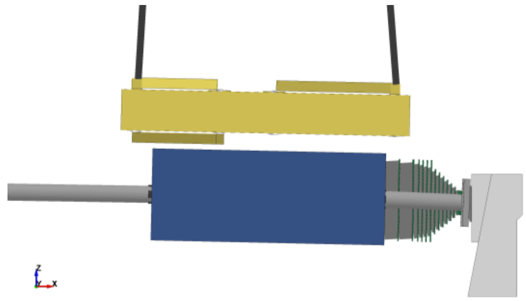

(a)

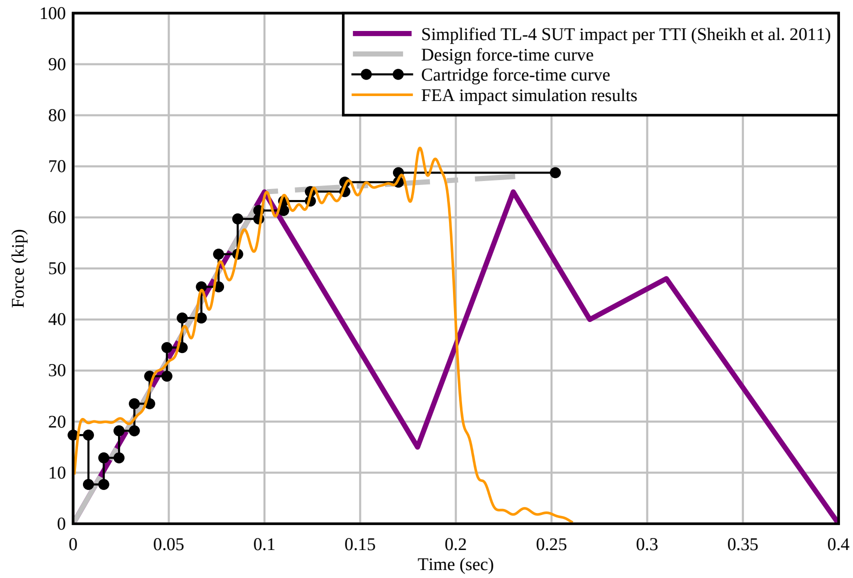

(b)

Figure 4.9 FEA impact simulation: (a) Side elevation view at end of impact; (b) Force-time results from FEA impact simulation compared to the (anticipated) force-time curve design

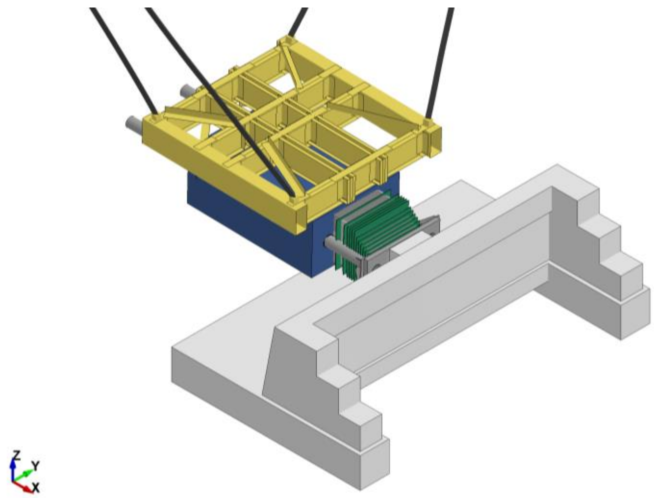

Figure 4.10 FEA impact simulation (isometric view) at end of impact with preliminary impact test specimen design

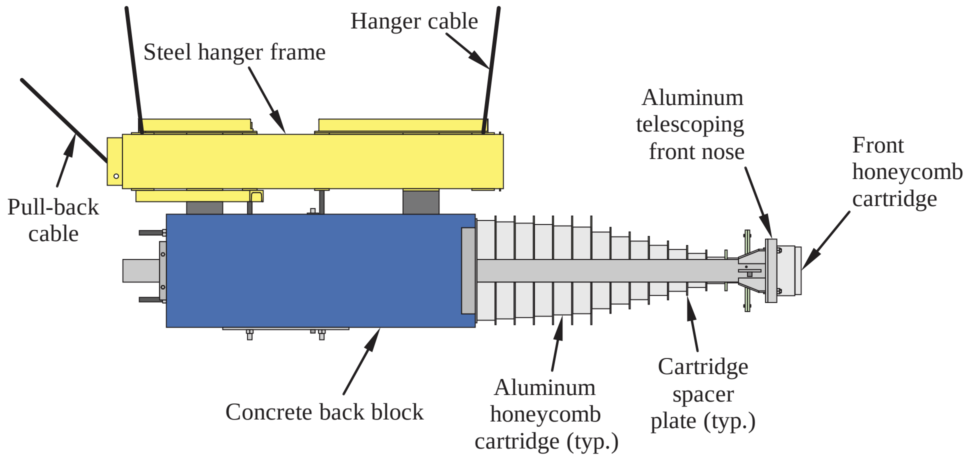

Figure 4.11 Overall design and major components of the pendulum impactor

4.3 Pendulum impactor fabrication

The impactor fabrication drawings were then used—with minor modifications and the development of additional fabrication sequence drawings—to fabricate the pendulum impactor. The following section provides an overview of the completed pendulum impactor fabrication. The fabricated impactor was then used in pendulum impact tests to investigate the structural adequacy of an FRC railing.

The pendulum impactor consists of three major components: (1) the steel hanger frame, (2) the concrete back block, and (3) the aluminum front nose. The steel hanger frame (shown in Figure 4.12) was repurposed for the present study to provide a method for connecting the 10,000-lb impactor to the pendulum towers (i.e., the hanger frame contains four connection points for hanging the impactor from the pendulum towers). Meanwhile, the concrete back block encompasses the majority of the designed 10,000-lb weight of the pendulum impactor. Additionally, the concrete block contains two embedded steel guide tubes. These guide tubes provide two longitudinal (pipe) voids through the concrete block for smaller diameter aluminum pipes, which attach to the aluminum front nose, to pass through. Correspondingly, the aluminum front nose was designed to deliver the impact (i.e., kinetic) energy of the impactor to the concrete railing, with the use of consumable aluminum honeycomb cartridges.

Figure 4.12 Repurposed steel hanger frame

As shown in the additionally developed fabrication sequence drawings in Appendix F, four steel channels were bolted to the existing steel hanger frame. Then, with the hanger frame suspended above the lab floor, formwork for the concrete block was positioned beneath the hanger frame. With the steel channels still connected to the hanger frame, the steel front face of the concrete block and all remaining steel components—to be embedded within the concrete block, such as rebar and the steel guide tubes—were positioned within the concrete block formwork (see Figures 4.13 through 4.16). With all steel components positioned within the formwork, concrete was placed through the steel hanger frame into the formwork, forming the concrete block. After a sufficient curing period, the formwork was removed, and the concrete block was formed/fabricated.

Figure 4.13 Steel hanger frame suspended above the concrete block formwork with embedded steel components correctly positioned

Figure 4.14 Embedded steel components within the concrete block formwork

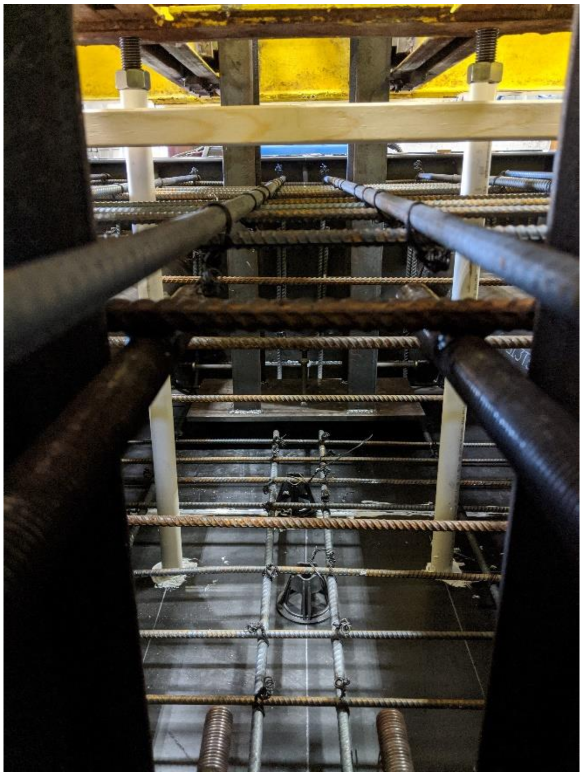

Figure 4.15 Embedded steel positioned inside the concrete block formwork

Figure 4.16 Steel hanger frame and concrete formwork ready for concrete placement

Figure 4.17 Formed concrete block connected to the steel hanger frame

To fabricate the front nose of the impactor, solid aluminum stock materials were ordered and delivered to Velocity Machine Works, a fabrication shop located in Tallahassee, FL. After machining and assembling the components, the aluminum front nose portion of the impactor was completed.

With the concrete block formed and with the aluminum front nose fabricated, strips of Teflon (3/8-in. thick x 1-in. wide x 4-in. long) were adhered—using fast setting epoxy—to the inside (rounded) surfaces of the steel guide tubes (as shown in Figure 4.18 and Figure 4.19). In total, 16 Teflon strips were installed inside the tubes, with 4 at each end or opening of each tube. The Teflon strips were installed to provide a low-friction interface between the aluminum tubes on the front nose and the steel guide tubes inside the concrete block. By reducing friction, the Teflon strips allow the front nose to telescope and pass through the impactor more easily (with minimal energy loss due to friction) during the duration of an impact test. Once the Teflon strips were installed, the aluminum front nose was placed inside the concrete block, as shown in Figure 4.20 and Figure 4.21, and the fabrication of the pendulum impactor was complete.

After completing the fabrication process of the pendulum impactor, the main components of the impactor were weighed, and it was determined that the (measured) total weight of the impactor is 10,333 lb (333 lb greater than the design). Due to the fact that the impactor (as fabricated) was found to have more mass than was designed, test protocols were revised (i.e., the drop height was reduced to 15 ft, to account for additional weight of the impactor to ensure that the intended impact energy of 155 kip-ft was maintained for testing, also reducing the intended impact speed to 21.2 mph [31.1 ft/sec]).

Figure 4.18 Teflon strips positioned within the steel guide tubes with magnets to hold them in place while the adhesive sets

Figure 4.19 Teflon strips adhered within the steel guide tube

Figure 4.20 Complete pendulum impactor: Fabricated aluminum front nose placed inside the concrete block

Figure 4.21 Complete pendulum impactor: Aluminum front nose placed inside the concrete block and the front nose tubes protruding out the back of the block

CHAPTER 5
FULL-SCALE RAILING PENDULUM IMPACT TEST PROGRAM

5.1 Overview

With the newly developed pendulum impactor constructed, a remaining task in the present study was to evaluate the structural adequacy of the proposed full-scale FRC traffic railing. To enable direct comparison of the proposed FRC railing to the standard R/C railing, three FRC and three standard FDOT traffic railing impact specimens were impact tested. Experimental impact test results of the two types were used to evaluate the structural adequacy of the proposed FRC traffic railing. In this chapter, a description of specimen development, construction, and installation is described (with test results shown in subsequent chapters).

5.1.1 Full-scale railing specimen design with integrated bridge deck

Concrete traffic railings are typically long, continuous elements (e.g., traffic railings can span more than 50-ft long). However, it was impractical to experimentally impact test a typical length of railing (i.e., a 50-ft specimen could not be used with the FDOT pendulum facility). Consequently, a shorter length impact specimen (shown in Figure 5.1) was designed to recreate longitudinal railing conditions with the following considerations:

- The selected railing length is greater than the expected ‘critical length’ as defined by AASHTO LRFD design. As shown in Appendix A, the ‘critical length’ of railing (i.e., length over which a yield line failure pattern was predicted to occur) was computed to be approximately 9 ft, for the standard FDOT 36-in. SSTR. Therefore, the length of the specimen is 13 ft (greater than 9 ft), to provide enough length for the expected yield line failure pattern to form.
- Because the traffic railing is relatively short in length, end supports (also referred to as ‘buttresses’) were placed at each end of the traffic railing specimen (Figure 5.1). Without the end supports, the 13-ft long specimen was expected to fail as a simple cantilever wall—preventing the more ‘realistic’ traffic railing yield line failure pattern from forming. With the end-support buttresses, the 13-ft specimen was expected to fail similar to the yield line pattern that would occur for a more typical (i.e., longer) traffic railing.
- One of the most common uses of traffic railings is along highway bridges. Therefore, the impact specimen includes a typical bridge deck portion beneath the railing (the preliminary geometry of the test specimen design is provided in Figure 5.2). Additionally, the proposed traffic railing contains connection reinforcement that extends into the deck below. Including the deck portion of the specimen allowed impact testing of the barrier-deck system usingtypical connection reinforcement configurations and a typical FDOT bridge deck configuration (see Figure 5.3).

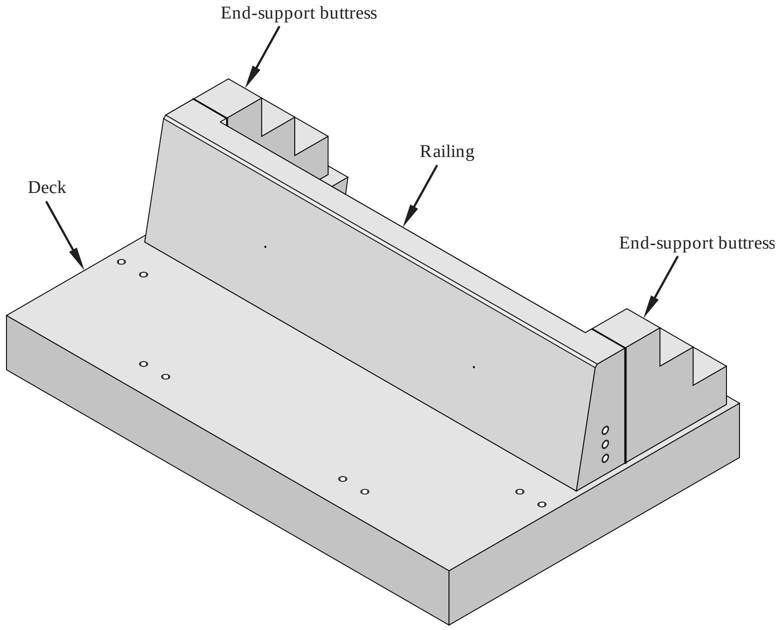

Figure 5.1 Main components of the pendulum impact test specimen

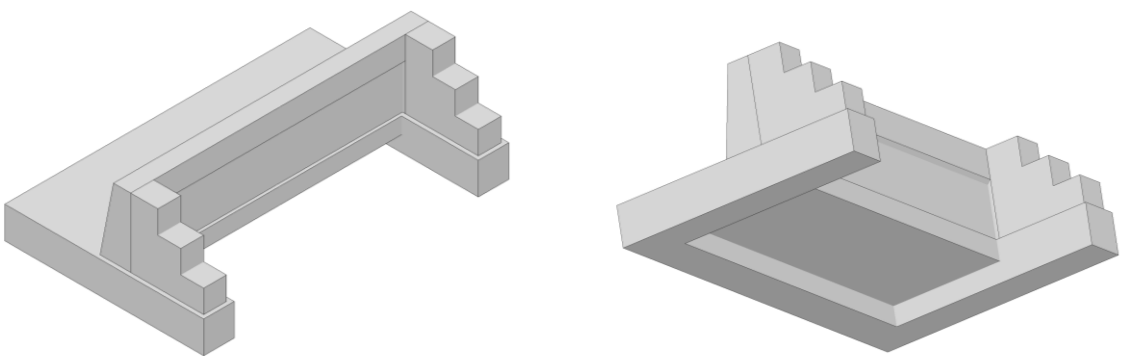

(a) (b)

Figure 5.2 Preliminary FEA model of deck-railing impact test specimen: (a) Back isometric view; (b) Isometric view underneath—to show how the central deck portion of the specimen is elevated, similar to a typical bridge deck overhang

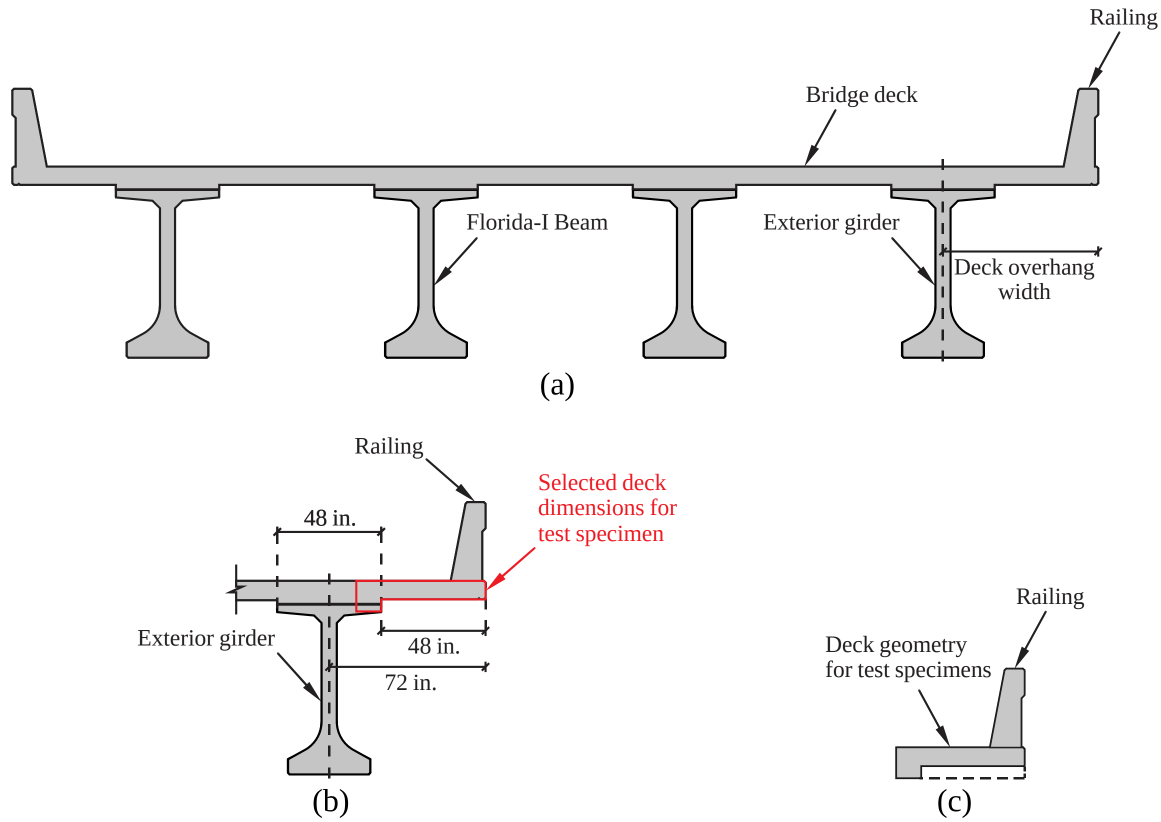

Figure 5.3 Approach for selecting cross-sectional deck dimensions: (a) Typical bridge cross-section; (b) Exterior girder and railing; (c) Selected geometry for test specimen

With these consideration, the final impact test specimen design—of either FRC or R/C configuration—consists of three separate components: (1) deck, (2) railing, and (3) end-support buttresses, as shown in Figure 5.1. The design of the standard R/C test specimen follows FDOT Standard Plans Index 521-427 (FDOT, 2020a), where the standard reinforcement within the 36-in. single-slope traffic railing is implemented (i.e., reinforcement within the standard R/C railing portion of the test specimen follows the reinforcing plan specified by FDOT, as shown in Figure 5.4).

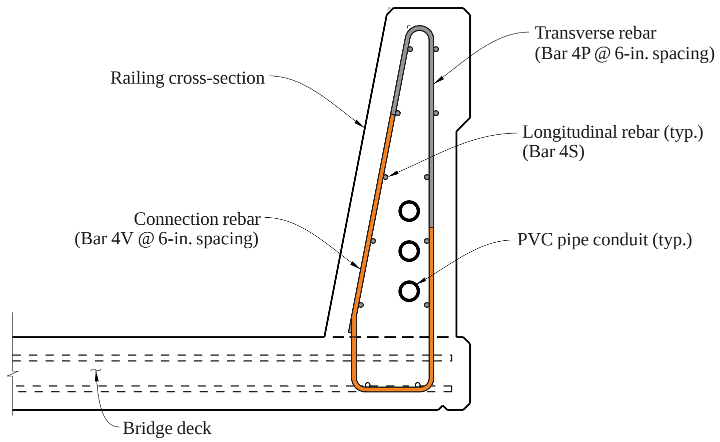

Figure 5.4 Standard 36-in. single-slope traffic railing (after FDOT 2020a)

Correspondingly, the design of the proposed FRC test specimen is derived from the FDOT Standard Plans Index 521-427 (FDOT, 2020a). However, for the FRC railing test specimen, FRC is relied upon to replace the majority of the reinforcement within the railing cross-section. Only the connection reinforcement (bar 4V with the “contractor’s option” to bend the top of the 4V connection bar) was retained, while all remaining reinforcing bars (i.e., longitudinal bars 4S and shear bars 4P) within the standard FDOT 36-in. single-slope railing were omitted (see Figure 5.5). Construction drawings developed for both the standard R/C and proposed FRC test specimens (provided in Appendix G) were then used to construct and form each test specimen (R/C or FRC) for impact testing.

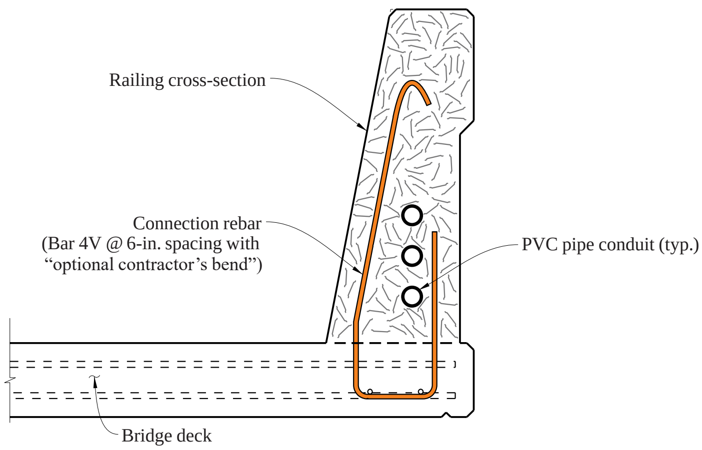

Figure 5.5 FRC 36-in. single-slope traffic railing

5.1.2 Construction of test specimens

All test specimens were first constructed inside the FDOT structures research laboratory and subsequently moved outside with a crane to the pendulum testing area. To begin the construction process for each test specimen, the reinforcing bars for the deck portion of the test specimen were first tied together and placed into the previously constructed deck formwork (shown in Appendix G)—which is a cast-in-place form that was constructed for the present study. Additional connection bars—between the deck and railing (i.e., 4V bars)—and end-support buttress bars were also installed within the deck formwork (Figure 5.6 and Figure 5.7) during this first construction stage.

Figure 5.6 Reinforcing bars positioned inside deck formwork

Figure 5.7 Deck-to-railing connection bars and end-support buttress reinforcement positioned inside deck formwork

With bars for the deck portion of the specimen in place, an FDOT approved Class II deck concrete (a conventional 4500-psi strength concrete that meets FDOT mixture design requirements for concrete bridge decks) was placed (Figure 5.8) and adequately vibrated to form the deck portion of each test specimen. Mixture design details and the specific concrete mixture quantities used in the delivered deck concrete are provided in Appendix D. After placement and hardening of the deck concrete, formwork for the railing portion of the test specimen was attached above the deck.

Figure 5.8 Deck concrete placement

For construction of standard R/C railing specimens, the conventional railing reinforcement was subsequently placed within the rail formwork (Figure 5.9a). With the railing reinforcement accurately positioned, an FDOT approved Class II (other than bridge deck) concrete (a conventional 3400-psi strength concrete that meets FDOT mixture design requirements for the 36-in. SSTR) was placed and adequately vibrated to form the railing and buttress regions of an R/C test specimen (Figure 5.9b). Mixture design details and the specific concrete mixture quantities used in the delivered railing concrete are provided in Appendix D.

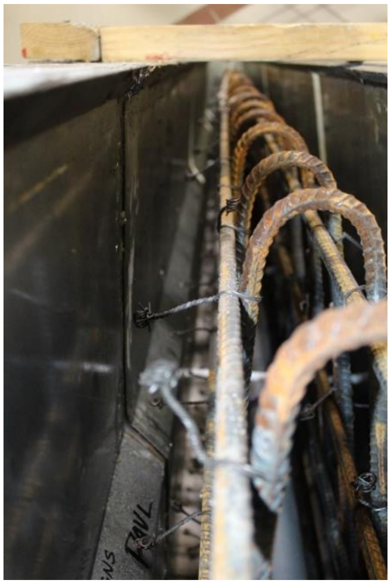

(a)

(b)

Figure 5.9 Construction of railing portion of R/C test specimen: (a) Railing reinforcement positioned inside railing formwork; (b) Railing concrete placed and formed

For construction of FRC railing specimens, because the FRC railing design only includes the 4V connection bars (which were already cast within the deck), the railing and buttress portions of the test specimen were ready to be cast (Figure 5.10). Following the same procedure as detailed in the ‘scaled-up FRC production at the ready-mix batch plant level’ section (where an FRC mixture that was developed for the present study was produced on a larger scale in coordination with a batch plant and with additional on-site mixing), FRC (1% hooked-end steel fiber) was produced and used to form the railing portion of the FRC test specimens. Leftover concrete (without fiber) was used to form the buttress regions of the test specimen. Mixture design details and details of the procedure used to produce FRC are provided in Appendix D. After adequate time for curing (around 3 days), components of the deck and railing formwork were removed and the construction phase of each test specimen was complete (Figure 5.11).

(a) (b)

Figure 5.10 Construction of FRC test specimen: (a) Deck concrete cast with railing formwork in position; (b) Railing reinforcement positioned inside railing formwork

Figure 5.11 Completed (FRC) test specimen

5.1.3 Installation of test specimens

After providing additional time for curing (approximately 7 days after casting the railing), each test specimen was then lifted by crane (Figure 5.12) and moved across the FDOT structures laboratory and placed onto a truck bed. Afterwards, the truck was driven outside, where an additional crane was used to move the specimen off of the truck bed and into position on the pendulum foundation (Figures 5.13 through 5.15). It should be noted that the total weight of a test specimen was approximately 20 kip and no noticeable cracking occurred during the lifting/transportation process in any of the test specimens.

Figure 5.12 Test specimen lifted out of the formwork by crane

Figure 5.13 Test specimen being moved into position on the pendulum foundation

Figure 5.14 Impact test specimen in position on pendulum foundation

Figure 5.15 Backside of impact specimen after being positioned onto the pendulum foundation (with temporary HSS lifting element still connected)

Once positioned, the test specimen was anchored to the pendulum foundation—using the anchoring plan developed as part of the impact testing procedure, which is provided in Appendix H. As depicted in Figure 5.16, a number of steel components were used to anchor the test specimen to the pendulum foundation beneath—preventing the test specimen from lateral movement or sliding as a rigid body, and only allowing the railing portion of the test specimen to deflect under impact loading.

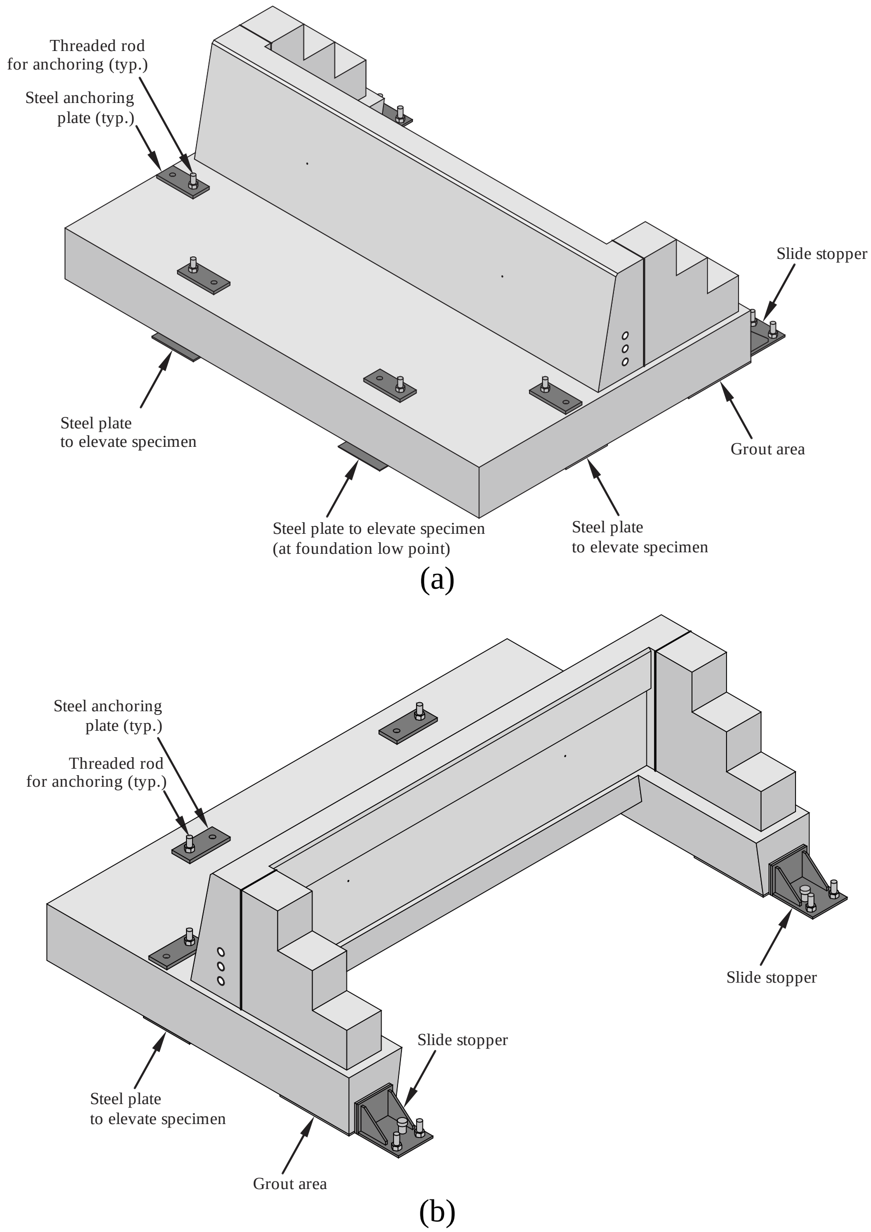

Figure 5.16 Diagram of impact test specimen with additional anchoring elements placed:
(a) Front isometric view; (b) Back isometric view

When the deck portion of the test specimen was formed, PVC pipes were cast within the deck concrete to create 8 total openings, which pass vertically through the deck. Each of these 8 openings were positioned within the deck to coincide with an ‘anchor point’—a fixture location—on the pendulum foundation. Anchoring was completed by first passing 4 threaded rods—which were fastened to the foundation—through the deck at 4 of the 8 openings. Although 8 openings were included in the design of the test specimen, it was later determined that only 4 of the 8 locations were necessary for the anchoring process. Steel anchoring plates (see Figure 5.16, with holes for a threaded rod to pass through) were then placed on top of the deck with a leveled grout surface and fastened with a threaded nut. Each of the four threaded rods were then post-tensioned—using a loading assembly provided by FDOT—to a 35-kip force. The 35-kip post-tension force (per threaded rod) was selected such that post-tensioning would produce a total 140-kip normal force (acting on the test specimen). Assuming a static coefficient of friction of 0.5, a 70-kip frictional force would then be relied upon to resist the maximum design impact force applied to the specimen—as the primary method for preventing lateral rigid body movement of the test specimen. Photographs taken during the post-tensioning process for one of the threaded rods is shown in Figure 5.17 and Figure 5.18.

Figure 5.17 Post-tensioning fourth (front right) threaded bar for anchoring test specimen to pendulum foundation with the FDOT loading assembly

Figure 5.18 Anchored test specimen

In the unlikely (but possible) event that post-tensioning would not produce adequate friction to resist lateral (rigid body) sliding of the test specimen, an additional (secondary) mechanism was used with the anchoring/installation process. As depicted in Figure 5.16b, behind each end-support buttress at the foundation/deck level, a steel 'slide stopper' was installed. Each slide stopper was designed to transfer a 35-kip lateral force from the deck to the foundation and prevent sliding of the test specimen. As part of the developed anchoring plan, to accommodate possible construction tolerances of the test specimen, a small gap (about 0.5-in.) between each steel slide stopper and test specimen was included. After the test specimen was post-tensioned, and with the slide stoppers installed on the foundation, grout was used to fill the gap between the slide stopper and test specimen (see Figure 5.19), completing the anchoring sequence. With the test specimen anchoring sequence complete, the aluminum loading wedge—which was used to provide a vertical impact surface on the front face of the sloped railing, preventing redirection of the impactor front nose during impact—was adhered to the railing (see Figure 5.20), and the aluminum honeycomb was installed in the impactor nose (see Figure 5.21), completing the installation stage of testing.

Figure 5.19 Placing grout between test specimen and small reaction element (steel slide stopper) as a secondary reaction system to prevent specimen from sliding during impact testing

Figure 5.20 Aluminum loading wedge adhered to front face of railing

Figure 5.21 Pendulum impactor and impact test specimen prepared and ready for testing (with instrumentation in place)

5.2 Instrumentation plan

For each pendulum impact test, a collection of high-speed data acquisition systems were used to record data during testing. Specifically, the following instrumentation components/sensors were used:

- Contact tape switches
- Optical break beams
- Accelerometers
- High-speed cameras
- Laser displacement sensors
- Concrete strain gages
- Rebar strain gages

The overall instrumentation plan for each test specimen (of either R/C or FRC configuration) is depicted in Figure 5.22 and is further detailed in Appendix I. The data acquisition rates were 2000 frames/sec for each high-speed camera and 10 kHz per channel for all other sensors. Sensors positioned on (i.e., attached to) the exterior faces of each test specimen are also depicted in Figure 5.23.

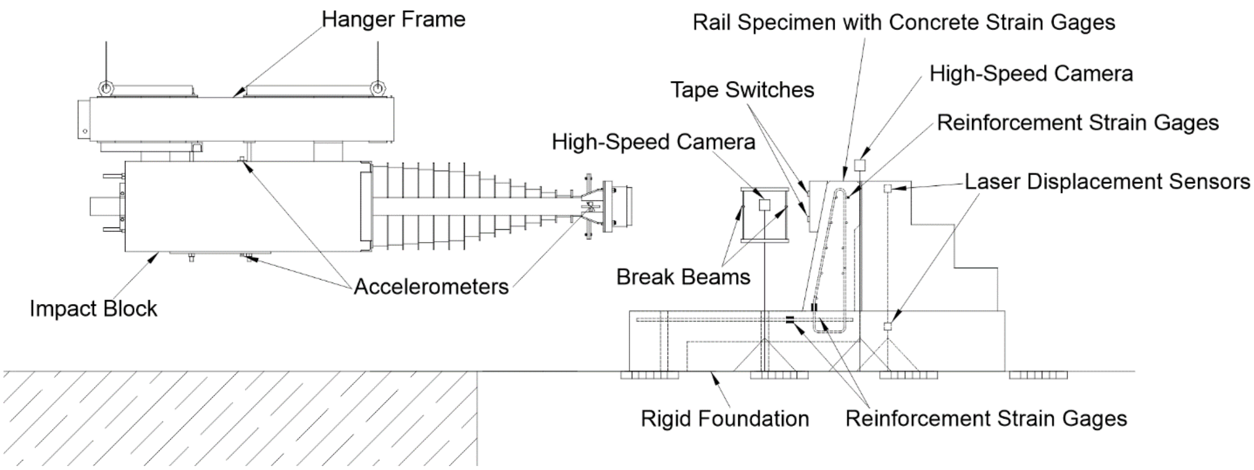

Figure 5.22 Instrumentation plan used in pendulum impact testing

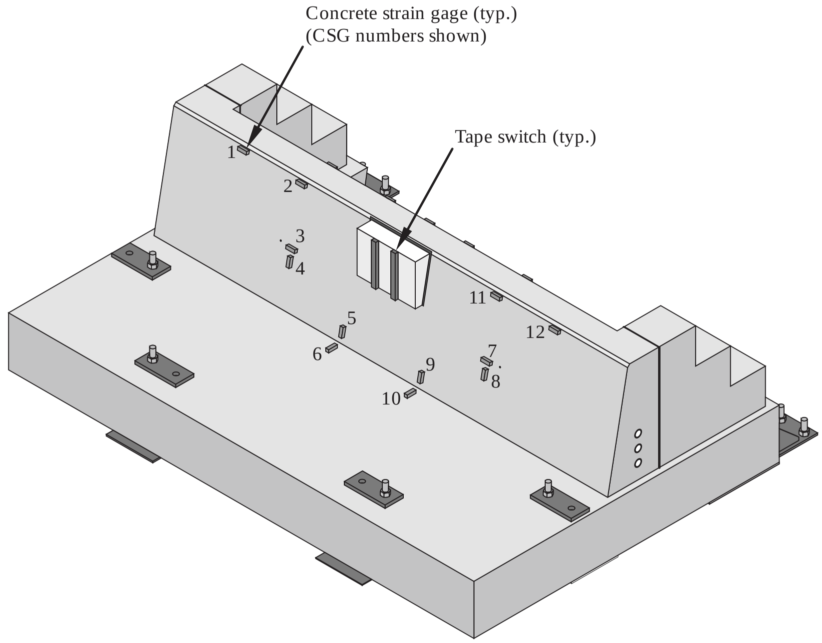

(a)

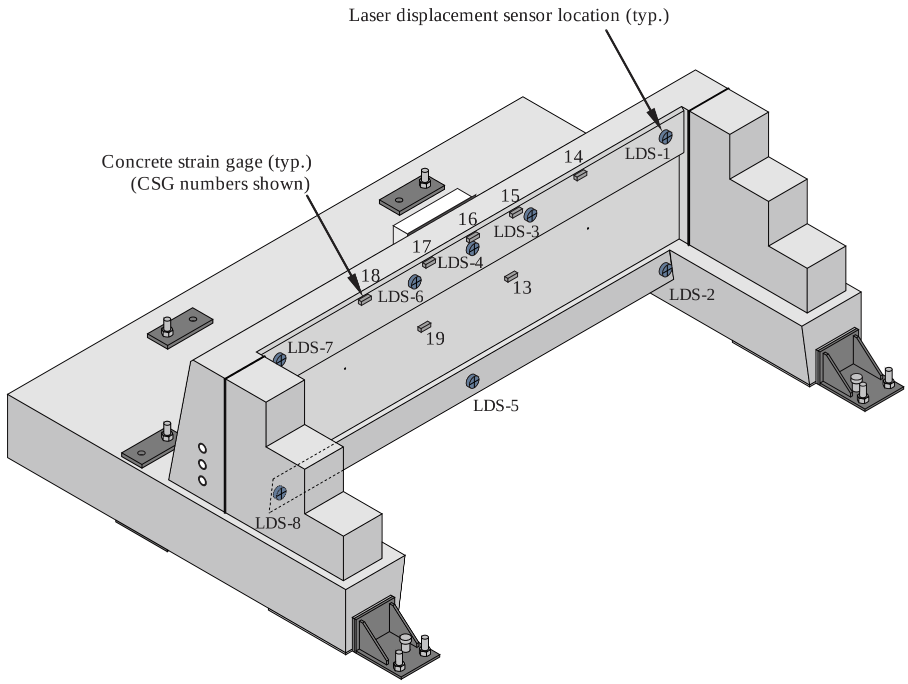

(b)

Figure 5.23 External instrumentation: (a) Front concrete strain gage and tape switch sensor locations; (b) Back concrete strain gage and laser displacement sensor locations

5.2.1 Contact tape switches

Pressure sensitive contact tape switches were installed with each test specimen primarily for detecting the initial time of impact. Specifically, two tape switches were placed on the impact face of the aluminum loading wedge (Figure 5.24). Tape switches are used to detect a change in pressure and are activated when the pendulum impactor comes into contact with the loading wedge (i.e., when depressed, the gage produces a change in voltage reading, signaling the starting time of impact). Although each tape switch activates independently, two tape switches were used with each impact test to ensure that the data acquisition system had been properly triggered. Specification of the 18-in. long disposable tape switches are provided in Table 5.1.

Figure 5.24 Tape switches adhered to the impact face of the aluminum loading wedge

Table 5.1 Specifications for pressure sensitive tape switches

Manufacturer	Tapeswitch Corporation
Ribbon switch type	131-A
Actuation force	60 oz.
Switch lengths used	18 in.
Dimensions	3/4" in. wide, 3/16 in. thick
Minimum bend radius	1 in.

5.2.2 Optical break beams

Infrared optical break beam sensors were used to quantify the impact velocity of each test. An individual break beam sensor set consists of one transmitter and one receiver. As shown in the instrumentation plan (Appendix I), two sets of beak beams were positioned in front of the test specimen at a 12-in. spacing and were mounted on a stand to elevate the sensors to the designated impact height (Figure 5.25). For each break beam set, the transmitter emits an infrared beam and is received by the other receiving end. If the infrared beam is blocked (in this case, when the impactor swings and crosses the path of the beam), a change in current will be produced, causing an increase in recorded voltage data. By placing break beam set 1 ahead of break beam set 2 by 1 ft, the duration of time over which the impactor moved 1 ft (i.e., the velocity) could be quantified just prior to impact (and compared to the target/design impact velocity). Break beam specifications are provided in Table 5.2.

(a)

(b)

Figure 5.25 Optical break beam sensors: (a) Close up of an individual sensor; (b) Break beam sensors positioned for testing

Table 5.2 Specifications for optical break beams

Manufacturer	Balluff
Receiver model	BLS 18KF-NA-1PP-S4-C
Transmitter model	BLS 18KF-XX-1P-S4-L
Range	65 ft

5.2.3 Accelerometers

Accelerometers were used with testing to acquire acceleration data of the impactor. The acceleration data may then be multiplied by the impactor mass to (indirectly) quantify the time-varying impact force that is applied to the test specimen. To capture the acceleration in various locations of the impactor, four triaxial accelerometers were utilized with each test:

- One 25g accelerometer on the top of the impactor block
- One 25g accelerometer on the bottom of the impactor block
- One 400g accelerometer on the front left side of the impactor nose
- One 400g accelerometer on the front right side of the impactor nose

Accelerometer locations are depicted and shown in Figure 5.26 and Figure 5.27. For each accelerometer, a calibration datasheet (provided by the manufacturer) was used for converting voltage readings into acceleration data sets. A summary of accelerometer specifications is provided in Table 5.3.

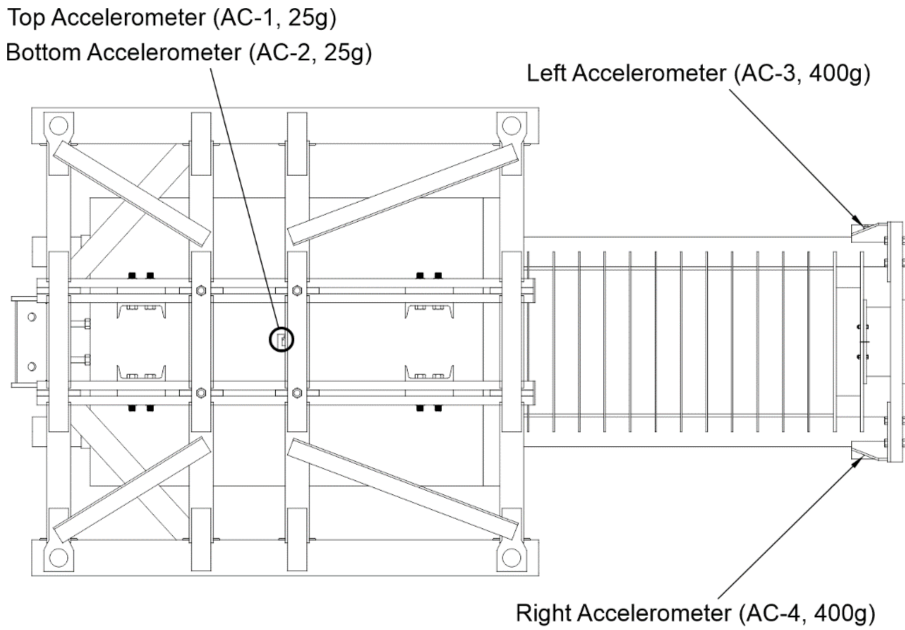

Figure 5.26 Accelerometers installed on pendulum impactor (top view)

(a)

(b)

(c)

(d)

Figure 5.27 Accelerometers installed on the pendulum impactor: (a) AC-1 mounted to the top of the concrete back block; (b) AC-2 mounted to the bottom of the concrete back block; (c) AC-3 mounted to the left mounting plate on the aluminum front nose; (d) AC-4 mounted to the right mounting plate on the aluminum front nose

Table 5.3 Specifications for accelerometers

Manufacturer	Model number	Serial number	Label	Range (g)	Bandwidth (Hz)
Dytran Instruments, Inc	7503D4	11355	AC-1	25	10,000
Dytran Instruments, Inc	7503D4	11356	AC-2	25	10,000
Dytran Instruments, Inc	7503D8	11367	AC-3	400	10,000
Dytran Instruments, Inc	7503D8	11368	AC-4	400	10,000

5.2.4 High speed cameras

High-speed video cameras (shown in Figure 5.28) were used to visually record the impact test at a rate of 2000 frames/sec (Table 5.4). During each impact test, two high-speed cameras were utilized with: (1) one focused on the front impact region of the test (from the side view perspective), recording the crush deformation of the aluminum honeycomb cartridges, and (2) the other focused above the height of the railing (from the side view perspective, looking down the longitudinal direction of the railing), capturing any lateral railing movement. Both cameras were positioned on the same side of the railing.

Figure 5.28 High-speed digital video camera

Table 5.4 Specifications for high-speed cameras

Manufacturer	Integrated Design Tools (IDT)
Distributor	Dynamic Imaging, LLC
Camera model	MotionXtra N-3
Image resolution	1280 x 1024
Frame rate	1000 fps (frames/sec)
Frame rate (plus mode)	2000 fps (frames/sec)
Memory	1.25GB
Maximum recording time	0.76 sec.

5.2.5 Laser displacement sensors

Eight laser displacement sensors positioned behind the test specimen (Figure 5.29) were used to capture lateral displacements (and potentially rigid motion of the specimen) at various locations on the specimen (on the railing and deck elevations). Specifications of the laser displacement sensors are provided in Table 5.5.

Figure 5.29 Laser displacement sensor mounted behind a test specimen

Table 5.5 Specifications for laser displacement sensors

Manufacturer	MTI Instruments
Model	LTS-300-200
Measurement range	7.8 in.
Accuracy	0.03%

5.2.6 Concrete strain gages

Bonded electrical resistance concrete strain gages (Figure 5.30) were used to capture concrete strain levels at select locations on the surface of the specimen. For each test specimen, nineteen strain gages were installed at various locations on the concrete railing and deck. The processed strain data were used to infer the stresses which were compared between tests. Specifications for concrete strain gages are detailed in Table 5.6.

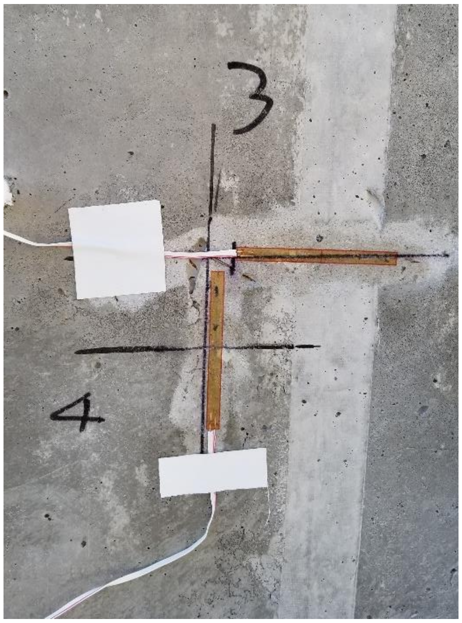

Figure 5.30 Concrete strain gages (3 and 4) adhered to concrete railing surface

Table 5.6 Specifications for concrete strain gages

Manufacturer	Kyowa Electronic Instruments
Model	KC-80-120-A1-11L3M3R
Gage length	80 mm
Gage width	0.6 mm
Strain limit	1.8%

5.2.7 Rebar strain gages

Before the deck or railing portion of the test specimen was cast (i.e., prior to concrete placement), additional bonded electrical resistance strain gages were attached to select steel reinforcing bars (Figure 5.31). Rebar strain gages were used to measure rebar strain and infer rebar stress levels (providing the ability to determine whether or not the reinforcement had yielded). For each test specimen, fifteen electrical rebar strain gages were installed. Specifications for rebar strain gages are detailed in Table 5.7.

Figure 5.31 Strain gage attached to deck reinforcing bar and protected with waterproof tape

Table 5.7 Specifications for rebar strain gages

Manufacturer	Kyowa Electronic Instruments
Model	KFGS-5-120-C1-11L3M3R
Gage length	5 mm
Gage width	1.4 mm
Strain limit	5.0%

CHAPTER 6
FULL-SCALE CENTER OF RAILING (COR) IMPACT TEST RESULTS

6.1 Introduction

As discussed in earlier chapters, a key objective of this study was to experimentally investigate the structural adequacy of the proposed FRC traffic railing. To achieve this objective, a series of pendulum impact tests were conducted on six railing test specimens following the procedures discussed earlier in this report. In this chapter, results from four of the six full-scale railing impact tests are discussed. These four specimens are referred to as ‘center of railing’ (COR) test specimens (two FRC and two R/C). The test specimens were 13-ft long, were supported at each end (using end-support buttresses), and the impact occurred at the centerline of the specimens in the impact direction (i.e., 6.5 ft from either end), as previously discussed (recall Figures 5.1 and 5.16). The remaining two test specimens, which were added to the test matrix after conducting the first full-scale pendulum impact test, are discussed in the following chapter.

Results for the COR impact tests are organized by the two railing types (i.e., FRC and R/C railing) and are followed with a comparison of the four COR test results. A summary of the overall COR test program is provided in Table 6.1. Hardened mechanical properties for the concrete material used to cast and form each pendulum impact test specimen (such as concrete compressive strength) are provided in Appendix E.

Table 6.1 Full-scale COR impact test summary

Impact test specimen	Test date	Drop height (ft)	Impact speed (mph) [ft/sec]	Impact energy (kip-ft)
FRC COR 1	9/02/2020	15	21.3 [31.2]	156.3
FRC COR 2	1/06/2021	15	21.2 [31.1]	155.3
R/C COR 1	10/30/2020	15	21.2 [31.1]	155.3
R/C COR 2	12/09/2020	15	20.5 [30.0]	144.5

6.2 FRC railing

6.2.1 Impact testing of FRC COR specimen 1

On September 2, 2020, full-scale pendulum impact testing for FRC COR test specimen 1 was conducted. The pendulum impactor was dropped from the required 15-ft drop height (Figure 6.1). Because this was the first full-scale pendulum impact test for the present study, this test was used for two purposes: (1) to verify the design of the pendulum impactor and (2) to verify that the FRC railing (with 1% hooked-end steel fiber) was structurally adequate. Although numerical (finite element) predictions indicated that the FRC railing would adequately resist the pendulum impact, it was not certain. Therefore, this first test was only partially instrumented (i.e., instrumentation that would be damaged if the FRC railing failed was not included with this first test). Instrumentation components included with the first FRC test specimen were accelerometers, break beams, high-speed cameras, and tape switches. Details of the instrumentation plan used during impact testing are provided in Appendix I.

Figure 6.1 Impactor pulled back to 15-ft drop height (prior to release)

Sequential images taken from high-speed camera 1 (HSC-1) over the impact duration are provided in Figure 6.2, starting with the first instant of impact and including the point in time when maximum crush depth on the crushable front nose (i.e., maximum impact force) was reached. Additional images from high-speed camera 2 (HSC-2) are provided in Figure 6.3, where no horizontal displacement was observed, indicating that the FRC specimen successfully resisted the designed impact. A photograph of the test specimen after completion of the impact test is shown in Figure 6.4. After completion of the impact test, no damage or cracking was found in the railing or deck concrete.

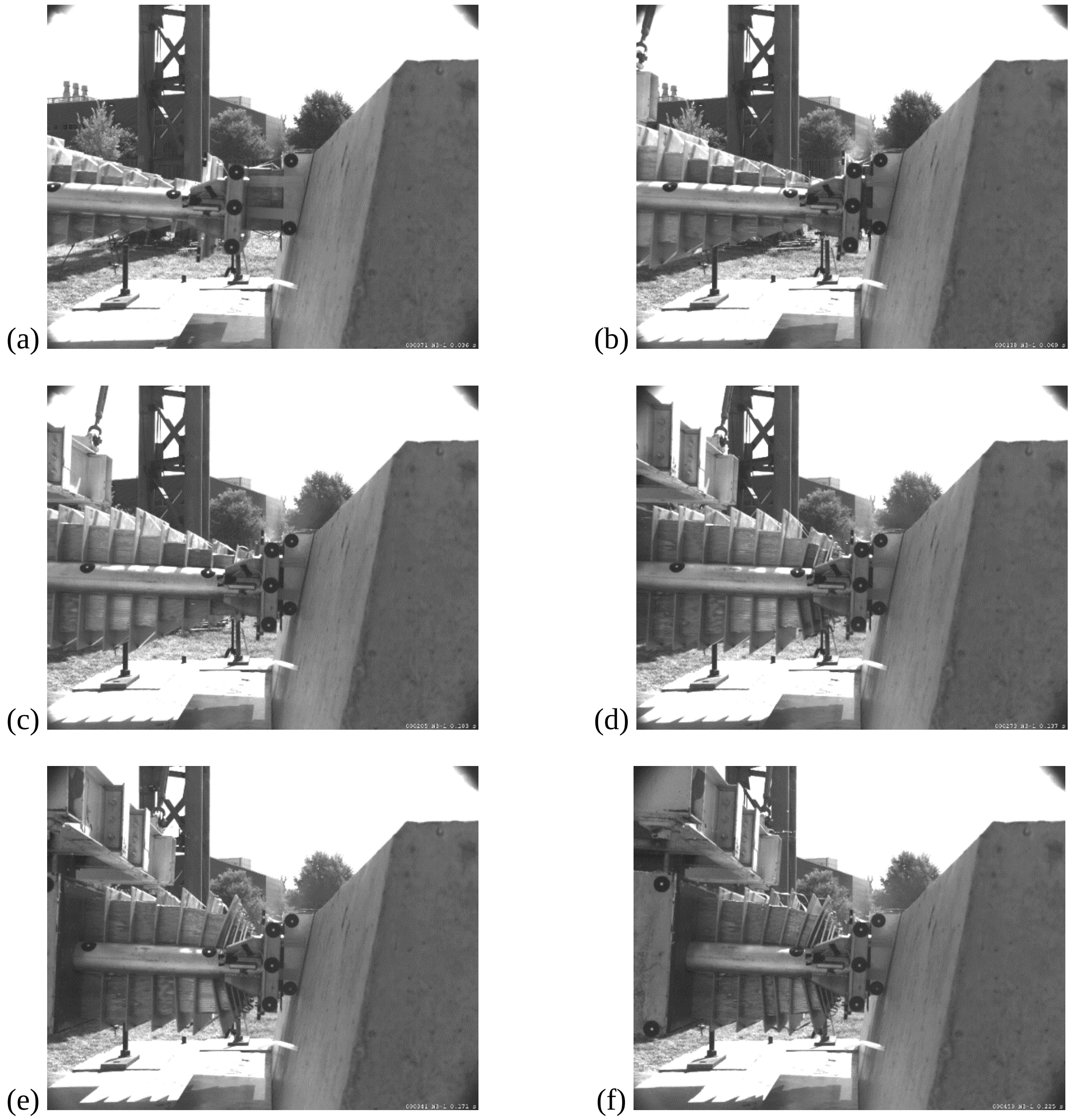

Figure 6.2 High-speed video frames from HSC-1 (FRC COR test 1) showing crush deformation of aluminum honeycomb: (a) At initial impact; (b) – (e) Intermediate frames; (f) At peak impact force

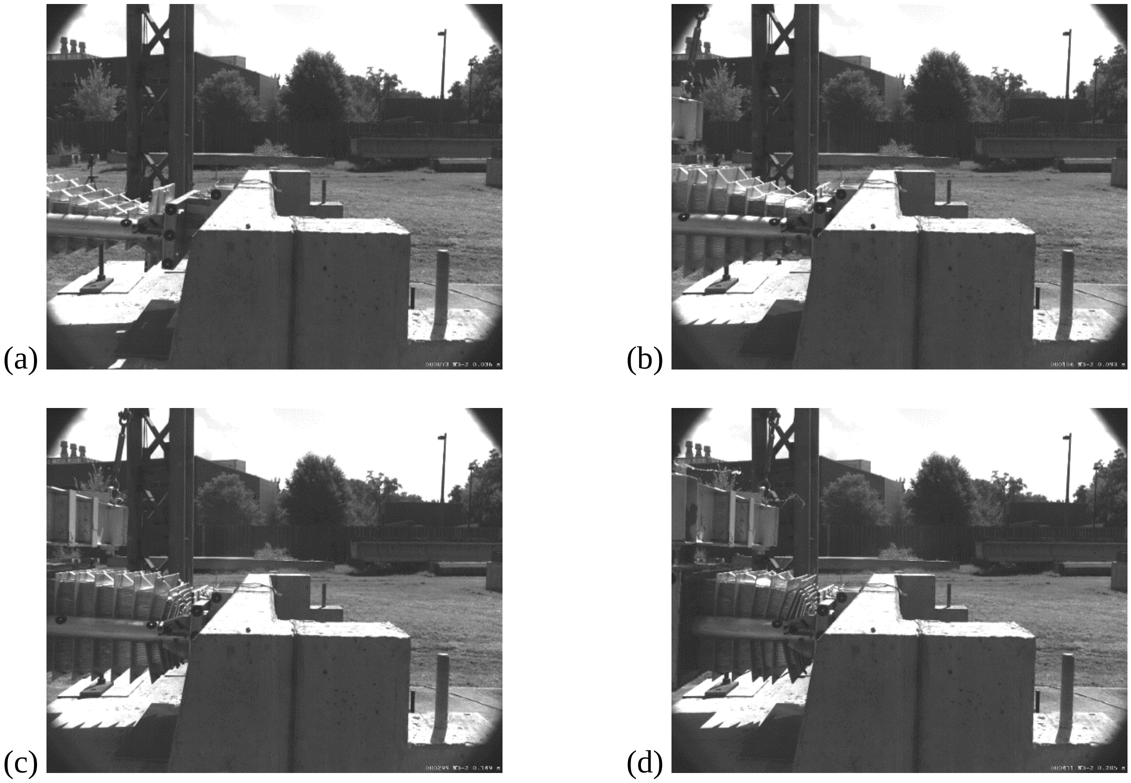

Figure 6.3 High-speed video frames from HSC-2 (FRC COR test 1): (a) At start of impact; (b) – (c) Intermediate frames; (d) At peak impact force

Figure 6.4 FRC COR test 1 specimen after completion of impact test

Break beam voltage data from FRC impact test 1 are provided in Figure 6.5, and were used to quantify the impact velocity. As shown in the instrumentation plan (Appendix I), two sets of break beams were placed in front of the impact test specimen at a 1-ft spacing. For each break beam, after the impactor was released and when the impactor crossed the path of the sensor, a change in voltage was observed. Since break beam 1 was placed 1 ft ahead of break beam 2, the duration of time over which the impactor moved 1 ft was quantified just prior to impact. For FRC test 1, the impact velocity was determined to be 31.2 ft/sec—compared to the design impact velocity of 31.1 ft/sec (a 0.3% difference). Tape switch data were used to determine the time at which the impact began and are shown in Figure 6.6. Note that all impact test data has been shifted such that the initiation of impact begins at 0.1 s (using the spike in tape switch voltage).

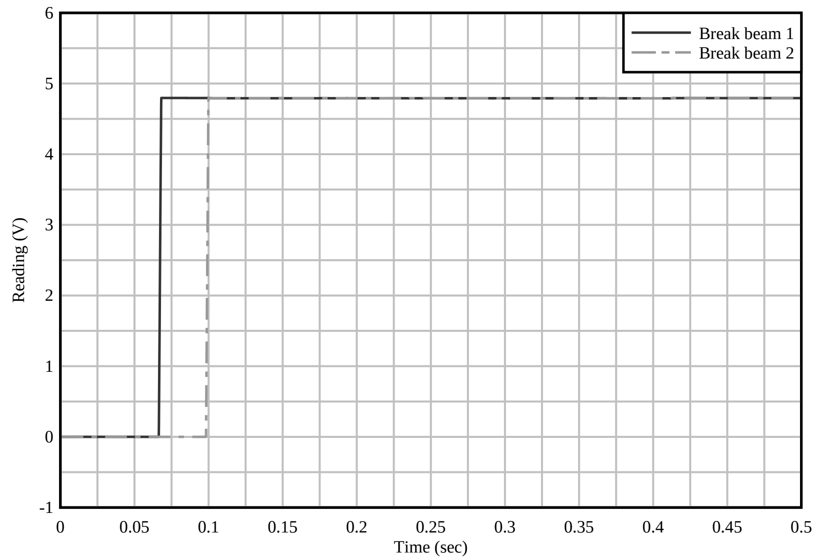

Figure 6.5 Break beam data for FRC COR test 1

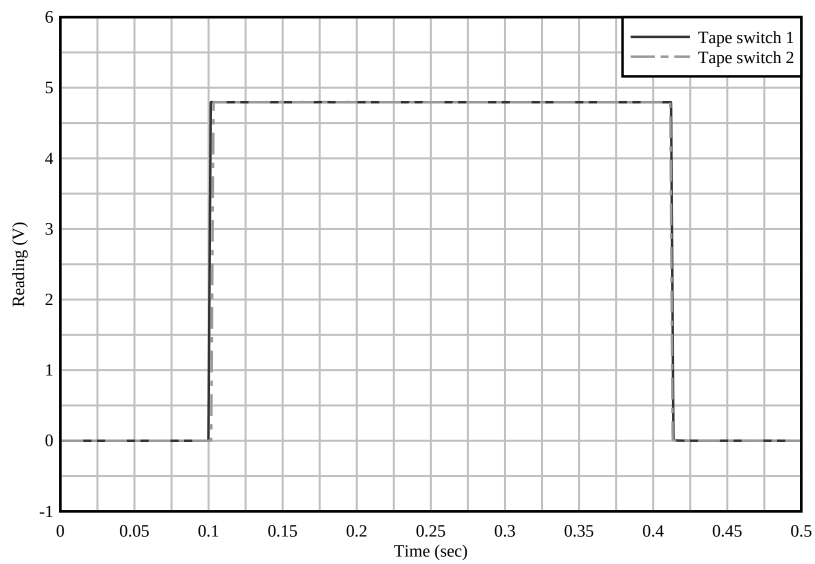

Figure 6.6 Tape switch data for FRC COR test 1

Measured accelerations from the two accelerometers on the concrete back block (AC-1 & AC-2) in the impact direction (i.e., local Y direction of the accelerometer) are shown in Figure 6.7. Correspondingly, measured accelerations from the two accelerometers on the aluminum front nose (AC-3 & AC-4) in the impact direction (local Y direction) are shown in Figure 6.8. As expected, acceleration values are negative because of the impactor deceleration during impact. Furthermore, a more gradual deceleration of the back block is clearly shown in the AC-1 and AC-2 data when compared with the more instantaneous impact that occurred with the front nose (as expected), producing more fluctuations in AC-3 and AC-4 data.

Accelerations were then multiplied by mass to quantify the impact forces that were applied to the standard FRC railing. Specifically, back block accelerations (AC-1 & AC-2) were multiplied by the 9850-lb back block mass (composed of the steel hanger frame and concrete block), while the front nose accelerations (AC-3 & AC-4) were multiplied by the 350-lb front nose mass (composed of the aluminum front nose components). The two back block forces (from AC-1 & AC-2) were then averaged and are shown in Figure 6.9, while the two front nose forces (from AC-3 & AC-4) were averaged and are shown in Figure 6.10.

The total applied impact force was then computed by combining the two averages from the back block and front nose, which is shown in Figure 6.11. In comparison with the designed/predicted maximum impact forces (shown in Figure 6.12, which provides the predicted impact force over time from previous FEA impact simulations), the maximum observed impact force from FRC test 1 was found to be 72.8 kip (5.8% greater than the originally designed 68.8-kip peak impact force, recall Figure 4.5 and Table 4.2).

General conclusions from this first test were: (1) that the pendulum impactor successfully delivered the designed force-time curve (as shown by the similarities of the two curves provided in Figure 6.12), and (2) that the developed FRC railing was structurally adequate to resist the designed pendulum impact condition (as indicated by the lack of damage to the test specimen and by the small railing deflection [<0.1 in.] estimated from the high-speed video). Because of these successful results, the subsequent testing included additional instrumentation (e.g., strain gages and laser displacement sensors).

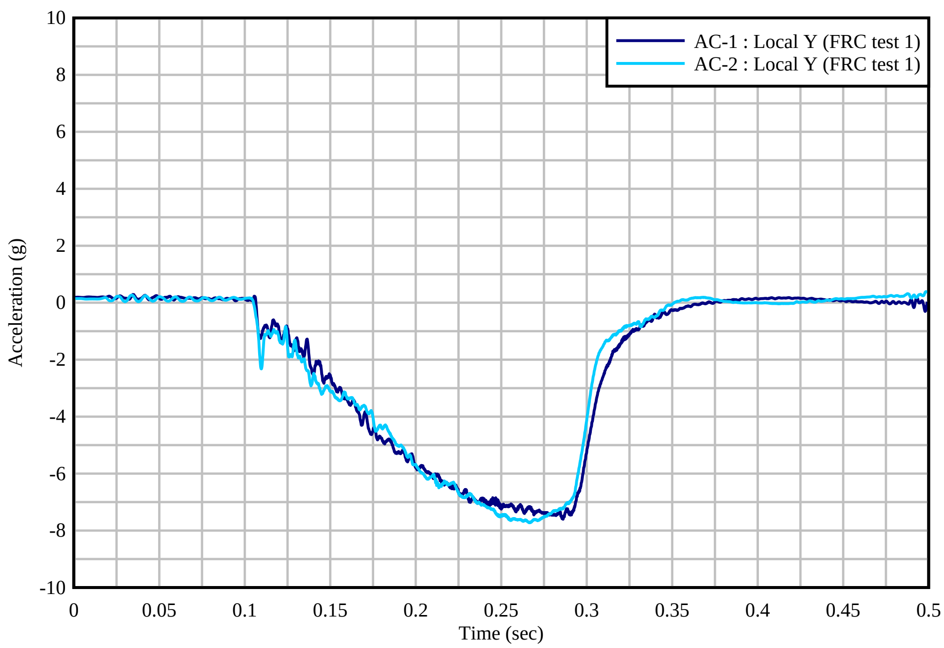

Figure 6.7 Raw concrete back block acceleration data (AC-1 & AC-2) for FRC COR test 1 (in the impact direction, local Y direction of accelerometer)

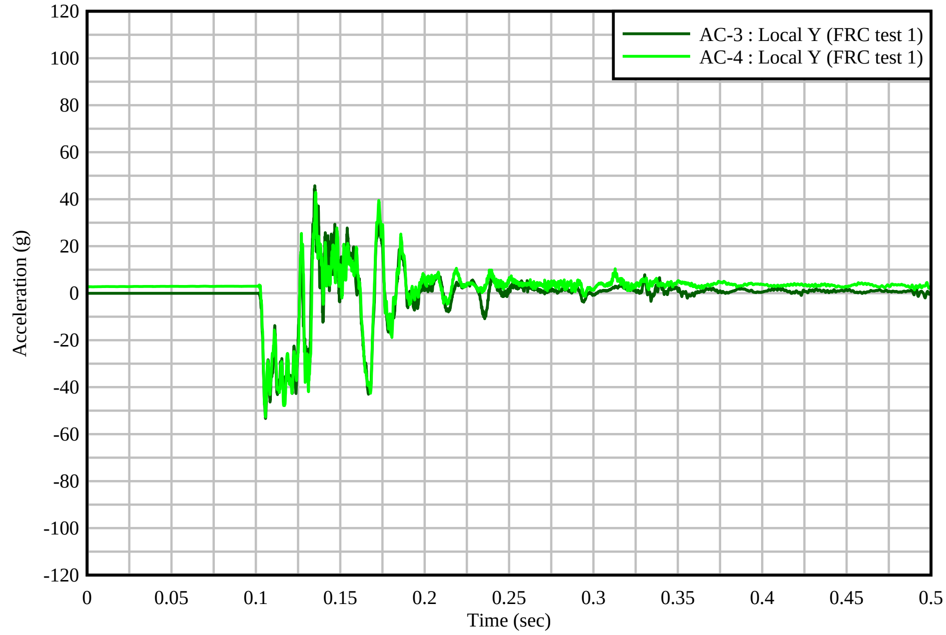

Figure 6.8 Raw front nose acceleration data (AC-3 & AC-4) for FRC COR test 1 (in the impact direction, local Y direction of accelerometer)

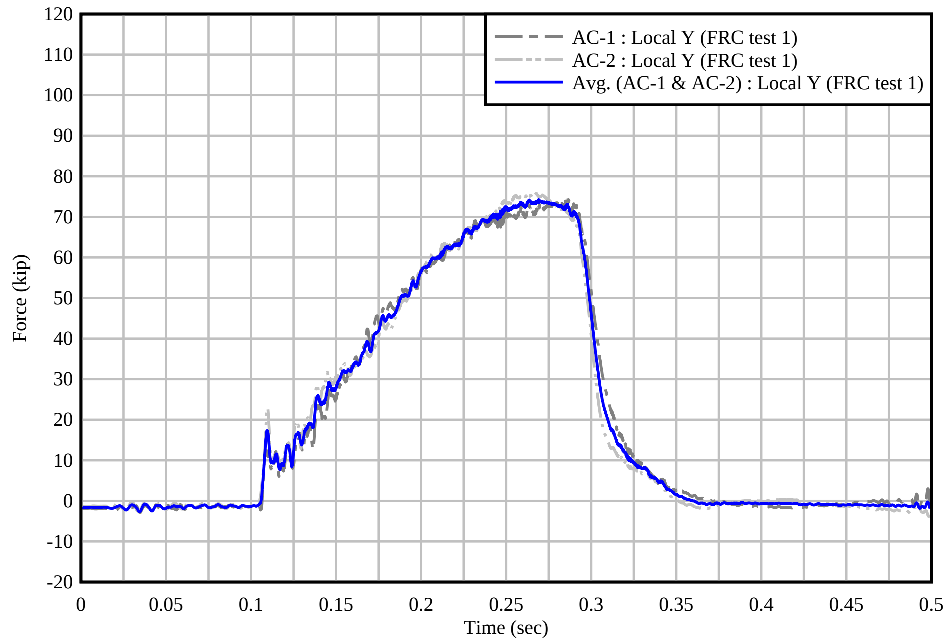

Figure 6.9 Computed impact forces from back block for FRC COR test 1

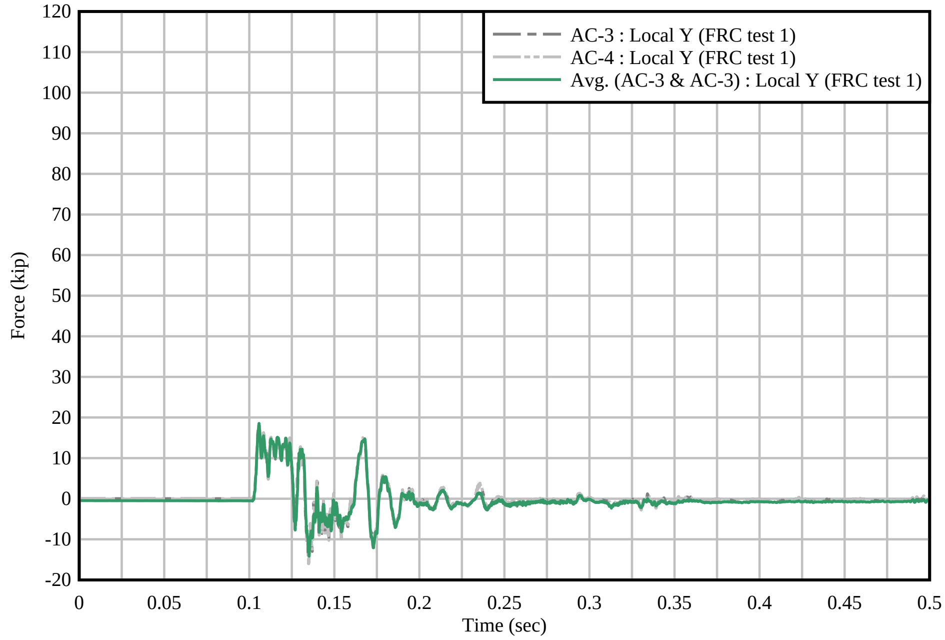

Figure 6.10 Computed impact forces from front nose for FRC COR test 1

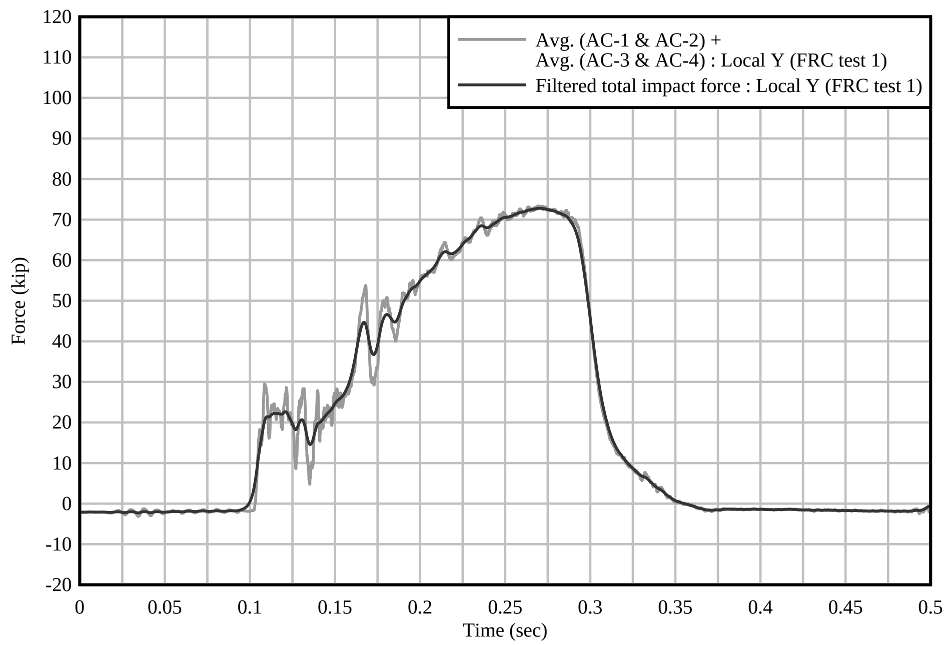

Figure 6.11 Raw and filtered total computed impact force for FRC COR test 1

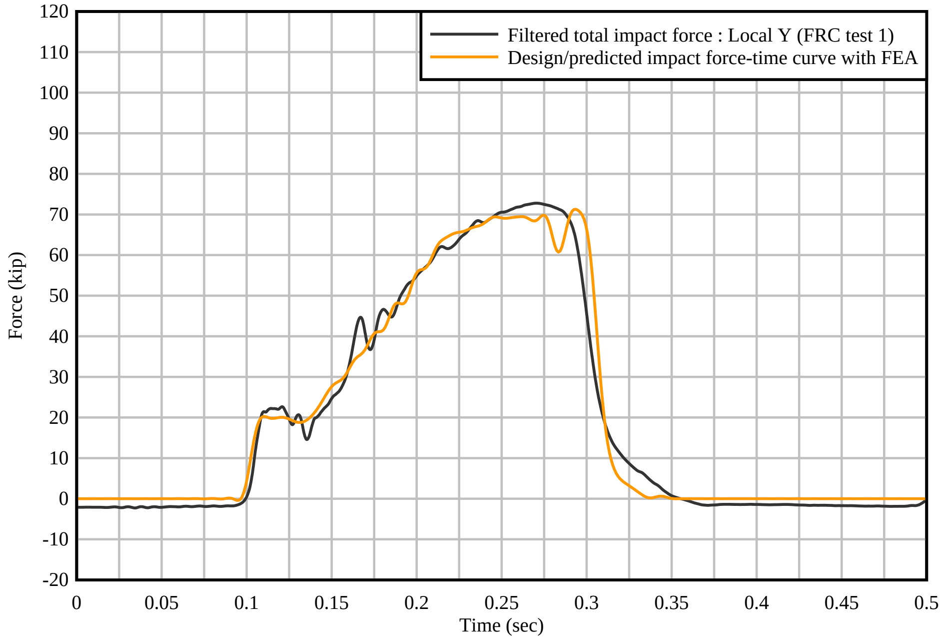

Figure 6.12 Filtered total experimental impact force for FRC COR test 1 compared to FEA prediction

6.2.2 Impact testing of FRC COR specimen 2

On January 6, 2021, full-scale pendulum impact testing for FRC COR test specimen 2 was conducted—where the pendulum impactor was dropped from 15 ft. Instrumentation components included with the second FRC test specimen were accelerometers, break beams, high-speed cameras, tape switches, laser displacement sensors, internal reinforcement strain gages, and external concrete strain gages. Additional details of the instrumentation plan used during impact testing are provided in Appendix I.

Sequential images taken from high-speed camera 1 (HSC-1) over the impact duration are provided in Figure 6.13, starting with the first instant of impact and including the point in time when the maximum crush depth on the crushable front nose (i.e., maximum impact force) was reached. Additional images from high-speed camera 2 (HSC-2) are provided in Figure 6.14, where no discernable sliding of the test specimen was observed. A photograph of the test specimen after completion of the impact test is shown in Figure 6.15. No damage or cracking was found in the railing or deck concrete after completion of the test.

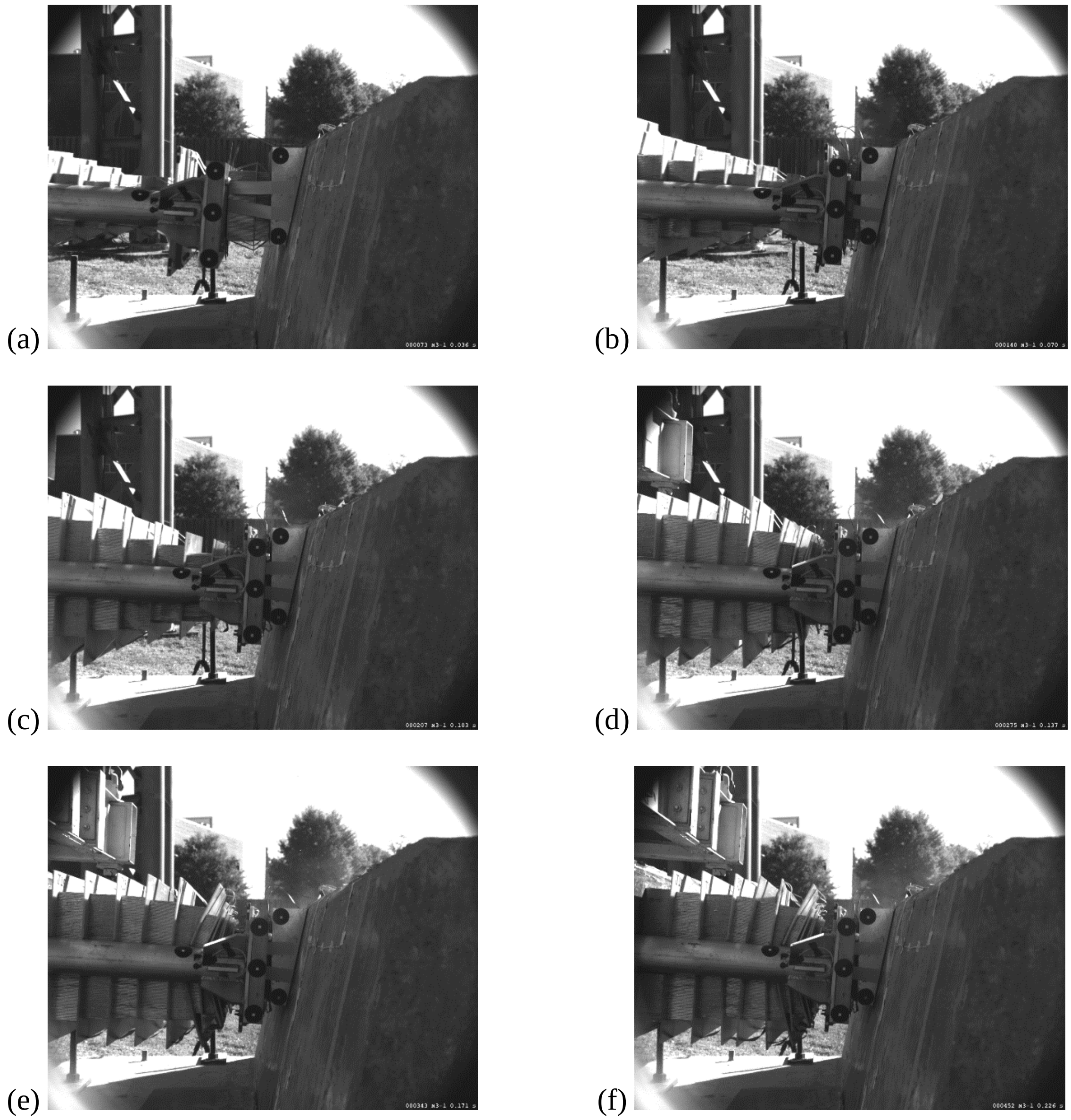

Figure 6.13 High-speed video frames from HSC-1 (FRC COR test 2) showing crush deformation of aluminum honeycomb: (a) At initial impact; (b) – (e) Intermediate frames; (f) At peak impact force

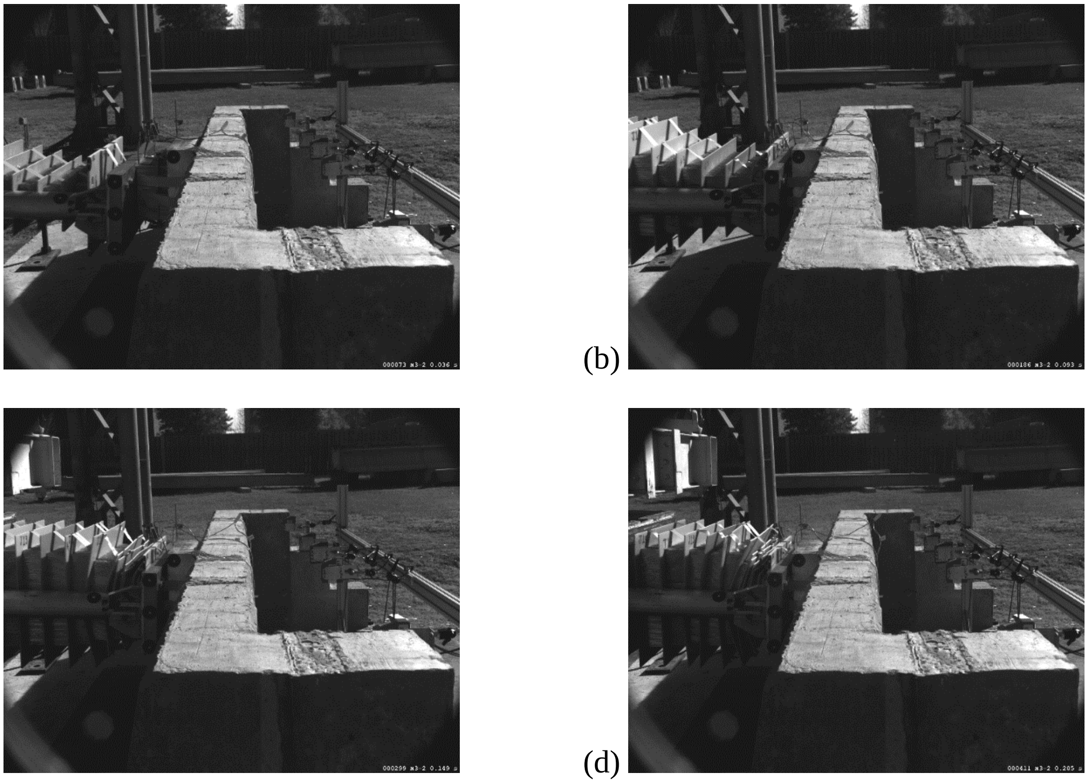

Figure 6.14 High-speed video frames from HSC-2 (FRC COR test 2): (a) At start of impact; (b) – (c) Intermediate frames; (d) At peak impact force

Figure 6.15 FRC COR test 2 specimen after completion of impact test

Break beam voltage data from FRC impact test 2 are provided in Figure 6.16, and were used to quantify the impact velocity. For FRC test 2, the impact velocity was determined to be 31.06 ft/sec—compared to the design impact velocity of 31.1 ft/sec (a 0.1% difference). Tape switch data are shown in Figure 6.17. Note that all impact test data has been shifted such that the initiation of impact begins at 0.1 s (using the spike in tape switch voltage).

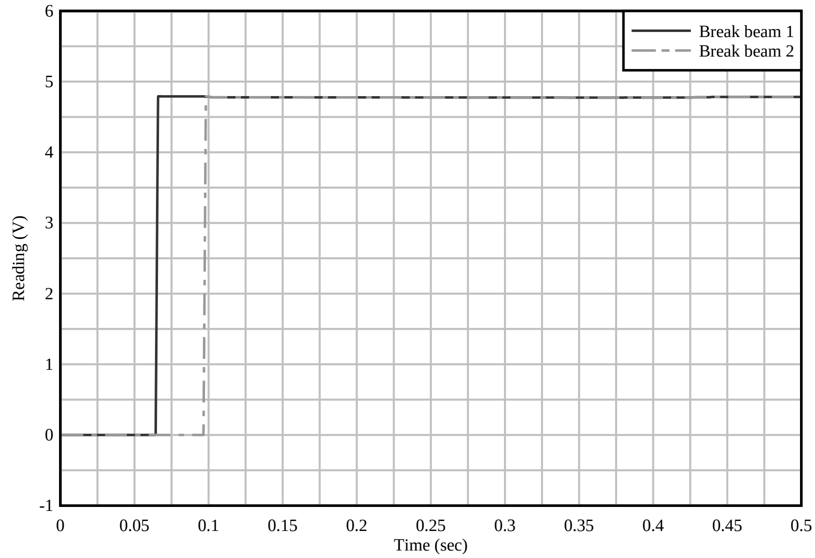

Figure 6.16 Break beam data for FRC COR test 2

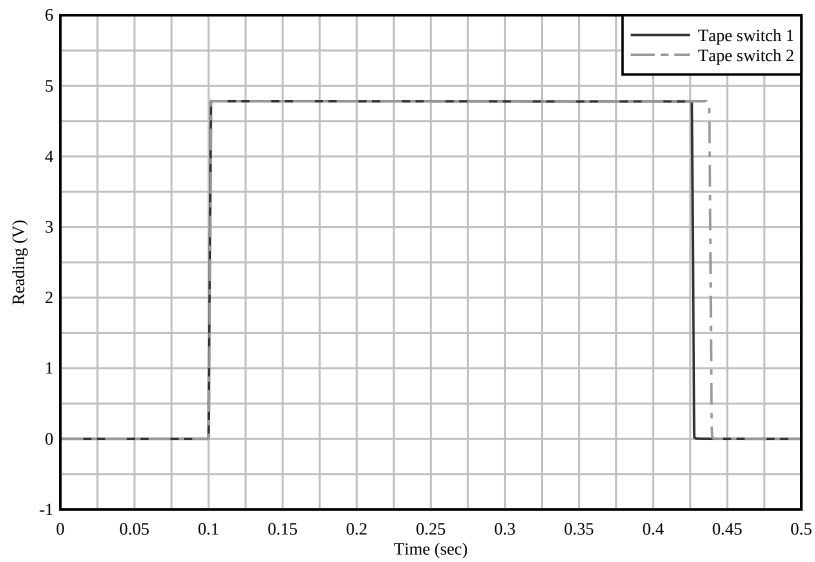

Figure 6.17 Tape switch data for FRC COR test 2

Measured accelerations from the two accelerometers on the concrete back block (AC-1 & AC-2) in the impact direction (i.e., local Y direction of the accelerometer) are shown in Figure 6.18. Correspondingly, measured accelerations from the two accelerometers on the aluminum front nose (AC-3 & AC-4) in the impact direction (local Y direction) are shown in Figure 6.19. Computed and averaged back block impact forces (from AC-1 & AC-2) are shown in Figure 6.20, while the computed and averaged front nose impact forces (from AC-3 & AC-4) are shown in Figure 6.21.

The total applied impact force (computed by combining the averages of the back block and front nose) is shown in Figure 6.22. In comparison with the designed/predicted maximum impact forces (shown in Figure 6.23, which provides the predicted impact force over time from previous FEA impact simulations), the maximum observed impact force from FRC test 2 was found to be 72.6 kip (5.5% greater than the originally designed 68.8-kip peak impact force).

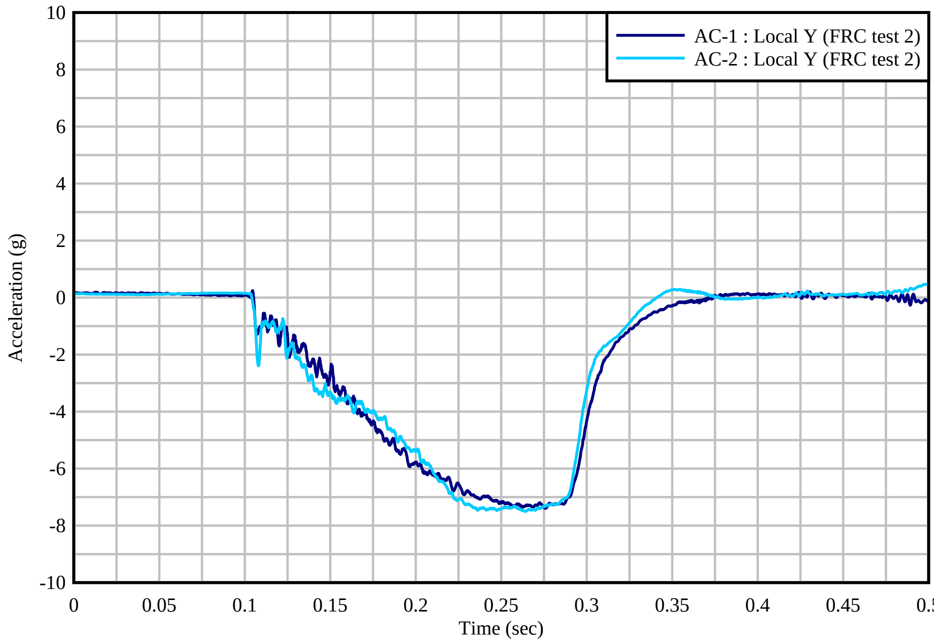

Figure 6.18 Raw concrete back block acceleration data (AC-1 & AC-2) for FRC COR test 2
(in the impact direction, local Y direction of accelerometer)

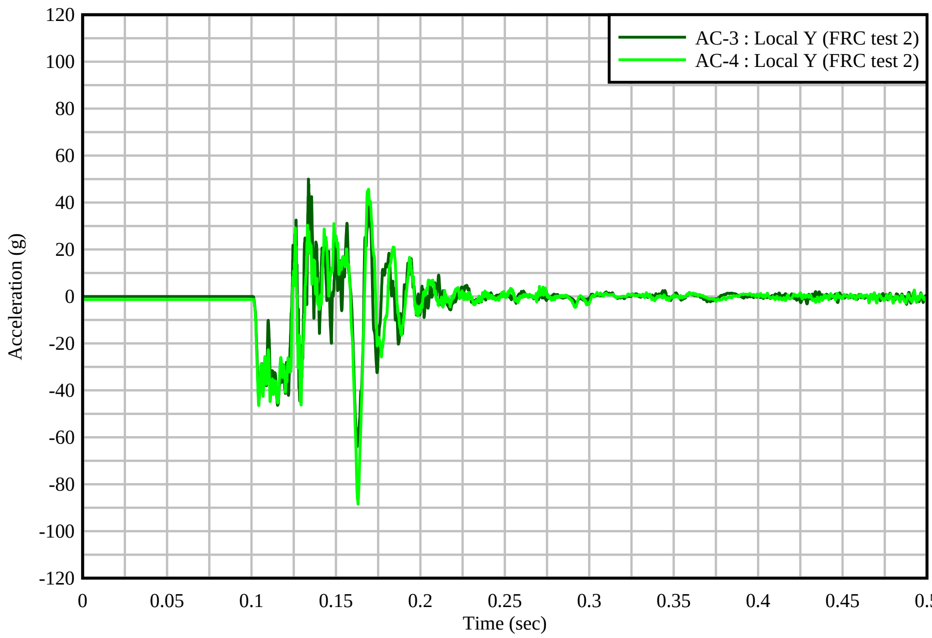

Figure 6.19 Raw front nose acceleration data (AC-3 & AC-4) for FRC COR test 2
(in the impact direction, local Y direction of accelerometer)

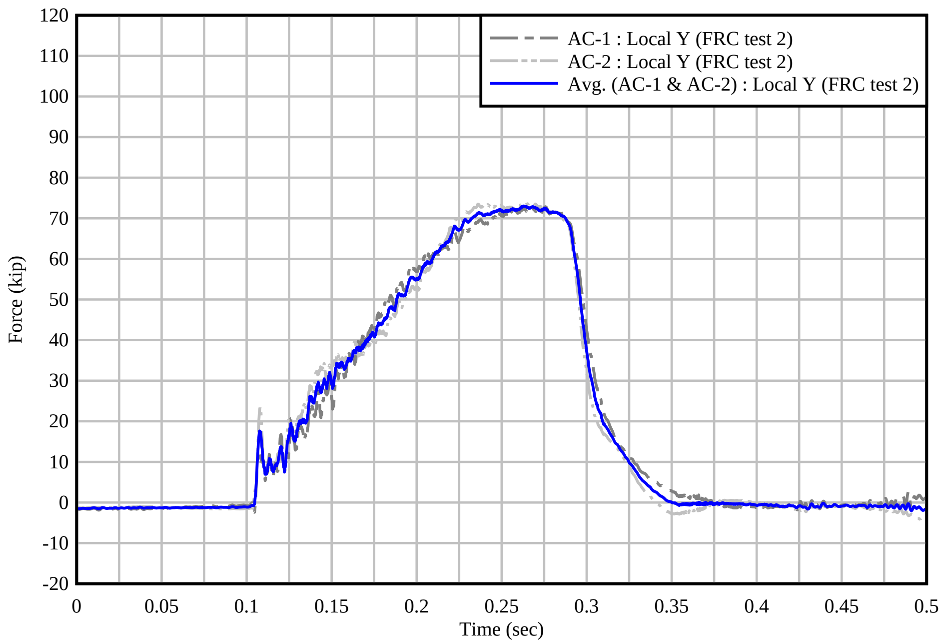

Figure 6.20 Computed impact forces from back block for FRC COR test 2

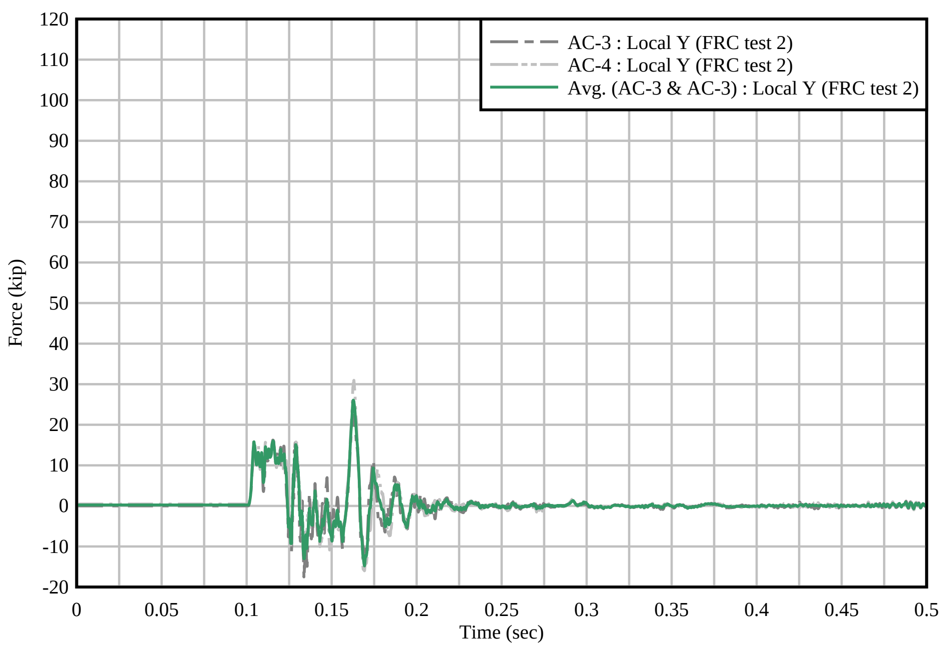

Figure 6.21 Computed impact forces from front nose for FRC COR test 2

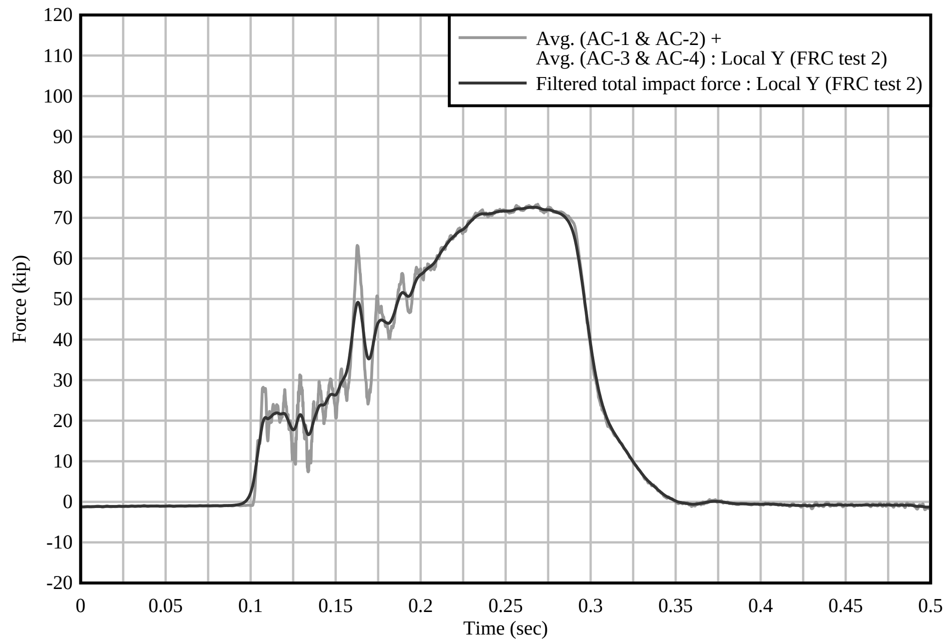

Figure 6.22 Raw and filtered total computed impact force for FRC COR test 2

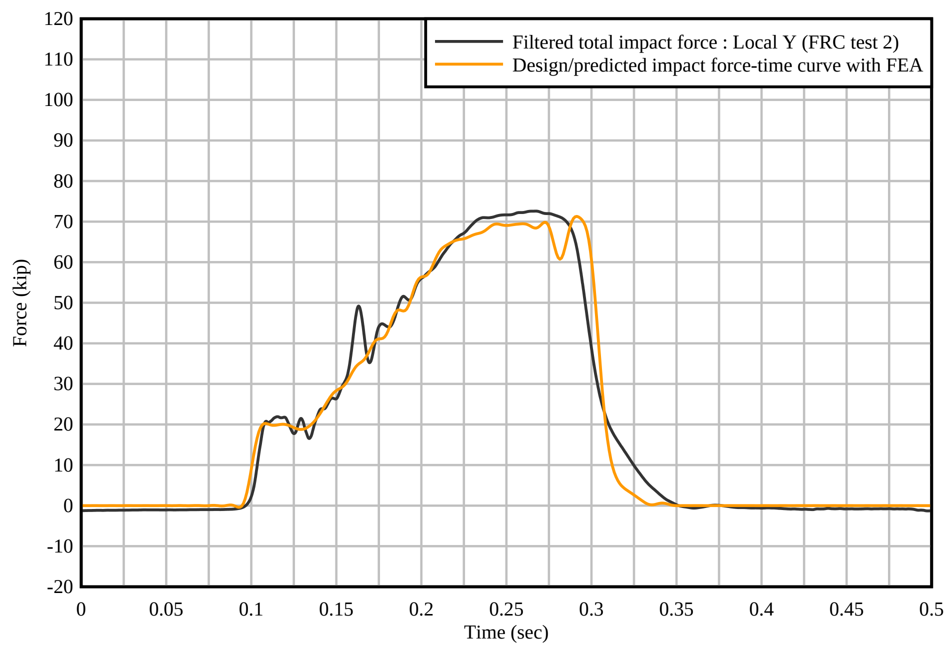

Figure 6.23 Filtered total experimental impact force for FRC COR test 2 compared to FEA prediction

During the second FRC COR impact test, lateral deflections of the railing and any rigid sliding of the test specimen that occurred were captured with laser displacement sensors positioned behind the specimen. Further, external concrete strain measurements in the railing and deck were taken at locations along the front and back faces of the specimen. Specific locations of the laser displacement sensors (LDS) and external concrete strain gages (CSG) are depicted in Figure 5.23 (and further detailed in Appendix I).

Laser displacement data captured during FRC test 2 are provided in Figure 6.24, where it is shown that the maximum displacement occurred at the center of the railing (LDS-4) with a magnitude of 0.049 in., near the time at which the peak impact force was reached. After completion of the impact, the measured displacements effectively reduced to zero, indicating that no sliding occurred and that there was no permanent deformation of the railing.

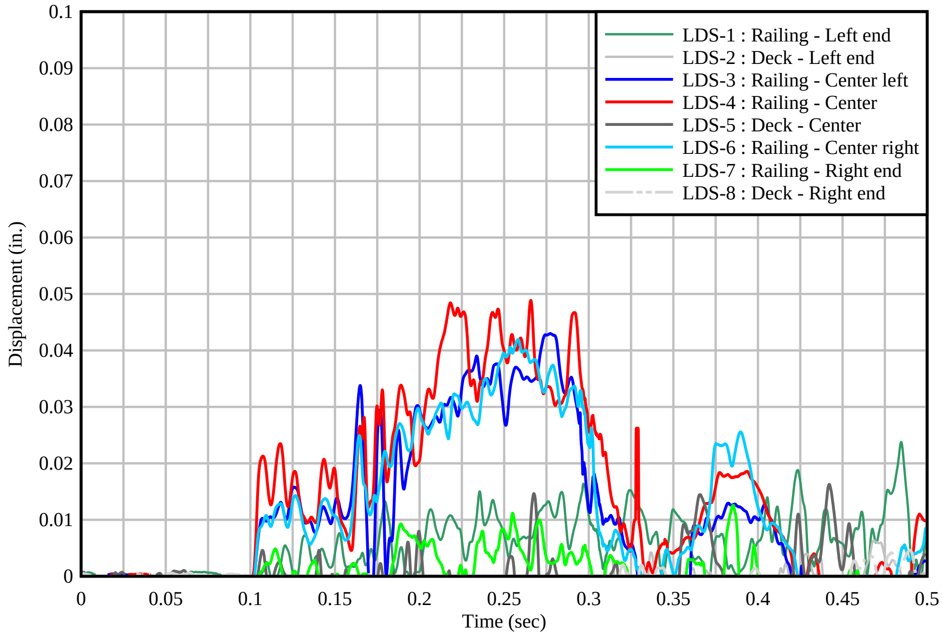

Figure 6.24 Laser displacement sensor data from FRC test 2

External strain gage readings for the top front face of the railing are provided in Figure 6.25. Strain readings for the bottom (i.e., lower half and toe) of the railing front face are provided in Figure 6.26 and Figure 6.27, and readings for the back face of the railing are provided in Figure 6.28. Although some strain levels exceeded the approximate rupture strain for 3400-psi strength concrete, no cracking was found in the railing or deck after visual inspection.

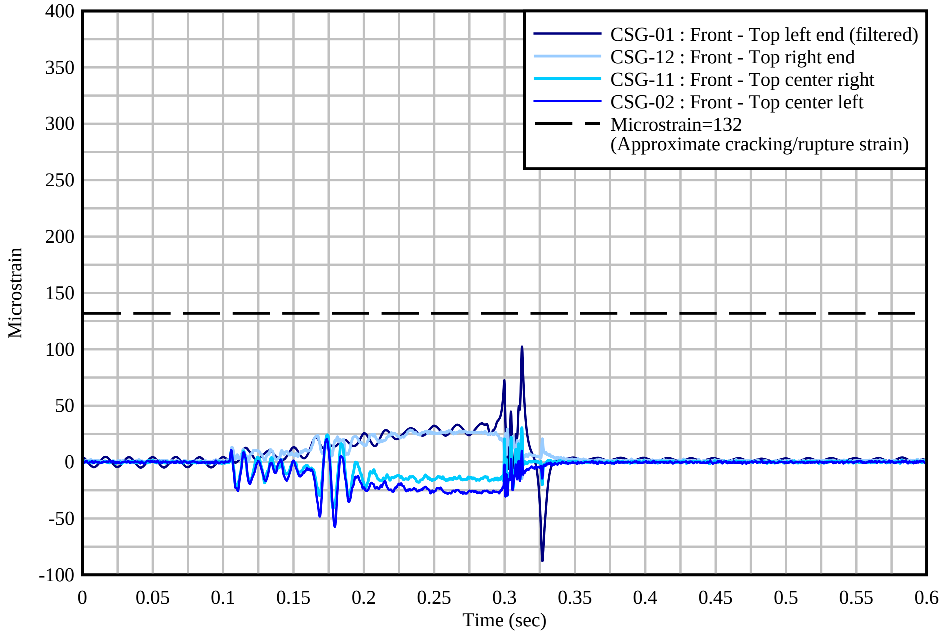

Figure 6.25 External concrete strain gage data for locations on the top front face of the railing during FRC COR test 2

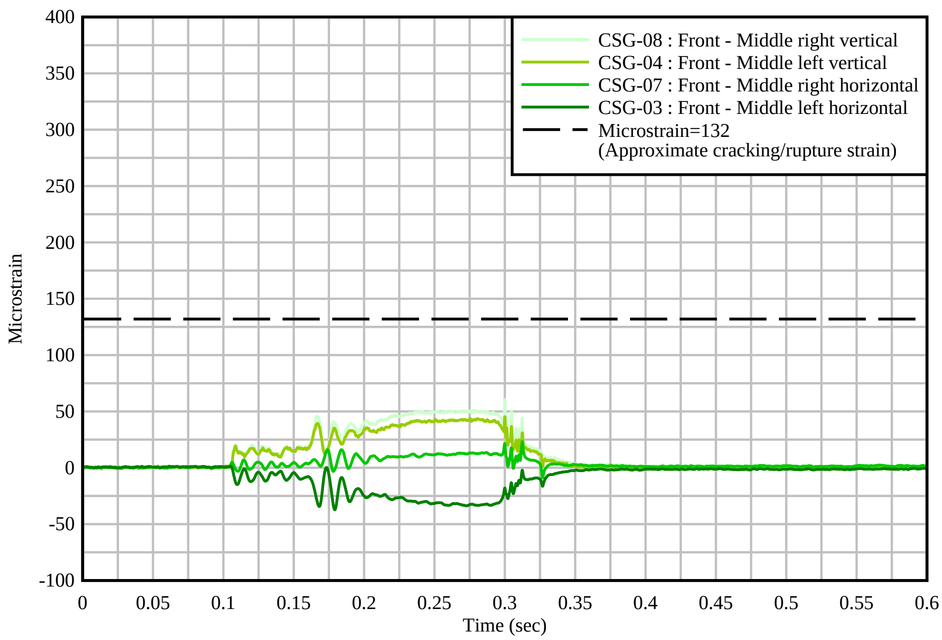

Figure 6.26 External concrete strain gage data for locations on the lower front face of the railing during FRC COR test 2

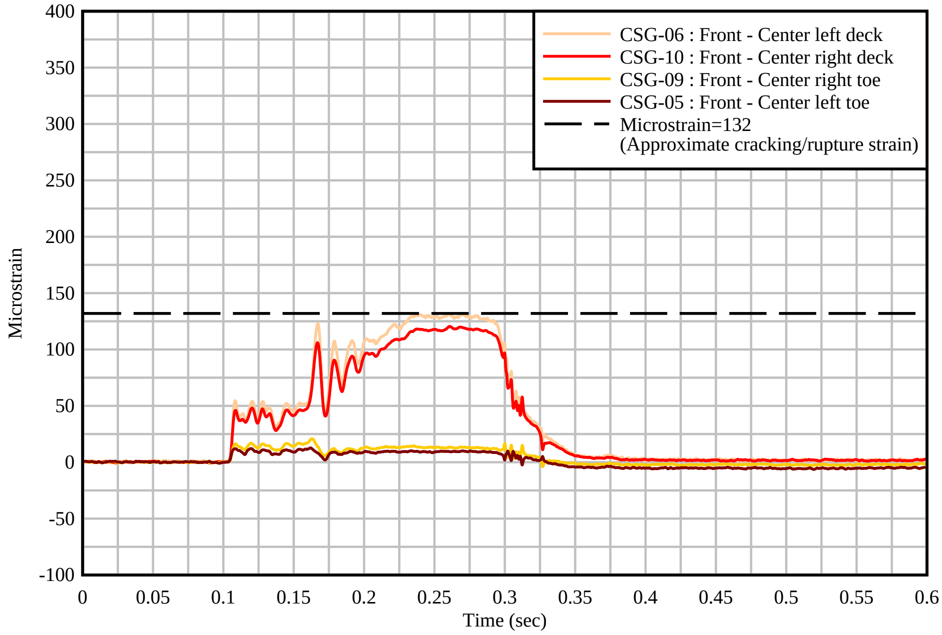

Figure 6.27 External concrete strain gage data for locations at the toe of the railing and deck during FRC COR test 2

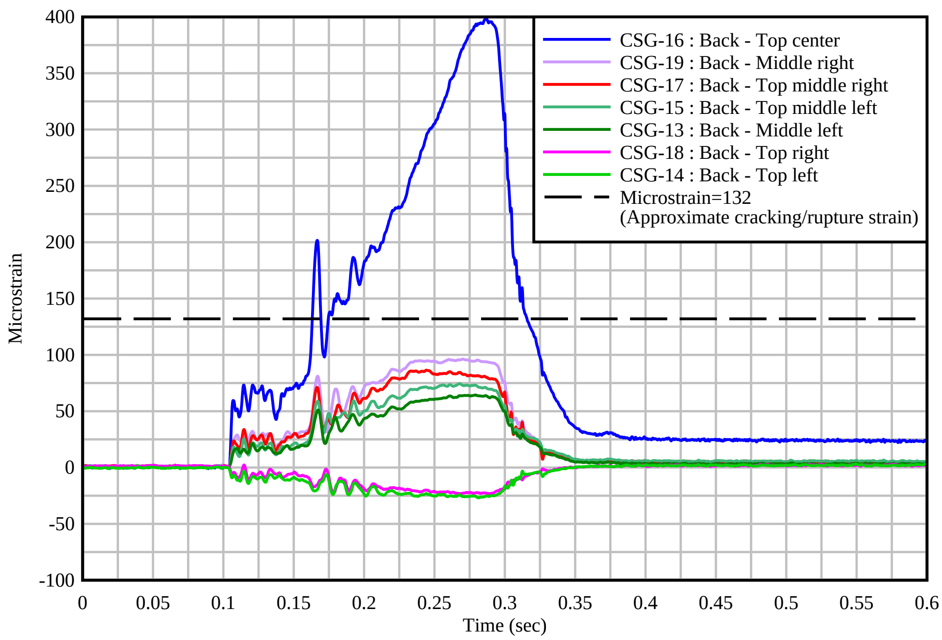

Figure 6.28 External concrete strain gage data for locations on the back face of the railing during FRC COR test 2

Readings from rebar strain gages are provided in Figure 6.29. Note that one rebar strain gage (RSG-7) reading is not included because the gage was damaged during the casting process and did not provide data during testing. Specific locations of the deck and connection (4V) rebar gages are provided in Appendix I. Maximum strain levels in the deck and railing steel reinforcement are well below yielding strain (2000 microstrain) indicating that the test specimen successfully resisted the pendulum impact. However, rebar strain values did not return to zero, indicating that some permanent strain in the reinforcement may have occurred. None the less, the specimen successfully resisted the impact with minimal damage.

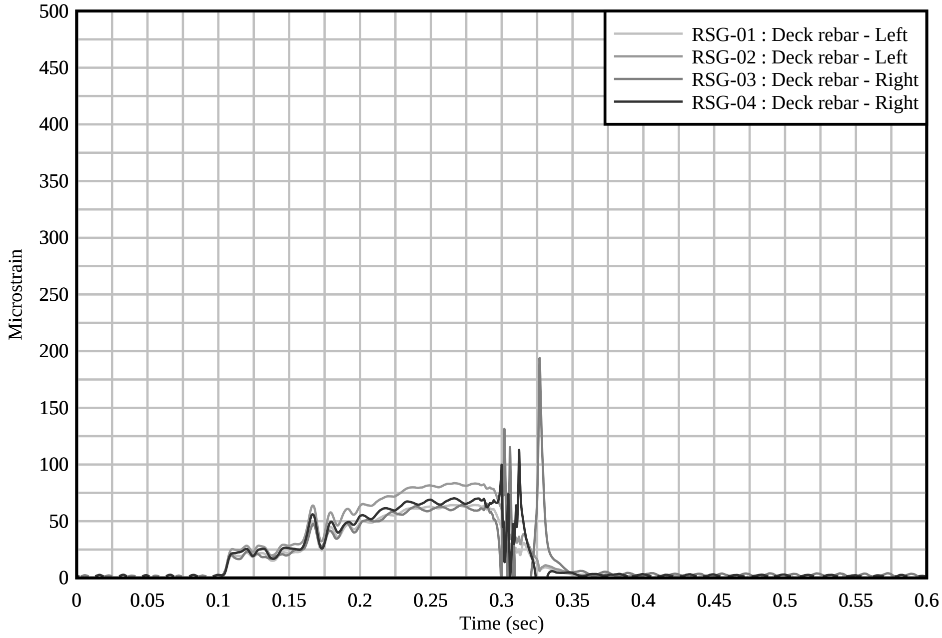

(a)

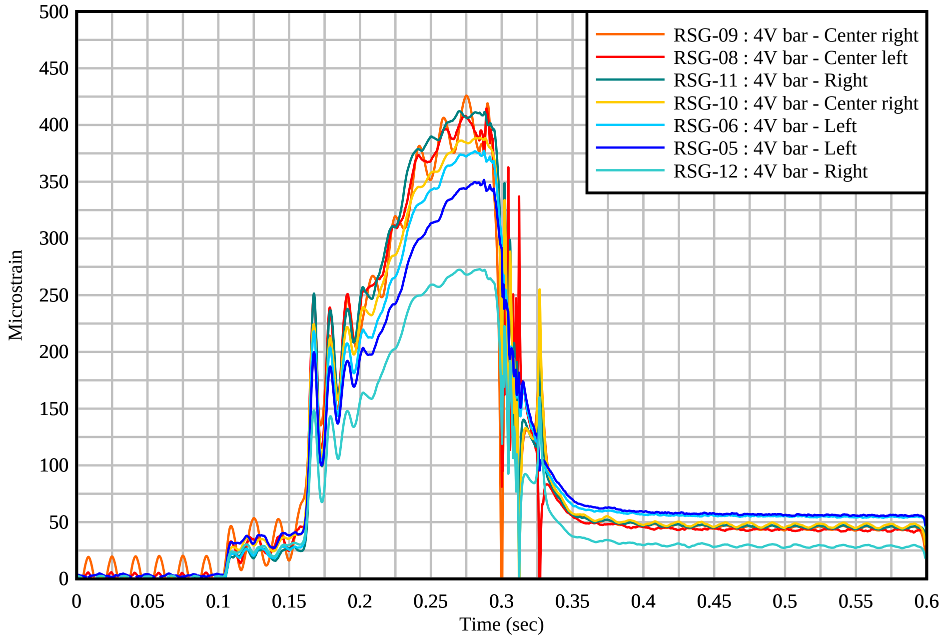

(b)

Figure 6.29 Internal rebar strain gage data during FRC COR test 2:
(a) Deck rebar; (b) Railing rebar

6.3 Standard (R/C) railing

6.3.1 Impact testing of R/C COR specimen 1

On October 30, 2020, full-scale pendulum impact testing for R/C COR test specimen 1 was conducted. The pendulum impactor was dropped from the required 15-ft drop height (Figure 6.30). Instrumentation components included with the first R/C COR test specimen were accelerometers, break beams, high-speed cameras, tape switches, laser displacement sensors, internal reinforcement strain gages, and external concrete strain gages. Additional details of the instrumentation plan used during impact testing are provided in Appendix I.

Figure 6.30 Impactor pulled back to 15-ft drop height (prior to release)

Sequential images taken from high-speed camera 1 (HSC-1) over the impact duration are provided in Figure 6.31, starting with the first instant of impact and including the point in time when maximum crush depth on the crushable front nose (i.e., maximum impact force) was reached. As shown in Figure 6.31e – 6.31h, about halfway through the impact, the adhesive used to hold the aluminum loading wedge in place on the face of the railing failed. As a result, the latter half of the impact occurred without the adhesive holding the wedge in position, allowing the wedge to slide up the surface of the railing as the impact continued. Once the total kinetic energy of the impactor was delivered to the test specimen, the remaining upwards momentum of the loading wedge caused the wedge to continue to slide up the face of the railing, eventually losing contact with the impactor and railing. Although the wedge sliding up the face of the railing was not preferable (and was not anticipated), the maximum design impact force—based on acceleration data (discussed later)—was still achieved, indicating that the test was a success.

Additional images from high-speed camera 2 (HSC-2) are provided in Figure 6.32, where an insignificant horizontal displacement was observed (i.e., a minor lateral rigid body motion of the test specimen occurred). This was confirmed with laser displacement data, which is discussed later. A photograph of the test specimen after completion of the impact test is shown in Figure 6.33. After completion of the impact test, no damage or cracking was found in the railing or deck concrete.

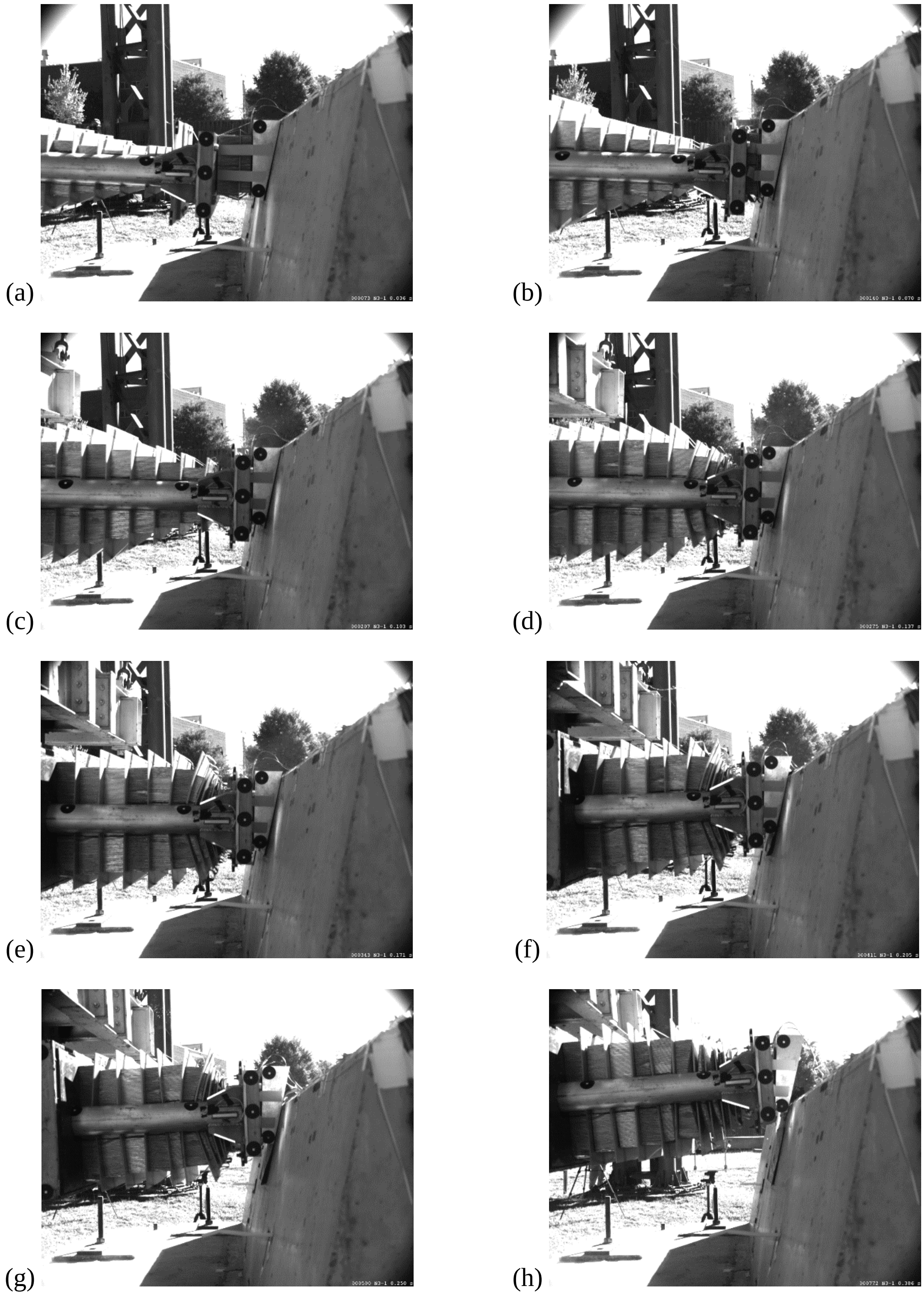

Figure 6.31 High-speed video frames from HSC-1 (R/C COR test 1) showing crush deformation of aluminum honeycomb: (a) At initial impact; (b) – (e) Intermediate frames; (f) At peak impact force; (g) – (h) Sliding and separation of loading wedge

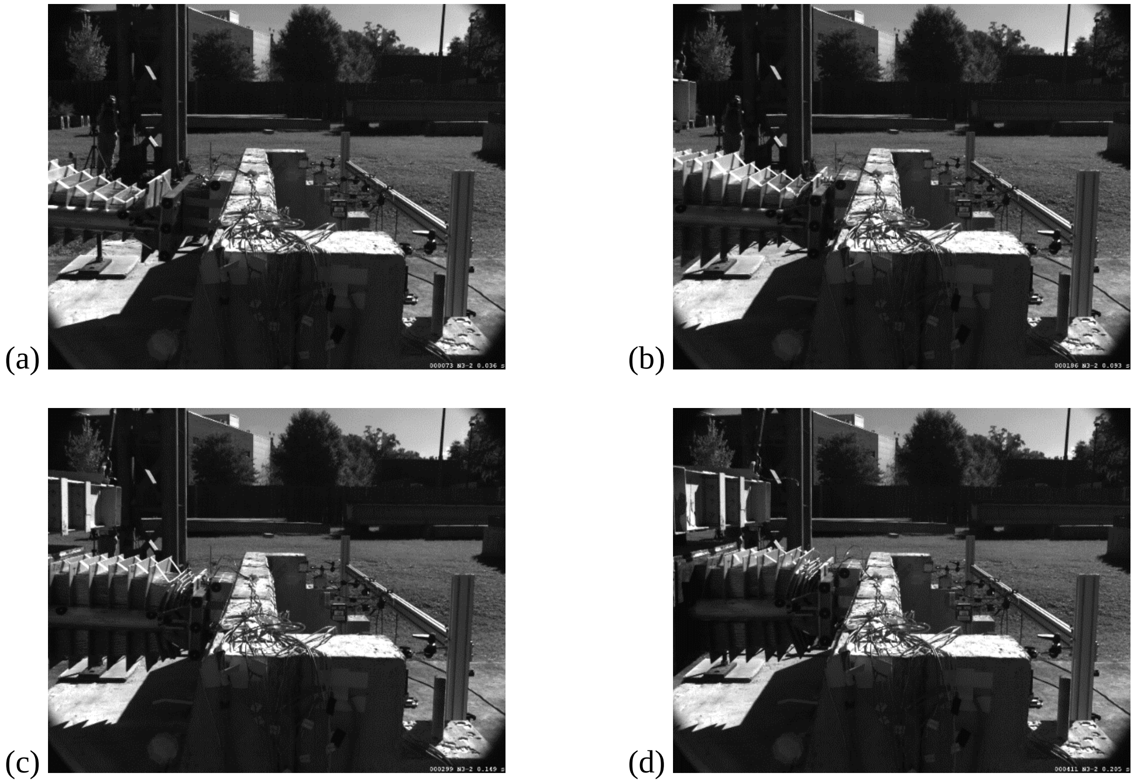

Figure 6.32 High-speed video frames from HSC-2 (R/C COR test 1): (a) At start of impact; (b) – (c) Intermediate frames; (d) At peak impact force

Figure 6.33 R/C COR 1 test specimen after completion of impact test

Break beam voltage data from R/C impact test 1 are provided in Figure 6.34, and were used to quantify the impact velocity. As shown in the instrumentation plan (Appendix I), two sets of break beams were placed in front of the impact test specimen at a 1-ft spacing. For each break beam, after the impactor was released and when the impactor crossed the path of the sensor, a change in voltage was observed. Since break beam 1 was placed 1 ft ahead of break beam 2, the duration of time over which the impactor moved 1 ft was quantified just prior to impact. For R/C test 1, the impact velocity was determined to be 31.3 ft/sec—compared to the design impact velocity of 31.1 ft/sec (a 0.6% difference). Tape switch data were used to determine the time at which the impact began and are shown in Figure 6.35. Note that all impact test data has been shifted such that the initiation of impact begins at 0.1 s (using the spike in tape switch voltage).

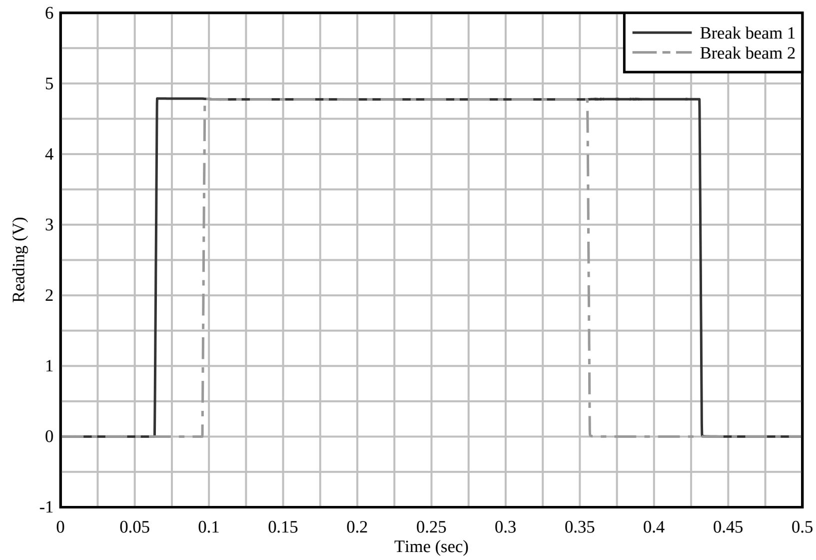

Figure 6.34 Break beam data for R/C COR test 1

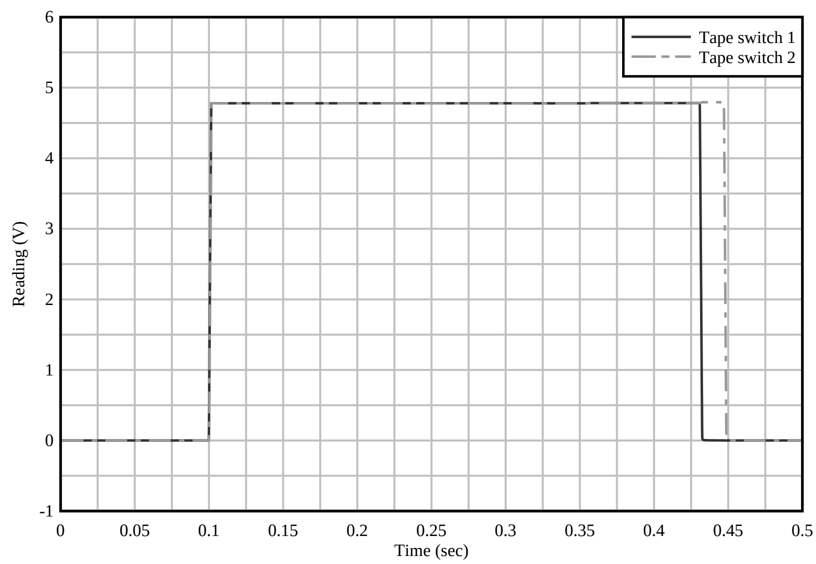

Figure 6.35 Tape switch data for R/C COR test 1

As shown in the instrumentation plan (Appendix I), four triaxial accelerometers—two mounted on the impactor concrete back block and two mounted on the aluminum front nose—were used to measure impactor accelerations during the pendulum impact test. Measured accelerations from the two accelerometers on the concrete back block (AC-1 & AC-2) in the impact direction (i.e., local Y direction of the accelerometer) are shown in Figure 6.36. Correspondingly, measured accelerations from the two accelerometers on the aluminum front nose (AC-3 & AC-4) in the impact direction (local Y direction) are shown in Figure 6.37. As expected, acceleration values are negative because of the impactor deceleration during impact. Furthermore, a more gradual deceleration of the back block is clearly shown in the AC-1 and

AC-2 data when compared with the more instantaneous impact that occurred with the front nose (as expected), producing more fluctuations in AC-3 and AC-4 data.

Accelerations were then multiplied by mass to quantify the impact forces that were applied to the standard R/C railing. Specifically, back block accelerations (AC-1 & AC-2) were multiplied by the 9850-lb back block mass (composed of the steel hanger frame and concrete block), while the front nose accelerations (AC-3 & AC-4) were multiplied by the 350-lb front nose mass (composed of the aluminum front nose components). The two back block forces (from AC-1 & AC-2) were then averaged and are shown in Figure 6.38, while the two front nose forces (from AC-3 & AC-4) were averaged and are shown in Figure 6.39.

The total applied impact force was then computed by combining the two averages from the back block and front nose, which is shown in Figure 6.40. In comparison with the designed/predicted maximum impact forces (shown in Figure 6.41, which provides the predicted impact force over time from previous FEA impact simulations), the maximum observed impact force from R/C test 1 was found to be 71.5 kip (3.9% greater than the originally designed 68.8-kip peak impact force).

As shown in Figure 6.36, acceleration measurements from AC-2—the accelerometer beneath the concrete back block—were noticeably influenced by the undesired and unexpected sliding of the aluminum loading wedge. Specifically, the (designed) gradual increase in acceleration magnitude and peak impact force were not entirely captured with AC-2. However, after averaging and combining data from all four accelerometers, with the total peak impact force and overall duration of impact similar to the designed force-time curve, these results indicate that the wedge sliding only had minimal influence on the impact test.

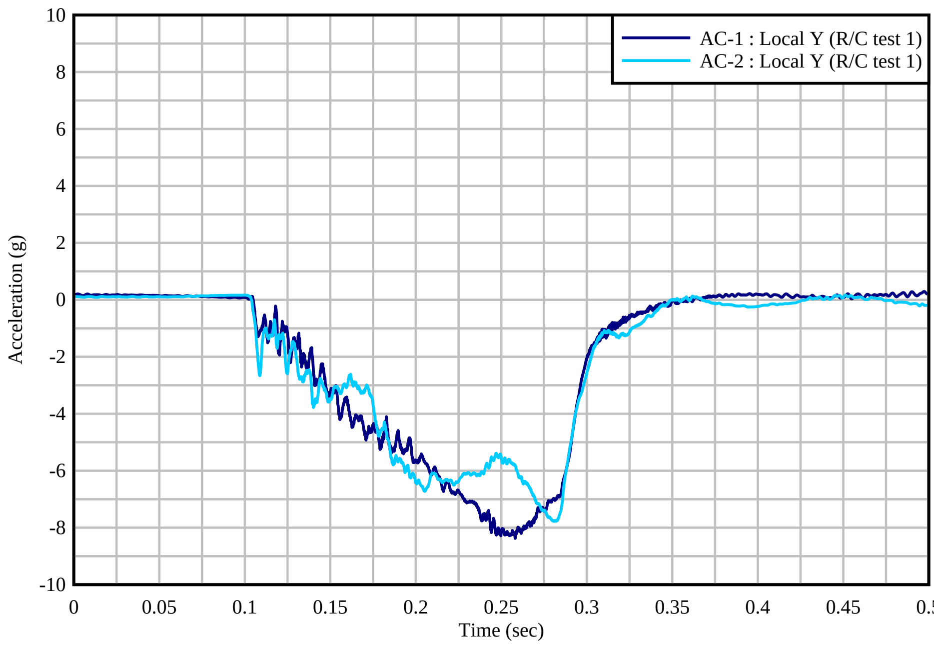

Figure 6.36 Raw concrete back block acceleration data (AC-1 & AC-2) for R/C COR test 1 (in the impact direction, local Y direction of accelerometer)

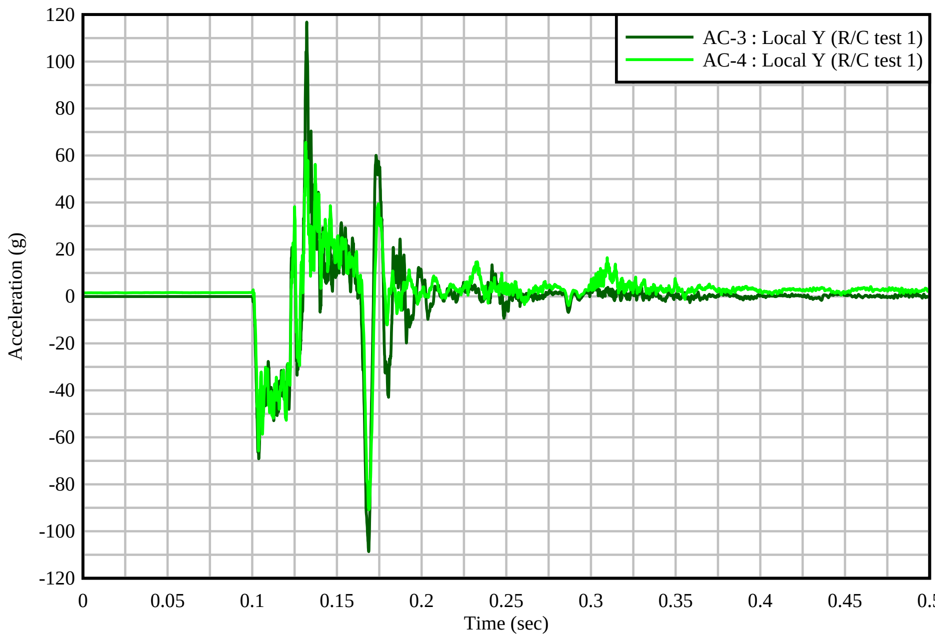

Figure 6.37 Raw front nose acceleration data (AC-3 & AC-4) for R/C COR test 1 (in the impact direction, local Y direction of accelerometer)

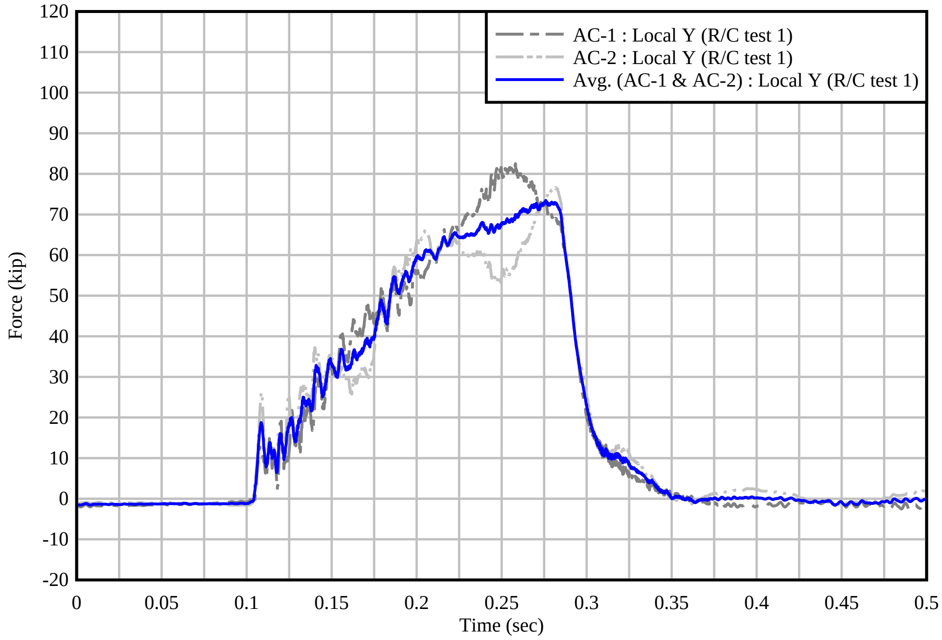

Figure 6.38 Computed impact forces from back block for R/C COR test 1

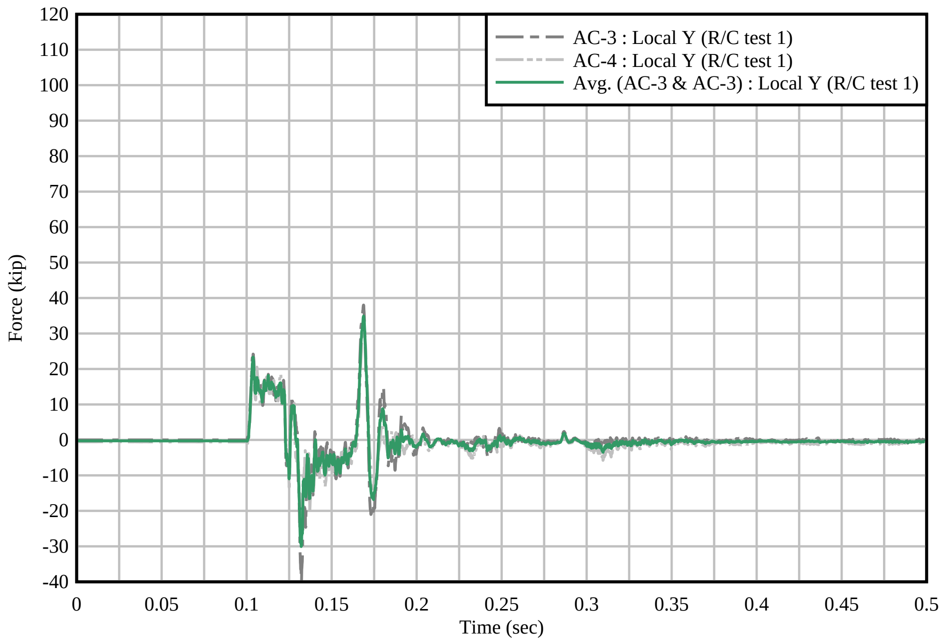

Figure 6.39 Computed impact forces from front nose for R/C COR test 1

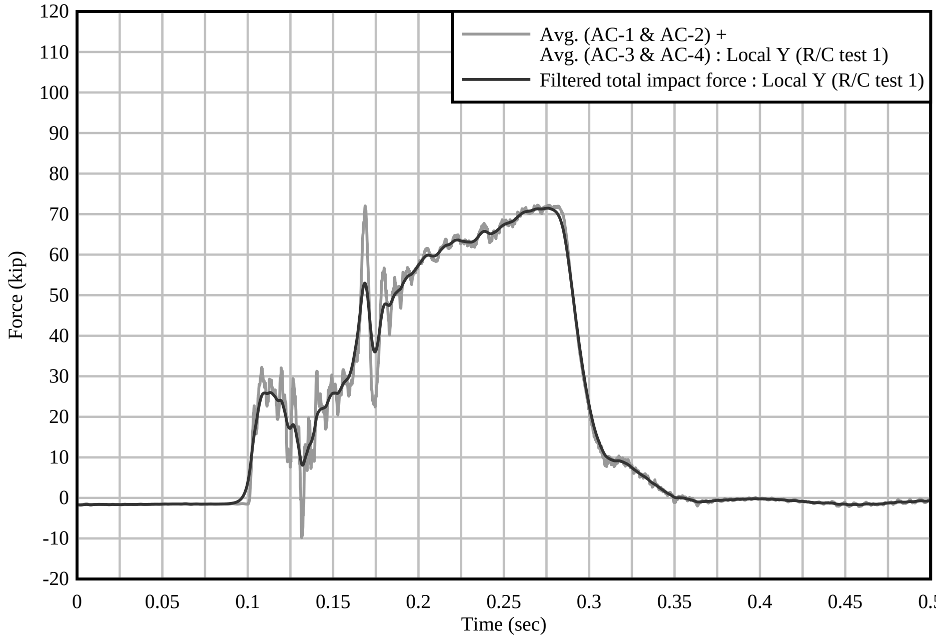

Figure 6.40 Raw and filtered total computed impact force for R/C COR test 1

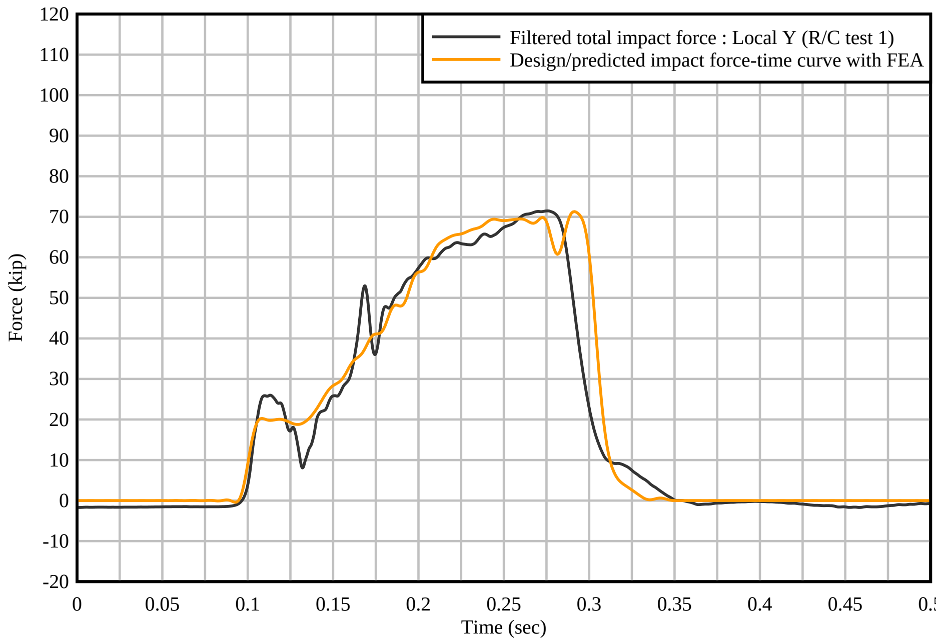

Figure 6.41 Filtered total experimental impact force for R/C COR test 1 compared to FEA prediction

During the impact test, lateral deflections of the railing and any rigid sliding of the test specimen that occurred were captured with laser displacement sensors positioned behind the specimen. Further, external concrete strain measurements in the railing and deck were taken at locations along the front and back faces of the specimen. Specific locations of the laser displacement sensors (LDS) and external concrete strain gages (CSG) are depicted in Figure 5.23 (and further detailed in Appendix I).

Laser displacement data captured during R/C test 1 are provided in Figure 6.42, where it is shown that the maximum displacement occurred at the center of the railing (LDS-4) with a magnitude of 0.067 in., when the peak impact force was applied. After completion of the impact, the measured displacements did not return to zero, confirming that some (minimal) horizontal sliding occurred. Had only the railing deflected and no rigid sliding of the specimen occurred, displacement data at the deck level (LDS-2, LDS-5, LDS-8) would be zero. However, displacement at LDS-2 and LDS-8 are non-zero and are of a similar magnitude to the railing displacements. Also note that data from LDS-1 and LDS-5 are not included, because the data from those sensors were inaccurate and no useful information could be discerned.

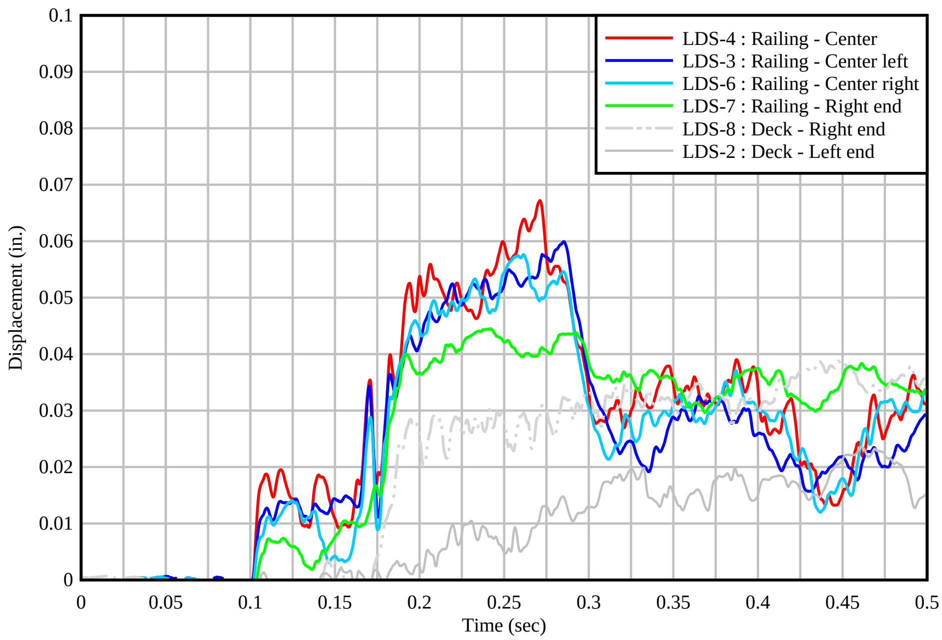

Figure 6.42 Laser displacement sensor data for R/C COR test 1

Readings from external concrete strain gages are provided in Figures 6.43 through 6.46. More specifically, external gage readings for the top front face of the railing are provided in Figure 6.43. Strain readings for the bottom (i.e., lower half and toe) of the railing front face are provided in Figure 6.44 and Figure 6.45, and readings for the back face of the railing are provided in Figure 6.46. Although some strain levels reached the approximate tensile rupture strain for 3400-psi strength concrete, no cracking was found in the railing or deck after visual inspection.

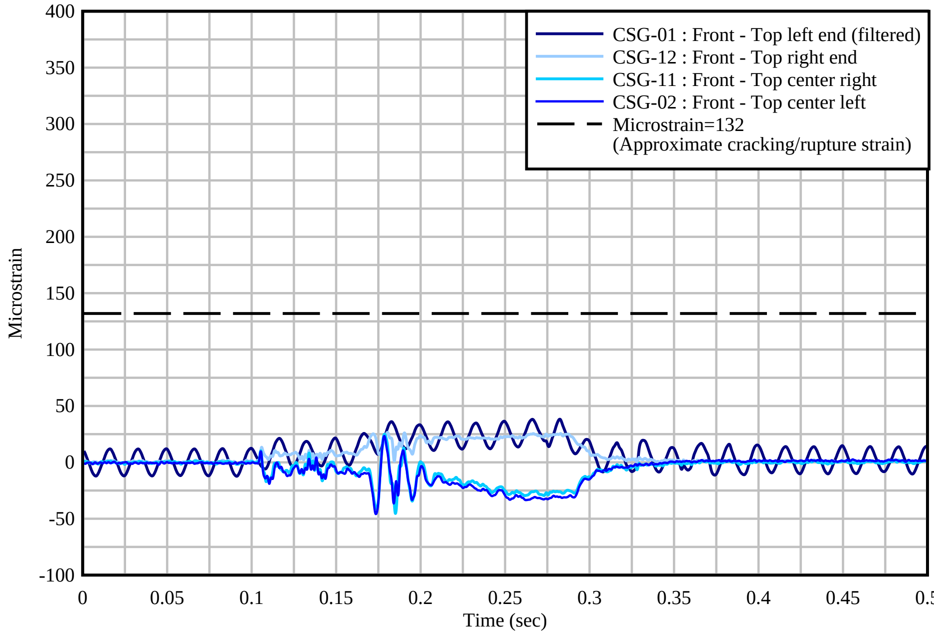

Figure 6.43 External concrete strain gage data for locations on the top front face of the railing during R/C COR test 1

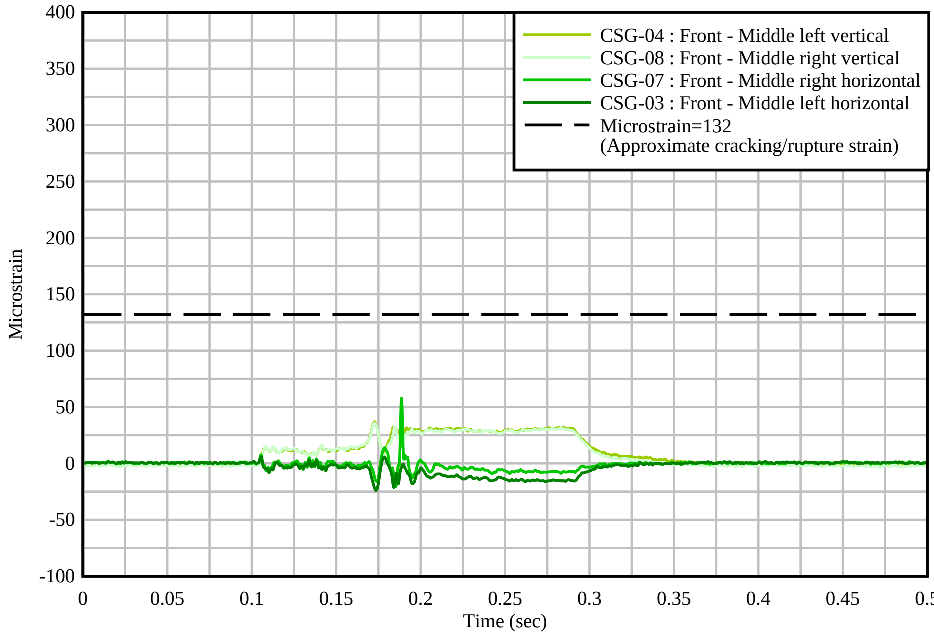

Figure 6.44 External concrete strain gage data for locations on the lower front face of the railing during R/C COR test 1

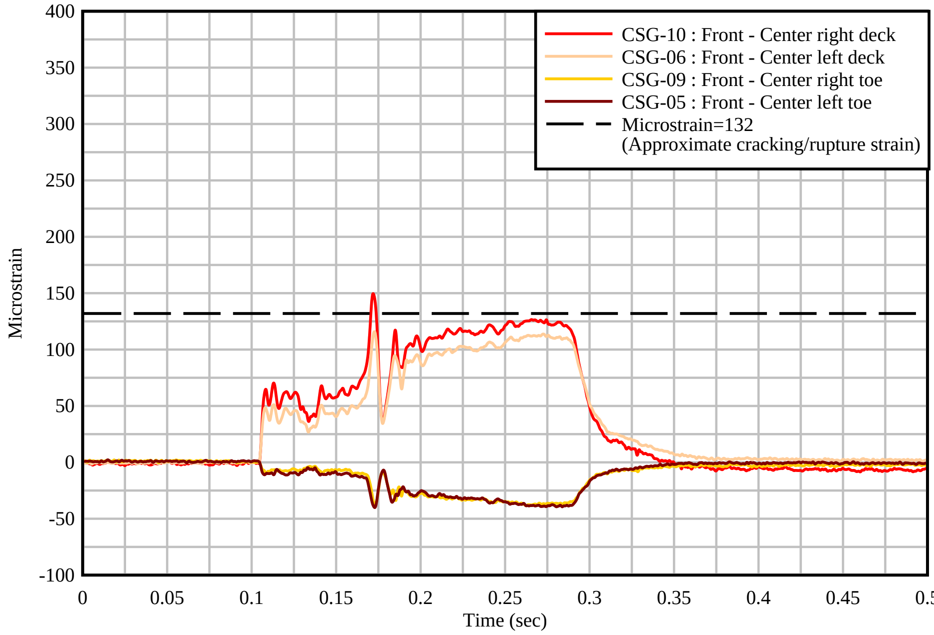

Figure 6.45 External concrete strain gage data for locations at the toe of the railing and deck during R/C COR test 1

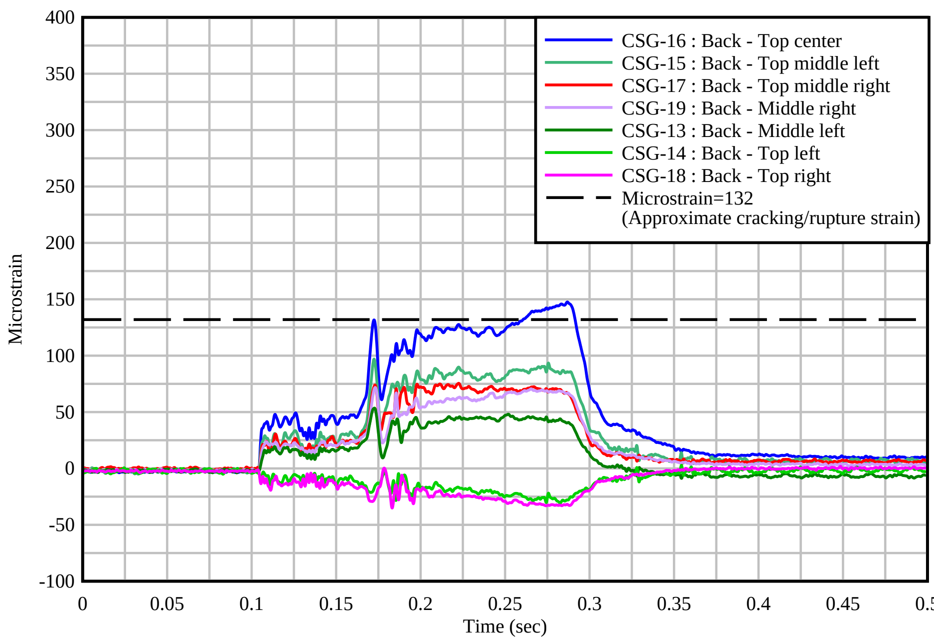

Figure 6.46 External concrete strain gage data for locations on the back face of the railing during R/C COR test 1

Readings from internal rebar strain gages are provided in Figure 6.47. Specific locations of the deck and connection (4V) rebar gages are provided in Appendix I. Maximum strain levels in the deck and railing steel reinforcement are well below yielding strain (2000 microstrain) indicating that the test specimen successfully resisted the pendulum impact with minimal damage. Note that some rebar strain gage readings are not included because the gages were damaged during the casting process and did not provide any data during testing (e.g., RSG-03, RSG-11, RSG-13, RSG-14, RSG-15 had zero readings during the test).

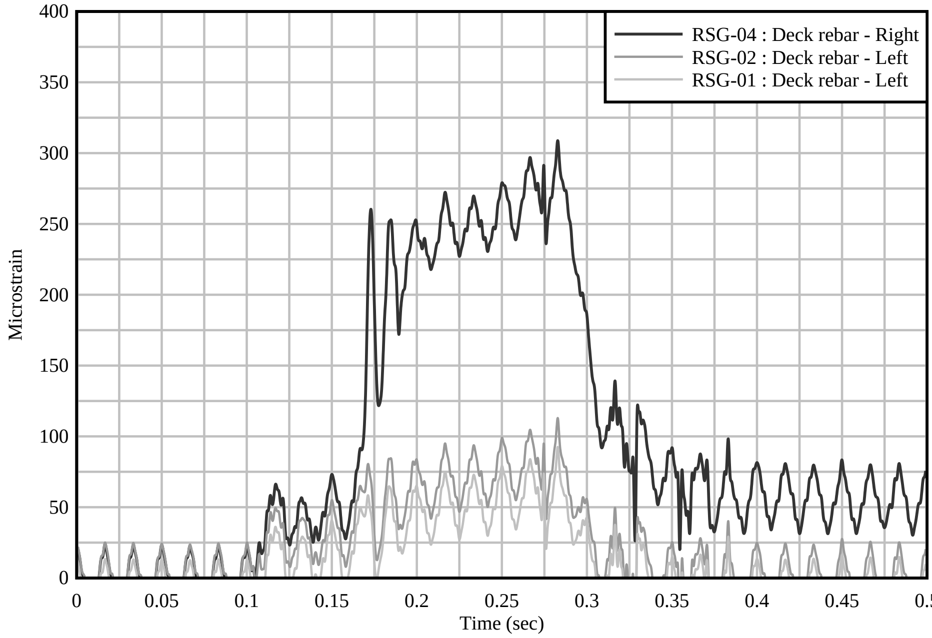

(a)

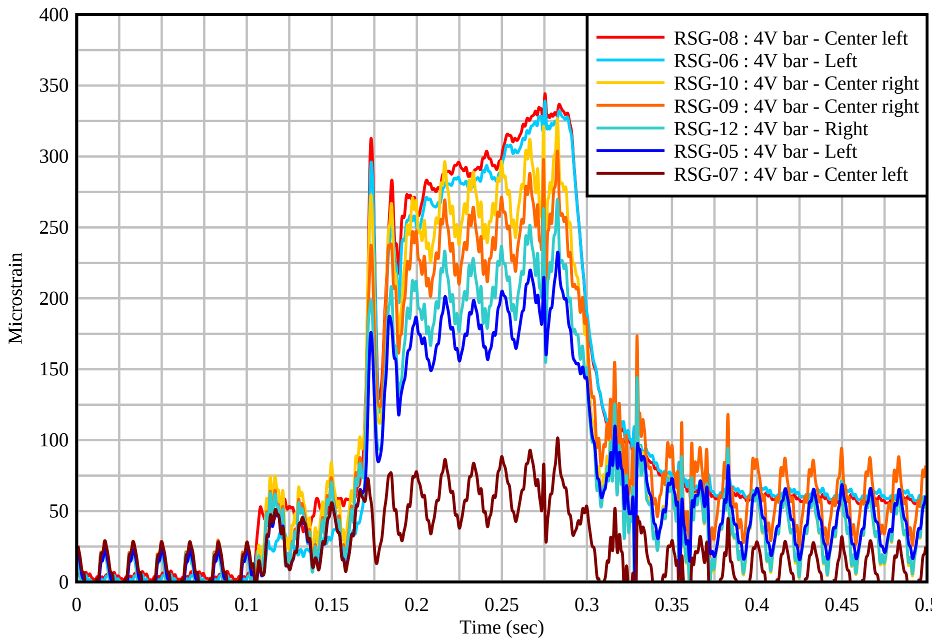

(b)

Figure 6.47 Internal rebar strain gage data during R/C COR test 1:
(a) Deck rebar; (b) Railing rebar

6.3.2 Impact testing of R/C COR specimen 2

On December 9, 2020, full-scale pendulum impact testing for R/C COR test specimen 2 was conducted—where the pendulum impactor was dropped from 15 ft. Instrumentation included with R/C test specimen 2 was the same as described for R/C test 1. Sequential images taken from high-speed camera 1 (HSC-1) over the impact duration are provided in Figure 6.48, starting with the first instant of impact and including the point in time when the maximum crush depth on the crushable front nose (i.e., maximum impact force) was reached. Unlike R/C COR test 1, for R/C COR test 2, the adhesive used to hold the aluminum loading wedge did not fail. Additional images from high-speed camera 2 (HSC-2) are provided in Figure 6.49, where no sliding of the test specimen was observed. A photograph of the test specimen after completion of the impact test is shown in Figure 6.50. After completion of the impact test, no damage or cracking was found in the railing or deck concrete.

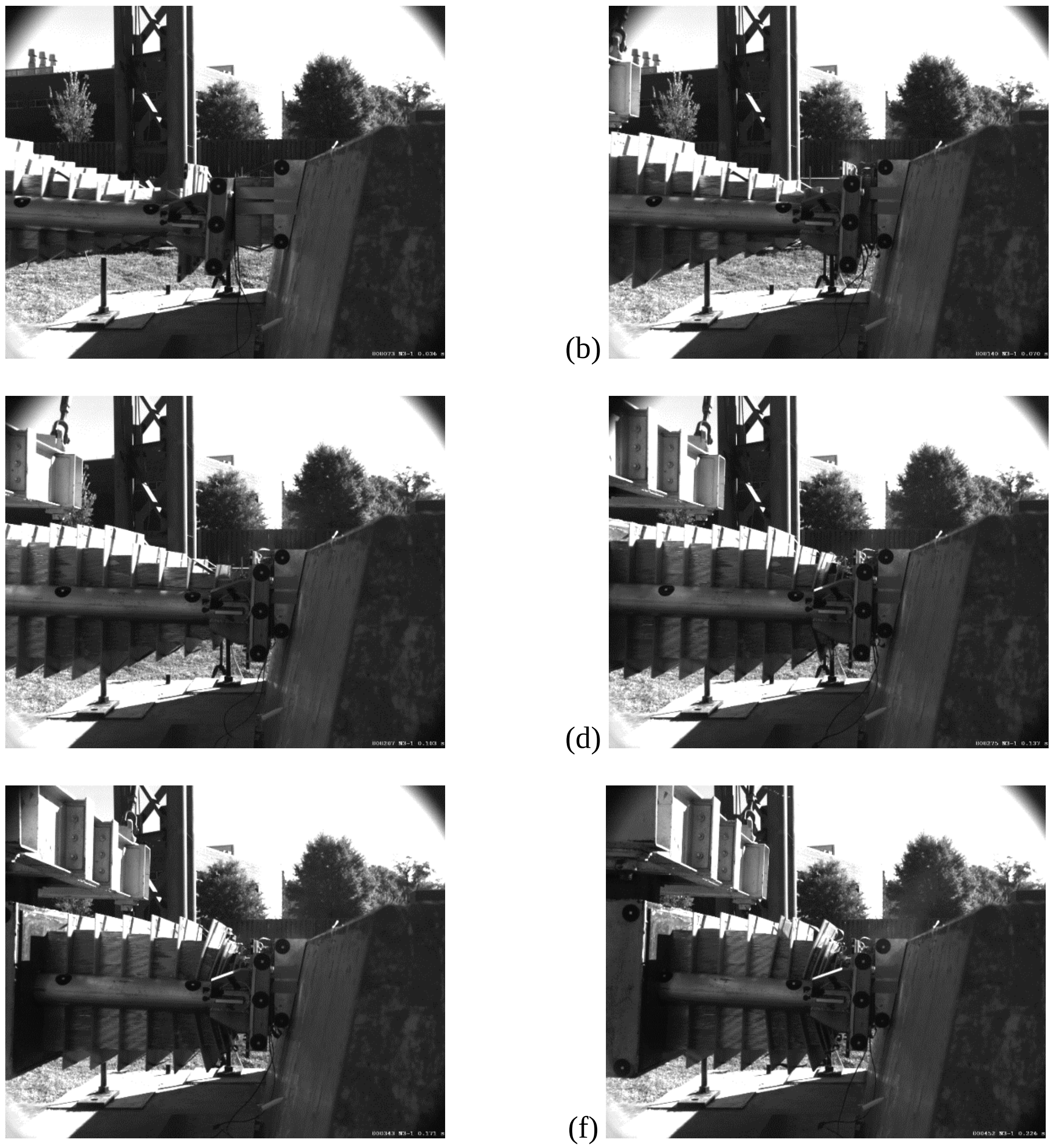

Figure 6.48 High-speed video frames from HSC-1 (R/C COR test 2) showing crush deformation of aluminum honeycomb: (a) At initial impact; (b) – (e) Intermediate frames; (f) At peak impact force

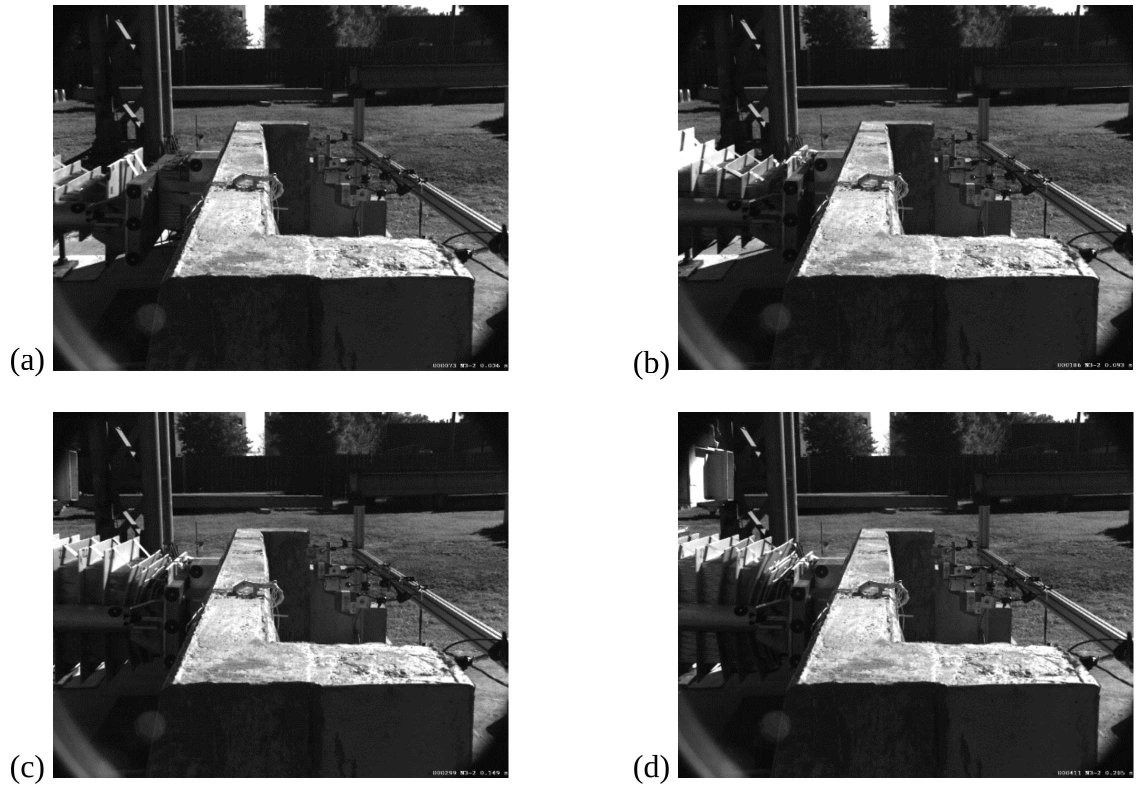

Figure 6.49 High-speed video frames from HSC-2 (R/C COR test 2): (a) At start of impact; (b) – (c) Intermediate frames; (d) At peak impact force

Figure 6.50 R/C COR test 2 specimen after completion of impact test

Break beam voltage data from R/C impact test 2 are provided in Figure 6.51, and were used to quantify the impact velocity. For R/C test 2, the impact velocity was determined to be 30.0 ft/sec—compared to the design impact velocity of 31.1 ft/sec (a 3.5% difference). Tape switch data are shown in Figure 6.52. Note that all impact test data has been shifted such that the initiation of impact begins at 0.1 s (using the spike in tape switch voltage).

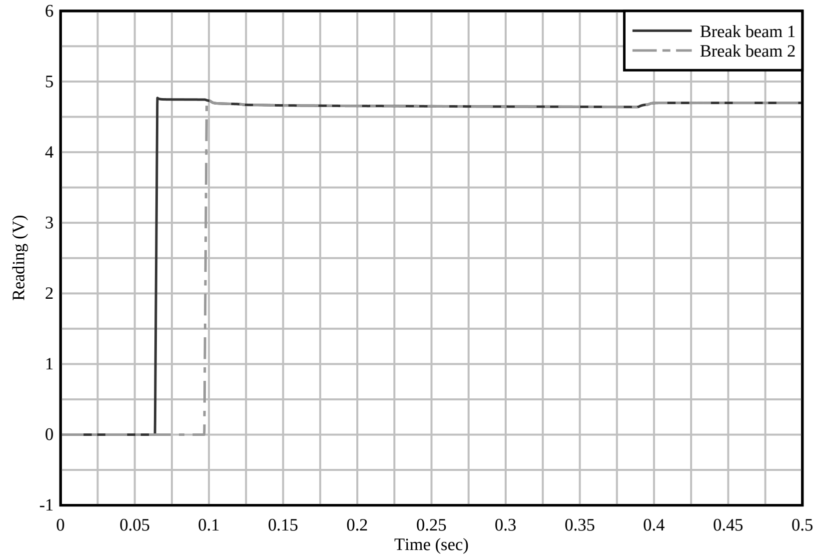

Figure 6.51 Break beam data for R/C COR test 2

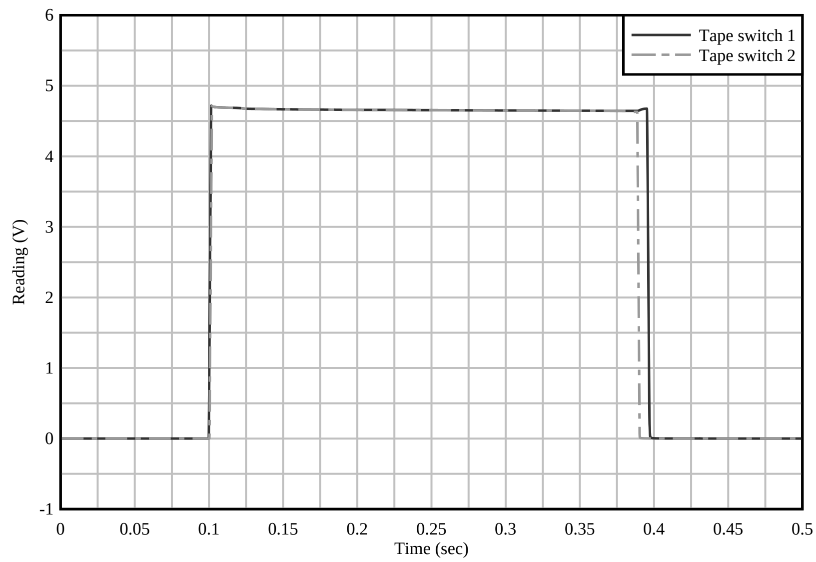

Figure 6.52 Tape switch data for R/C COR test 2

Measured accelerations from the two accelerometers on the concrete back block (AC-1 & AC-2) in the impact direction (i.e., local Y direction of the accelerometer) are shown in Figure 6.53. Correspondingly, measured accelerations from the two accelerometers on the aluminum front nose (AC-3 & AC-4) in the impact direction (local Y direction) are shown in Figure 6.54. Computed and averaged back block impact forces (from AC-1 & AC-2) are shown in Figure 6.55, while the computed and averaged front nose impact forces (from AC-3 & AC-4) are shown in Figure 6.56.

The total applied impact force (computed by combining the averages of the back block and front nose) is shown in Figure 6.57. In comparison with the designed/predicted maximum impact forces (shown in Figure 6.58, which provides the predicted impact force over time from previous FEA impact simulations), the maximum observed impact force from R/C test 2 was found to be 74.3 kip (7.9% greater than the originally designed 68.8-kip peak impact force).

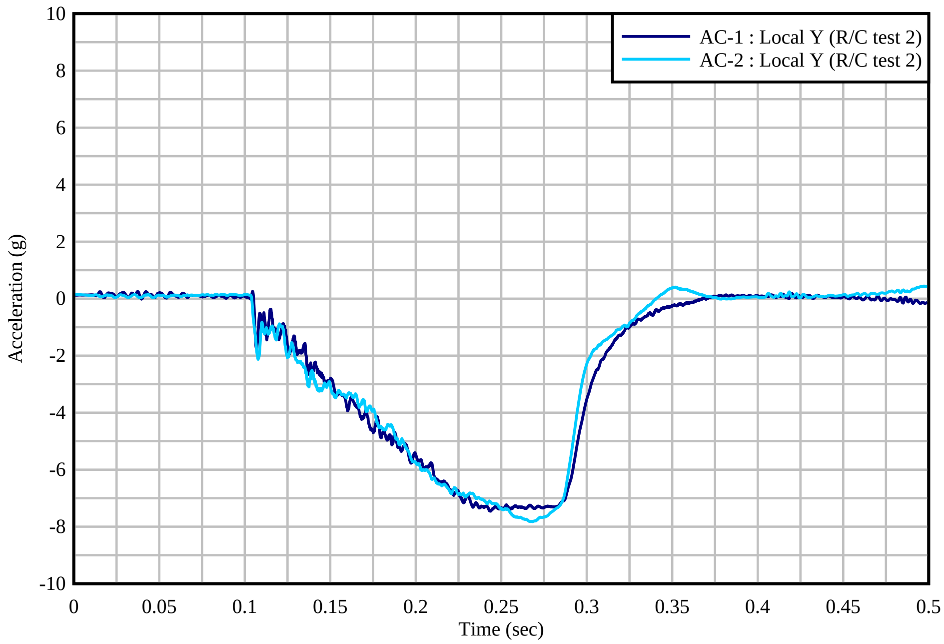

Figure 6.53 Raw concrete back block acceleration data (AC-1 & AC-2) for R/C COR test 2 (in the impact direction, local Y direction of accelerometer)

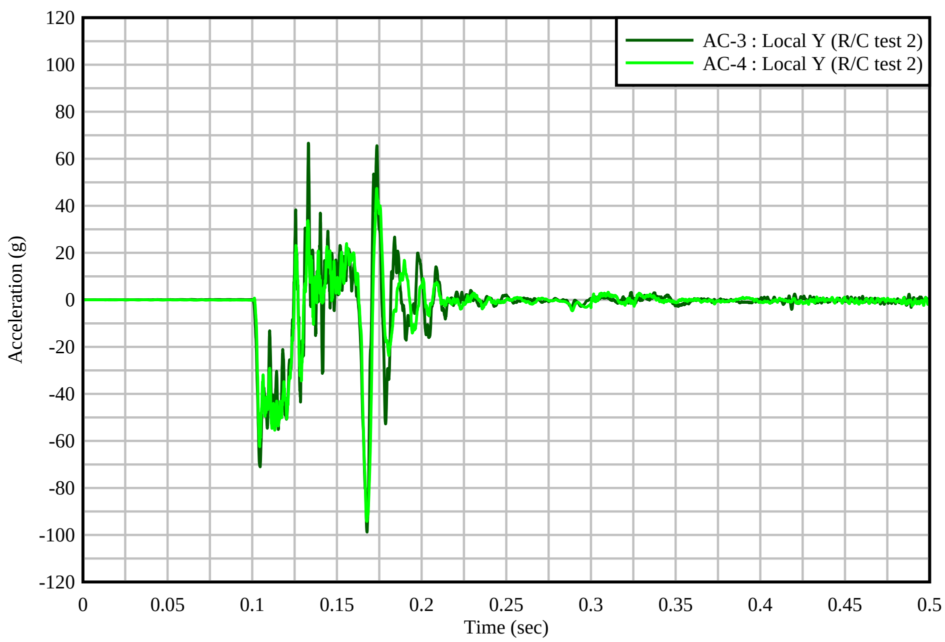

Figure 6.54 Raw front nose acceleration data (AC-3 & AC-4) for R/C COR test 2 (in the impact direction, local Y direction of accelerometer)

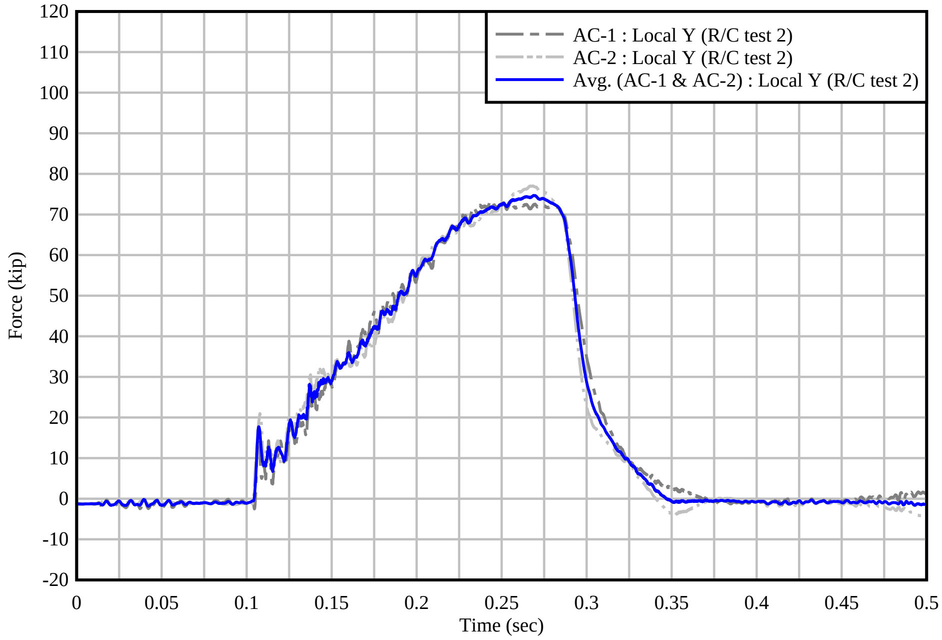

Figure 6.55 Computed impact forces from back block for R/C COR test 2

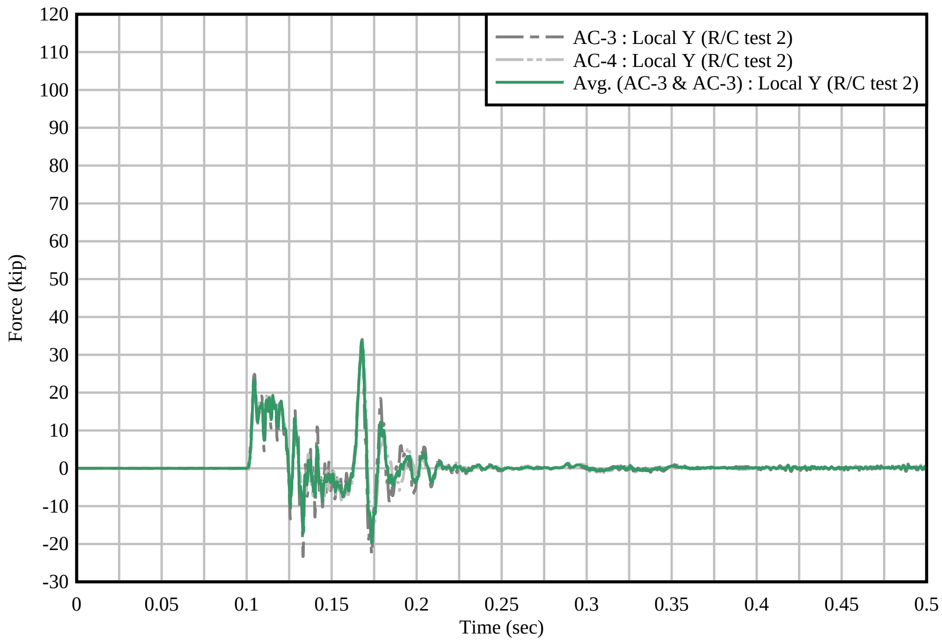

Figure 6.56 Computed impact forces from front nose for R/C COR test 2

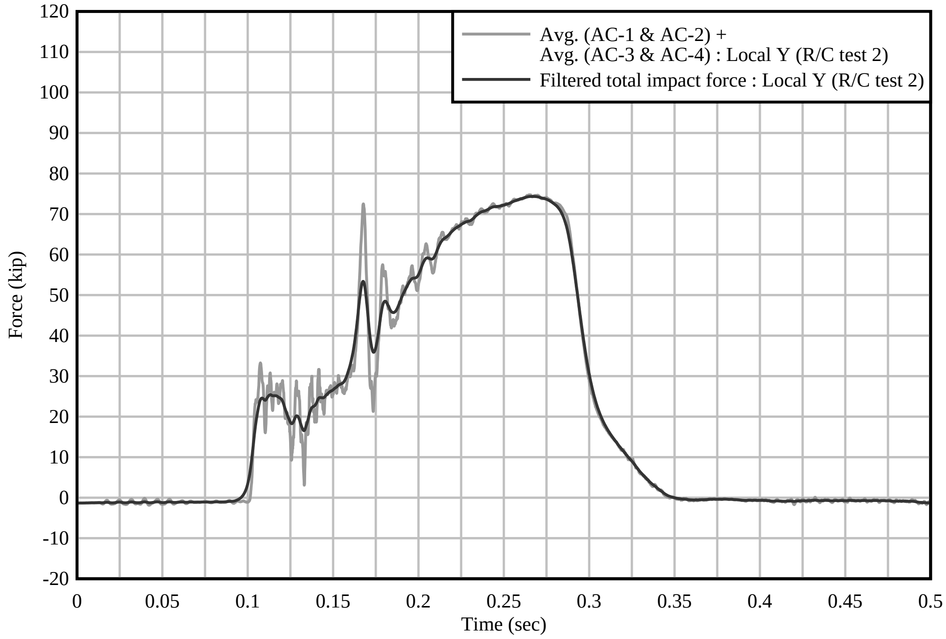

Figure 6.57 Raw and filtered total computed impact force for R/C COR test 2

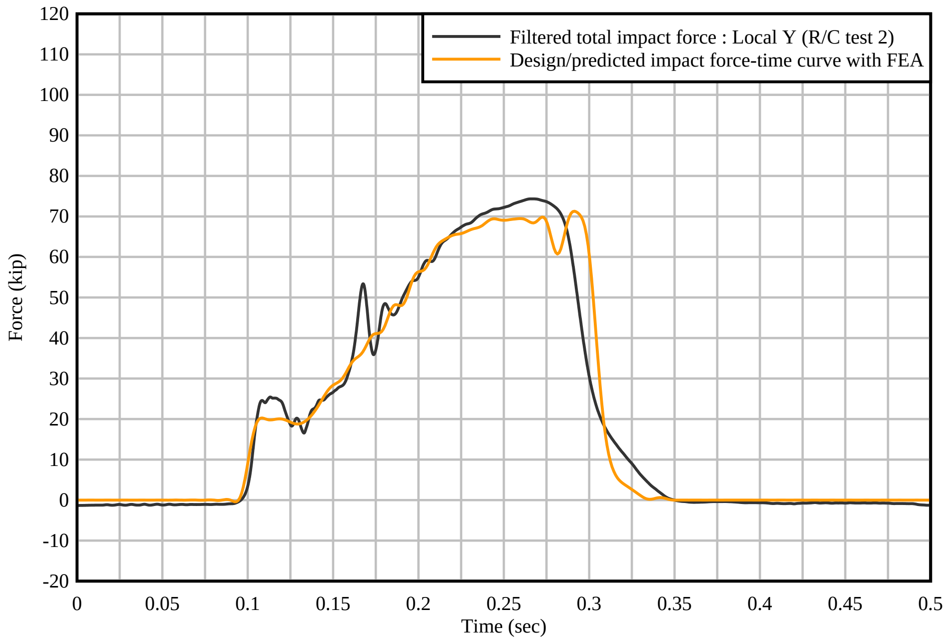

Figure 6.58 Filtered total experimental impact force for R/C COR test 2 compared to FEA prediction

Laser displacement data captured during R/C COR test 2 are provided in Figure 6.59. Based on the unusual and sporadic behavior displayed in the displacement data, it was determined that the laser data from R/C test 2 were not useful and did not provide any discernable trends. A probable cause of the sporadic data was that the frame/stand used to hold the laser gages in position was influenced by the impact test (meaning that some movement of the gages unassociated with the displacements/deflections of the test specimen were captured).

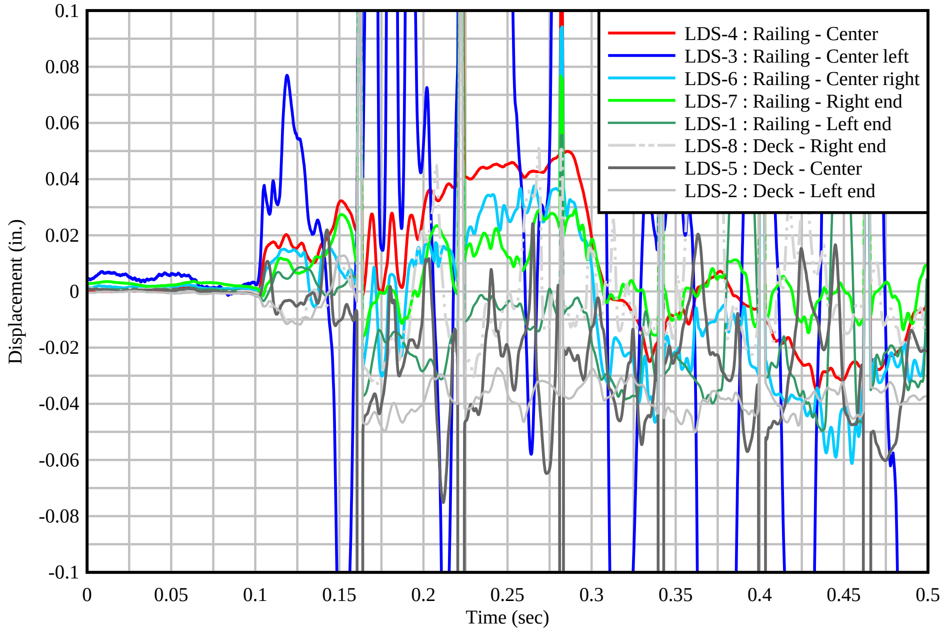

Figure 6.59 Laser displacement sensor data from R/C COR test 2

Concrete strain gage readings for the top front face of the railing are provided in Figure 6.60. Strain readings for the bottom (i.e., lower half and toe) of the railing front face are provided in Figure 6.61 and Figure 6.62, and readings for the back face of the railing are provided in Figure 6.63. Although some strain levels exceeded the approximate rupture strain for 3400-psi strength concrete, no visible cracks were found in the railing or deck during visual inspection.

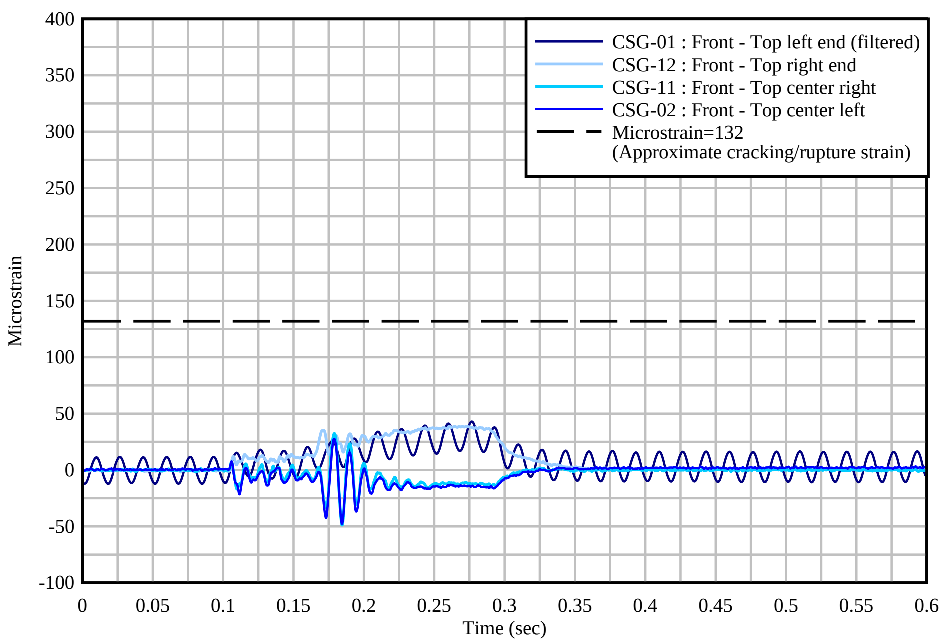

Figure 6.60 External concrete strain gage data for locations on the top front face of the railing during R/C COR test 2

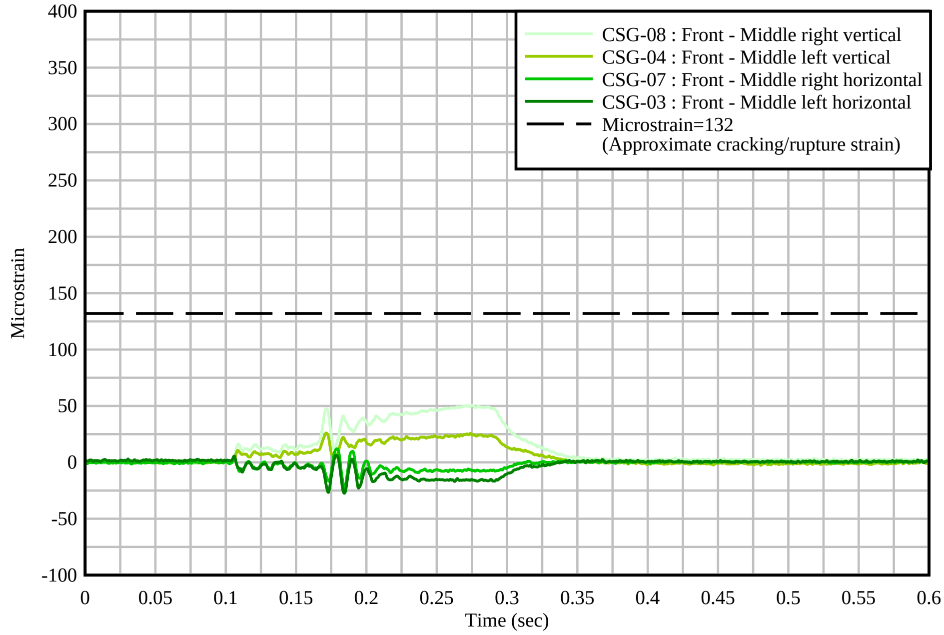

Figure 6.61 External concrete strain gage data for locations on the lower front face of the railing during R/C COR test 2

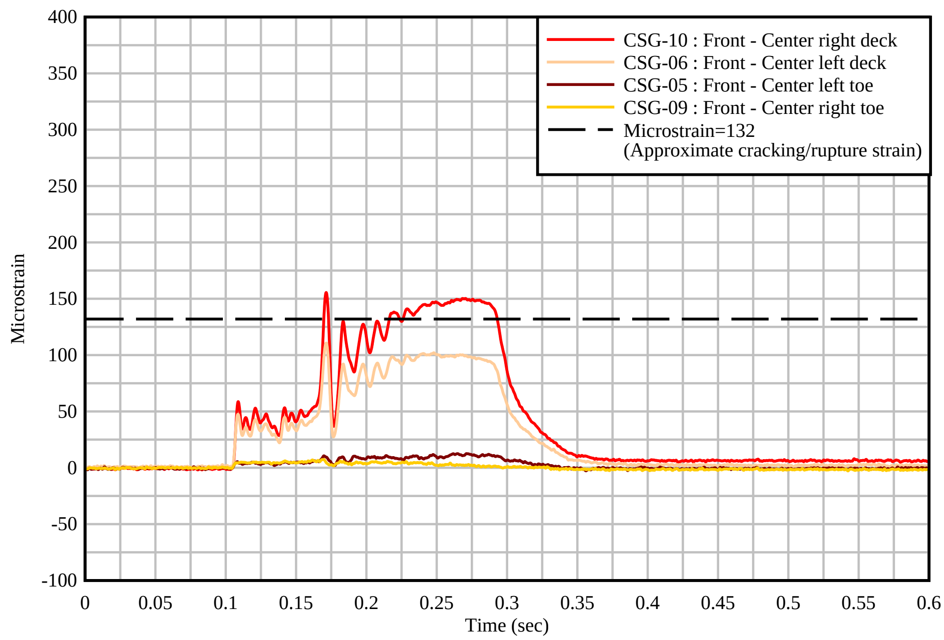

Figure 6.62 External concrete strain gage data for locations at the toe of the railing and deck during R/C COR test 2

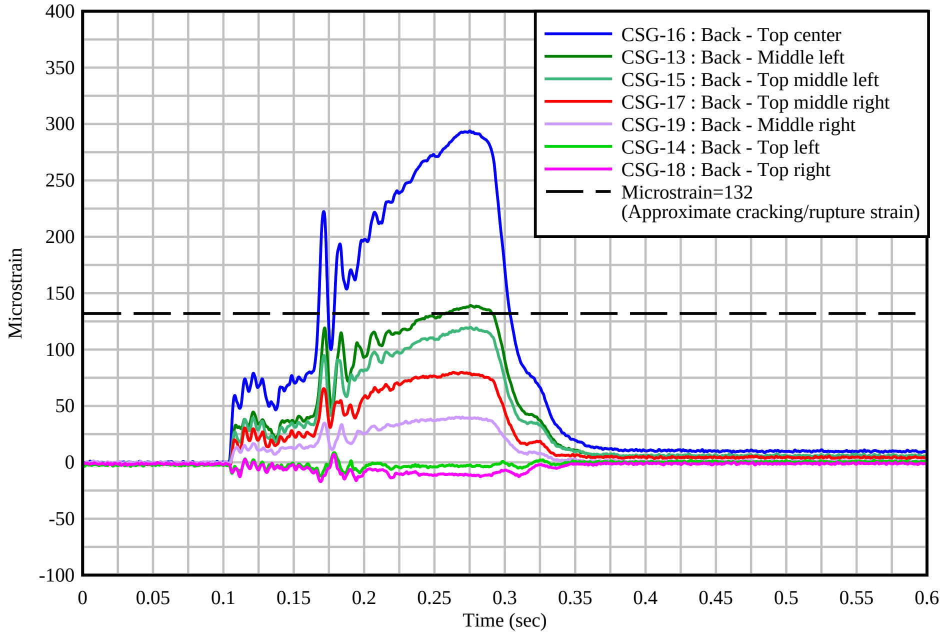

Figure 6.63 External concrete strain gage data for locations on the back face of the railing during R/C COR test 2

Readings from internal rebar strain gages are provided in Figure 6.64. Specific locations of the deck and connection (4V) rebar gages are provided in Appendix I. Maximum strain levels in the deck and railing steel reinforcement are well below yielding strain (2000 microstrain) indicating that the test specimen successfully resisted the pendulum impact. Note that a significant number of rebar strain gage readings are not included because the gages were damaged during the casting process and did not provide data during testing (e.g., RSG-6, RSG-8, RSG-10, RSG-12, RSG-14, RSG-15 are zero).

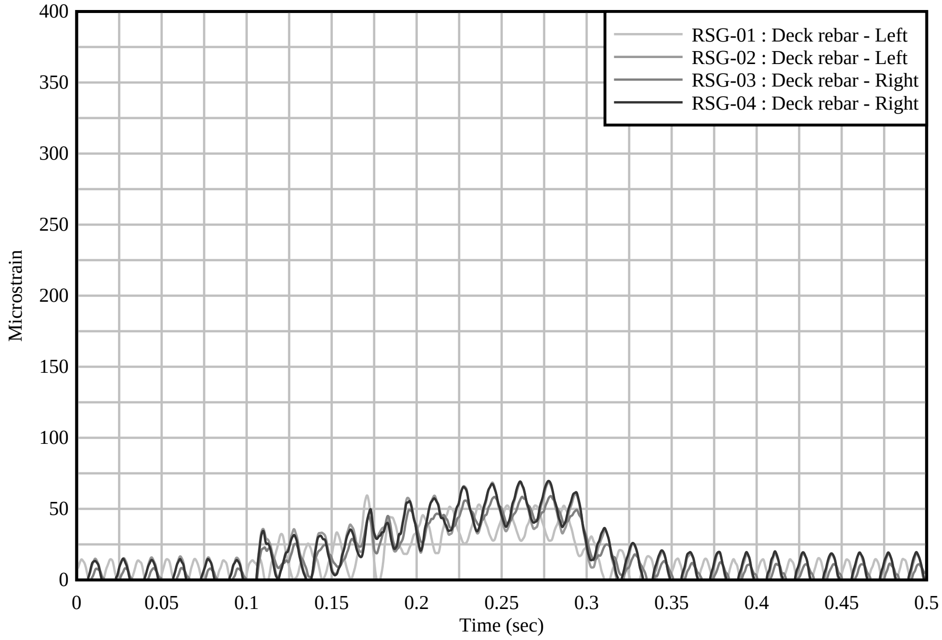

(a)

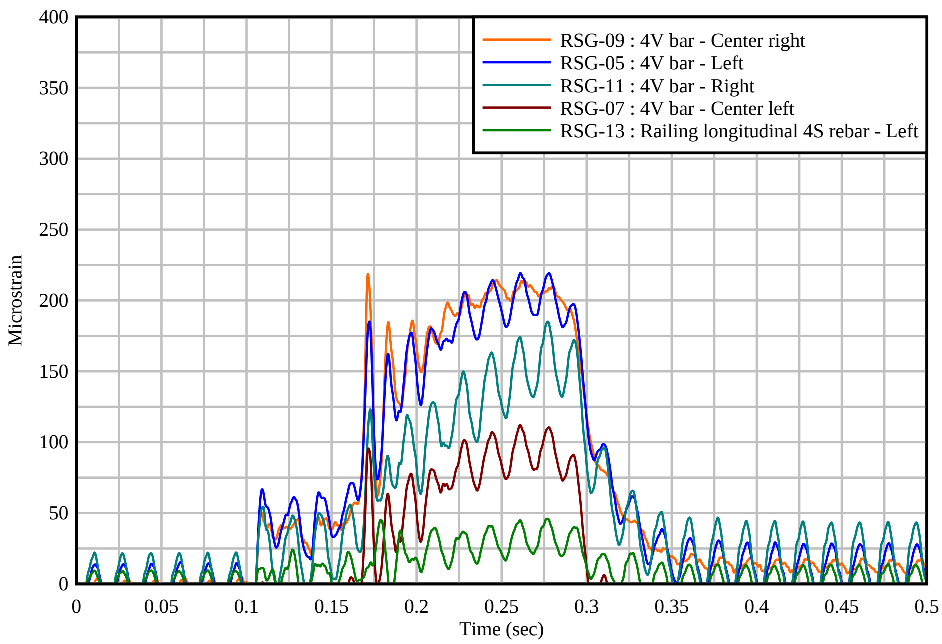

(b)

Figure 6.64 Internal rebar strain gage data during R/C COR test 2:
(a) Deck rebar; (b) Railing rebar

6.4 Comparison of FRC and R/C COR test specimen results

Selected data from testing of both COR specimen types are compared, to evaluate the performance of the proposed FRC railing and to establish whether the FRC railing system behaved similar to the traditional R/C FDOT railing under comparable impact loads.

6.4.1 Overview

As discussed, the following specimen configurations were pendulum impact tested:

- Partially-instrumented FRC COR test specimen 1
- Fully-instrumented FRC COR test specimen 2
- Fully-instrumented R/C COR test specimen 1
- Fully-instrumented R/C COR test specimen 2

Because there was only one fully-instrumented FRC test specimen (i.e., because laser displacements and strain gage data were not part of FRC specimen 1 testing), only some comparisons of collected instrumentation data could be made between all four impact tests. Furthermore, some instrumentation components from each test could not be used for comparison.

6.4.2 Comparison of COR acceleration data and pendulum impact forces

For each of the four COR tests, accelerometers located on the pendulum impactor were used to measure deceleration of the impactor over the duration of impact. Acceleration data were subsequently used to indirectly measure the impact force applied to each test specimen. As shown in Figure 6.65, a similar force-time curve was achieved with each of the four tests and each test was found to adequately follow the designed force-time curve—which was designed to produce impact forces similar to the transverse component of a TL-4 vehicle impact test.

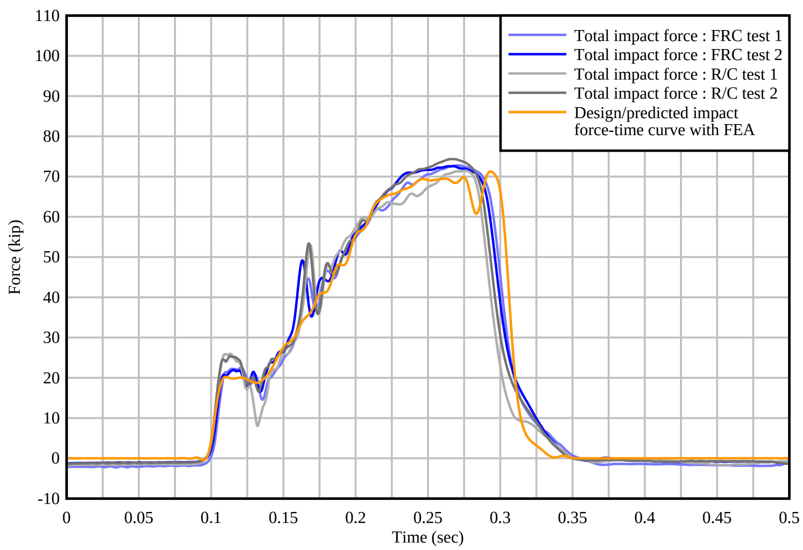

Figure 6.65 Total impact force for each traffic railing impact test

6.4.3 Comparison of COR laser displacement data

For FRC COR test 2 and R/C COR test 1, laser displacement sensors were used to capture lateral deflections at various locations on the back face of the railing. (As previously discussed, displacements were not captured during FRC COR test 1 and displacements recorded during R/C test 2 were unusable due to support-stand vibrations). As opposed to comparing all LDS data from the two available tests, only the largest observed displacements (from LDS-4, located behind the center of the railing shown in Figure 5.23b) are compared in Figure 6.66. As shown, the maximum displacement for each test was similar in magnitude and relatively small (less than 0.07 in.). Although only two of the four tests provided useful displacement data, it was shown with high-speed video that the other two specimens (FRC test 1 and R/C test 2) performed similarly, with comparable small displacements as estimated from the high-speed video recordings, suggesting that the proposed FRC railing is structurally adequate (with repeated test specimen productions).

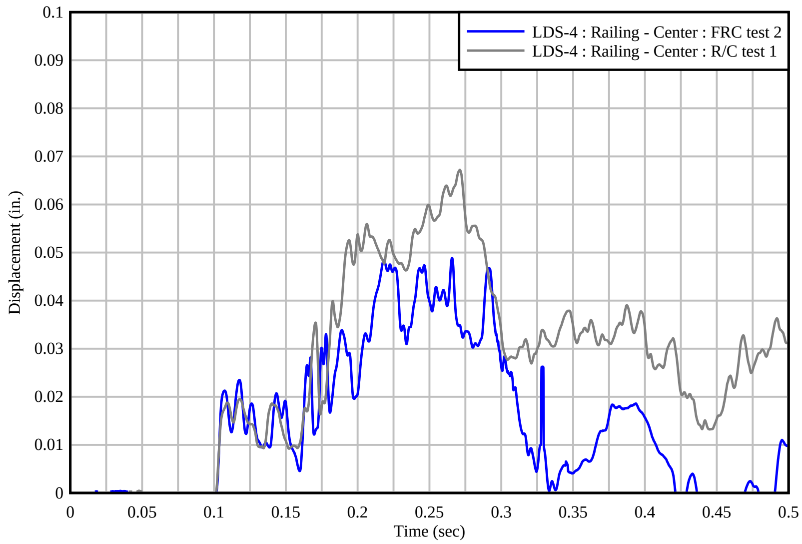

Figure 6.66 Comparison of captured displacements

6.4.4 Comparison of COR external concrete strain gage data

For three of the four COR tests (FRC test 1, R/C test 1, R/C test 2), external concrete strain measurements in the railing and deck were taken at locations along the front and back sides of the test specimen. Recorded external strain data from a select number of gage locations are compared in Figure 6.67 and Figure 6.68.

Gages on the deck near the toe of the railing (CSG-6 and CSG-10) were found to capture the largest strain levels for the front (impact) side of the specimen. In some tests, CSG-6 strains (located to the left of the specimen centerline and to the left of the loading wedge) were found to be largest in magnitude for the front side of the specimen. In other instances, data from CSG-10 strains (located to the right of the specimen centerline and to the right of the loading wedge) were found to be highest for the front side. Because these two gages were located at mirrored distances from the centerline of the test specimen, and because they were found to be similar in magnitude over the impact duration, CSG-6 and CSG-10 data from each test were averaged and are compared in Figure 6.67. As shown, similar strain levels were found for each of the three impact tests, another indication that the FRC railing performed similarly to the standard R/C railing.

For the back side of the test specimen, strain levels from gage CSG-16 were found to be largest in magnitude (in each of the three tests) because this gage was positioned at the centerline of the test specimen (directly behind the impact location). Therefore, strain levels on the back side of the specimen at gage CSG-16 are compared in Figure 6.68. The maximum transient strain level for FRC test 2 was found to be larger in magnitude than the two standard R/C tests (over 33% greater than R/C test 2), however the residual (post impact) strains were all minimal in magnitude (for both R/C and FRC specimens). This finding was consistent with the fact that no visible surface cracks were found on any of the test specimens after impact testing.

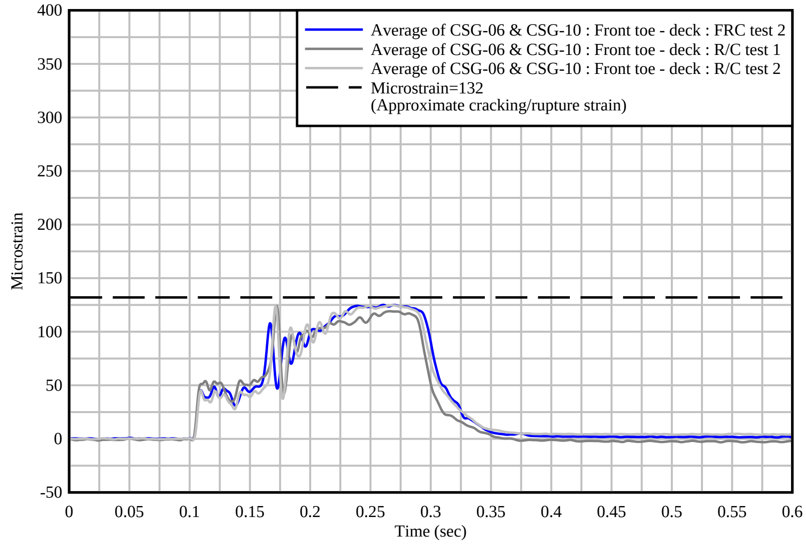

Figure 6.67 Comparison of external concrete strain gages on the deck near the railing toe (on the front side of the impact specimen)

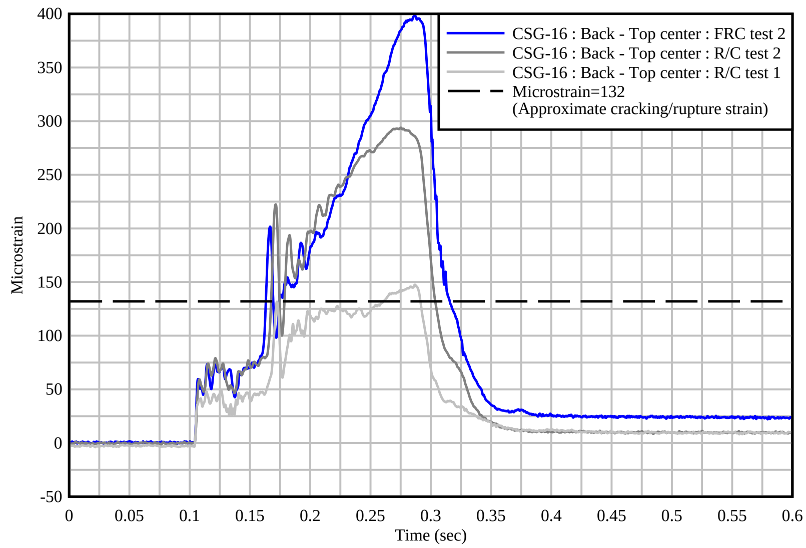

Figure 6.68 Comparison of external concrete strain gages located at the center of the specimen (on back side of the impact specimen)

6.4.5 Comparison of COR internal steel rebar strain gage data

Using the three available test data sets, selected rebar strain gage measurements are compared. For the deck reinforcement, the largest observed strains are compared in Figure 6.69, where it is shown that the FRC test was larger than R/C COR test 2, but less than R/C COR test 1. For the connection (4V) reinforcement (the only reinforcement within the railing cross-section of both specimen types), the FRC specimen was found to have a higher strain than the two R/C specimens, as shown in Figure 6.70. Overall, the maximum strain in the reinforcement for any of the three tests is well below the rebar yield strain (2000 microstrain). A comparison of strain levels between each test (for external or internal gages) show that there was some variability between tests, even when comparing the two R/C COR tests. Overall, however, the results suggest that the FRC railing performed in a manner similar to the conventional R/C specimen.

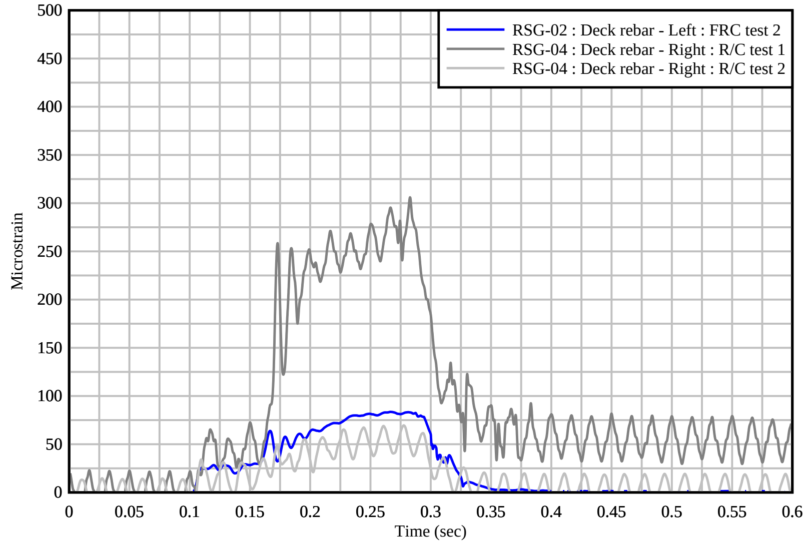

Figure 6.69 Comparison of internal strain gages located on the top deck rebar

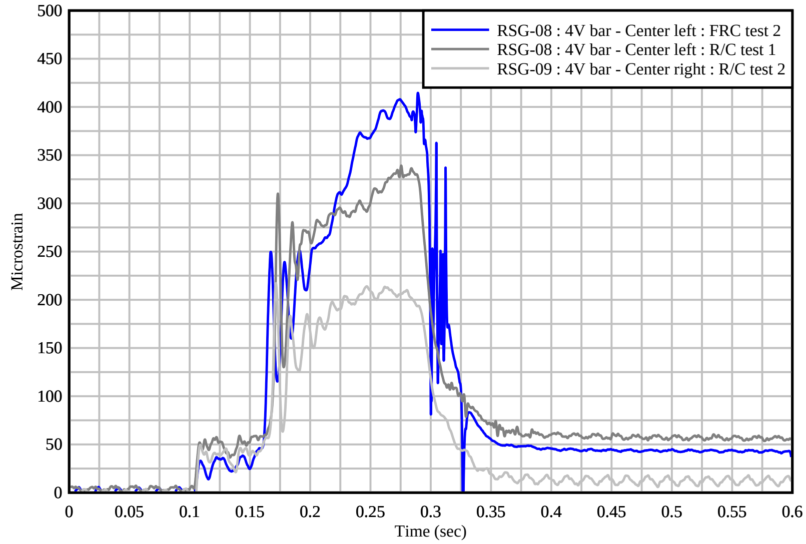

Figure 6.70 Comparison of internal strain gages located on the railing connection rebar

CHAPTER 7
FULL-SCALE END OF RAILING (EOR) IMPACT TEST RESULTS

7.1 Introduction

An ‘end of railing’ (EOR) test specimen configuration (Figure 7.1) was included in the impact test matrix to investigate the relative performance of FRC and R/C rails under end impact loading conditions. The EOR specimen configuration was shorter in length (8-ft) than the ‘center of railing’ (COR) specimen configuration discussed in the previous chapter. Additionally, each EOR specimen was only supported at one end (i.e., only one end-support buttress was used). The other end of the railing was free (i.e., without an end-support buttress), with the impact load applied near the free end. This test configuration was termed an ‘end of railing’ (EOR) impact configuration because it was used to evaluate the railing strength near a termination point of the railing (i.e., where the railing segment ends, which typically occurs at a construction joint or at the end of a bridge span).

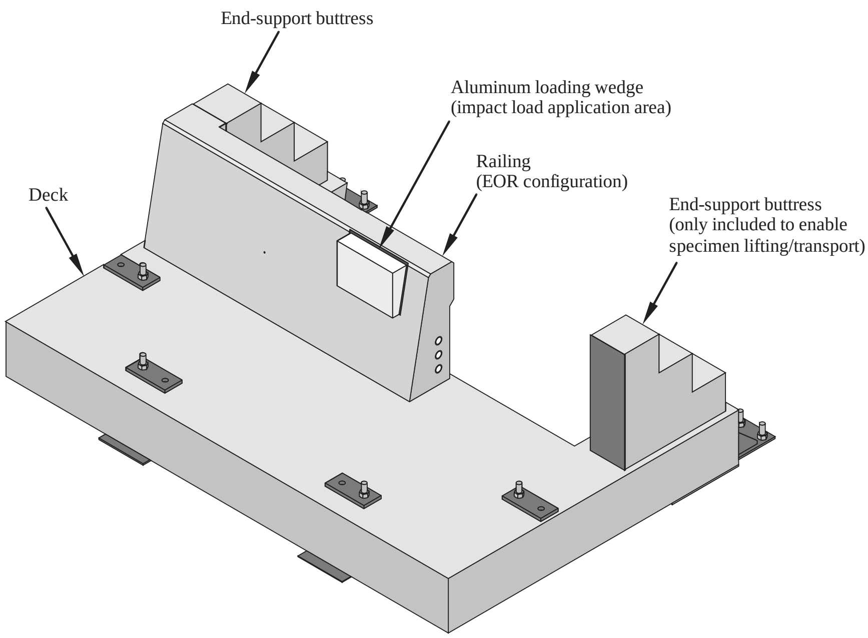

Figure 7.1 Main components of EOR specimen

In comparison to an interior impact location (i.e., a COR impact condition, where the impact occurs at an interior location along the railing length), if an impact occurs near the end of a railing segment, the railing capacity is reduced (because the impact occurs near an unsupported end) and the failure pattern is expected to follow the yield line failure pattern detailed in Section 13 of *AASHTO LRFD Bridge Design* (2017). Therefore, this additional configuration was employed to further investigate the capacity of the proposed FRC railing. This test was only added to the test matrix after confirming that the proposed FRC railing could withstand impact at an interior location (i.e., with a COR test). It was expected that the EOR impact tests would produce more damage in the railing (i.e., more concrete cracking) and higher deflection levels than the COR impact tests.

In this chapter, results from two full-scale railing impact tests are discussed, where one FRC EOR specimen and one R/C EOR specimen were tested (see Appendix G for EOR specimen construction drawings). Results for the EOR impact tests are organized by the two railing types (i.e., FRC and R/C railing) and are followed with a comparison of the EOR test results. A summary of the overall EOR test program is provided in Table 7.1. The instrumentation plan for the EOR configuration was similar to the COR test, with only a few gage locations changed (due to the shorter railing length and due to the different expected cracking pattern). External instrumentation components used during EOR tests are illustrated in Figure 7.2 (with additional instrumentation plans for EOR specimens detailed in Appendix I). Hardened mechanical properties for the concrete material used to cast and form each pendulum impact test specimen (such as concrete compressive strength) are provided in Appendix E.

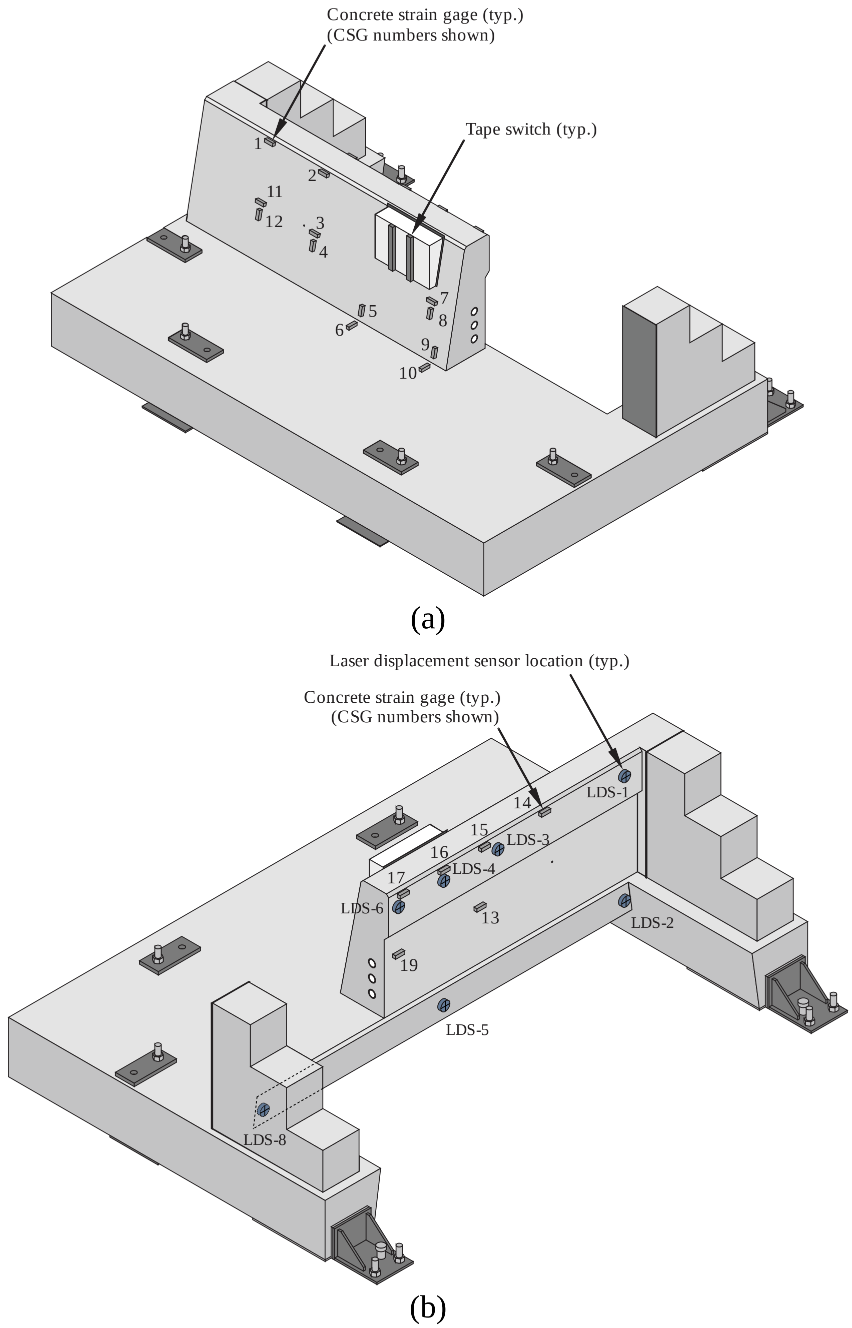

Figure 7.2 External EOR instrumentation: (a) Front concrete strain gage and tape switch sensor locations; (b) Back concrete strain gage and laser displacement sensor locations

Table 7.1 Full-scale EOR impact test summary

Impact test specimen	Test date	Drop height (ft)	Impact speed (mph) [ft/sec]	Impact energy (kip-ft)
FRC EOR 1 (FRC test 3)	2/23/2021	15	21.04 [30.9]	153.0
R/C EOR 1 (R/C test 3)	4/06/2021	15	20.99 [30.8]	152.0

7.2 FRC railing

7.2.1 Impact testing of FRC EOR specimen 1 (FRC test specimen 3)

On February 23, 2021, full-scale pendulum impact testing of the FRC EOR test specimen (FRC test specimen 3, Figure 7.3) was conducted—where the pendulum impactor was dropped from 15 ft. Instrumentation components included with the FRC EOR test specimen were accelerometers, break beams, high-speed cameras, tape switches, laser displacement sensors, internal reinforcement strain gages, and external concrete strain gages. Additional details of the instrumentation plan used during impact testing are provided in Appendix I.

Figure 7.3 FRC EOR specimen prepared and ready for pendulum impact testing (with instrumentation in place)

Sequential images taken from high-speed camera 1 (HSC-1) over the impact duration are provided in Figure 7.4, starting with the first instant of impact and including the point in time when the maximum crush depth on the crushable front nose (i.e., maximum impact force) was reached. Additional images from high-speed camera 2 (HSC-2) are provided in Figure 7.5, where no discernable sliding of the test specimen was observed. Photographs of the test specimen after completion of the impact test are shown in Figures 7.6 and 7.7.

For the FRC EOR test, diagonal cracks were found on the front and back faces of the railing and were similar to the predicted failure pattern in AASHTO LRFD (2017). Cracks found in the test specimen were marked with a black marker to more clearly document where cracking occurred (with photographs). The largest measured crack on the front (impact) face of the FRC EOR specimen was approximately 0.035-in. wide, located near the top of the railing and was the closest crack to the supported end. The largest crack on the back (non-impact) face of the railing was approximately 0.015-in. wide, near the free end of the railing.

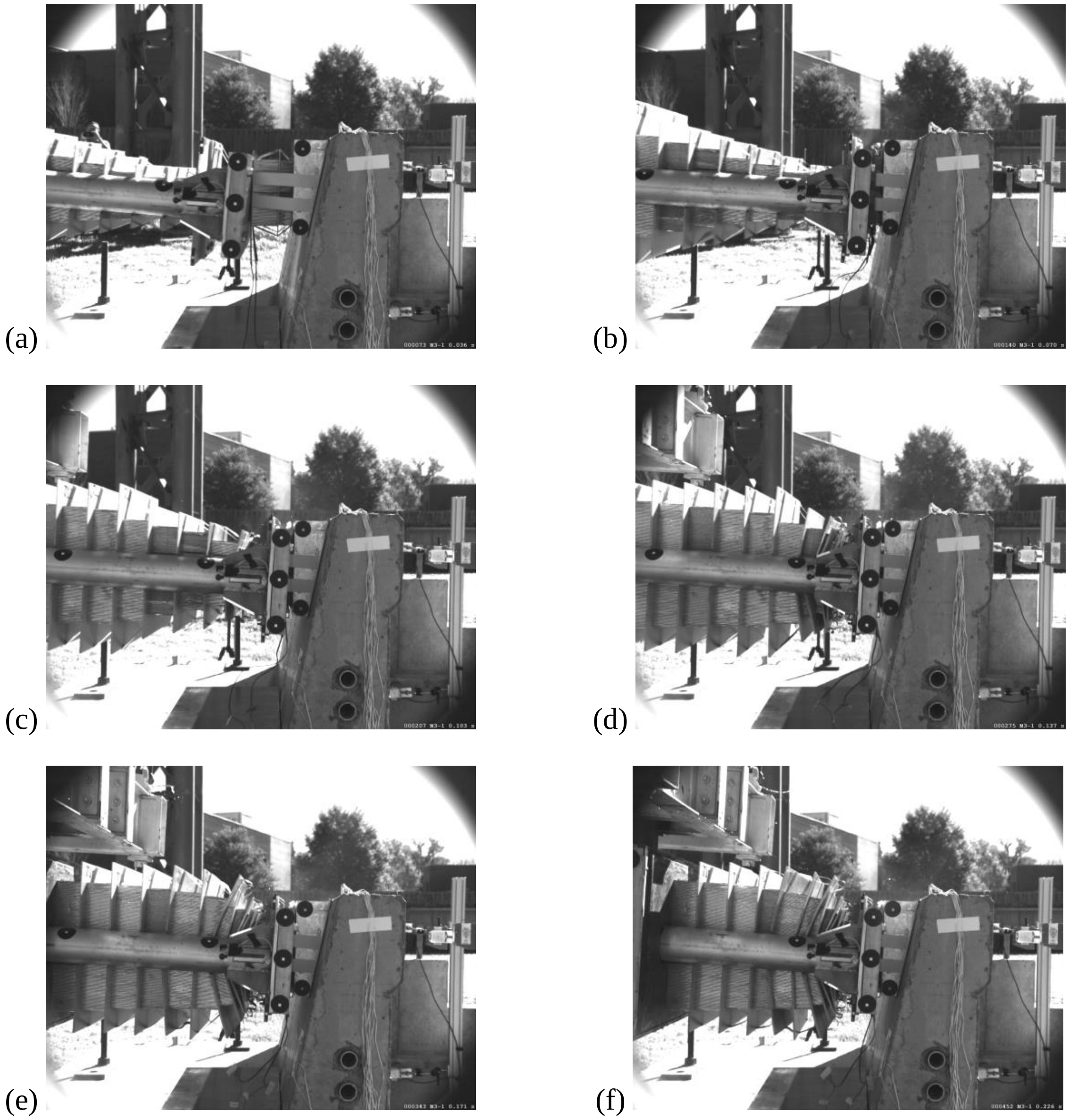

Figure 7.4 High-speed video frames from HSC-1 (FRC EOR test 1) showing crush deformation of aluminum honeycomb: (a) At initial impact; (b) – (e) Intermediate frames; (f) At peak impact force

(a) 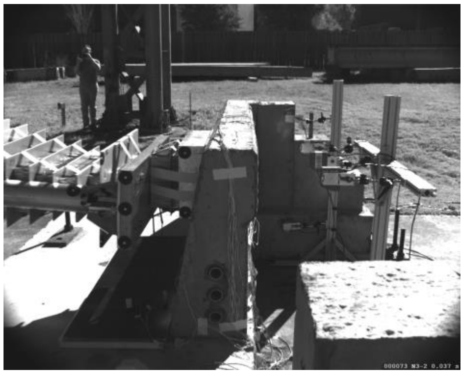 (b) 

(c) 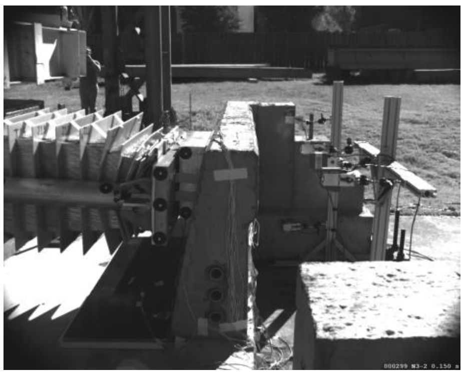 (d) 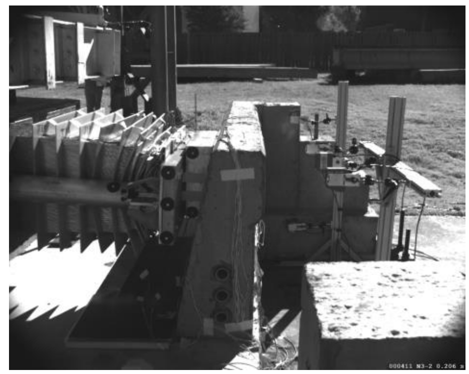

Figure 7.5 High-speed video frames from HSC-2 (FRC EOR test 1): (a) At start of impact; (b) – (c) Intermediate frames; (d) At peak impact force

Figure 7.6 FRC EOR test 1 specimen after completion of impact test

(a)

(b)

Figure 7.7 Cracking found on FRC EOR test 1 specimen: (a) On front railing face; (b) On back railing face

Break beam voltage data from FRC EOR impact test 1 are provided in Figure 7.8, and were used to quantify the impact velocity. For FRC EOR test 1, the impact velocity was determined to be 30.9 ft/sec—compared to the design impact velocity of 31.1 ft/sec (a 0.7% difference). Tape switch data are shown in Figure 7.9. Note that all impact test data has been shifted such that the initiation of impact begins at 0.1 s (using the spike in tape switch voltage).

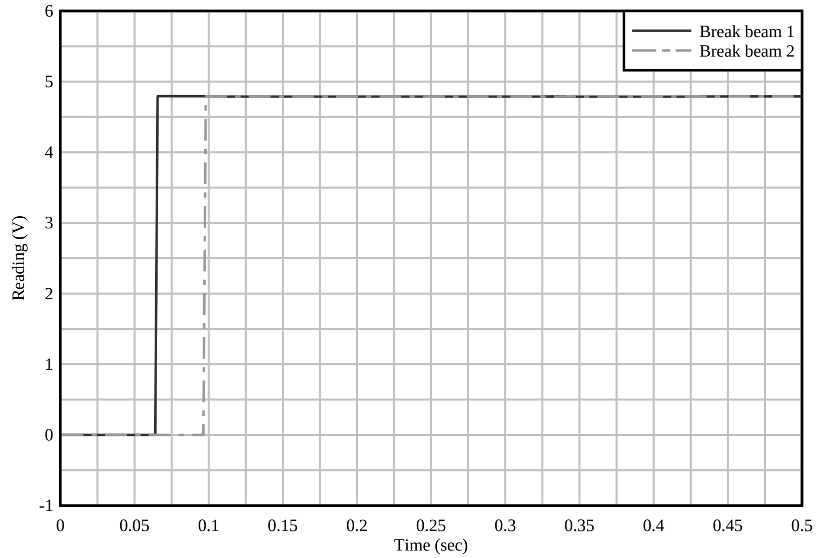

Figure 7.8 Break beam data for FRC EOR test 1

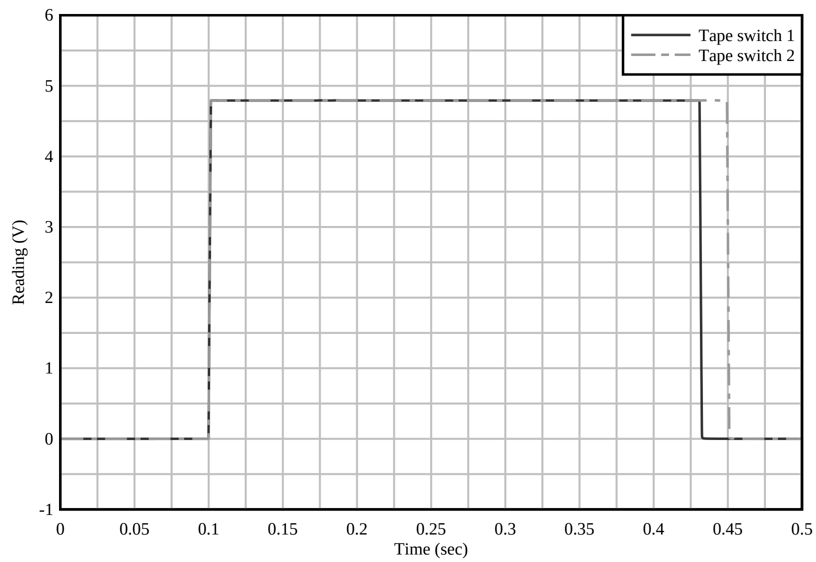

Figure 7.9 Tape switch data for FRC EOR test 1

Measured accelerations from the two accelerometers on the concrete back block (AC-1 & AC-2) in the impact direction (i.e., local Y direction of the accelerometer) are shown in Figure 7.10. Correspondingly, measured accelerations from the two accelerometers on the aluminum front nose (AC-3 & AC-4) in the impact direction (local Y direction) are shown in Figure 7.11. Computed and averaged back block impact forces (from AC-1 & AC-2) are shown in Figure 7.12, while the computed and averaged front nose impact forces (from AC-3 & AC-4) are shown in Figure 7.13.

The total applied impact force (computed by combining the averages of the back block and front nose) is shown in Figure 7.14. In comparison with the designed/predicted maximum impact forces (shown in Figure 7.15, which provides the predicted impact force over time from previous FEA impact simulations), the maximum observed impact force from FRC EOR test 1 was found to be 74.2 kip (7.8% greater than the originally designed 68.8-kip peak impact force, recall Figure 4.5 and Table 4.2).

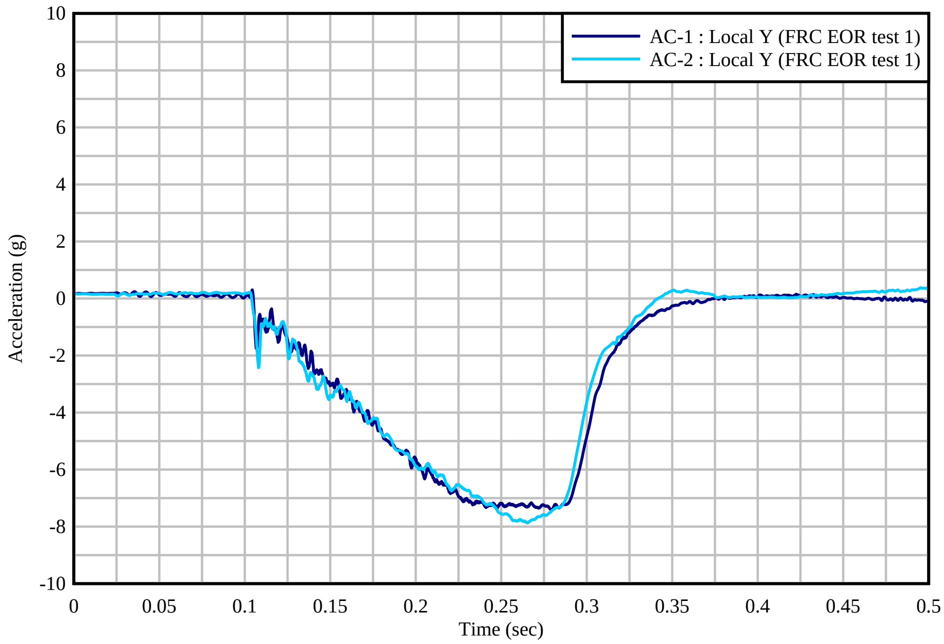

Figure 7.10 Raw concrete back block acceleration data (AC-1 & AC-2) for FRC EOR test 1 (in the impact direction, local Y direction of accelerometer)

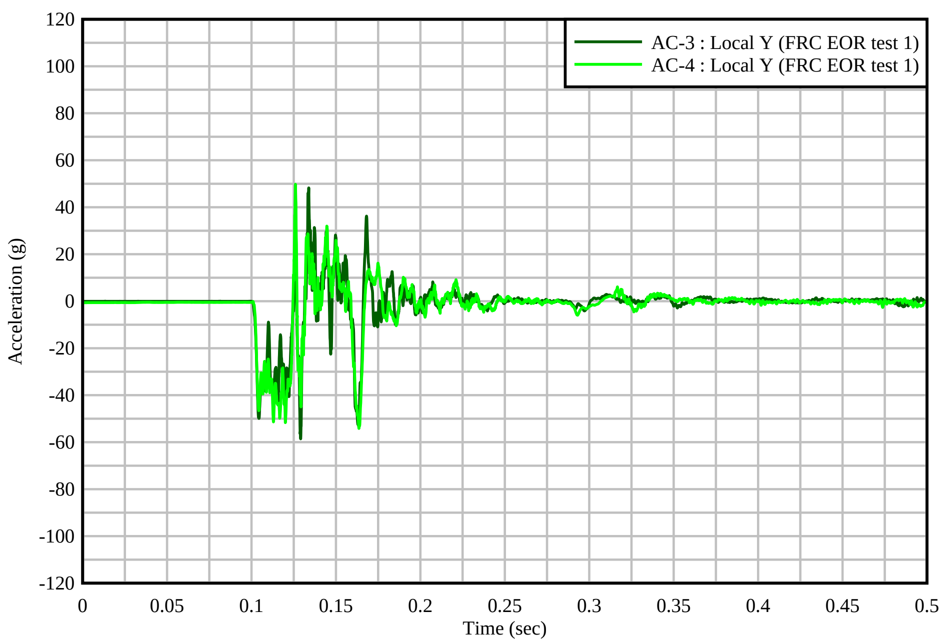

Figure 7.11 Raw front nose acceleration data (AC-3 & AC-4) for FRC EOR test 1 (in the impact direction, local Y direction of accelerometer)

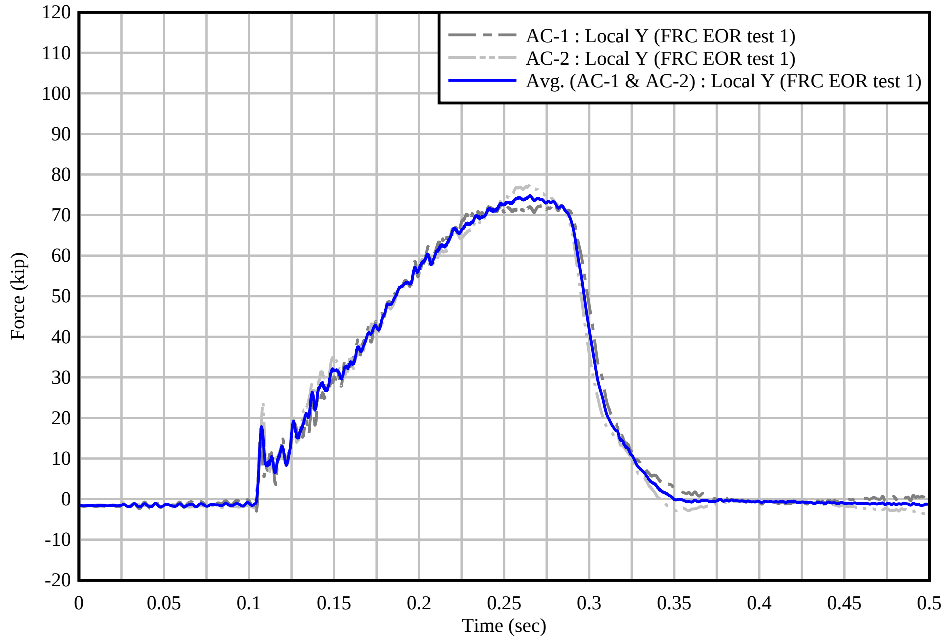

Figure 7.12 Computed impact forces from back block for FRC EOR test 1

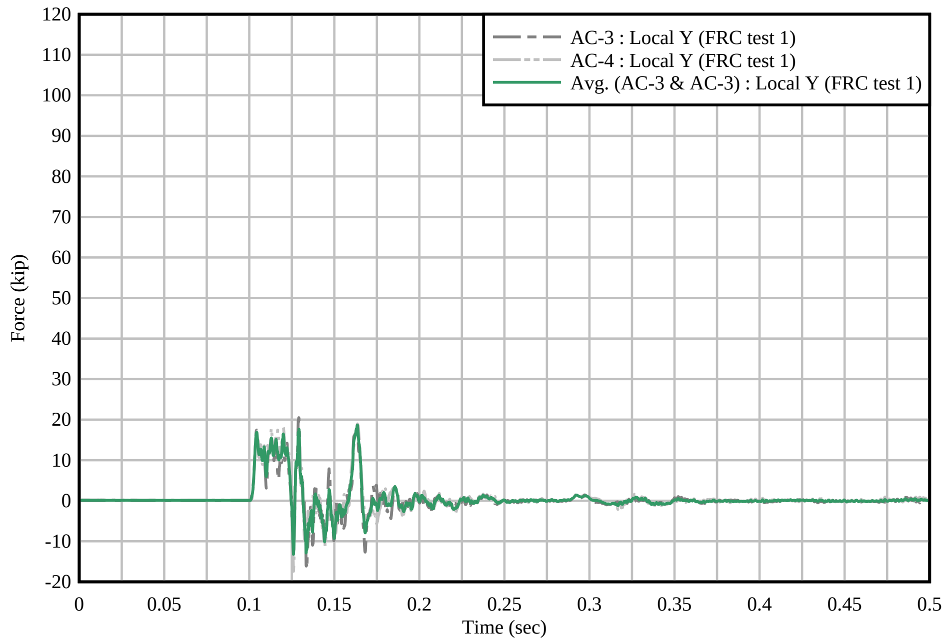

Figure 7.13 Computed impact forces from front nose for FRC EOR test 1

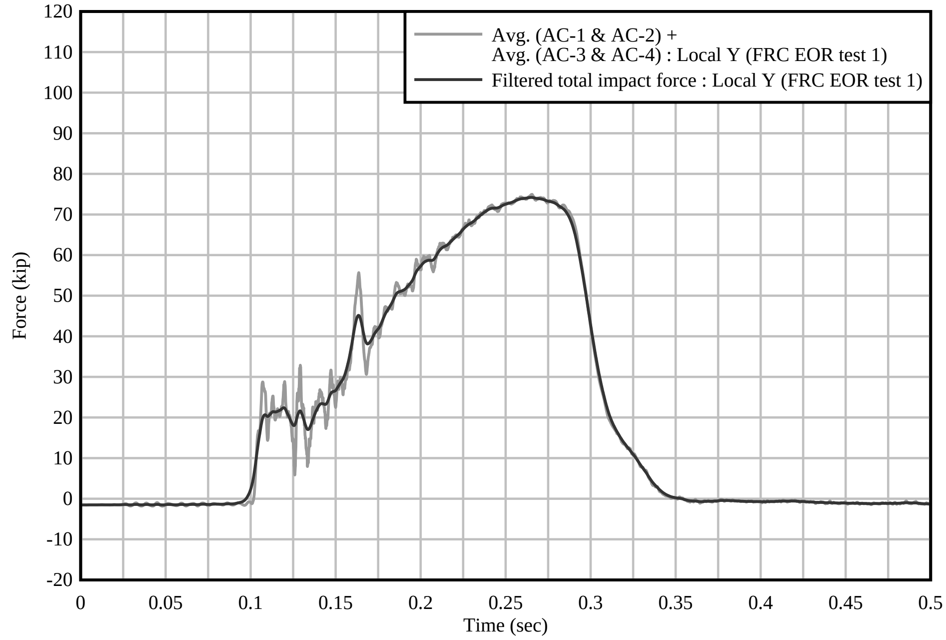

Figure 7.14 Raw and filtered total computed impact force for FRC EOR test 1

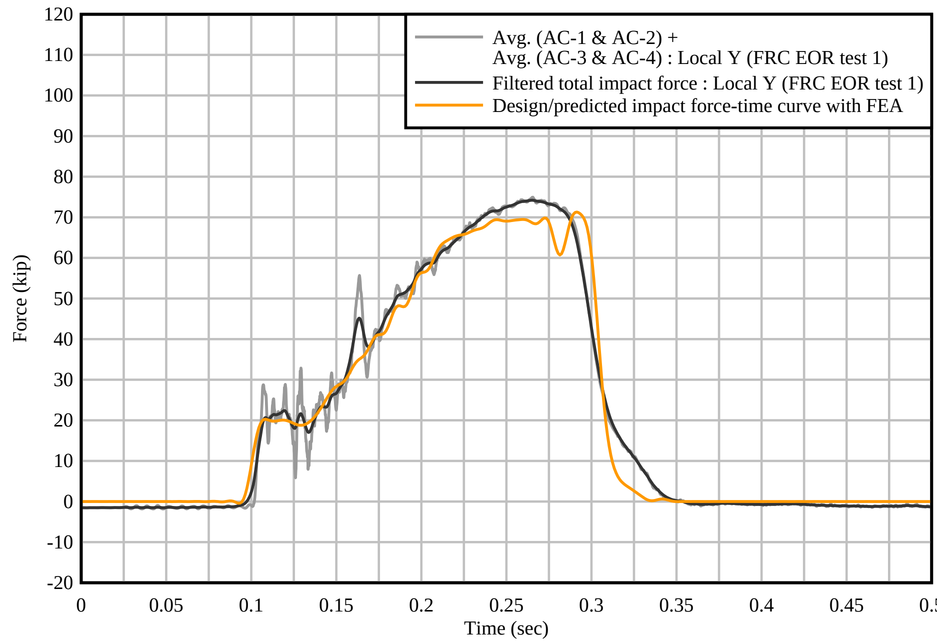

Figure 7.15 Filtered total experimental impact force for FRC EOR test 1 compared to FEA prediction

During the FRC EOR impact test, lateral deflections of the railing and any rigid sliding of the test specimen that occurred were captured with laser displacement sensors positioned behind the specimen. Further, external concrete strain measurements in the railing and deck were taken at locations along the front and back faces of the specimen. Specific locations of the laser displacement sensors (LDS) and external concrete strain gages (CSG) are depicted in Figure 7.2 (and further detailed in Appendix I).

Laser displacement data captured during FRC EOR test 1 are provided in Figure 7.16, where it is shown that the maximum displacement occurred at the free end of the railing (LDS-6) with a magnitude of 0.40 in., near the time at which the peak impact force was applied. After completion of the impact, the maximum railing displacement reduced to approximately 0.12 in. (LDS-6), indicating that some permanent deformation occurred. Displacement sensors located along the deck of the specimen (LDS-2 and LDS-5) were found to record negative displacement values, indicating that there was some movement (less than 0.1 in.) in the deck—positive values indicate that the location on the specimen moved towards the sensor and negative values indicate that the location on the specimen moved further away from the sensor. Without readings from LDS-8 (the only sensor: at the far end of the specimen; and, without a railing portion above the deck) and without additional sensor readings at the deck level, it was not possible to discern why there were inidications of a small permanent set in the LDS-5 data.

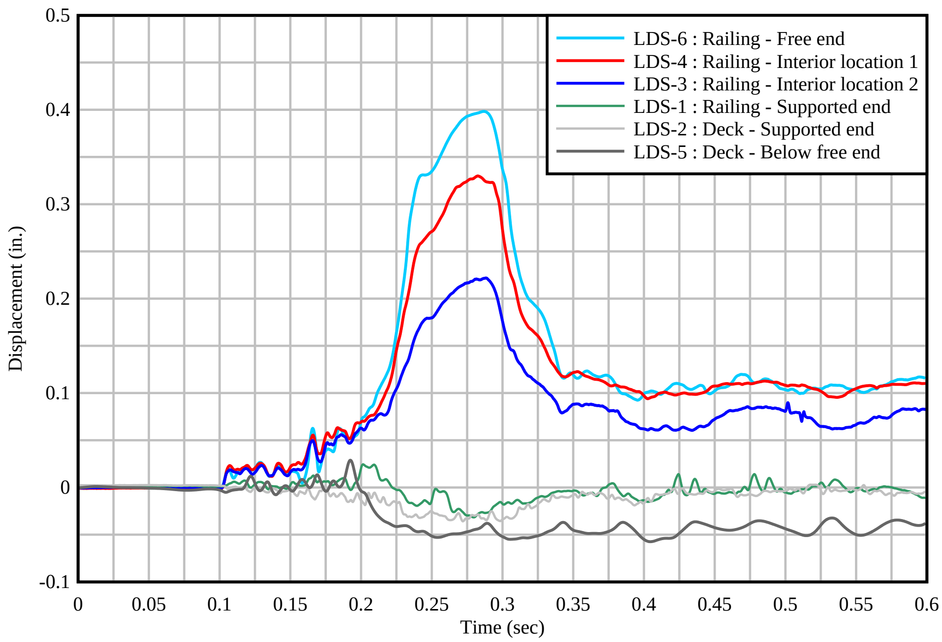

Figure 7.16 Laser displacement sensor data from FRC EOR test 1

External strain gage readings for the front (impact) face of the FRC EOR test are provided in Figures 7.17 and 7.18. As previously shown in Figure 7.7, diagonal cracks formed on the front face of the railing. As a result of the cracking, multiple concrete strain gages on the railing front face were found to reach the maximum gage limit. Once the gage limit was exceeded, readings from the gages were no longer accurate. Gage readings where the strain limit was reached (indicating that cracking occurred at the gage location) are shown in Figure 7.17, while the other (remaining) gages (with lower strain level readings) located on the front side of the EOR specimen are provided in Figure 7.18.

Strain readings for the back (non-impact) side of the FRC EOR are provided in Figure 7.19. Similar to the front side, CSG-16 was found to reach the maximum gage limit as a result of the cracking that formed on the back side of the railing. The remaining gages were found to record strain levels near or below the approximate rupture strain.

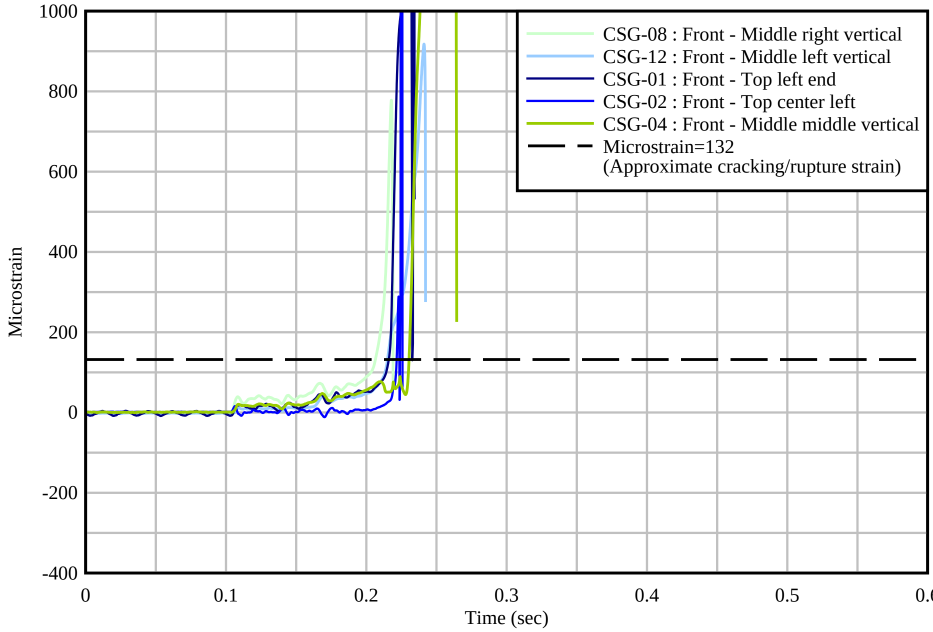

Figure 7.17 Concrete strain gage data for locations with out of range readings on the front face of the railing (due to cracking) for FRC EOR test 1

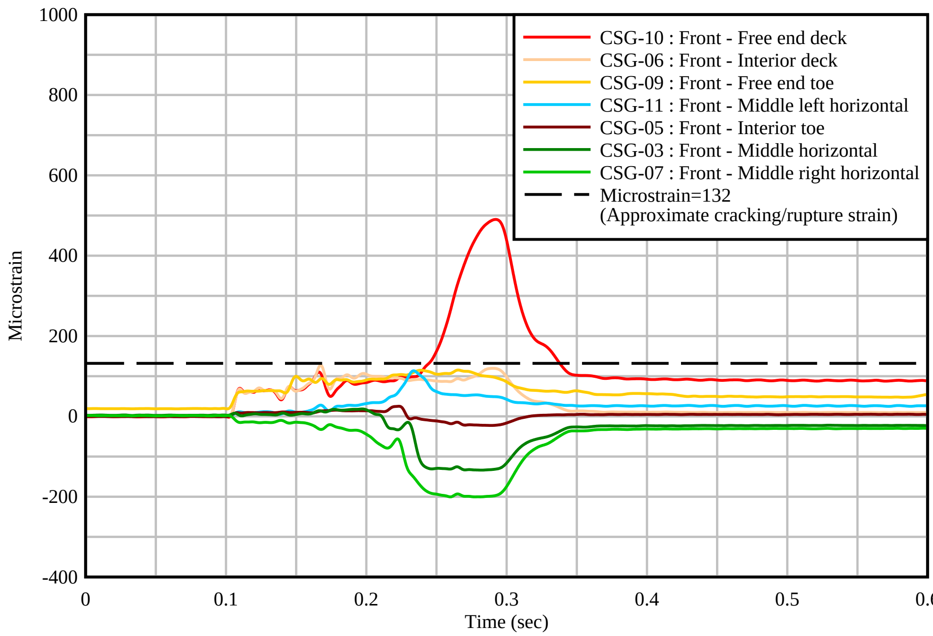

Figure 7.18 Concrete strain gage data for locations with in range readings on the front face of the railing for FRC EOR test 1

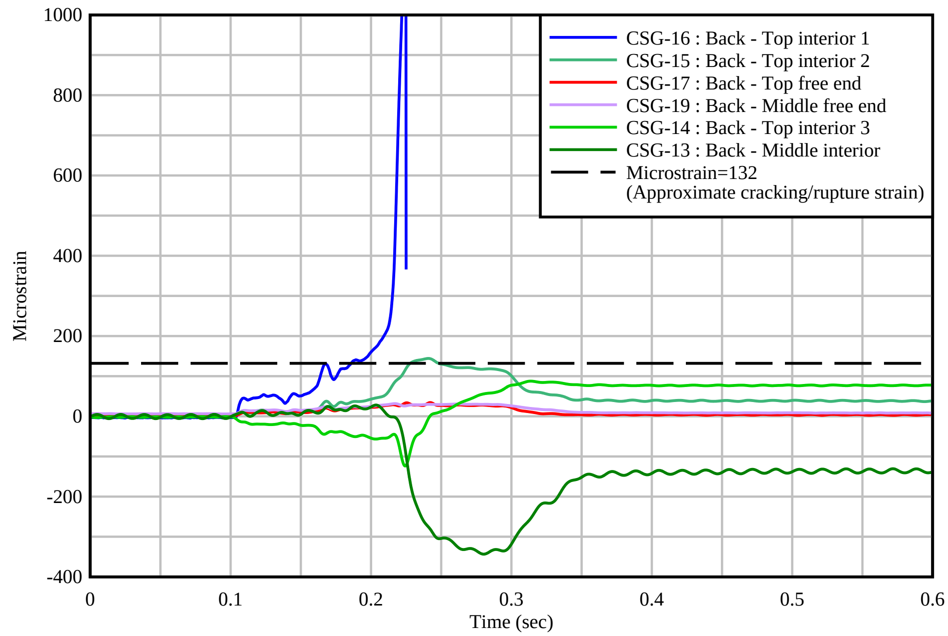

Figure 7.19 Concrete strain gage data for locations on the back (non-impact) face of the railing during FRC EOR test 1

Readings from rebar strain gages are provided in Figure 7.20. Note that two rebar strain gages (RSG-3 and RSG-7) are not included because the gages were damaged during the casting process and did not provide data during testing. Specific locations of the deck and connection (4V) rebar gages are provided in Appendix I. Maximum strain levels in the deck rebar (Figure 7.20a) were found to be below the yield strain (2000 microstrain). However, gages located on the 4V connection bars (connecting the railing to the deck) were found to reach strain levels above the yield strain of the rebar (Figure 7.20b), indicating that some permanent strain occurred.

As expected, some damage did occur in the FRC EOR impact test, but the specimen successfully resisted the designed impact. For purposes of comparison, a conventional R/C EOR specimen was impact tested and was used to determine the relative structural integrity of the FRC railing under an end segment impact condition.

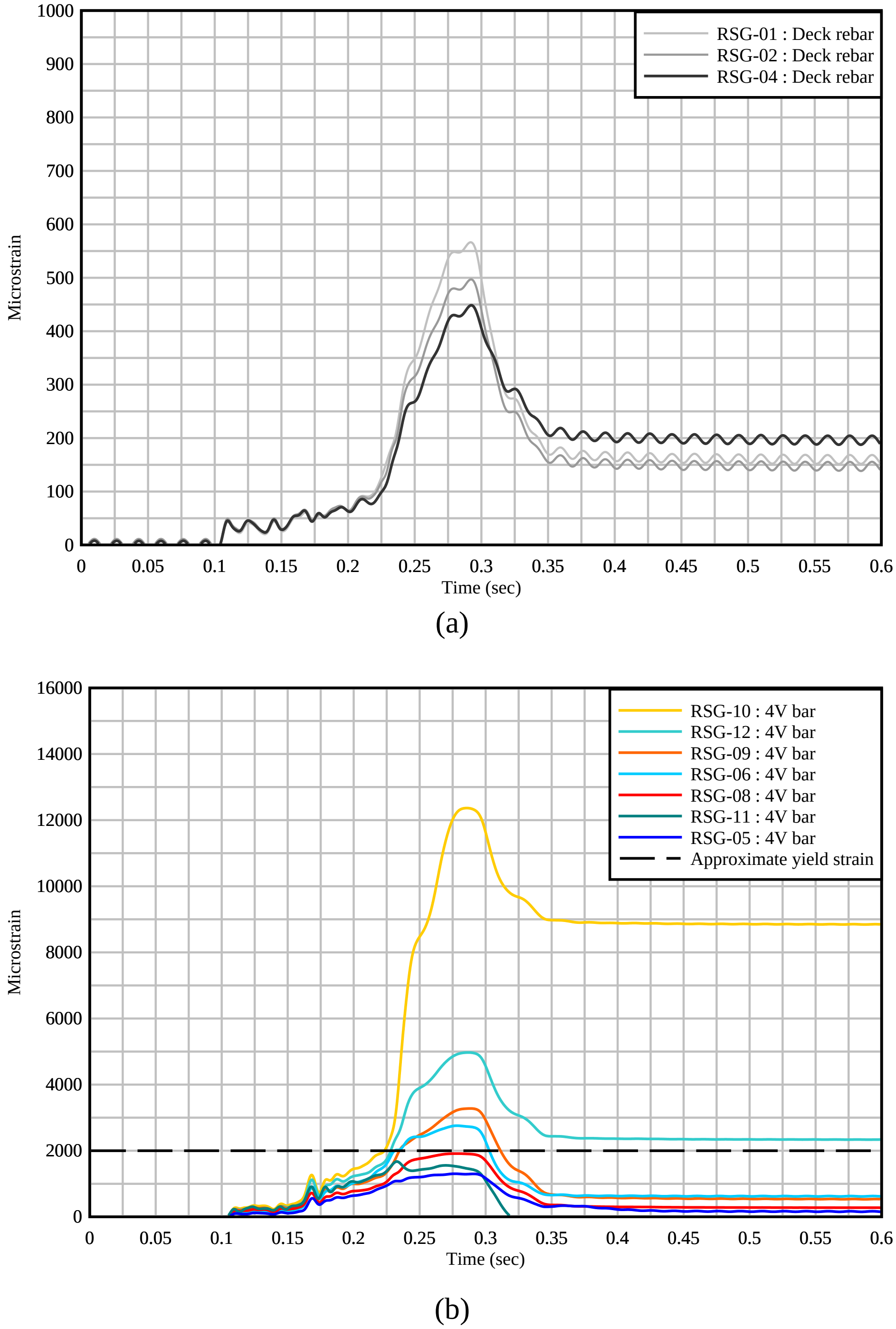

Figure 7.20 Internal rebar strain gage data during FRC EOR test 1:
(a) Deck rebar; (b) Railing rebar

7.3 Standard (R/C) railing

7.3.1 Impact testing of R/C EOR specimen 1 (R/C test specimen 3)

On April 6, 2021, full-scale pendulum impact testing of the R/C EOR test specimen (R/C test specimen 3) was conducted—where the pendulum impactor was dropped from 15 ft. Instrumentation components included with the R/C EOR test specimen were accelerometers, break beams, high-speed cameras, tape switches, laser displacement sensors, internal reinforcement strain gages, and external concrete strain gages. Additional details of the instrumentation plan used during impact testing are provided in Appendix I.

It should be noted that, in certain areas, concrete consolidation of the R/C EOR specimen was relatively poor due to inadequate concrete vibration during casting (producing a poor surface condition and areas of 'honeycombing' near the bottom of the railing, as shown in Figure 7.21). Because cast-in-place formwork was used, the poor quality of the concrete consolidation was not known until after the formwork was removed. Despite the honeycombing, it was decided that the specimen would still be used for testing. However, when comparing the R/C EOR test results to the FRC EOR results, it should be noted that the poor concrete consolidation may have caused some (small but unknown) reduction in the resistance strength of the R/C EOR specimen.

(a)

(b)

Figure 7.21 Poor concrete consolidation of R/C EOR specimen 1 prior to testing:
(a) Front face of railing; (b) Bottom of the (cross-sectional) railing face at free end

Sequential images taken from high-speed camera 1 (HSC-1) over the impact duration are provided in Figure 7.22, starting with the first instant of impact and including the point in time when the maximum crush depth on the crushable front nose (i.e., maximum impact force) was reached. Additional images from high-speed camera 2 (HSC-2) are provided in Figure 7.23, where no discernable sliding of the test specimen was observed. Photographs of the test specimen after completion of the impact test is shown in Figures 7.24 and 7.25.

For the R/C EOR test, diagonal cracks were found on the front and back faces of the railing (similar to the FRC EOR test). Cracks found in the test specimen were marked with a black marker to more clearly document where cracking occurred (with photographs). The largest measured crack on the front (impact) face of the FRC EOR specimen was approximately 0.015-in. wide, located near the top of the railing half-way between the end-support and the loading wedge. The largest crack on the back (non-impact) face of the railing was also approximately 0.015-in. wide, near the free end of the railing.

Figure 7.22 High-speed video frames from HSC-1 (R/C EOR test 1) showing crush deformation of aluminum honeycomb: (a) At initial impact; (b) – (e) Intermediate frames; (f) At peak impact force

(a)  (b) 

(c)  (d) 

Figure 7.23 High-speed video frames from HSC-2 (R/C EOR test 1): (a) At start of impact; (b) – (c) Intermediate frames; (d) At peak impact force

Figure 7.24 R/C EOR test 1 specimen after completion of impact test

(a)

(b)

Figure 7.25 Cracking found on R/C EOR test 1 specimen: (a) On front railing face; (b) On back railing face

Break beam voltage data from R/C EOR impact test 1 are provided in Figure 7.26, and were used to quantify the impact velocity. As shown in the instrumentation plan (Appendix I), two sets of break beams were placed in front of the impact test specimen at a 1-ft spacing. For each break beam, after the impactor was released and when the impactor crossed the path of the sensor, a change in voltage was observed. Since break beam 1 was placed 1 ft ahead of break beam 2, the duration of time over which the impactor moved 1 ft was quantified just prior to impact. For R/C EOR test 1, the impact velocity was determined to be 30.8 ft/sec—compared to the design impact velocity of 31.1 ft/sec (a 1.0% difference). Tape switch data were used to determine the time at which the impact began and are shown in Figure 7.27. Note that all impact test data has been shifted such that the initiation of impact begins at 0.1 s (using the spike in tape switch voltage).

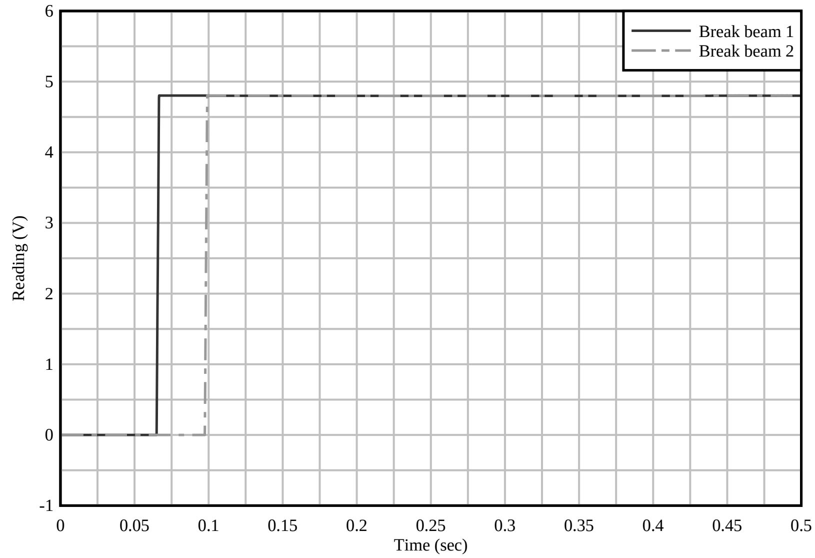

Figure 7.26 Break beam data for R/C EOR test 1

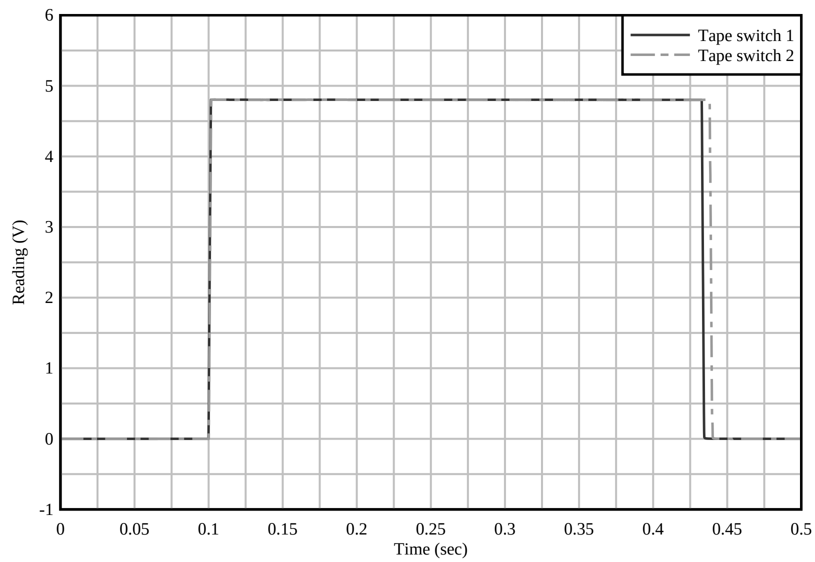

Figure 7.27 Tape switch data for R/C EOR test 1

Measured accelerations from the two accelerometers on the concrete back block (AC-1 & AC-2) in the impact direction (i.e., local Y direction of the accelerometer) are shown in Figure 7.28. Correspondingly, measured accelerations from the two accelerometers on the aluminum front nose (AC-3 & AC-4) in the impact direction (local Y direction) are shown in Figure 7.29. Computed and averaged back block impact forces (from AC-1 & AC-2) are shown in Figure 7.30, while the computed and averaged front nose impact forces (from AC-3 & AC-4) are shown in Figure 7.31.

The total applied impact force (computed by combining the averages of the back block and front nose) is shown in Figure 7.32. In comparison with the designed/predicted maximum impact forces (shown in Figure 7.33, which provides the predicted impact force over time from previous FEA impact simulations), the maximum observed impact force from R/C EOR test 1 was found to be 76.9 kip (11.7% greater than the originally designed 68.8-kip peak impact force).

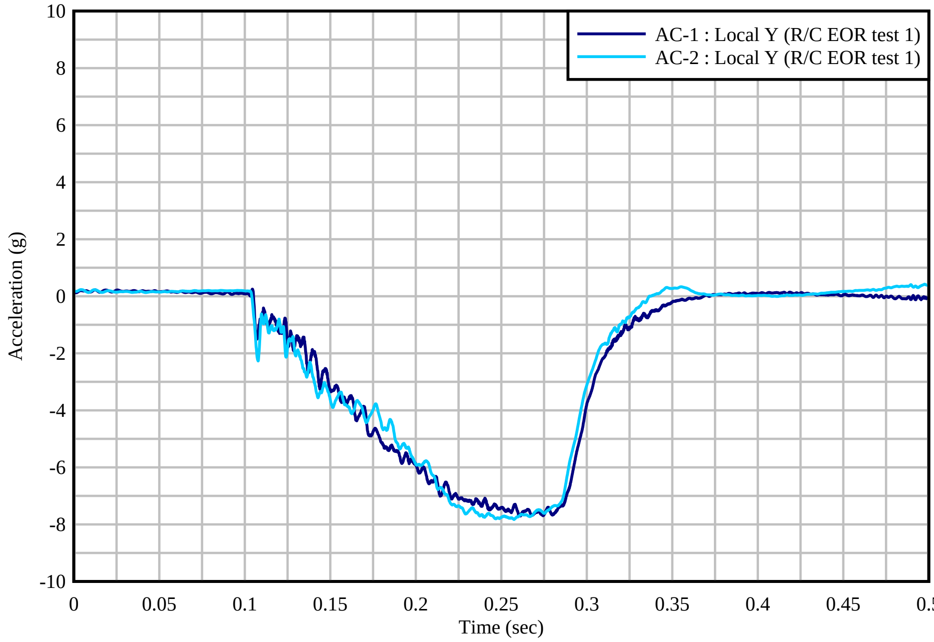

Figure 7.28 Raw concrete back block acceleration data (AC-1 & AC-2) for R/C EOR test 1 (in the impact direction, local Y direction of accelerometer)

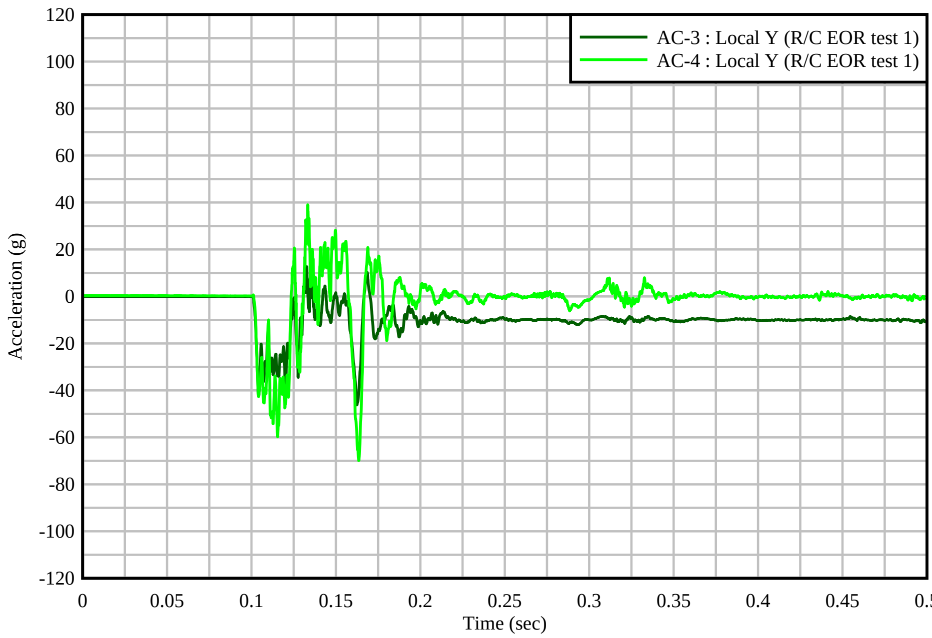

Figure 7.29 Raw front nose acceleration data (AC-3 & AC-4) for R/C COR test 1 (in the impact direction, local Y direction of accelerometer)

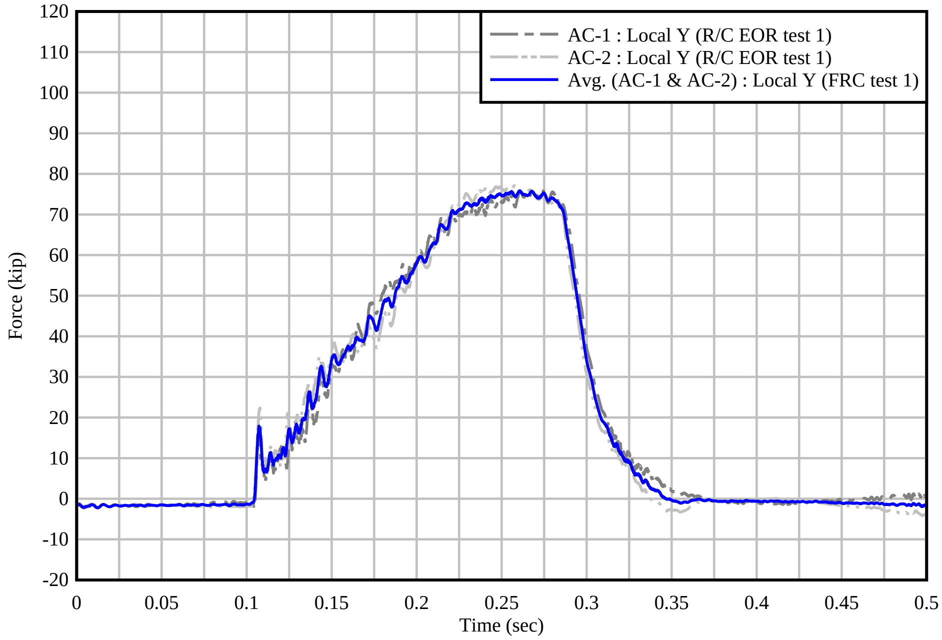

Figure 7.30 Computed impact forces from back block for R/C EOR test 1

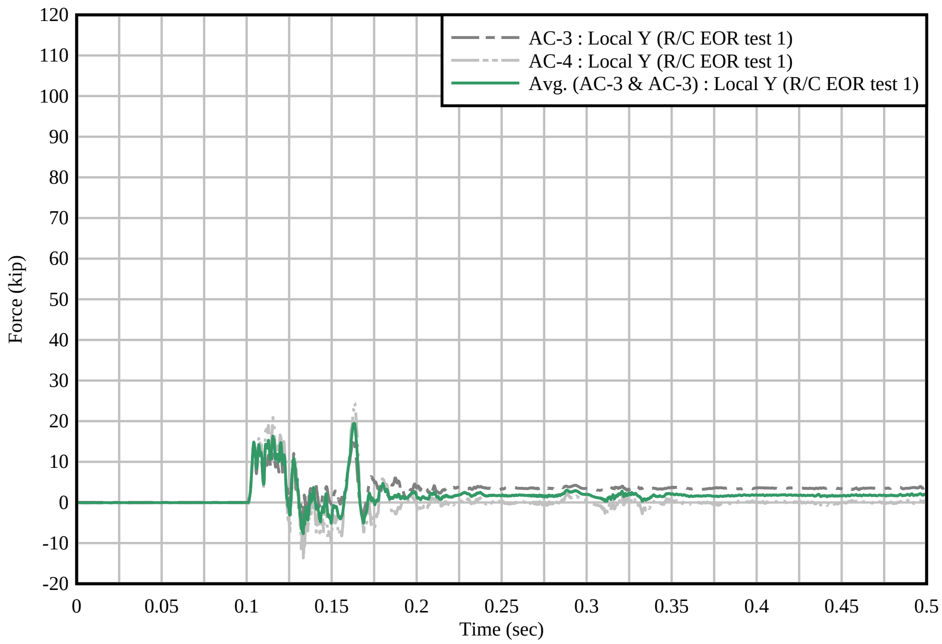

Figure 7.31 Computed impact forces from front nose for R/C EOR test 1

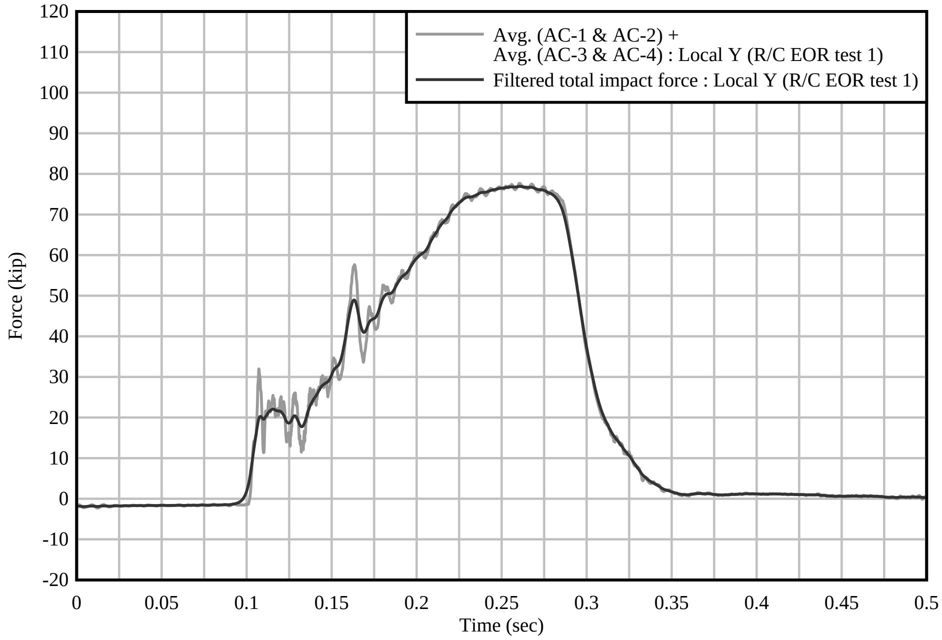

Figure 7.32 Raw and filtered total computed impact force for R/C EOR test 1

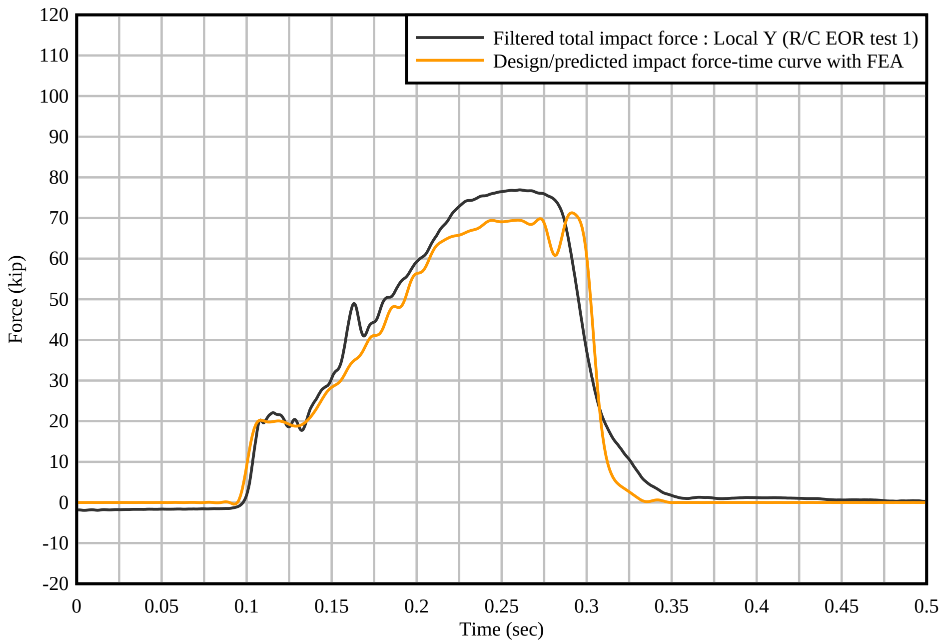

Figure 7.33 Filtered total experimental impact force for R/C EOR test 1 compared to FEA prediction

During the R/C EOR impact test, lateral deflections of the railing and any rigid sliding of the test specimen that occurred were captured with laser displacement sensors positioned behind the specimen. Further, external concrete strain measurements in the railing and deck were taken at locations along the front and back faces of the specimen. Specific locations of the laser displacement sensors (LDS) and external concrete strain gages (CSG) are depicted in Figure 7.2 (and further detailed in Appendix I).

Laser displacement data captured during R/C EOR test 1 are provided in Figure 7.34, where it is shown that the maximum displacement occurred at the free end of the railing (LDS-6) with a magnitude of 0.42 in., near the time at which the peak impact force was applied. After completion of the impact, the maximum railing displacement reduced to approximately 0.14 in. (LDS-6), indicating that some permanent deformation occurred. Displacement sensors located along the deck of the specimen (LDS-2, LDS-5, and LDS-8) were found to record negative displacement values, indicating that there was some movement (less than 0.1 in.) in the deck—positive values indicate that the location on the specimen moved towards the sensor and negative values indicate that the location on the specimen moved further away from the sensor.

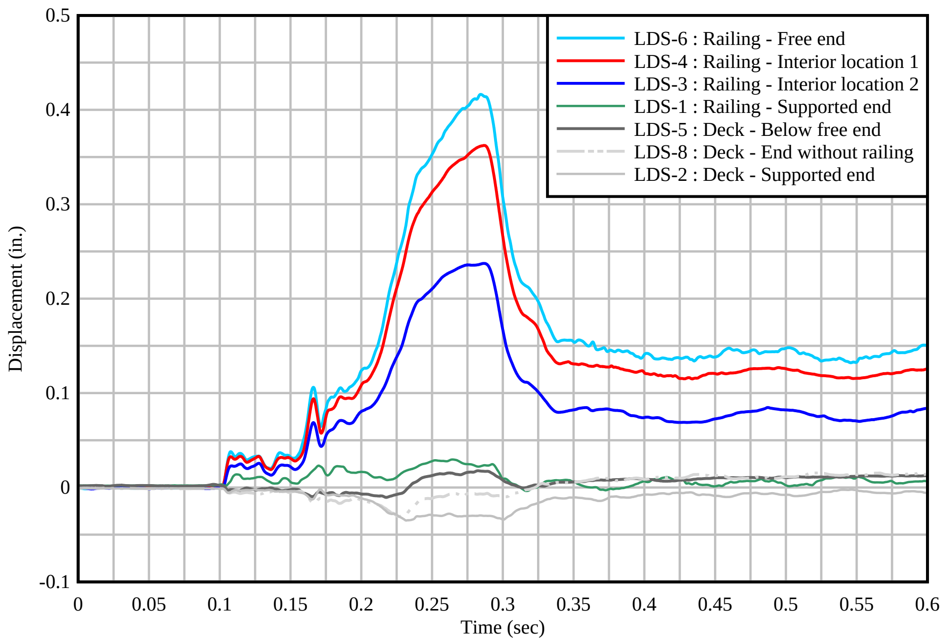

Figure 7.34 Laser displacement sensor data from R/C EOR test 1

Concrete strain gage readings for the front (impact) face of the R/C EOR test are provided in Figures 7.35 and 7.36. As previously mentioned, the surface condition of the R/C EOR specimen near the toe of the railing was relatively poor due to inadequate consolidation during casting. Consequently, a number of the concrete strain gages were shifted upwards (by about 3 in.) to ensure that the gages were properly adhered to the surface.

As previously shown in Figure 7.25, cracks formed on the front face of the railing. As a result of the cracking, a few of the concrete strain gages on the railing front face were found to reach the maximum gage limit. Once the gage limit was exceeded, readings from the gages were no longer accurate. Gage readings where the strain limit was reached (indicating that cracking occurred at the gage location) are shown in Figure 7.35, while the other (remaining) gages (with lower strain level readings) located on the front face of the EOR specimen are provided in Figure 7.36.

Concrete strain readings for the back (non-impact) face of the R/C EOR are provided in Figure 7.37. Unlike the front side, no back-side gages were found to reach the maximum gage limit as a result of the cracking, and all back-side strain readings were near or below the approximate concrete tensile rupture strain.

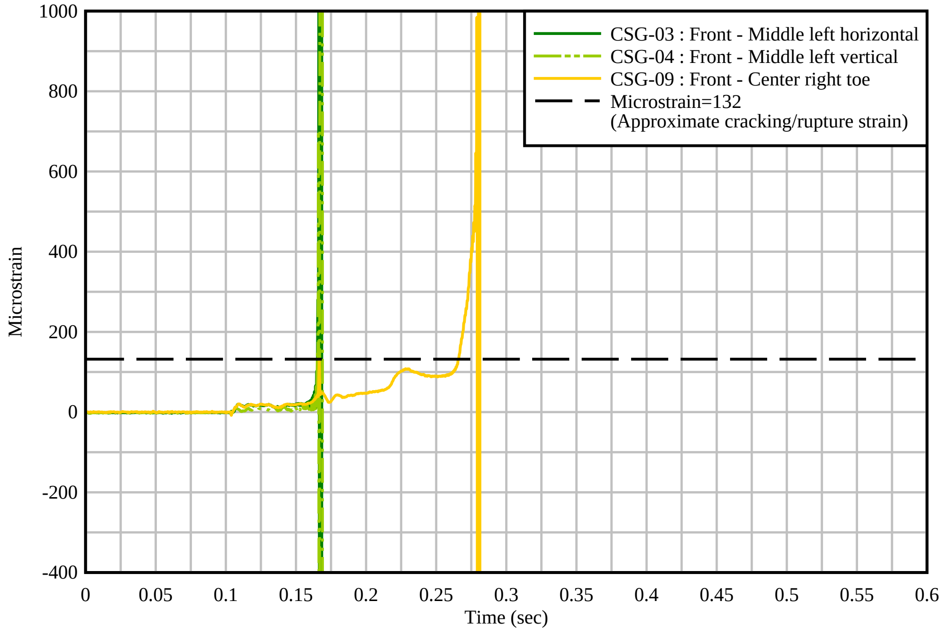

Figure 7.35 Concrete strain gage data for locations with out of range readings on the front face of the railing (due to cracking) for R/C EOR test 1

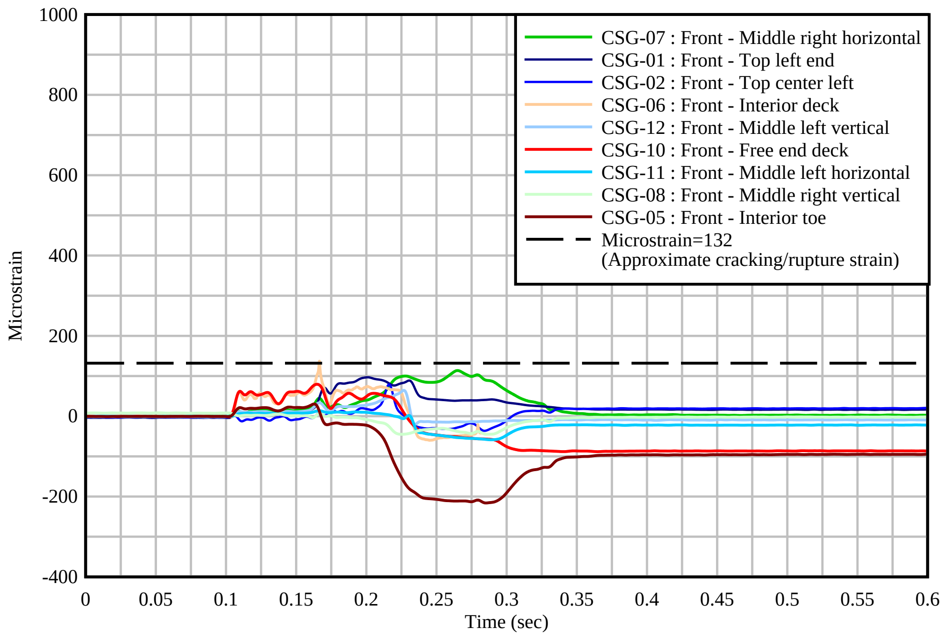

Figure 7.36 Concrete strain gage data for locations with in range readings on the front face of the railing for R/C EOR test 1

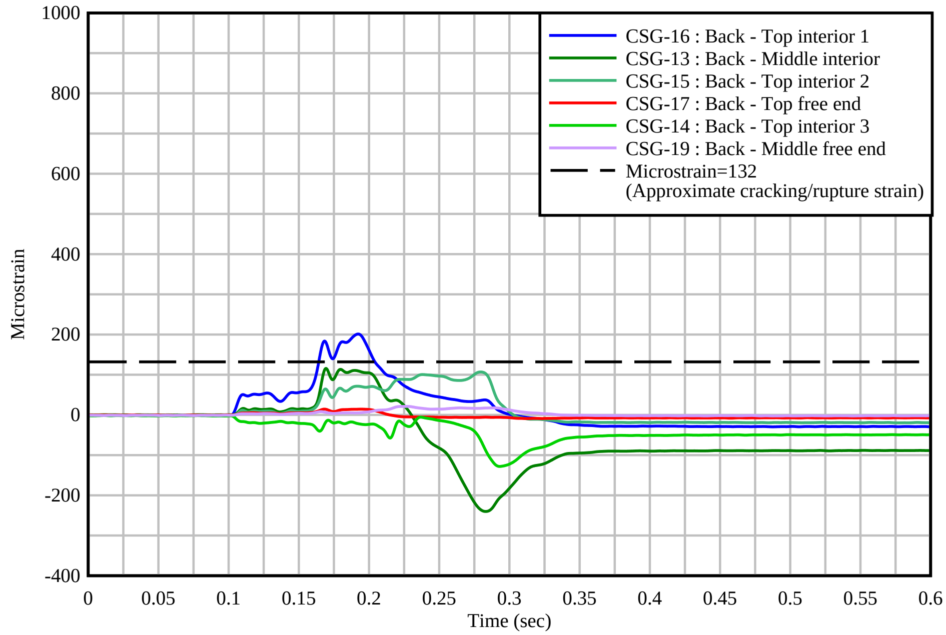

Figure 7.37 External concrete strain gage data for locations on the back face of the railing during R/C EOR test 1

Readings from internal rebar strain gages are provided in Figure 7.38. Specific locations of the deck and connection (4V) rebar gages are provided in Appendix I. Maximum strain levels in the deck rebar (Figure 7.38a) were found to be below the steel yield strain (2000 microstrain). However, a number of gages located on the 4V connection bars (connecting the railing to the deck) were found to reach strain levels above the rebar yield strain (Figure 7.38b), indicating that some permanent strain occurred.

As expected, some damage did occur in the R/C EOR impact test, but the specimen successfully resisted the designed impact. For purposes of evaluating the structural adequacy of the FRC EOR specimen, test results from both EOR impact tests (FRC and R/C) are compared in the following section.

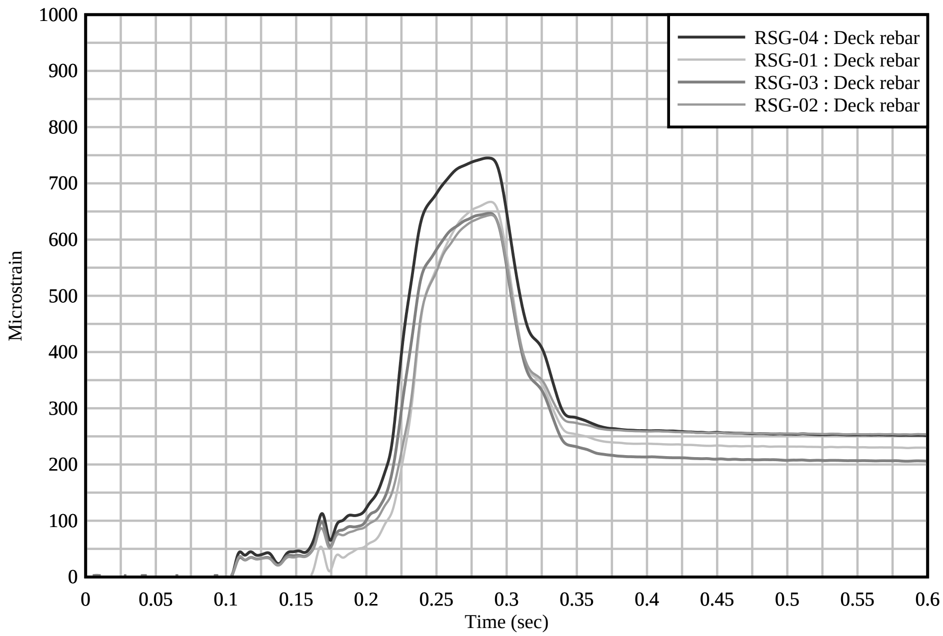

(a)

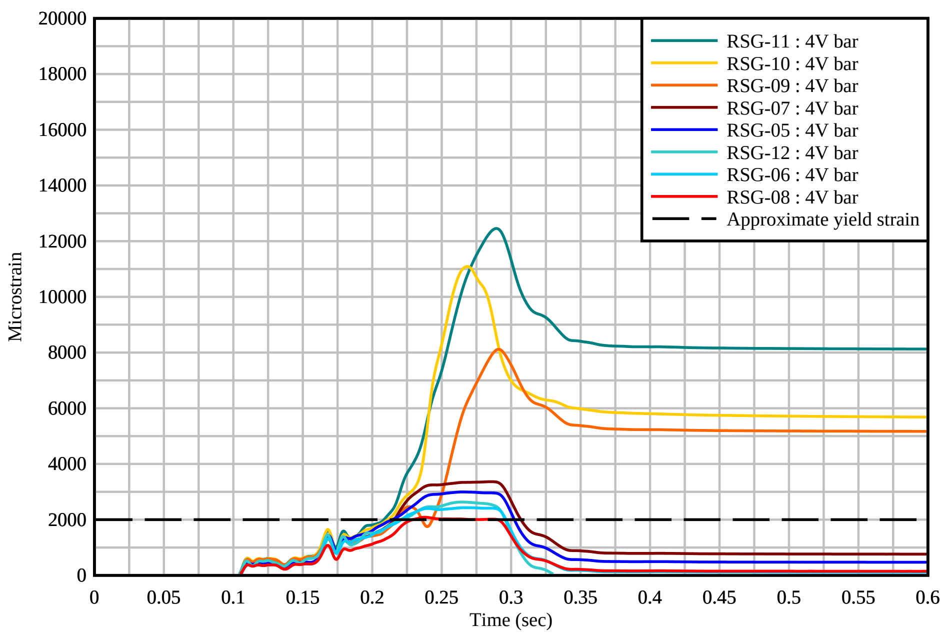

(b)

Figure 7.38 Internal rebar strain gage data during R/C EOR test 1:
(a) Deck rebar; (b) Railing rebar

7.4 Comparison of FRC and R/C EOR test specimen results

Selected data from testing of both EOR specimen types are compared, to evaluate the performance of the proposed FRC railing and to establish whether the FRC railing system was structurally similar to the traditional R/C FDOT railing.

7.4.1 Overview

As discussed, the following EOR specimen configurations were pendulum impact tested:

- Fully-instrumented FRC EOR test specimen 1
- Fully-instrumented R/C EOR test specimen 1

Although some differences were found when comparing test results of the two EOR types, the FRC EOR specimen performed adequately, withstanding the designed impact condition, as did the R/C EOR specimen. In the following sections, recorded data are compared, providing evidence that the proposed FRC railing is structurally similar to the conventional R/C FDOT railing.

7.4.2 Comparison of EOR acceleration data and pendulum impact forces

For each of the two EOR tests, accelerometers located on the pendulum impactor were used to measure deceleration of the impactor over the duration of impact. Acceleration data were subsequently used to compute the impact force applied to each test specimen. As shown in Figure 7.39, a similar force-time curve was achieved with each of the two tests and each test was found to adequately follow the designed force-time curve—which was intended to produce impact forces similar to the transverse component of a TL-4 vehicle impact test.

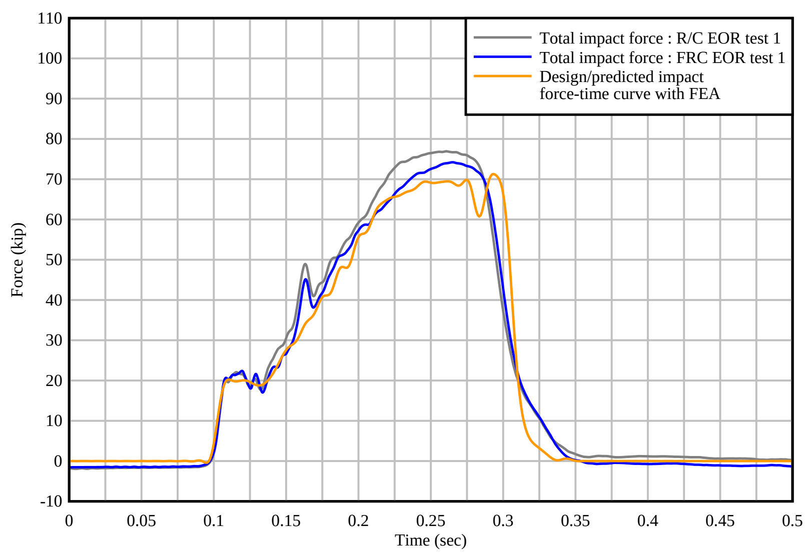

Figure 7.39 Total impact force for each traffic railing impact test

7.4.3 Comparison of EOR laser displacement data

For FRC EOR test 1 and R/C EOR test 1, laser displacement sensors were used to capture lateral deflections at various locations on the back face of the railing. As opposed to comparing all LDS data from the two available tests, the three gages closest to the free end of the EOR specimen (LDS-3, LDS-4, LDS-6)—which were found to have the highest displacement levels—are compared between the two EOR specimen types in Figure 7.40 (refer to Figure 7.2 for specific gage locations). As shown, the displacement levels were similar in magnitude at each set of corresponding gage locations for tests. Such similarities of displacement indicate that the FRC railing performed in a manner that was structurally similar to the R/C railing.

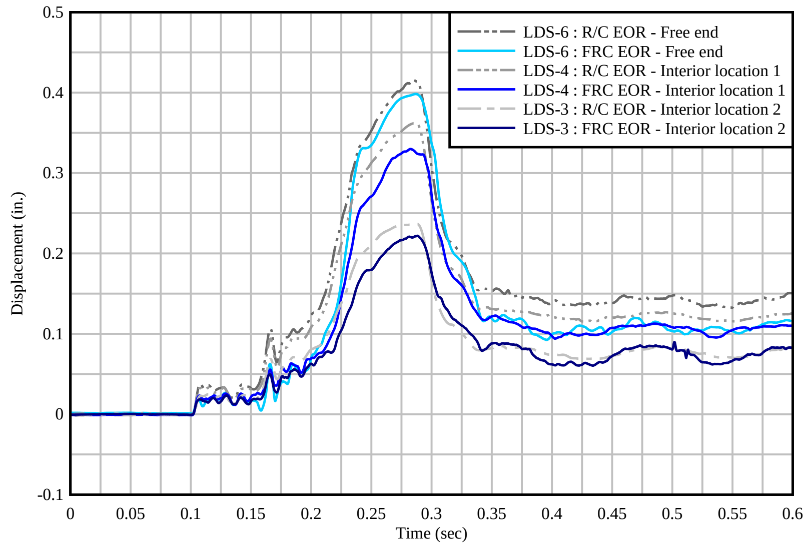

Figure 7.40 Comparison of displacements

7.4.4 Comparison of EOR external concrete strain gage data and cracking patterns

It is difficult to compare external strain gage data between the two EOR types for a number of reasons. Mainly, gage readings for some critical locations on the FRC EOR specimen were found to reach maximum strain limits of the gages, limiting the available concrete strain data. However, concrete gages with the highest reading levels (that did not exceed the gage limit, due to cracking) in the FRC EOR test—located on the deck near the toe of the railing—are compared with the R/C EOR test in Figure 7.41. Smaller deck surface strains were measured on the R/C EOR specimen than on the FRC specimen, possibly as a result of honeycombing in the R/C specimen and consequent compromised surface integrity at the rail-to-deck interface. Another possibility is that cracks may have formed in the deck under the gages to such a degree as to have a more significant effect on the FRC gage as compared to that of the R/C gage, thus leading to a marked and unexpected difference in strain measurements. Nevertheless, barrier crack patterns were found to be comparable in both EOR specimen types (as shown in Figures 7.42 and 7.43), indicating the similar structural behavior of the two specimens.

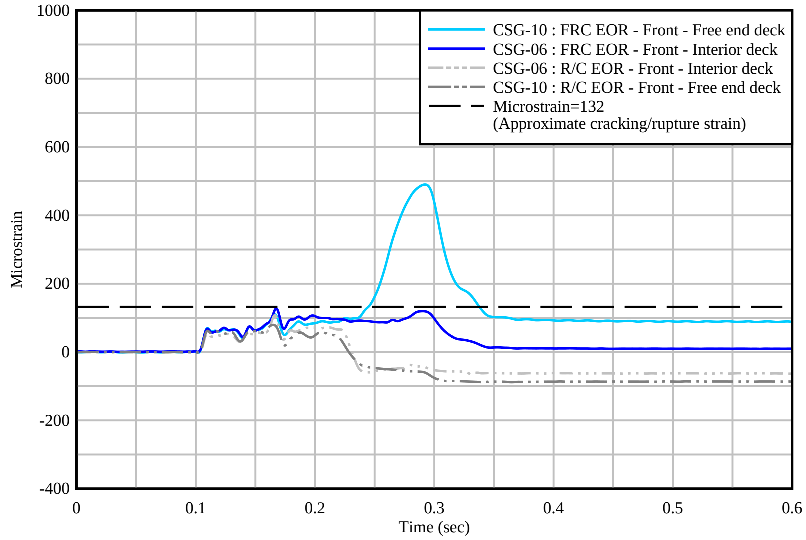

Figure 7.41 Comparison of external concrete strain gages on the deck near the railing toe

(a)

(b)

Figure 7.42 Comparison of crack pattern on the front (impact) face of EOR railing specimens: (a) FRC EOR specimen; (b) R/C EOR specimen

(a)

(b)

Figure 7.43 Comparison of crack pattern on the back (non-impact) face of EOR railing specimens: (a) FRC EOR specimen; (b) R/C EOR specimen

7.4.5 Comparison of EOR internal steel rebar strain gage data

As with the external concrete strain gages, only selected strain measurements from internal gages located on steel reinforcing bars are compared between the two EOR tests. Deck rebar strain readings are compared in Figure 7.44, where it is shown that the R/C test strains were relatively larger than the FRC EOR test strains. Similarly, comparing the connection (4V) reinforcement (the only reinforcement within the railing cross-section of both specimen types), the R/C and FRC specimens had similar maximum strain levels as shown in Figure 7.45 (i.e., comparing RSG-10 FRC data to RSG-11 R/C data). Overall, the rebar strain levels in both specimen types were generally similar, which suggest that the FRC railing performed in a manner similar to the conventional R/C specimen.

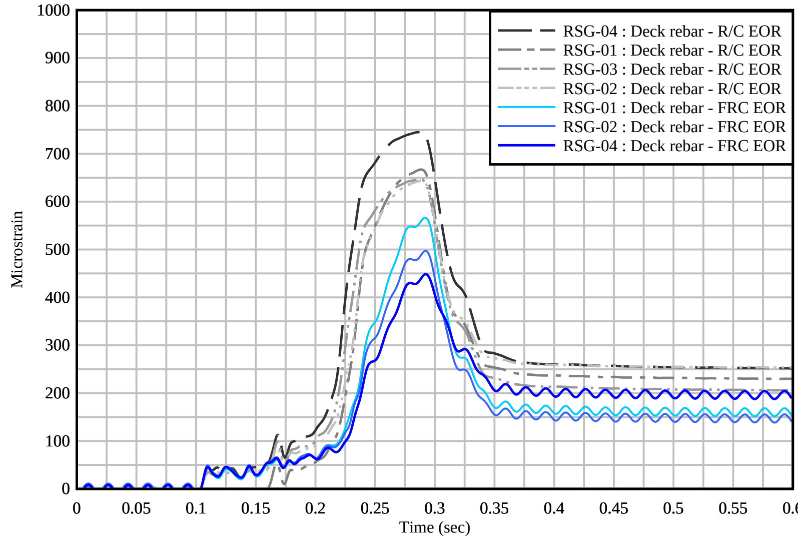

Figure 7.44 Comparison of internal strain gages located on the top deck rebar

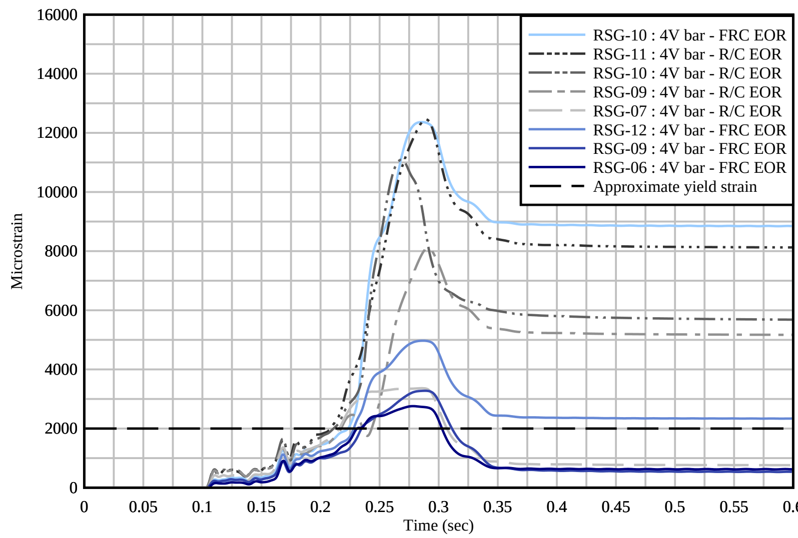

Figure 7.45 Comparison of internal strain gages located on the railing connection rebar

CHAPTER 8
SUMMARY, CONCLUSIONS, RECOMMENDATIONS, AND FUTURE DIRECTIONS

8.1 Summary and conclusions

In the present study, FRC was investigated as a possible means of reducing the quantity of steel reinforcing bars within a concrete traffic railing by using steel fibers to augment the typical deck-to-railing connection rebar for impact strength. Due to the wide variety of commercially available fibers, a number of different types of fibers were considered and evaluated for the proposed application. Based on the evaluated mechanical properties of the designed trial FRC mixtures (which were derived from a conventional slip-form concrete railing mixture, and were developed with the consideration of slip-form applications), an FRC mixture employing 2-in. long hooked-end steel fiber with a 1% fiber volume was selected for full-scale FRC railing impact testing.

To facilitate direct comparisons between the proposed FRC traffic railing and a conventional R/C railing, test specimens of each configuration with an integrated bridge deck were pendulum impact tested. The pendulum impactor and test protocols used during impact testing were developed and designed in the present study to deliver similar impact conditions to those prescribed in AASHTO LRFD and AASHTO MASH for a TL-4 vehicle impact.

As was shown with large-scale pendulum impact testing, the proposed FRC railing was largely successful and the FRC railing specimens performed adequately, each withstanding the designed impact, as did the conventional R/C railing specimens. As a result of the similarities discussed between the FRC and R/C railing specimens that were pendulum impact tested, it is concluded that the developed FRC railing (repeated in Figure 8.1, employing the FRC mixture detailed in Table 8.1) exhibits comparable structural strength to the conventional R/C railing and may be considered for future implementation (i.e., installed on roadways).

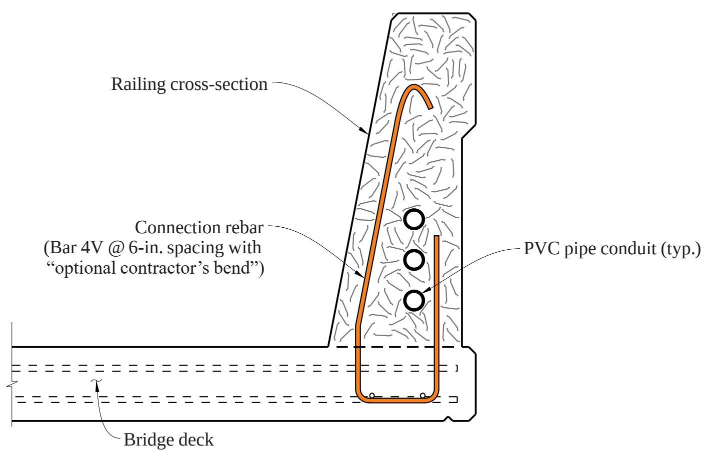

Figure 8.1 Final (investigated) FRC 36-in. single-slope traffic railing

Table 8.1 Mixture constituents and proportions for the final (developed) FRC mixture design

Product	Quantity	Units
Cement – Type IL	424	lb/cy
Fly Ash – Class F	133	lb/cy
#67 Stone – Coarse aggregate	1535	lb/cy
Silica Sand – Fine aggregate	1608	lb/cy
Water	267	lb/cy
	[32.0]	[gallons/cy]
Sika hooked-end steel fiber (1.0% fiber volume)	132.3	lb/cy
Darex AEA – Air-entraining admixture	4	fl oz/cy
MasterSet DELVO – Retarding admixture	28	fl oz/cy
MasterGlenium 7920 – High-range Water-reducing admixture	12	fl oz/cy

However, before full implementation of the FRC railing may be achieved, additional recommendations provided in the following section should be considered. These recommendations include additional steps needed to demonstrate whether the proposed FRC mixture may be successfully used in slip-form railing construction as well as potential laboratory tests that may be required—similar to 28-day compressive strength requirements—in order to ensure suitability of the FRC material.

8.2 Recommendations

The following items should be considered (and/or addressed) prior to full (roadway) implementation:

1. The ability to slip-form the developed FRC mixture should be further investigated and demonstrated.

2. FRC flexural tests should be used (and/or required) during implementation to ensure suitable FRC (hardened) mechanical properties are achieved during construction.

8.2.1 Ability to slip-form

As a demonstration of concept, the FRC traffic railing in the present study (Figure 8.1) was formed using cast-in-place construction techniques. Although the final FRC mixture used in railing test specimen production was derived from a slip-form mixture (Table 8.1), slip-form construction techniques were not employed. Therefore, the developed mixture should be further investigated using slip-form techniques, and equipment, to ensure that it is either applicable 'as is', or to identify any mixture modifications that would be needed for implementation using slip-form construction equipment.

8.2.2 FRC flexural strength tests

In the present study, hardened FRC mechanical properties—specifically, from EN 14651 (2005) CMOD flexural tests—were used to determine which FRC trial mixture was most suitable for the proposed application (in an FRC railing). Similar to compressive strength requirements for a concrete mixture that is delivered to a job site (i.e., used to cast a concrete structural component), it is recommended that *both* minimum FRC compressive strength and minimum residual tensile strength be required. Small flexural beam (prism) samples may be cast from the mixtures used during construction and should subsequently be used to evaluate the (hardened) mechanical properties of the FRC mixture employed at the job site.

In Section 3.4.2, design strength calculations for the 36-in. FRC single-slope traffic railing (SSTR) were discussed (and are further detailed in Appendix A). As a review of the calculations, to compute the design strength of the FRC railing, the design calculations for the standard 36-in. FDOT SSTR were modified by removing reinforcing (flexural and shear) steel within the railing cross-section and instead assuming a simplified tensile stress block for FRC (per ACI Committee 544, 2018). The required FRC tensile design strength (f_{ctd}) was then iteratively revised until the FRC railing design strength was found to be equivalent to the previously computed standard FDOT SSTR design strength (i.e., values of f_{ctd} were iterated until the 36-in. FRC SSTR design strength was found to be equivalent to the 105.5-kip railing resistance load computed for the conventional R/C FDOT 36-in. SSTR).

Based on the FRC design calculations, the *design* tensile strength (f_{ctd}) required for the FRC SSTR was determined to be approximately 250 psi. In comparison, for the implemented FRC mixture (with Sika 2-in. long hooked-end steel fiber with a 1% volume), (per EN 14651) the average load corresponding to $CMOD_4$ (0.138 in.) was found to produce a residual flexural tensile strength of 887 psi. Following the design approach in ACI (ACI Committee 544, 2018), to correlate experimental flexural (residual) tensile strength—found using the CMOD test—to (uniform) design tensile strength, the average experimental (flexural) strength is divided by 3. Using this design approach, the computed design strength for the developed mixture is 295 psi (i.e., 887/3 = 295). Since the design strength of the developed FRC mixture was greater than the computed 250-psi value assumed in the FRC railing design worksheet to achieve an equivalent railing strength, it was assumed that using this FRC mixture would produce FRC material strength properties that are sufficient for a 36-in. FRC SSTR—which was subsequently confirmed with experimental pendulum impact testing.

Therefore, it is recommended that flexural tests following guidance provided in ACI (ACI Committee 544, 2018) should be used (and/or required) to ensure correct implementation of the FRC railing. As detailed in ACI (ACI Committee 544, 2018), either the EN 14651 (2005) FRC flexural test or the ASTM C1609 (2012) FRC flexural test may be used to evaluate the flexural (residual) tensile strength of the FRC mixture. Furthermore, since the railing design strength may be considered an ultimate limit design state, residual strength values at $CMOD_4$ or L/150 should be used—from EN 14651 or ASTM C1609 testing, respectively.

8.3 Future implementation

Full implementation of FRC bridge rails will require that FDOT establish specifications for the development and approval of FRC barrier mixtures, as well as quality control procedures for material testing during construction. In this study, small beam tests provided an effective approach to addressing these issues when used in conjunction with the ACI design approach mentioned above and the AASHTO bridge rail yield line analysis procedure. It is recommended that FDOT develop FRC mixtures that are suitable for slip-forming procedures and that also establish compressive and residual tensile strength requirements that provide equivalent barrier performance to the current FDOT R/C SSTR design.

REFERENCES

AASHTO (American Association of State Highway and Transportation Officials) (2016). *Manual for Assessing Safety Hardware (MASH): 2nd Edition*, American Association of State Highway and Transportation Officials, Washington, D.C.

AASHTO (2017). *LRFD Bridge Design Specifications: 8th Edition*, American Association of State Highway and Transportation Officials, Washington, D.C.

ACI Committee 544 (1999). *Measurement of Properties of Fiber Reinforced Concrete*. ACI544.2R-89, Reapproved 1999, ACI Committee 544 Report, ACI: Farmington Hills, MI, USA.

ACI Committee 544 (2002). *State-of-the-Art Report on Fiber Reinforced Concrete*. ACI544.1R-96, Reapproved 2002, ACI Committee 544 Report, ACI: Farmington Hills, MI, USA.

ACI Committee 544 (2008). *Guide for Specifying, Proportioning, and Production of Fiber-Reinforced Concrete*. ACI544.3R-08, ACI Committee 544 Report, ACI: Farmington Hills, MI, USA.

ACI Committee 544 (2009). *Design Considerations for Steel Fiber Reinforced Concrete*. ACI544.4R-88, Reapproved 2009, ACI Committee 544 Report, ACI: Farmington Hills, MI, USA.

ACI Committee 544 (2016). *Report on Design and Construction of Fiber-Reinforced Precast Concrete Tunnel Segments*. ACI544.7R-16, ACI Committee 544 Report, ACI: Farmington Hills, MI, USA.

ACI Committee 544 (2018). *Guide for Design with Fiber-Reinforced Concrete*. ACI544.4R-18, ACI Committee 544 Report, ACI: Farmington Hills, MI, USA.

ASTM A820-16 (2016). *Standard Specification for Steel Fibers for Fiber-Reinforced Concrete*. ASTM International.

ASTM C1018-97 (1997). *Standard Test Method for Flexural Toughness and First-Crack Strength of Fiber-Reinforced Concrete (Using Beam with Third-Point Loading)*. ASTM International.

ASTM C1116-10 (2010). *Standard Specification for Fiber-Reinforced Concrete*. ASTM International.

ASTM C1399-10 (2015). *Standard Test Method for Obtaining Average Residual-Strength of Fiber-Reinforced Concrete*. ASTM International.

ASTM C143-15 (2015). *Standard Test Method for Slump of Hydraulic-Cement Concrete*. ASTM International.

ASTM C1609-19 (2019). *Standard Test Method for Flexural Performance of Fiber-Reinforced Concrete (Using Beam with Third-Point Loading)*. ASTM International.

ASTM C31-17 (2017). *Standard Practice for Making and Curing Concrete Test Specimens in the Field*. ASTM International.

ASTM C39-17 (2017). *Standard Test Method for Compressive Strength of Cylindrical Concrete Specimens*. ASTM International.

ASTM C496-11 (2011). *Standard Test Method for Splitting Tensile Strength of Cylindrical Concrete Specimens*. ASTM International.

ASTM C995-01 (2001). *Standard Test Method for Time of Flow of Fiber-Reinforced Concrete Through Inverted Slump Cone*. ASTM International.

Banthia, N. and Trottier, J.F. (1994). *Concrete reinforced with deformed steel fibers, part I: bond-slip mechanisms*. ACI Materials Journal, 91 (5), pp. 435-446.

Banthia, N. and Sappakittipakorn, M. (2007). *Toughness enhancement in steel fiber reinforced concrete through fiber hybridization*. Cement and Concrete Research, 37 (9), pp. 1366-1372.

Bencardino, F., Rizzuti, L., Spadea, G., and Swamy, R.N. (2010). *Experimental evaluation of fiber reinforced concrete fracture properties*. Composites Part B: Engineering, 41 (1), pp. 17-24.

Bindiganavile, V., Banthia, N., and Aarup, B. (2002). *Impact response of ultra-high-strength fiber-reinforced cement composite*. ACI Materials Journal, 99 (6), pp. 543-548.

Carmona, S., Aguado, A. and Molins, C. (2013). *Characterization of the properties of steel fiber reinforced concrete by means of the generalized Barcelona test*. Construction and Building Materials, 48, pp. 592–600.

Charron, J.P., Niamba, E., and Massicotte, B. (2011). *Static and dynamic behavior of high-and ultrahigh-performance fiber-reinforced concrete precast bridge parapets*. Journal of Bridge Engineering, 16 (3), pp. 413-421.

Chen, W.F. (1970). *Double-punch test for tensile strength of concrete*. Journal of Materials, 67, pp. 993-995.

Consolazio, G., Getter, D., and Kantrales, G. (2014). *Validation and Implementation of Bridge Design Specifications for Barge Impact Loading*, Structures Research Report No. 2014/87294, University of Florida, Gainesville, FL.

Consolazio, G., Hamilton, H.R., Groetaers, M., and Innocent, D. (2016). *Pendulum Impact Testing of Metallic, Non-metallic, and Hybrid Sign Posts*, Structures Research Report No. 2016/113605-113606, University of Florida, Gainesville, FL.

EN 14651 (2005). *Test method for metallic fibered concrete – measuring the flexural tensile strength (limit of proportionality (LOP), residual)*. European Standard.

FDOT (2020a). *Standard Plans Index 521-427: Traffic Railing – 36" Single-Slope*, Florida Department of Transportation, Tallahassee, FL.

FDOT (2020b). *Standard Specifications for Road and Bridge Construction*, Florida Department of Transportation, Tallahassee, FL.

Gomaco (2017). GT-6300 Barrier/Parapet. Retrieved April 2, 2017, from https://gomaco.com/

Green, L. (1997). *So You Want to Slipfrom Median Barriers*. Retrieved from ConcreteConstruction.net. http://www.concreteconstruction.net/how-to/construction/so-you-want-to-slipform-median-barriers_o

Green, L. (1997). So you want to slipform Median Barriers. *Concrete Construction*. Retrieved from ConcreteConstruction.net

Groetaers, M., Consolazio, G., and Wagner, D. (2016). *Development of an 1100C Crushable Nose Surrogate Vehicle for Low-Speed Impact Testing of Breakaway Hardware*. Transportation Research Record, 2588 (1), pp. 126-136. https://doi.org/10.3141/2588-14

Hrynyk, T. and Vecchio, F. (2014). *Behavior of steel fiber-reinforced concrete slabs under impact load*. ACI Structural Journal, 111 (5), pp. 1213-1224.

Kosa, K. and Naaman, A. (1990). *Corrosion of steel fiber reinforced concrete*. Materials Journal, 87 (1), pp. 27-37.

Kosmatka, S., Kerkhoff, B., and Panarese, W. (2003). *Design and Control of Concrete Mixtures: 14th edition*, Portland Cement Association, Skokie, Illinois, USA.

Livermore Software Technology (LST). (2020). *LS-DYNA keyword user's manual*. Livermore, CA.

Markovic, I. (2006). *High-Performance Hybrid-Fibre Concrete*. Doctoral thesis, Department of Concrete Structures, Delft University of Technology, The Netherlands.

Murray, Y. (2007). *Users Manual for LS-DYNA Concrete Material Model 159*. Federal Highway Administration, (May), 77.

NCHRP (1981), Michie, J.D. *NCHRP Report 230: Recommended Procedures for the Safety Performance Evaluation of Highway Appurtenances*, Transportation Research Board (TRB), National Research Council, Washington, D.C.

NCHRP (1993), Ross, H., Sicking, D., Zimmer, R., and Michie, J. *NCHRP Report 350: Recommended Procedures for the Safety Performance Evaluation of Highway Features*, Transportation Research Board (TRB), National Research Council, Washington, D.C.

Ong, K.C.G., Basheerkhan, M., and Paramasivam, P. (1999). *Resistance of fibre concrete slabs to low velocity projectile impact*. Cement and Concrete Composites, 21 (5), pp. 391-401.

Othman, H. and Marzouk, H. (2016). *Impact Response of Ultra-High-Performance Reinforced Concrete Plates*. ACI Structural Journal, 113 (6), pp. 1325-1334.

Paegle, I. (2015). *Characterization and modeling of fiber reinforced concrete for structural applications in beams and plates*. Doctoral dissertation, Department of Civil Engineering, Technical University of Denmark, Denmark.

Pekmezci, B.Y., Voigt, T., Wang, K., and Shah, P. (2007). *Low Compaction Energy Concrete for Improved Slipform Casting of Concrete Pavements*. ACI Materials Journal, 104 (3), pp. 251-258.

Ray, G. and H. Halm (1965). *Fifteen Years of Slip-Form Paving*. Journal of the American Concrete Institute, 62 (2), pp. 145-159.

Sheikh, N., Bligh, R., and Menges, W. (2011). *Determination of minimum height and lateral design load for MASH test level 4 bridge rails*, Test Report No. 9-1002-5, Texas Transportation Institute (TTI), College Station, TX.

Sika (2017). *Fiber-reinforced Sprayed Concrete*. Retrieved from http://sika.com/

Silvestri-Dobrovolny, C., Schulz, N., Moran, S., Skinner, T., Bligh, R., and Williams, W. (2017). *MASH Equivalency of NCHRP Report 350-Approved Bridge Railings*, Project No. 20-07/Task 395 TTI Project 607141, Texas A&M Transportation Institute, College Station, TX.

TxDOT (2019). *Bridge Division Standard: Traffic Rail Single Slope (Type SSTR)*, Texas Department of Transportation, Austin, TX.

TGRMCC (2017). *Fiber Reinforced Concrete*. Retrieved from http://tgrmcc.com/

Voigt, T., Mbele, J.J., Wang, K. and Shah, P. (2010). *Using Fly Ash, Clay, and Fibers for Simultaneous Improvement of Concrete Green Strength and Consolidatability for Slip-Form Pavement*. Journal of Materials in Civil Engineering, 22 (2), pp. 196-206.

Wang, K., Shah, S. P., and Voigt, T. (2008). *Self-Consolidating Concrete for Slip-Form Construction: Properties and Test Methods*. Proceedings of Advances in Civil Engineering Materials—The 50-Year Teach and Research Anniversary of Professor Sun Wei, pp. 161-172.

Yin, S., Tuladhar, R., Shi, F., Combe, M., Collister, T. and Sivakugan, N., (2015). *Use of macro plastic fibres in concrete: a review*. Construction and Building Materials, 93, pp.180-188.

Yoo, D.Y., Banthia, N. and Yoon, Y.S. (2017). *Impact resistance of reinforced ultra-high-performance concrete beams with different steel fibers*. ACI Structural Journal, 114(1), pp. 113-124.

Zayed, T., Sharifi, M. R., Baciu, S., and Amer, M. (2008). *Slip-Form Application to Concrete Structures*. Journal of Construction Engineering and Management, 134 (3), pp. 157-168.

Zheng, W.; A. K. H. Kwan, and P.K.K. Lee (2001). *Direct tensions test of concrete*. Materials Journal, 98 (1), pp. 63-71.

Zollo, R. F. (1997). *Fiber-reinforced concrete: an overview after 30 years of development*. Cement and Concrete Composites, 19 (2), pp. 107-122.

APPENDIX A
LRFD DESIGN STRENGTH CALCULATIONS
FOR FDOT 36-IN. SINGLE-SLOPE TRAFFIC RAILING (INDEX NO. 521-427)

Presented in this appendix is a calculation worksheet that was prepared to evaluate the strength of the current (standard R/C) FDOT 36-in. single-slope traffic railing (per AASHTO LRFD Design equations, which are based on a yield line analysis approach).

▶ References [hidden]

FDOT Index 427 Bridge Rail Design Check
(based on AASHTO LRFD Section A13)

Table A13.2-1—Design Forces for Traffic Railings

Design Forces and Designations	Railing Test Levels					
	TL-1	TL-2	TL-3	TL-4	TL-5	TL-6
F_t Transverse (kips)	13.5	27.0	54.0	54.0	124.0	175.0
F_L Longitudinal (kips)	4.5	9.0	18.0	18.0	41.0	58.0
F_v Vertical (kips) Down	4.5	4.5	4.5	18.0	80.0	80.0
L_t and L_L (ft)	4.0	4.0	4.0	3.5	8.0	8.0
L_v (ft)	18.0	18.0	18.0	18.0	40.0	40.0
H_e (min) (in.)	18.0	20.0	24.0	32.0	42.0	56.0
Minimum H Height of Rail (in.)	27.0	27.0	27.0	32.0	42.0	90.0

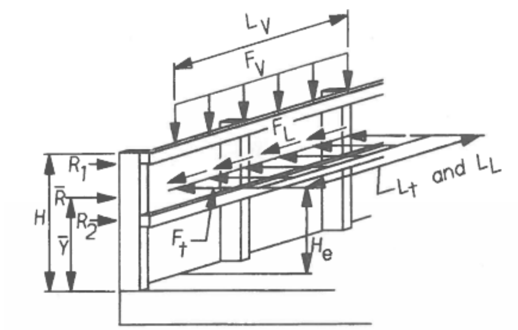

Figure A13.2-1—Metal Bridge Railing Design Forces, Vertical Location, and Horizontal Distribution Length

Design based on Test Level 4 (TL-4)

$F_t = 54 \cdot kip$ ***Transverse Design Force (recommended to be*** 80kips ***by TTI per MASH)***

$F_L = 18 \cdot kip$ ***Longitudinal Design Force***

$F_V = 18kip$ ***Vertical Design Force Down***

$L_t = 3.5ft$

$L_L = 3.5ft$

$L_V = 18ft$

$H_e = 32in$ ***Minimum height of applied load***

$H = 36in$ ***Height of railing (see railing details below)***

The design of the railing is based on a yield line analysis which has three variables:

M_w ***: the flexural resistance of the wall (railing) about its vertical axis (kip-ft)***

M_b ***: the flexural resistance of the top beam (if present) [i.e., any additional flexural capacity in addition to*** M_w***] (kip-ft)***

M_c ***: the flexural resistance of cantilevered walls about an axis parallel to the longitudinal axis of the bridge [i.e., the flexural capacity of the railing about its horizontal axis] (kip-ft/ft)***

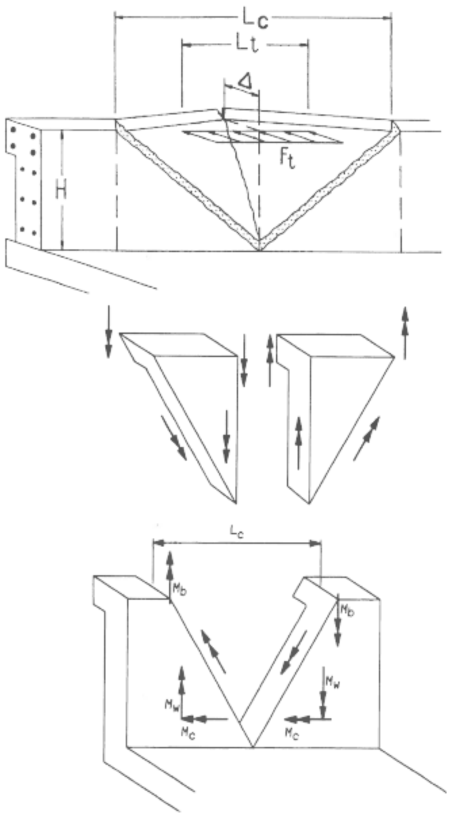

Figure CA13.3.1-1—Yield Line Analysis of Concrete Parapet Walls for Impact within Wall Segment

The interior region is considered to have three yield lines. Two of the yield lines have tension on the inside face of the railing and the remaining yield line has tension on the outside face of the railing.

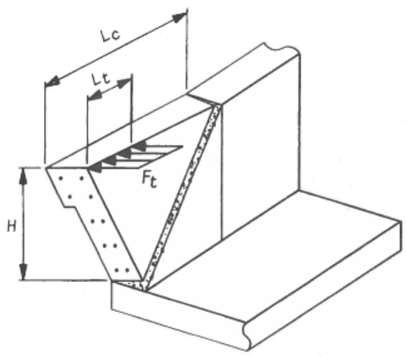

Figure CA13.3.1-2—Yield Line Analysis of Concrete Parapet Walls for Impact near End of Wall Segment

The end region failure mechanism is assumed to have one yield line that has tension on the inside face of the railing.

Note: It is recommended that in addition to inclined yield lines, one-way cantilever resistance of the rail should be investigated for rail segments with lengths less than twice L_c *(for internal regions). (Possible consideration for a bridge rail test specimen.)*

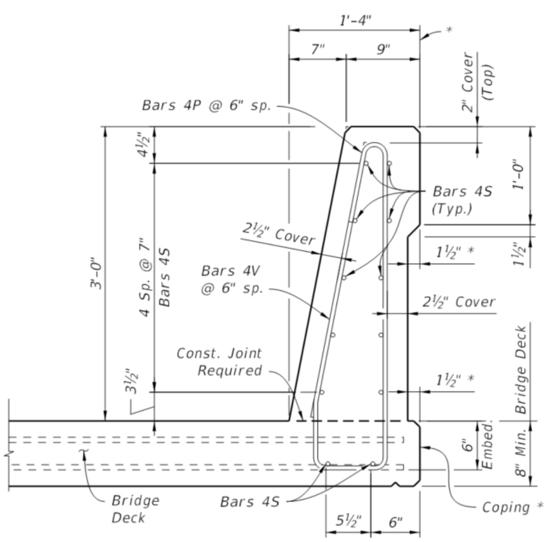

SECTION A-A
TYPICAL SECTION THRU TRAFFIC RAILING
(Section thru Bridge Deck shown, Section thru Approach Slab and Retaining Walls similar)

FDOT Traffic Railing [Index 521-427] - 36-in. Single-Slope

Longitudinal rebar layout (with details removed for clarity) and separated into 5 different zones:

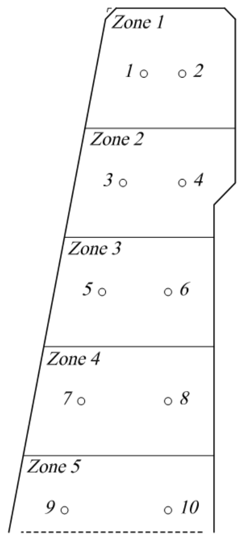

Rotated for clarity/comprehension:

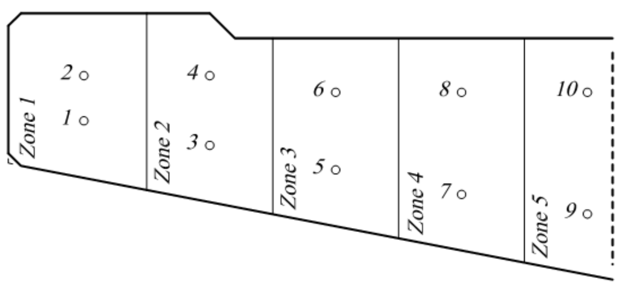

Zones separated with dimensions measured in AutoCAD:

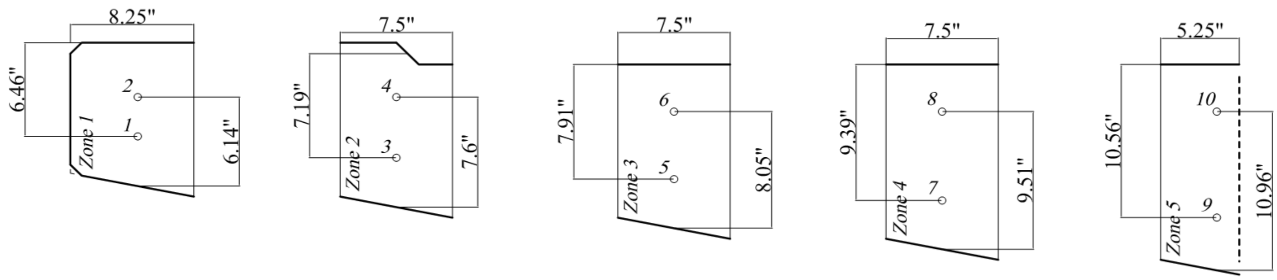

Determine $M_b + M_w$***:***

Using: $\phi \cdot M_n = \phi \cdot A_s \cdot f_y \cdot \left(d - \frac{a}{2}\right)$ ***where*** $\phi = 1.0$ ***(for Extreme Event Limit States)***

Longitudinal reinforcing bars are No. 4, $A_s = As4 = 0.2 \cdot in^2$ ***and assume*** $f_y = 60ksi$

Concrete for FDOT traffic railings is required to have $f'_c = 3400psi$

From the details provided by the FDOT, determine the width (b) of each zone and depth (d) of each rebar (when in tension):

Zone	***Width (b)***	***Depth of interior bar***	***Depth of exterior bar***
1	$b_{zone1} = 8.25in$	$d_{bar1} = 6.46in$	$d_{bar2} = 6.14in$
2	$b_{zone2} = 7.5in$	$d_{bar3} = 7.19in$	$d_{bar4} = 7.6in$
3	$b_{zone3} = 7.5in$	$d_{bar5} = 7.91in$	$d_{bar6} = 8.05in$
4	$b_{zone4} = 7.5in$	$d_{bar7} = 9.39in$	$d_{bar8} = 9.51in$
5	$b_{zone5} = 5.25in$	$d_{bar9} = 10.56in$	$d_{bar10} = 10.96in$

Compute the depth (a) of each separate zone:

$$a_1 = \frac{A_s \cdot f_y}{0.85 \cdot f'_c \cdot b_{zone1}} = 0.50 \cdot in \qquad a_2 = \frac{A_s \cdot f_y}{0.85 \cdot f'_c \cdot b_{zone1}} = 0.50 \cdot in$$

$$a_3 = \frac{A_s \cdot f_y}{0.85 \cdot f'_c \cdot b_{zone2}} = 0.55 \cdot in \qquad a_4 = \frac{A_s \cdot f_y}{0.85 \cdot f'_c \cdot b_{zone2}} = 0.55 \cdot in$$

$$a_5 = \frac{A_s \cdot f_y}{0.85 \cdot f'_c \cdot b_{zone3}} = 0.55 \cdot in \qquad a_6 = \frac{A_s \cdot f_y}{0.85 \cdot f'_c \cdot b_{zone3}} = 0.55 \cdot in$$

$$a_7 = \frac{A_s \cdot f_y}{0.85 \cdot f'_c \cdot b_{zone4}} = 0.55 \cdot in \qquad a_8 = \frac{A_s \cdot f_y}{0.85 \cdot f'_c \cdot b_{zone4}} = 0.55 \cdot in$$

$$a_9 = \frac{A_s \cdot f_y}{0.85 \cdot f'_c \cdot b_{zone5}} = 0.79 \cdot in \qquad a_{10} = \frac{A_s \cdot f_y}{0.85 \cdot f'_c \cdot b_{zone5}} = 0.79 \cdot in$$

Compare to an average compression zone depth:

$$a_{avg} = \frac{5 \cdot A_s \cdot f_y}{0.85 \cdot f'_c \cdot H} = 0.58 \cdot in$$

Bar #	***ϕMn (interior or exterior face)***
1	$\phi M_{n1} = \phi \cdot A_s \cdot f_y \cdot \left(d_{bar1} - \frac{a_1}{2}\right) = 6.21 \cdot kip \cdot ft$
2	$\phi M_{n2} = \phi \cdot A_s \cdot f_y \cdot \left(d_{bar2} - \frac{a_2}{2}\right) = 5.89 \cdot kip \cdot ft$
3	$\phi M_{n3} = \phi \cdot A_s \cdot f_y \cdot \left(d_{bar3} - \frac{a_3}{2}\right) = 6.91 \cdot kip \cdot ft$
4	$\phi M_{n4} = \phi \cdot A_s \cdot f_y \cdot \left(d_{bar4} - \frac{a_4}{2}\right) = 7.32 \cdot kip \cdot ft$
5	$\phi M_{n5} = \phi \cdot A_s \cdot f_y \cdot \left(d_{bar5} - \frac{a_5}{2}\right) = 7.63 \cdot kip \cdot ft$
6	$\phi M_{n6} = \phi \cdot A_s \cdot f_y \cdot \left(d_{bar6} - \frac{a_6}{2}\right) = 7.77 \cdot kip \cdot ft$
7	$\phi M_{n7} = \phi \cdot A_s \cdot f_y \cdot \left(d_{bar7} - \frac{a_7}{2}\right) = 9.11 \cdot kip \cdot ft$
8	$\phi M_{n8} = \phi \cdot A_s \cdot f_y \cdot \left(d_{bar8} - \frac{a_8}{2}\right) = 9.23 \cdot kip \cdot ft$
9	$\phi M_{n9} = \phi \cdot A_s \cdot f_y \cdot \left(d_{bar9} - \frac{a_9}{2}\right) = 10.16 \cdot kip \cdot ft$
10	$\phi M_{n10} = \phi \cdot A_s \cdot f_y \cdot \left(d_{bar10} - \frac{a_{10}}{2}\right) = 10.56 \cdot kip \cdot ft$

$$M_{w\ interior} = \phi M_{n1} + \phi M_{n3} + \phi M_{n5} + \phi M_{n7} + \phi M_{n9} = 40.03 \cdot kip \cdot ft$$

$$M_{w\ exterior} = \phi M_{n2} + \phi M_{n4} + \phi M_{n6} + \phi M_{n8} + \phi M_{n10} = 40.78 \cdot kip \cdot ft$$

For an interior region of railing, there are two yield lines with interior tension and one yield line with exterior tension:

$$M_w = \frac{2 \cdot M_{w\ interior} + M_{w\ exterior}}{3} = 40.28 \cdot kip \cdot ft$$

This approach considers both the top beam and remaining (wall) railing all together, therefore, will be used for the AASHTO equations below.

Determine M_c **:**

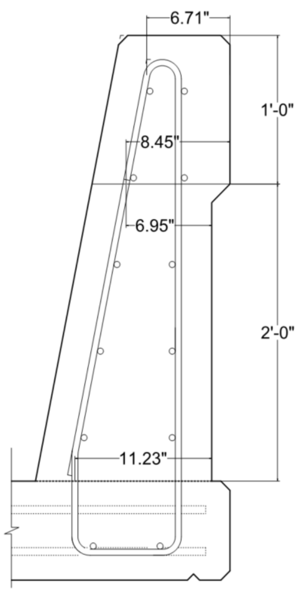

Average the top and bottom depth of the vertical reinforcing bars:

$$d_{average} = \left(\frac{6.71in + 8.45in}{2}\right)\cdot\left(\frac{12in}{36in}\right) + \left(\frac{6.95in + 11.23in}{2}\right)\cdot\left(\frac{24in}{36in}\right) = 8.59\cdot in$$

$b = 12in$ ***Assume a unit length of railing as 1 ft***

$spacing = 6in$ ***Spacing of vertical reinforcement***

$A_{s\ per\text{-}ft} = As4\cdot\frac{12in}{spacing} = 0.4\cdot in^2$ ***Vertical (shear) reinforcement is spaced every 6 in., therefore two bars every 12 in.***

$a = \frac{A_{s\ per\text{-}ft}\cdot f_y}{0.85\cdot f'_c\cdot b} = 0.69\cdot in$ ***Depth of concrete in compression***

$$M_c = \frac{\phi\cdot A_{s\ per\text{-}ft}\cdot f_y\cdot\left(d_{average} - \frac{a}{2}\right)}{b} = 16.48\cdot\frac{kip\cdot ft}{ft}$$

Compute the critical wall length and the bridge rail resistance capacity (using equations given in AASHTO):

$$L_c = \frac{L_t}{2} + \sqrt{\left(\frac{L_t}{2}\right)^2 + \frac{8\cdot H\cdot\left(M_b + M_w\right)}{M_c}} = 9.61\ ft$$ ***(Eqn. A13.3.1-2)*** $\alpha = atan\left(\frac{H}{L_c \div 2}\right) = 32\cdot deg$

$$R_w = \left(\frac{2}{2\cdot L_c - L_t}\right)\cdot\left(8M_b + 8\cdot M_w + \frac{M_c\cdot L_c^{\,2}}{H}\right) = 105.5\cdot kip$$ ***(Eqn. A13.3.1-1)***

which is greater than the specified design load of 54kip ***(and the recommended*** 80kip ***design load per TTI)***

To confirm, compute the minimum load for the yield mechanism:

$n = 500 \quad lim1 = 0.01 \quad lim2 = 1.2 \quad inc = \frac{lim2 - lim1}{n} \quad i = 0..n \quad \alpha_i = lim1 + i \cdot inc$

$$L_c = \frac{2 \cdot H}{\tan(\alpha)}$$

$$F_t(\alpha) = \frac{8 \cdot M_b}{\frac{2 \cdot H}{\tan(\alpha)} - \frac{L_t}{2}} + \frac{8 \cdot M_w}{\frac{2 \cdot H}{\tan(\alpha)} - \frac{L_t}{2}} + \frac{M_c \cdot \left(\frac{2 \cdot H}{\tan(\alpha)}\right)^2}{H \cdot \left(\frac{2 \cdot H}{\tan(\alpha)} - \frac{L_t}{2}\right)}$$

Eq. (15.8) [from "Design of highway bridges an LRFD approach (3rd ed)" by Barker and Puckett (2013)]

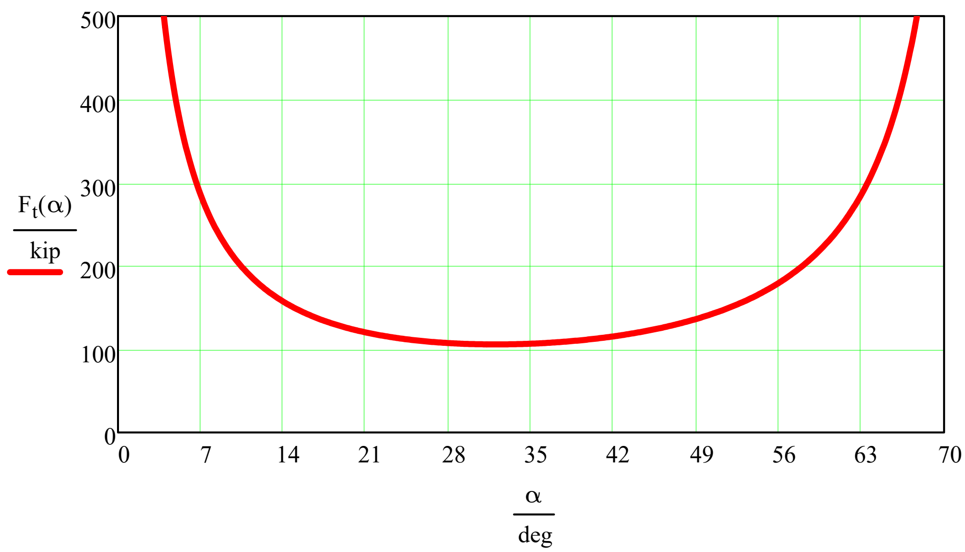

$\min(F_t(\alpha)) = 105.5 \cdot kip \quad F_t(32deg) = 105.5 \cdot kip \quad L_c = \frac{2 \cdot H}{\tan(32deg)} = 9.60 \cdot ft$

APPENDIX B
LRFD DESIGN STRENGTH CALCULATIONS FOR FRC 36-IN. SINGLE-SLOPE TRAFFIC RAILING

Presented in this appendix is a calculation worksheet that was prepared to evaluate the strength of the proposed FRC 36-in. single-slope traffic railing (per AASHTO LRFD Design equations, which are based on a yield line analysis approach). In this worksheet, the FRC design tensile strength (f_{ctd}) was iterated until the total strength of the FRC railing was equivalent to the standard R/C railing presented in Appendix A.

▶ References

FDOT Index 427 Bridge Rail Design with FRC (based on AASHTO Section A13.3)

Table A13.2-1—Design Forces for Traffic Railings

Design Forces and Designations	Railing Test Levels					
	TL-1	TL-2	TL-3	TL-4	TL-5	TL-6
F_t Transverse (kips)	13.5	27.0	54.0	54.0	124.0	175.0
F_L Longitudinal (kips)	4.5	9.0	18.0	18.0	41.0	58.0
F_v Vertical (kips) Down	4.5	4.5	4.5	18.0	80.0	80.0
L_t and L_L (ft)	4.0	4.0	4.0	3.5	8.0	8.0
L_v (ft)	18.0	18.0	18.0	18.0	40.0	40.0
H_e (min) (in.)	18.0	20.0	24.0	32.0	42.0	56.0
Minimum H Height of Rail (in.)	27.0	27.0	27.0	32.0	42.0	90.0

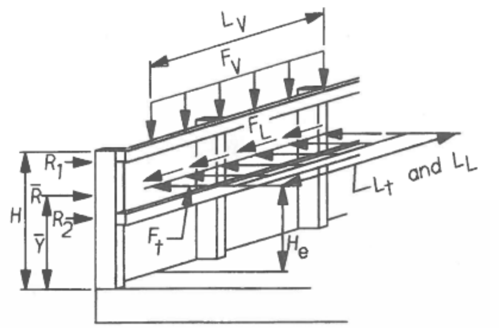

Figure A13.2-1—Metal Bridge Railing Design Forces, Vertical Location, and Horizontal Distribution Length

Design based on Test Level 4 (TL-4)

$F_t = 54 \cdot kip$ — ***Transverse Design Force***

$F_L = 18 \cdot kip$ — ***Longitudinal Design Force***

$F_V = 18kip$ — ***Vertical Design Force Down***

$L_t = 3.5ft$

$L_L = 3.5ft$

$L_V = 18ft$

$H_e = 32in$ — ***Minimum height of applied load***

$H = 36in$ — ***Height of railing (see railing details below)***

The design of the railing is based on a yield line analysis which has three variables:

M_w ***: the flexural resistance of the wall (railing) about its vertical axis (kip-ft)***

M_b ***: the flexural resistance of the top beam (if present) [i.e., any additional flexural capacity in addition to*** M_w ***] (kip-ft)***

M_c ***: the flexural resistance of cantilevered walls about an axis parallel to the longitudinal axis of the bridge [i.e., the flexural capacity of the railing about its horizontal axis] (kip-ft/ft)***

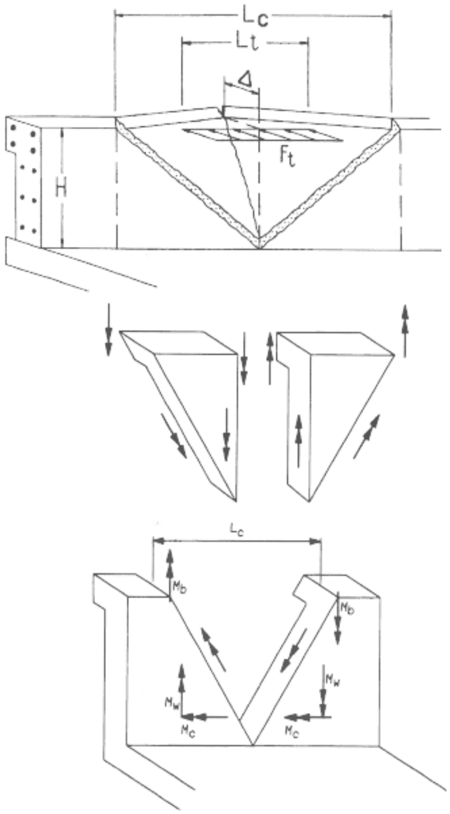

Figure CA13.3.1-1—Yield Line Analysis of Concrete Parapet Walls for Impact within Wall Segment

the yield lines have tension on the inside face of the railing and the remaining yield line has tension on the outside face of the railing.

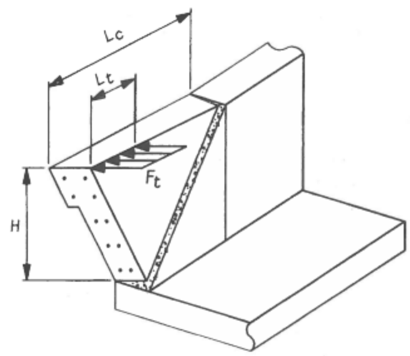

Figure CA13.3.1-2—Yield Line Analysis of Concrete Parapet Walls for Impact near End of Wall Segment

The end region failure mechanism is assumed to have one yield line that has tension on the inside face of the railing.

Note: It is recommended that in addition to inclined yield lines, one-way cantilever resistance of the rail should be investigated for rail segments with lengths less than twice L_c ***(for internal regions). (Possible consideration for a bridge rail test specimen.)***

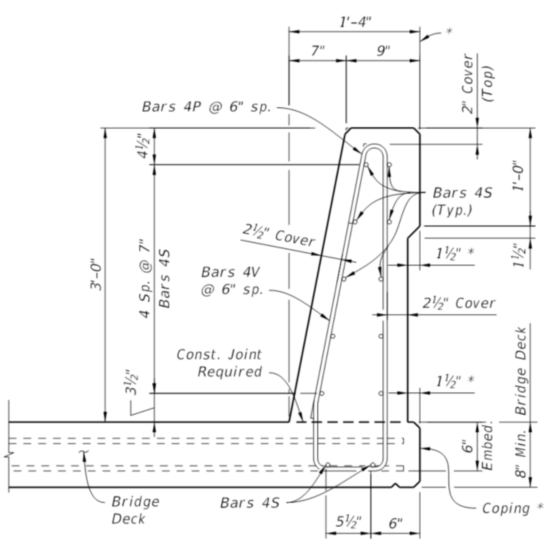

SECTION A-A
TYPICAL SECTION THRU TRAFFIC RAILING
(Section thru Bridge Deck shown, Section thru Approach Slab and Retaining Walls similar)

FDOT Traffic Railing [Index 521-427] - 36 in. Single-Slope

Longitudinal rebar layout (with details removed for clarity) separated into 5 different zones:

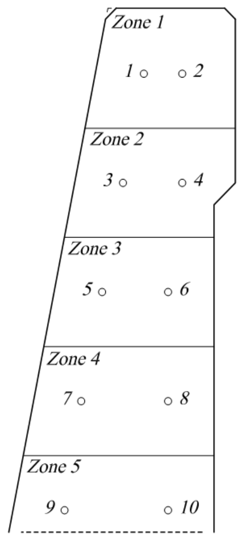

Rotated for clarity/comprehension:

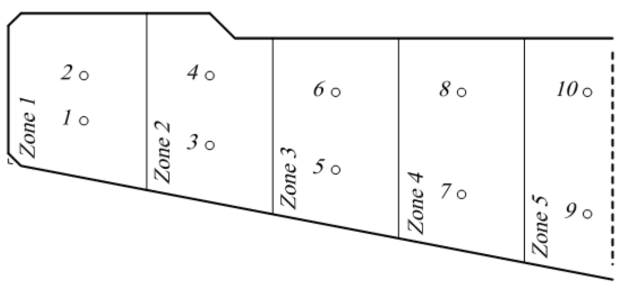

Zones separated with dimensions measured in AutoCAD (Note: for FRC, rebar is removed):

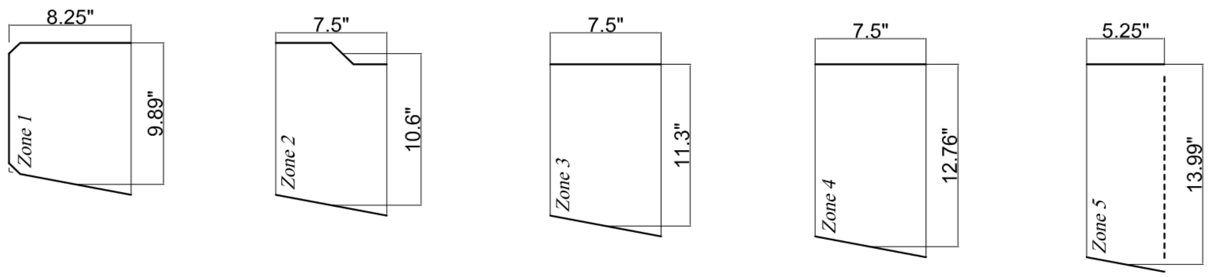

Determine $M_b + M_w$ ***:***

Use a simplified stress distribution for FRC in the tension zone (from ACI-544):

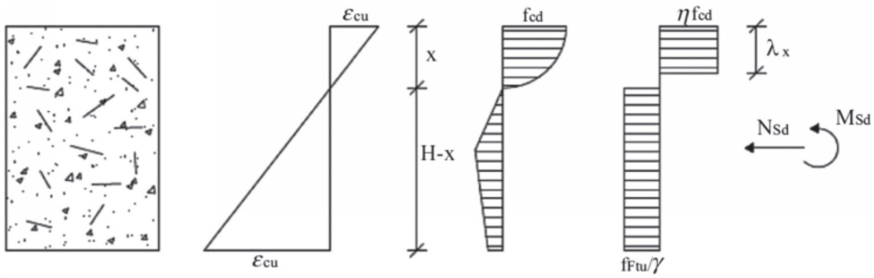

Fig. 10.1b—FRC constitutive law used for design of segments against ultimate loads in Monte Lirio tunnel (Caratelli et al. 2012).

To satisfy equilibrium:

$$C_{concrete} = T_{concrete}$$

$$0.85 \cdot f'_c \cdot a \cdot b = f_{ctd} \cdot (h - c) \cdot b$$

$$0.85 \cdot f'_c \cdot \beta_1 \cdot c = f_{ctd}(h - c)$$

First must solve for the depth of the neutral axis:

$$c = \frac{f_{ctd} \cdot h}{0.85 \cdot f'_c \cdot \beta_1 + f_{ctd}}$$

With c ***, can then find the capacity:***

$$a = \beta_1 \cdot c$$

$$M_n = f_{ctd} \cdot (h - c) \cdot b \cdot \left(\frac{h - c}{2} + c - \frac{a}{2} \right)$$

Compute the capacity for each separate zone:

Concrete for FDOT traffic railings is required to have $f'_c = 3400psi$ ***and therefore*** $\beta_1 = 0.85$

Assuming the tensile strength of FRC is $f_{ctd} = 250psi$ ***. This value can be iterated until a desired railing capacity is achieved. Additionally, using the Helix Design Program [based on a specified fiber content (percent volume)], the FRC tensile stress ( ) is an output value in the program (which can be verified with laboratory testing).***

From the details provided by the FDOT, determine the width (b) and height (h) of each zone:

Zone	***Width (b)***	***Height (h)***
1	$b_{zone1} = 8.25in$	$h_{zone1} = 9.89in$
2	$b_{zone2} = 7.5in$	$h_{zone2} = 10.6in$
3	$b_{zone3} = 7.5in$	$h_{zone3} = 11.3in$
4	$b_{zone4} = 7.5in$	$h_{zone4} = 12.76in$
5	$b_{zone5} = 5.25in$	$h_{zone5} = 13.99in$

Compute the depth (a) of each separate zone:

$$c_{zone1} = \frac{f_{ctd} \cdot h_{zone1}}{0.85 \cdot f'_c \cdot \beta_1 + f_{ctd}} = 0.91 \cdot in \qquad a_{zone1} = \beta_1 \cdot c_{zone1} = 0.78 \cdot in$$

$$c_{zone2} = \frac{f_{ctd} \cdot h_{zone2}}{0.85 \cdot f'_c \cdot \beta_1 + f_{ctd}} = 0.98 \cdot in \qquad a_{zone2} = \beta_1 \cdot c_{zone2} = 0.83 \cdot in$$

$$c_{zone3} = \frac{f_{ctd} \cdot h_{zone3}}{0.85 \cdot f'_c \cdot \beta_1 + f_{ctd}} = 1.04 \cdot in \qquad a_{zone3} = \beta_1 \cdot c_{zone3} = 0.89 \cdot in$$

$$c_{zone4} = \frac{f_{ctd} \cdot h_{zone4}}{0.85 \cdot f'_c \cdot \beta_1 + f_{ctd}} = 1.18 \cdot in \qquad a_{zone4} = \beta_1 \cdot c_{zone4} = 1 \cdot in$$

$$c_{zone5} = \frac{f_{ctd} \cdot h_{zone5}}{0.85 \cdot f'_c \cdot \beta_1 + f_{ctd}} = 1.29 \cdot in \qquad a_{zone5} = \beta_1 \cdot c_{zone5} = 1.1 \cdot in$$

Zone #	***Mn (interior or exterior face)***
1	$M_{n1} = f_{ctd} \cdot (h_{zone1} - c_{zone1}) \cdot b_{zone1} \cdot \left(\frac{h_{zone1} - c_{zone1}}{2} + c_{zone1} - \frac{a_{zone1}}{2} \right) = 7.73 \cdot kip \cdot ft$
2	$M_{n2} = f_{ctd} \cdot (h_{zone2} - c_{zone2}) \cdot b_{zone2} \cdot \left(\frac{h_{zone2} - c_{zone2}}{2} + c_{zone2} - \frac{a_{zone2}}{2} \right) = 8.08 \cdot kip \cdot ft$
3	$M_{n3} = f_{ctd} \cdot (h_{zone3} - c_{zone3}) \cdot b_{zone3} \cdot \left(\frac{h_{zone3} - c_{zone3}}{2} + c_{zone3} - \frac{a_{zone3}}{2} \right) = 9.18 \cdot kip \cdot ft$
4	$M_{n4} = f_{ctd} \cdot (h_{zone4} - c_{zone4}) \cdot b_{zone4} \cdot \left(\frac{h_{zone4} - c_{zone4}}{2} + c_{zone4} - \frac{a_{zone4}}{2} \right) = 11.71 \cdot kip \cdot ft$
5	$M_{n5} = f_{ctd} \cdot (h_{zone5} - c_{zone5}) \cdot b_{zone5} \cdot \left(\frac{h_{zone5} - c_{zone5}}{2} + c_{zone5} - \frac{a_{zone5}}{2} \right) = 9.85 \cdot kip \cdot ft$

$$M_{w\ interior/exterior} = M_{n1} + M_{n2} + M_{n3} + M_{n4} + M_{n5} = 46.55 \cdot kip \cdot ft$$

For an interior region of railing, there are two yield lines with interior tension and one yield line with exterior tension, but for FRC, all three yield lines have the same capacity:

$$M_w = M_{w\ interior/exterior} = 46.55 \cdot kip \cdot ft$$

This approach considers both the top beam and remaining (wall) railing all together, therefore, will be used for AASHTO equations below.

Compare to a simplified (rectangular) railing shape:

$h_{simple} = 9in$ ***width of the top of the railing***

$b_{simple} = H = 36 \cdot in$

$$c_{simple} = \frac{f_{ctd} \cdot h_{simple}}{0.85 \cdot f'_c \cdot \beta_1 + f_{ctd}} = 0.83 \cdot in \qquad a_{simple} = \beta_1 \cdot c_{simple} = 0.71 \cdot in$$

$$M_{n\ simple} = f_{ctd} \cdot (h_{simple} - c_{simple}) \cdot b_{simple} \cdot \left(\frac{h_{simple} - c_{simple}}{2} + c_{simple} - \frac{a_{simple}}{2} \right) = 27.95 \cdot kip \cdot ft$$

Determine M_c **:**

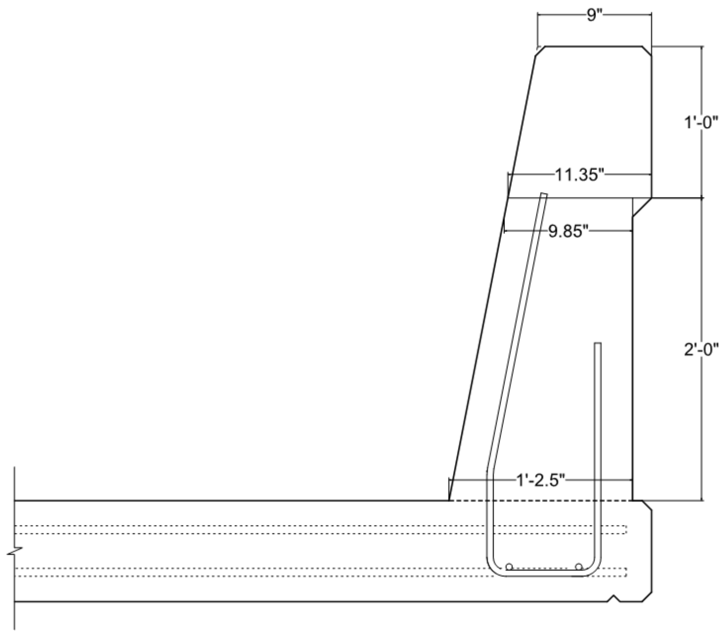

Average the top and bottom height (h), which is the horizontal dimension of the railing:

$$h_{average} = \left(\frac{9in + 11.35in}{2}\right)\cdot\left(\frac{12in}{36in}\right) + \left(\frac{9.85in + 14.5in}{2}\right)\cdot\left(\frac{24in}{36in}\right) = 11.51\cdot in$$

$b_{vertical} = 12in$ ***Assume a unit length of railing as 1 ft***

$$c_{vertical} = \frac{f_{ctd}\cdot h_{average}}{0.85\cdot f'_c\cdot \beta_1 + f_{ctd}} = 1.06\cdot in \qquad a_{vertical} = \beta_1\cdot c_{vertical} = 0.9\cdot in$$

$$M_c = \frac{f_{ctd}\cdot\left(h_{average} - c_{vertical}\right)\cdot b_{vertical}\cdot\left(\frac{h_{average} - c_{vertical}}{2} + c_{vertical} - \frac{a_{vertical}}{2}\right)}{b_{vertical}} = 15.23\cdot\frac{kip\cdot ft}{ft}$$

Compute the critical wall length and the bridge rail resistance capacity (using equations given in AASHTO):

$$L_c = \frac{L_t}{2} + \sqrt{\left(\frac{L_t}{2}\right)^2 + \frac{8\cdot H\cdot\left(M_b + M_w\right)}{M_c}} = 10.49\ ft \qquad \textit{(A13.3.1-2)} \qquad \theta = atan\left(\frac{H}{L_c \div 2}\right) = 29.8\cdot deg$$

$$R_w = \left(\frac{2}{2\cdot L_c - L_t}\right)\cdot\left(8M_b + 8\cdot M_w + \frac{M_c\cdot {L_c}^2}{H}\right) = 106.5\cdot kip \qquad \textit{(A13.3.1-1)}$$

which is greater than the specified design load of 54kip ***(and the recommended*** 80kip ***design load per TTI)***

APPENDIX C
SPECIMEN FORMWORK AND TRIAL PRODUCTION DRAWINGS

Presented in this appendix are formwork fabrication drawings. The formwork was designed for forming (i.e., casting) a large-scale 'trial FRC railing production specimen' (without an integrated bridge deck), and was also designed for forming the separate railing and deck portions of subsequent pendulum impact test specimens.

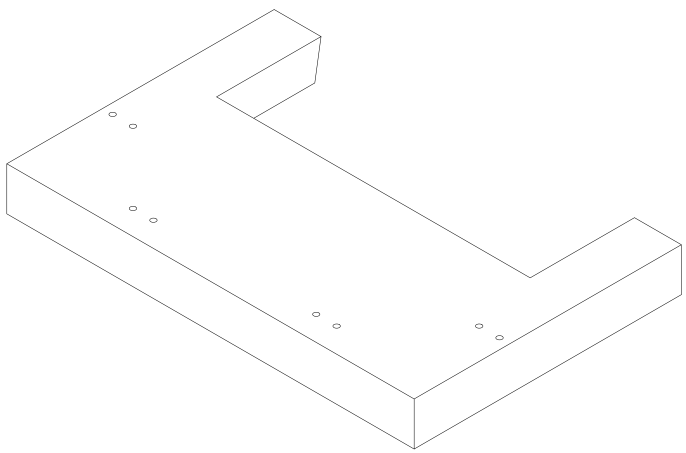

DECK PORTION OF IMPACT SPECIMEN
FRONT ISOMETRIC VIEW

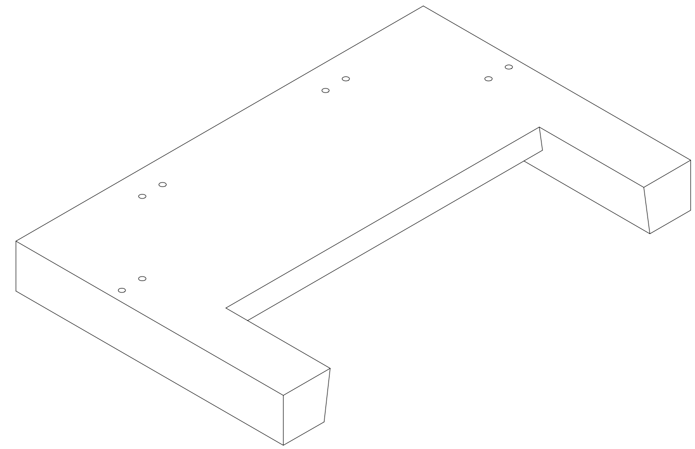

DECK PORTION OF IMPACT SPECIMEN
BACK ISOMETRIC VIEW

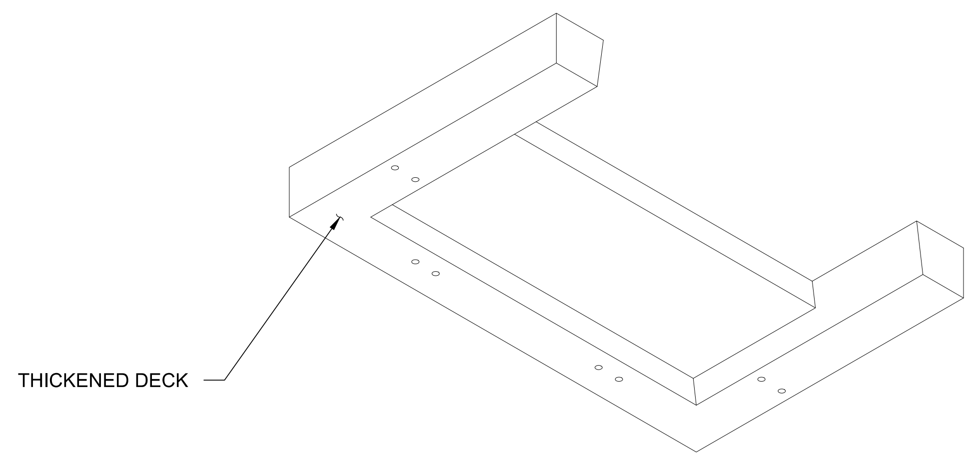

DECK PORTION OF IMPACT SPECIMEN
BOTTOM ISOMETRIC VIEW

Fiber-Reinforced Concrete Traffic Railings for Impact Loading				*Revisions:*
Deck formwork	*2019-12-20*	*University of Florida*	*Sheet 1 of 23*	

DECK PORTION OF IMPACT SPECIMEN
PLAN VIEW

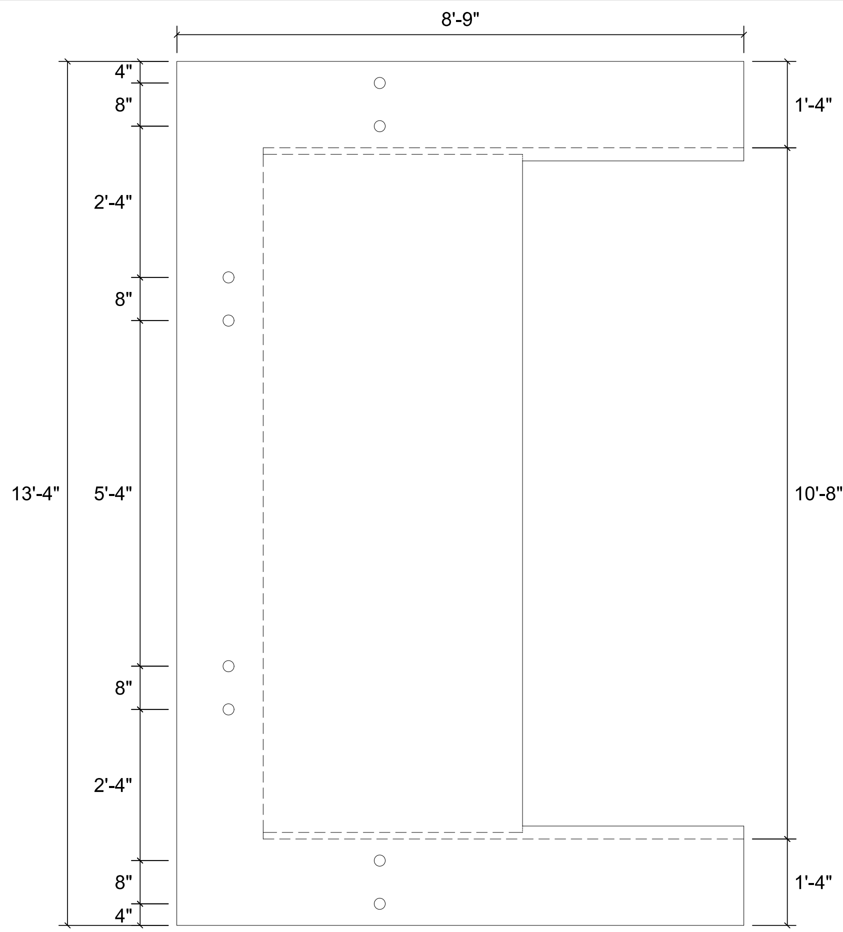

DECK PORTION OF IMPACT SPECIMEN
SIDE ELEVATION VIEW

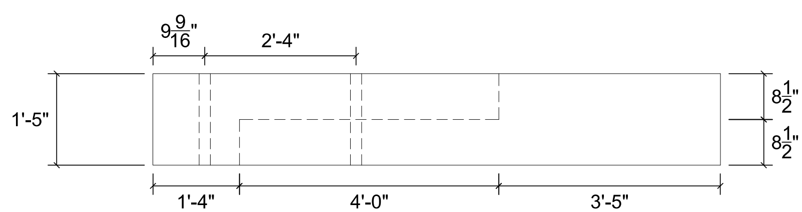

Fiber-Reinforced Concrete Traffic Railings for Impact Loading				*Revisions:*
Deck formwork	*2019-12-20*	*University of Florida*	*Sheet 2 of 23*	

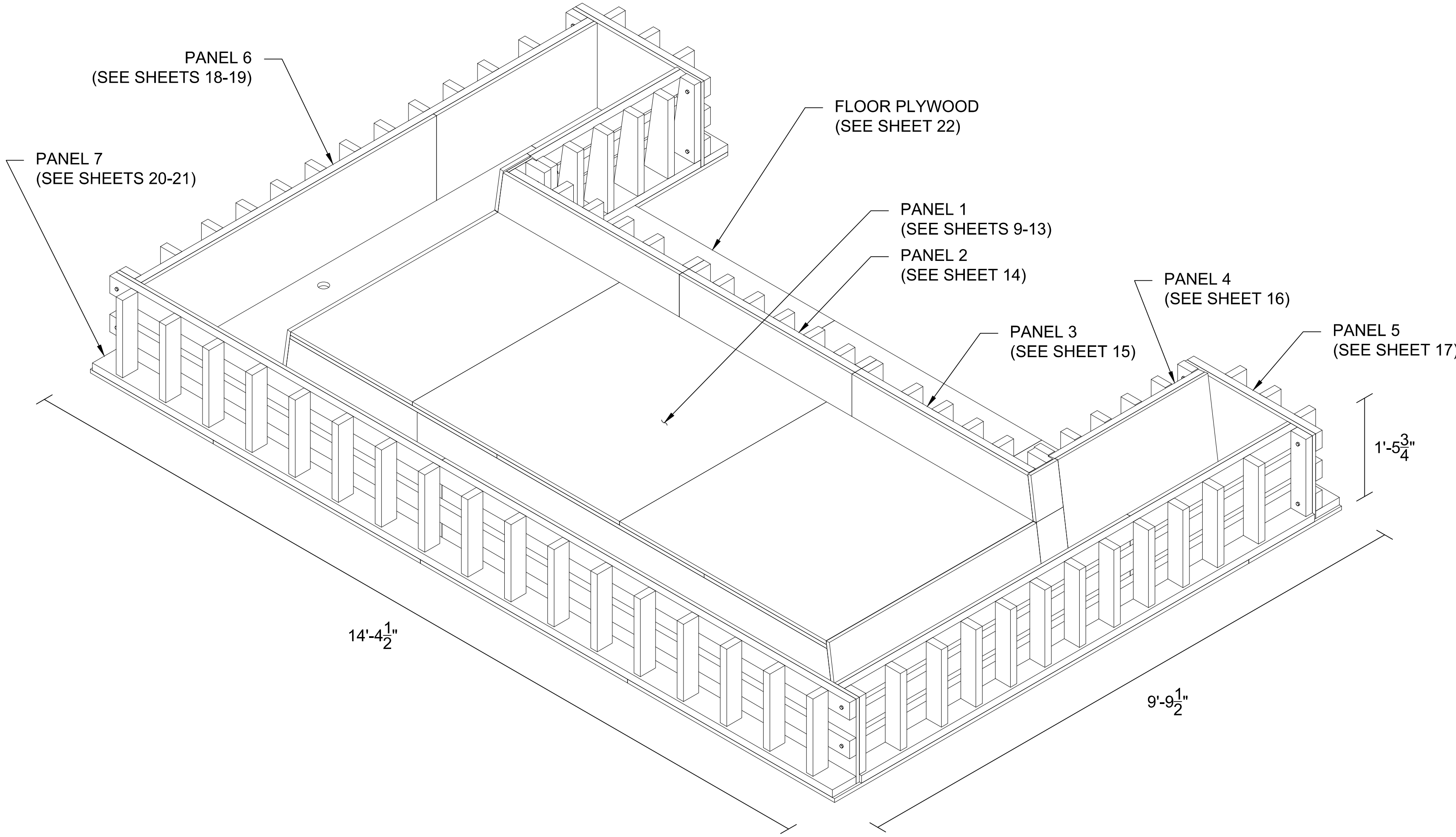

DECK FORMWORK
FRONT ISOMETRIC VIEW

Fiber-Reinforced Concrete Traffic Railings for Impact Loading				Revisions:
Deck formwork	2019-12-20	University of Florida	Sheet 3 of 23	

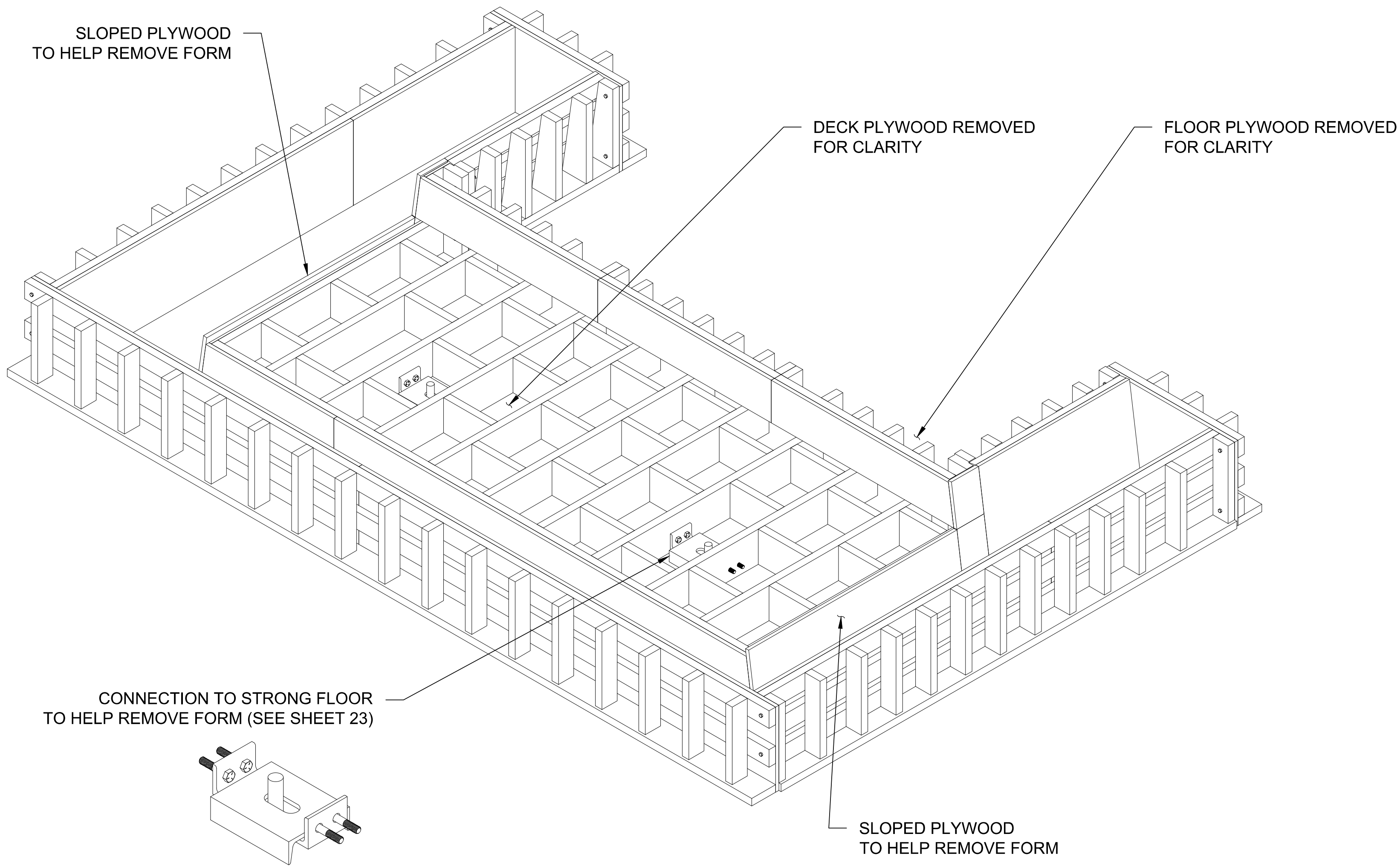

STRONG FLOOR CONNECTION HARDWARE
FRONT ISOMETRIC VIEW

DECK FORMWORK
FRONT ISOMETRIC VIEW

Fiber-Reinforced Concrete Traffic Railings for Impact Loading				Revisions:
Deck formwork	2019-12-20	University of Florida	Sheet 4 of 23	

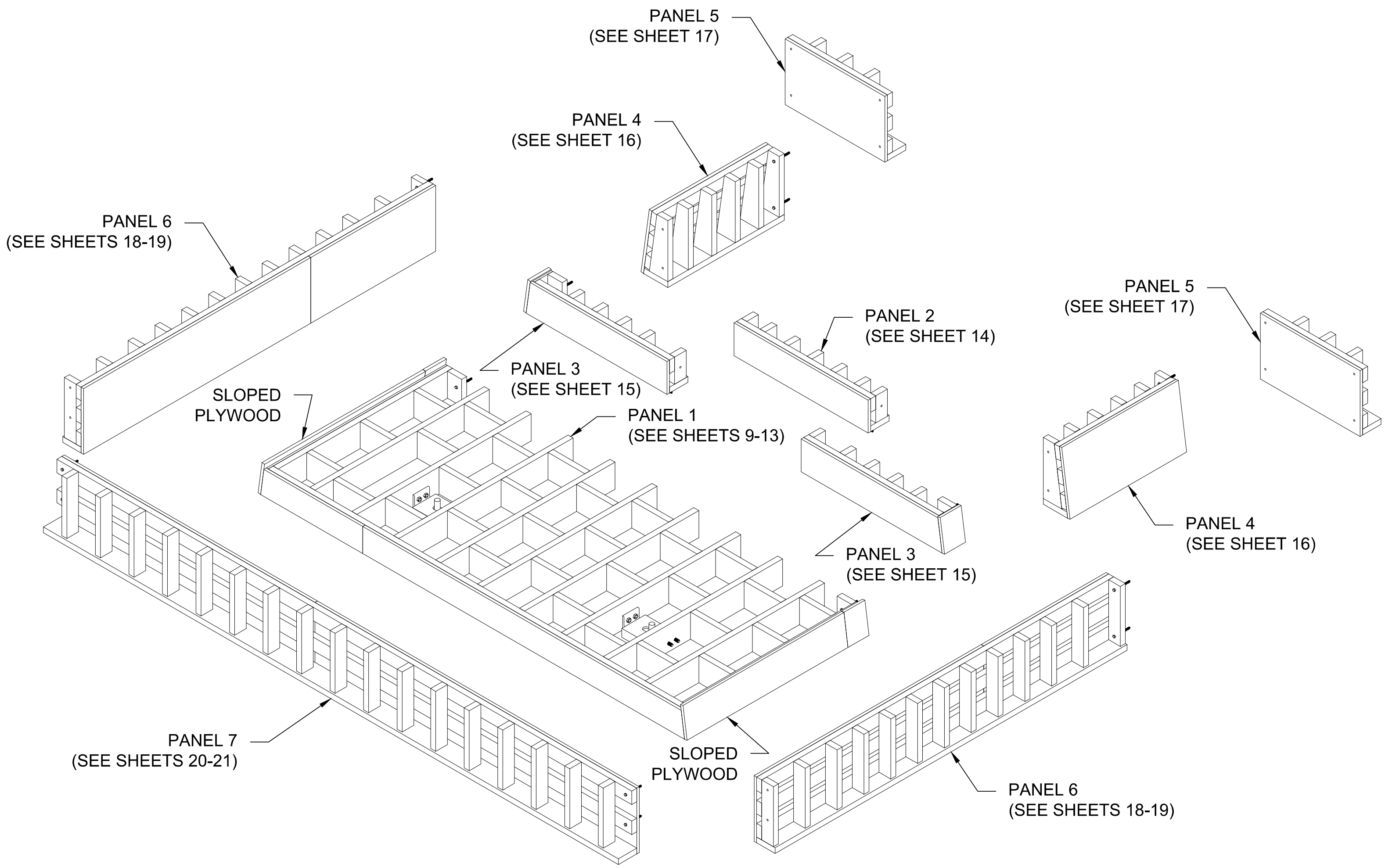

DECK FORMWORK
FRONT ISOMETRIC VIEW

Fiber-Reinforced Concrete Traffic Railings for Impact Loading				*Revisions:*	
Deck formwork	*2019-12-20*	*University of Florida*	*Sheet 5 of 23*		

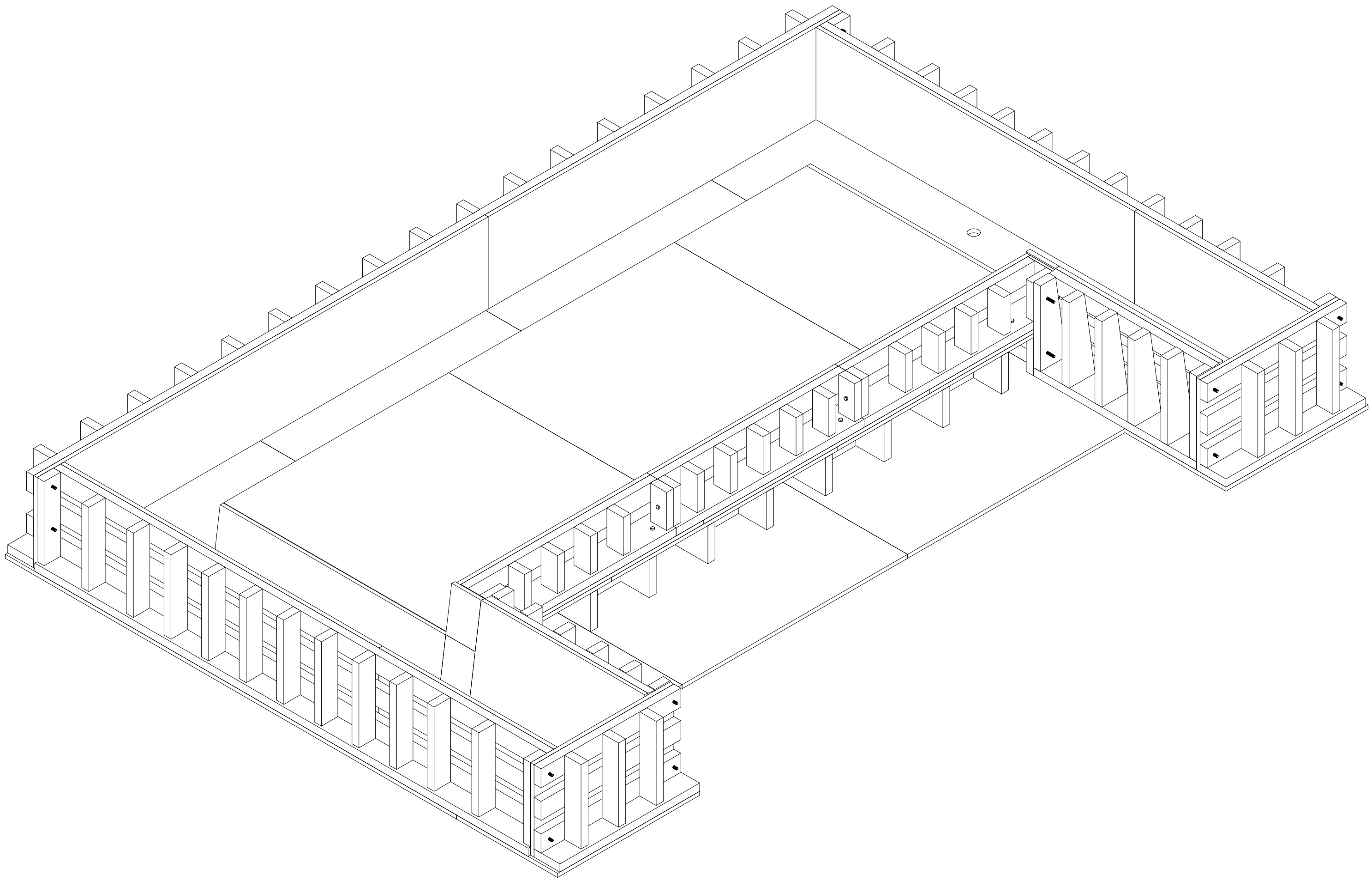

DECK FORMWORK
BACK ISOMETRIC VIEW

Fiber-Reinforced Concrete Traffic Railings for Impact Loading				*Revisions:*	
Deck formwork	*2019-12-20*	*University of Florida*	*Sheet 6 of 23*		

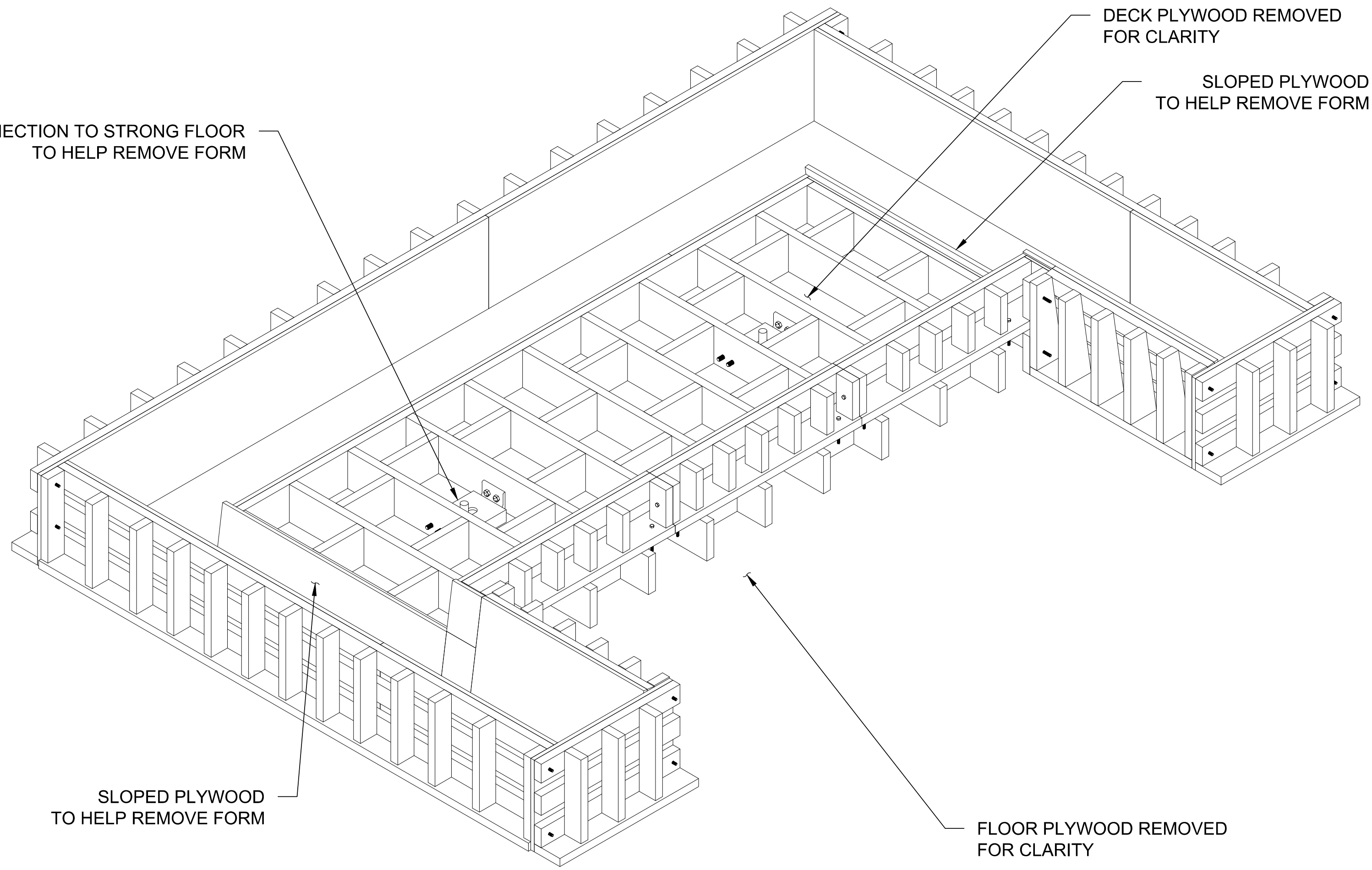

DECK FORMWORK
BACK ISOMETRIC VIEW

Fiber-Reinforced Concrete Traffic Railings for Impact Loading				*Revisions:*		
Deck formwork	*2019-12-20*	*University of Florida*	*Sheet 7 of 23*			

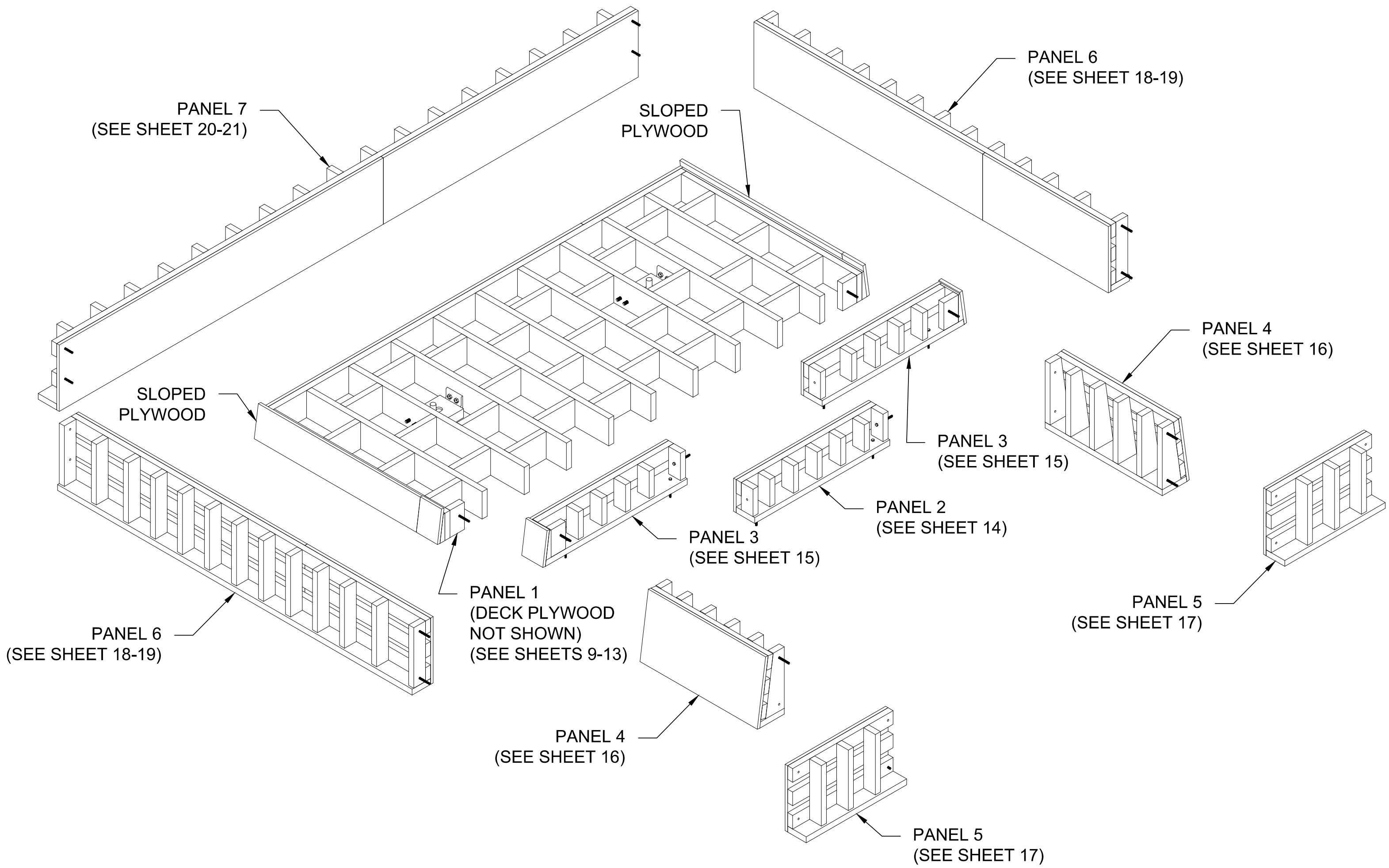

DECK FORMWORK
BACK ISOMETRIC VIEW

Fiber-Reinforced Concrete Traffic Railings for Impact Loading				*Revisions:*
Deck formwork	*2019-12-20*	*University of Florida*	*Sheet 8 of 23*	

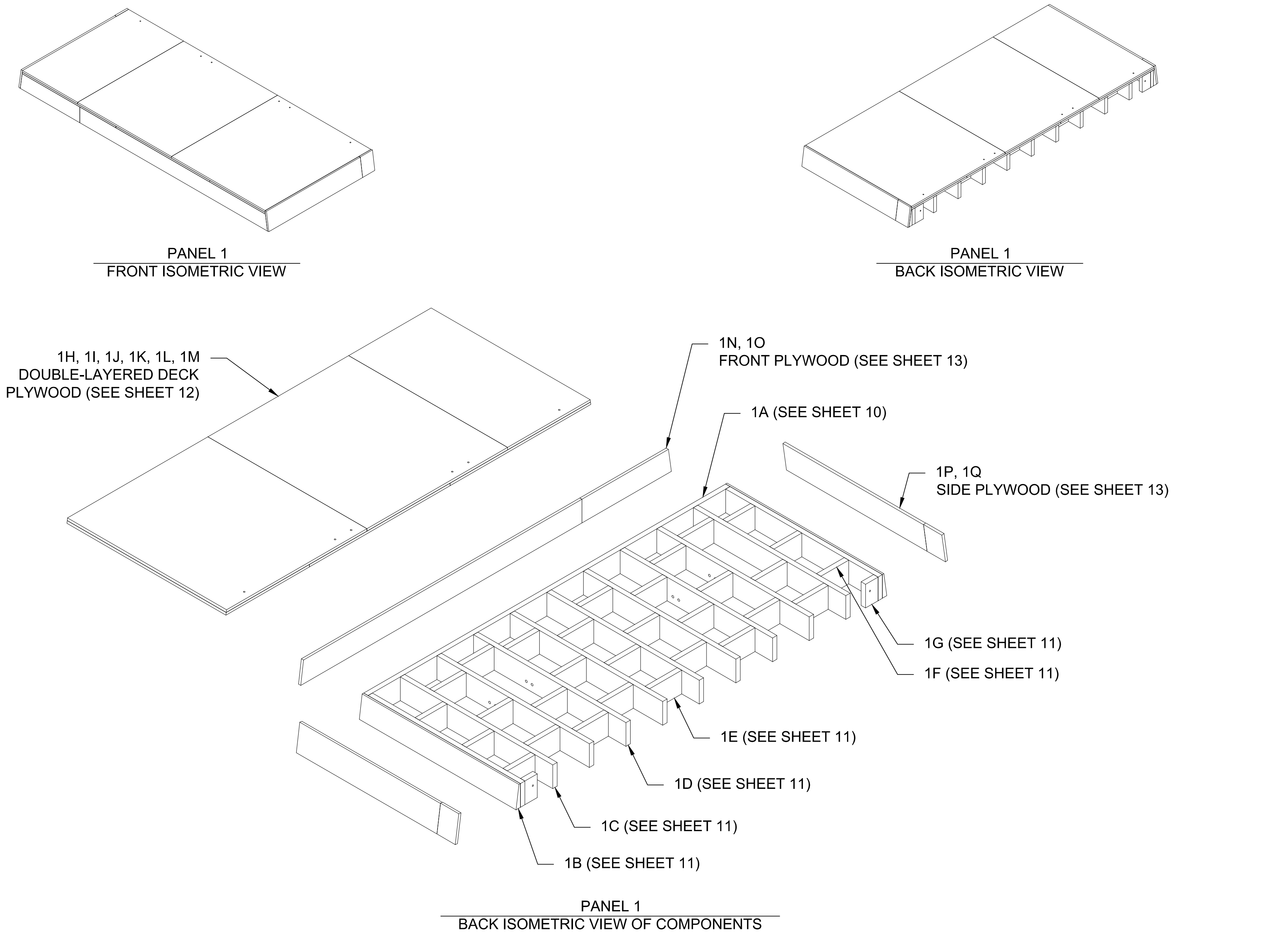

Fiber-Reinforced Concrete Traffic Railings for Impact Loading				*Revisions:*
Deck formwork	*2019-12-20*	*University of Florida*	*Sheet 9 of 23*	

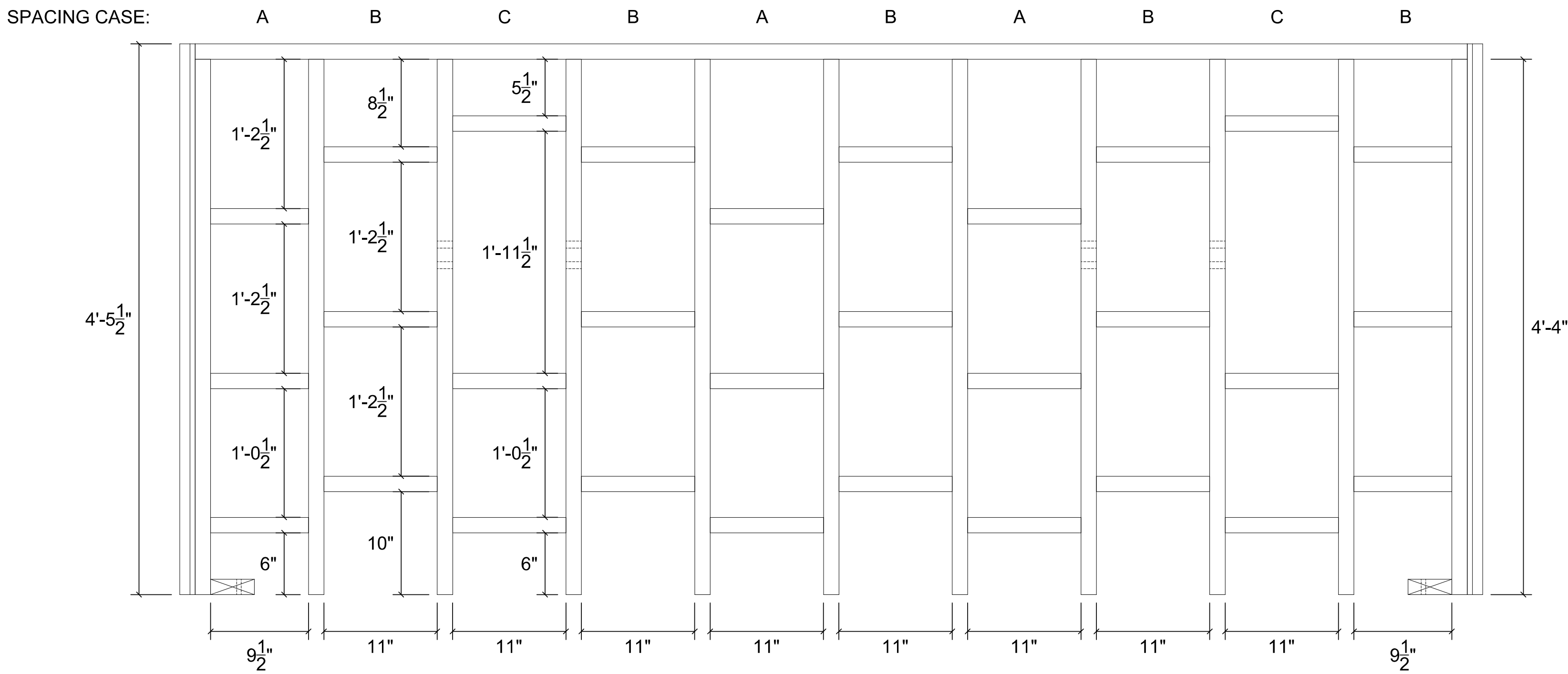

PANEL 1 SPACING
PLAN VIEW

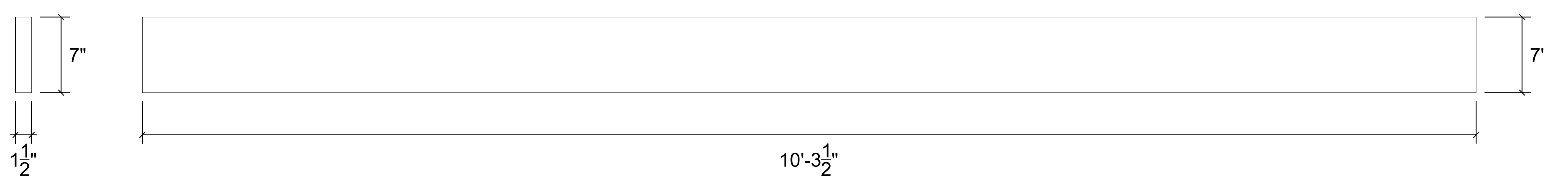

1A: 2x8
QTY: 1

Fiber-Reinforced Concrete Traffic Railings for Impact Loading				*Revisions:*
Deck formwork	*2019-12-20*	*University of Florida*	*Sheet 10 of 23*	

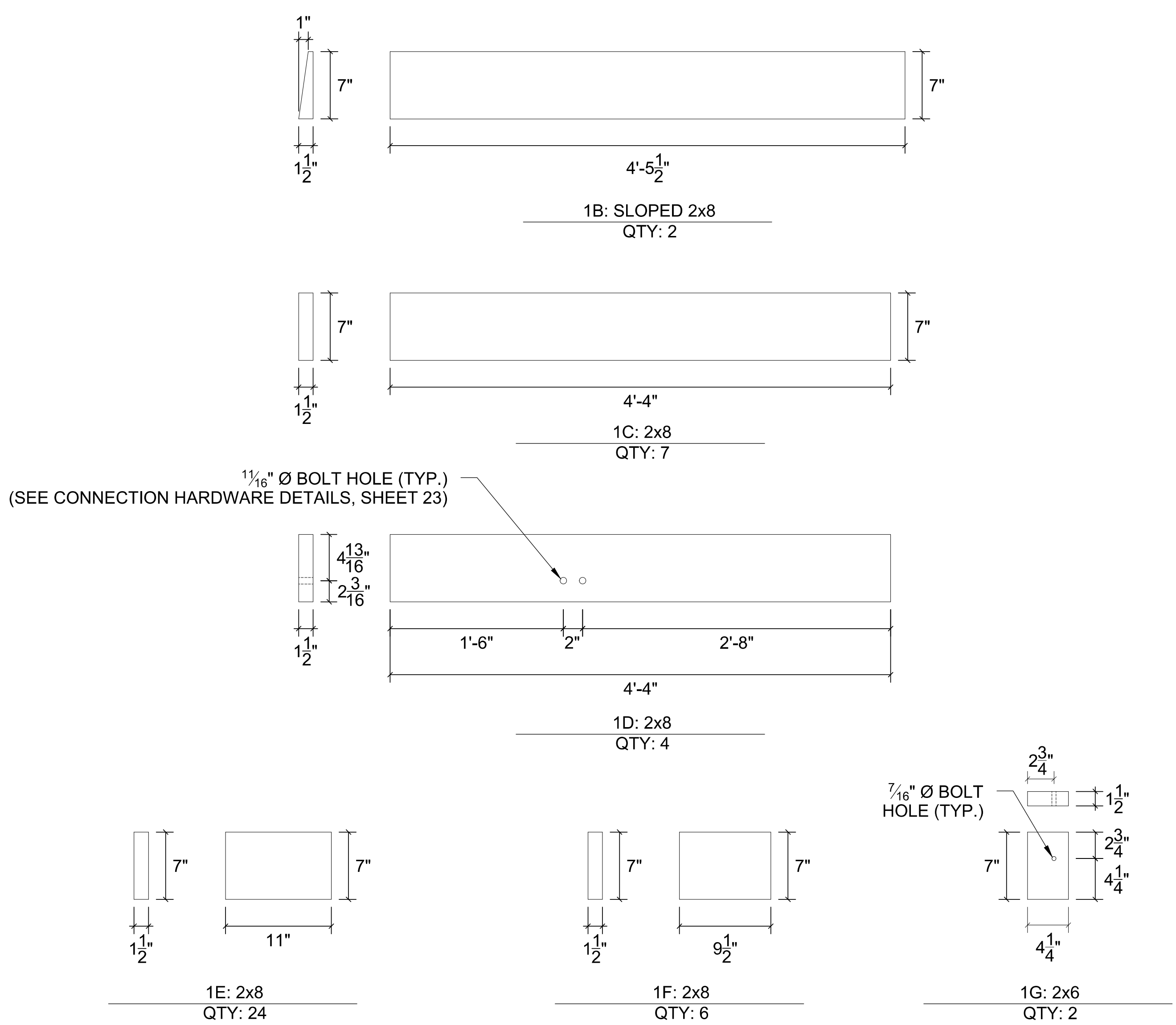

Fiber-Reinforced Concrete Traffic Railings for Impact Loading				*Revisions:*	*Revised 1G details*	
Deck formwork	*2020-01-10*	*University of Florida*	*Sheet 11 of 23*			

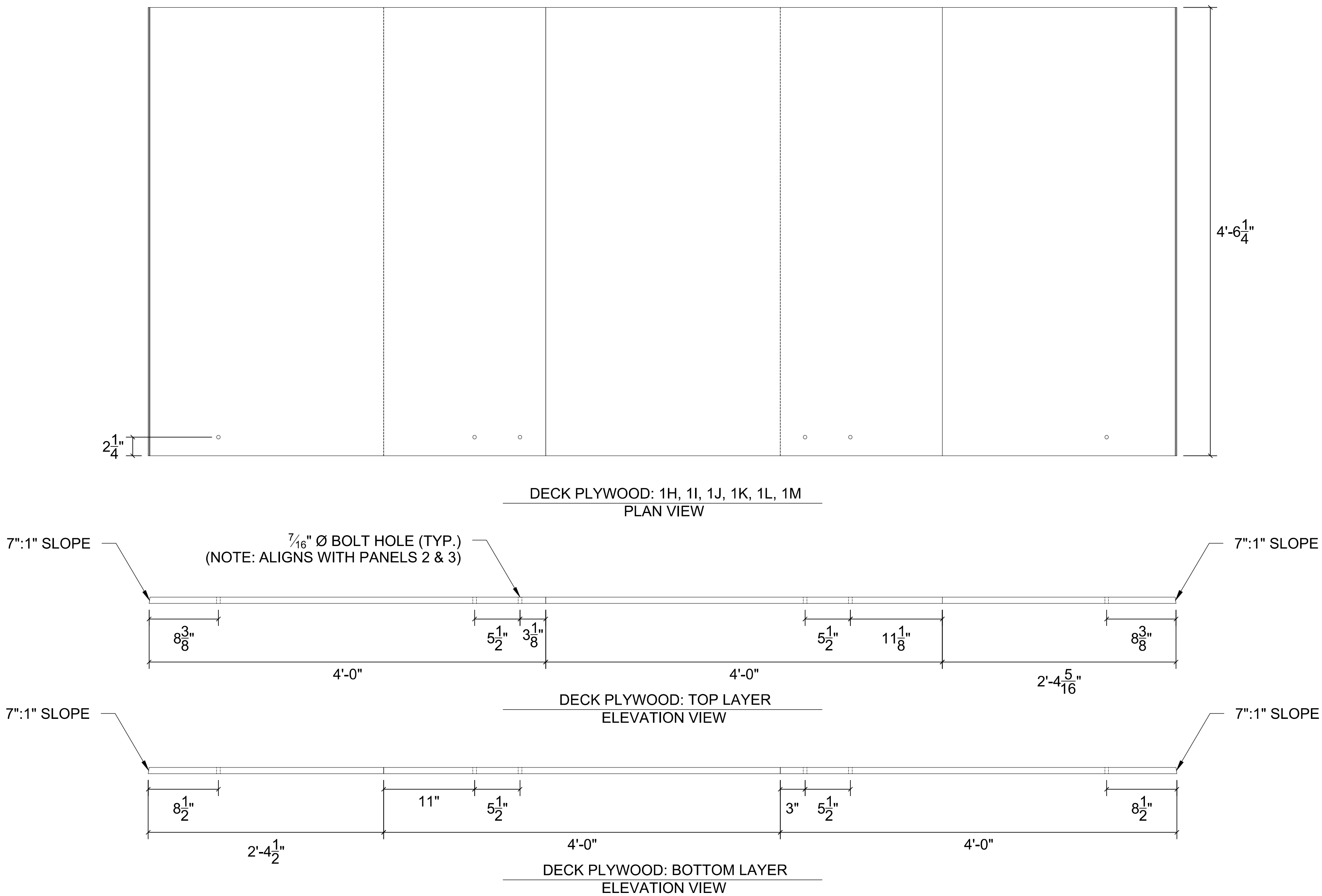

Fiber-Reinforced Concrete Traffic Railings for Impact Loading				*Revisions:*
Deck formwork	*2019-12-20*	*University of Florida*	*Sheet 12 of 23*	

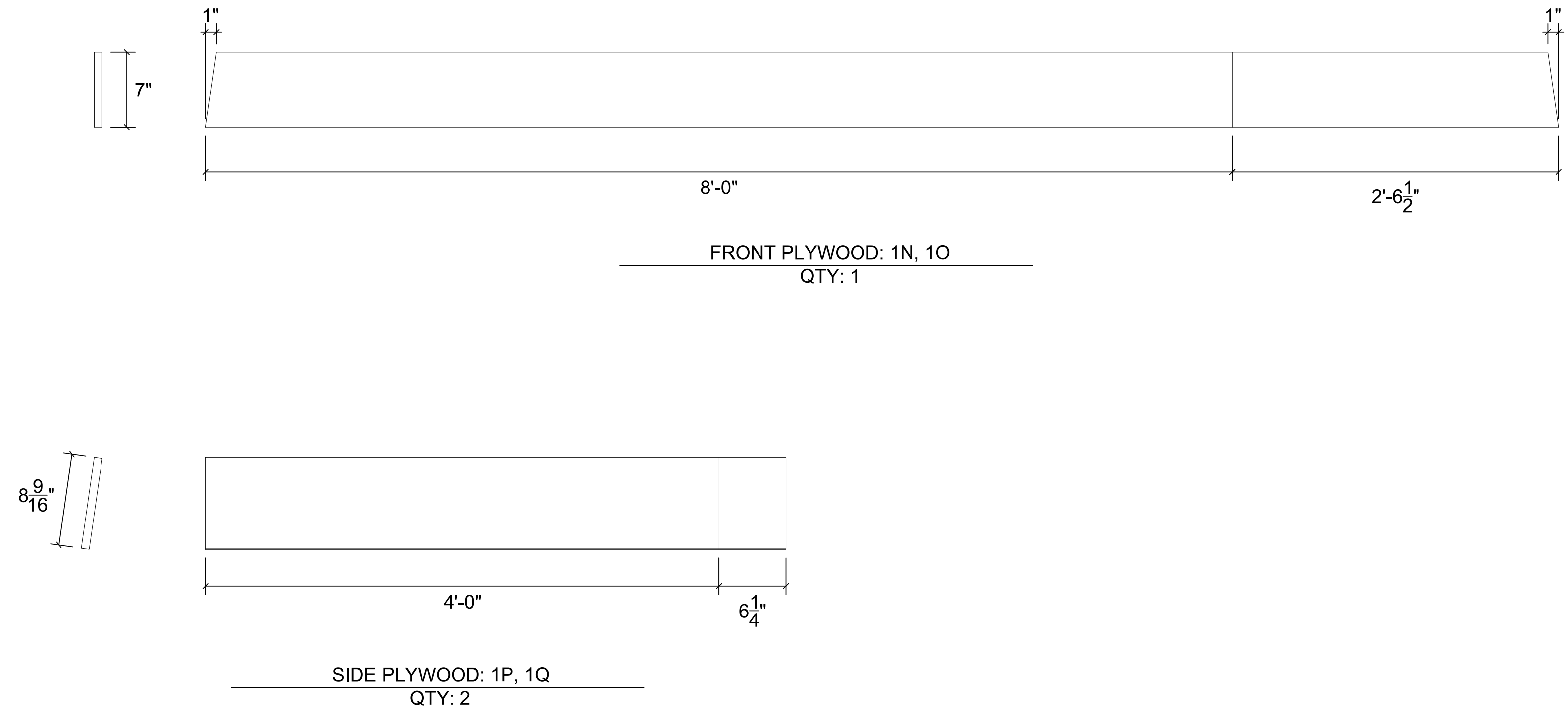

Fiber-Reinforced Concrete Traffic Railings for Impact Loading				*Revisions:*		
Deck formwork	*2019-12-20*	*University of Florida*	*Sheet 13 of 23*			

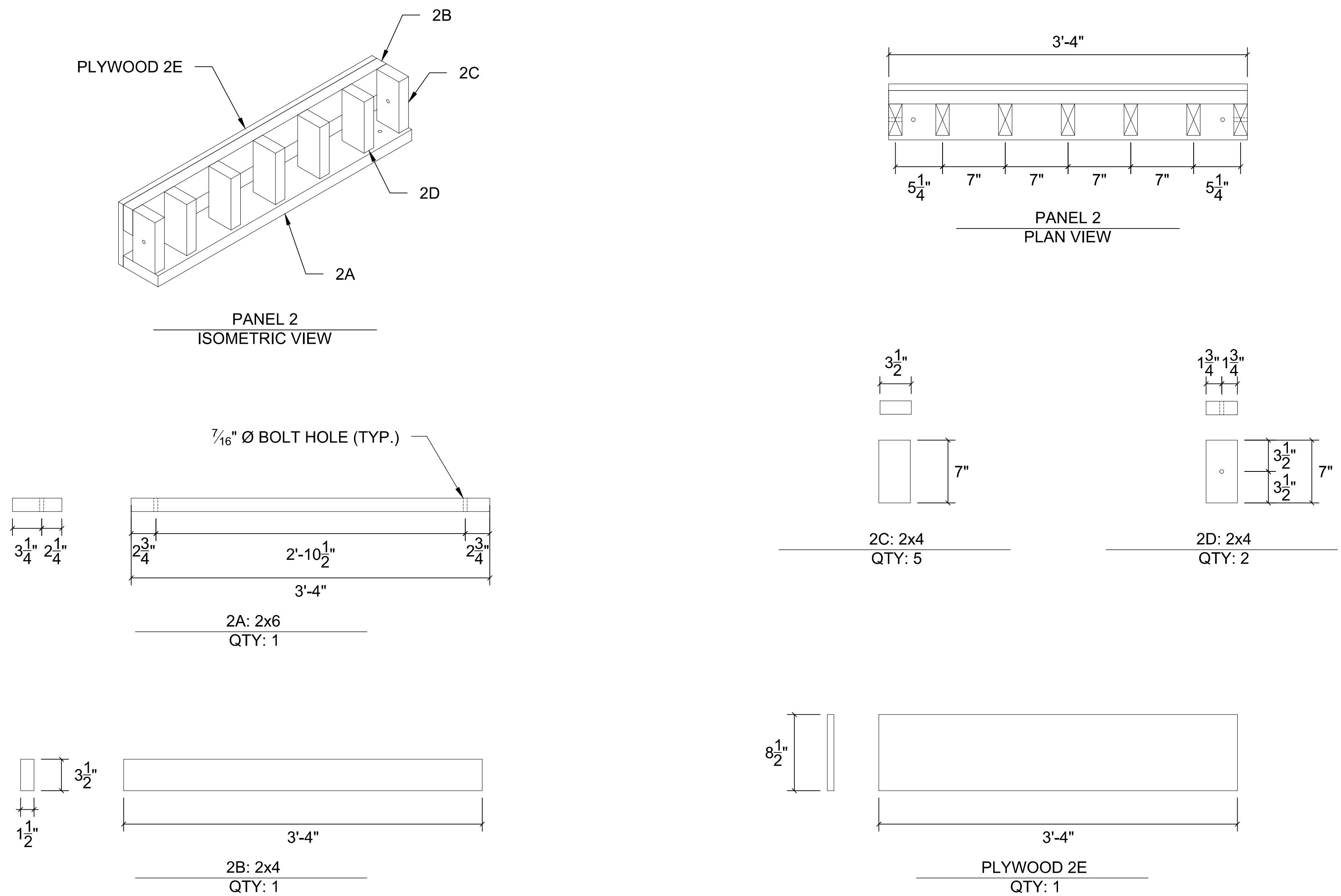

Fiber-Reinforced Concrete Traffic Railings for Impact Loading				*Revisions:*
Deck formwork	*2019-12-20*	*University of Florida*	*Sheet 14 of 23*	

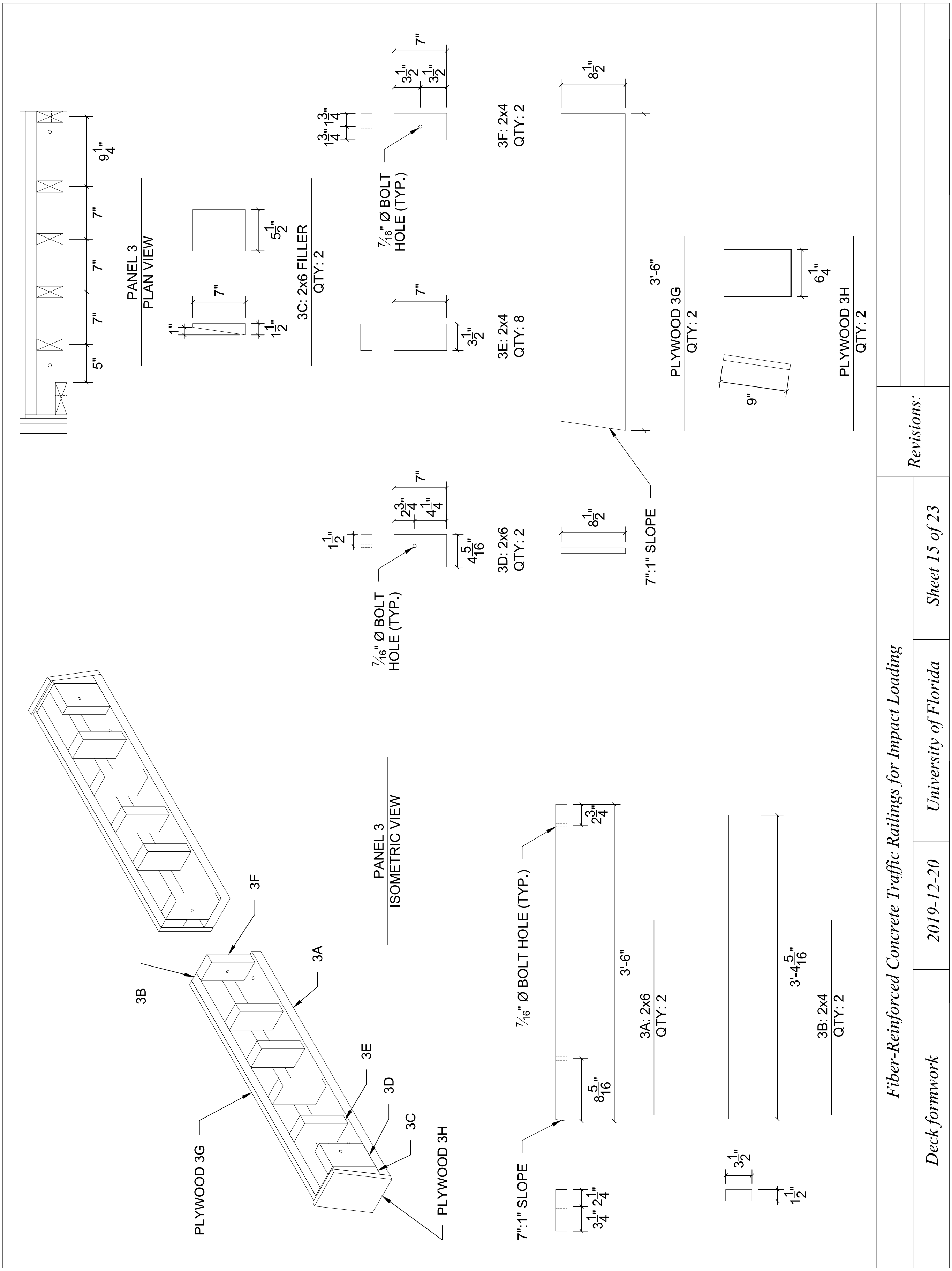
PANEL 3
PLAN VIEW
PANEL 3
ISOMETRIC VIEW
3A
3B
3C
3D
3E
3F
PLYWOOD 3G
PLYWOOD 3H
3C: 2x6 FILLER
QTY: 2
3D: 2x6
QTY: 2
3E: 2x4
QTY: 8
3F: 2x4
QTY: 2
PLYWOOD 3G
QTY: 2
PLYWOOD 3H
QTY: 2
3A: 2x6
QTY: 2
3B: 2x4
QTY: 2
7/16" Ø BOLT HOLE (TYP.)
7":1" SLOPE
3'-6"
3'-4 5/16"
Revisions:
Fiber-Reinforced Concrete Traffic Railings for Impact Loading
Deck formwork
2019-12-20
University of Florida
Sheet 15 of 23

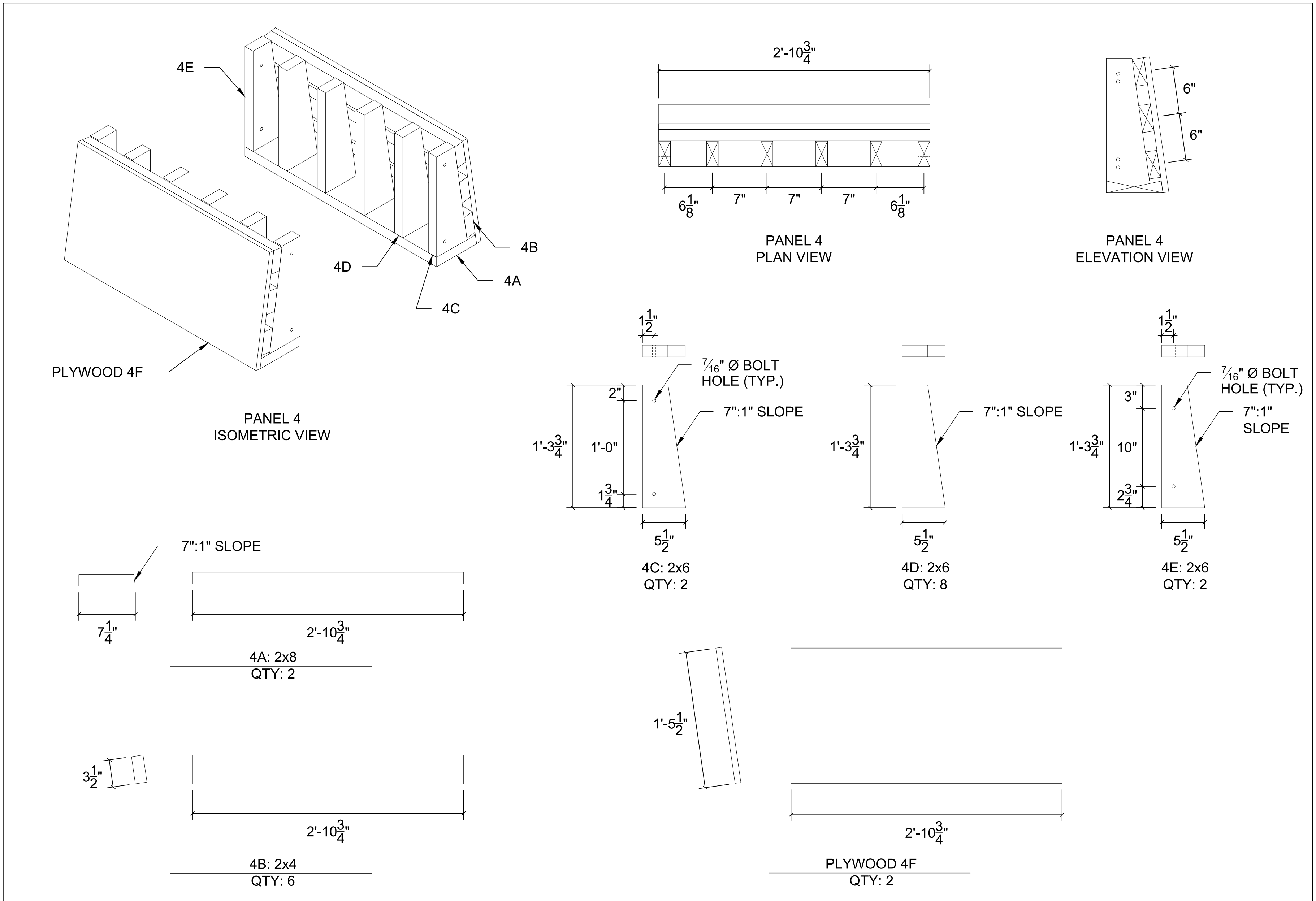

Fiber-Reinforced Concrete Traffic Railings for Impact Loading

Deck formwork | *2019-12-20* | *University of Florida* | *Sheet 16 of 23*

Revisions:

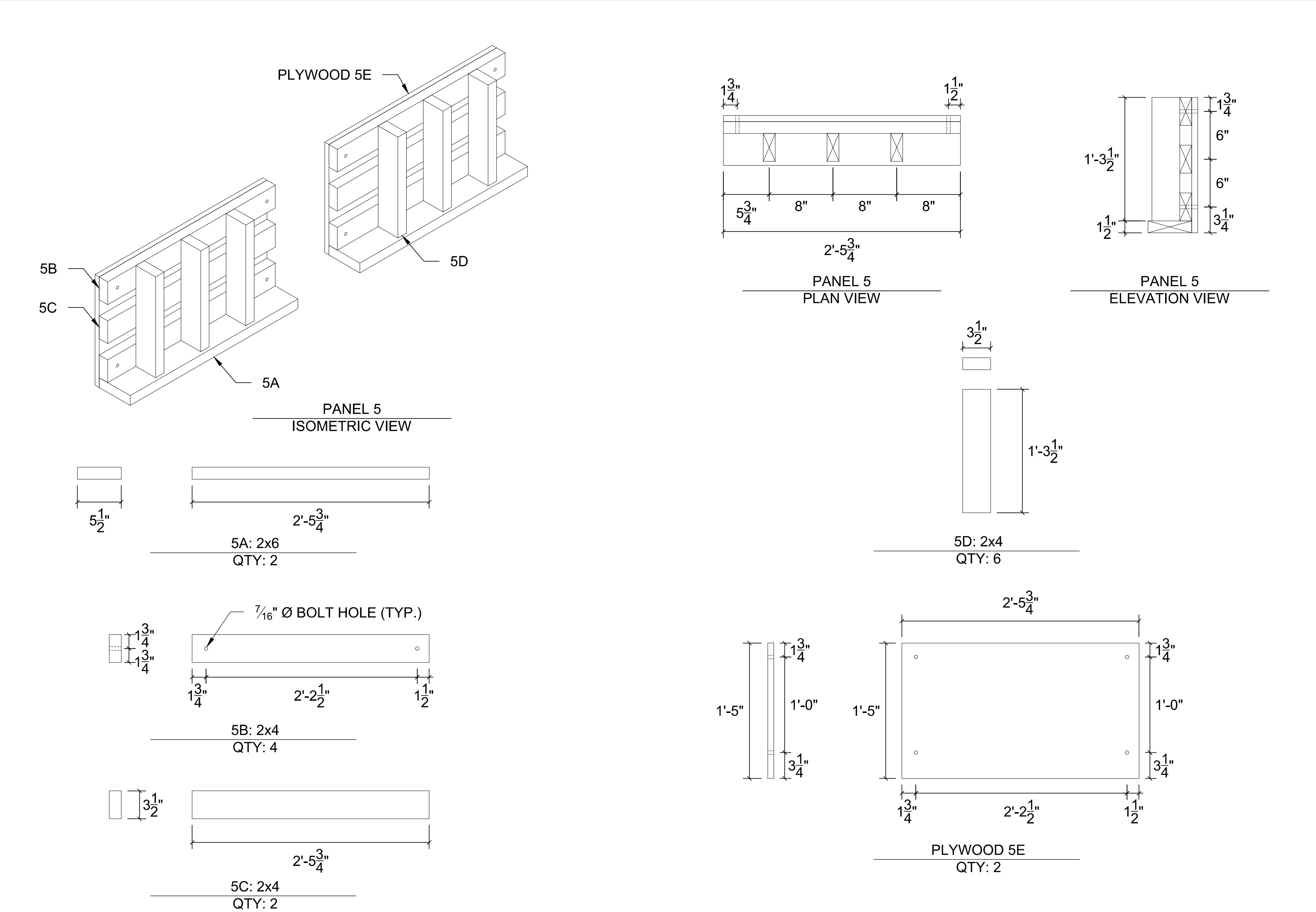

Fiber-Reinforced Concrete Traffic Railings for Impact Loading				*Revisions:*
Deck formwork	*2019-12-20*	*University of Florida*	*Sheet 17 of 23*	

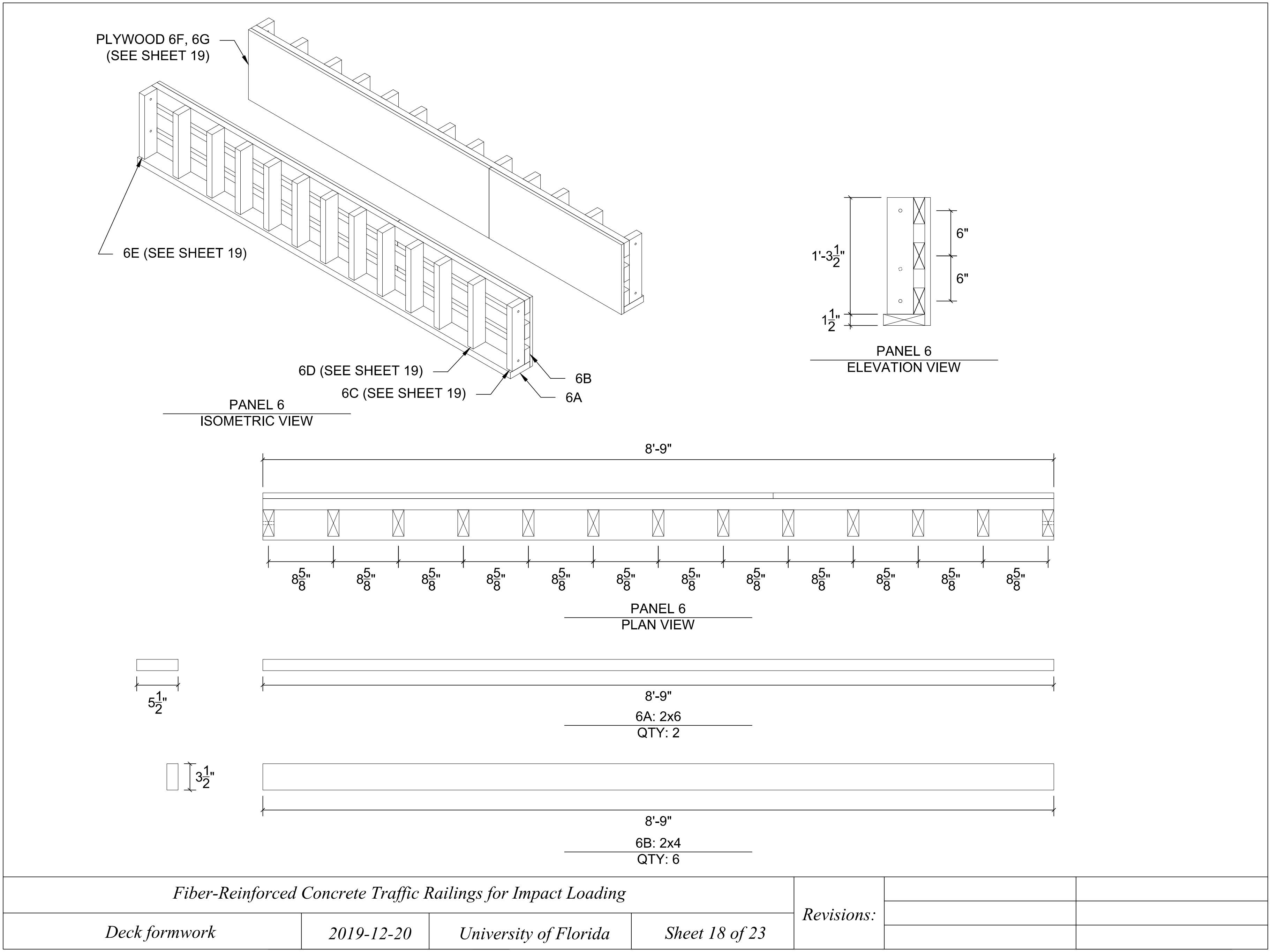
PLYWOOD 6F, 6G
(SEE SHEET 19)
6E (SEE SHEET 19)
6D (SEE SHEET 19)
6C (SEE SHEET 19)
6B
6A
PANEL 6
ISOMETRIC VIEW
6"
6"
1'-3 1/2"
1 1/2"
PANEL 6
ELEVATION VIEW
8'-9"
8 5/8"
PANEL 6
PLAN VIEW
5 1/2"
8'-9"
6A: 2x6
QTY: 2
3 1/2"
8'-9"
6B: 2x4
QTY: 6
Fiber-Reinforced Concrete Traffic Railings for Impact Loading
Revisions:
Deck formwork
2019-12-20
University of Florida
Sheet 18 of 23

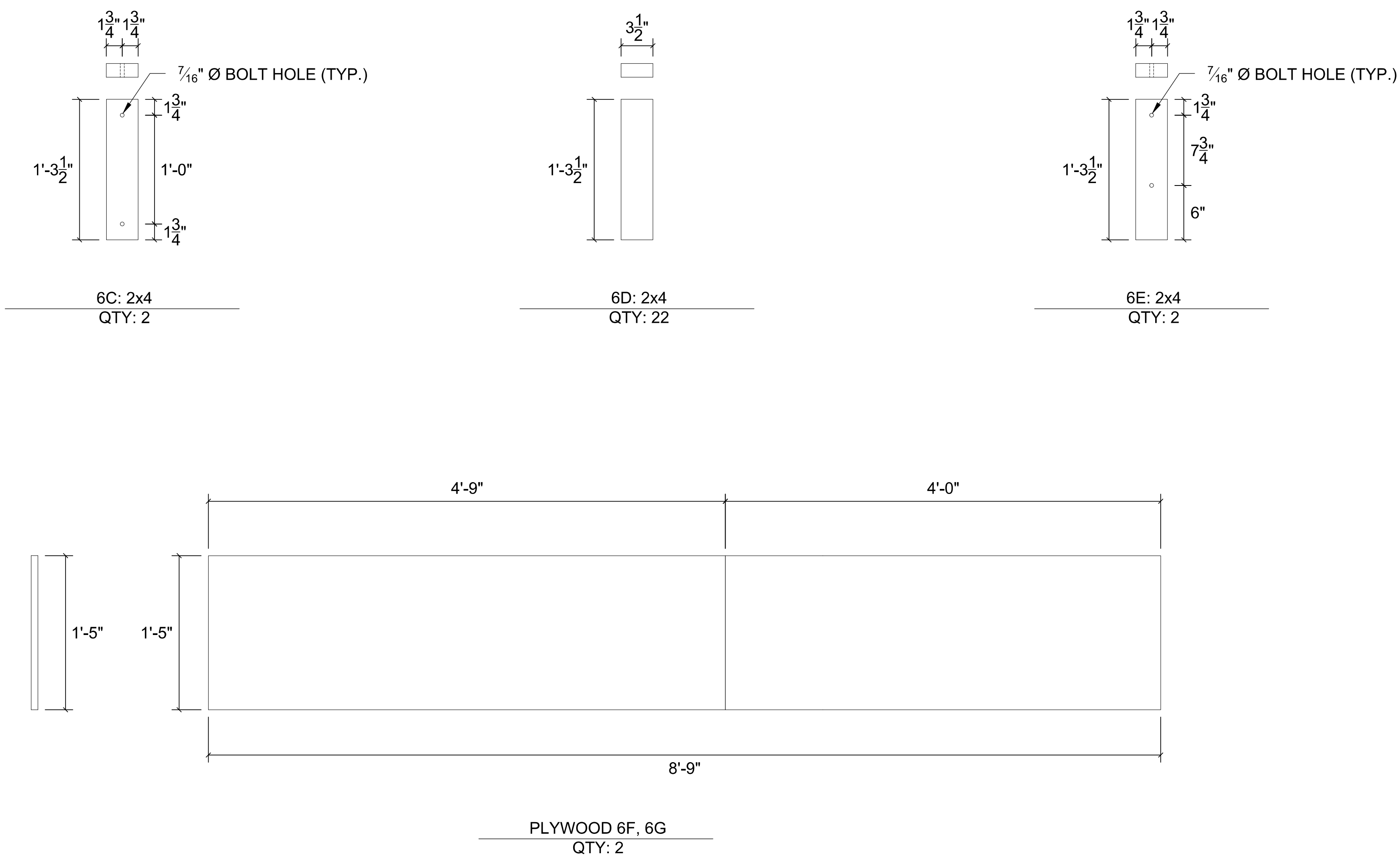

Fiber-Reinforced Concrete Traffic Railings for Impact Loading				*Revisions:*
Deck formwork	*2019-12-20*	*University of Florida*	*Sheet 19 of 23*	

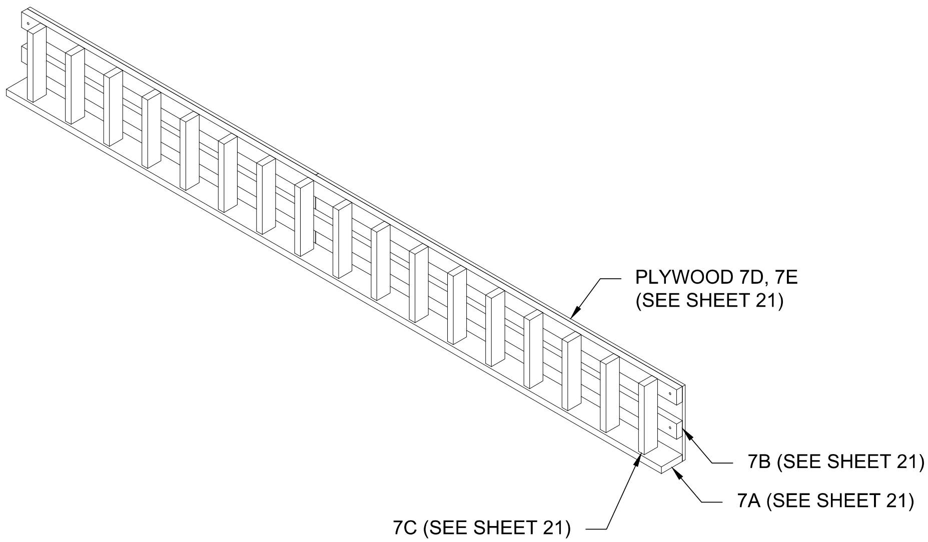

PANEL 7
ISOMETRIC VIEW

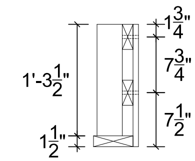

PANEL 7
ELEVATION VIEW

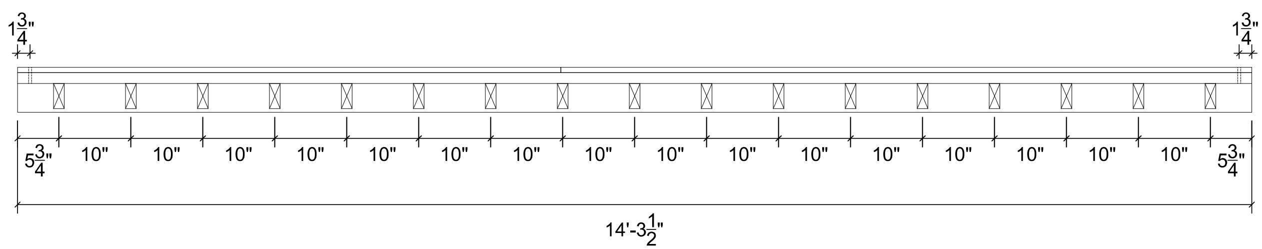

PANEL 7
PLAN VIEW

Fiber-Reinforced Concrete Traffic Railings for Impact Loading				*Revisions:*	
Deck formwork	*2019-12-20*	*University of Florida*	*Sheet 20 of 23*		

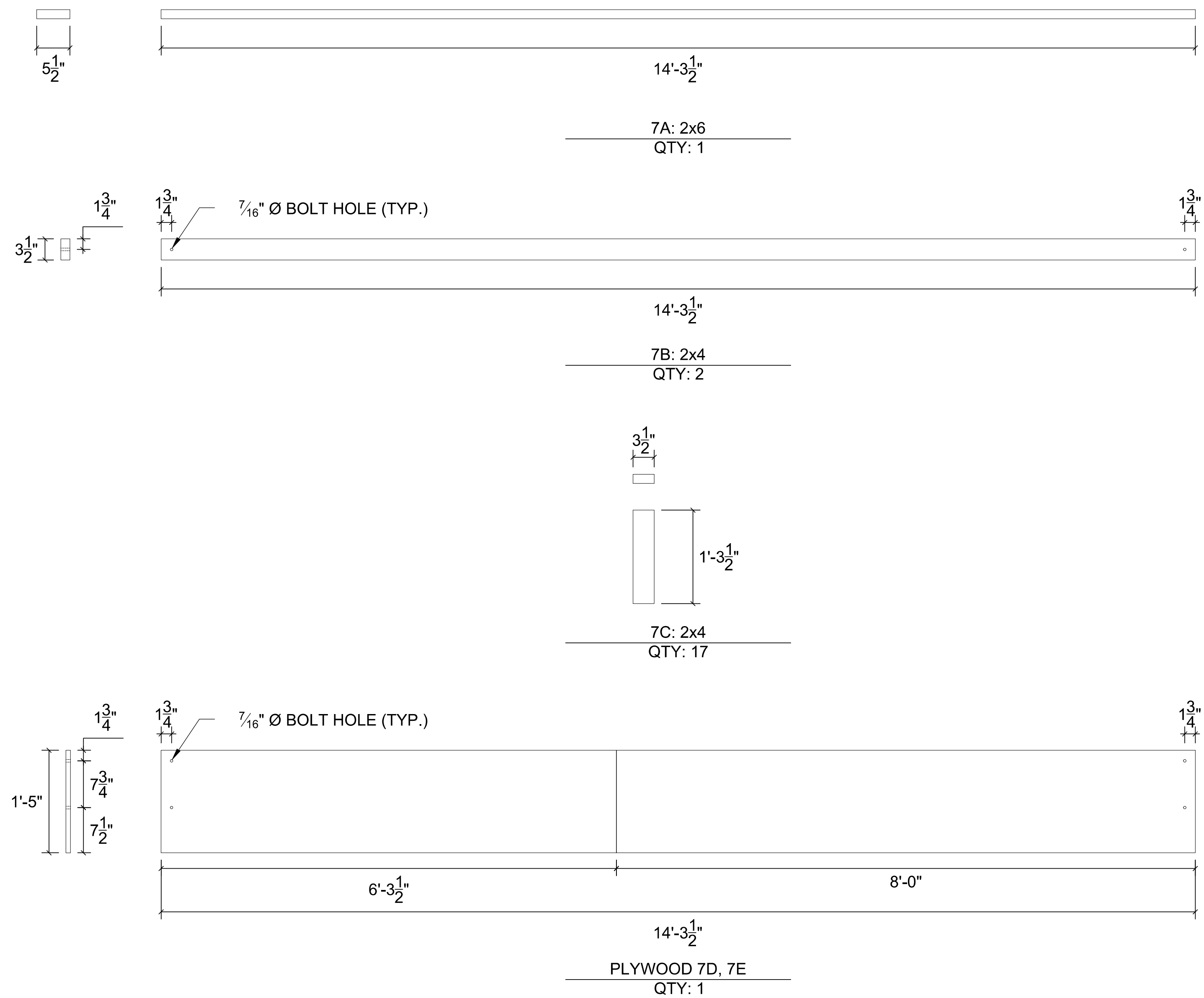

Fiber-Reinforced Concrete Traffic Railings for Impact Loading				*Revisions:*		
Deck formwork	*2019-12-20*	*University of Florida*	*Sheet 21 of 23*			

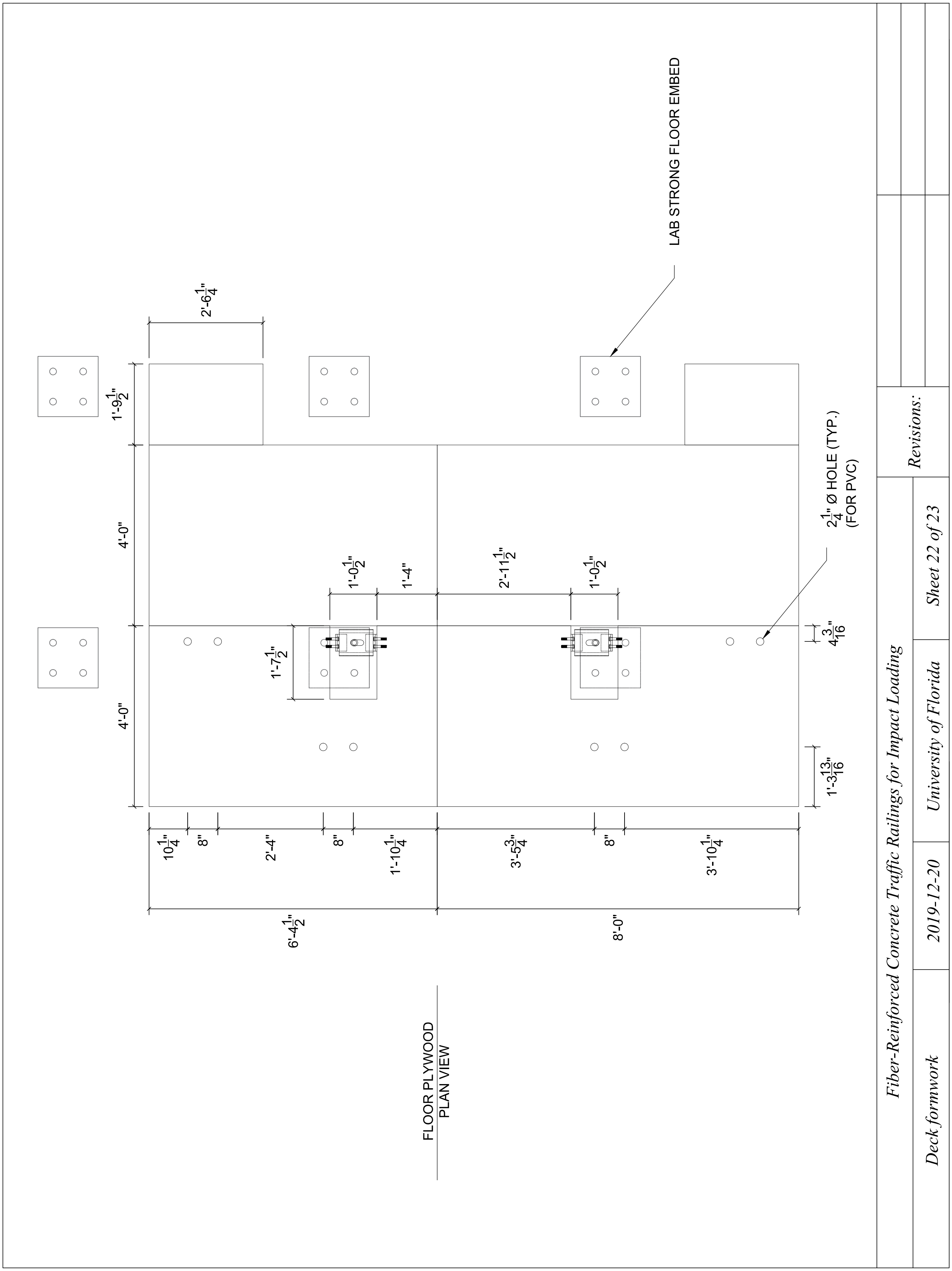
LAB STRONG FLOOR EMBED
2'-6 1/4"
1'-9 1/2"
4'-0"
4'-0"
1'-0 1/2"
1'-4"
2'-11 1/2"
1'-0 1/2"
1'-7 1/2"
2 1/4" Ø HOLE (TYP.)
(FOR PVC)
4 3/16"
1'-3 13/16"
10 1/4"
8"
2'-4"
8"
1'-10 1/4"
3'-5 3/4"
8"
3'-10 1/4"
6'-4 1/2"
8'-0"
FLOOR PLYWOOD
PLAN VIEW
Revisions:
Fiber-Reinforced Concrete Traffic Railings for Impact Loading
Deck formwork
2019-12-20
University of Florida
Sheet 22 of 23

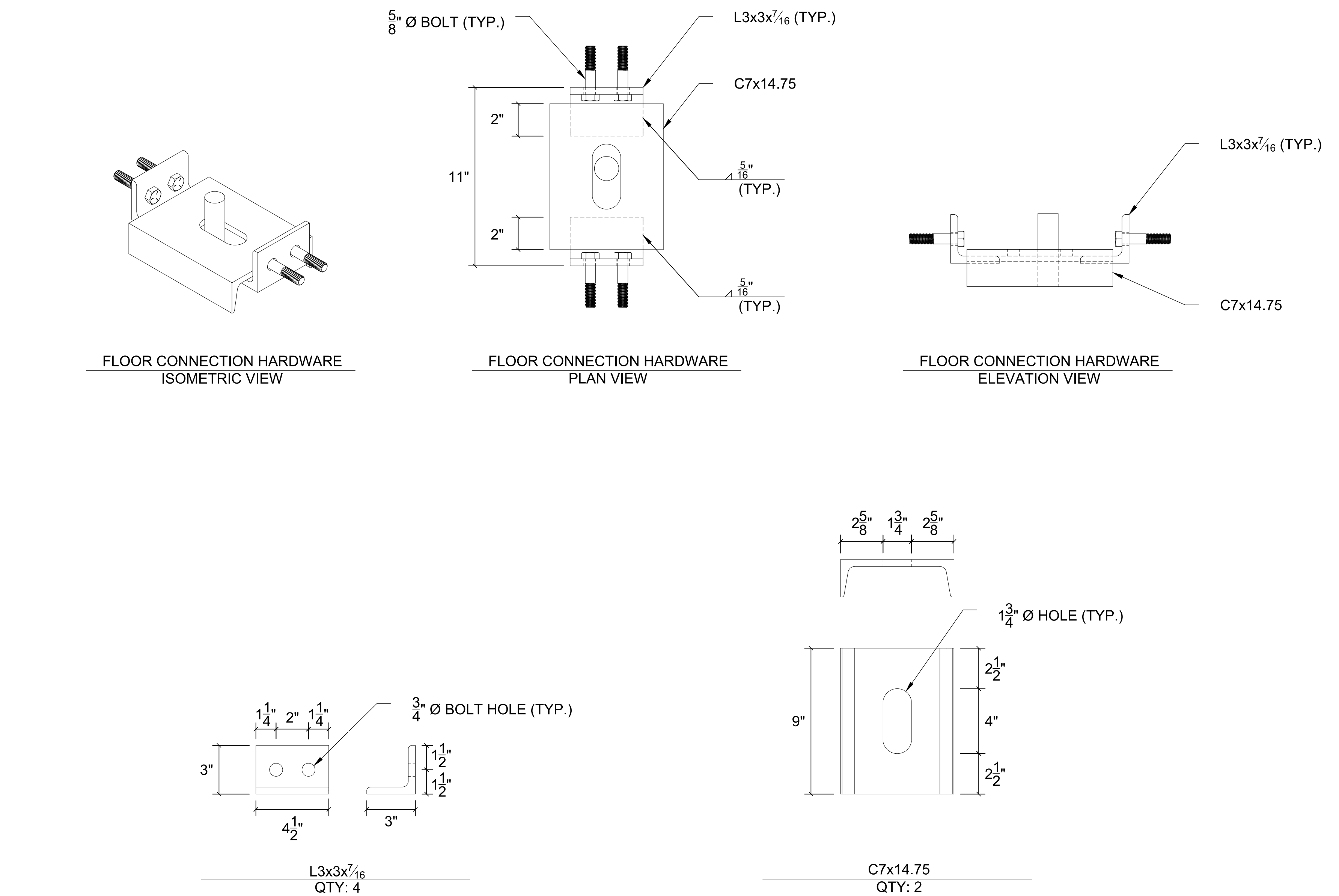

Fiber-Reinforced Concrete Traffic Railings for Impact Loading				Revisions:
Deck formwork	2019-12-20	University of Florida	Sheet 23 of 23	

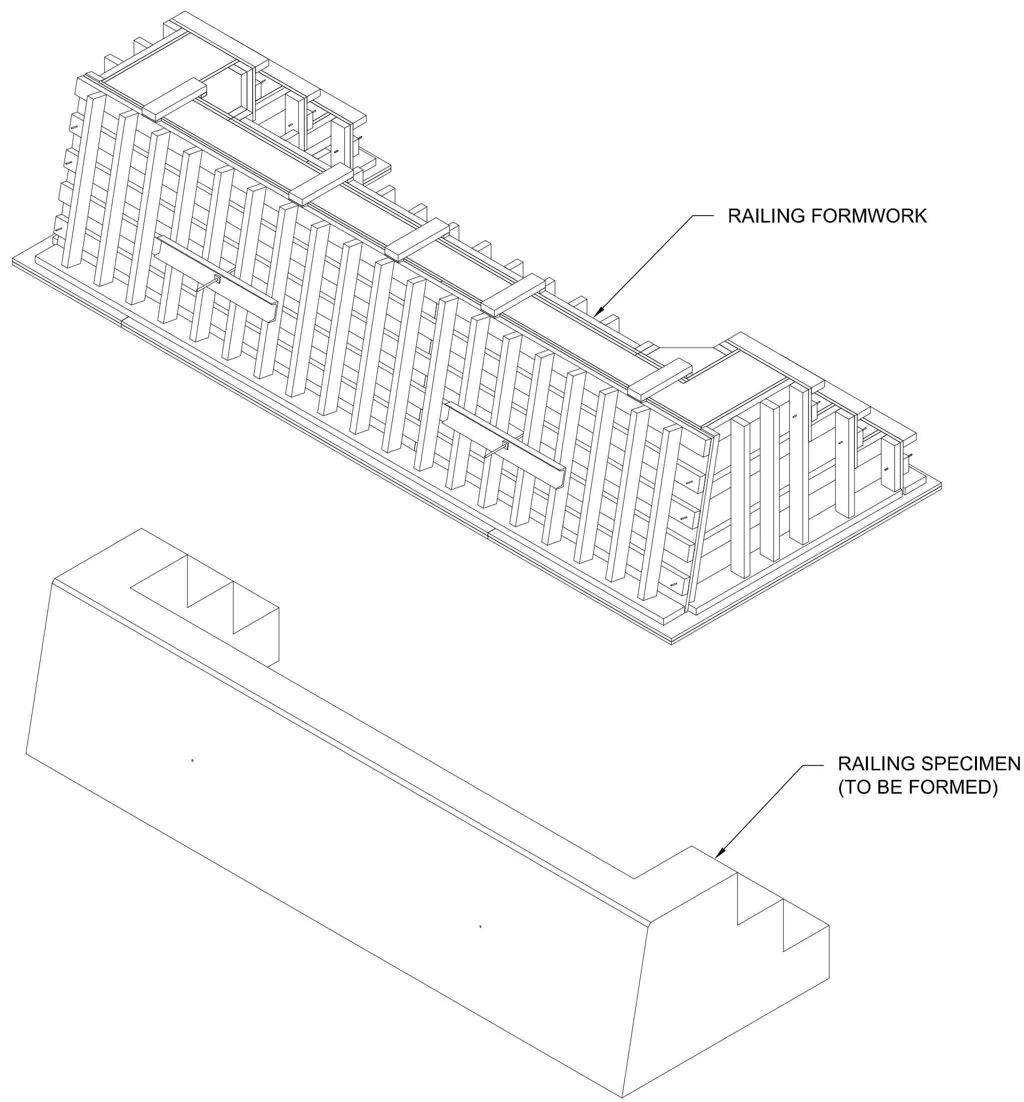

ISOMETRIC VIEW

Fiber-Reinforced Concrete Traffic Railings for Impact Loading				*Revisions:*		
Railing formwork (concept)	*2019-03-04*	*University of Florida*	*Sheet 1 of 16*			

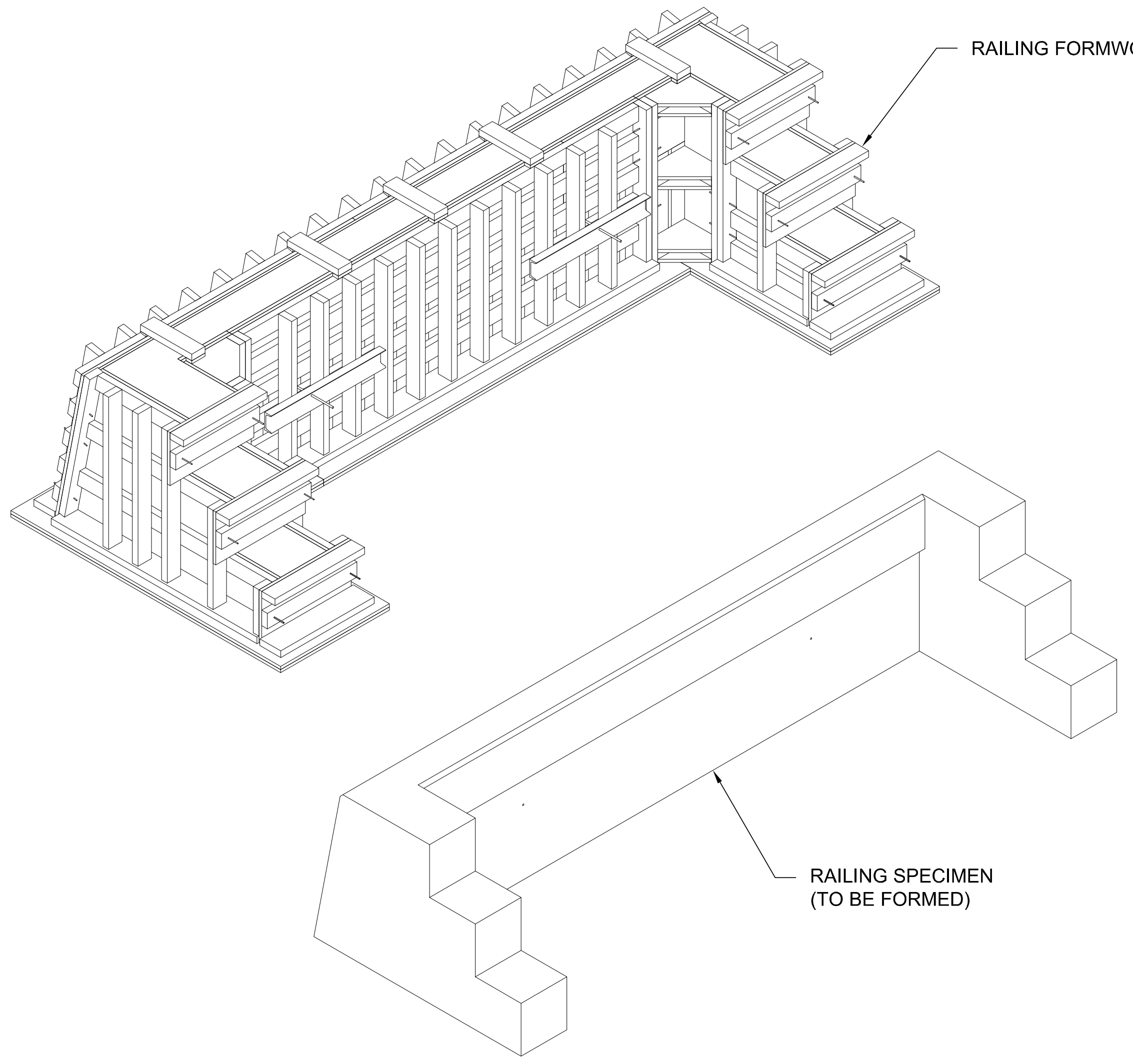

ISOMETRIC VIEW

Fiber-Reinforced Concrete Traffic Railings for Impact Loading				*Revisions:*	
Railing formwork (concept)	*2019-03-04*	*University of Florida*	*Sheet 2 of 16*		

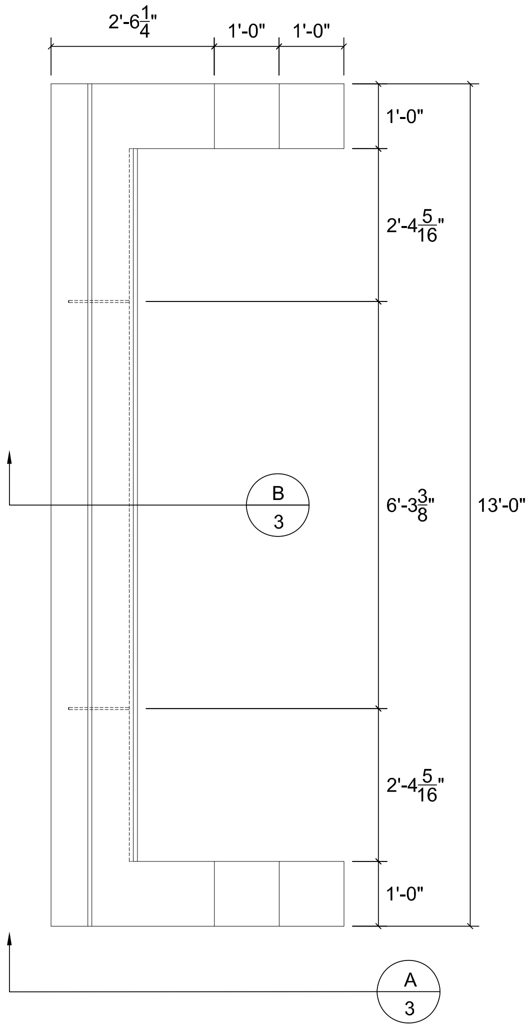

PLAN VIEW
OF CONCRETE RAILING SPECIMEN

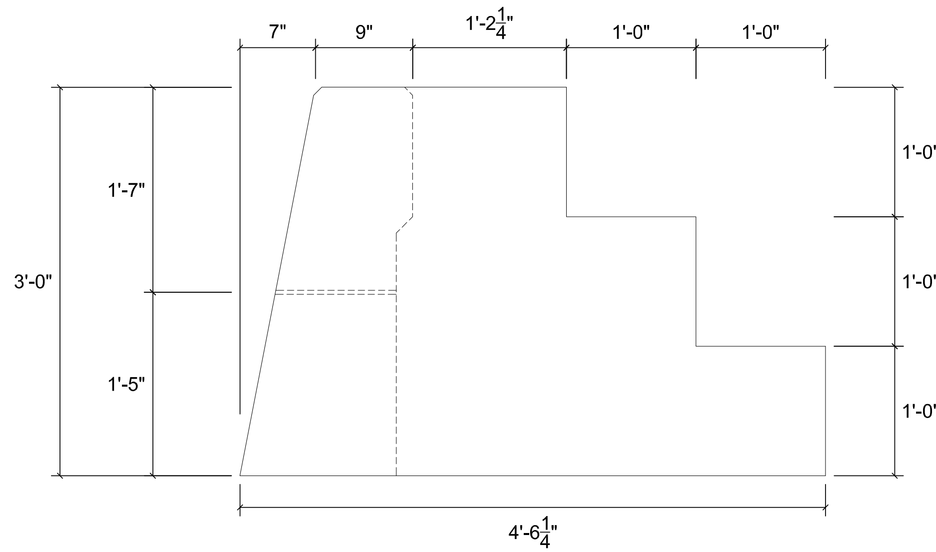

A-3 SIDE ELEVATION VIEW

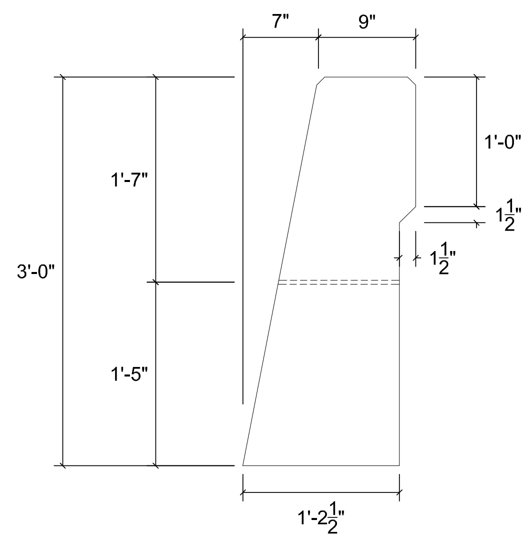

B-3 SIDE ELEVATION VIEW

Fiber-Reinforced Concrete Traffic Railings for Impact Loading				*Revisions:*
Railing formwork (concept)	*2019-03-04*	*University of Florida*	*Sheet 3 of 16*	

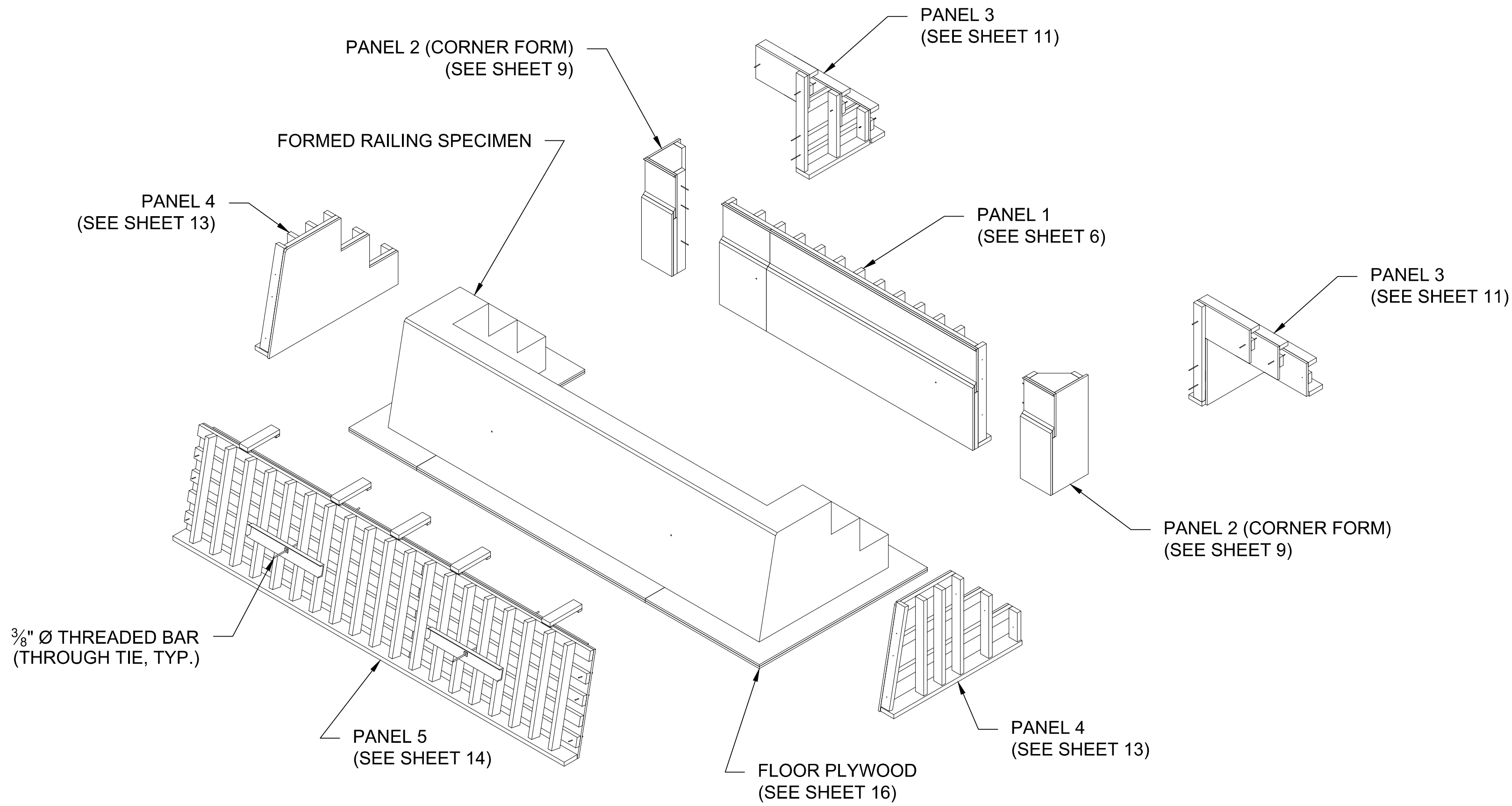

ISOMETRIC VIEW

Fiber-Reinforced Concrete Traffic Railings for Impact Loading				*Revisions:*	
Railing formwork (concept)	*2019-03-04*	*University of Florida*	*Sheet 4 of 16*		

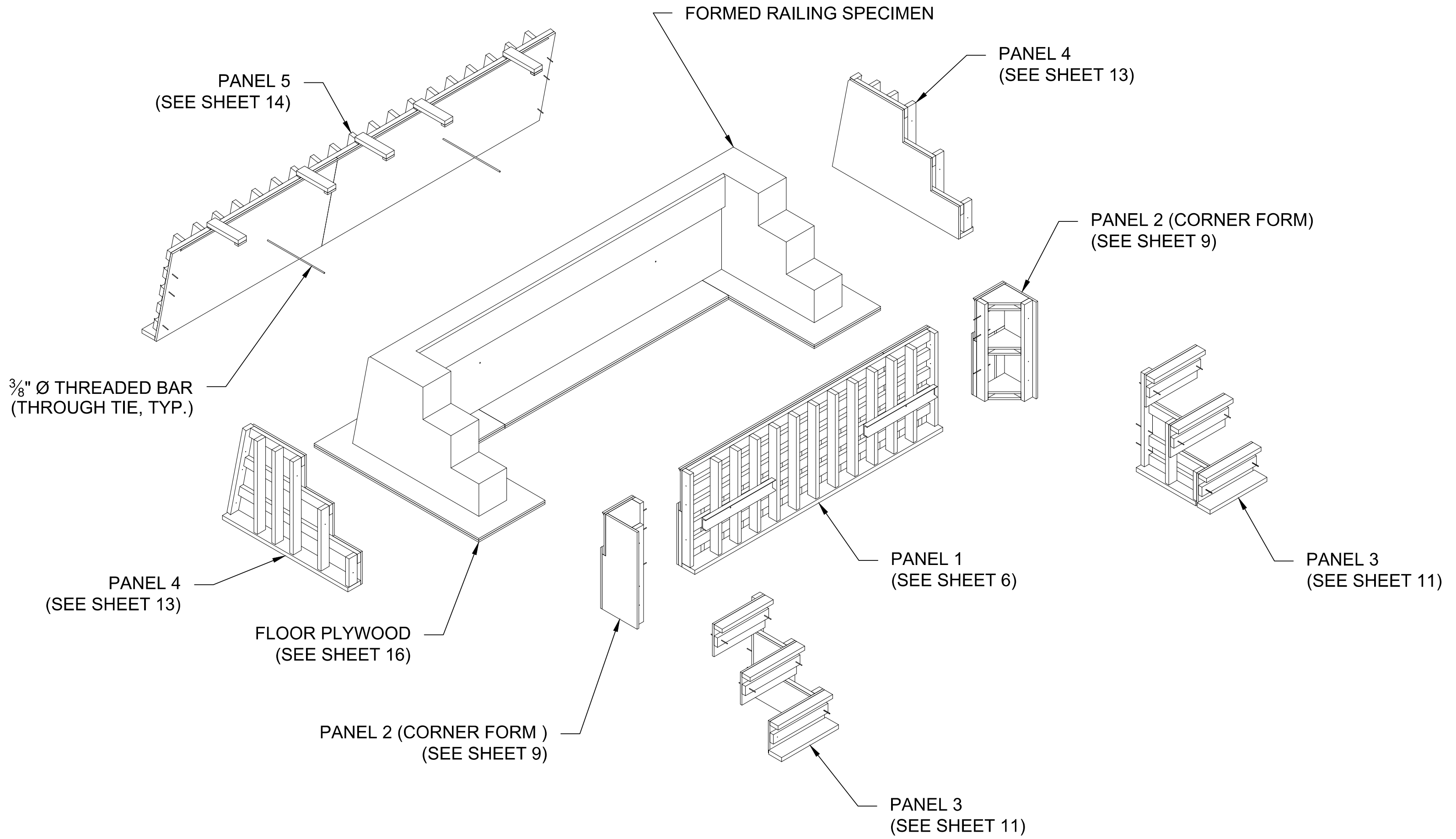

ISOMETRIC VIEW

Fiber-Reinforced Concrete Traffic Railings for Impact Loading				*Revisions:*
Railing formwork (concept)	*2019-03-04*	*University of Florida*	*Sheet 5 of 16*	

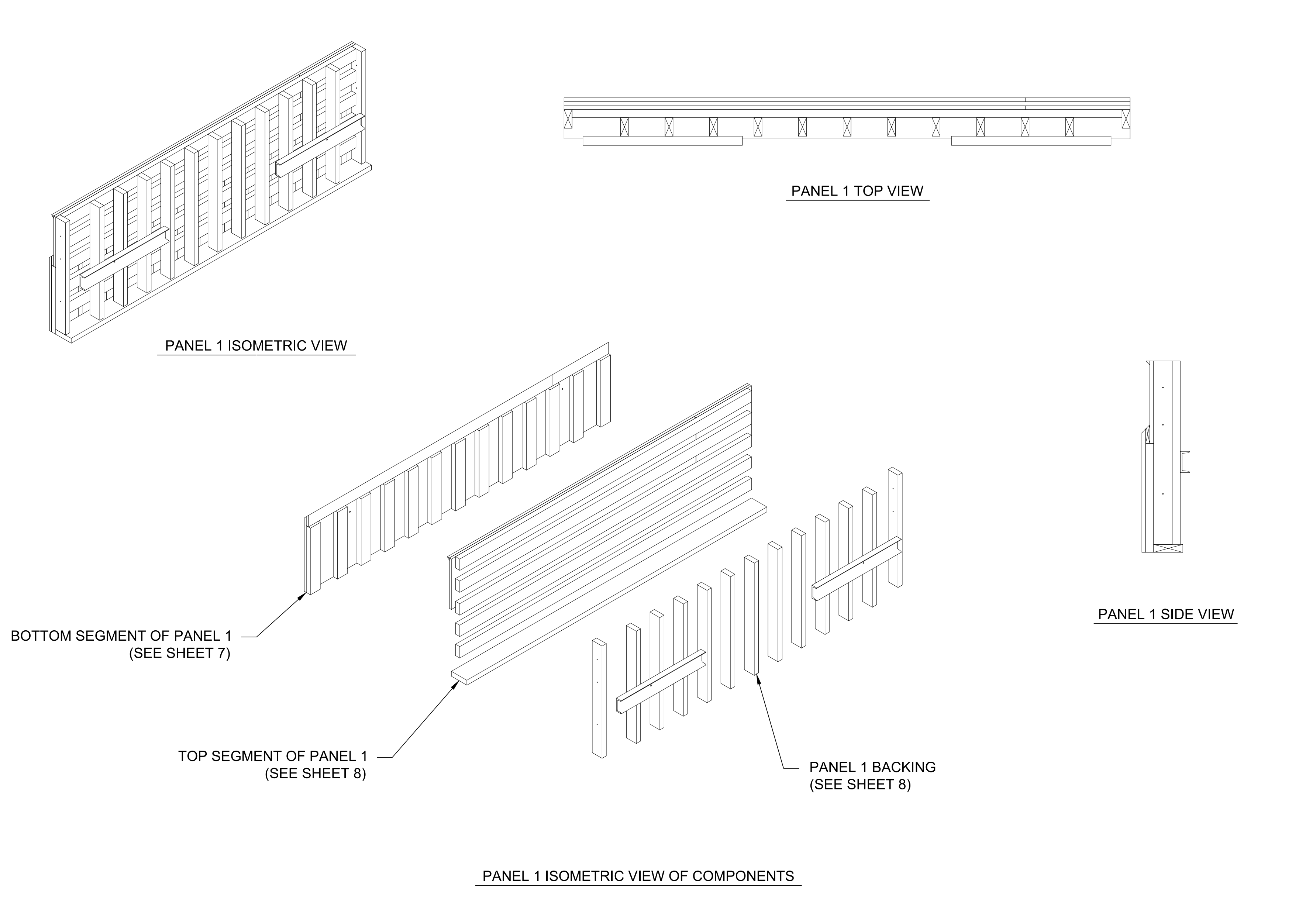

Fiber-Reinforced Concrete Traffic Railings for Impact Loading				*Revisions:*	
Railing formwork (concept)	*2019-03-04*	*University of Florida*	*Sheet 6 of 16*		

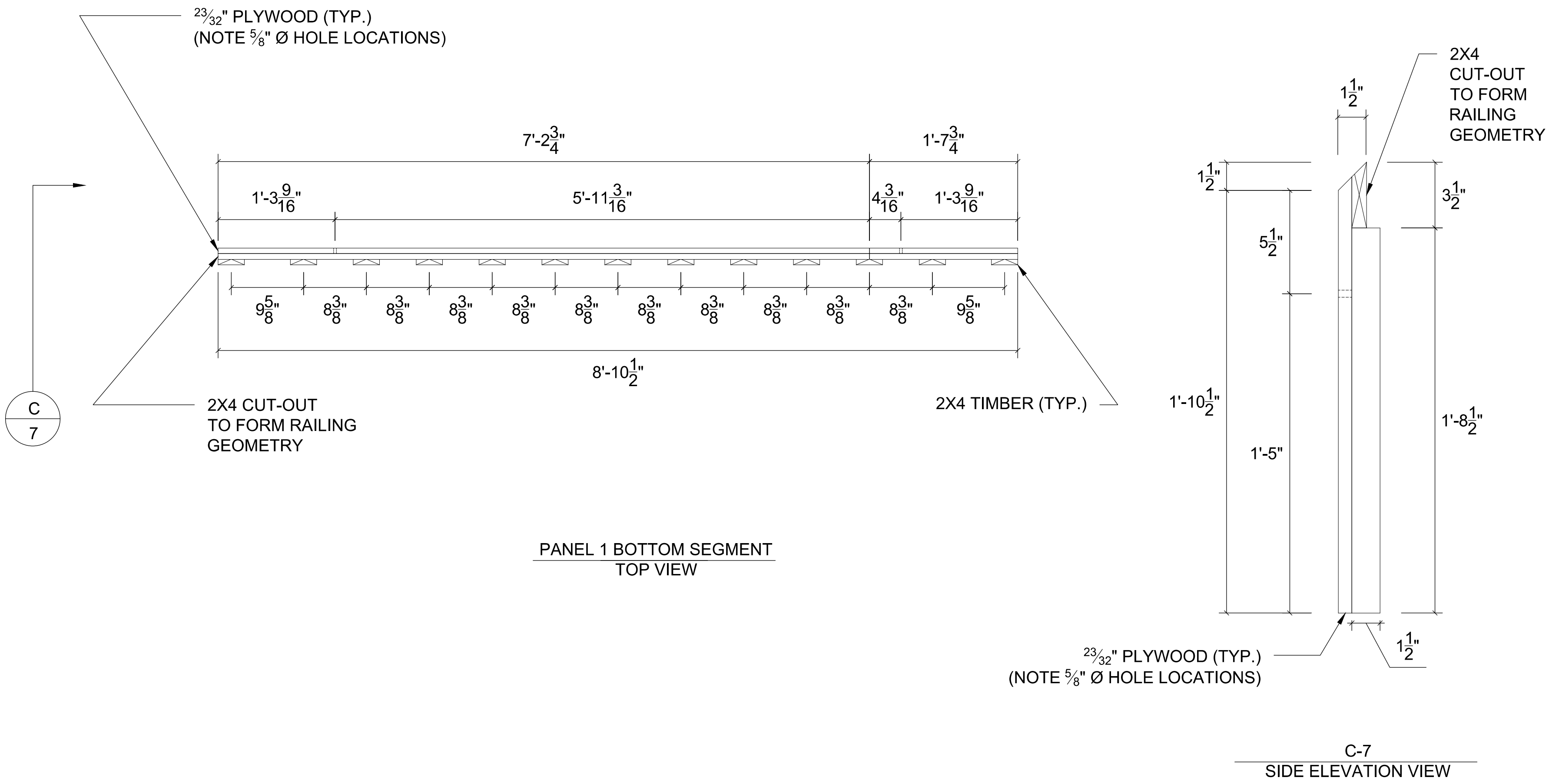

Fiber-Reinforced Concrete Traffic Railings for Impact Loading				*Revisions:*
Railing formwork (concept)	*2019-03-04*	*University of Florida*	*Sheet 7 of 16*	

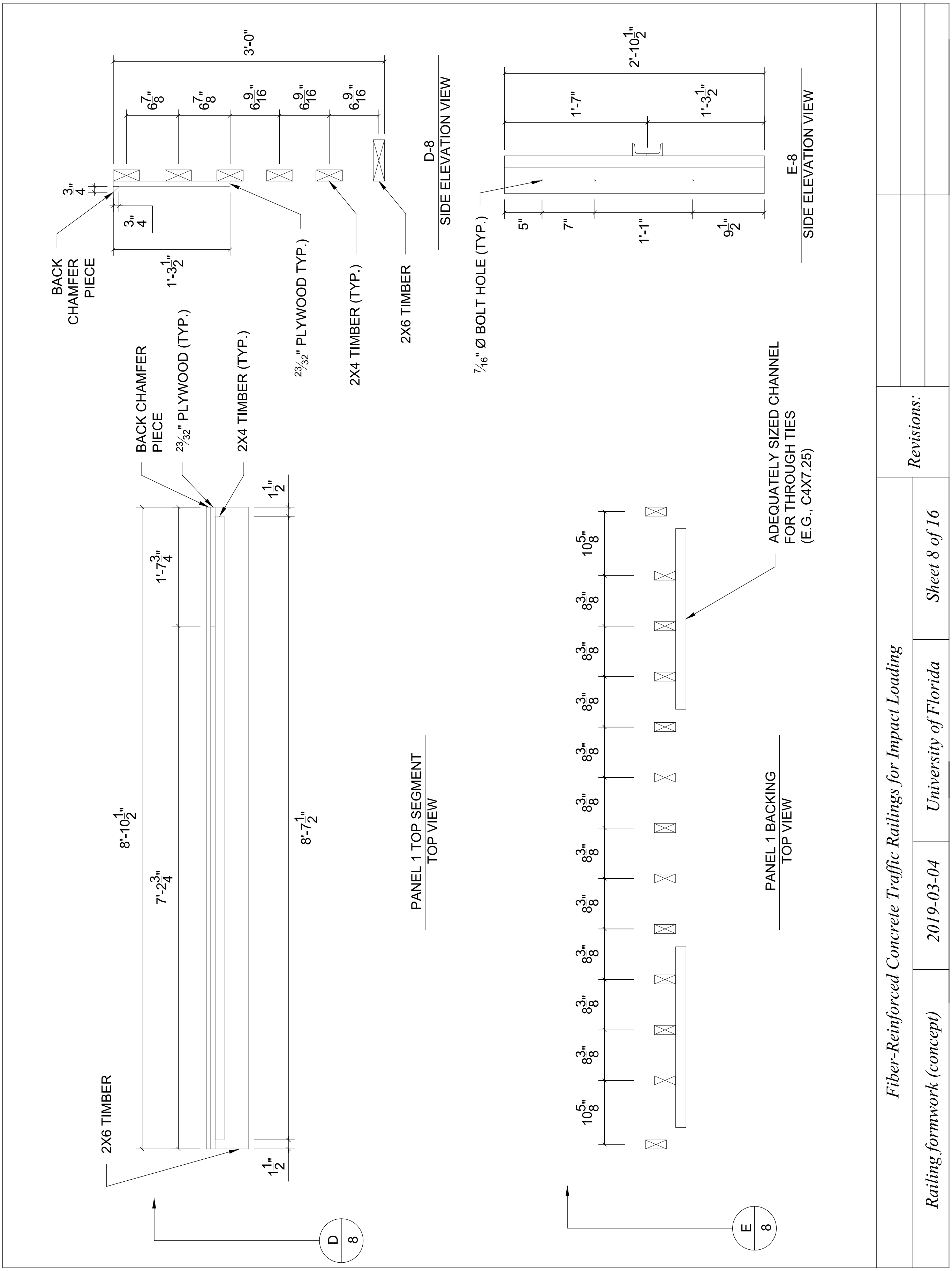

2X6 TIMBER
8'-10 1/2"
7'-2 3/4"
1'-7 3/4"
8'-7 1/2"
1 1/2"
1 1/2"
BACK CHAMFER PIECE
23/32" PLYWOOD (TYP.)
2X4 TIMBER (TYP.)
PANEL 1 TOP SEGMENT TOP VIEW
D 8
BACK CHAMFER PIECE
3/4"
3/4"
1'-3 1/2"
6 7/8"
6 7/8"
6 9/16"
6 9/16"
6 9/16"
3'-0"
23/32" PLYWOOD TYP.)
2X4 TIMBER (TYP.)
2X6 TIMBER
D-8 SIDE ELEVATION VIEW
10 5/8"
8 3/8"
8 3/8"
8 3/8"
8 3/8"
8 3/8"
8 3/8"
8 3/8"
8 3/8"
8 3/8"
8 3/8"
8 3/8"
10 5/8"
PANEL 1 BACKING TOP VIEW
ADEQUATELY SIZED CHANNEL FOR THROUGH TIES (E.G., C4X7.25)
E 8
7/16" Ø BOLT HOLE (TYP.)
5"
7"
1'-1"
9 1/2"
1'-7"
1'-3 1/2"
2'-10 1/2"
E-8 SIDE ELEVATION VIEW
Fiber-Reinforced Concrete Traffic Railings for Impact Loading
Railing formwork (concept)
2019-03-04
University of Florida
Sheet 8 of 16
Revisions:

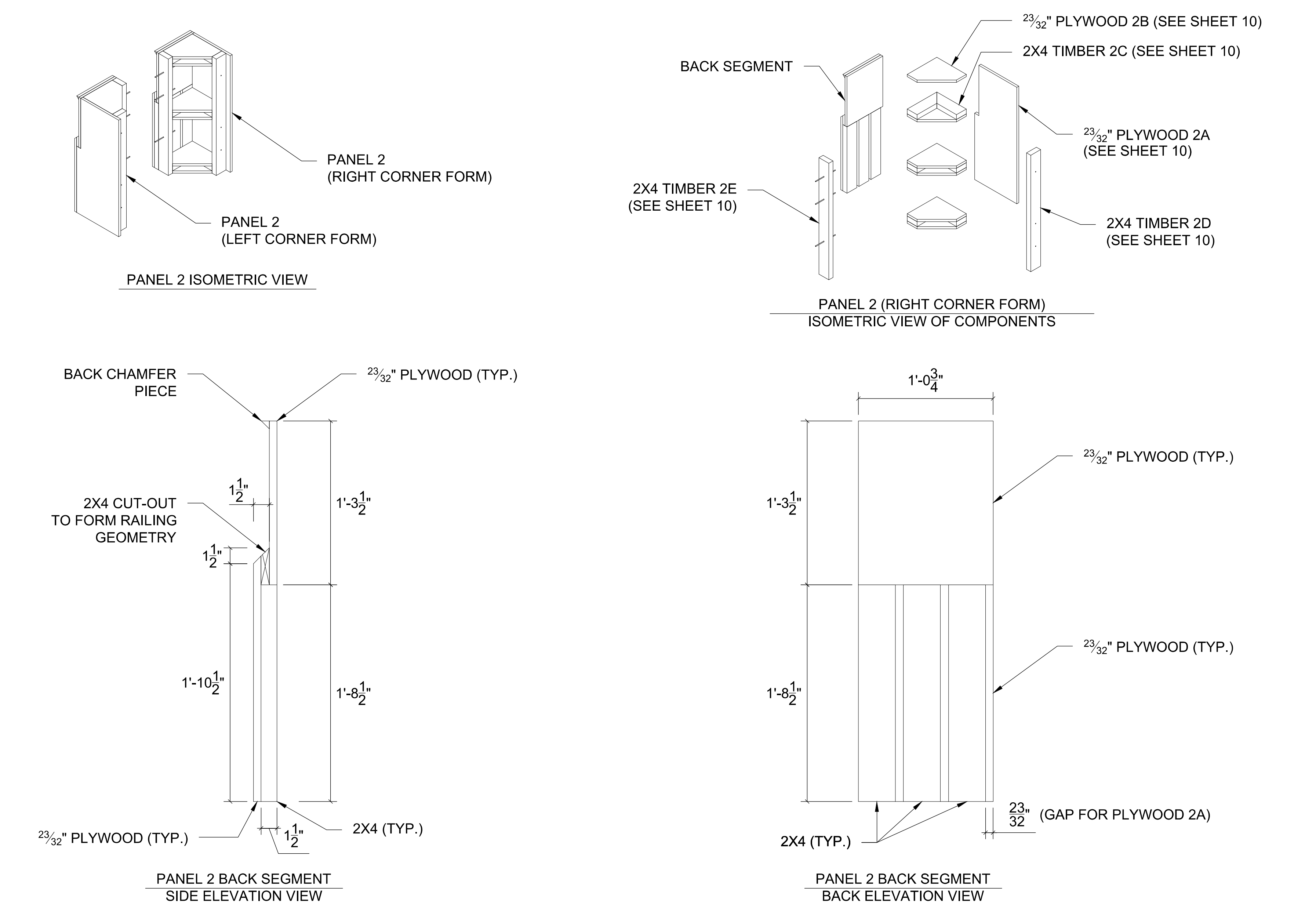

Fiber-Reinforced Concrete Traffic Railings for Impact Loading				*Revisions:*
Railing formwork (concept)	*2019-03-04*	*University of Florida*	*Sheet 9 of 16*	

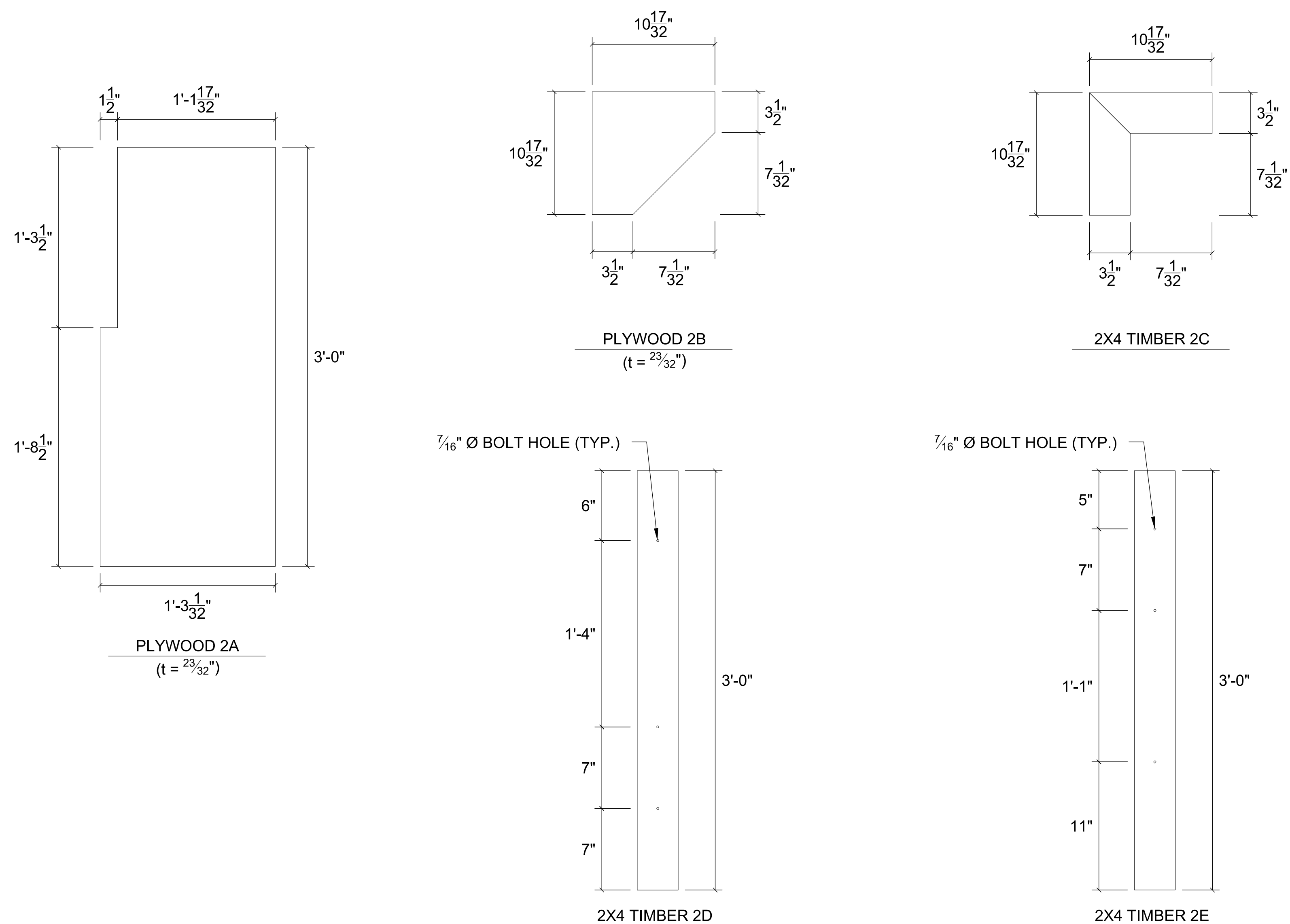

Fiber-Reinforced Concrete Traffic Railings for Impact Loading				*Revisions:*
Railing formwork (concept)	*2019-03-04*	*University of Florida*	*Sheet 10 of 16*	

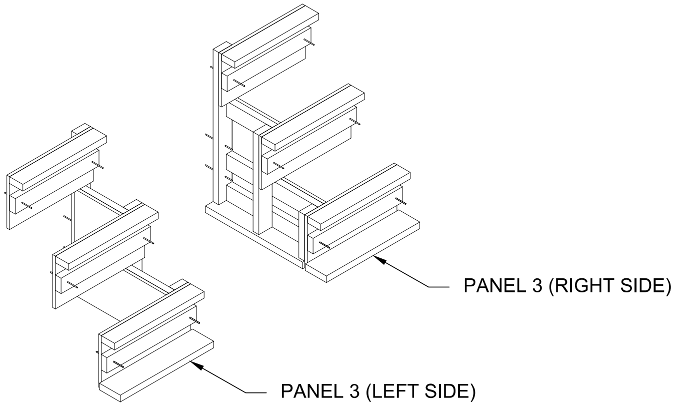

PANEL 3 ISOMETRIC VIEW

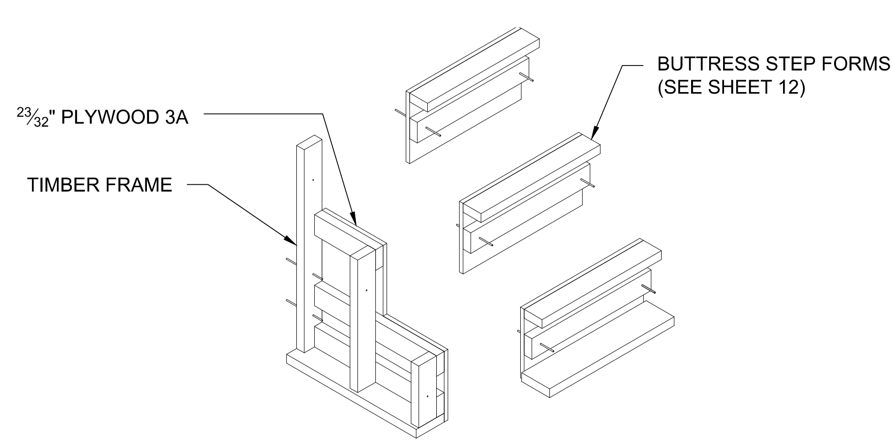

PANEL 3 ISOMETRIC VIEW OF COMPONENTS
(RIGHT SIDE)

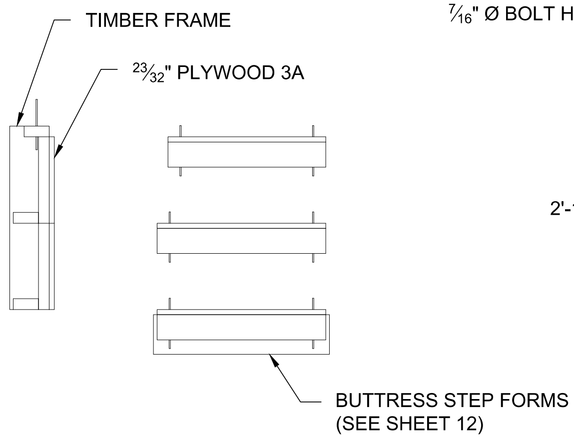

PANEL 3 TOP VIEW OF COMPONENTS
(RIGHT SIDE)

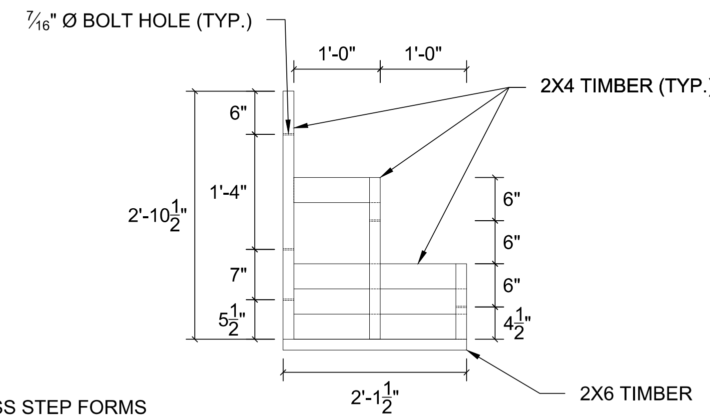

TIMBER FRAME SIDE ELEVATION VIEW

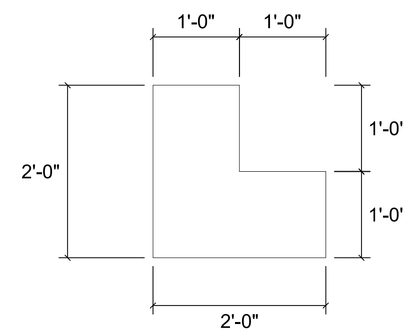

PLYWOOD 3A
(t = $^{23}/_{32}$")

Fiber-Reinforced Concrete Traffic Railings for Impact Loading				*Revisions:*
Railing formwork (concept)	*2019-03-04*	*University of Florida*	*Sheet 11 of 16*	

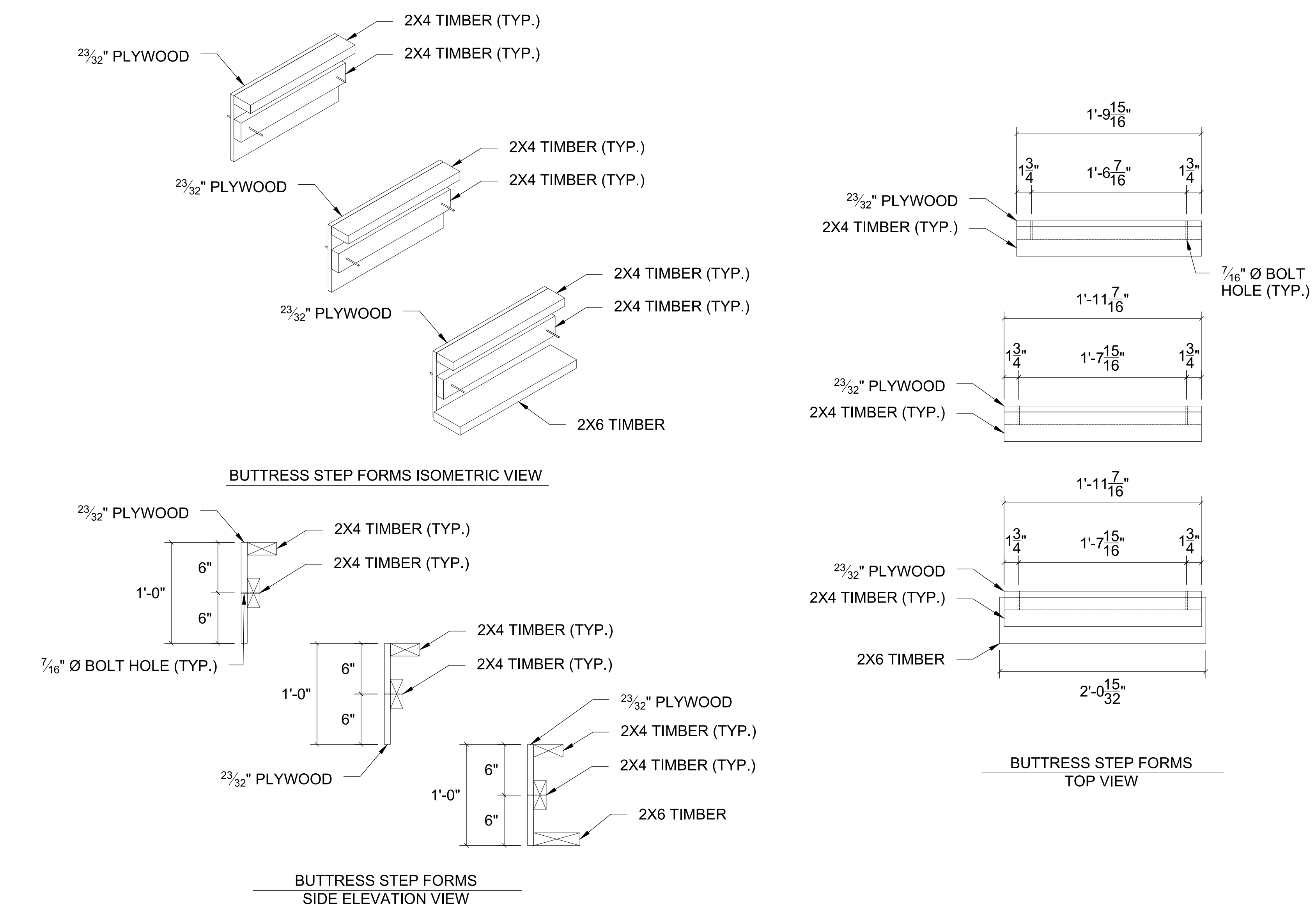

Fiber-Reinforced Concrete Traffic Railings for Impact Loading

Railing formwork (concept) | *2019-03-04* | *University of Florida* | *Sheet 12 of 16* | *Revisions:*

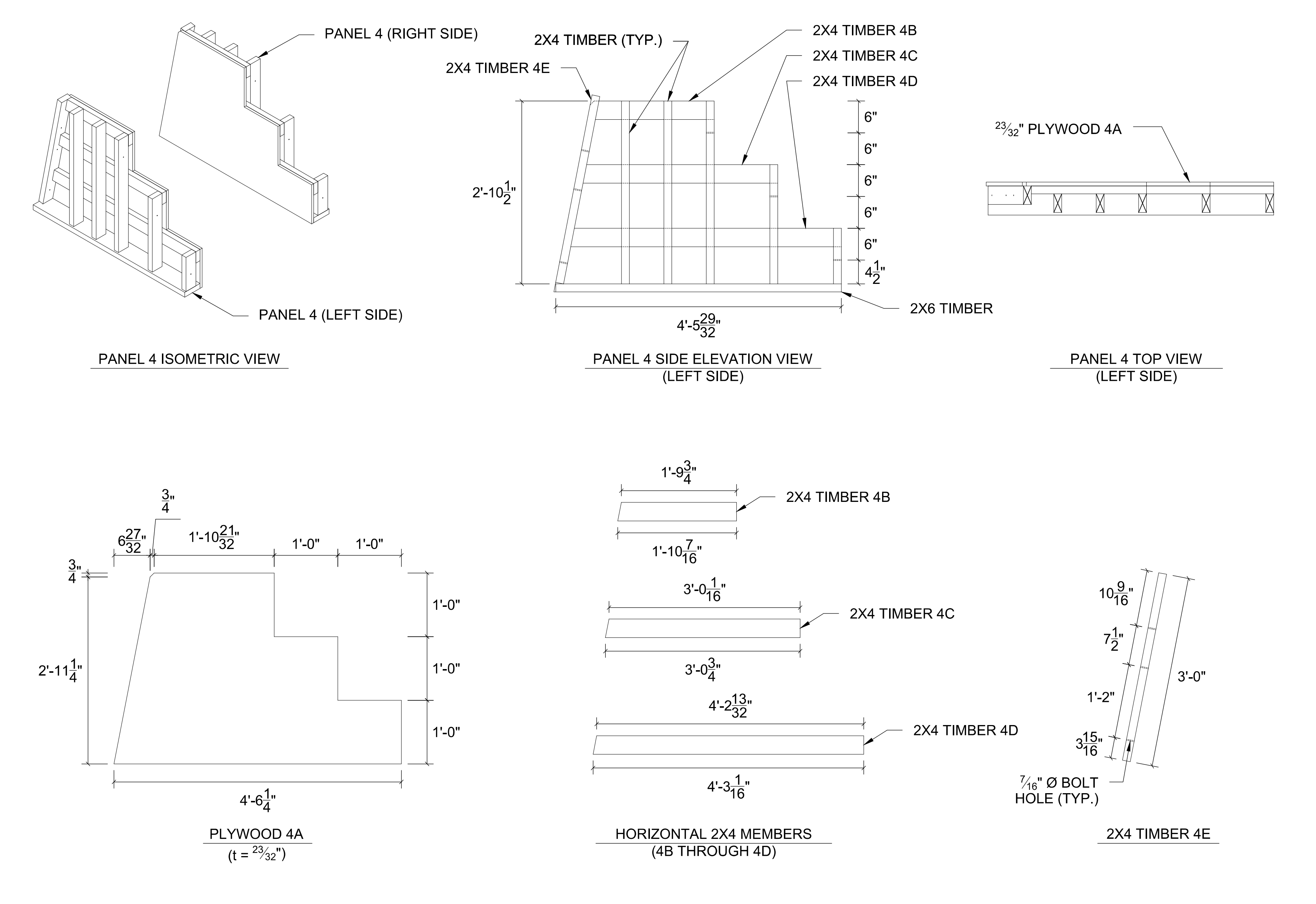

Fiber-Reinforced Concrete Traffic Railings for Impact Loading				*Revisions:*
Railing formwork (concept)	*2019-03-04*	*University of Florida*	*Sheet 13 of 16*	

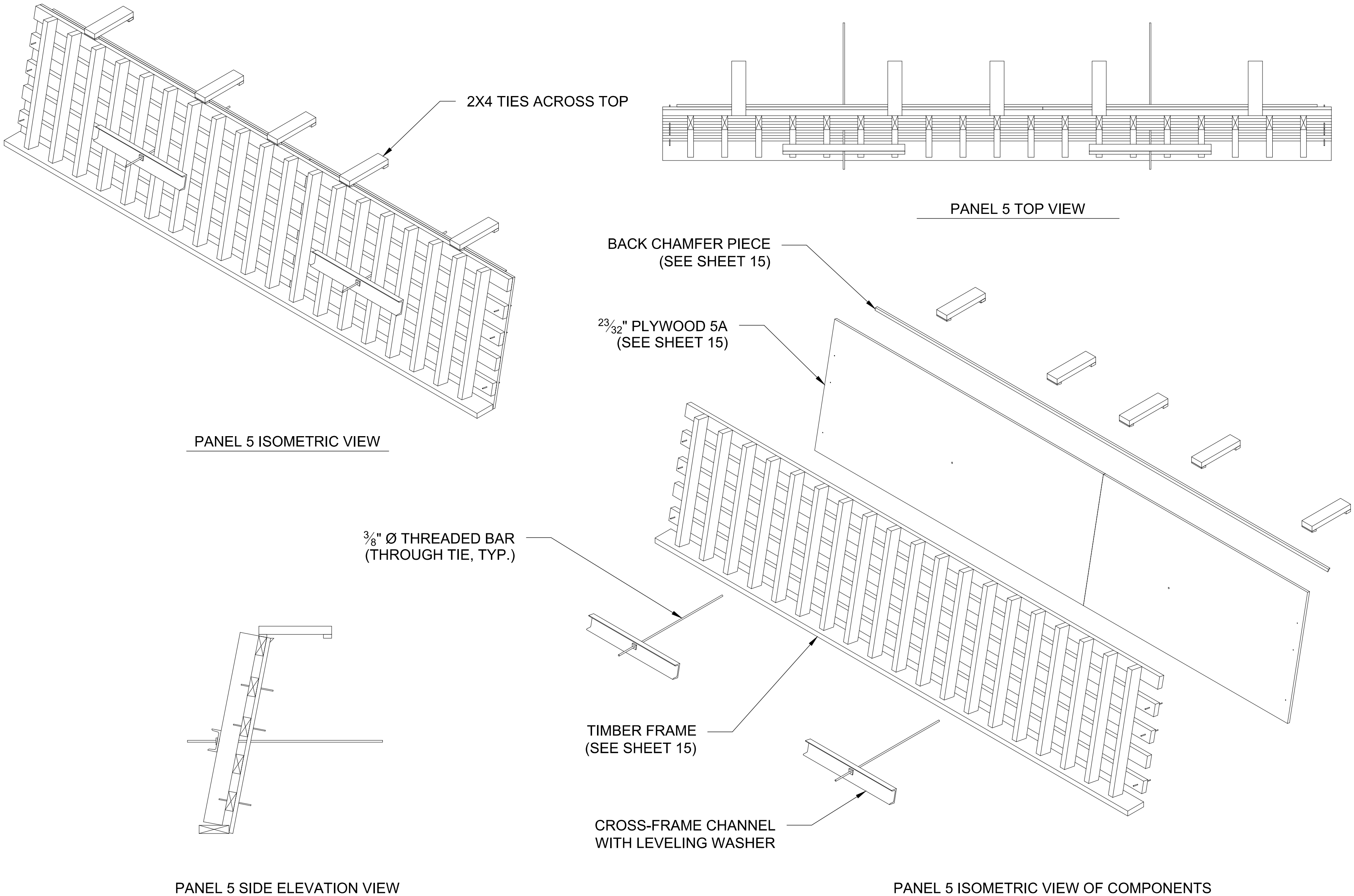

Fiber-Reinforced Concrete Traffic Railings for Impact Loading				*Revisions:*
Railing formwork (concept)	*2019-03-04*	*University of Florida*	*Sheet 14 of 16*	

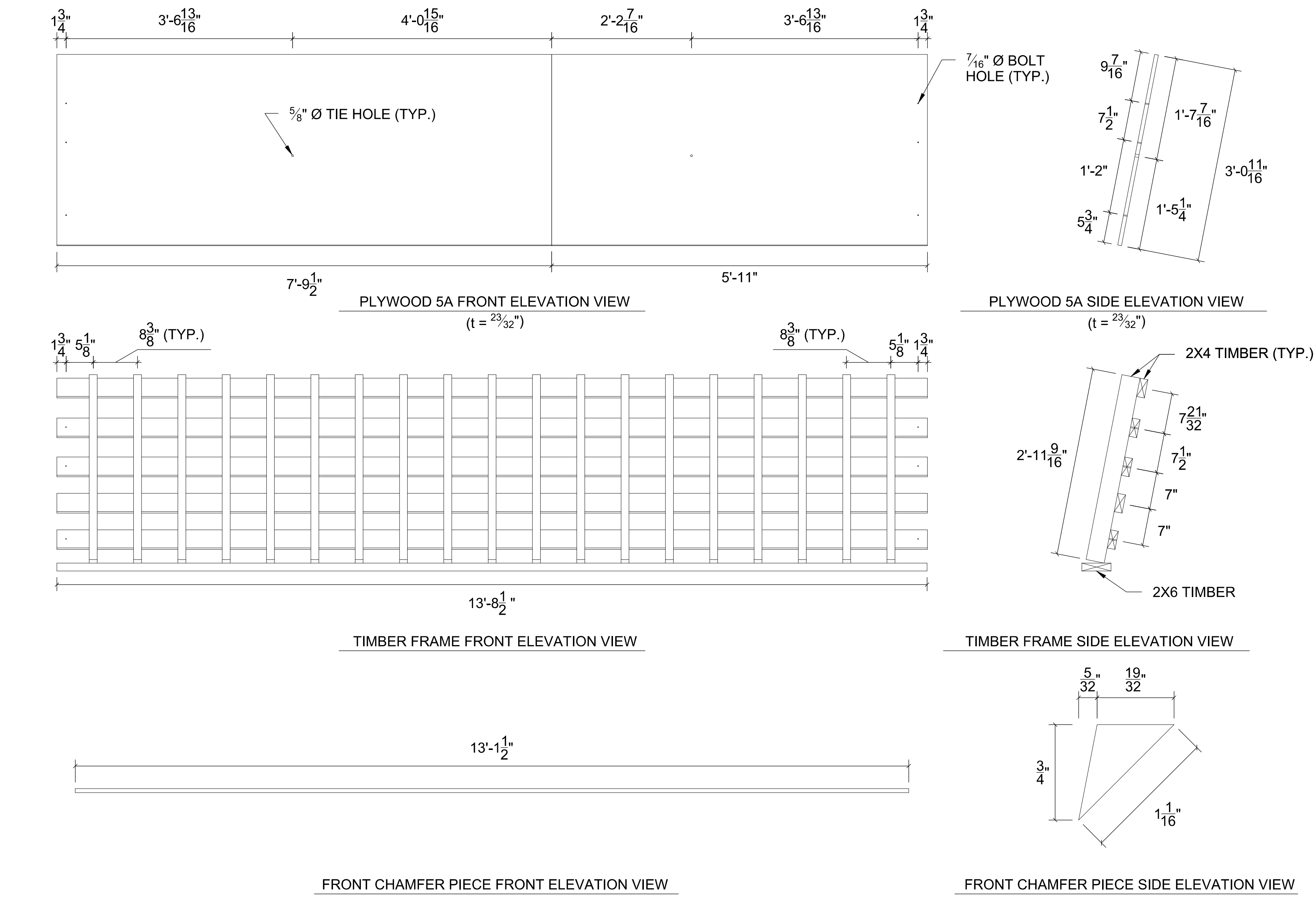

Fiber-Reinforced Concrete Traffic Railings for Impact Loading				*Revisions:*
Railing formwork (concept)	*2019-03-04*	*University of Florida*	*Sheet 15 of 16*	

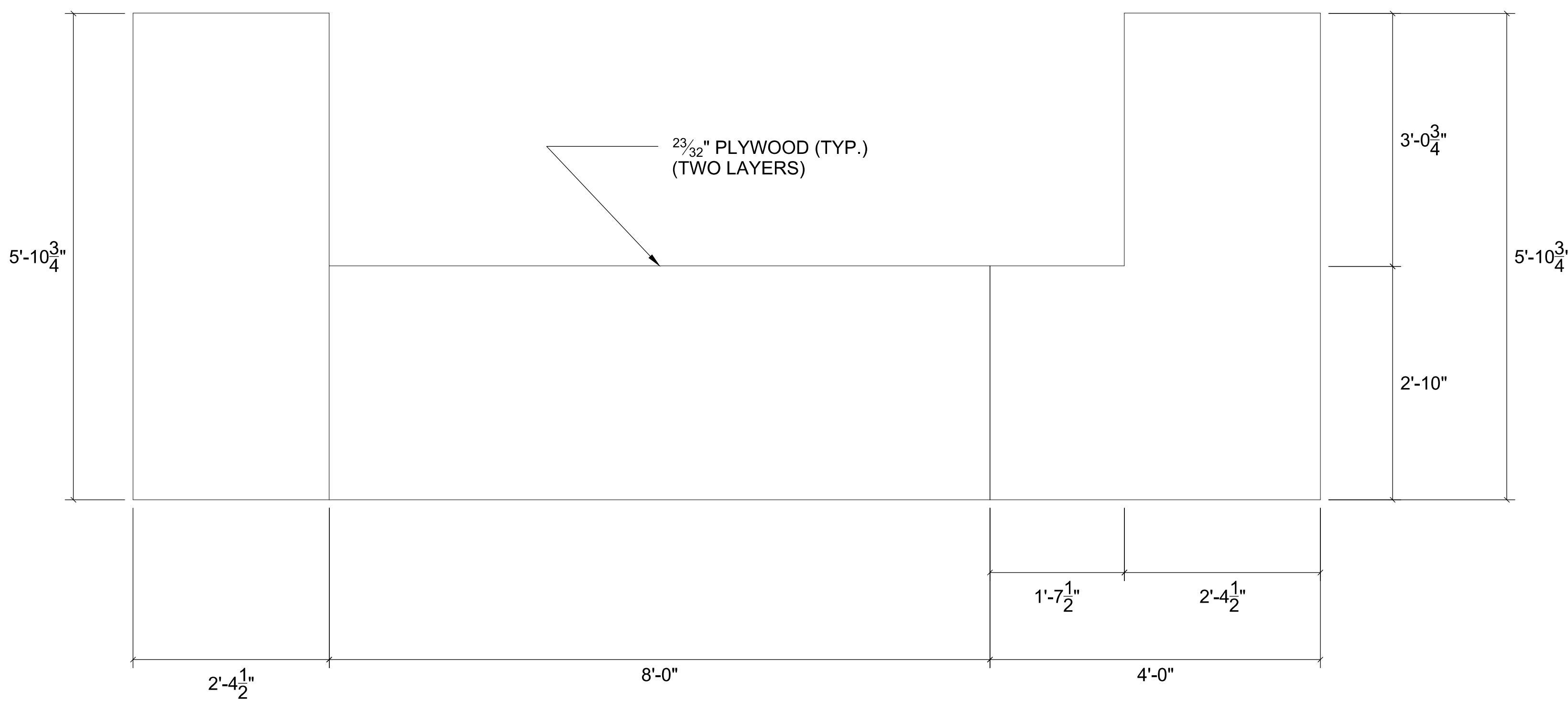

FLOOR PLYWOOD TOP VIEW

Fiber-Reinforced Concrete Traffic Railings for Impact Loading				*Revisions:*
Railing formwork (concept)	*2019-03-04*	*University of Florida*	*Sheet 16 of 16*	

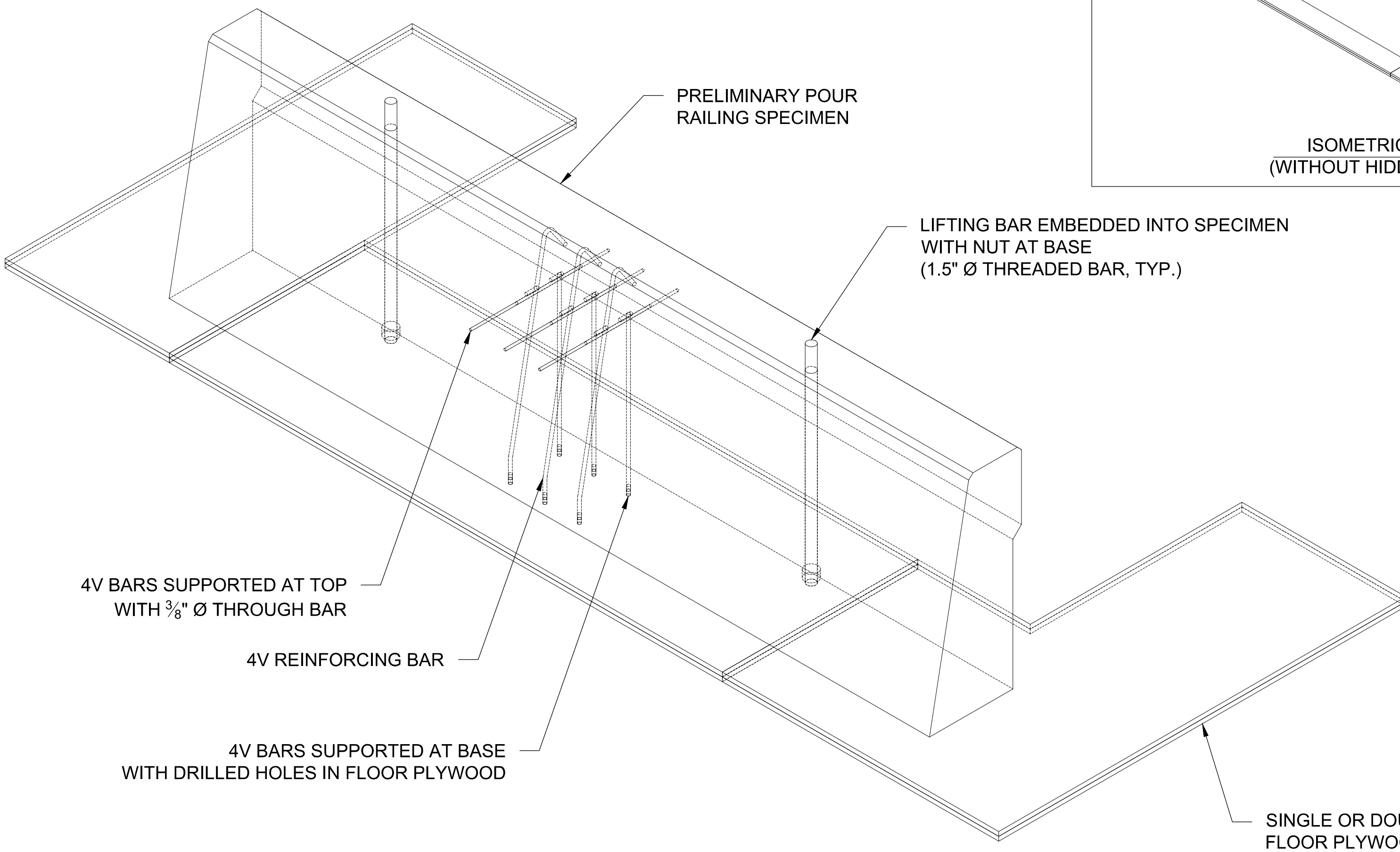

ISOMETRIC VIEW
(WITH EMBEDDED BARS SHOWN)

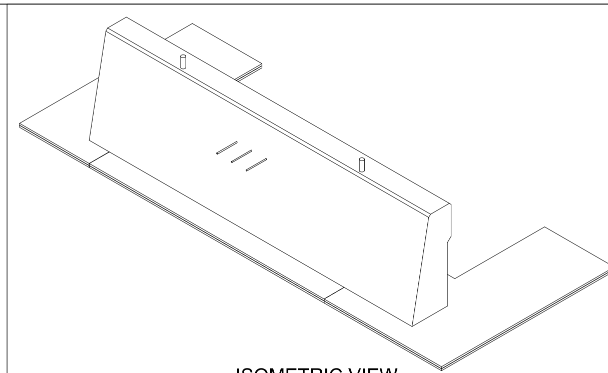

ISOMETRIC VIEW
(WITHOUT HIDDEN LINES)

Fiber-Reinforced Concrete Traffic Railings for Impact Loading				*Revisions:*		
Preliminary Pour Specimen	*2019-05-16*	*University of Florida*	*Sheet 1 of 7*			

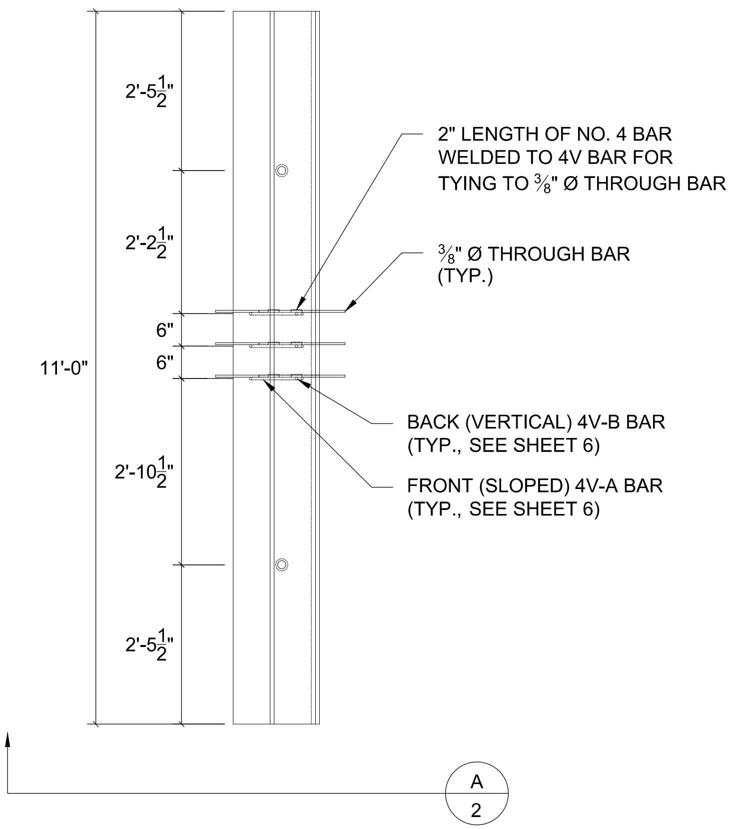

PLAN VIEW
CONCRETE RAILING SPECIMEN

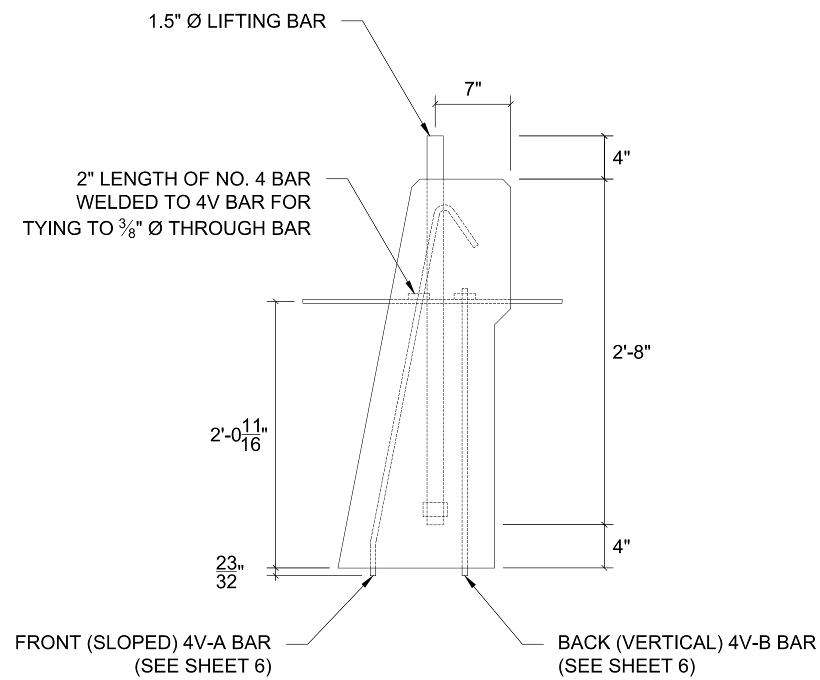

A-2 SIDE ELEVATION VIEW

Fiber-Reinforced Concrete Traffic Railings for Impact Loading				*Revisions:*
Preliminary Pour Specimen	*2019-05-16*	*University of Florida*	*Sheet 2 of 7*	

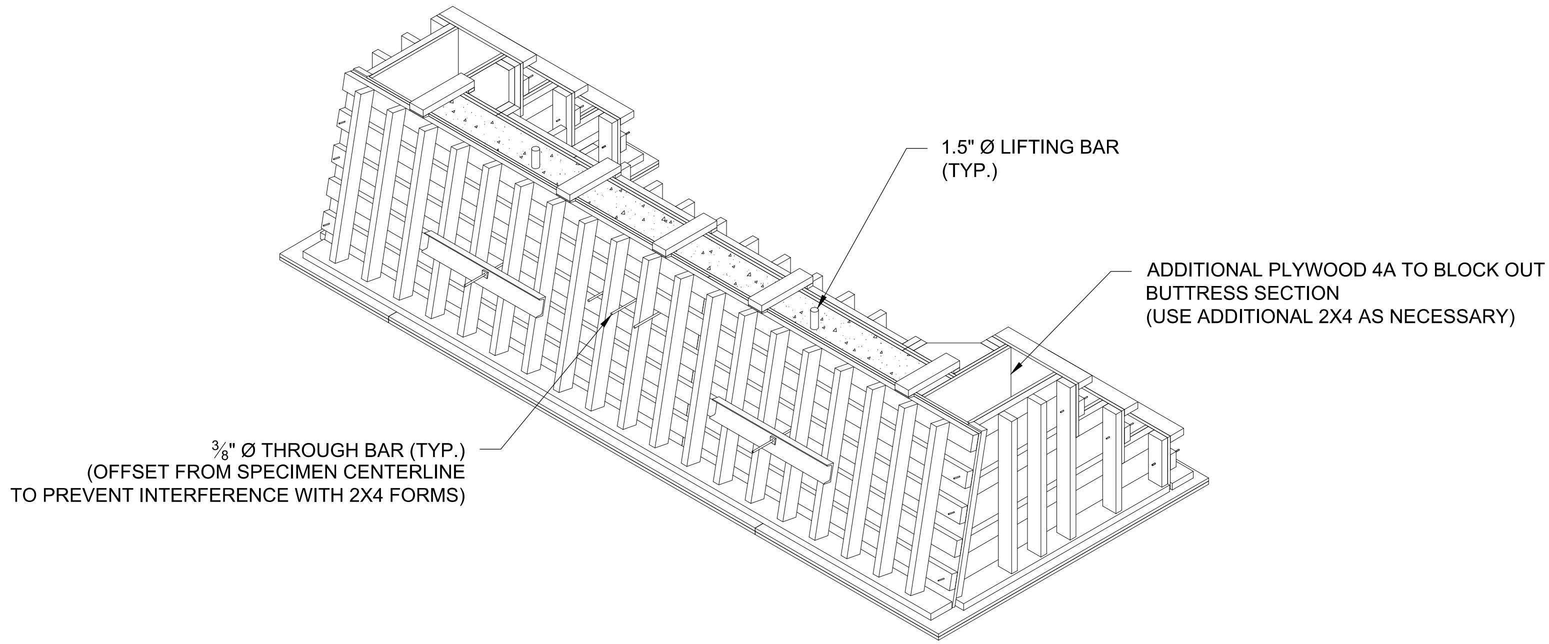

ISOMETRIC VIEW

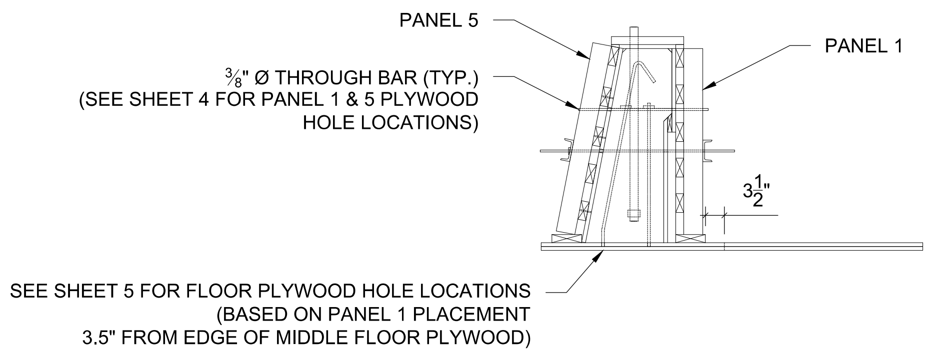

SIDE ELEVATION VIEW
(ONLY PANELS 1 & 5 SHOWN FOR CLARITY)

Fiber-Reinforced Concrete Traffic Railings for Impact Loading				*Revisions:*		
Preliminary Pour Specimen	*2019-05-16*	*University of Florida*	*Sheet 3 of 7*			

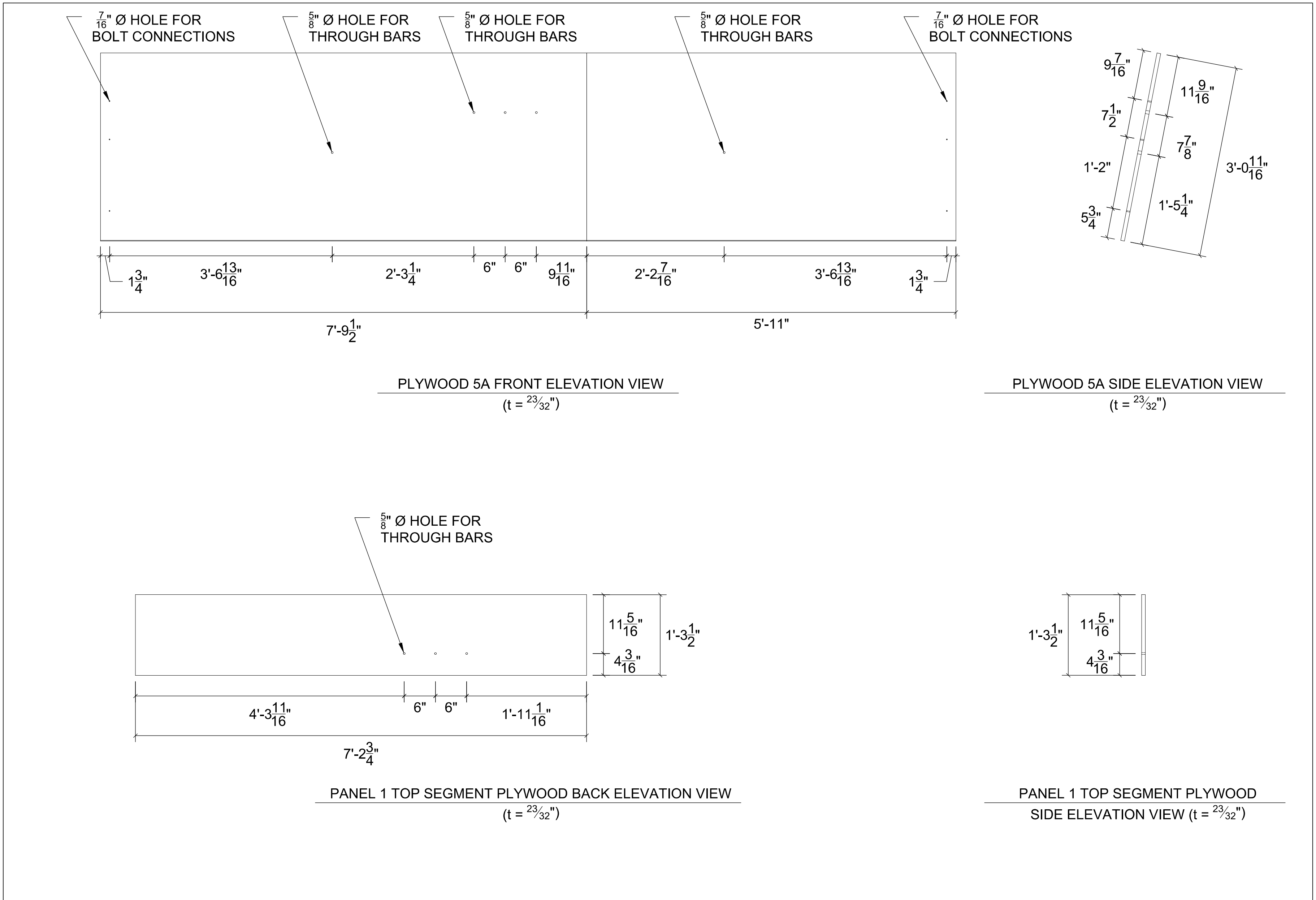

Fiber-Reinforced Concrete Traffic Railings for Impact Loading				*Revisions:*
Preliminary Pour Specimen	*2019-05-16*	*University of Florida*	*Sheet 4 of 7*	

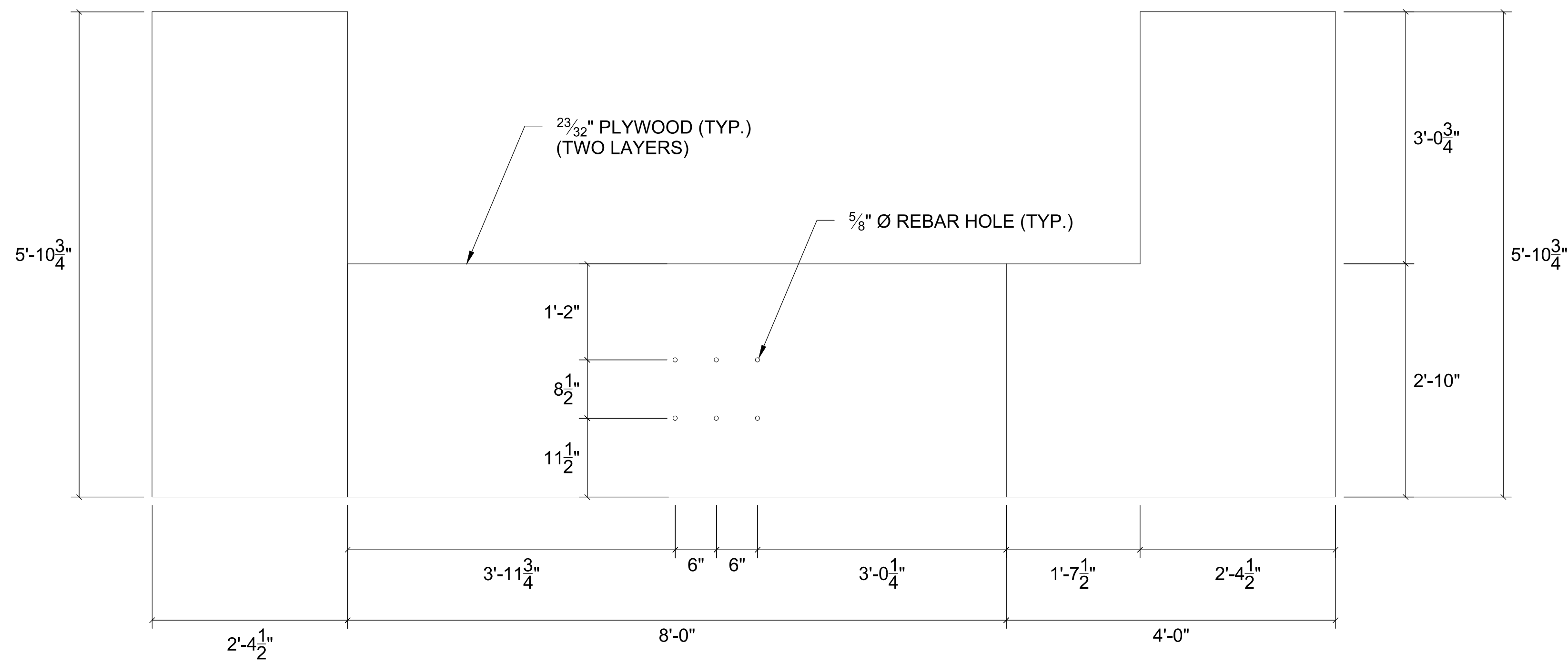

SINGLE OR DOUBLE-LAYERED FLOOR PLYWOOD PLAN VIEW

(t = 23⁄32")

Fiber-Reinforced Concrete Traffic Railings for Impact Loading

Preliminary Pour Specimen | *2019-05-16* | *University of Florida* | *Sheet 5 of 7* | *Revisions:*

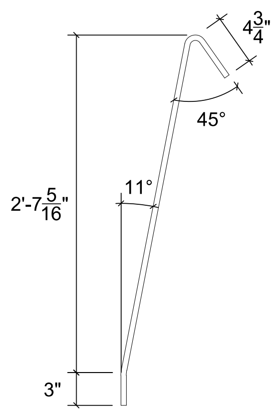

BAR 4V-A

BAR SIZE: #4, LENGTH=3'-3 13/16", QTY:3

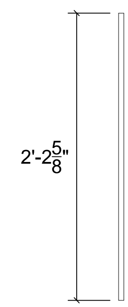

BAR 4V-B

BAR SIZE: #4, LENGTH=2'-2 5/8", QTY:3

Fiber-Reinforced Concrete Traffic Railings for Impact Loading				*Revisions:*		
Preliminary Pour Specimen	*2019-05-16*	*University of Florida*	*Sheet 6 of 7*			

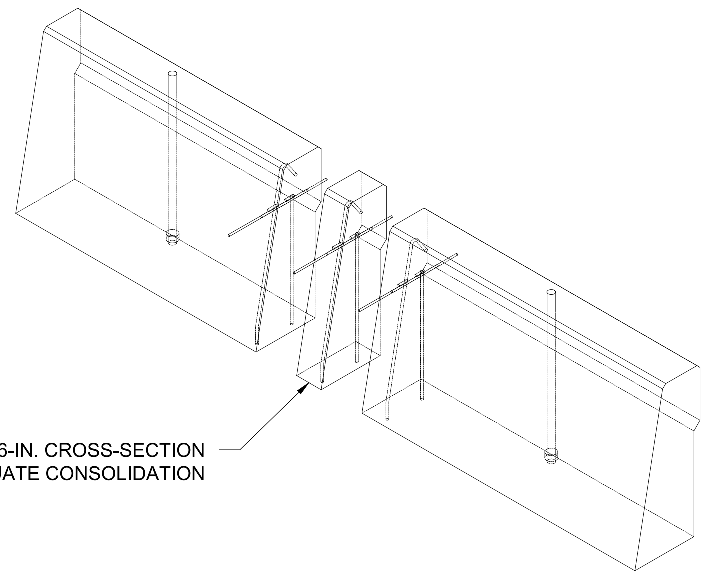

ISOMETRIC VIEW
(WITH EMBEDDED BARS SHOWN)

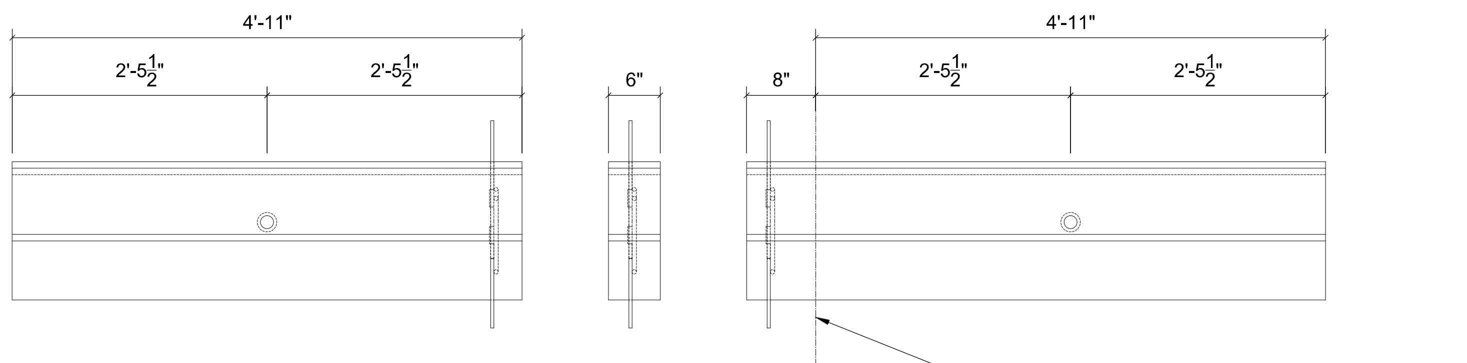

TOP VIEW
(WITH EMBEDDED BARS SHOWN)

Fiber-Reinforced Concrete Traffic Railings for Impact Loading				*Revisions:*
Preliminary Pour Specimen	*2019-05-16*	*University of Florida*	*Sheet 7 of 7*	

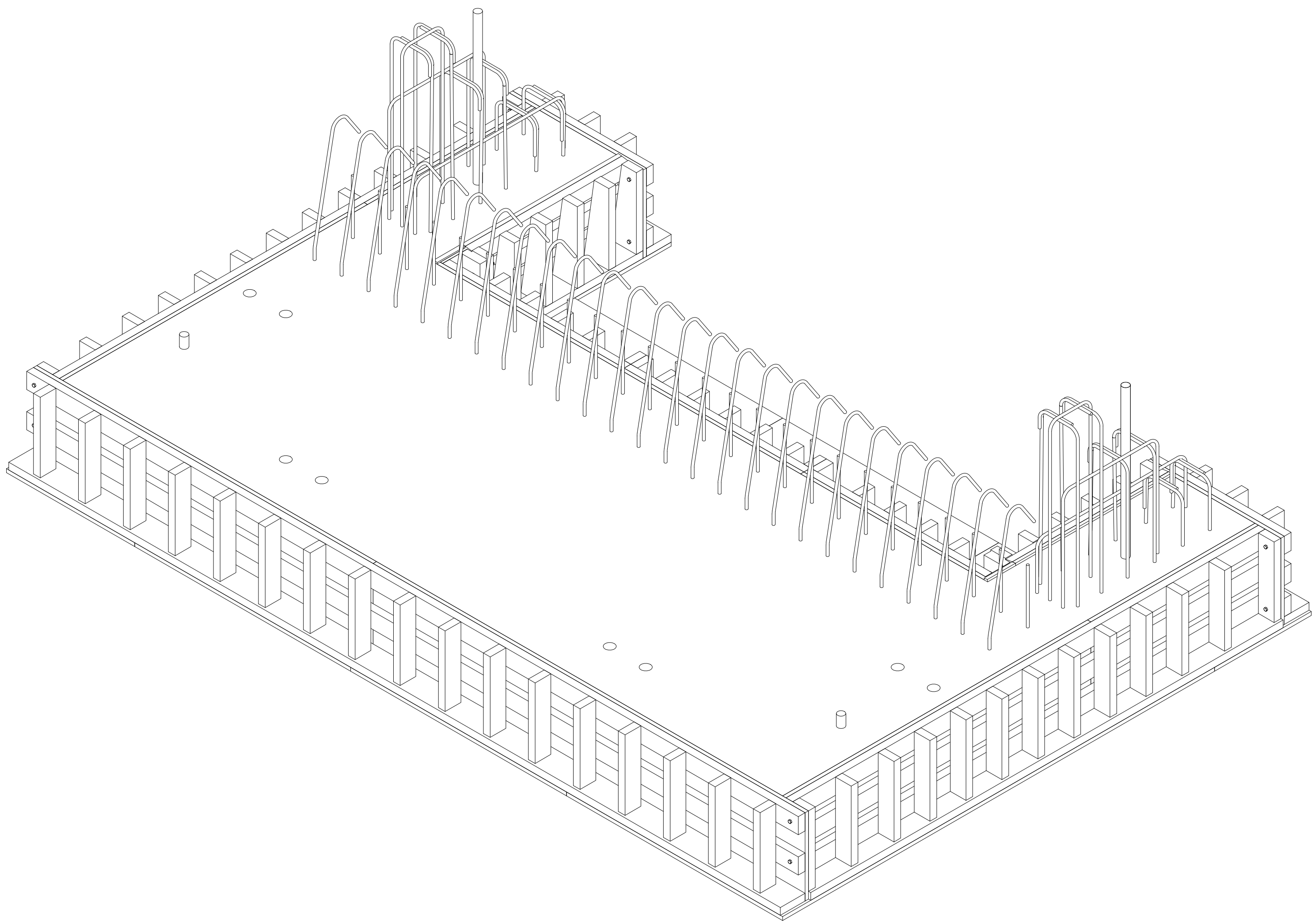

ISOMETRIC VIEW
AFTER DECK CONCRETE PLACEMENT

Fiber-Reinforced Concrete Traffic Railings for Impact Loading				*Revisions:*	
Deck and Railing formwork	*2020-04-03*	*University of Florida*	*Sheet 01 of 04*		

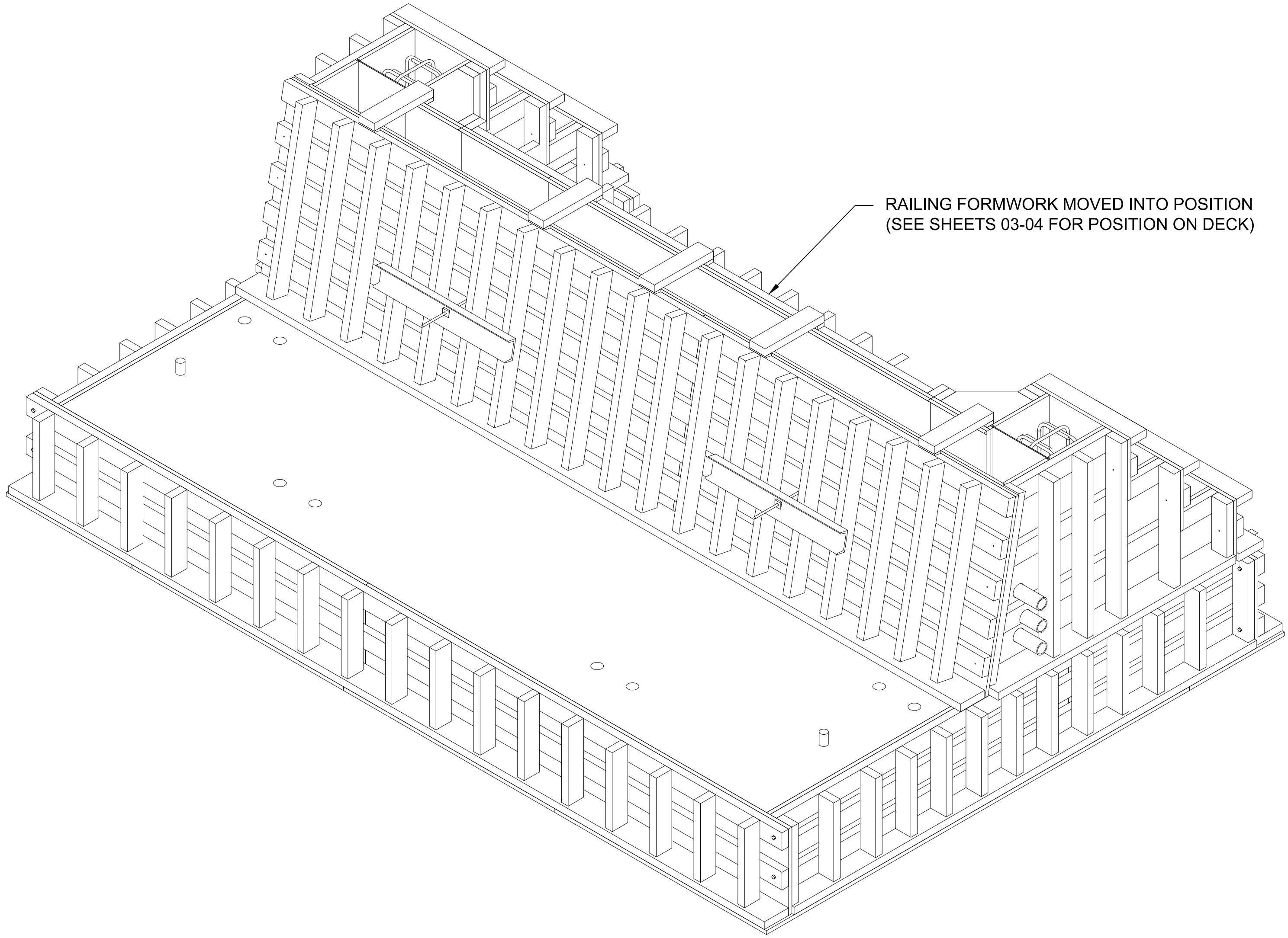

ISOMETRIC VIEW
AFTER DECK CONCRETE PLACEMENT

Fiber-Reinforced Concrete Traffic Railings for Impact Loading				*Revisions:*		
Deck and Railing formwork	*2020-04-03*	*University of Florida*	*Sheet 02 of 04*			

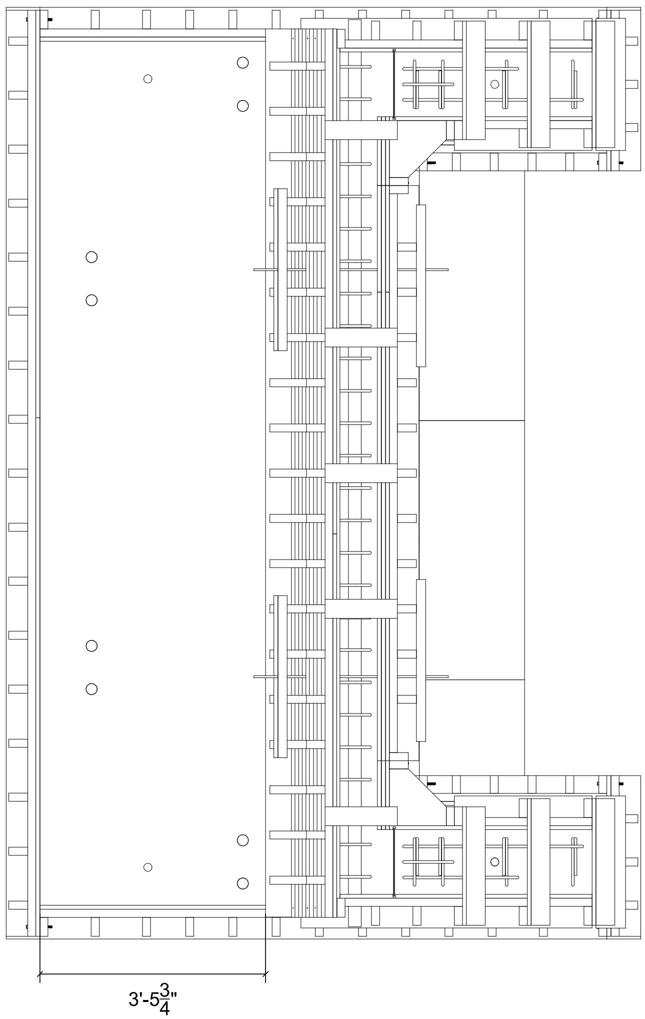

PLAN VIEW
RAILING FORMWORK POSITIONED ON DECK

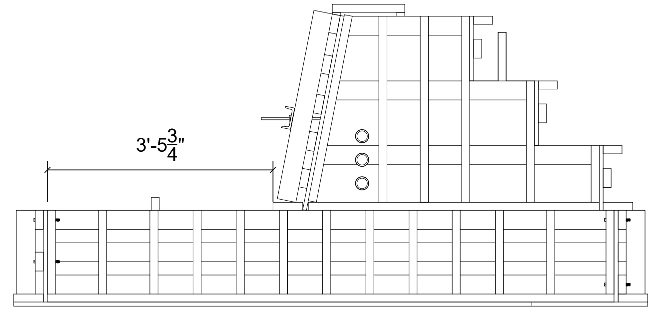

SIDE ELEVATION VIEW
RAILING FORMWORK POSITIONED ON DECK

Fiber-Reinforced Concrete Traffic Railings for Impact Loading				*Revisions:*		
Deck and Railing formwork	*2020-04-03*	*University of Florida*	*Sheet 03 of 04*			

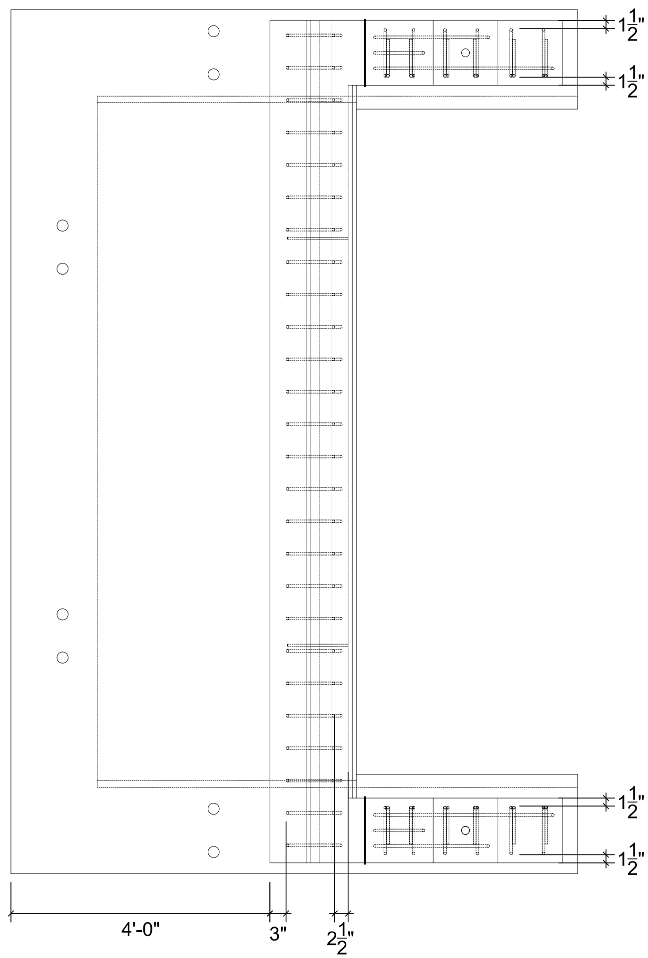

PLAN VIEW
CONCRETE COVER FOR RAILING REBAR

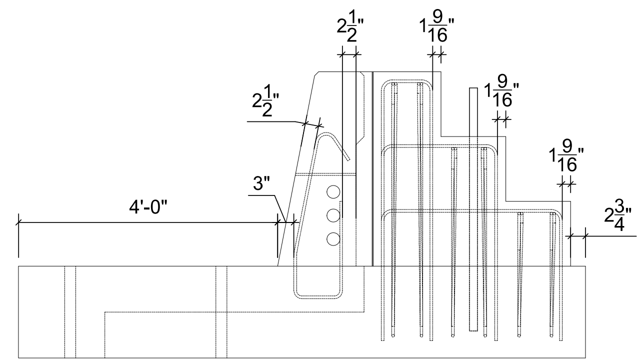

SIDE ELEVATION VIEW
CONCRETE COVER FOR RAILING REBAR

Fiber-Reinforced Concrete Traffic Railings for Impact Loading				*Revisions:*	
Deck and Railing formwork	*2020-04-03*	*University of Florida*	*Sheet 04 of 04*		

APPENDIX D
LARGE-SCALE TRIAL MIXTURE PRODUCTION DETAILS AND BATCH-PLANT MIXTURES FOR SPECIMEN PRODUCTION

Presented in this appendix are batch-plant concrete mixture details and large-scale FRC mixture production details used to cast full-scale railing test specimens. The mixture designs and production details are organized in the following order:

- Mixture details used to cast the deck and railing portions of FRC test specimens
- Mixture details used to cast the deck and railing portions of standard R/C test specimens

FRC railing concrete mixture design
excluding fiber

SMYRNA READY MIX CONCRETE
"QUALITY CONCRETE, UNMATCHED SERVICE"

CONCRETE MIX DESIGN

MIX ID: 34091 3400 PSI CONCRETE 5/1/2020
CLASS II SLIP FORM

CONTRACTOR: FDOT RESEARCH
PROJECT: RESEARCH PROJECT
USE: SLIP FORM

	WEIGHTS PER CUBIC YARD	(SATURATED, SURFACE DRY)		
				YIELD, CU FT
CEMENT	TYPE I/II ASTM C150, LB.	424		2.16
FLYASH	TYPE F ASTM C618, LB.	133	23.88%	0.88
SAND	FDOT NATURAL SAND,ASTM C33 LB.	1608		8.47
STONE	FDOT #67 GRANITE ASTM C33 , LB.	1535		10.47
STONE	#89 GRANITE ASTM C33 LB.	0		0.00
WATER	(GAL-US)	32		4.27
TOTAL AIR, %		3.5	+/- 2.5	0.945
			TOTAL	27.20

AIR ENTRAINMENT, OZ-US	1 TO 6
HR WATER REDUCER, OZ/100WT-US	2 TO 4
RETARDER, OZ/100WT-US	5.0
FIBER	TBD
WATER/CEMENT RATIO. LBS/LB	0.48
SLUMP, IN	6.0 +/- 1.0
CONCRETE UNIT WEIGHT, PCF	145.83

TEST RESULTS OBTAINED FROM A LIKE OR SIMILAR MIX DESIGN
PER ACI 301; 4.3.2

COMMENT: CUSTOMER TO PUT FIBER IN AT JOB

JUSTIN SPOONER

FDOT DELIVERY TICKET

Financial Project No.:		Serial No.:	3005740
Plant No.:	55-136	Date:	6/20/2019
Concrete Supplier:	SRM	Delivered to:	Jeff
Phone No.:	850-576-4141	Phone No.:	561-632-4076
Address:	2222 MILL ST	Address:	E. Paul Dirac
	Tallahassee, Fl 32310		Leon

Truck No. 1562	DOT Class II 3400 Slip	DOT Mix No. 03-2212SF	Cubic Yards This Load 3
Allowable Water 22	Time Loaded 10:10 AM	Mixing Revs 70	Yards Delivered 3

Cement	Source: Argos	Type: I 1L	Amount: 1270	Fly Ash or Slag	Source: BORAL	Brand:	Type: F	Amount: 400
Coarse Agg.	Pit No.: GA553	% Moist: 2	Amount: 4700	Air Entrainment	Source: WR Grace	Brand:	Type: Darex AEA	Amount: 11
Fine Agg.	Pit No.: 50-382	% Moist: 3.9	Amount: 5020	Admixture	Source: BASF	Brand:	Type: Rearder (Retarder)	Amount: 20
Batch Water (gal or lbs)			Amount: 29	Admixture	Source: BASF	Brand:	Type: Super (High-range WRDA)	Amount: 30

ification that the concrete batched was produced and
›artment specification requirements for structural concrete.

J525-536-67-090-0	J SPOONER
CTQP Technician Identification Number	Signature of Batch Plant Operator

Arrival Time at Jobsite		Number of Revs. upon arrival at Jobsite	
Water added at Jobsite		Additional mixing revs. with added water	
Time concrete completely discharged		Total number of revolutions	
Initial slump	Initial Air	Initial Concrete Temp	Initial W/C Ratio
Acceptance Slump	Acceptance Air	Acceptance Temp	Acceptance W/C Ratio

that the maximum specified water cementitious ratio was not
›ed in compliance with Department specification requirements.

CTQP Technician Identification Number	Signature of Contractors Representative

FRC trial railing mixture

2019-06-20: Attempt #2 scaled-up FRC mixture design vs truck delivery mixture

Batch size (cy)	3
Batch size (ft^3)	81

	Natural moisture (%)	Absorption (%)	Difference (%)
#67 stone - Coarse aggregate	2.00%	0.53%	1.47%
Sand - Fine aggregate	3.90%	0.40%	3.50%

Mix Design				
Product	Quantity	Units	SG	Volume/cy (ft^3/cy)
Cement - Type 1L	424	lb/cy	3.15	2.16
Fly ash - Class F	133	lb/cy	2.37	0.90
#67 stone - Coarse aggregate	1535	lb/cy	2.80	8.79
Sand - Fine aggregate	1608	lb/cy	2.63	9.80
Water	267	lb/cy	1.00	4.28
	32.0	gallons/cy		
Air	3.5%	-		0.95
Fiber - Sika hooked-end (1% volume)	132.26	lb/cy	7.85	0.27
WR Grace Darex AEA - Air entraining Admixture	4	fl oz/cy	-	
MasterSet DELVO - Retarding Admixture	28	fl oz/cy	-	
MasterGlenium 7920 - High-range WRDA	12	fl oz/cy	-	

Mix info	
Total volume	27.1 ft^3
Total mass	4099.26 lb/cy
Unit weight	151.07 lb/ft^3
Total cm/cy	557.00 lb/cy
w/c	0.630
w/cm	0.479
% fly ash	23.88%
sand/agg	0.512

Fiber dosage	
Fiber type	Sika hooked-end steel fiber
SG	7.85
Dosage by volume	1%
Unit weight	489.84 lb/ft^3
Fiber dosage	132.26 lb/cy
FRC batch size	1.59 cy
FRC batch size	42.9 ft^3
Total fiber quantity	210.3 lb
Number of buckets	9 buckets
Fiber wt per bucket	23.4 lb/bucket

Adjustments for moisture		
Aggregate weight adjustments for natural moisture		
#67 stone - Coarse aggregate	1565.7	lb/cy
Sand - Fine aggregate	1670.7	lb/cy
Water weight adjustment based on absorption and natural moisture		
Water from #67 stone - Coarse aggregate	22.5	lb/cy
Water from Sand - Fine aggregate	56.3	lb/cy
Water adjustment	-78.8	lb/cy
	-9.5	gallons/cy
Water (adjusted mix quantity)	188.2	lb/cy
	22.6	gallons/cy

Total content added to the truck (from delivery ticket)		Units	Design quantities (with moisture adjustments)		Difference	
Cement - Type 1L	1270.0	lb	1272.0	lb	-2.0	lb
Fly ash - Class F	400.0	lb	399.0	lb	1.0	lb
#67 stone - Coarse aggregate	4700.0	lb	4697.1	lb	2.9	lb
Sand - Fine aggregate	5020.0	lb	5012.1	lb	7.9	lb
Water	241.7	lb	564.7	lb	-323.0	lb
	29.0	gallons	67.8	gallons	-38.8	gallons
WR Grace Darex AEA - Air entraining Admixture	11.0	fl oz	12.0	fl oz	-1.0	fl oz
MasterSet DELVO - Retarding Admixture	20.0	fl oz	84.0	fl oz	-64.0	fl oz
MasterGlenium 7920 - High-range WRDA	30.0	fl oz	36	fl oz	-6	fl oz

ADDED 15 GALLONS OF WATER UPON DELIVERY

366.7 lbs of water added to truck mix

44.0 gallons of water added to truck mix

23.8 remaining gallons for design

Mix Design based on truck delivery quantities					% Difference
Product	Quantity	Units	SG	Volume/cy (ft^3/cy)	from design
Cement - Type 1L	423.3	lb/cy	3.15	2.15	-0.2%
Fly ash - Class F	133.3	lb/cy	2.37	0.90	0.3%
#67 stone - Coarse aggregate	1535.3	lb/cy	2.80	8.79	0.0%
Sand - Fine aggregate	1608.1	lb/cy	2.63	9.80	0.0%
Water	259.0	lb/cy	1.00	4.15	-3.0%
	31.1	gallons/cy			-3.0%
Air	3.5%	-		0.95	0.0%
Fiber - Sika hooked-end (1% volume)	132.3	lb/cy	7.85	0.27	0.0%
WR Grace Darex AEA - Air entraining Admixture	3.7	fl oz/cy	-		-8.3%
MasterSet DELVO - Retarding Admixture	6.7	fl oz/cy	-		-76.2%
MasterGlenium 7920 - High-range WRDA	10.0	fl oz/cy	-		-16.7%

Mix info based on truck delivery	
Total volume	27.01 ft^3
Total mass	4091.33 lb/cy
Unit weight	151.49 lb/ft^3
Total cm/cy	556.67 lb/cy
w/c	0.61
w/cm	0.47
% fly ash	23.95%
sand/agg	0.51

Deck concrete mixture design
for FRC specimen 1

1616395

CONCRETE MIX DESIGN

07-1239-10

Producer: Cemex, Inc. - Concrete Division | Class II Bridge Deck (4500 PSI) / Conventional | Effective Date: 4/14/2020

Aggregrate Correction Factor: 0.6 | Environment: Extremely Aggressive | Hot Weather

Source of Materials

Product	Quantity		Production Facility
921: Cement - Type II (MH)	495	Pound(s)	CMT08 - Cemex - Brooksville, FL (South)
929: Fly Ash - Class F	124	Pound(s)	FA43 - Cemex (MRT) - Tampa, FL (Zonguldak, Turkey)
901: C10 - #57 Stone	1728	Pound(s)	87090 - CEMEX
902: F01 - Silica Sand (Concrete)	1180	Pound(s)	50471 - A MINING GROUP, LLC
Isosphere 5004 [924-000-041 - Admixture for Concrete - Air Entraining]	4	FL OZ	CEMEX Admix USA, LLC
Isoplast 1440 [924-003-062 - Admixture for Concrete Type D]	29.7	FL OZ	CEMEX Admix USA, LLC
Water	32.7	GAL	
Water	272	LB	

Calculated Values

Theoretical Unit Weight	140.7	PCF
Theoretical Yield	27.00	CF
Water Contributed from Admixture(s)	0.0	LB

Producer Data

Mix Design Limits*

Water to Cementitious Materials Ratio <= 0.44

**See Contract Documents for Limits not displayed*

Special Use Instructions:

Deck concrete mixture design
for FRC specimen 2

CONCRETE MIX DESIGN
03-2177-02

Producer: Smyrna Ready Mix	Class II Bridge Deck (4500 PSI) / Increased Slump	Effective Date: 3/6/2019
Aggregrate Correction Factor: 0.2	Environment: Extremely Aggressive	Hot Weather

Source of Materials

Product	Quantity		Production Facility
921: Cement - Type II (MH)	489	Pound(s)	CMT29 - Suwannee American Cement - Branford, FL
929: Fly Ash - Class F	122	Pound(s)	FA45 - Boral - Bucks, AL (Barry)
901: C12 - #67 Stone	1900	Pound(s)	GA553 - JUNCTION CITY MINING
902: F01 - Silica Sand (Concrete)	1255	Pound(s)	50471 - A MINING GROUP, LLC
MasterAir AE 90 (MB-AE 90) [924-000-014 - Admixture for Concrete - Air Entraining]	.6	FL OZ	BASF Construction Chemicals, LLC
MasterSet DELVO (Delvo) [924-003-021 - Admixture for Concrete Type D]	30.6	FL OZ	BASF Construction Chemicals, LLC
MasterGlenium 7920 [924-005-093 - Admixture for Concrete Type F]	12.2	FL OZ	BASF Construction Chemicals, LLC
Water	32.5	GAL	
Water	271	LB	

Calculated Values

Theoretical Unit Weight	149.5	PCF
Theoretical Yield	27.01	CF
Water Contributed from Admixture(s)	0.0	LB

Producer Data

Mix Design Limits*

Slump = 5 +/- 1.5 in

Water to Cementitious Materials Ratio <= 0.44

**See Contract Documents for Limits not displayed*

Special Use Instructions: Extended Transit Time: 2 Hours 30 Minutes

FRC-2 deck concrete
2020-10-26: SRM Class II deck truck delivery mixture

Financial Project No.:		Serial No.:	4036127
Plant No.:	55-503	Date:	10/26/2020
Concrete Supplier:	Smyrna Ready Mix	Deliver To:	FDOT
Phone Number:	850-575-3888	Phone No.:	561-632-4076
Address:	5379 Capitol Circle Tallahassee, Fl 32305	Address:	2007 Paul Dirac

Truck No. 4033		DOT Class Class II 4500 DECK		DOT Mix No. 03-2177-04		Cubic Yards This Load 4		
Allowable Jobsite water 30		Time Loaded 8:35		Mixing Revolutions		Cubic Yards Total Today 4		
Cement	Argos (Source)	IL (Type)	1950 (Amount)	Fly Ash or Slag		Boral (Source)	Class F (Type)	550 (Amount)
Coarse Agg.	GA553 (Pit No.)	1.1 (% Moisture)	7880 (Amount)	Air Entraining	BASF (Source)	AE 90 (Brand)	--- (Type)	4 (Amount)
Fine Agg.	50-382 (Pit No.)	3.7 (% Moisture)	5280 (Amount)	Admixture	BASF (Source)	Retarder (Brand)	D (Type)	73 (Amount)
Batch Water (gals or lbs)			70 (Amount)	Admixture	BASF (Source)	7920 (Brand)	G (Type)	61 (Amount)
				Admixture	BASF (Source)	SRA 020 (Brand)	S (Type)	0 (Amount)

Issuance of this ticket constitutes certification that the concrete batched was produced and information recorded in compliance with Department specification requirements for Structural Concrete.

E351810854210
CTQP Technician Identification Number

Signature of Batcher Plant Operator

Arrival Time At Jobsite: 9:05		Number of Revolutions Upon Arrival At Job Site 129	
Water Added At Job Site (gals or lbs)		Additional Mixing Revolutions With Added Water	
Time Concrete Completely Discharged		Total Number of Revolutions	
Initial Slump	Initial Air	Initial Concrete Temperature	Initial W/C Ratio
Acceptance Slump	Acceptance Air	Acceptance Concrete Temperature	Acceptance W/C Ratio

Issuance of this ticket constitutes certification that the maximum specified water cementitious ratio was not exceeded and the batch was delivered and placed in compliance with Department specification requirements.

FRC-2 deck concrete
2020-10-26: SRM Class II deck design vs truck delivery mixture

Batch size (cy)	4
Batch size (ft^3)	108

	Natural moisture (%)	Absorption (%)	Difference (%)
#67 stone - Coarse aggregate	1.10%	0.53%	0.57%
Sand - Fine aggregate	3.70%	0.40%	3.30%

Mix Design				
Product	Quantity	Units	SG	Volume/cy (ft^3/cy)
Cement - Type 1L	489	lb/cy	3.15	2.49
Fly ash - Class F	122	lb/cy	2.37	0.82
#67 stone - Coarse aggregate	1900	lb/cy	2.80	10.87
Sand - Fine aggregate	1255	lb/cy	2.63	7.65
Water	271	lb/cy	1.00	4.34
	32.5	gallons/cy		
Air	3.5%	-		0.95
Fiber - Sika hooked-end (1% volume)	0	lb/cy	7.85	0.00
AE 90 - Air entraining Admixture	0.6	fl oz/cy	-	
MasterSet DELVO - Retarding Admixture	30.6	fl oz/cy	-	
MasterGlenium 7920 - High-range WRDA	12.2	fl oz/cy	-	

Mix info		
Total volume	**27.1**	**ft^3**
Total mass	4037.00	lb/cy
Unit weight	148.84	lb/ft^3
Total cm/cy	611.00	lb/cy
w/c	0.554	
w/cm	0.444	
% fly ash	19.97%	
sand/agg	0.398	

Adjustments for moisture		
Aggregate weight adjustments for natural moisture		
#67 stone - Coarse aggregate	1920.9	lb/cy
Sand - Fine aggregate	1301.4	lb/cy
Water weight adjustment based on absorption and natural moisture		
Water from #67 stone - Coarse aggregate	10.7	lb/cy
Water from Sand - Fine aggregate	41.4	lb/cy
Water adjustment	-52.2	lb/cy
	-6.3	gallons/cy
Water (adjusted mix quantity)	218.8	lb/cy
	26.3	gallons/cy

Total content added to the truck (from delivery ticket)		Units	Design quantities (with moisture adjustments)	Difference	
Cement - Type 1L	1950.0	lb	1956.0 lb	-6.0 lb	
Fly ash - Class F	550.0	lb	488.0 lb	62.0 lb	
#67 stone - Coarse aggregate	7880.0	lb	7683.6 lb	196.4 lb	
Sand - Fine aggregate	5280.0	lb	5205.7 lb	74.3 lb	
Water	583.3	lb	875.4 lb	-292.1 lb	
	70.0	gallons	105.0 gallons	-35.0 gallons	<--- Total number of gallons that may be added to the truck (if negative)
WR Grace Darex AEA - Air entraining Admixture	4.0	fl oz	2.4 fl oz	1.6 fl oz	** Measured 4" slump upon delivery. Added 6 gallons of water and measured a 4.5" slump.
MasterSet DELVO - Retarding Admixture	73.0	fl oz	122.4 fl oz	-49.4 fl oz	** So they added 3 more gallons and did not take the time to measure another slump
MasterGlenium 7920 - High-range WRDA	61.0	fl oz	48.8 fl oz	12.2 fl oz	

Mix Design based on truck delivery quantities					% Difference
Product	Quantity	Units	SG	Volume/cy (ft^3/cy)	from design
Cement - Type 1L	487.5	lb/cy	3.15	2.48	-0.3%
Fly ash - Class F	137.5	lb/cy	2.37	0.93	12.7%
#67 stone - Coarse aggregate	1948.3	lb/cy	2.80	11.15	2.5%
Sand - Fine aggregate	1271.2	lb/cy	2.63	7.75	1.3%
Water	259.0	lb/cy	1.00	4.15	-4.4%
	31.1	gallons/cy			-4.4%
Air	3.5%	-		0.95	0.0%
Fiber - Sika hooked-end (1% volume)	0.0	lb/cy	7.85	0.00	
WR Grace Darex AEA - Air entraining Admixture	1.0	fl oz/cy	-		66.7%
MasterSet DELVO - Retarding Admixture	18.3	fl oz/cy	-		-40.4%
MasterGlenium 7920 - High-range WRDA	15.3	fl oz/cy	-		25.0%

Mix info based on truck delivery		
Total volume	**27.40**	**ft^3**
Total mass	4103.49	lb/cy
Unit weight	149.75	lb/ft^3
Total cm/cy	625.00	lb/cy
w/c	0.53	
w/cm	0.41	
% fly ash	22.00%	
sand/agg	0.39	

FRC railing concrete mixture design
excluding fiber

SMYRNA READY MIX CONCRETE
"QUALITY CONCRETE, UNMATCHED SERVICE"

CONCRETE MIX DESIGN

MIX ID: 34091 3400 PSI CONCRETE 5/1/2020
CLASS II SLIP FORM

CONTRACTOR: FDOT RESEARCH
PROJECT: RESEARCH PROJECT
USE: SLIP FORM

	WEIGHTS PER CUBIC YARD	(SATURATED, SURFACE DRY)		YIELD, CU FT
CEMENT	TYPE I/II ASTM C150, LB.	424		2.16
FLYASH	TYPE F ASTM C618, LB.	133	23.88%	0.88
SAND	FDOT NATURAL SAND,ASTM C33 LB.	1608		8.47
STONE	FDOT #67 GRANITE ASTM C33 , LB.	1535		10.47
STONE	#89 GRANITE ASTM C33 LB.	0		0.00
WATER	(GAL-US)	32		4.27
TOTAL AIR, %		3.5	+/- 2.5	0.945
			TOTAL	27.20

AIR ENTRAINMENT, OZ-US	1 TO 6
HR WATER REDUCER, OZ/100WT-US	2 TO 4
RETARDER, OZ/100WT-US	5.0
FIBER	TBD
WATER/CEMENT RATIO. LBS/LB	0.48
SLUMP, IN	6.0 +/- 1.0
CONCRETE UNIT WEIGHT, PCF	145.83

TEST RESULTS OBTAINED FROM A LIKE OR SIMILAR MIX DESIGN
PER ACI 301; 4.3.2

COMMENT: CUSTOMER TO PUT FIBER IN AT JOB

JUSTIN SPOONER

FRC-1 railing concrete
2020-05-04: FRC railing truck delivery mixture

DELIVERY TICKET FOR NONSTRUCTURAL CONCRETE

Financial Project No.		Serial No.	4032567
Plant No.:	55-503	Date:	5/4/2020
Concrete Supplier:	Smyrna Ready Mix	Deliver To:	University of Florida
Phone Number:	850-576-4141	Phone No.	561-632-4076
Address:	5379 Capitol Circle Tallahassee, Fl 32305	Address:	2007 East Paul Dr

Truck No. 4037	DOT Class NS 3400	DOT Mix No. 03-2176-02	Cubic Yards This Load 3
Batch Time 10:10	Time Arrived	Time Discharged	Cubic Yards Delivered Today 3
Allowable Jobsite Water Addition 20		Jobsite Slump	

Cement	Argos (Source)	IL (Type)	1380	Fly Ash	BORAL (Brand)	CLASS F (Type)	390 (Amount)
Coarse Agg.	GA553 (PIT NO)	1.1 (% Moisture)	4520 (Amount)	Air Entraining Admix	AE 90 (Brand)	BASF (Source)	5 (Amount)
Fine Agg.	50-382 (PIT NO)	3.7 (% Moisture)	4920 (Amount)	Admixture	Retarder (Brand)	BASF (Source)	87 (Amount)
Batch Water (gals or lbs)			40 (Amount)	Admixture	WR (7920) (Brand)	BASF (Source)	51 (Amount)

Issuance of this ticket constitutes certification that the concrete batched was produced and information recorded in compliance with Department specification requirements (347-5).

Signature of Batcher Plant Operator

FRC-1 railing concrete

2020-05-04: FRC railing design vs truck delivery mixture

Batch size (cy)	3
Batch size (ft^3)	81

	Natural moisture (%)	Absorption (%)	Difference (%)
#67 stone - Coarse aggregate	1.10%	0.53%	0.57%
Sand - Fine aggregate	3.70%	0.40%	3.30%

Mix Design				
Product	Quantity	Units	SG	Volume/cy (ft^3/cy)
Cement - Type 1L	424	lb/cy	3.15	2.16
Fly ash - Class F	133	lb/cy	2.37	0.90
#67 stone - Coarse aggregate	1535	lb/cy	2.80	8.79
Sand - Fine aggregate	1608	lb/cy	2.63	9.80
Water	267	lb/cy	1.00	4.28
	32.0	gallons/cy		
Air	3.5%	-		0.95
Fiber - Sika hooked-end (1% volume)	132.26	lb/cy	7.85	0.27
AE 90 - Air entraining Admixture	3.7	fl oz/cy	-	
MasterSet DELVO - Retarding Admixture	27	fl oz/cy	-	
MasterGlenium 7920 - High-range WRDA	10	fl oz/cy	-	

Mix info		
Total volume	**27.1**	**ft^3**
Total mass	4099.26	lb/cy
Unit weight	151.07	lb/ft^3
Total cm/cy	557.00	lb/cy
w/c	0.630	
w/cm	0.479	
% fly ash	23.88%	
sand/agg	0.512	

Fiber dosage		
Fiber type	Sika hooked-end steel fiber	
SG	7.85	
Dosage by volume	1%	
Unit weight	489.84	lb/ft^3
Fiber dosage	132.26	lb/cy
FRC batch size	1.86	cy
FRC batch size	50.3	ft^3
Total fiber quantity	246.4	lb
Number of buckets	10	buckets
Fiber wt per bucket	24.6	lb/bucket

Adjustments for moisture		
Aggregate weight adjustments for natural moisture		
#67 stone - Coarse aggregate	1551.9	lb/cy
Sand - Fine aggregate	1667.5	lb/cy
Water weight adjustment based on absorption and natural moisture		
Water from #67 stone - Coarse aggregate	8.7	lb/cy
Water from Sand - Fine aggregate	53.1	lb/cy
Water adjustment	-61.7	lb/cy
	-7.4	gallons/cy
Water (adjusted mix quantity)	205.3	lb/cy
	24.6	gallons/cy

Total content added to the truck (from delivery ticket)		Units	Design quantities (with moisture adjustments)		Difference		
Cement - Type 1L	1380.0	lb	1272.0	lb	108.0	lb	
Fly ash - Class F	390.0	lb	399.0	lb	-9.0	lb	
#67 stone - Coarse aggregate	4520.0	lb	4655.7	lb	-135.7	lb	
Sand - Fine aggregate	4920.0	lb	5002.5	lb	-82.5	lb	
Water	333.3	lb	615.8	lb	-282.4	lb	
	40.0	gallons	73.9	gallons	-33.9	gallons	<--- Total number of gallons that may be added to the truck (if negative)
WR Grace Darex AEA - Air entraining Admixture	5.0	fl oz	11.1	fl oz	-6.1	fl oz	*** added 9+3 gallons to truck delivery
MasterSet DELVO - Retarding Admixture	87.0	fl oz	81.0	fl oz	6.0	fl oz	
MasterGlenium 7920 - High-range WRDA	51.0	fl oz	30	fl oz	21	fl oz	

Mix Design based on truck delivery quantities					% Difference
Product	Quantity	Units	SG	Volume/cy (ft^3/cy)	from design
Cement - Type 1L	460.0	lb/cy	3.15	2.34	8.5%
Fly ash - Class F	130.0	lb/cy	2.37	0.88	-2.3%
#67 stone - Coarse aggregate	1490.1	lb/cy	2.80	8.53	-2.9%
Sand - Fine aggregate	1579.3	lb/cy	2.63	9.62	-1.8%
Water	259.0	lb/cy	1.00	4.15	-3.0%
	31.1	gallons/cy			-3.0%
Air	3.5%	-		0.95	0.0%
Fiber - Sika hooked-end (1% volume)	132.3	lb/cy	7.85	0.27	0.0%
WR Grace Darex AEA - Air entraining Admixture	1.7	fl oz/cy	-		-55.0%
MasterSet DELVO - Retarding Admixture	29.0	fl oz/cy	-		7.4%
MasterGlenium 7920 - High-range WRDA	17.0	fl oz/cy	-		70.0%

Mix info based on truck delivery		
Total volume	**26.74**	**ft^3**
Total mass	4050.67	lb/cy
Unit weight	151.50	lb/ft^3
Total cm/cy	590.00	lb/cy
w/c	0.56	
w/cm	0.44	
% fly ash	22.03%	
sand/agg	0.51	

FRC-1 railing concrete mixing procedure

Name: Jeff Honig
Date: 5/04/2020
Mix: FRC impact railing production
FRC mix design no. 14
(Documented over Zoom)
Temp: 73 deg. F at 10:53 am
79 deg. F at 11:53 am

Time	Procedure
10:10 am	Batch time at plant
10:36 am	Truck arrived to lab
10:40 am	Started to fill buttress
10:44 am	Standard slump measured: 3.75 in.
10:48 am	9 gallons of water added to truck mix
10:51 am	Standard slump measured: 6.75 in.
10:53 am	3 gallons of water added to truck mix
10:58 am	Standard slump measured: 8.5 in.
11:00 am	Started to fill first small drop bucket and transfer to UHPC mixer - Had trouble using bucket chute
11:13 am	Added second small drop bucket to mixer
11:17 am	Turned on UHPC mixer and started adding fiber
11:21 am	All 5 buckets of fiber added to mixer
11:24 am	Turned off mixer and dumped to larger drop bucket below
11:31 am	FRC slump measured: 4.50 in.
11:33 am	Start to fill railing formwork - Filled railing 14.75in. from top of form - Leaking along the bottom of form
11:46 am	Standard slump measured: 5.50 in. (for second lift)
11:52 am	Transport first small bucket to mixer
12:02 pm	Transport second small bucket to mixer
12:06 pm	Turned on mixer for second lift
12:06 pm	Slowly added 10 fl oz of Chryso Premia 150 superplasticizer AND 10 fl oz of water (mixed together)
12:06 pm	Started adding fiber
12:10 pm	Finished adding fiber
12:12 pm	Turned off mixer
12:18 pm	FRC slump measured: 5.50 in.
12:33 pm	Finished filling railing formwork
12:45 pm	Finished filling buttress regions

Time	Test	Measurement
10:44 am	Slump (from truck)	3.75 in.
10:51 am	Slump (from truck)	6.75 in.
10:58 am	Slump (from truck)	8.50 in.
11:31 am	FRC slump (lift 1)	4.50 in.
11:46 am	Slump (from truck)	5.50 in.
12:06 pm	Added plasticizer	
12:18 pm	FRC slump (lift 2)	5.50 in.

FRC-2 railing concrete
2020-11-09: FRC railing truck delivery mixture

Financial Project No.:	
Plant No.:	55-503
Concrete Supplier:	Smyrna Ready Mix
Phone Number:	850-575-3888
Address:	5379 Capitol Circle Tallahassee, Fl 32305

Serial No.:	4036451
Date:	11/9/2020
Deliver To:	FDOT
Phone No.:	561-632-4076
Address:	2007 Paul Dirac

Truck No. 4037	DOT Class CLASS II 3400 Slip	DOT Mix No.	Cubic Yards This Load 3
Allowable Jobsite water 30	Time Loaded 9:35	Mixing Revolutions	Cubic Yards Total Today 3

Material	Source / Pit No.	Type / % Moisture	Amount
Cement	Argos (Source)	IL (Type)	1280
Coarse Agg.	GA553 (Pit No.)	1.1 (% Moisture)	4720
Fine Agg.	50-382 (Pit No.)	3.7 (% Moisture)	5040
Batch Water (gals or lbs)			43

Material	Source	Brand	Type	Amount
Fly Ash or Slag	Boral		Class F	450
Air Entraining	BASF	AE 90	---	4
Admixture	BASF	Retarder	D	87
Admixture	BASF	7920	G	48
Admixture	BASF	SRA 020	S	0

Issuance of this ticket constitutes certification that the concrete batched was produced and information recorded in compliance with Department specification requirements for Structural Concrete.

E351810854210
CTQP Technician Identification Number

Signature of Batcher Plant Operator

Arrival Time At Jobsite:		Number of Revolutions Upon Arrival At Job Site	
Water Added At Job Site (gals or lbs)		Additional Mixing Revolutions With Added Water	
Time Concrete Completely Discharged		Total Number of Revolutions	
Initial Slump	Initial Air	Initial Concrete Temperature	Initial W/C Ratio
Acceptance Slump	Acceptance Air	Acceptance Concrete Temperature	Acceptance W/C Ratio

Issuance of this ticket constitutes certification that the maximum specified water cementitious ratio was not exceeded and the batch was delivered and placed in compliance with Department specification requirements.

FRC-2 railing concrete
2020-11-09: FRC railing design vs truck delivery mixture

Batch size (cy)	3
Batch size (ft^3)	81

	Natural moisture (%)	Absorption (%)	Difference (%)
#67 stone - Coarse aggregate	1.10%	0.53%	0.57%
Sand - Fine aggregate	3.70%	0.40%	3.30%

Mix Design				
Product	Quantity	Units	SG	Volume/cy (ft^3/cy)
Cement - Type 1L	424	lb/cy	3.15	2.16
Fly ash - Class F	133	lb/cy	2.37	0.90
#67 stone - Coarse aggregate	1535	lb/cy	2.80	8.79
Sand - Fine aggregate	1608	lb/cy	2.63	9.80
Water	267	lb/cy	1.00	4.28
	32.0	gallons/cy		
Air	3.5%	-		0.95
Fiber - Sika hooked-end (1% volume)	132.26	lb/cy	7.85	0.27
AE 90 - Air entraining Admixture	3.7	fl oz/cy	-	
MasterSet DELVO - Retarding Admixture	27	fl oz/cy	-	
MasterGlenium 7920 - High-range WRDA	10	fl oz/cy	-	

Mix info		
Total volume	**27.1**	**ft^3**
Total mass	4099.26	lb/cy
Unit weight	151.07	lb/ft^3
Total cm/cy	557.00	lb/cy
w/c	0.630	
w/cm	0.479	
% fly ash	23.88%	
sand/agg	0.512	

Fiber dosage		
Fiber type	Sika hooked-end steel fiber	
SG	7.85	
Dosage by volume	1%	
Unit weight	489.84	lb/ft^3
Fiber dosage	132.26	lb/cy
FRC batch size	1.86	cy
FRC batch size	50.3	ft^3
Total fiber quantity	246.4	lb
Number of buckets	10	buckets
Fiber wt per bucket	24.6	lb/bucket

Adjustments for moisture		
Aggregate weight adjustments for natural moisture		
#67 stone - Coarse aggregate	1551.9	lb/cy
Sand - Fine aggregate	1667.5	lb/cy
Water weight adjustment based on absorption and natural moisture		
Water from #67 stone - Coarse aggregate	8.7	lb/cy
Water from Sand - Fine aggregate	53.1	lb/cy
Water adjustment	-61.7	lb/cy
	-7.4	gallons/cy
Water (adjusted mix quantity)	205.3	lb/cy
	24.6	gallons/cy

Total content added to the truck (from delivery ticket)		Units	Design quantities (with moisture adjustments)		Difference		
Cement - Type 1L	1280.0	lb	1272.0	lb	8.0	lb	
Fly ash - Class F	450.0	lb	399.0	lb	51.0	lb	
#67 stone - Coarse aggregate	4720.0	lb	4655.7	lb	64.3	lb	
Sand - Fine aggregate	5040.0	lb	5002.5	lb	37.5	lb	
Water	358.3	lb	615.8	lb	-257.4	lb	
	43.0	gallons	73.9	gallons	-30.9	gallons	<--- Total number of gallons that may be added to the truck (if negative)
WR Grace Darex AEA - Air entraining Admixture	4.0	fl oz	11.1	fl oz	-7.1	fl oz	*** added 12 and 3 gallons to truck delivery
MasterSet DELVO - Retarding Admixture	87.0	fl oz	81.0	fl oz	6.0	fl oz	
MasterGlenium 7920 - High-range WRDA	48.0	fl oz	30	fl oz	18	fl oz	

Mix Design based on truck delivery quantities					% Difference
Product	Quantity	Units	SG	Volume/cy (ft^3/cy)	from design
Cement - Type 1L	426.7	lb/cy	3.15	2.17	0.6%
Fly ash - Class F	150.0	lb/cy	2.37	1.01	12.8%
#67 stone - Coarse aggregate	1556.0	lb/cy	2.80	8.91	1.4%
Sand - Fine aggregate	1617.8	lb/cy	2.63	9.86	0.6%
Water	259.0	lb/cy	1.00	4.15	-3.0%
	31.1	gallons/cy			-3.0%
Air	3.5%	-		0.95	0.0%
Fiber - Sika hooked-end (1% volume)	132.3	lb/cy	7.85	0.27	0.0%
WR Grace Darex AEA - Air entraining Admixture	1.3	fl oz/cy	-		-64.0%
MasterSet DELVO - Retarding Admixture	29.0	fl oz/cy	-		7.4%
MasterGlenium 7920 - High-range WRDA	16.0	fl oz/cy	-		60.0%

Mix info based on truck delivery		
Total volume	**27.31**	**ft^3**
Total mass	4141.79	lb/cy
Unit weight	151.63	lb/ft^3
Total cm/cy	576.67	lb/cy
w/c	0.61	
w/cm	0.45	
% fly ash	26.01%	
sand/agg	0.51	

FRC-2 railing concrete mixing procedure

Name: Jeff Honig
Date: 11/09/2020
Mix: FRC impact railing production
FRC mix design no. 14
(Documented over Zoom)

Time	Procedure
9:35 am	Batch time at plant
10:04 am	Truck arrived to lab
10:10 am	Started to fill buttress
10:10 am	Standard slump measured: 2.75 in.
10:13 am	12 gallons of water added to truck mix
10:18 am	Standard slump measured: 3.25 in.
10:20 am	3 gallons of water added to truck mix
10:23 am	Standard slump measured: 8.0 in.
10:27 am	Started to fill large drop bucket and transfer to UHPC mixer
10:30 am	Added large drop bucket to mixer
10:33 am	Turned on UHPC mixer and started adding fiber
10:38 am	All 5 buckets of fiber added to mixer
10:40 am	Turned off mixer and dumped to first small drop bucket below
10:43 am	FRC slump measured: 7.50 in.
10:49 am	Start to fill railing formwork
10:52 am	Continued with second small bucket from first lift - Filled railing 17.25 in. from top of form
11:02 am	- Leaking along the bottom of form
11:07 am	Standard slump measured: 7.25 in. (for second lift)
11:11 am	Transport large bucket to mixer
11:18 am	Added concrete to mixer
11:20 am	Turned on mixer for second lift
11:20 am	Started adding fiber
11:27 pm	Finished adding fiber
11:29 am	Turned off mixer
11:33 am	FRC slump measured: 5.0 in.
11:45 am	Finished filling railing formwork and continued to vibrate
12:14 pm	Finished filling buttress regions

Time	Test	Measurement
10:10 am	Slump (from truck)	2.75 in.
10:18 am	Slump (from truck)	3.25 in.
10:23 am	Slump (from truck)	8.00 in.
10:43 am	FRC slump (lift 1)	7.50 in.
11:07 am	Slump (from truck) (did not need to add plasticizer)	7.25 in.
11:33 am	FRC slump (lift 2)	5.00 in.

FRC-3 (EOR) railing concrete
2021-01-21: FRC railing truck delivery mixture

Financial Project No.:		Serial No.:	4037863
Plant No.:	55-503	Date:	1/21/2021
Concrete Supplier:	Smyrna Ready Mix	Deliver To:	FDOT
Phone Number:	850-575-3888	Phone No.:	561-632-4076
Address:	5379 Capitol Circle Tallahassee, Fl 32305	Address:	2007 Paul Dirac

Truck No. **4007**	DOT Class **CLASS**	DOT Mix No. **03-2176-02sf**	Cubic Yards This Load **3**
Allowable Jobsite water **30**	Time Loaded **8:45**	Mixing Revolutions	Cubic Yards Total Today **3**

Cement	Argos	IL	1400	Fly Ash or Slag		Boral	Class F	425
	Source	Type	Amount			Source	Type	Amount
Coarse Agg.	GA553	1.1	4800	Air Entraining	BASF	AE 90	---	2
	Pit No.	% Moisture	Amount		Source	Brand	Type	Amount
Fine Agg.	50-382	3.7	4950	Admixture	BASF	Retarder	D	0
	Pit No.	% Moisture	Amount		Source	Brand	Type	Amount
Batch Water (gals or lbs)			44	Admixture	BASF	7920	G	51
			Amount		Source	Brand	Type	Amount
				Admixture	BASF	SRA 020	S	0
					Source	Brand	Type	Amount

Issuance of this ticket constitutes certification that the concrete batched was produced and information recorded in compliance with Department specification requirements for Structural Concrete.

E351810854210
CTQP Technician Identification Number

Signature of Batcher Plant Operator

Arrival Time At Jobsite:		Number of Revolutions Upon Arrival At Job Site 110	
Water Added At Job Site (gals or lbs)		Additional Mixing Revolutions With Added Water	
Time Concrete Completely Discharged		Total Number of Revolutions	
Initial Slump	Initial Air	Initial Concrete Temperature	Initial W/C Ratio
Acceptance Slump	Acceptance Air	Acceptance Concrete Temperature	Acceptance W/C Ratio

Issuance of this ticket constitutes certification that the maximum specified water cementitious ratio was not exceeded and the batch was delivered and placed in compliance with Department specification requirements.

FRC-3 (EOR) railing concrete
2021-01-21: FRC railing design vs truck delivery mixture

Batch size (cy)	3
Batch size (ft^3)	81

	Natural moisture (%)	Absorption (%)	Difference (%)
#67 stone - Coarse aggregate	1.10%	0.53%	0.57%
Sand - Fine aggregate	3.70%	0.40%	3.30%

Mix Design				
Product	Quantity	Units	SG	Volume/cy (ft^3/cy)
Cement - Type 1L	424	lb/cy	3.15	2.16
Fly ash - Class F	133	lb/cy	2.37	0.90
#67 stone - Coarse aggregate	1535	lb/cy	2.80	8.79
Sand - Fine aggregate	1608	lb/cy	2.63	9.80
Water	267	lb/cy	1.00	4.28
	32.0	gallons/cy		
Air	3.5%	-		0.95
Fiber - Sika hooked-end (1% volume)	132.26	lb/cy	7.85	0.27
AE 90 - Air entraining Admixture	3.7	fl oz/cy	-	
MasterSet DELVO - Retarding Admixture	27	fl oz/cy	-	
MasterGlenium 7920 - High-range WRDA	10	fl oz/cy	-	

Mix info		
Total volume	**27.1**	**ft^3**
Total mass	4099.26	lb/cy
Unit weight	151.07	lb/ft^3
Total cm/cy	557.00	lb/cy
w/c	0.630	
w/cm	0.479	
% fly ash	23.88%	
sand/agg	0.512	

Fiber dosage		
Fiber type	Sika hooked-end steel fiber	
SG	7.85	
Dosage by volume	1%	
Unit weight	489.84	lb/ft^3
Fiber dosage	132.26	lb/cy
FRC batch size	1.86	cy
FRC batch size	50.3	ft^3
Total fiber quantity	246.4	lb
Number of buckets	10	buckets
Fiber wt per bucket	24.6	lb/bucket

Adjustments for moisture		
Aggregate weight adjustments for natural moisture		
#67 stone - Coarse aggregate	1551.9	lb/cy
Sand - Fine aggregate	1667.5	lb/cy
Water weight adjustment based on absorption and natural moisture		
Water from #67 stone - Coarse aggregate	8.7	lb/cy
Water from Sand - Fine aggregate	53.1	lb/cy
Water adjustment	-61.7	lb/cy
	-7.4	gallons/cy
Water (adjusted mix quantity)	205.3	lb/cy
	24.6	gallons/cy

Total content added to the truck (from delivery ticket)		Units	Design quantities (with moisture adjustments)		Difference		
Cement - Type 1L	1400.0	lb	1272.0	lb	128.0	lb	
Fly ash - Class F	425.0	lb	399.0	lb	26.0	lb	
#67 stone - Coarse aggregate	4800.0	lb	4655.7	lb	144.3	lb	
Sand - Fine aggregate	4950.0	lb	5002.5	lb	-52.5	lb	
Water	366.7	lb	615.8	lb	-249.1	lb	
	44.0	gallons	73.9	gallons	-29.9	gallons	<--- Total number of gallons that may be added to the truck (if negative)
WR Grace Darex AEA - Air entraining Admixture	2.0	fl oz	11.1	fl oz	-9.1	fl oz	** added 15 and gallons to truck delivery
MasterSet DELVO - Retarding Admixture	0.0	fl oz	81.0	fl oz	-81.0	fl oz	** slump 1 = 3"
MasterGlenium 7920 - High-range WRDA	51.0	fl oz	30	fl oz	21	fl oz	** slump 2 = 8.75"

Mix Design based on truck delivery quantities					% Difference
Product	Quantity	Units	SG	Volume/cy (ft^3/cy)	from design
Cement - Type 1L	466.7	lb/cy	3.15	2.37	10.1%
Fly ash - Class F	141.7	lb/cy	2.37	0.96	6.5%
#67 stone - Coarse aggregate	1582.4	lb/cy	2.80	9.06	3.1%
Sand - Fine aggregate	1589.0	lb/cy	2.63	9.68	-1.2%
Water	259.0	lb/cy	1.00	4.15	-3.0%
	31.1	gallons/cy			-3.0%
Air	3.5%	-		0.95	0.0%
Fiber - Sika hooked-end (1% volume)	132.3	lb/cy	7.85	0.27	0.0%
WR Grace Darex AEA - Air entraining Admixture	0.7	fl oz/cy	-		-82.0%
MasterSet DELVO - Retarding Admixture	0.0	fl oz/cy	-		-100.0%
MasterGlenium 7920 - High-range WRDA	17.0	fl oz/cy	-		70.0%

Mix info based on truck delivery		
Total volume	**27.44**	**ft^3**
Total mass	4170.94	lb/cy
Unit weight	152.02	lb/ft^3
Total cm/cy	608.33	lb/cy
w/c	0.56	
w/cm	0.43	
% fly ash	23.29%	
sand/agg	0.50	

Deck concrete mixture design
for R/C test specimens (same as FRC 2)

CONCRETE MIX DESIGN
03-2177-02

Producer: Smyrna Ready Mix	Class II Bridge Deck (4500 PSI) / Increased Slump	Effective Date: 3/6/2019
Aggregrate Correction Factor: 0.2	Environment: Extremely Aggressive	Hot Weather

Source of Materials

Product	Quantity		Production Facility
921: Cement - Type II (MH)	489	Pound(s)	CMT29 - Suwannee American Cement - Branford, FL
929: Fly Ash - Class F	122	Pound(s)	FA45 - Boral - Bucks, AL (Barry)
901: C12 - #67 Stone	1900	Pound(s)	GA553 - JUNCTION CITY MINING
902: F01 - Silica Sand (Concrete)	1255	Pound(s)	50471 - A MINING GROUP, LLC
MasterAir AE 90 (MB-AE 90) [924-000-014 - Admixture for Concrete - Air Entraining]	.6	FL OZ	BASF Construction Chemicals, LLC
MasterSet DELVO (Delvo) [924-003-021 - Admixture for Concrete Type D]	30.6	FL OZ	BASF Construction Chemicals, LLC
MasterGlenium 7920 [924-005-093 - Admixture for Concrete Type F]	12.2	FL OZ	BASF Construction Chemicals, LLC
Water	32.5	GAL	
Water	271	LB	

Calculated Values

Theoretical Unit Weight	149.5	PCF
Theoretical Yield	27.01	CF
Water Contributed from Admixture(s)	0.0	LB

Producer Data

Mix Design Limits*

Slump = 5 +/- 1.5 in

Water to Cementitious Materials Ratio <= 0.44

**See Contract Documents for Limits not displayed*

Special Use Instructions: Extended Transit Time: 2 Hours 30 Minutes

RC-1 deck concrete
2020-06-29: SRM Class II deck truck delivery mixture

Financial Project No.:		Serial No.:	4033679
Plant No.:	55-503	Date:	6/29/2020
Concrete Supplier:	Smyrna Ready Mix	Deliver To:	Jeff Honing
Phone Number:	850-575-3888	Phone No.:	561-632-4076
Address:	5379 Capitol Circle Tallahassee, Fl 32305	Address:	2007 E. Paul Dirac DR

Truck No. 1680	DOT Class Class II 4500 Deck	DOT Mix No. 03-2177-02	Cubic Yards This Load 4
Allowable Jobsite water 20	Time Loaded 9:27	Mixing Revolutions	Cubic Yards Total Today 4

	Source	Type	Amount
Cement	Argos	IL	1900

	Pit No.	% Moisture	Amount
Coarse Agg.	GA553	1.1	7800
Fine Agg.	50-382	3.7	4900
Batch Water (gals or lbs)			76

	Source	Brand	Type	Amount
Fly Ash or Slag	Boral		Class F	490
Air Entraining	BASF	AE 90	---	4
Admixture	BASF	Retarder	D	60
Admixture	BASF	7920	G	73
Admixture	BASF	SRA 020	S	0

Issuance of this ticket constitutes certification that the concrete batched was produced and information recorded in compliance with Department specification requirements for Structural Concrete.

2000848
CTQP Technician Identification Number

Signature of Batcher Plant Operator

Arrival Time At Jobsite:		Number of Revolutions Upon Arrival At Job Site	
Water Added At Job Site (gals or lbs)		Additional Mixing Revolutions With Added Water	
Time Concrete Completely Discharged		Total Number of Revolutions	
Initial Slump	Initial Air	Initial Concrete Temperature	Initial W/C Ratio
Acceptance Slump	Acceptance Air	Acceptance Concrete Temperature	Acceptance W/C Ratio

Issuance of this ticket constitutes certification that the maximum specified water cementitious ratio was not exceeded and the batch was delivered and placed in compliance with Department specification requirements.

RC-1 deck concrete

2020-06-29: SRM Class II deck design vs truck delivery mixture

Batch size (cy)	4
Batch size (ft^3)	108

	Natural moisture (%)	Absorption (%)	Difference (%)
#67 stone - Coarse aggregate	1.10%	0.53%	0.57%
Sand - Fine aggregate	3.70%	0.40%	3.30%

Mix Design				
Product	Quantity	Units	SG	Volume/cy (ft^3/cy)
Cement - Type 1L	489	lb/cy	3.15	2.49
Fly ash - Class F	122	lb/cy	2.37	0.82
#67 stone - Coarse aggregate	1900	lb/cy	2.80	10.87
Sand - Fine aggregate	1255	lb/cy	2.63	7.65
Water	271	lb/cy	1.00	4.34
	32.5	gallons/cy		
Air	3.5%	-		0.95
Fiber - Sika hooked-end (1% volume)	0	lb/cy	7.85	0.00
AE 90 - Air entraining Admixture	0.6	fl oz/cy	-	
MasterSet DELVO - Retarding Admixture	30.6	fl oz/cy	-	
MasterGlenium 7920 - High-range WRDA	12.2	fl oz/cy	-	

Mix info		
Total volume	**27.1**	**ft^3**
Total mass	4037.00	lb/cy
Unit weight	148.84	lb/ft^3
Total cm/cy	611.00	lb/cy
w/c	0.554	
w/cm	0.444	
% fly ash	19.97%	
sand/agg	0.398	

Adjustments for moisture		
Aggregate weight adjustments for natural moisture		
#67 stone - Coarse aggregate	1920.9	lb/cy
Sand - Fine aggregate	1301.4	lb/cy
Water weight adjustment based on absorption and natural moisture		
Water from #67 stone - Coarse aggregate	10.7	lb/cy
Water from Sand - Fine aggregate	41.4	lb/cy
Water adjustment	-52.2	lb/cy
	-6.3	gallons/cy
Water (adjusted mix quantity)	218.8	lb/cy
	26.3	gallons/cy

Total content added to the truck (from delivery ticket)		Units	Design quantities (with moisture adjustments)		Difference		
Cement - Type 1L	1900.0	lb	1956.0	lb	-56.0	lb	
Fly ash - Class F	490.0	lb	488.0	lb	2.0	lb	
#67 stone - Coarse aggregate	7800.0	lb	7683.6	lb	116.4	lb	
Sand - Fine aggregate	4900.0	lb	5205.7	lb	-305.7	lb	
Water	633.3	lb	875.4	lb	-242.1	lb	
	76.0	gallons	105.0	gallons	-29.0	gallons	<--- Total number of gallons that may be added to the truck (if negative)
WR Grace Darex AEA - Air entraining Admixture	4.0	fl oz	2.4	fl oz	1.6	fl oz	
MasterSet DELVO - Retarding Admixture	60.0	fl oz	122.4	fl oz	-62.4	fl oz	
MasterGlenium 7920 - High-range WRDA	73.0	fl oz	48.8	fl oz	24.2	fl oz	

Mix Design based on truck delivery quantities					% Difference
Product	Quantity	Units	SG	Volume/cy (ft^3/cy)	from design
Cement - Type 1L	475.0	lb/cy	3.15	2.42	-2.9%
Fly ash - Class F	122.5	lb/cy	2.37	0.83	0.4%
#67 stone - Coarse aggregate	1928.6	lb/cy	2.80	11.04	1.5%
Sand - Fine aggregate	1179.7	lb/cy	2.63	7.19	-6.0%
Water	259.0	lb/cy	1.00	4.15	-4.4%
	31.1	gallons/cy			-4.4%
Air	3.5%	-		0.95	0.0%
Fiber - Sika hooked-end (1% volume)	0.0	lb/cy	7.85	0.00	
WR Grace Darex AEA - Air entraining Admixture	1.0	fl oz/cy	-		66.7%
MasterSet DELVO - Retarding Admixture	15.0	fl oz/cy	-		-51.0%
MasterGlenium 7920 - High-range WRDA	18.3	fl oz/cy	-		49.6%

Mix info based on truck delivery		
Total volume	**26.57**	**ft^3**
Total mass	3964.73	lb/cy
Unit weight	149.24	lb/ft^3
Total cm/cy	597.50	lb/cy
w/c	0.55	
w/cm	0.43	
% fly ash	20.50%	
sand/agg	0.38	

RC-2 deck concrete
2020-08-31: SRM Class II deck truck delivery mixture

Financial Project No.:			Serial No.:	4034906
Plant No.:	55-503		Date:	8/31/2020
Concrete Supplier:	Smyrna Ready Mix		Deliver To:	University Of Florida
Phone Number:	850-575-3888		Phone No.:	850-921-7111
Address:	5379 Capitol Circle		Address:	2007 Paul Dirac
	Tallahassee, Fl 32305			

Truck No. 4038		DOT Class Class II 4500 DECK		DOT Mix No. 03-2177-04		Cubic Yards This Load 4	
Allowable Jobsite water 30		Time Loaded 9:15		Mixing Revolutions		Cubic Yards Total Today 4	
Cement	Argos (Source)	IL (Type)	1950 (Amount)	Fly Ash or Slag	Boral (Source)	Class F (Type)	500 (Amount)
Coarse Agg.	GA553 (Pit No.)	1.1 (% Moisture)	7800 (Amount)	Air Entraining	BASF (Source) / AE 90 (Brand)	--- (Type)	4 (Amount)
Fine Agg.	50-382 (Pit No.)	3.7 (% Moisture)	5080 (Amount)	Admixture	BASF (Source) / Retarder (Brand)	D (Type)	72 (Amount)
Batch Water (gals or lbs)			68 (Amount)	Admixture	BASF (Source) / 7920 (Brand)	G (Type)	60 (Amount)
				Admixture	BASF (Source) / SRA 020 (Brand)	S (Type)	0 (Amount)

Issuance of this ticket constitutes certification that the concrete batched was produced and information recorded in compliance with Department specification requirements for Structural Concrete.

E351810854210
CTQP Technician Identification Number

Signature of Batcher Plant Operator

Arrival Time At Jobsite:		Number of Revolutions Upon Arrival At Job Site	
Water Added At Job Site (gals or lbs)		Additional Mixing Revolutions With Added Water	
Time Concrete Completely Discharged		Total Number of Revolutions	
Initial Slump	Initial Air	Initial Concrete Temperature	Initial W/C Ratio
Acceptance Slump	Acceptance Air	Acceptance Concrete Temperature	Acceptance W/C Ratio

Issuance of this ticket constitutes certification that the maximum specified water cementitious ratio was not exceeded and the batch was delivered and placed in compliance with Department specification requirements.

RC-2 deck concrete

2020-08-31: SRM Class II deck design vs truck delivery mixture

Batch size (cy)	4	
Batch size (ft^3)	108	

	Natural moisture (%)	Absorption (%)	Difference (%)
#67 stone - Coarse aggregate	1.10%	0.53%	0.57%
Sand - Fine aggregate	3.70%	0.40%	3.30%

Mix Design				
Product	Quantity	Units	SG	Volume/cy (ft^3/cy)
Cement - Type 1L	489	lb/cy	3.15	2.49
Fly ash - Class F	122	lb/cy	2.37	0.82
#67 stone - Coarse aggregate	1900	lb/cy	2.80	10.87
Sand - Fine aggregate	1255	lb/cy	2.63	7.65
Water	271	lb/cy	1.00	4.34
	32.5	gallons/cy		
Air	3.5%	-		0.95
Fiber - Sika hooked-end (1% volume)	0	lb/cy	7.85	0.00
AE 90 - Air entraining Admixture	0.6	fl oz/cy	-	
MasterSet DELVO - Retarding Admixture	30.6	fl oz/cy	-	
MasterGlenium 7920 - High-range WRDA	12.2	fl oz/cy	-	

Mix info		
Total volume	27.1	ft^3
Total mass	4037.00	lb/cy
Unit weight	148.84	lb/ft^3
Total cm/cy	611.00	lb/cy
w/c	0.554	
w/cm	0.444	
% fly ash	19.97%	
sand/agg	0.398	

Adjustments for moisture		
Aggregate weight adjustments for natural moisture		
#67 stone - Coarse aggregate	1920.9	lb/cy
Sand - Fine aggregate	1301.4	lb/cy
Water weight adjustment based on absorption and natural moisture		
Water from #67 stone - Coarse aggregate	10.7	lb/cy
Water from Sand - Fine aggregate	41.4	lb/cy
Water adjustment	-52.2	lb/cy
	-6.3	gallons/cy
Water (adjusted mix quantity)	218.8	lb/cy
	26.3	gallons/cy

Total content added to the truck (from delivery ticket)		Units	Design quantities (with moisture adjustments)		Difference		
Cement - Type 1L	1950.0	lb	1956.0	lb	-6.0	lb	
Fly ash - Class F	500.0	lb	488.0	lb	12.0	lb	
#67 stone - Coarse aggregate	7800.0	lb	7683.6	lb	116.4	lb	
Sand - Fine aggregate	5080.0	lb	5205.7	lb	-125.7	lb	
Water	566.7	lb	875.4	lb	-308.7	lb	
	68.0	gallons	105.0	gallons	-37.0	gallons	<--- Total number of gallons that may be added to the truck (if negative)
WR Grace Darex AEA - Air entraining Admixture	4.0	fl oz	2.4	fl oz	1.6	fl oz	
MasterSet DELVO - Retarding Admixture	60.0	fl oz	122.4	fl oz	-62.4	fl oz	
MasterGlenium 7920 - High-range WRDA	72.0	fl oz	48.8	fl oz	23.2	fl oz	

Mix Design based on truck delivery quantities					% Difference
Product	Quantity	Units	SG	Volume/cy (ft^3/cy)	from design
Cement - Type 1L	487.5	lb/cy	3.15	2.48	-0.3%
Fly ash - Class F	125.0	lb/cy	2.37	0.85	2.5%
#67 stone - Coarse aggregate	1928.6	lb/cy	2.80	11.04	1.5%
Sand - Fine aggregate	1223.0	lb/cy	2.63	7.45	-2.5%
Water	259.0	lb/cy	1.00	4.15	-4.4%
	31.1	gallons/cy			-4.4%
Air	3.5%	-		0.95	0.0%
Fiber - Sika hooked-end (1% volume)	0.0	lb/cy	7.85	0.00	
WR Grace Darex AEA - Air entraining Admixture	1.0	fl oz/cy	-		66.7%
MasterSet DELVO - Retarding Admixture	15.0	fl oz/cy	-		-51.0%
MasterGlenium 7920 - High-range WRDA	18.0	fl oz/cy	-		47.5%

Mix info based on truck delivery		
Total volume	26.91	ft^3
Total mass	4023.06	lb/cy
Unit weight	149.49	lb/ft^3
Total cm/cy	612.50	lb/cy
w/c	0.53	
w/cm	0.42	
% fly ash	20.41%	
sand/agg	0.39	

R/C Railing concrete mixture design

CONCRETE MIX DESIGN
03-2176-02

Producer: Smyrna Ready Mix | Class II (3400 PSI) / Increased Slump | Effective Date: 3/7/2019

Aggregrate Correction Factor: 0.2 | Environment: Extremely Aggressive | Hot Weather

Source of Materials

Product	Quantity		Production Facility
921: Cement - Type II (MH)	416	Pound(s)	CMT29 - Suwannee American Cement - Branford, FL
929: Fly Ash - Class F	104	Pound(s)	FA45 - Boral - Bucks, AL (Barry)
901: C12 - #67 Stone	1900	Pound(s)	GA553 - JUNCTION CITY MINING
902: F01 - Silica Sand (Concrete)	1319	Pound(s)	50471 - A MINING GROUP, LLC
MasterAir AE 90 (MB-AE 90) [924-000-014 - Admixture for Concrete - Air Entraining]	.5	FL OZ	BASF Construction Chemicals, LLC
MasterSet DELVO (Delvo) [924-003-021 - Admixture for Concrete Type D]	26	FL OZ	BASF Construction Chemicals, LLC
MasterGlenium 7920 [924-005-093 - Admixture for Concrete Type F]	13	FL OZ	BASF Construction Chemicals, LLC
Water	33.2	GAL	
Water	277	LB	

Calculated Values

Theoretical Unit Weight	148.7	PCF
Theoretical Yield	27.01	CF
Water Contributed from Admixture(s)	0.0	LB

Producer Data

Mix Design Limits*

Slump = 5 +/- 1.5 in

Water to Cementitious Materials Ratio <= 0.53

**See Contract Documents for Limits not displayed*

Special Use Instructions: Extended Transit Time: 2 Hours 30 Minutes

RC-1 railing concrete
2020-07-16: SRM Class II railing truck delivery mixture

Financial Project No.:			Serial No.:	2005448
Plant No.:	50-466		Date:	7/16/2020
Concrete Supplier:	Smyrna Ready Mix		Deliver To:	UNIVERSITY OF FLORIDA
Phone Number:	850-575-3888		Phone No.:	
Address:	1800 Brickyard Rd. E		Address:	2007 E. PAUL DIRAC DR
	Midway, Fl. 32343			

Truck No. 4044		DOT Class CLASS II 3400 GRANITE		DOT Mix No. 34090		Cubic Yards This Load 3	
Allowable Jobsite water 6		Time Loaded 8:38		Mixing Revolutions 81		Cubic Yards Total Today 3	
Cement	SAC (Source)	I/II (Type)	1295 (Amount)	Fly Ash or Slag	Boral (Source)	Class F (Type)	305 (Amount)
Coarse Agg.	GA553 (Pit No.)	1.2 (% Moisture)	5790 (Amount)	Air Entraining	BASF (Source)	AE 90 (Brand)	--- (Type) / 3 (Amount)
Fine Agg.	50-471 (Pit No.)	3.2 (% Moisture)	4180 (Amount)	Admixture	BASF (Source)	Retarder (Brand)	D (Type) / 48 (Amount)
Batch Water (gals or lbs)			70 (Amount)	Admixture	BASF (Source)	7920 (Brand)	A (Type) / 32 (Amount)

Issuance of this ticket constitutes certification that the concrete batched was produced and information recorded in compliance with Department specification requirements for Structural Concrete.

F-500-436-56-062-0
CTQP Technician Identification Number

Signature of Batcher Plant Operator

Arrival Time At Jobsite:		Number of Revolutions Upon Arrival At Job Site	
Water Added At Job Site (gals or lbs)		Additional Mixing Revolutions With Added Water	
Time Concrete Completely Discharged		Total Number of Revolutions	
Initial Slump	Initial Air	Initial Concrete Temperature	Initial W/C Ratio
Acceptance Slump	Acceptance Air	Acceptance Concrete Temperature	Acceptance W/C Ratio

Issuance of this ticket constitutes certification that the maximum specified water cementitious ratio was not exceeded and the batch was delivered and placed in compliance with Department specification requirements.

CTQP Technician Identification Number

Signature of Contractor's Representative

RC-1 railing concrete

2020-07-16: SRM Class II railing design vs truck delivery mixture

Batch size (cy)	3	
Batch size (ft^3)	81	

	Natural moisture (%)	Absorption (%)	Difference (%)
#67 stone - Coarse aggregate	1.20%	0.53%	0.67%
Sand - Fine aggregate	3.20%	0.40%	2.80%

Mix Design				
Product	Quantity	Units	SG	Volume/cy (ft^3/cy)
Cement - Type II	416	lb/cy	3.15	2.12
Fly ash - Class F	104	lb/cy	2.37	0.70
#67 stone - Coarse aggregate	1900	lb/cy	2.80	10.87
Sand - Fine aggregate	1319	lb/cy	2.63	8.04
Water	277	lb/cy	1.00	4.44
	33.2	gallons/cy		
Air	3.0%	-		0.81
Fiber - Sika hooked-end (1% volume)	0	lb/cy	7.85	0.00
AE 90 - Air entraining Admixture	0.5	fl oz/cy	-	
MasterSet DELVO - Retarding Admixture	26	fl oz/cy	-	
MasterGlenium 7920 - High-range WRDA	13	fl oz/cy	-	

Mix info		
Total volume	27.0	ft^3
Total mass	4016.00	lb/cy
Unit weight	148.85	lb/ft^3
Total cm/cy	520.00	lb/cy
w/c	0.666	
w/cm	0.533	
% fly ash	20.00%	
sand/agg	0.410	

Adjustments for moisture		
Aggregate weight adjustments for natural moisture		
#67 stone - Coarse aggregate	1922.8	lb/cy
Sand - Fine aggregate	1361.2	lb/cy
Water weight adjustment based on absorption and natural moisture		
Water from #67 stone - Coarse aggregate	12.6	lb/cy
Water from Sand - Fine aggregate	36.9	lb/cy
Water adjustment	-49.6	lb/cy
	-5.9	gallons/cy
Water (adjusted mix quantity)	227.4	lb/cy
	27.3	gallons/cy

Total content added to the truck (from delivery ticket)		Units	Design quantities (with moisture adjustments)		Difference		
Cement - Type II	1295.0	lb	1248.0	lb	47.0	lb	
Fly ash - Class F	305.0	lb	312.0	lb	-7.0	lb	
#67 stone - Coarse aggregate	5790.0	lb	5768.4	lb	21.6	lb	
Sand - Fine aggregate	4180.0	lb	4083.6	lb	96.4	lb	
Water	583.3	lb	682.3	lb	-99.0	lb	
	70.0	gallons	81.9	gallons	-11.9	gallons	<--- Total number of gallons that may be added to the truck (if negative)
WR Grace Darex AEA - Air entraining Admixture	3.0	fl oz	1.5	fl oz	1.5	fl oz	
MasterSet DELVO - Retarding Admixture	32.0	fl oz	78.0	fl oz	-46.0	fl oz	
MasterGlenium 7920 - High-range WRDA	48.0	fl oz	39	fl oz	9	fl oz	

Mix Design based on truck delivery quantities					% Difference
Product	Quantity	Units	SG	Volume/cy (ft^3/cy)	from design
Cement - Type 1L	431.7	lb/cy	3.15	2.20	3.8%
Fly ash - Class F	101.7	lb/cy	2.37	0.69	-2.2%
#67 stone - Coarse aggregate	1906.8	lb/cy	2.80	10.91	0.4%
Sand - Fine aggregate	1348.7	lb/cy	2.63	8.22	2.3%
Water	259.0	lb/cy	1.00	4.15	-6.5%
	31.1	gallons/cy			-6.5%
Air	3.5%	-		0.95	16.7%
Fiber - Sika hooked-end (1% volume)	132.3	lb/cy	7.85	0.27	#DIV/0!
WR Grace Darex AEA - Air entraining Admixture	1.0	fl oz/cy	-		100.0%
MasterSet DELVO - Retarding Admixture	10.7	fl oz/cy	-		-59.0%
MasterGlenium 7920 - High-range WRDA	16.0	fl oz/cy	-		23.1%

Mix info based on truck delivery		
Total volume	27.38	ft^3
Total mass	4180.18	lb/cy
Unit weight	152.67	lb/ft^3
Total cm/cy	533.33	lb/cy
w/c	0.60	
w/cm	0.49	
% fly ash	19.06%	
sand/agg	0.41	

RC-2 railing concrete
2020-09-15: SRM Class II railing truck delivery mixture

Financial Project No.:		Serial No.:	4035230
Plant No.:	55-503	Date:	9/15/2020
Concrete Supplier:	Smyrna Ready Mix	Deliver To:	FDOT
Phone Number:	850-575-3888	Phone No.:	561-632-4076
Address:	5379 Capitol Circle Tallahassee, Fl 32305	Address:	2007 Paul Dirac

Truck No. 4006		DOT Class CLASS II 3400		DOT Mix No. 03-2176-02		Cubic Yards This Load 3	
Allowable Jobsite water 30		Time Loaded 8:55		Mixing Revolutions		Cubic Yards Total Today 3	
Cement	Argos (Source)	IL (Type)	1260 (Amount)	Fly Ash or Slag	Boral (Source)	Class F (Type)	310 (Amount)
Coarse Agg.	GA553 (Pit No.)	1.1 (% Moisture)	5760 (Amount)	Air Entraining	BASF (Source)	AE 90 (Brand)	--- (Type) / 3 (Amount)
Fine Agg.	50-382 (Pit No.)	3.7 (% Moisture)	4110 (Amount)	Admixture	BASF (Source)	Retarder (Brand)	D (Type) / 23 (Amount)
Batch Water (gals or lbs)			40 (Amount)	Admixture	BASF (Source)	7920 (Brand)	G (Type) / 42 (Amount)
				Admixture	BASF (Source)	Delvo (Brand)	S (Type) / 48 (Amount)

Issuance of this ticket constitutes certification that the concrete batched was produced and information recorded in compliance with Department specification requirements for Structural Concrete.

E351810854210
CTQP Technician Identification Number

Signature of Batcher Plant Operator

Arrival Time At Jobsite:		Number of Revolutions Upon Arrival At Job Site	
Water Added At Job Site (gals or lbs)		Additional Mixing Revolutions With Added Water	
Time Concrete Completely Discharged		Total Number of Revolutions	
Initial Slump	Initial Air	Initial Concrete Temperature	Initial W/C Ratio
Acceptance Slump	Acceptance Air	Acceptance Concrete Temperature	Acceptance W/C Ratio

Issuance of this ticket constitutes certification that the maximum specified water cementitious ratio was not exceeded and the batch was delivered and placed in compliance with Department specification requirements.

RC-2 railing concrete

2020-09-15: SRM Class II railing design vs truck delivery mixture

Batch size (cy)	3
Batch size (ft^3)	81

	Natural moisture (%)	Absorption (%)	Difference (%)
#67 stone - Coarse aggregate	1.10%	0.53%	0.57%
Sand - Fine aggregate	3.70%	0.40%	3.30%

Mix Design				
Product	Quantity	Units	SG	Volume/cy (ft^3/cy)
Cement - Type II	416	lb/cy	3.15	2.12
Fly ash - Class F	104	lb/cy	2.37	0.70
#67 stone - Coarse aggregate	1900	lb/cy	2.80	10.87
Sand - Fine aggregate	1319	lb/cy	2.63	8.04
Water	277	lb/cy	1.00	4.44
	33.2	gallons/cy		
Air	3.0%	-		0.81
Fiber - Sika hooked-end (1% volume)	0	lb/cy	7.85	0.00
AE 90 - Air entraining Admixture	0.5	fl oz/cy	-	
MasterSet DELVO - Retarding Admixture	26	fl oz/cy	-	
MasterGlenium 7920 - High-range WRDA	13	fl oz/cy	-	

Mix info		
Total volume	27.0	ft^3
Total mass	4016.00	lb/cy
Unit weight	148.85	lb/ft^3
Total cm/cy	520.00	lb/cy
w/c	0.666	
w/cm	0.533	
% fly ash	20.00%	
sand/agg	0.410	

Adjustments for moisture		
Aggregate weight adjustments for natural moisture		
#67 stone - Coarse aggregate	1920.9	lb/cy
Sand - Fine aggregate	1367.8	lb/cy
Water weight adjustment based on absorption and natural moisture		
Water from #67 stone - Coarse aggregate	10.7	lb/cy
Water from Sand - Fine aggregate	43.5	lb/cy
Water adjustment	-54.3	lb/cy
	-6.5	gallons/cy
Water (adjusted mix quantity)	222.7	lb/cy
	26.7	gallons/cy

Total content added to the truck (from delivery ticket)		Units	Design quantities (with moisture adjustments)		Difference		
Cement - Type II	1260.0	lb	1248.0	lb	12.0	lb	
Fly ash - Class F	310.0	lb	312.0	lb	-2.0	lb	
#67 stone - Coarse aggregate	5760.0	lb	5762.7	lb	-2.7	lb	
Sand - Fine aggregate	4110.0	lb	4103.4	lb	6.6	lb	
Water	333.3	lb	668.2	lb	-334.9	lb	
	40.0	gallons	80.2	gallons	-40.2	gallons	<--- Total number of gallons that may be added to the truck (if negative)
WR Grace Darex AEA - Air entraining Admixture	3.0	fl oz	1.5	fl oz	1.5	fl oz	
MasterSet DELVO - Retarding Admixture	48.0	fl oz	78.0	fl oz	-30.0	fl oz	
MasterGlenium 7920 - High-range WRDA	42.0	fl oz	39	fl oz	3	fl oz	

Mix Design based on truck delivery quantities					% Difference
Product	Quantity	Units	SG	Volume/cy (ft^3/cy)	from design
Cement - Type 1L	420.0	lb/cy	3.15	2.14	1.0%
Fly ash - Class F	103.3	lb/cy	2.37	0.70	-0.6%
#67 stone - Coarse aggregate	1898.9	lb/cy	2.80	10.87	-0.1%
Sand - Fine aggregate	1319.3	lb/cy	2.63	8.04	0.0%
Water	259.0	lb/cy	1.00	4.15	-6.5%
	31.1	gallons/cy			-6.5%
Air	3.5%	-		0.95	16.7%
Fiber - Sika hooked-end (1% volume)	132.3	lb/cy	7.85	0.27	#DIV/0!
WR Grace Darex AEA - Air entraining Admixture	1.0	fl oz/cy	-		100.0%
MasterSet DELVO - Retarding Admixture	16.0	fl oz/cy	-		-38.5%
MasterGlenium 7920 - High-range WRDA	14.0	fl oz/cy	-		7.7%

Mix info based on truck delivery		
Total volume	27.11	ft^3
Total mass	4132.78	lb/cy
Unit weight	152.45	lb/ft^3
Total cm/cy	523.33	lb/cy
w/c	0.62	
w/cm	0.49	
% fly ash	19.75%	
sand/agg	0.41	

APPENDIX E
HARDENED MECHANICAL PROPERTIES OF RAILING CONCRETE MIXTURES

Presented in this appendix are measured hardened mechanical properties of concrete test samples (4-in. x 8-in. cylinders and 4-in. x 4-in. x 14-in. flexural beam prisms) that were formed with the same concrete batches used to cast full-scale pendulum impact test specimens. Concrete compressive strengths are included for each of the impact test specimens at 28 days and at (or near) the day of pendulum impact testing. Furthermore, flexural mechanical properties of the FRC batch used to form the FRC EOR test specimen are provided in Figure E.1. Note that the flexural test results in Figure E.1 were measured following the ASTM C1609 flexural test (not the EN 14651 CMOD flexural test).

Table E.1 Average compressive strength of concrete deck samples at 28 days

Related test specimen	Concrete placement location	Cast date	Test date	Age (days)	Avg. compressive strength (psi)
FRC COR 1	Deck	-	-	-	Not tested
FRC COR 2	Deck	10/26/2020	11/23/2020	28	4449
FRC EOR	Deck	12/10/2020	1/11/2021	32	4969
R/C COR 1	Deck	6/29/2020	7/27/2020	28	4542
R/C COR 2	Deck	8/31/2020	9/28/2020	28	5138
R/C EOR	Deck	2/17/2021	3/17/2021	28	4480

Table E.2 Average compressive strength of concrete deck samples near day of impact testing

Related test specimen	Concrete placement location	Cast date	Test date	Age (days)	Avg. compressive strength (psi)
FRC COR 1	Deck	4/1/2020	9/2/2020	154	9618
FRC COR 2	Deck	10/26/2020	1/6/2021	72	5613
FRC EOR	Deck	12/10/2020	2/23/2021	75	5747
R/C COR 1	Deck	6/29/2020	10/30/2020	123	5027
R/C COR 2	Deck	8/31/2020	12/9/2020	100	6677
R/C EOR	Deck	2/17/2021	4/6/2021	48	5332

Table E.3 Average compressive strength of concrete or FRC railing samples at 28 days

Related test specimen	Concrete placement location	Cast date	Test date	Age (days)	Avg. compressive strength (psi)
FRC COR 1	Railing				Not tested
FRC COR 2	Railing	11/9/2020	12/7/2020	28	3475
FRC EOR	Railing	1/21/2021	2/18/2021	28	3340
R/C COR 1	Railing	7/16/2020	8/13/2020	28	4232
R/C COR 1	Railing	9/15/2020	10/13/2020	28	4105
R/C EOR	Railing	3/3/2021	3/31/2021	28	4474

Table E.4 Average compressive strength of concrete or FRC railing samples near day of testing

Related test specimen	Concrete placement location	Cast date	Test date	Age (days)	Avg. compressive strength (psi)
FRC COR 1	Railing	5/4/2020	9/2/2020	121	5986
FRC COR 2	Railing	11/9/2020	1/6/2021	58	4067
FRC EOR	Railing	1/21/2021	2/23/2021	33	3564
R/C COR 1	Railing	7/16/2020	10/30/2020	106	4972
R/C COR 1	Railing	9/15/2020	12/9/2020	85	5724
R/C EOR	Railing	3/3/2021	4/6/2021	34	4799

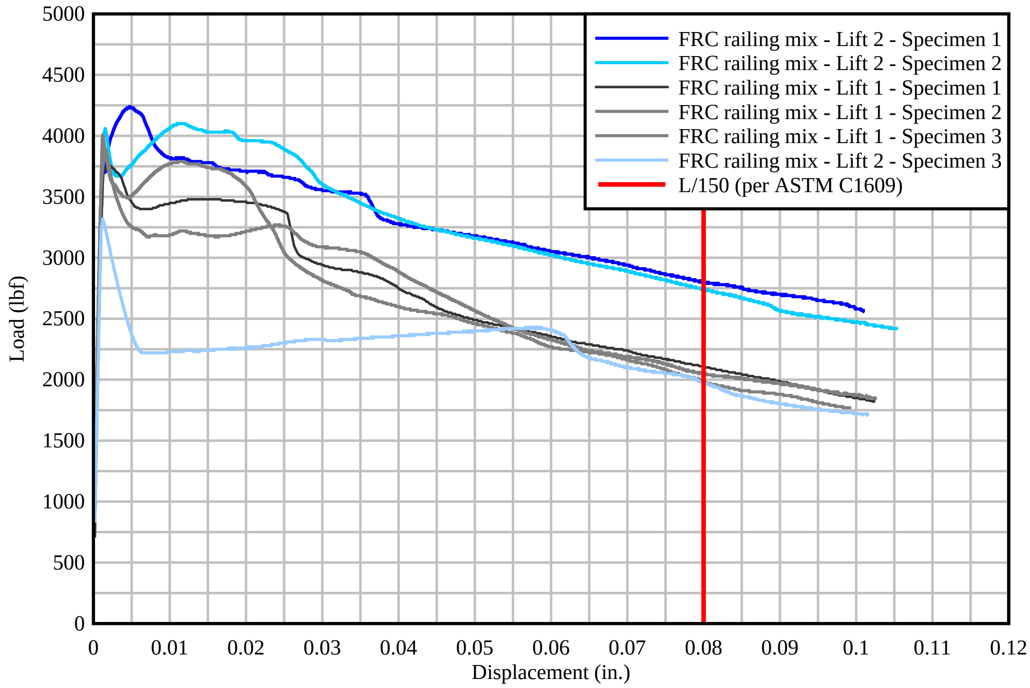

Figure E.1 ASTM C1609 flexural test results for FRC EOR mixture samples (using Sika hooked-end steel fibers at 1.0% fiber volume, mixture no. 13)

APPENDIX F
PENDULUM IMPACTOR FABRICATION DRAWINGS

Presented in this appendix are fabrication drawings of the pendulum impactor, consisting of three main components: (1) steel hanger frame, (2) concrete back block, and (3) aluminum front nose. The back block was designed as a rebar-reinforced concrete block (with approximately 500-lb of adjustable/removable steel weight plates) and was connected to a previously constructed steel hanger frame. The concrete back block contains steel guide tubes embedded within the concrete to allow the crushable front nose to telescope during a pendulum impact test. The front nose was made of high strength aluminum (6061 T6) and includes FRP spacer plates (which were placed between each aluminum honeycomb cartridge). The aluminum honeycomb cartridges (and their sizes) are also included in this drawing set.

After completing the fabrication process of the pendulum impactor, the main components of the impactor were weighed, and it was determined that the (measured) total weight of the impactor is 10,333 lb (333 lb greater than the design), with the steel hanger frame and concrete back block weighing 9850 lb and the front nose (including FRP spacer plates) weighing 483 lb.

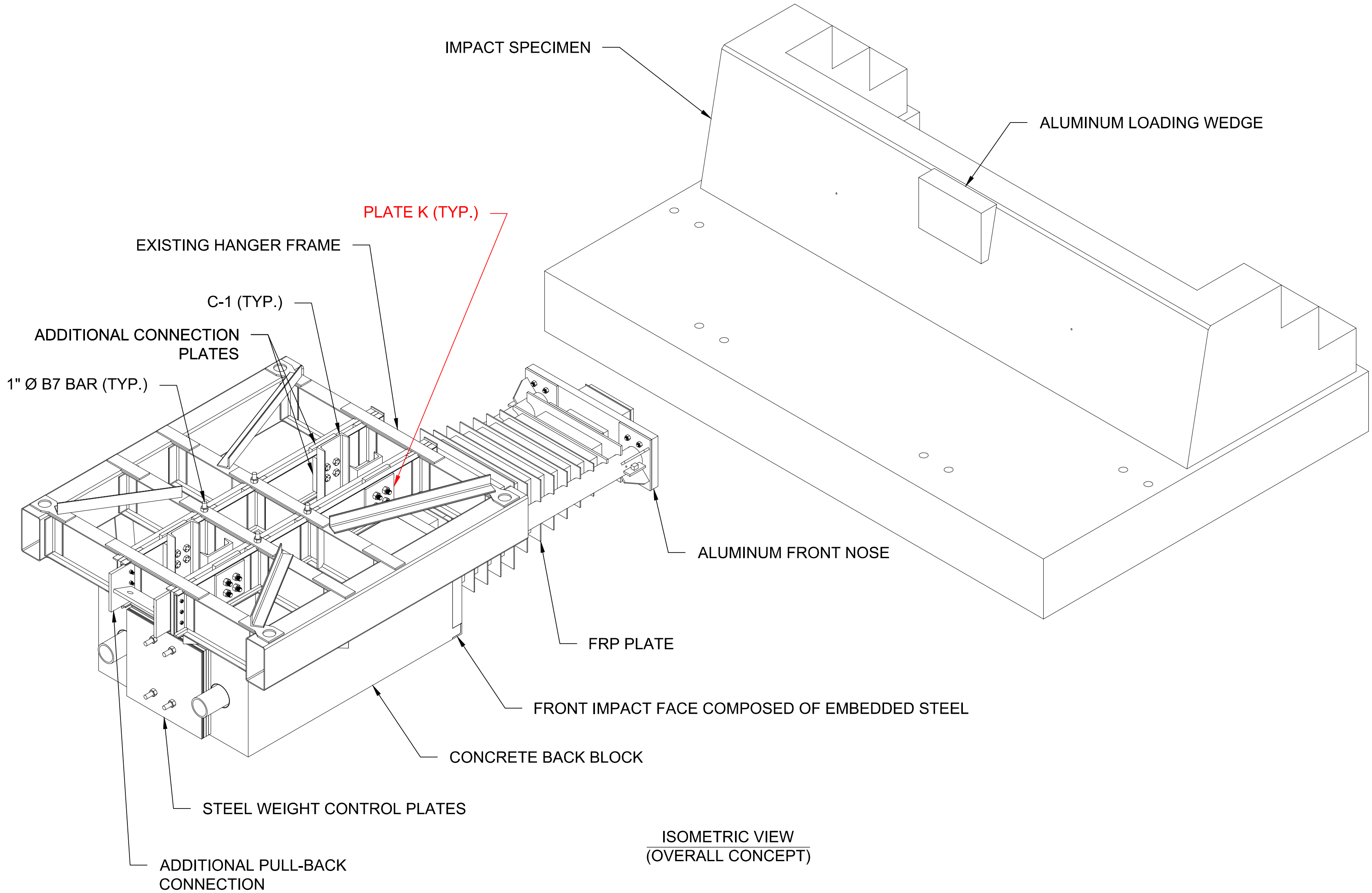

ISOMETRIC VIEW
(OVERALL CONCEPT)

Fiber-Reinforced Concrete Traffic Railings for Impact Loading				*Revisions:*	PLATE K ADDED	
Pendulum impactor	*2019-10-09*	*University of Florida*	*Sheet 01 of 38*			

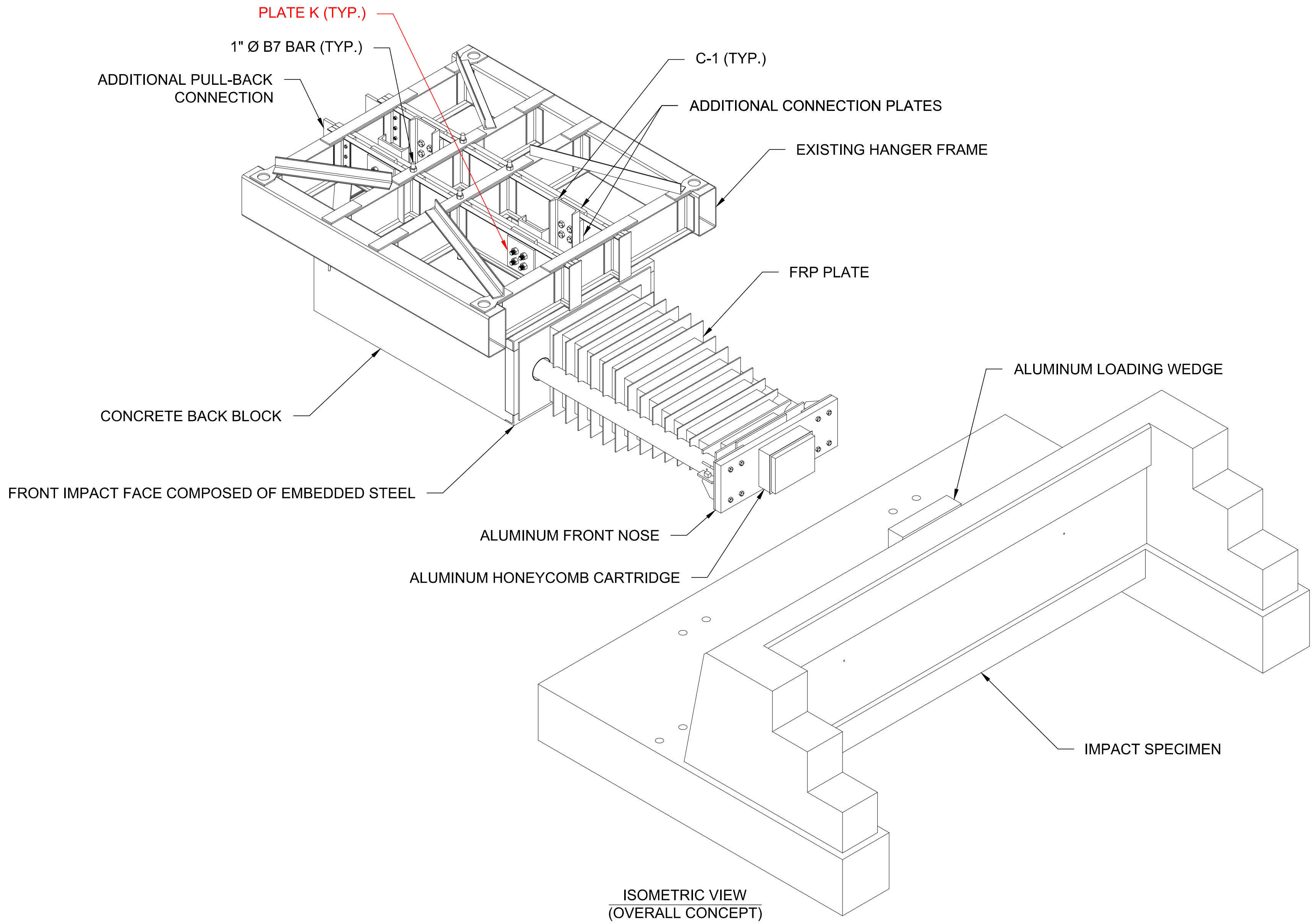

ISOMETRIC VIEW
(OVERALL CONCEPT)

Fiber-Reinforced Concrete Traffic Railings for Impact Loading				*Revisions:*	PLATE K ADDED
Pendulum impactor	*2019-10-09*	*University of Florida*	*Sheet 02 of 38*		

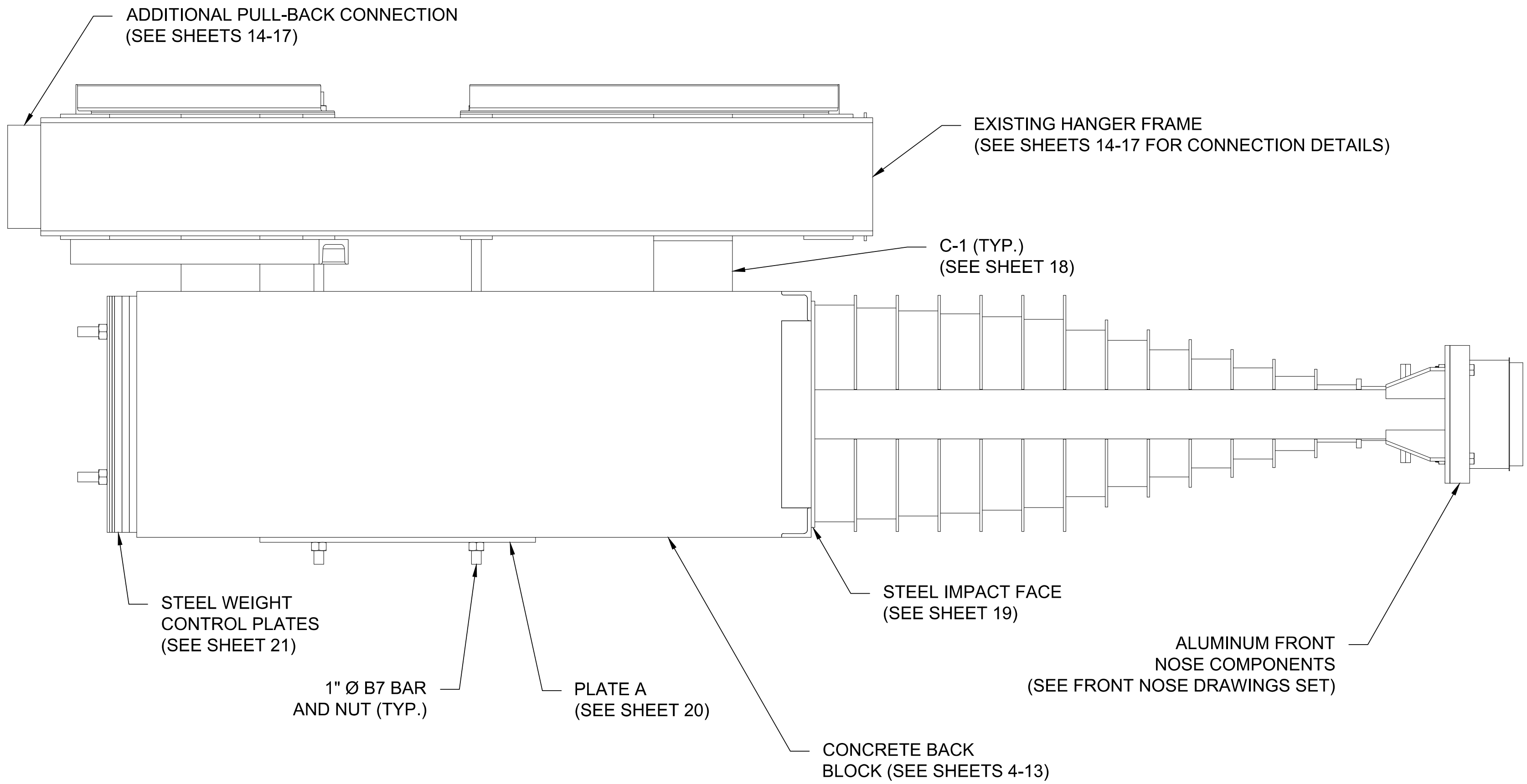

SIDE ELEVATION VIEW

Fiber-Reinforced Concrete Traffic Railings for Impact Loading				*Revisions:*	
Pendulum impactor	*2019-09-25*	*University of Florida*	*Sheet 03 of 38*		

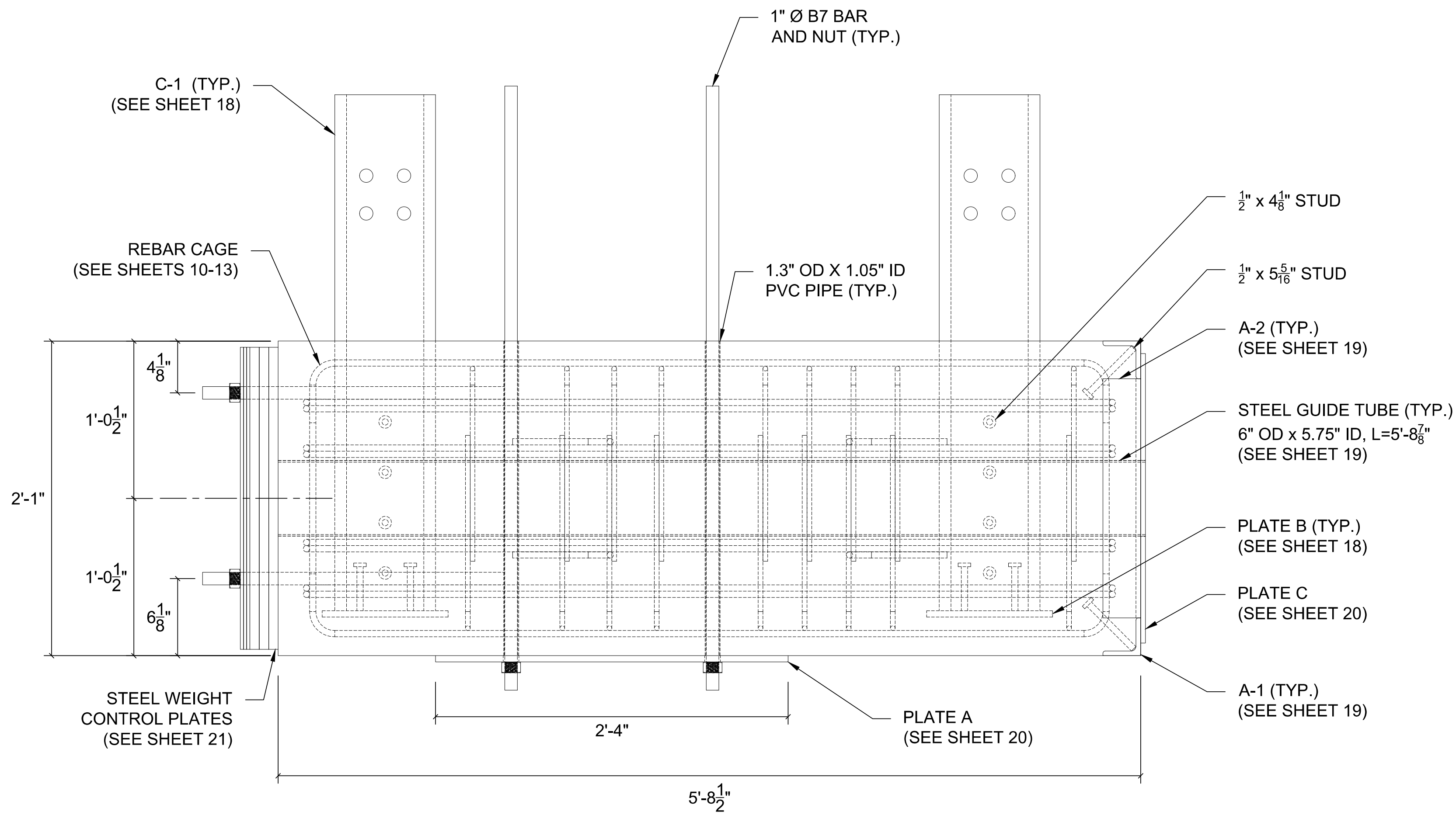

SIDE ELEVATION VIEW
(BACK BLOCK COMPONENTS)

Fiber-Reinforced Concrete Traffic Railings for Impact Loading				*Revisions:*	STUD LENGTH CHANGE:	$3\frac{1}{2}$" LENGTH TO $4\frac{1}{8}$" LENGTH
Pendulum impactor	*2019-09-25*	*University of Florida*	*Sheet 04 of 38*			5" LENGTH TO $5\frac{5}{16}$" LENGTH

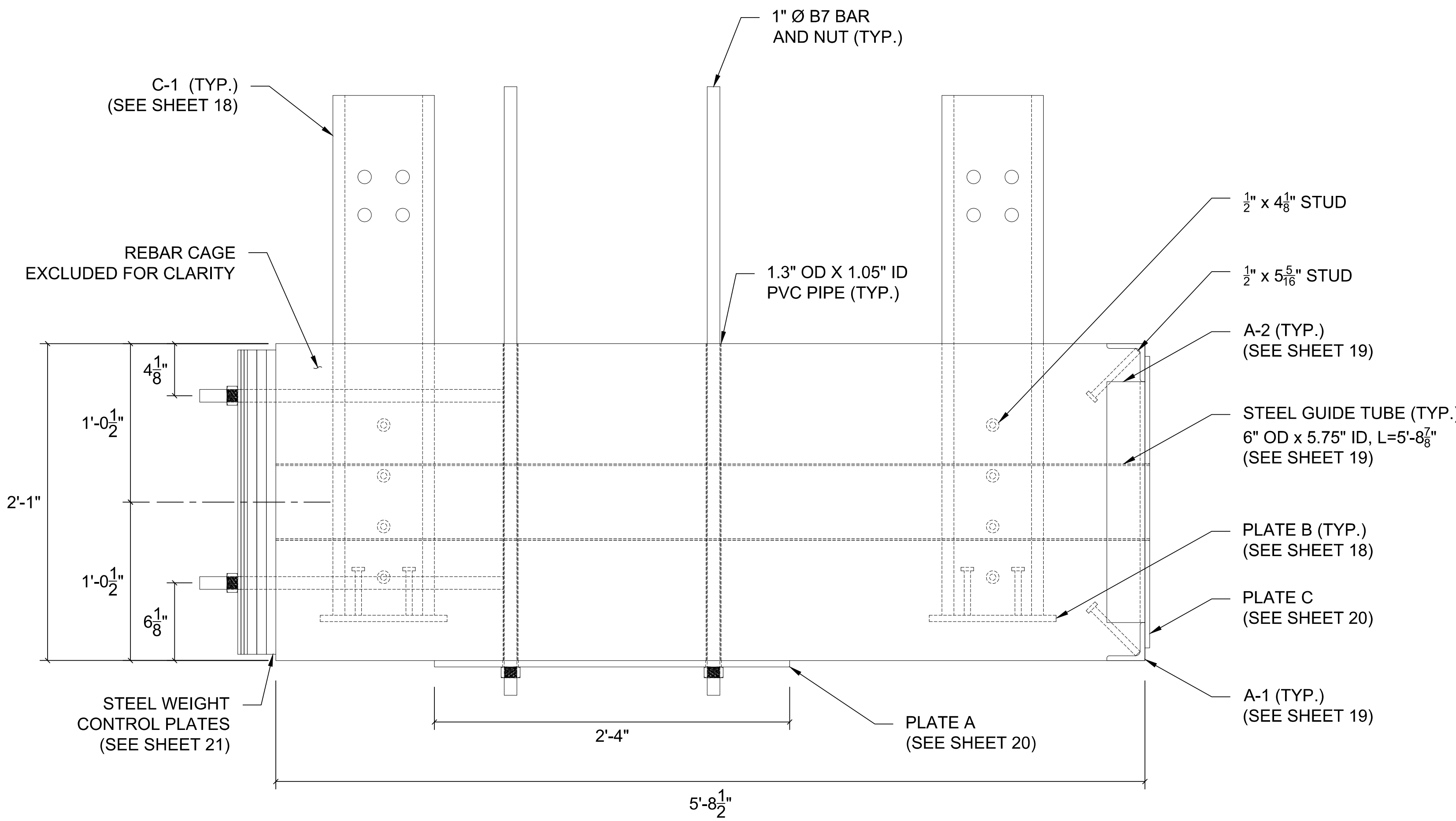

SIDE ELEVATION VIEW
(BACK BLOCK COMPONENTS, REBAR CAGE EXCLUDED)

Fiber-Reinforced Concrete Traffic Railings for Impact Loading				*Revisions:*		
Pendulum impactor	*2019-09-25*	*University of Florida*	*Sheet 05 of 38*			

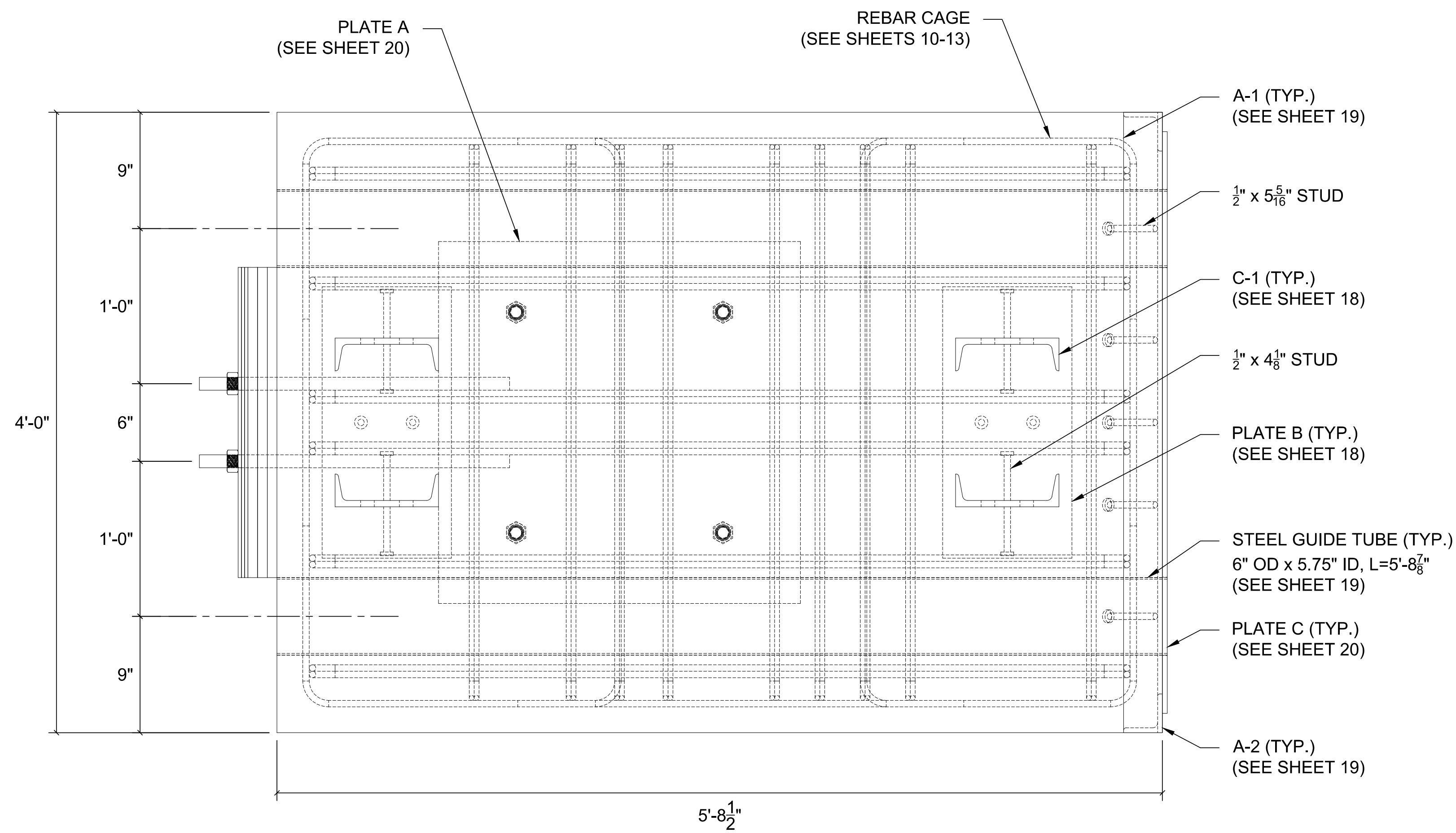

PLAN VIEW
(BACK BLOCK COMPONENTS)

Fiber-Reinforced Concrete Traffic Railings for Impact Loading				*Revisions:*	
Pendulum impactor	*2019-09-25*	*University of Florida*	*Sheet 06 of 38*		

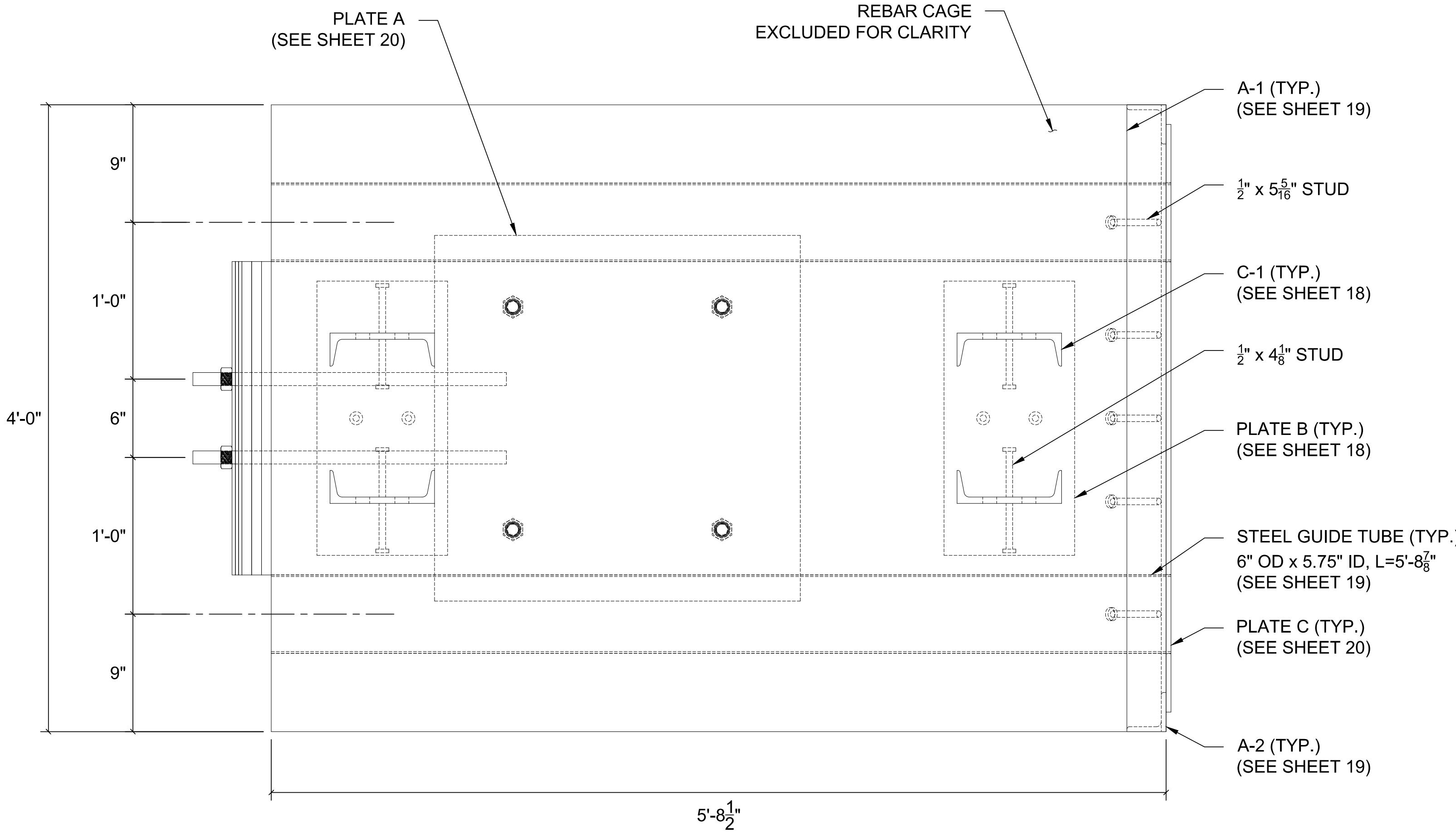

PLAN VIEW
(BACK BLOCK COMPONENTS, REBAR CAGE EXCLUDED)

Fiber-Reinforced Concrete Traffic Railings for Impact Loading				*Revisions:*
Pendulum impactor	*2019-09-25*	*University of Florida*	*Sheet 07 of 38*	

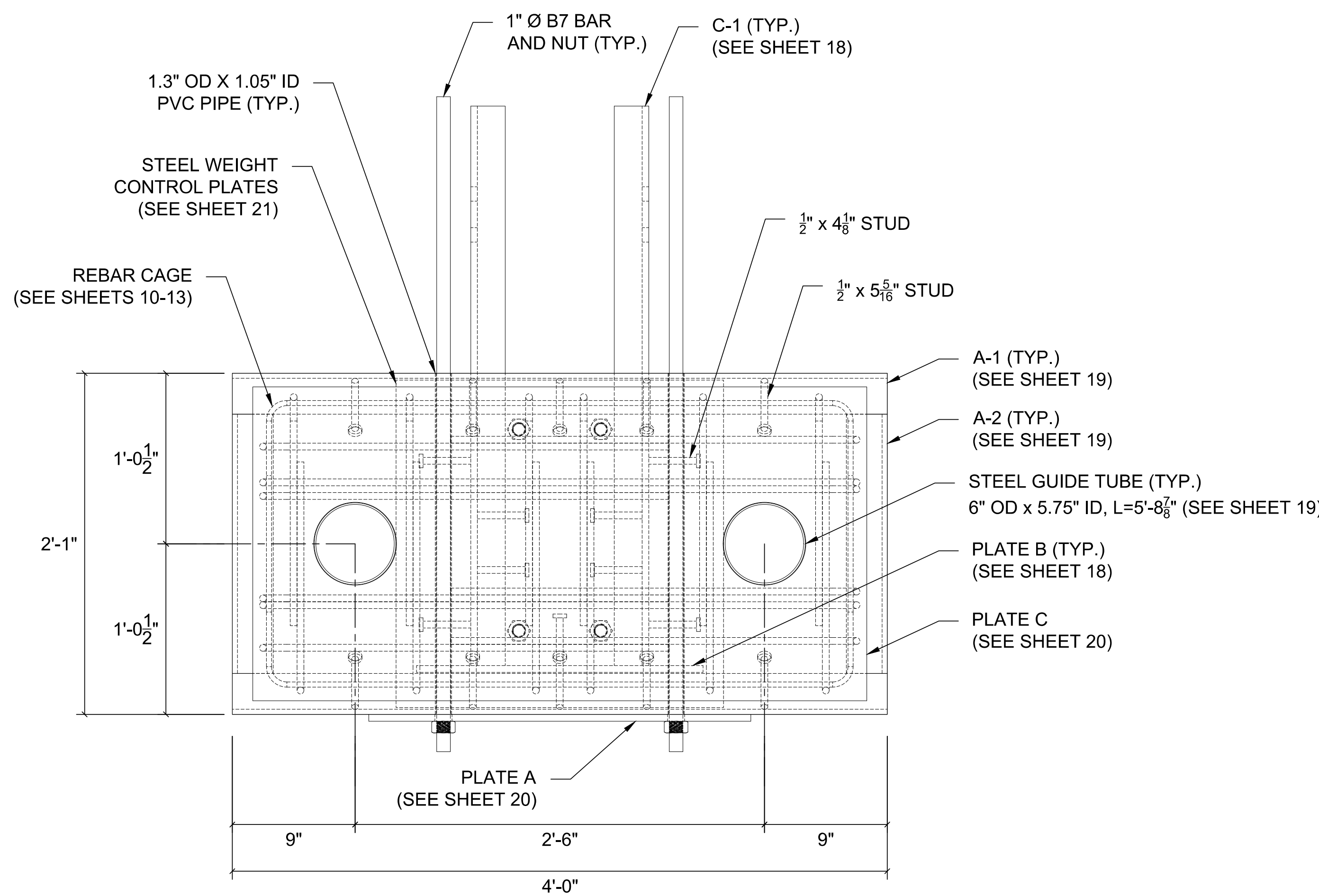

FRONT ELEVATION VIEW
(BACK BLOCK COMPONENTS)

Fiber-Reinforced Concrete Traffic Railings for Impact Loading				*Revisions:*
Pendulum impactor	*2019-09-25*	*University of Florida*	*Sheet 08 of 38*	

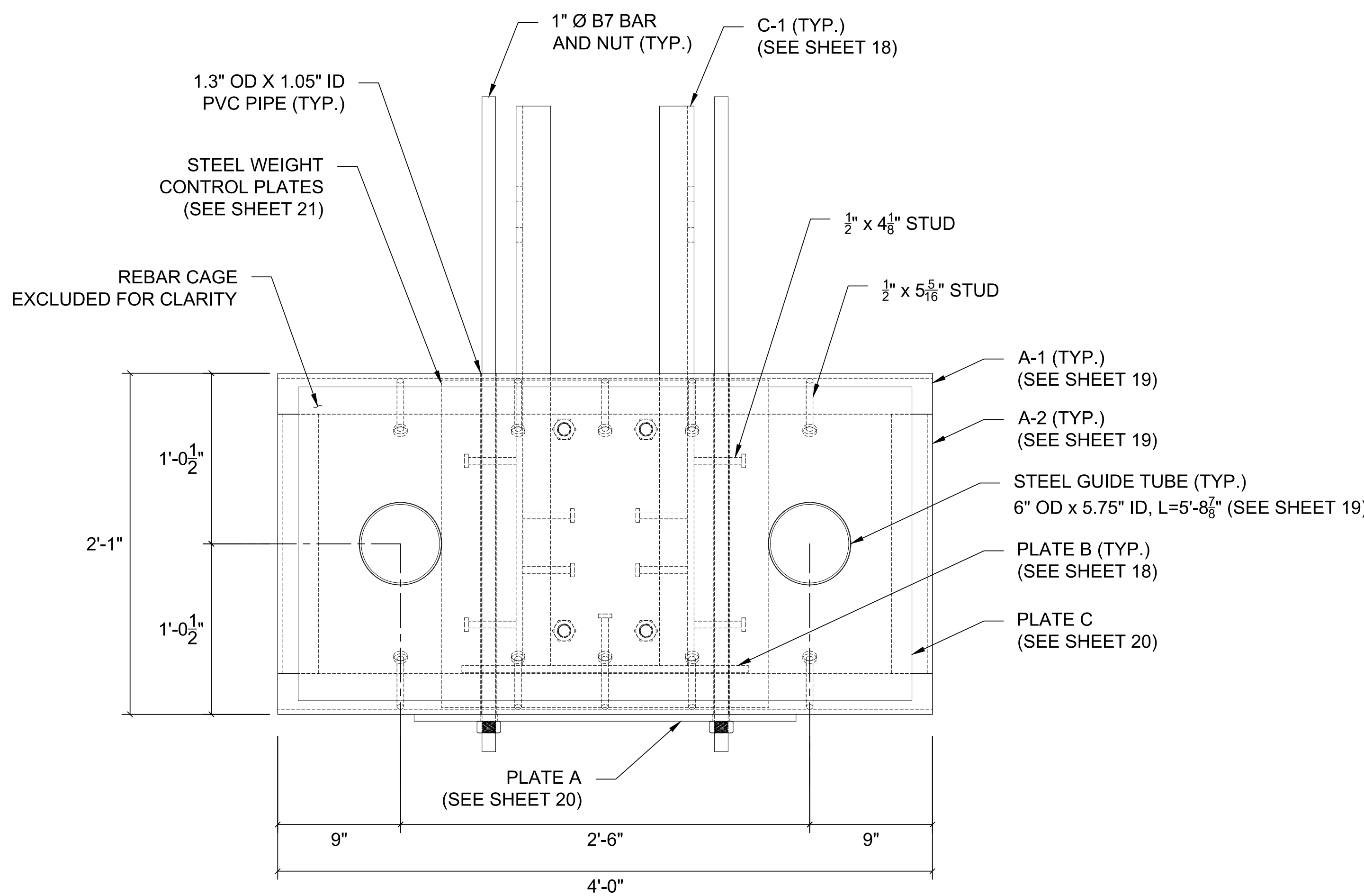

FRONT ELEVATION VIEW
(BACK BLOCK COMPONENTS, REBAR CAGE EXCLUDED)

Fiber-Reinforced Concrete Traffic Railings for Impact Loading				*Revisions:*
Pendulum impactor	*2019-09-25*	*University of Florida*	*Sheet 09 of 38*	

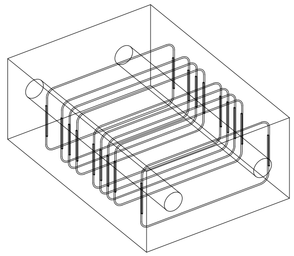

ISOMETRIC VIEW: 3A BARS

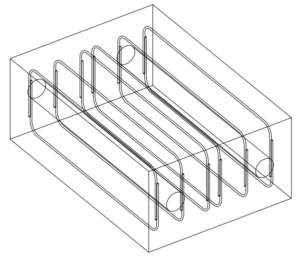

ISOMETRIC VIEW: 4A BARS

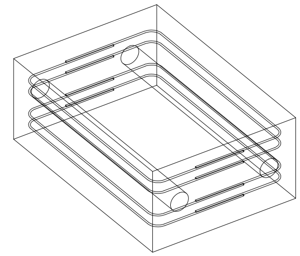

ISOMETRIC VIEW: 4B BARS

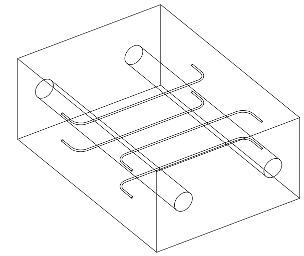

ISOMETRIC VIEW: 4C BARS

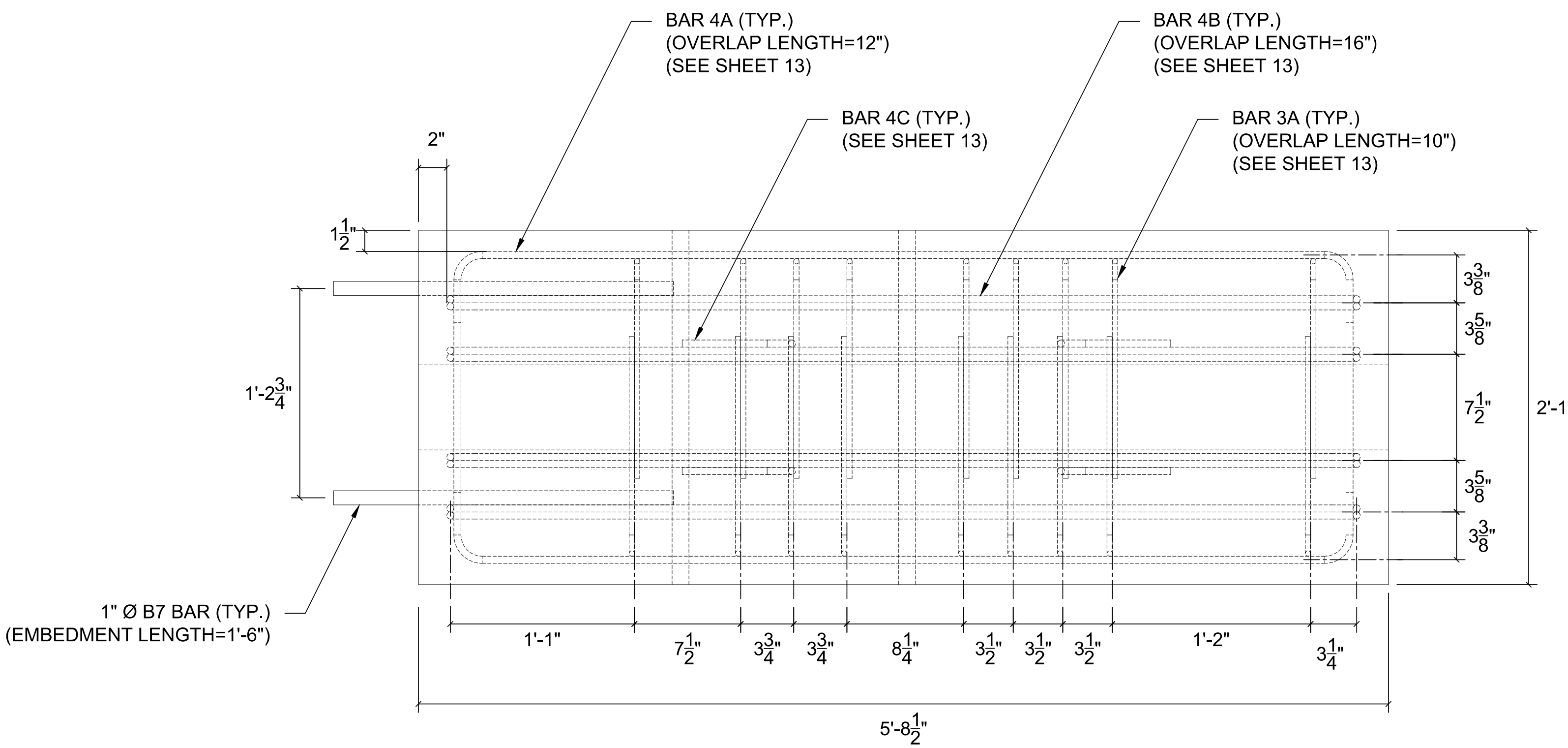

SIDE ELEVATION VIEW
(REBAR CAGE)

Fiber-Reinforced Concrete Traffic Railings for Impact Loading				*Revisions:*
Pendulum impactor	*2019-09-25*	*University of Florida*	*Sheet 10 of 38*	

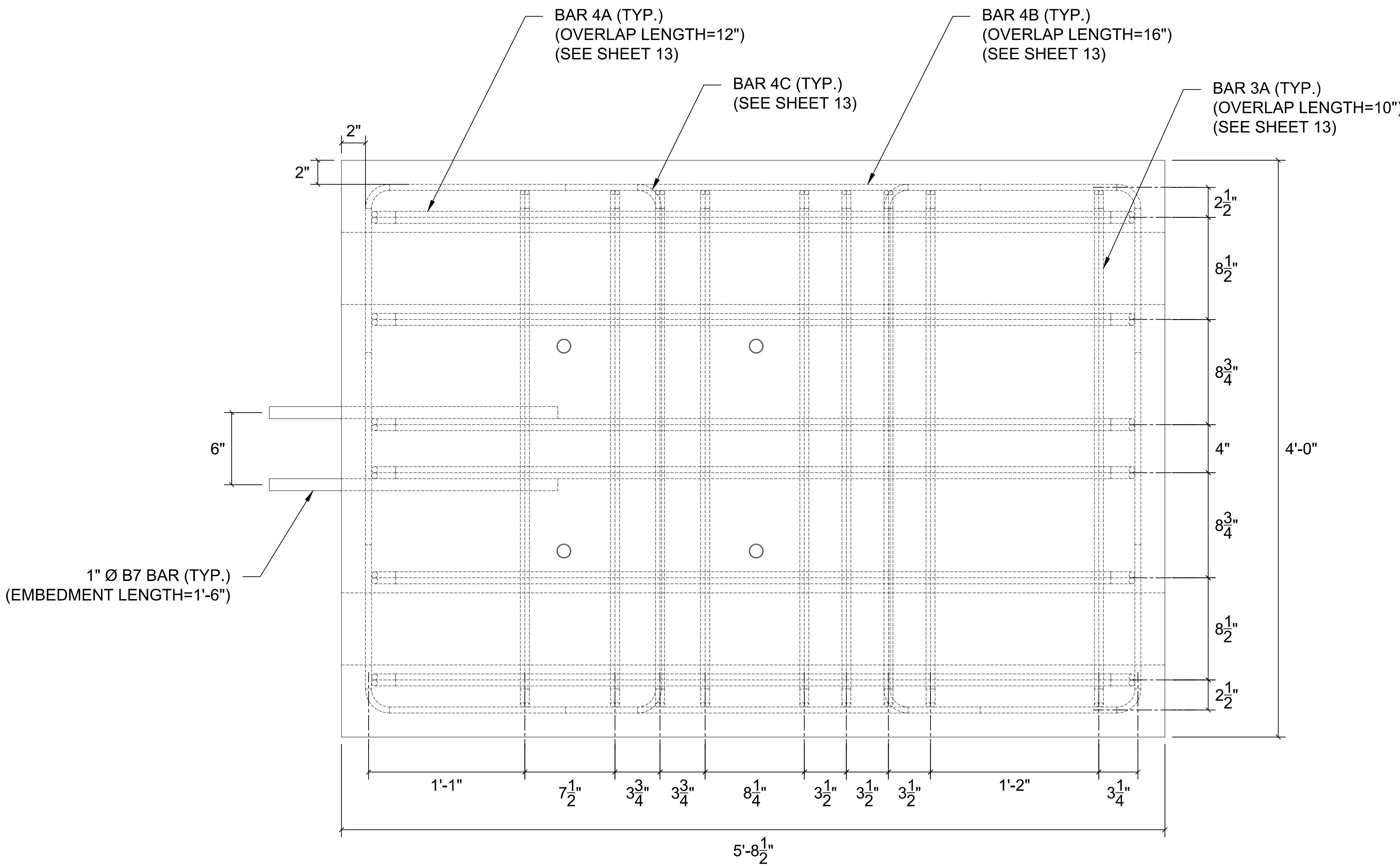

PLAN VIEW
(REBAR CAGE)

Fiber-Reinforced Concrete Traffic Railings for Impact Loading				*Revisions:*
Pendulum impactor	*2019-09-25*	*University of Florida*	*Sheet 11 of 38*	

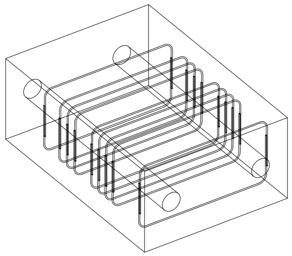

ISOMETRIC VIEW: 3A BARS

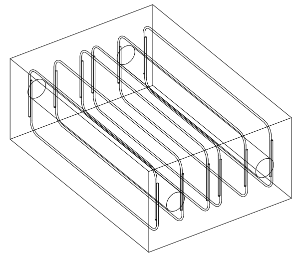

ISOMETRIC VIEW: 4A BARS

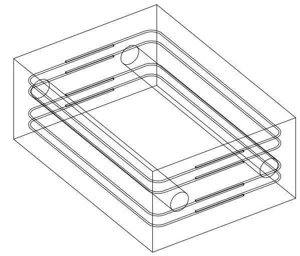

ISOMETRIC VIEW: 4B BARS

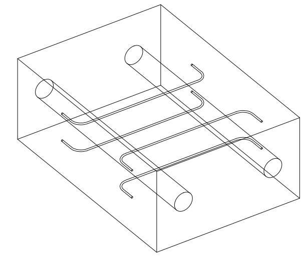

ISOMETRIC VIEW: 4C BARS

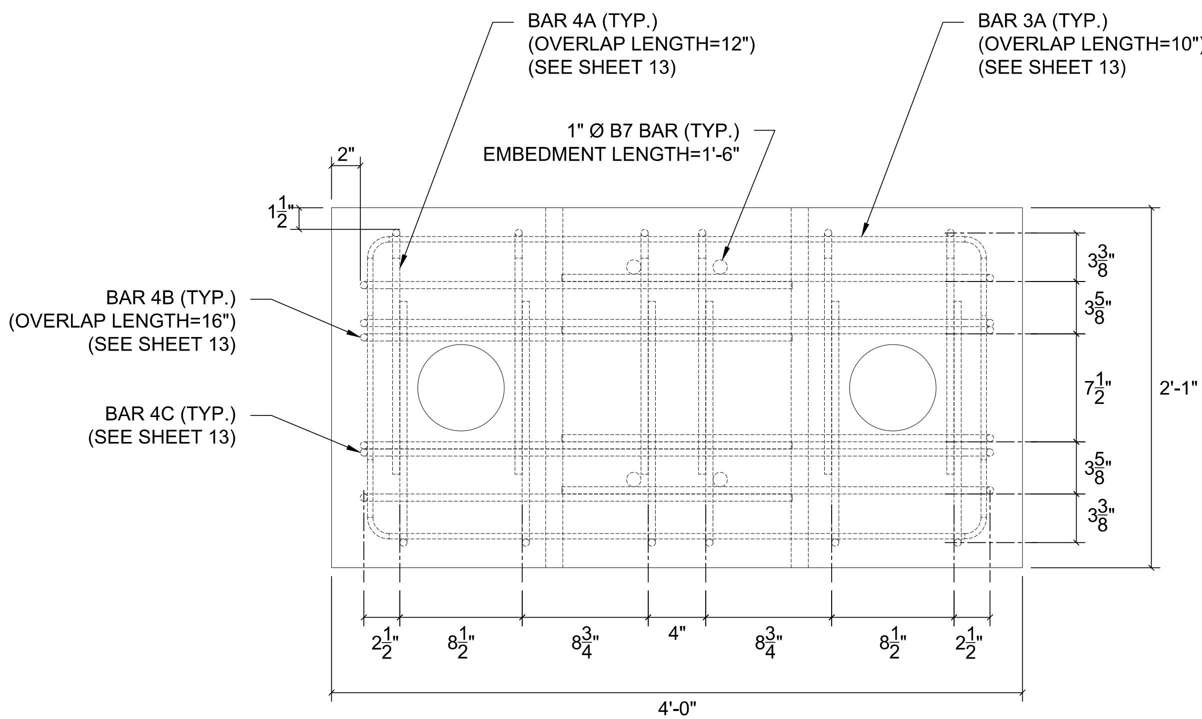

FRONT ELEVATION VIEW
(REBAR CAGE)

Fiber-Reinforced Concrete Traffic Railings for Impact Loading				*Revisions:*
Pendulum impactor	*2019-09-25*	*University of Florida*	*Sheet 12 of 38*	

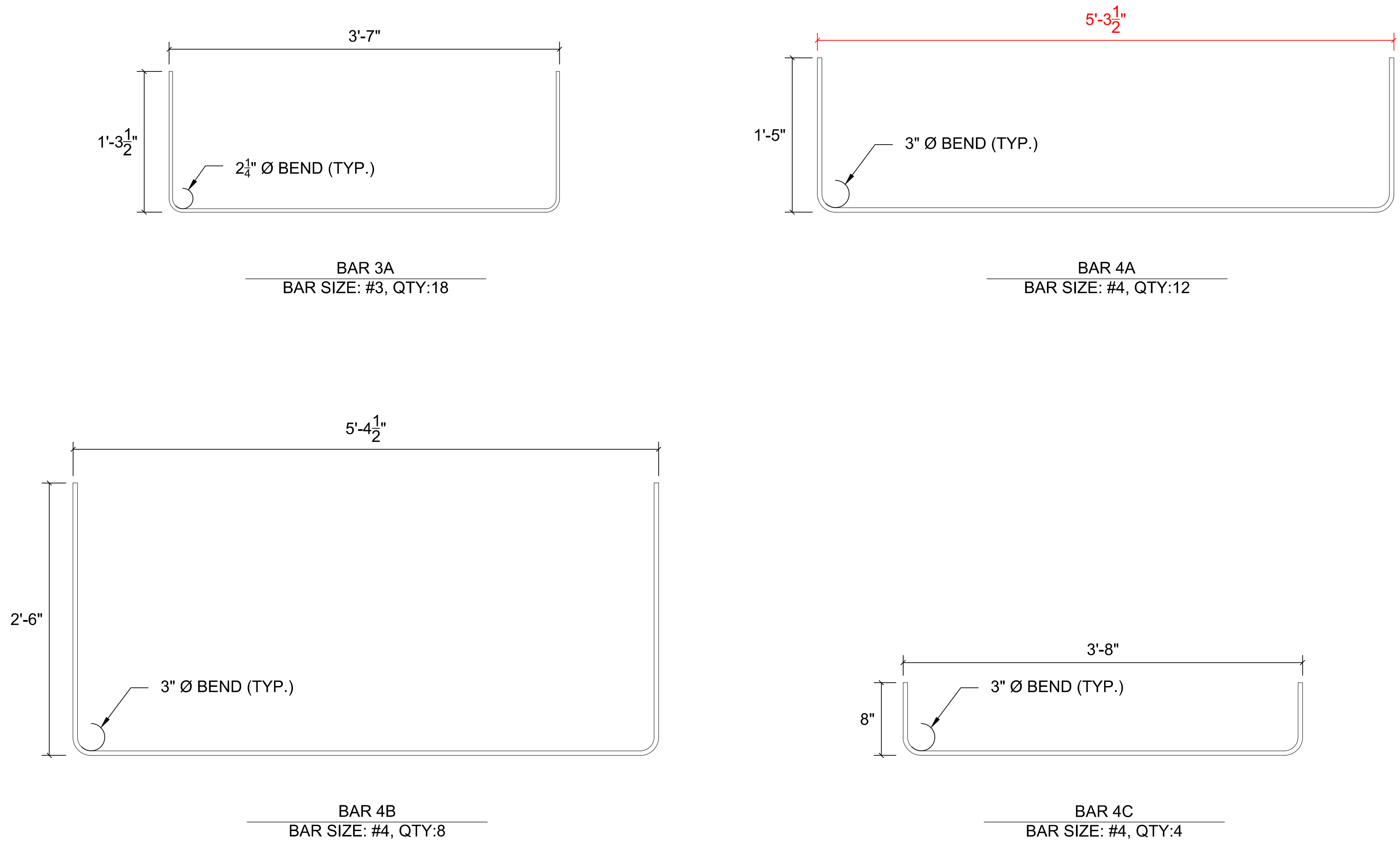

Fiber-Reinforced Concrete Traffic Railings for Impact Loading				*Revisions:*	BAR 4A LENGTH CORRECTED
Pendulum impactor	*2019-09-25*	*University of Florida*	*Sheet 13 of 38*		

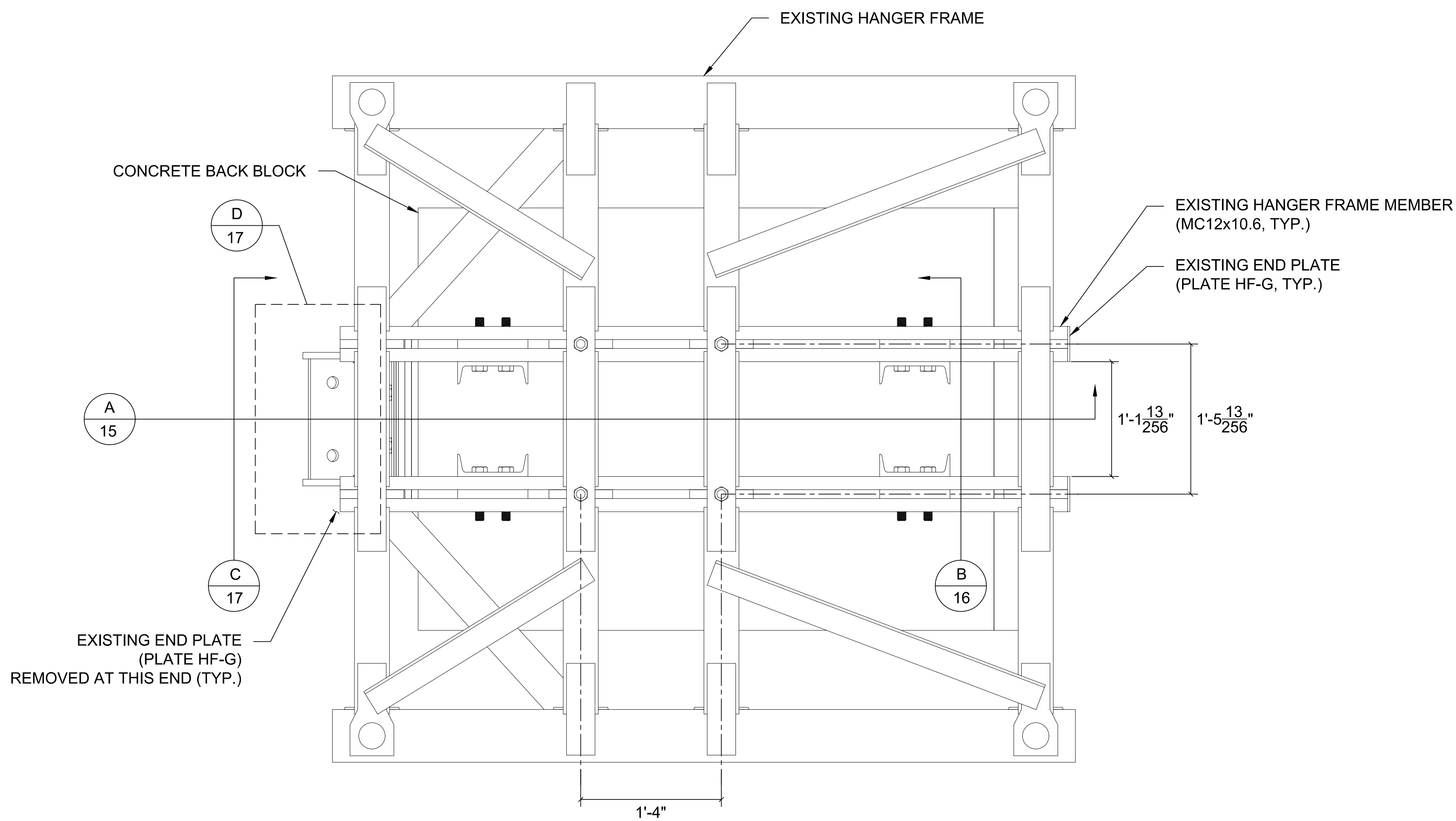

PLAN VIEW
(BACK BLOCK CONNECTION TO HANGER FRAME)

Fiber-Reinforced Concrete Traffic Railings for Impact Loading				*Revisions:*
Pendulum impactor	*2019-09-25*	*University of Florida*	*Sheet 14 of 38*	

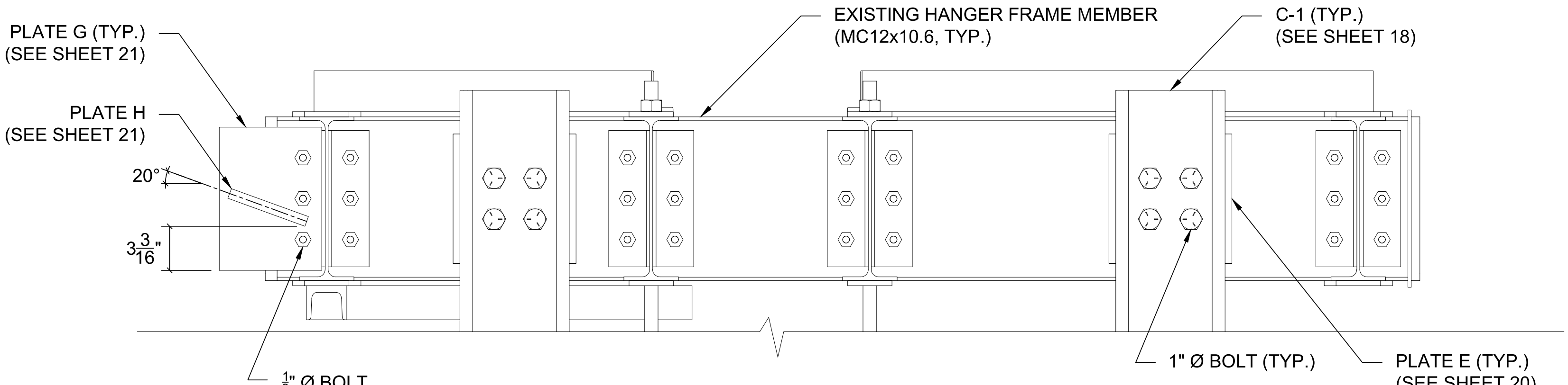

A-15: SIDE ELEVATION VIEW WITH C-1 ATTACHED
(BACK BLOCK CONNECTION TO HANGER FRAME AND PULL-BACK CONNECTION)

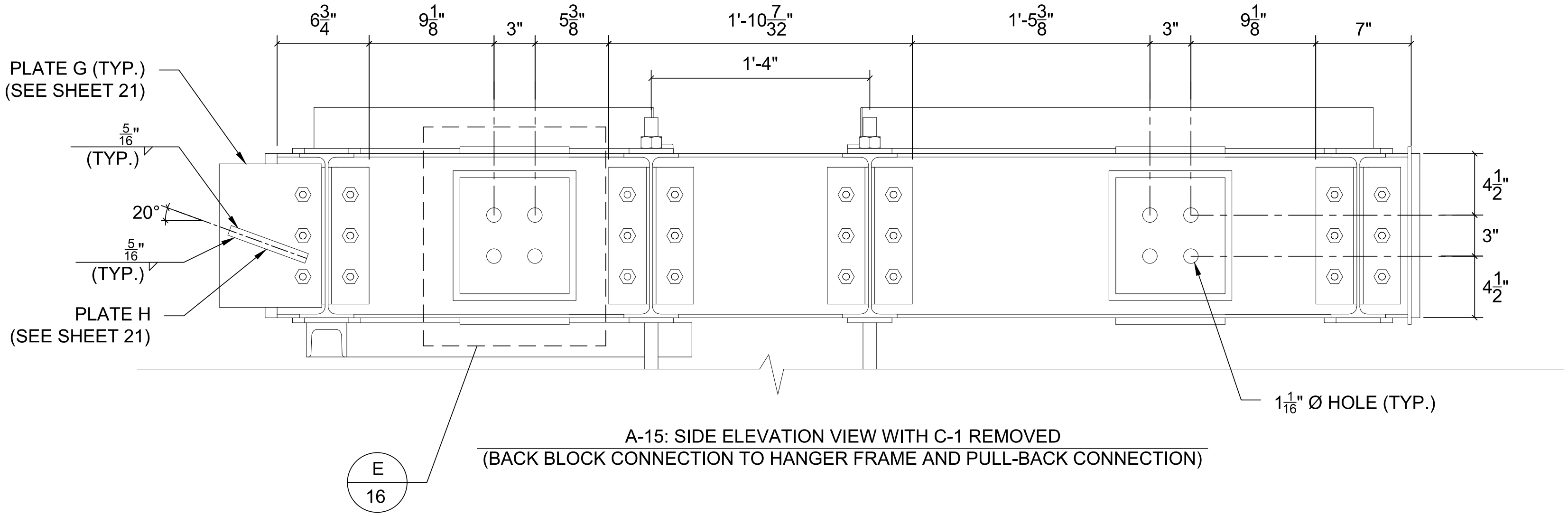

A-15: SIDE ELEVATION VIEW WITH C-1 REMOVED
(BACK BLOCK CONNECTION TO HANGER FRAME AND PULL-BACK CONNECTION)

Fiber-Reinforced Concrete Traffic Railings for Impact Loading				Revisions:
Pendulum impactor	*2019-09-25*	*University of Florida*	*Sheet 15 of 38*	

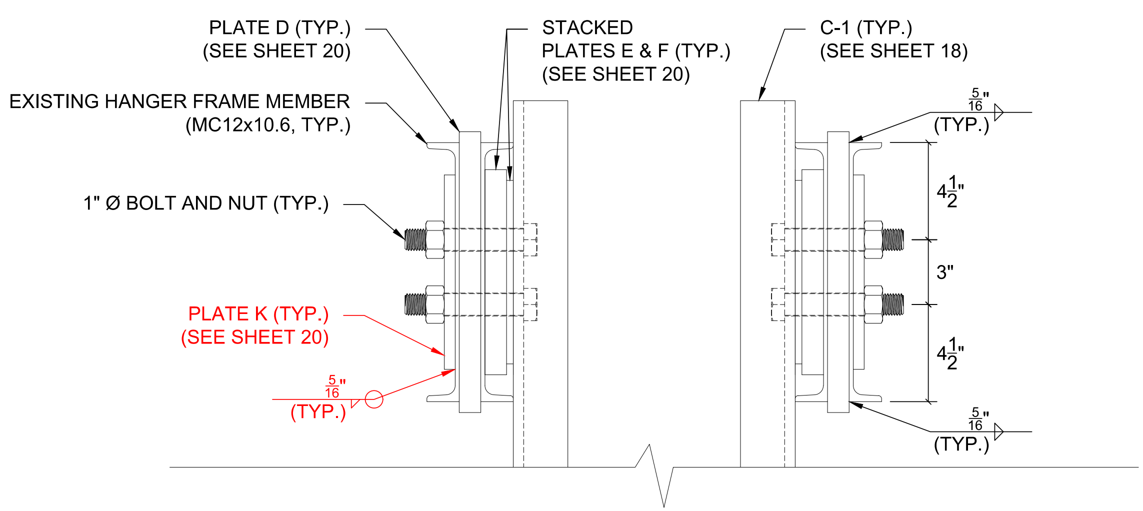

B-16: FRONT ELEVATION VIEW OF CONNECTION
(BACK BLOCK CONNECTION TO HANGER FRAME)

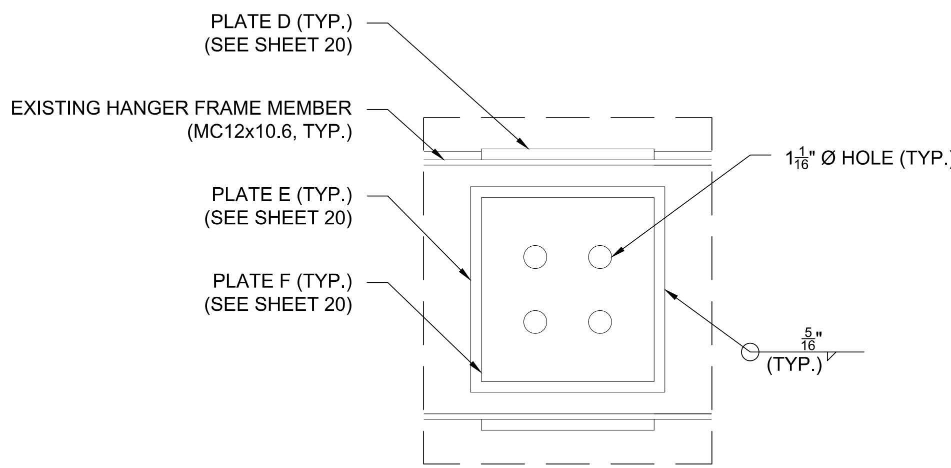

E-16: SIDE ELEVATION VIEW OF CONNECTION PLATES
(BACK BLOCK CONNECTION TO HANGER FRAME)

Fiber-Reinforced Concrete Traffic Railings for Impact Loading				*Revisions:*	PLATE K ADDED
Pendulum impactor	*2019-10-09*	*University of Florida*	*Sheet 16 of 38*		

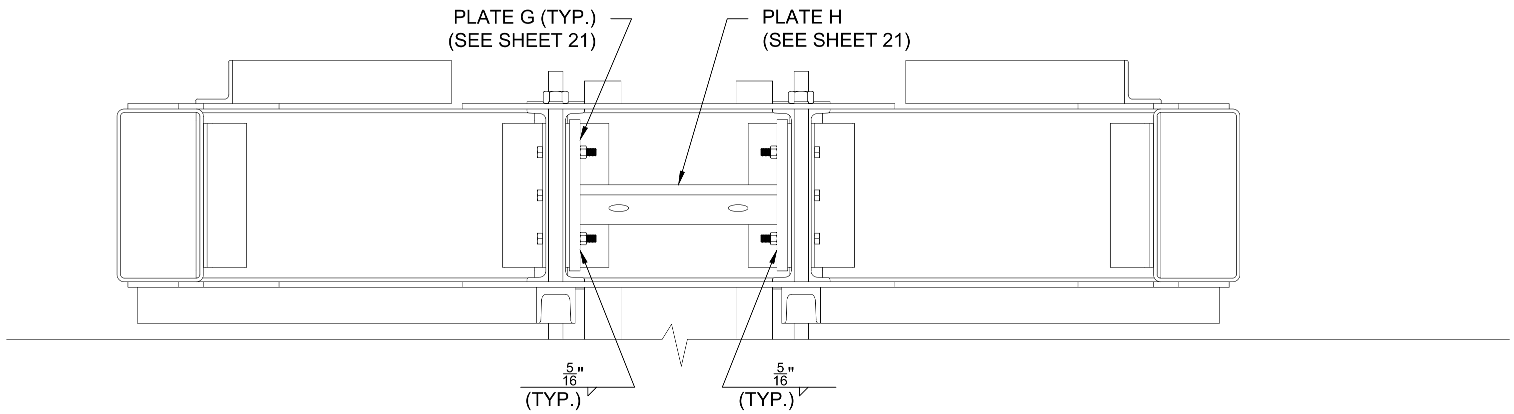

C-17: BACK ELEVATION VIEW OF PULL-BACK CONNECTION

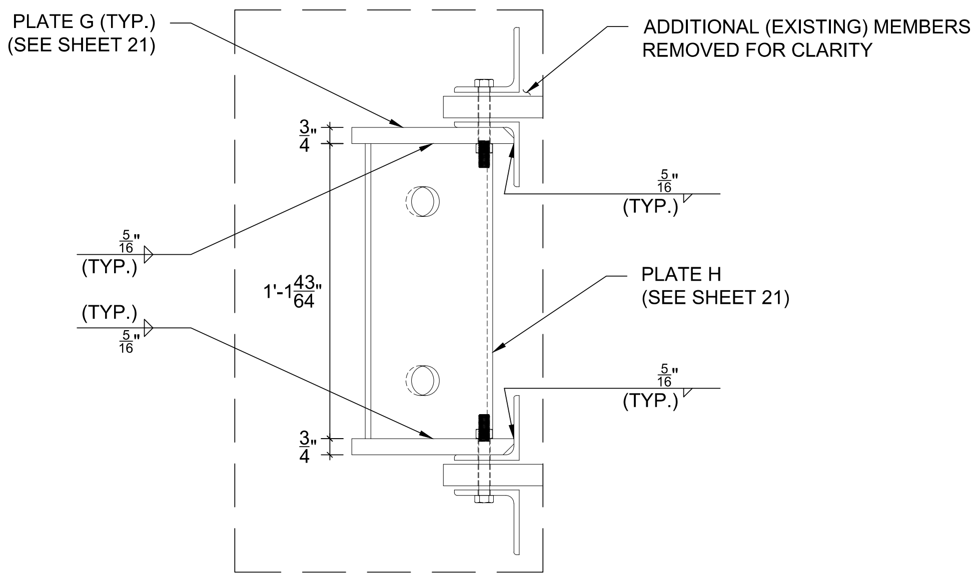

D-17: PLAN VIEW OF PULL-BACK CONNECTION

Fiber-Reinforced Concrete Traffic Railings for Impact Loading				*Revisions:*		
Pendulum impactor	*2019-09-25*	*University of Florida*	*Sheet 17 of 38*			

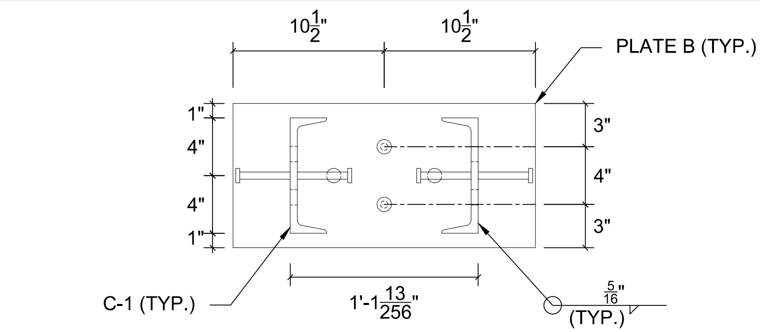

PLAN VIEW
(BACK BLOCK COMPONENTS, C-1 TO PLATE B CONNECTION)

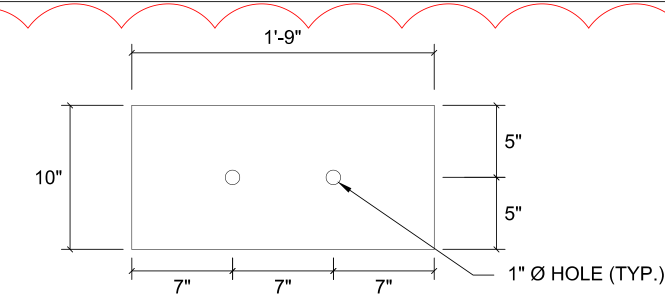

PLATE B
t = ½", A572-50, QTY:2

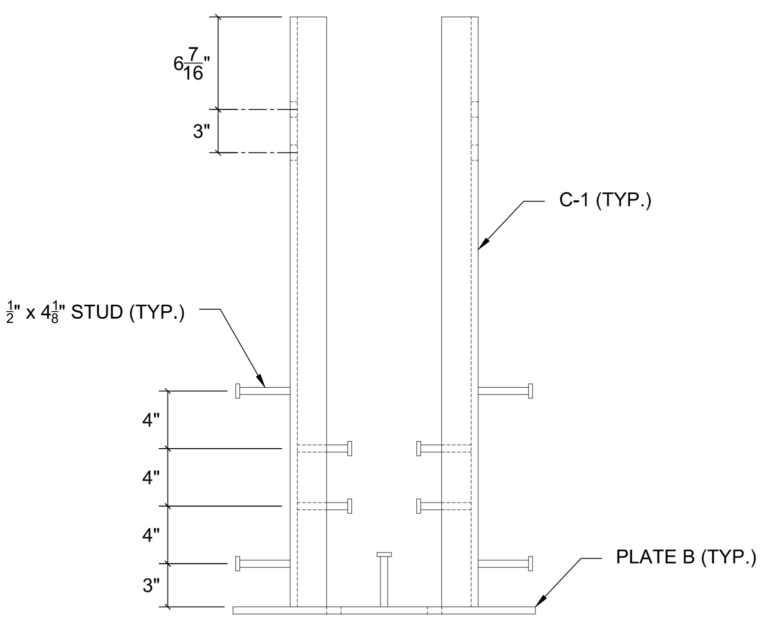

FRONT ELEVATION VIEW
(BACK BLOCK COMPONENTS, C-1 TO PLATE B CONNECTION)

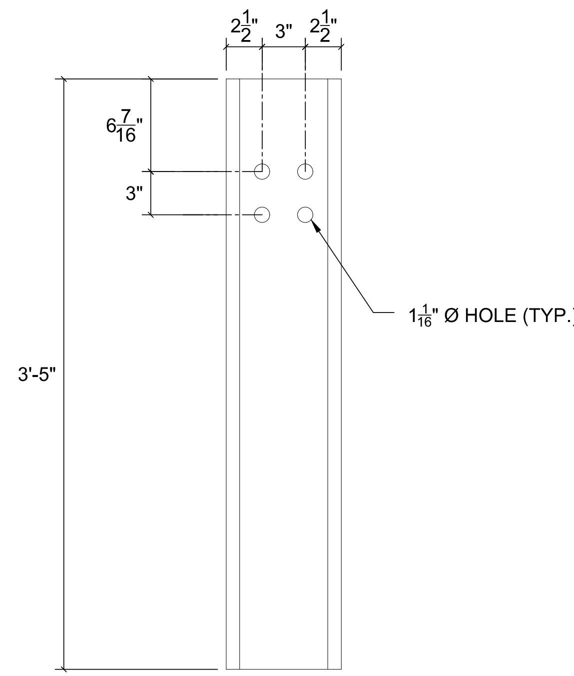

C-1
C8x18.75, A572-50, QTY: 4

Fiber-Reinforced Concrete Traffic Railings for Impact Loading				*Revisions:*	PLATE B: ADDED 1" Ø HOLES
Pendulum impactor	*2019-09-25*	*University of Florida*	*Sheet 18 of 38*		STUD LENGTH CHANGE: 3½" LENGTH TO 4⅛" LENGTH

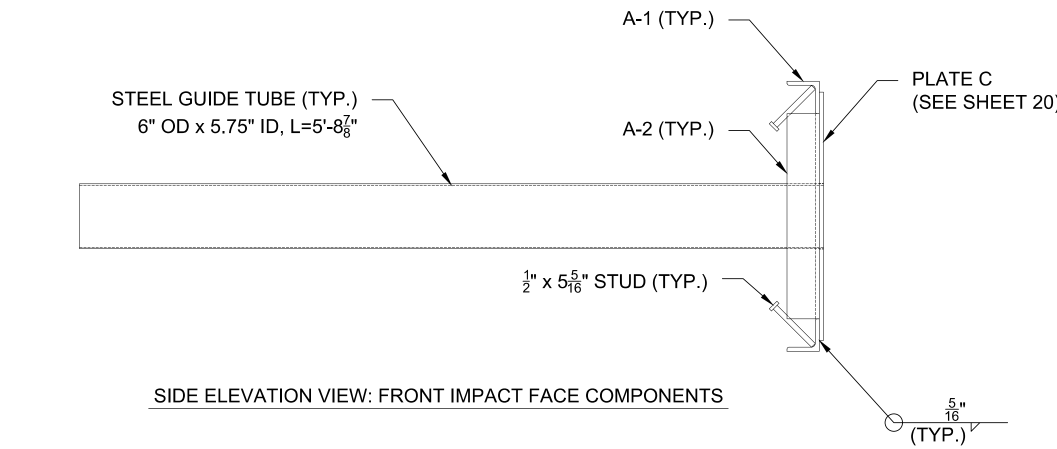

SIDE ELEVATION VIEW: FRONT IMPACT FACE COMPONENTS

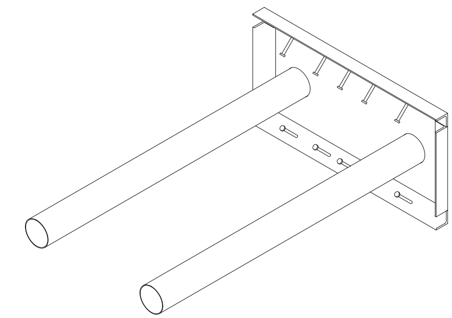

ISOMETRIC VIEW: FRONT IMPACT FACE COMPONENTS

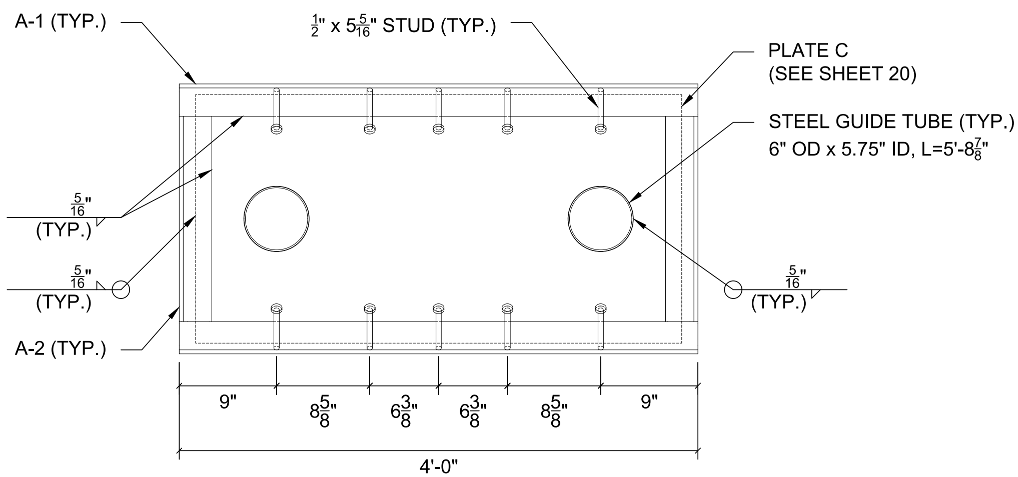

BACK ELEVATION VIEW: FRONT IMPACT FACE COMPONENTS

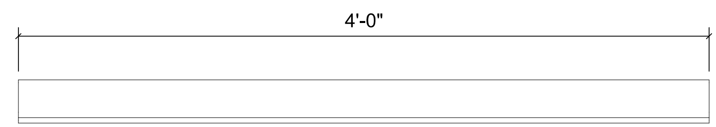

A-1

L3x3x$\frac{3}{8}$, A36, QTY: 2

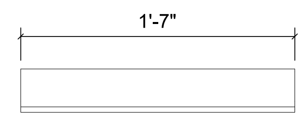

A-2

L3x3x$\frac{3}{8}$, A36, QTY: 2

Fiber-Reinforced Concrete Traffic Railings for Impact Loading				*Revisions:*	STUD LENGTH CHANGE:	5" LENGTH TO 5$\frac{5}{16}$" LENGTH
Pendulum impactor	*2019-09-25*	*University of Florida*	*Sheet 19 of 38*			

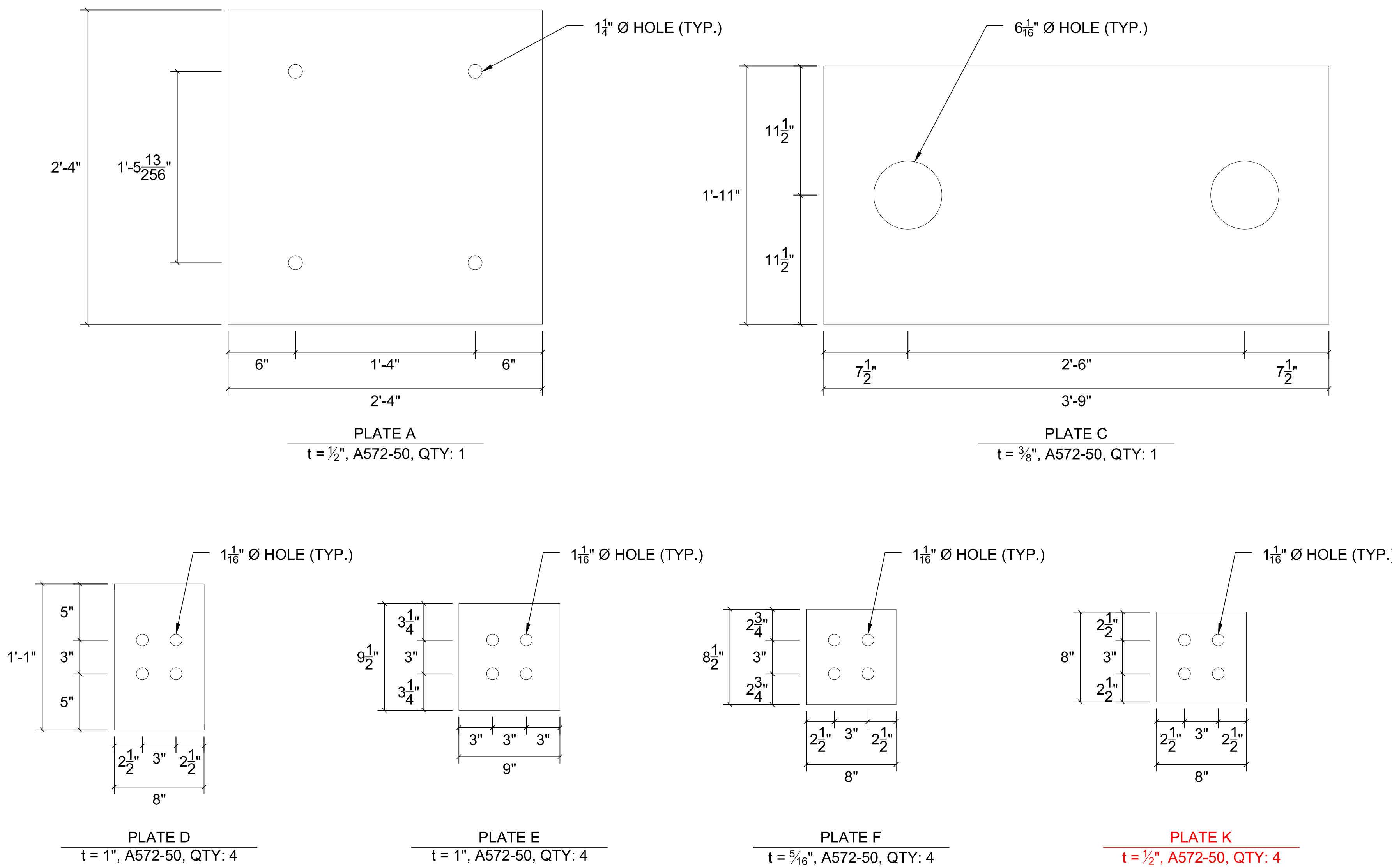

Fiber-Reinforced Concrete Traffic Railings for Impact Loading				*Revisions:*	PLATE K ADDED
Pendulum impactor	*2019-10-09*	*University of Florida*	*Sheet 20 of 38*		

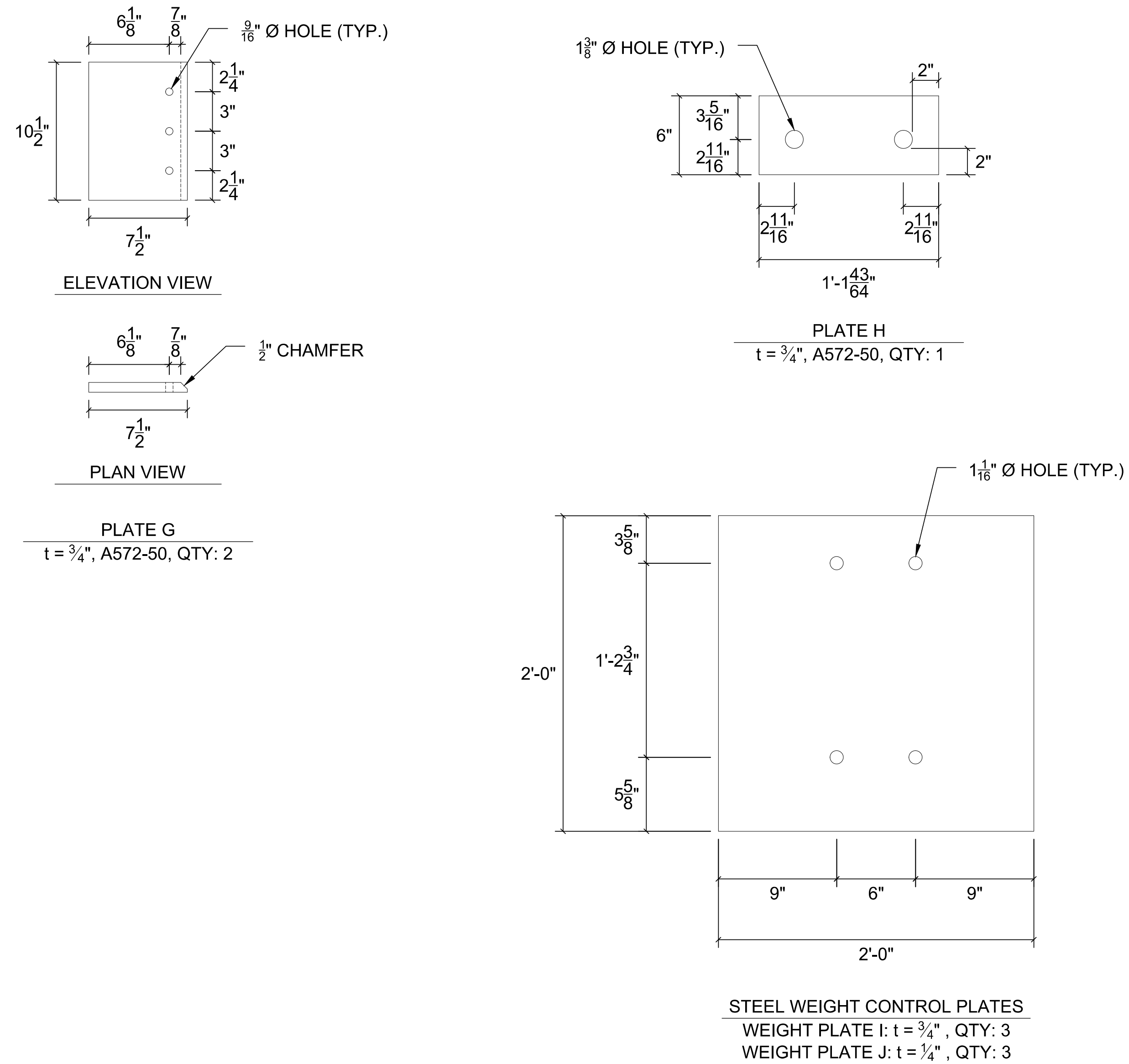

Fiber-Reinforced Concrete Traffic Railings for Impact Loading				*Revisions:*
Pendulum impactor	*2019-09-25*	*University of Florida*	*Sheet 21 of 38*	

SCHEDULE OF PLATES

NAME	QTY	NOTES
PLATE A	1	A572-50
PLATE B	2	A572-50
PLATE C	1	A572-50
PLATE D	4	A572-50
PLATE E	4	A572-50
PLATE F	4	A572-50
PLATE G	2	A572-50
PLATE H	1	A572-50
WEIGHT PLATE I	3	A36, t = ¾"
WEIGHT PLATE J	3	A36, t = ¼"
Plate K	4	A572-50

Fiber-Reinforced Concrete Traffic Railings for Impact Loading				*Revisions:*
Pendulum impactor	*2019-09-25*	*University of Florida*	*Sheet 22 of 38*	

SCHEDULE OF MEMBERS

NAME	SIZE	LENGTH	QTY	TOTAL LENGTH	NOTES
A-1	L3x3x3/8	4'-0"	2	8'-0"	A36
A-2	L3x3x3/8	1'-7"	2	3'-2"	A36
C-1	C8x18.75	3'-5"	4	13'-8"	A572-50
GUIDE TUBE	6" OD x 5.75" ID	5'-8 7/8"	2	11'-9 3/4"	304
B7 ROD	1 Ø	4'-0"	4	16'-0"	A193 GRADE B7
B7 ROD	1 Ø	2'-0"	4	8'-0"	A193 GRADE B7
PVC PIPE	1.3" OD X 1.05" ID	2'-1"	4	8'-4"	PVC
BOLTS	1 Ø	5 1/2"	16	-	A325
BOLTS	1/2" Ø	3 3/4"	6	-	A325
NUTS	1 Ø	-	28	-	A563
NUTS	1/2" Ø	-	6	-	A563
STUDS	1/2" Ø	4 1/8"	20	-	-
STUDS	1/2" Ø	5 5/16"	10	-	-

Fiber-Reinforced Concrete Traffic Railings for Impact Loading				*Revisions:*
Pendulum impactor	*2019-09-25*	*University of Florida*	*Sheet 23 of 38*	

REINFORCING BAR SCHEDULE	
NAME	QTY
BAR 3A	18
BAR 4A	12
BAR 4B	8
BAR 4C	4

Fiber-Reinforced Concrete Traffic Railings for Impact Loading

Pendulum impactor	*2019-09-25*	*University of Florida*	*Sheet 24 of 38*	*Revisions:*

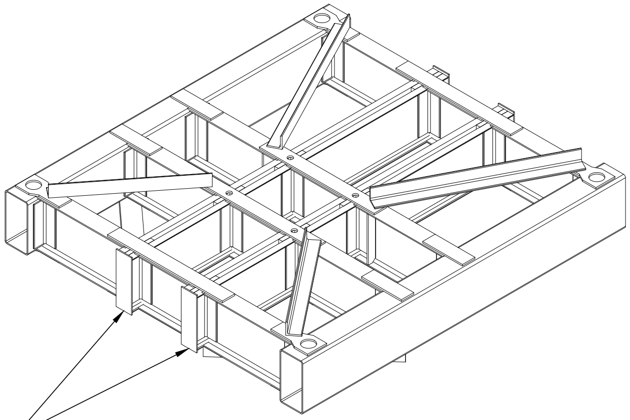

BACK ISOMETRIC VIEW
(FABRICATION SEQUENCE)

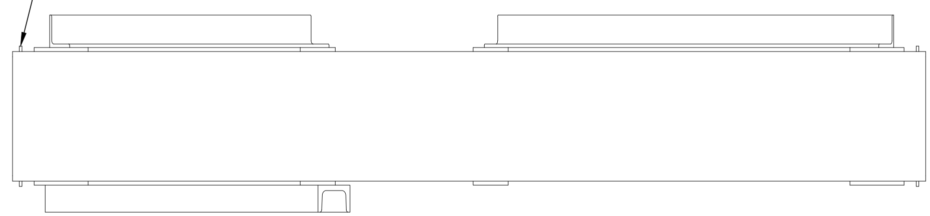

SIDE ELEVATION VIEW
(FABRICATION SEQUENCE)

FABRICATION SEQUENCE STEP 0:

- Existing hanger frame to be used for pendulum impactor
- SEE SHEET 14-17 for hanger frame connection details

Fiber-Reinforced Concrete Traffic Railings for Impact Loading				*Revisions:*
Pendulum impactor	*2019-09-25*	*University of Florida*	*Sheet 25 of 38*	

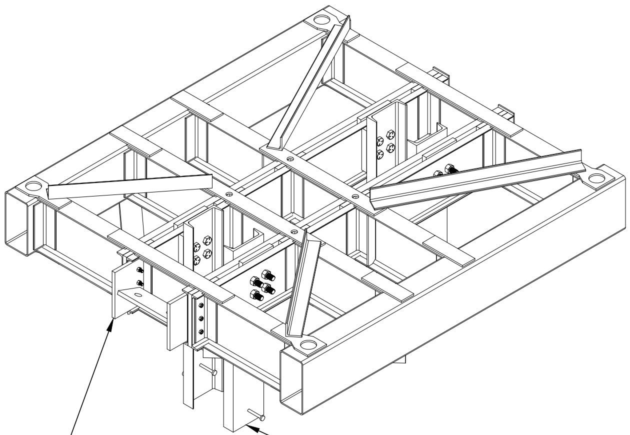

BACK ISOMETRIC VIEW
(FABRICATION SEQUENCE)

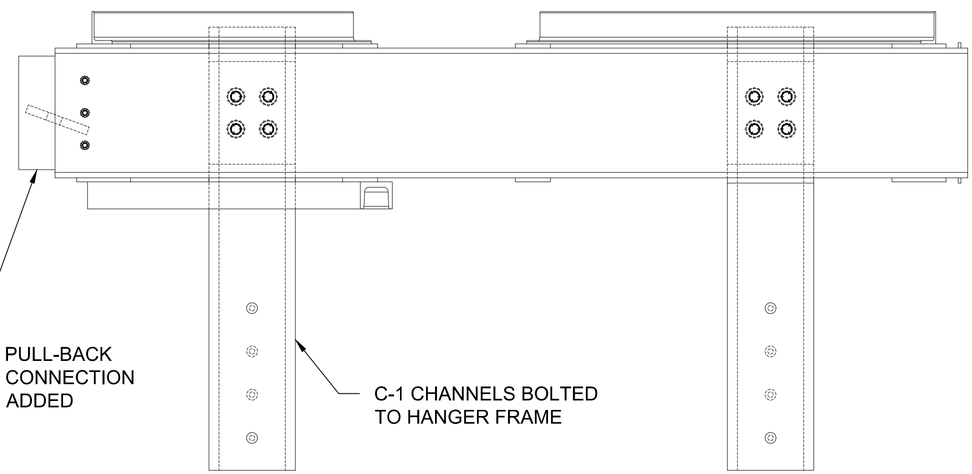

SIDE ELEVATION VIEW
(FABRICATION SEQUENCE)

FABRICATION SEQUENCE STEP 01:

- Remove both end plates (HF-G) from back of hanger frame
- Add pull-back connection plates (Plates G and Plate H) to the back of the hanger frame
- SEE SHEETS 14-17 for hanger frame connection details

- Add studs to C-1 channels before connecting C-1 channels to hanger frame
- Using Plates D, E, and F as templates (Sheet 20), add bolt holes to C-1 channels and to hanger frame
- SEE SHEET 18 for C-1 details

Fiber-Reinforced Concrete Traffic Railings for Impact Loading				Revisions:
Pendulum impactor	2019-09-25	University of Florida	Sheet 26 of 38	

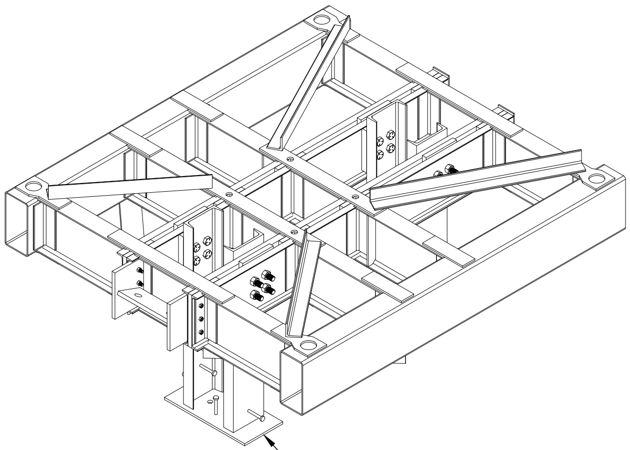

BACK ISOMETRIC VIEW
(FABRICATION SEQUENCE)

FABRICATION SEQUENCE STEP 02:
- Weld Plate B to the bottom of C-1 channels while connected to the hanger frame
- SEE SHEET 18 for Plate B welds
- NOTE: additional holes added to Plate B to prevent air pockets from forming when placing concrete (SEE SHEET 18)

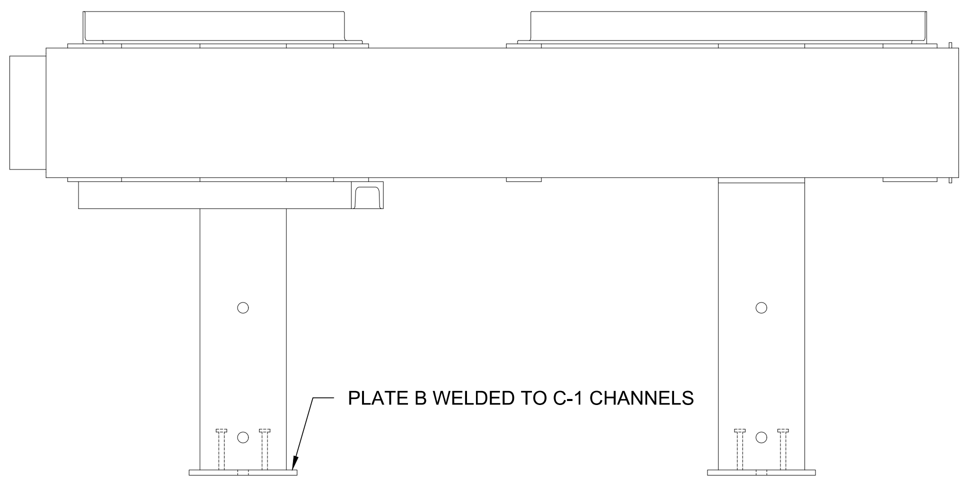

SIDE ELEVATION VIEW
(FABRICATION SEQUENCE)

Fiber-Reinforced Concrete Traffic Railings for Impact Loading				*Revisions:*
Pendulum impactor	*2019-09-25*	*University of Florida*	*Sheet 27 of 38*	

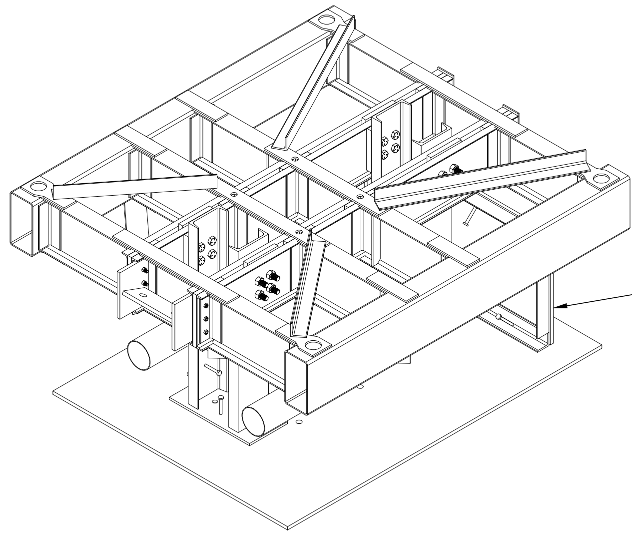

BACK ISOMETRIC VIEW
(FABRICATION SEQUENCE)

FABRICATION SEQUENCE STEP 03:
- Create/use a level and flat working surface
- Suspend hanger frame
- Position floor plywood
  (with holes for B7 bar and PVC cover)
- Position steel front impact face
- SEE SHEET 19 for front impact face details
- Position front panel of formwork
- SEE SHEETS 35-36 for formwork details

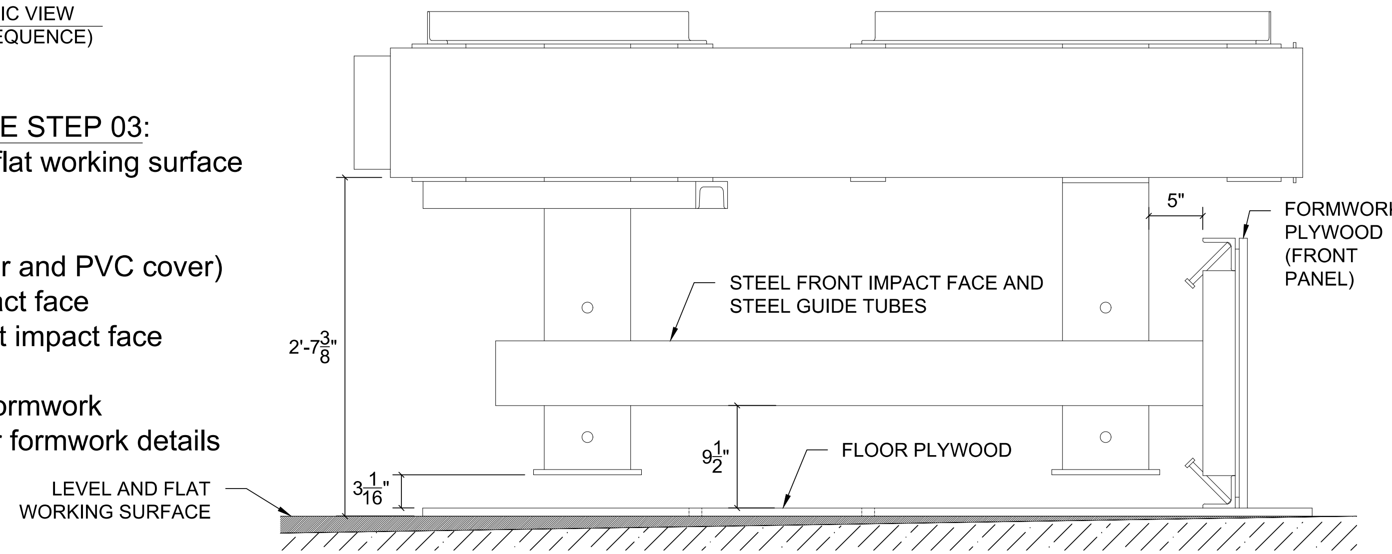

SIDE ELEVATION VIEW
(FABRICATION SEQUENCE)

Fiber-Reinforced Concrete Traffic Railings for Impact Loading				*Revisions:*
Pendulum impactor	*2019-09-25*	*University of Florida*	*Sheet 28 of 38*	

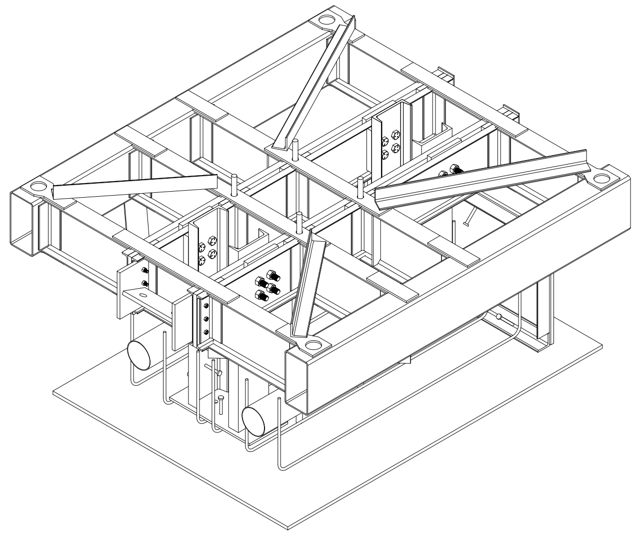

BACK ISOMETRIC VIEW
(FABRICATION SEQUENCE)

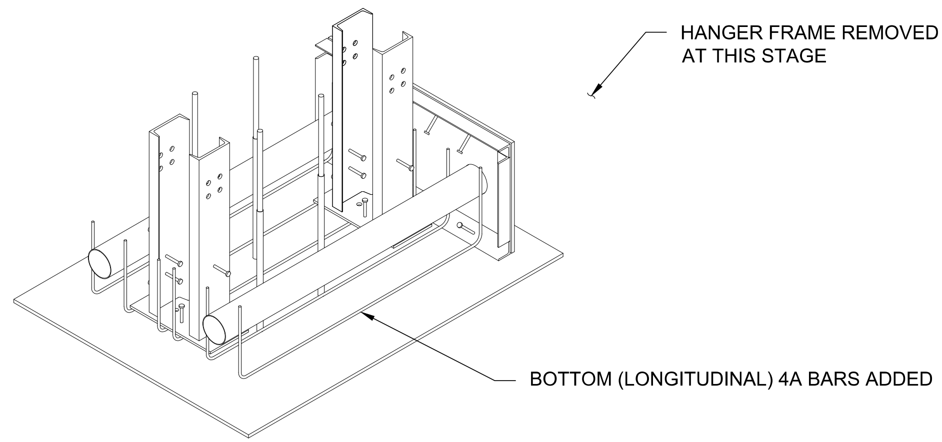

FABRICATION SEQUENCE STEP 04:

- Unbolt C-1 channels and remove hanger frame
- Add bottom (longitudinal) 4A bars
- Position B7 bar PVC cover through floor plywood
- SEE SHEETS 10-13 for rebar details

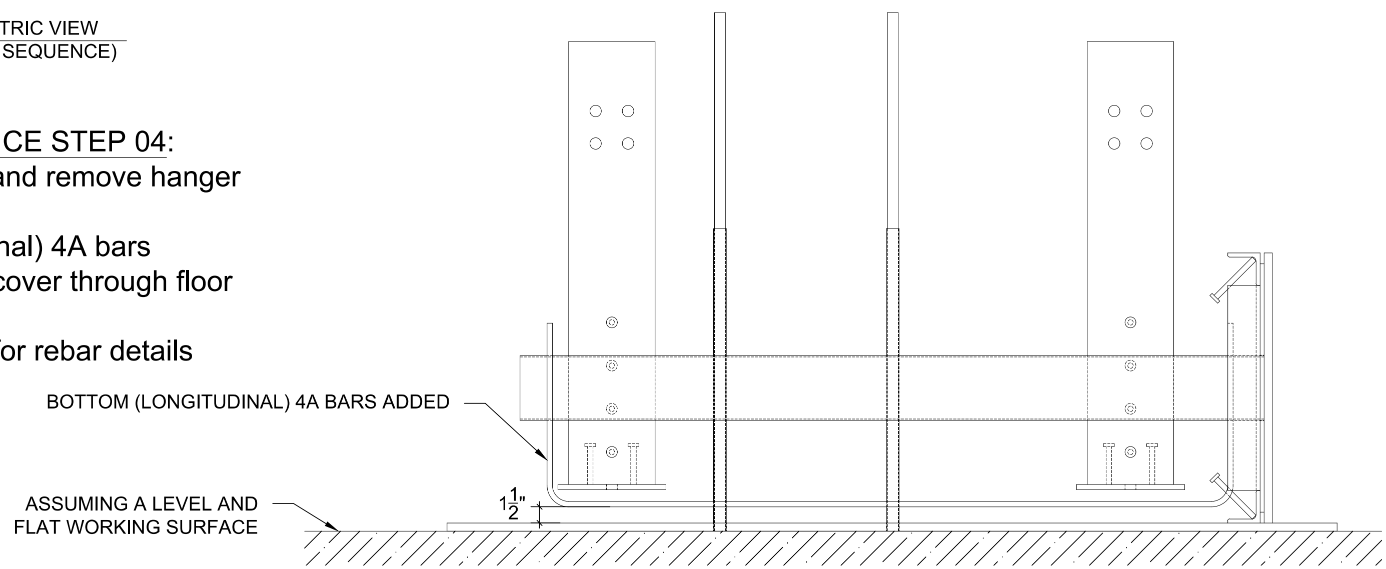

SIDE ELEVATION VIEW
(FABRICATION SEQUENCE)

Fiber-Reinforced Concrete Traffic Railings for Impact Loading				Revisions:
Pendulum impactor	2019-09-25	University of Florida	Sheet 29 of 38	

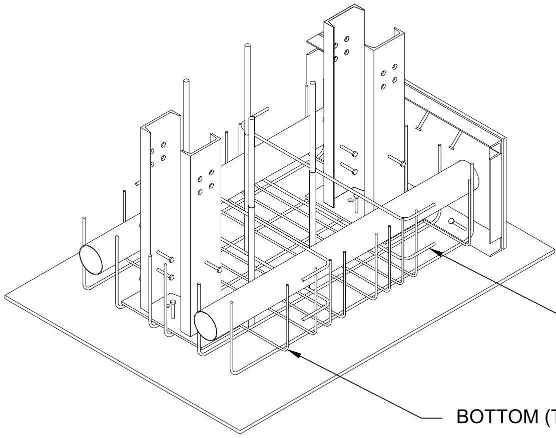

BACK ISOMETRIC VIEW
(FABRICATION SEQUENCE)

FABRICATION SEQUENCE STEP 05:
- Add bottom (transverse) 3A bars
- Add top and bottom (transverse) 4C bars
- SEE SHEETS 10-13 for rebar details

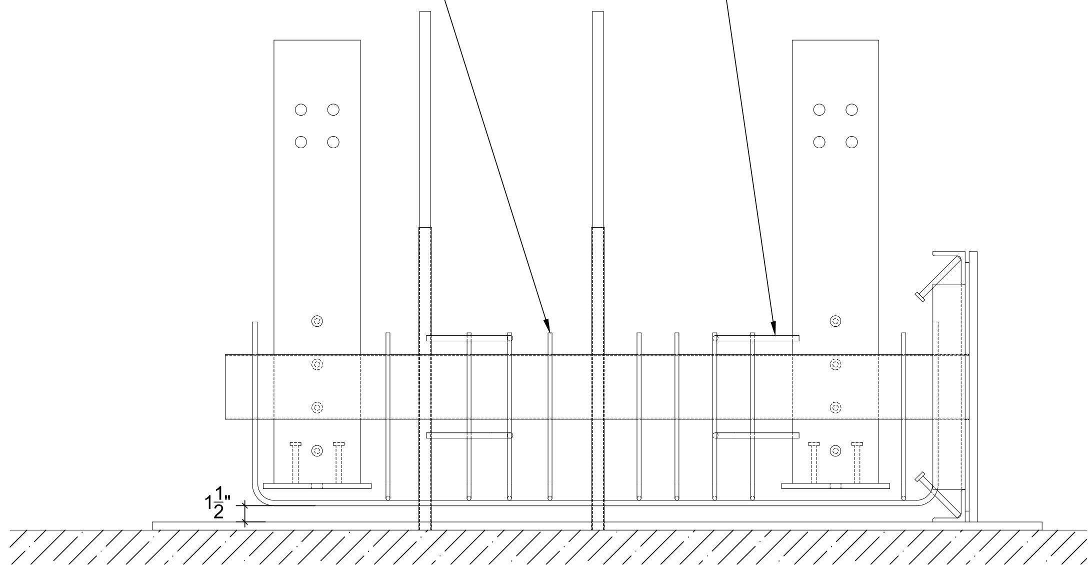

SIDE ELEVATION VIEW
(FABRICATION SEQUENCE)

Fiber-Reinforced Concrete Traffic Railings for Impact Loading				*Revisions:*
Pendulum impactor	*2019-09-25*	*University of Florida*	*Sheet 30 of 38*	

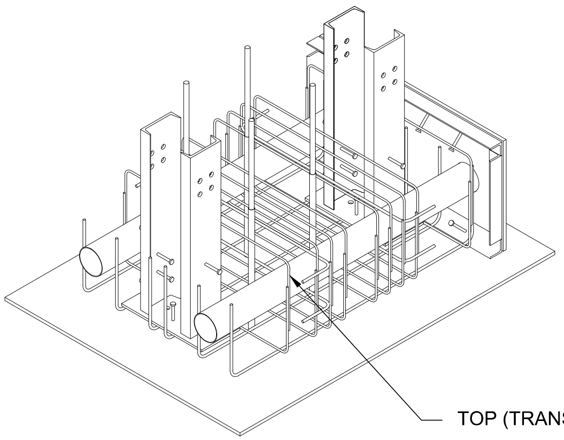

BACK ISOMETRIC VIEW
(FABRICATION SEQUENCE)

FABRICATION SEQUENCE STEP 06:
- Add top (transverse) 3A bars
- SEE SHEETS 10-13 for rebar details

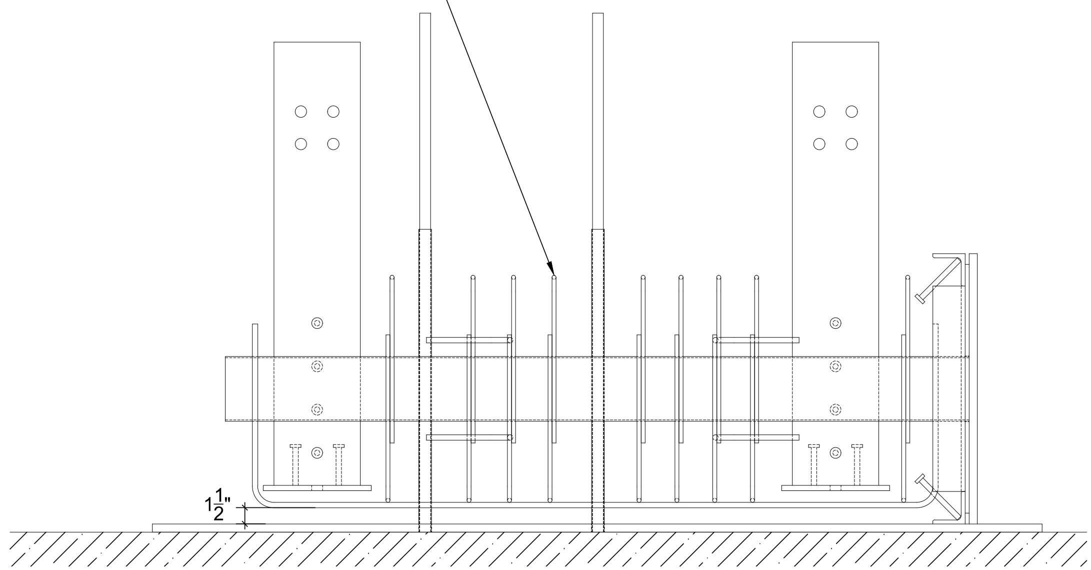

SIDE ELEVATION VIEW
(FABRICATION SEQUENCE)

Fiber-Reinforced Concrete Traffic Railings for Impact Loading				*Revisions:*
Pendulum impactor	*2019-09-25*	*University of Florida*	*Sheet 31 of 38*	

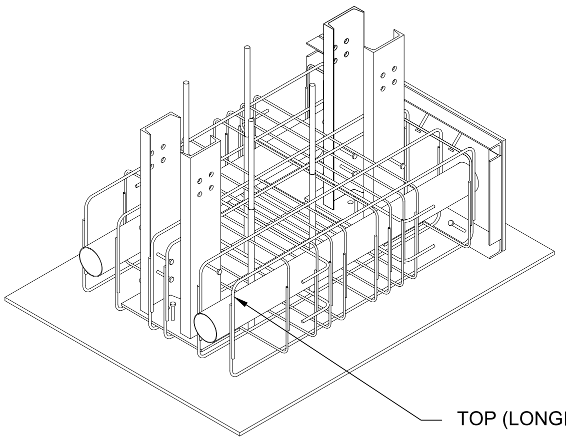

BACK ISOMETRIC VIEW
(FABRICATION SEQUENCE)

FABRICATION SEQUENCE STEP 07:
- Add top (longitudinal) 4A bars
- SEE SHEETS 10-13 for rebar details

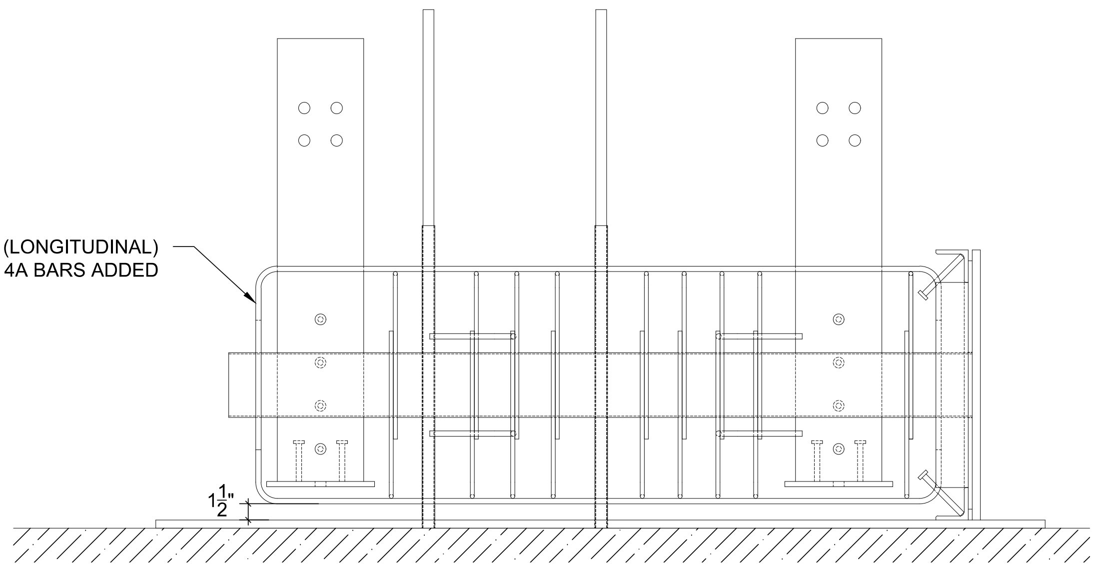

SIDE ELEVATION VIEW
(FABRICATION SEQUENCE)

Fiber-Reinforced Concrete Traffic Railings for Impact Loading				*Revisions:*	
Pendulum impactor	*2019-09-25*	*University of Florida*	*Sheet 32 of 38*		

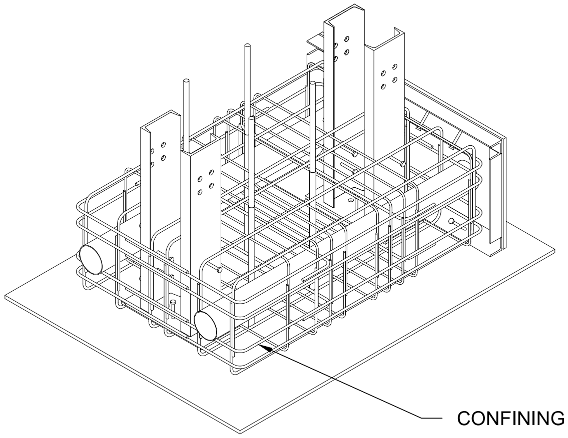

BACK ISOMETRIC VIEW
(FABRICATION SEQUENCE)

FABRICATION SEQUENCE STEP 08:
- Add confining 4B bars
- SEE SHEETS 10-13 for rebar details

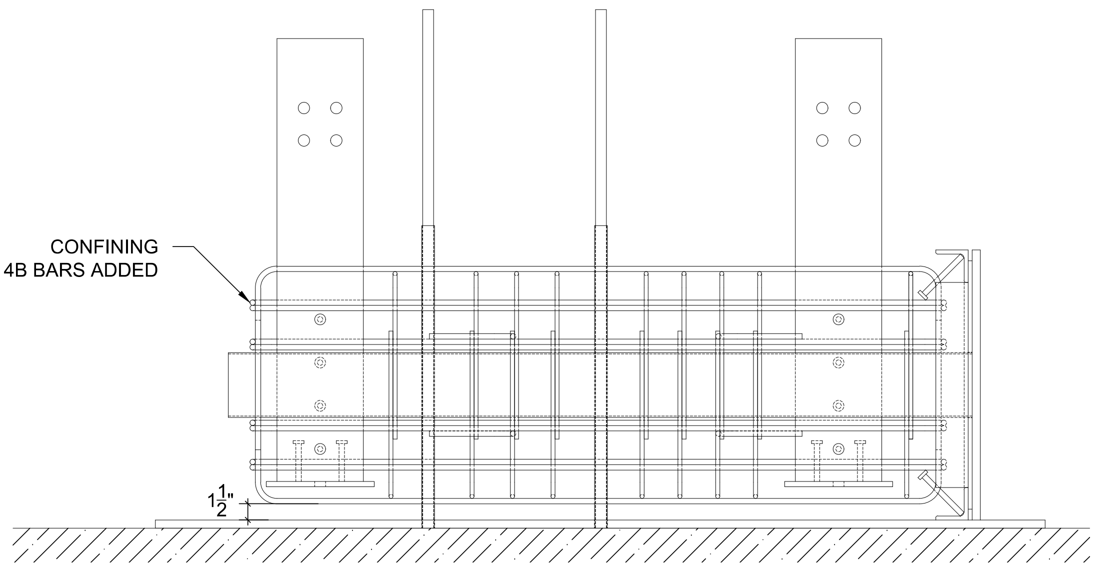

SIDE ELEVATION VIEW
(FABRICATION SEQUENCE)

Fiber-Reinforced Concrete Traffic Railings for Impact Loading				*Revisions:*
Pendulum impactor	*2019-09-25*	*University of Florida*	*Sheet 33 of 38*	

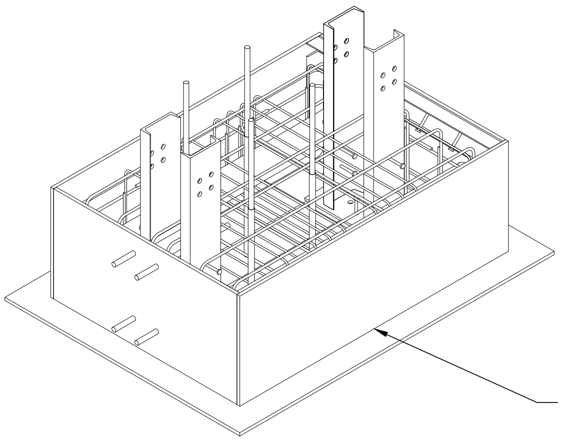

BACK ISOMETRIC VIEW
(FABRICATION SEQUENCE)

FABRICATION SEQUENCE STEP 09:
- Add remaining formwork
- (2x4s not shown) See SHEETS 35-36 for formwork details
- Add B7 bar to back of formwork (for steel weight plates)

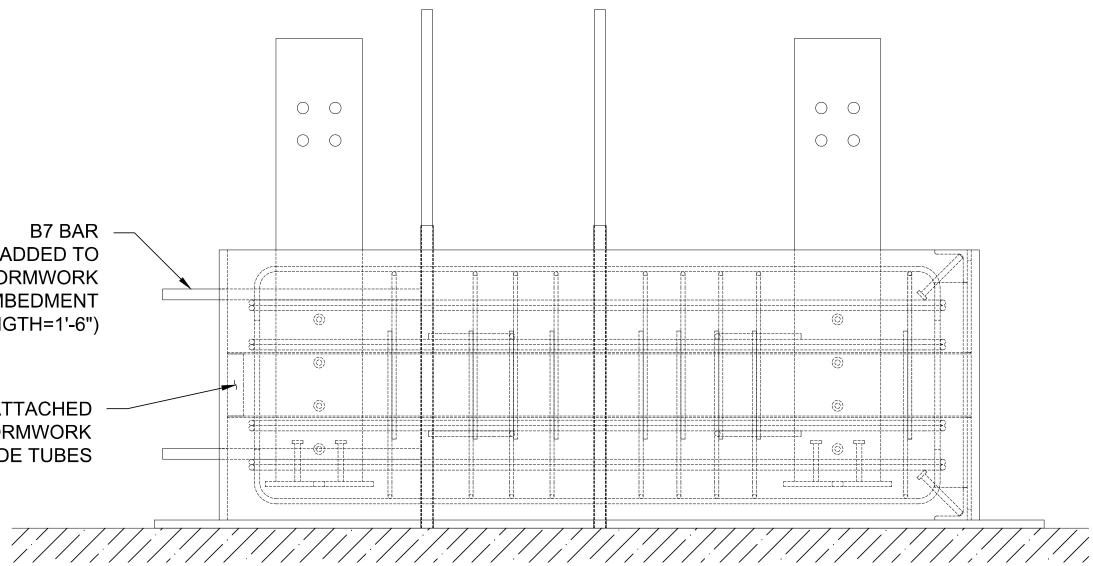

SIDE ELEVATION VIEW
(FABRICATION SEQUENCE)

Fiber-Reinforced Concrete Traffic Railings for Impact Loading				*Revisions:*		
Pendulum impactor	*2019-09-25*	*University of Florida*	*Sheet 34 of 38*			

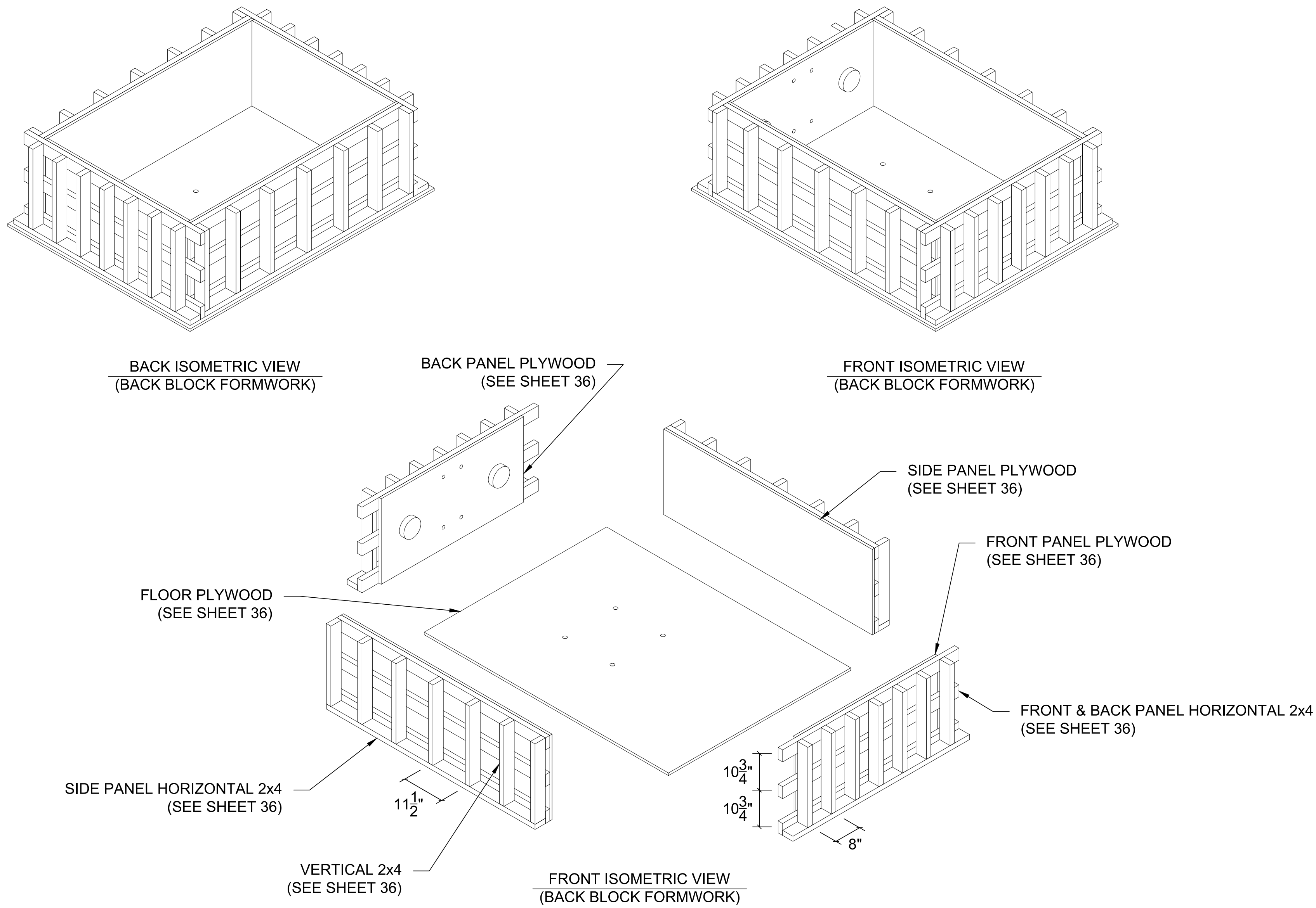

Fiber-Reinforced Concrete Traffic Railings for Impact Loading

Pendulum impactor	*2019-09-25*	*University of Florida*	*Sheet 35 of 38*	*Revisions:*

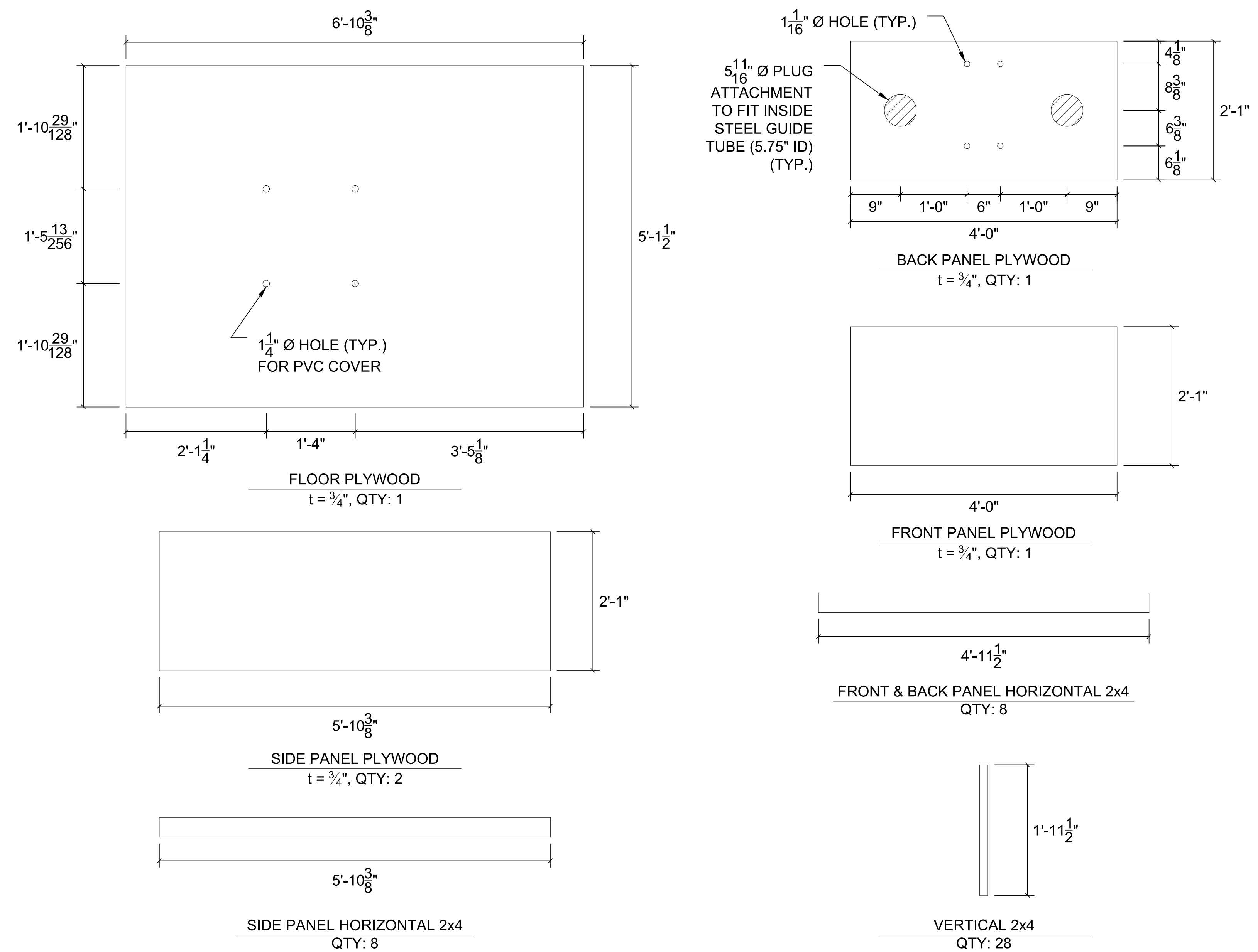

Fiber-Reinforced Concrete Traffic Railings for Impact Loading				*Revisions:*
Pendulum impactor	*2019-09-25*	*University of Florida*	*Sheet 36 of 38*	

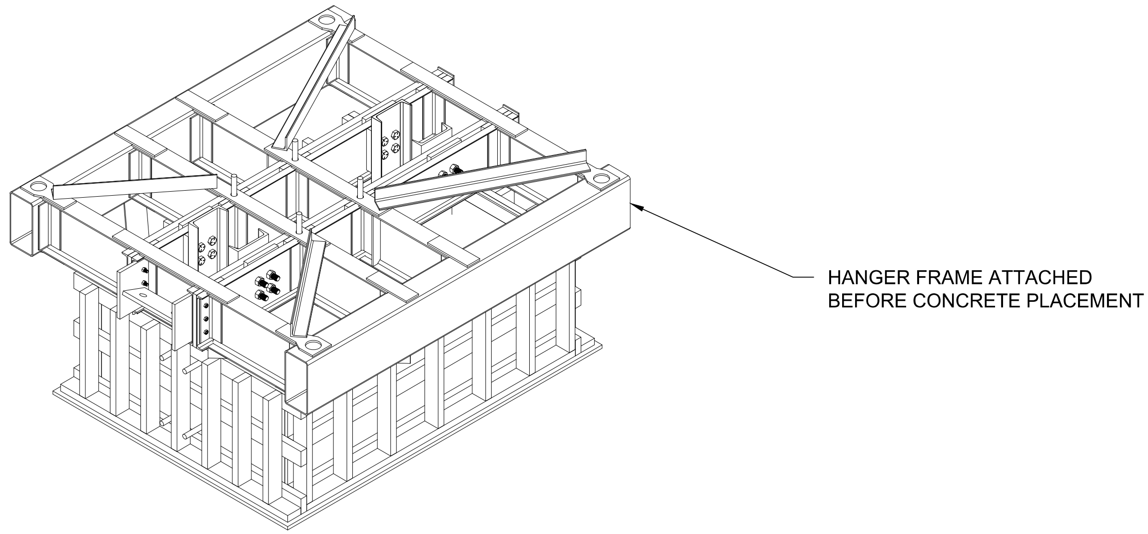

BACK ISOMETRIC VIEW
(FABRICATION SEQUENCE)

FABRICATION SEQUENCE STEP 10:
- Attach hanger frame
- Place concrete into formwork with hanger frame attached

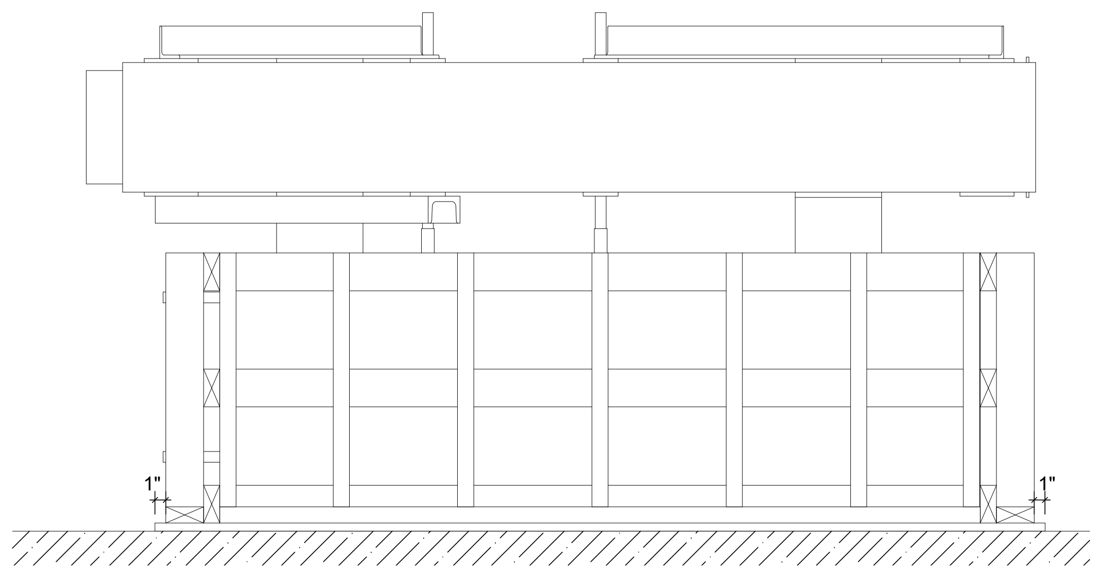

SIDE ELEVATION VIEW
(FABRICATION SEQUENCE)

Fiber-Reinforced Concrete Traffic Railings for Impact Loading			
Pendulum impactor	*2019-09-25*	*University of Florida*	*Sheet 37 of 38*

Revisions:

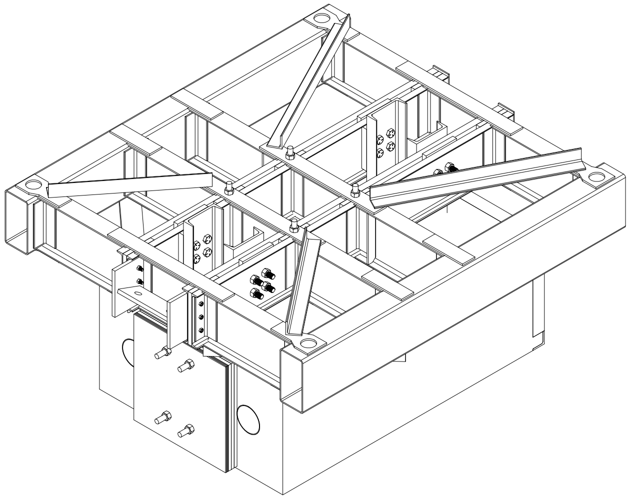

BACK ISOMETRIC VIEW
(FABRICATION SEQUENCE)

FABRICATION SEQUENCE STEP 11:
- Remove formwork
- Attach back weight plates
- Attach Plate A to bottom of the concrete block
- SEE SHEETS 20-21 for Plate A and weight control plate details

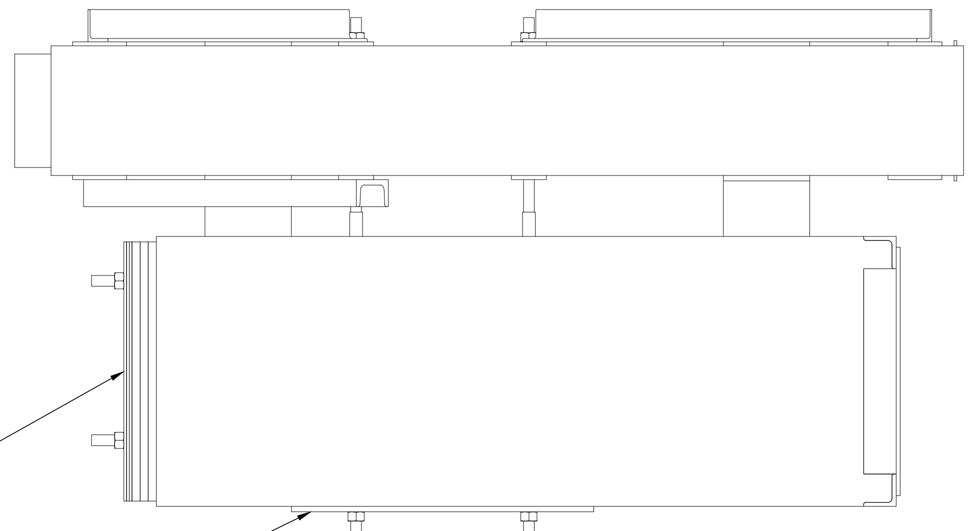

SIDE ELEVATION VIEW
(FABRICATION SEQUENCE)

Fiber-Reinforced Concrete Traffic Railings for Impact Loading				*Revisions:*
Pendulum impactor	*2019-09-25*	*University of Florida*	*Sheet 38 of 38*	

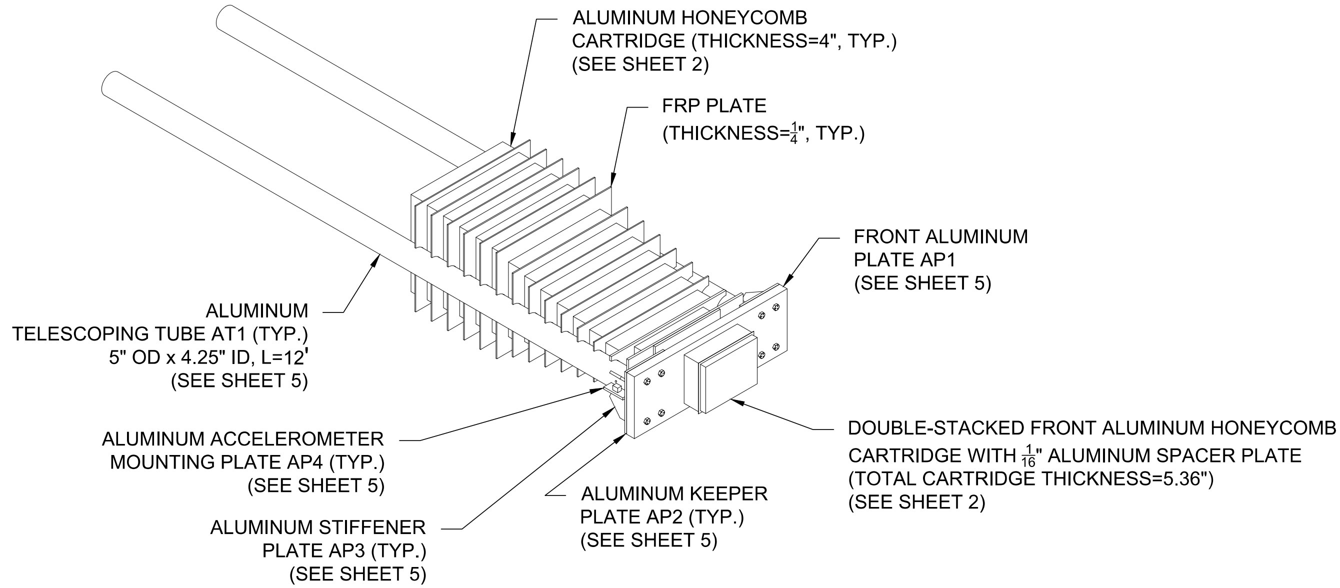

FRONT ISOMETRIC VIEW
(FRONT NOSE COMPONENTS)

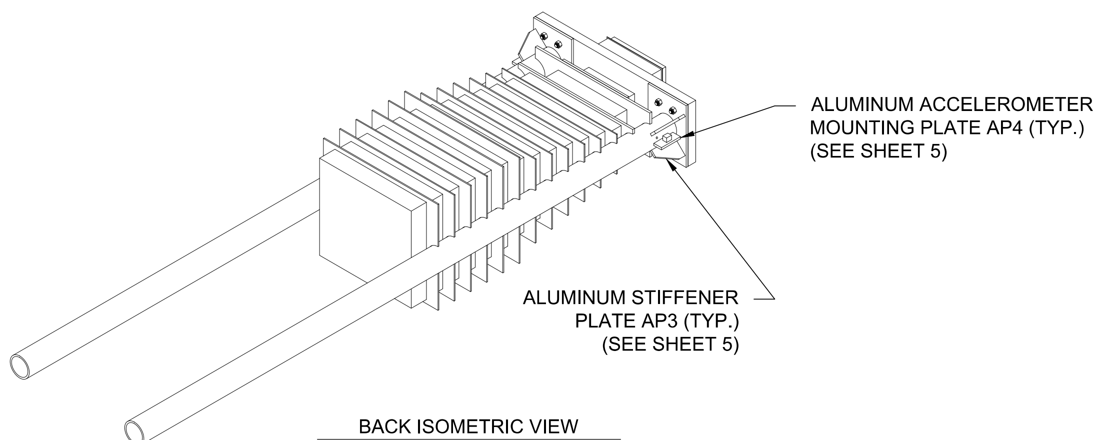

BACK ISOMETRIC VIEW
(FRONT NOSE COMPONENTS)

Fiber-Reinforced Concrete Traffic Railings for Impact Loading				*Revisions:*		
Pendulum impactor front nose	*2019-10-09*	*University of Florida*	*Sheet 01 of 05*			

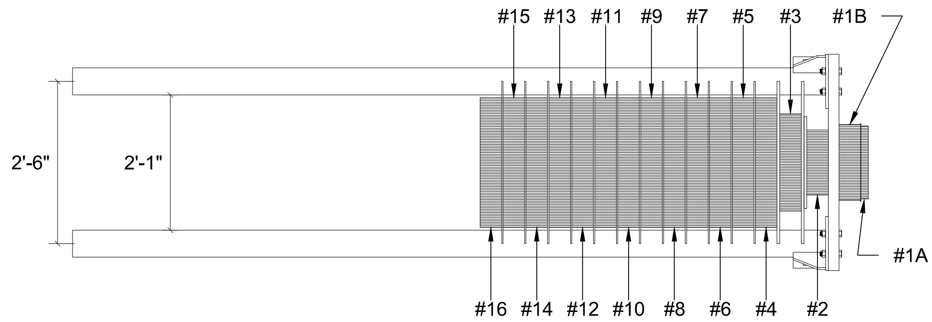

PLAN VIEW
(CARTRIDGE NUMBERING)

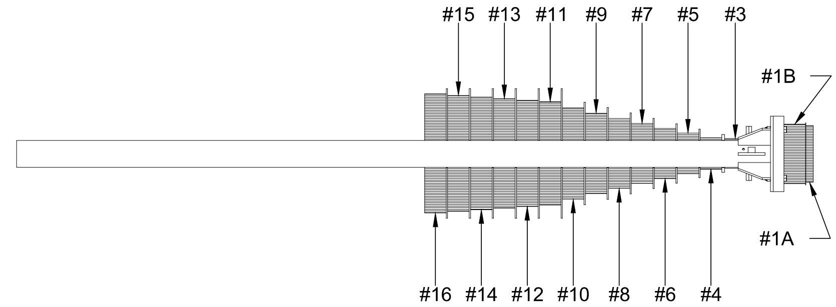

SIDE ELEVATION VIEW
(CARTRIDGE NUMBERING)

Table 1 Design dimensions and crush force for aluminum honeycomb cartridges

Cartridge #	Compressive strength (psi)	Vertical height (in.)	Lateral width (in.)	Thickness (in.)*	Design force (kip)
1A	130	10.50	13.50	1.36	18.4
1B	130	11.00	14.00	4.00	20.0
2	130	5.00	12.00	4.00	7.7
3	130	5.50	18.00	4.00	12.9
4	130	5.83	24.00	4.00	18.2
5	130	7.53	24.00	4.00	23.5
6	130	9.26	24.00	4.00	28.9
7	130	11.06	24.00	4.00	34.5
8	130	12.92	24.00	4.00	40.3
9	130	14.87	24.00	4.00	46.4
10	130	16.92	24.00	4.00	52.8
11	130	19.13	24.00	4.00	59.7
12	130	19.66	24.00	4.00	61.4
13	130	20.26	24.00	4.00	63.2
14	130	20.85	24.00	4.00	65.1
15	130	21.44	24.00	4.00	66.9
16	130	22.04	24.00	4.00	68.8

* Maximum thickness after cartridge pre-crushing

Fiber-Reinforced Concrete Traffic Railings for Impact Loading				*Revisions:*
Pendulum impactor front nose	*2019-10-09*	*University of Florida*	*Sheet 02 of 05*	

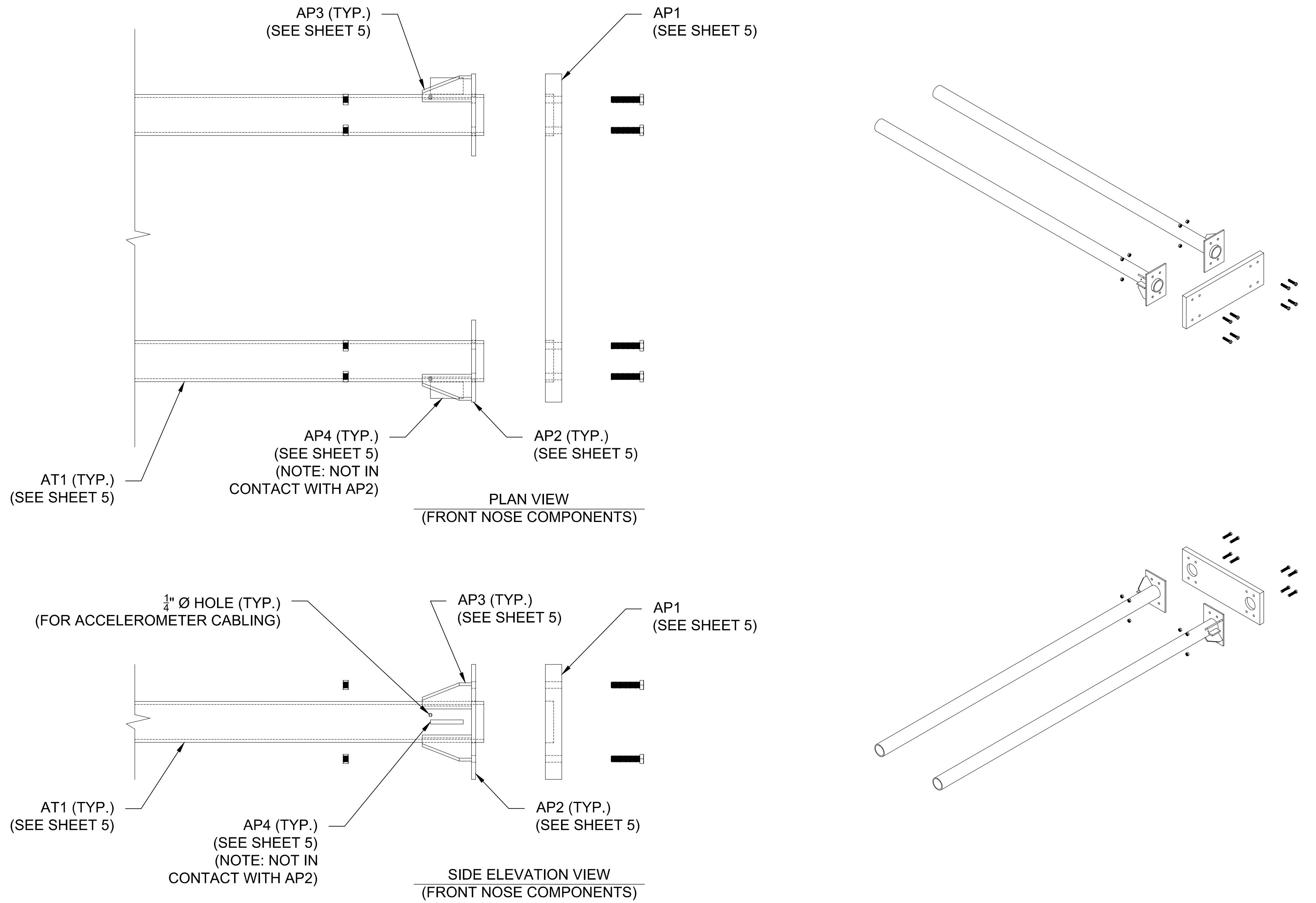

Fiber-Reinforced Concrete Traffic Railings for Impact Loading				*Revisions:*	
Pendulum impactor front nose	*2019-10-09*	*University of Florida*	*Sheet 03 of 05*		

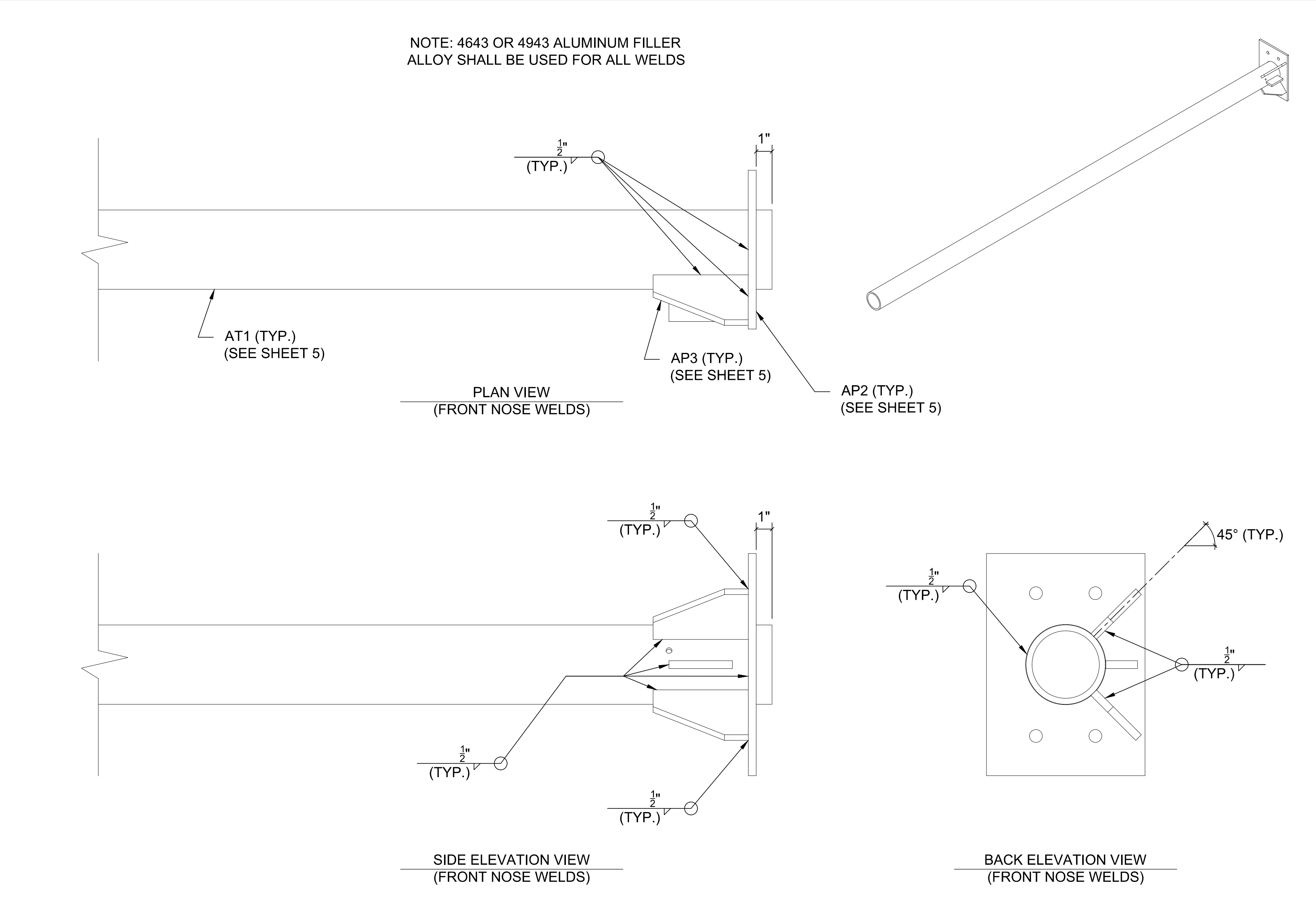

Fiber-Reinforced Concrete Traffic Railings for Impact Loading				*Revisions:*
Pendulum impactor front nose	*2019-10-09*	*University of Florida*	*Sheet 04 of 05*	

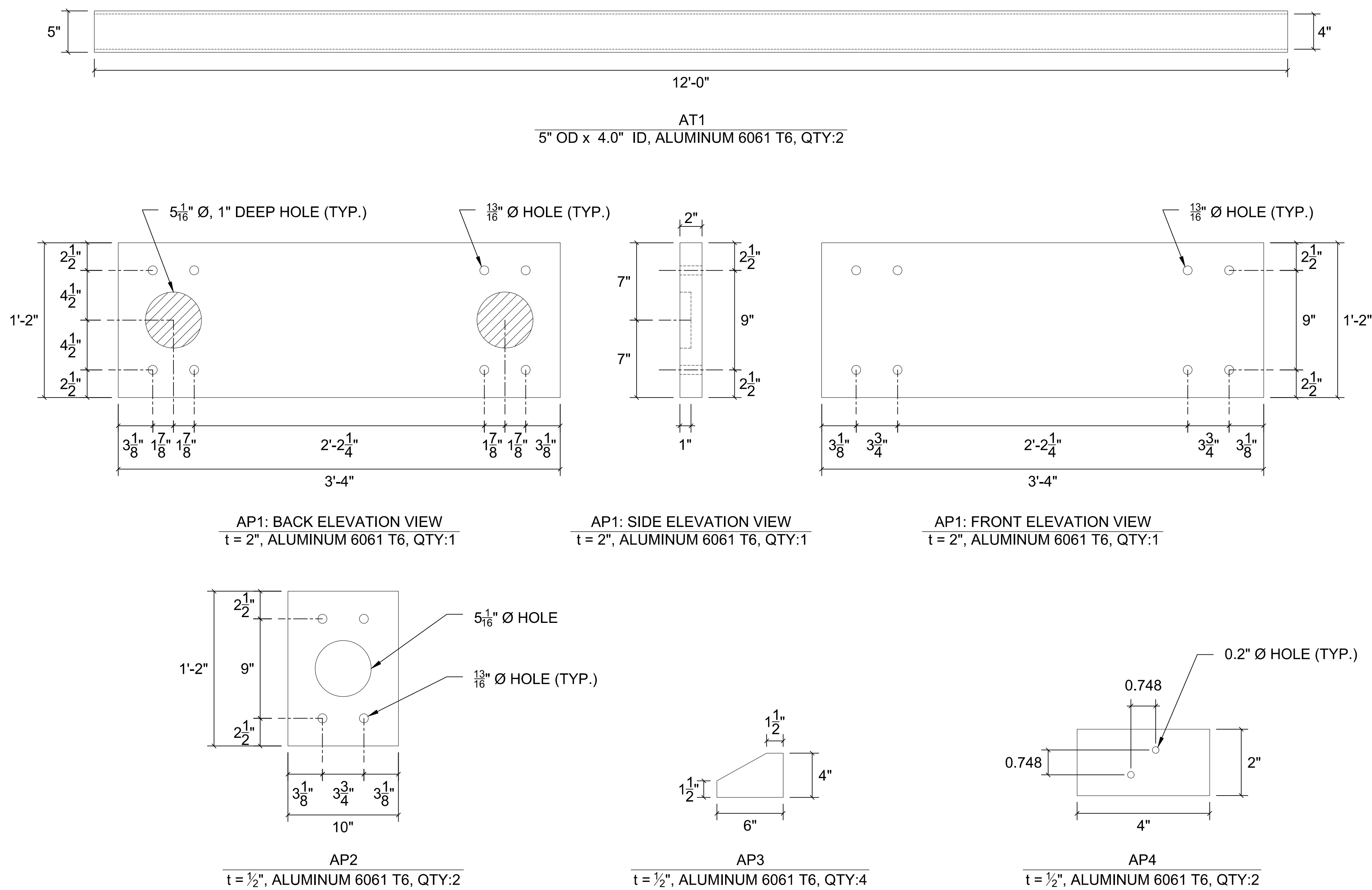

Fiber-Reinforced Concrete Traffic Railings for Impact Loading				*Revisions:*
Pendulum impactor front nose	*2019-10-09*	*University of Florida*	*Sheet 05 of 05*	

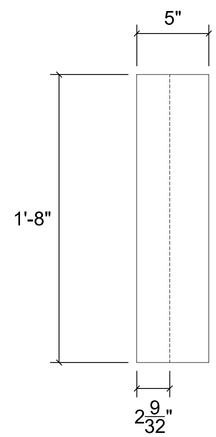

ALUMINUM LOADING WEDGE: PLAN VIEW
t = 5", ALUMINUM 6061 T6, QTY:1

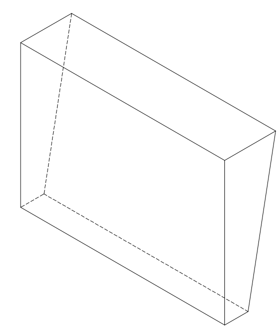

ALUMINUM LOADING WEDGE: ISOMETRIC VIEW
t = 5", ALUMINUM 6061 T6, QTY:1

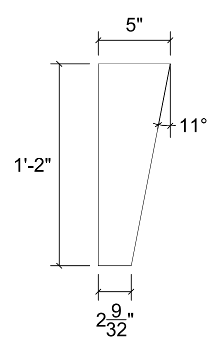

ALUMINUM LOADING WEDGE: SIDE ELEVATION VIEW
t = 5", ALUMINUM 6061 T6, QTY:1

Fiber-Reinforced Concrete Traffic Railings for Impact Loading				*Revisions:*
Pendulum impactor front nose	*2019-10-09*	*University of Florida*		

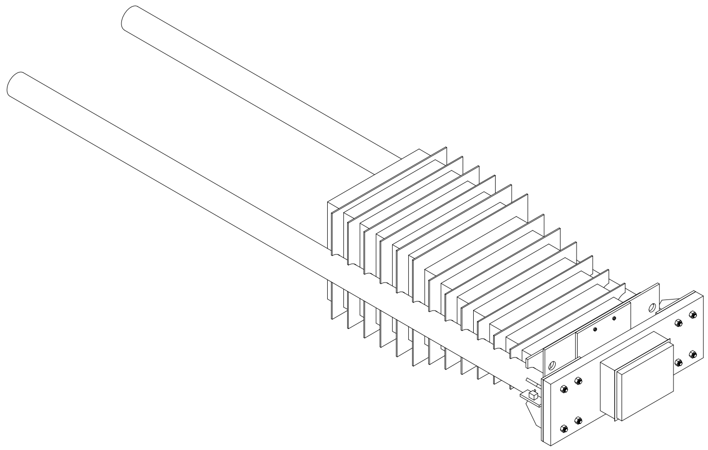

FRONT ISOMETRIC VIEW
(FRONT NOSE COMPONENTS)

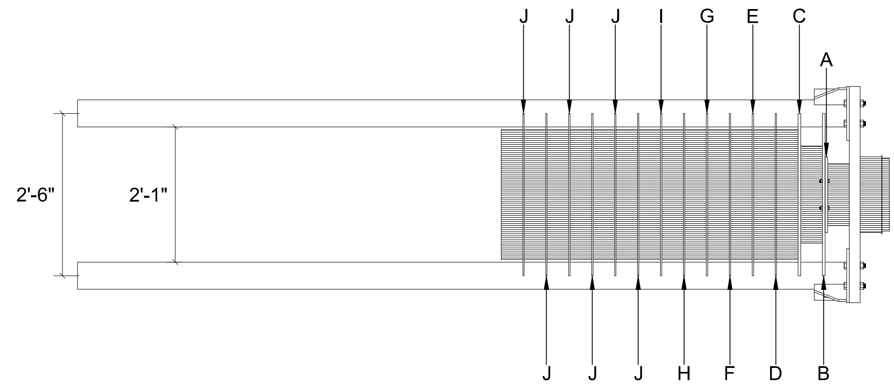

PLAN VIEW
(FRP PLATE LABELING)

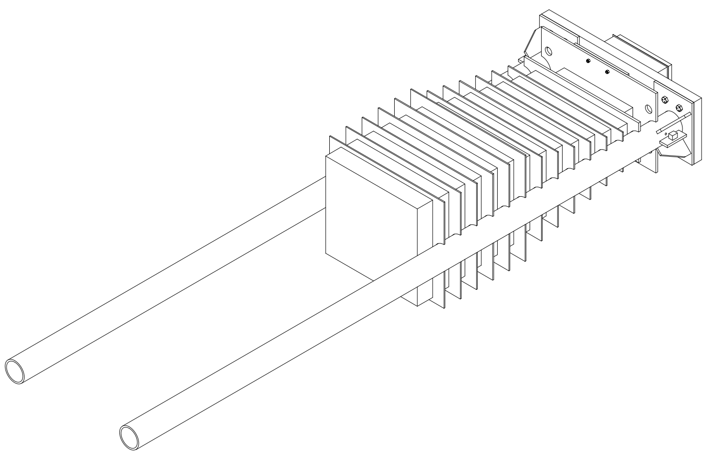

BACK ISOMETRIC VIEW
(FRONT NOSE COMPONENTS)

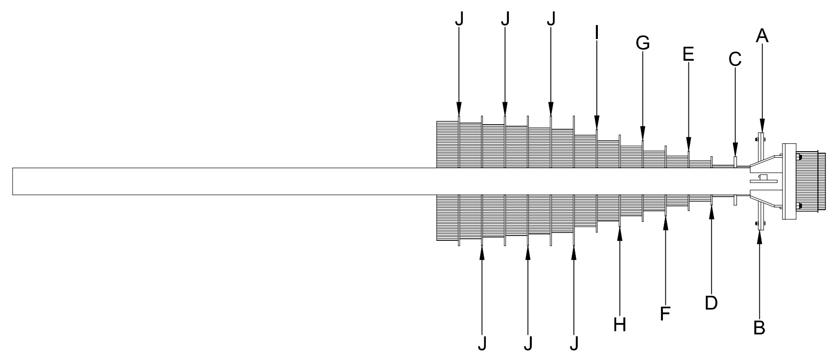

ELEVATION VIEW
(FRP PLATE LABELING)

Fiber-Reinforced Concrete Traffic Railings for Impact Loading				Revisions:
Front nose FRP plates	2020-01-17	University of Florida	Sheet 01 of 04	

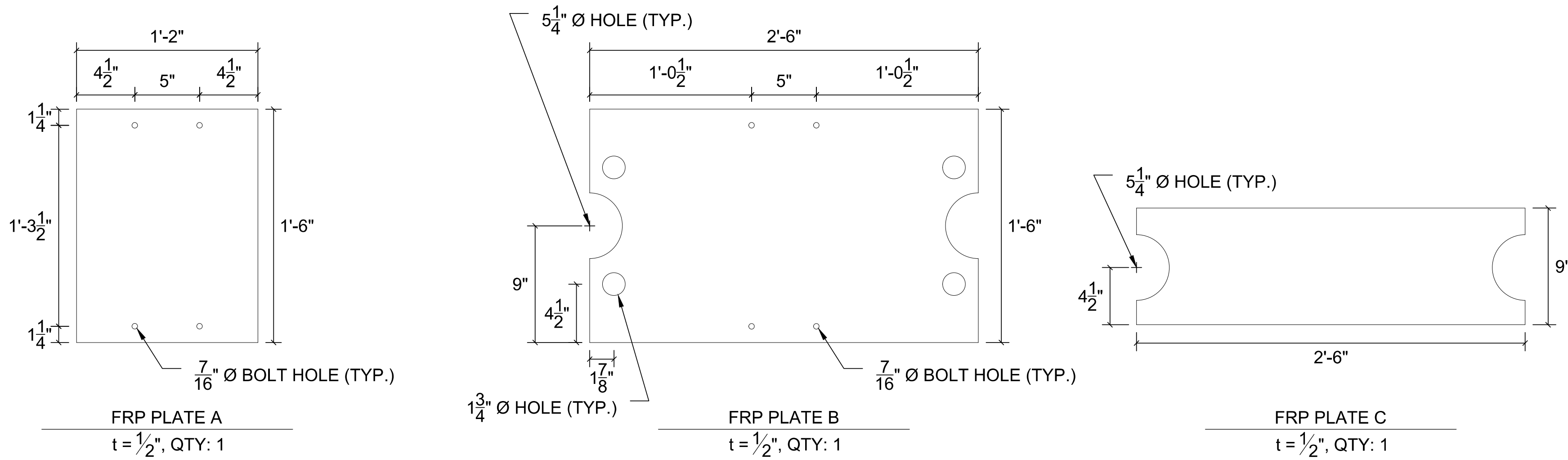

Fiber-Reinforced Concrete Traffic Railings for Impact Loading				*Revisions:*
Front nose FRP plates	*2020-01-17*	*University of Florida*	*Sheet 02 of 04*	

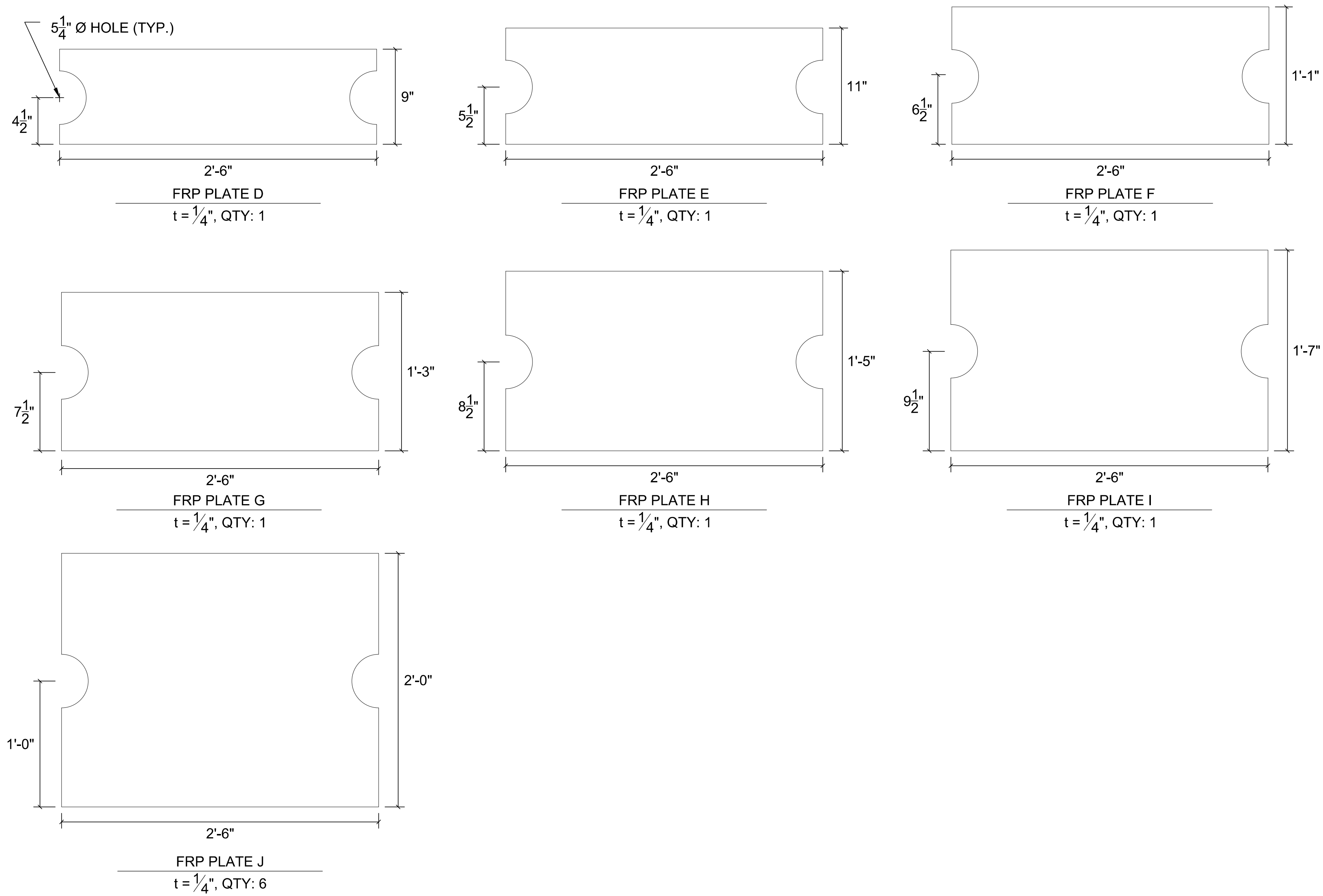

Fiber-Reinforced Concrete Traffic Railings for Impact Loading				*Revisions:*
Front nose FRP plates	*2020-01-17*	*University of Florida*	*Sheet 03 of 04*	

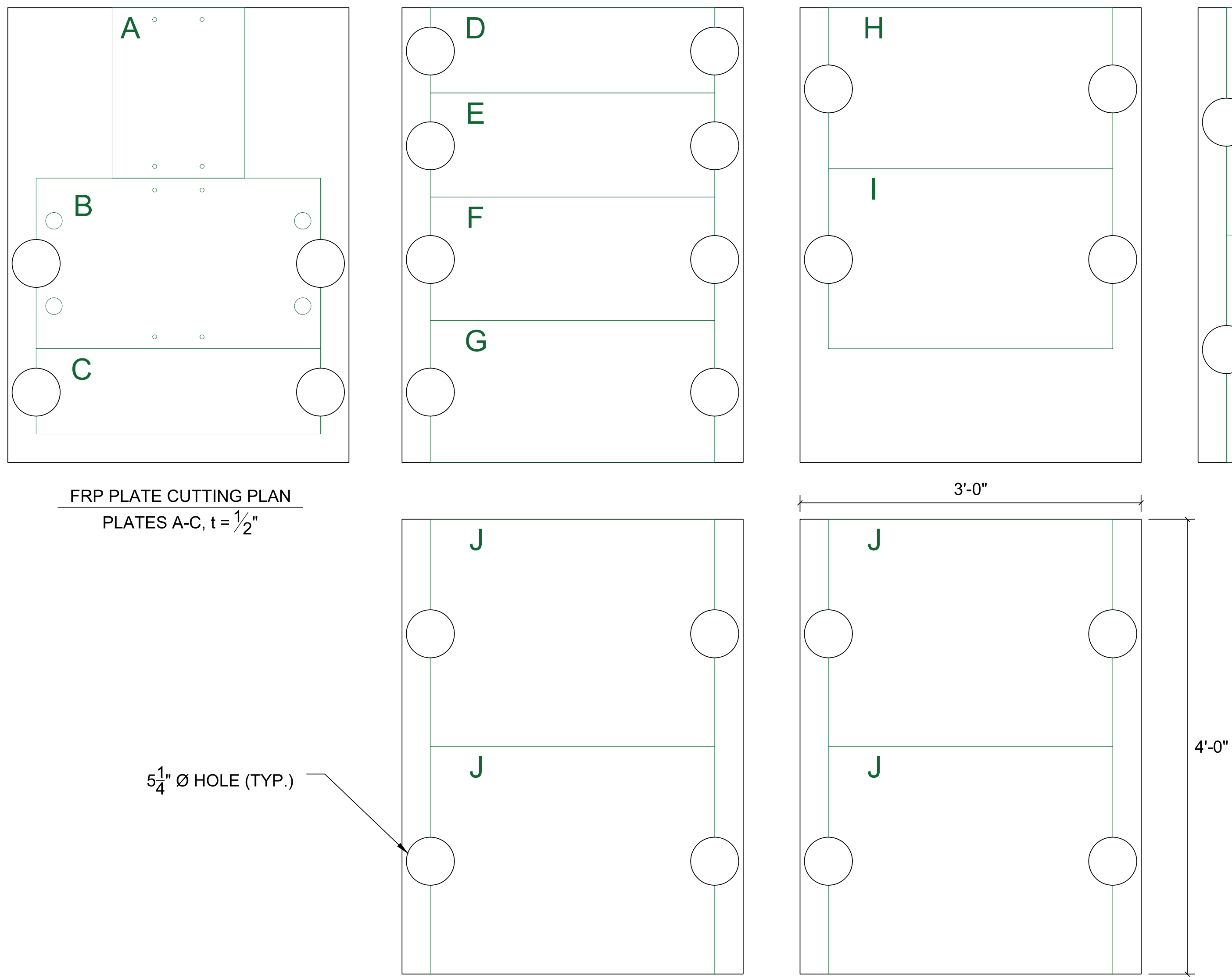

FRP PLATE CUTTING PLAN
PLATES A-C, t = $\frac{1}{2}$"

FRP PLATE CUTTING PLAN
PLATES D-J, t = $\frac{1}{4}$"

Fiber-Reinforced Concrete Traffic Railings for Impact Loading				*Revisions:*
Front nose FRP plates	*2020-01-17*	*University of Florida*	*Sheet 04 of 04*	

APPENDIX G
IMPACT TEST SPECIMEN (DECK AND RAILING) CONSTRUCTION DRAWINGS

Presented in this appendix are impact test specimen construction drawings. The series of drawings include the different specimen versions that were pendulum impact tested:

- FRC COR
- R/C COR
- FRC EOR
- R/C EOR

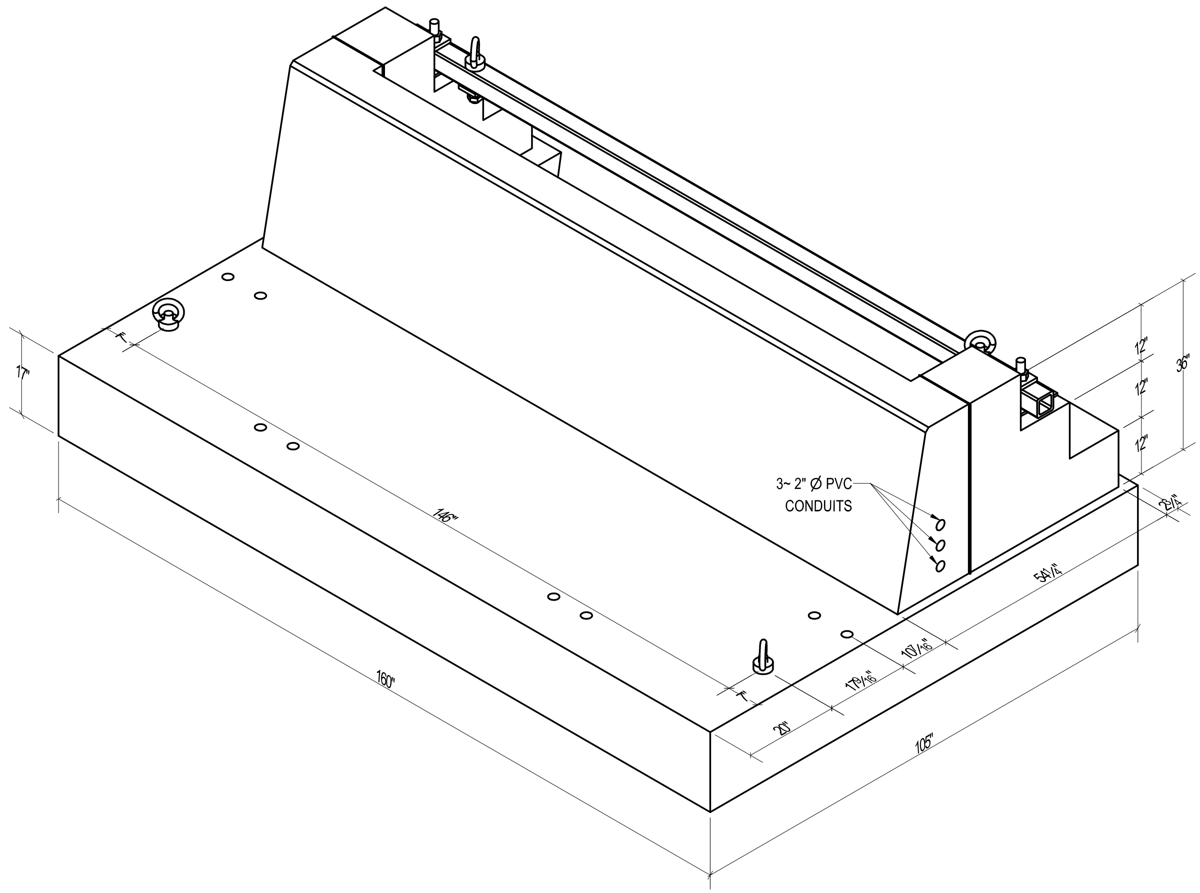

TEST SPECIMEN
FRONT ISOMETRIC VIEW

FRC REINFORCED TEST SPECIMEN				*Revision:*		
TEST SPECIMEN OVERVIEW	*5/19/2020*	*University of Florida*	*SHEET 1 OF 18*			

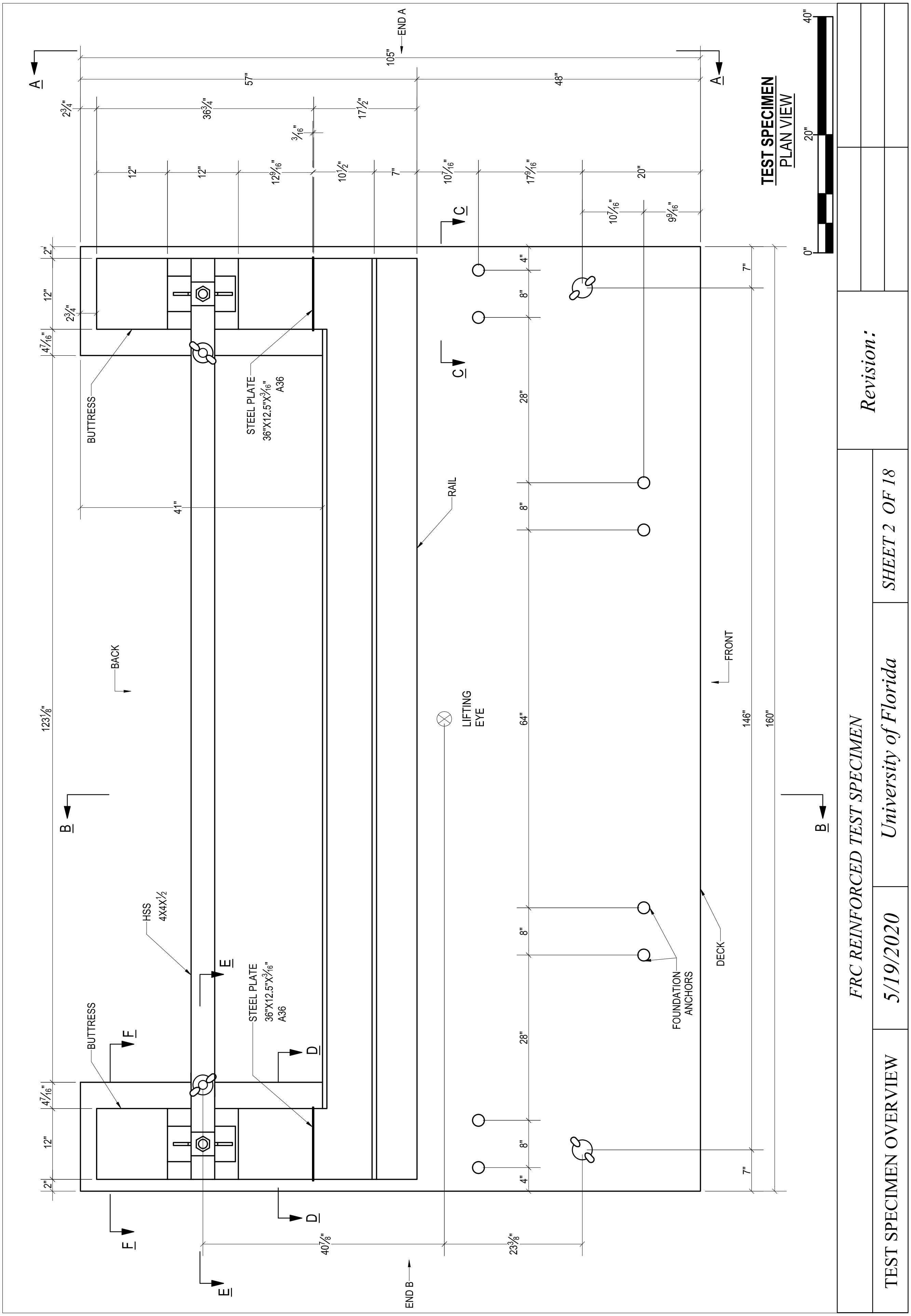
TEST SPECIMEN
PLAN VIEW
FRC REINFORCED TEST SPECIMEN
University of Florida
TEST SPECIMEN OVERVIEW
5/19/2020
SHEET 2 OF 18
Revision:
END A
END B
BUTTRESS
STEEL PLATE 36"X12.5"X3/16" A36
HSS 4X4X1/2
RAIL
BACK
FRONT
DECK
LIFTING EYE
FOUNDATION ANCHORS
0"
20"
40"
105"
57"
48"
123 1/8"
146"
160"
41"
64"
28"
40 7/8"
23 3/8"

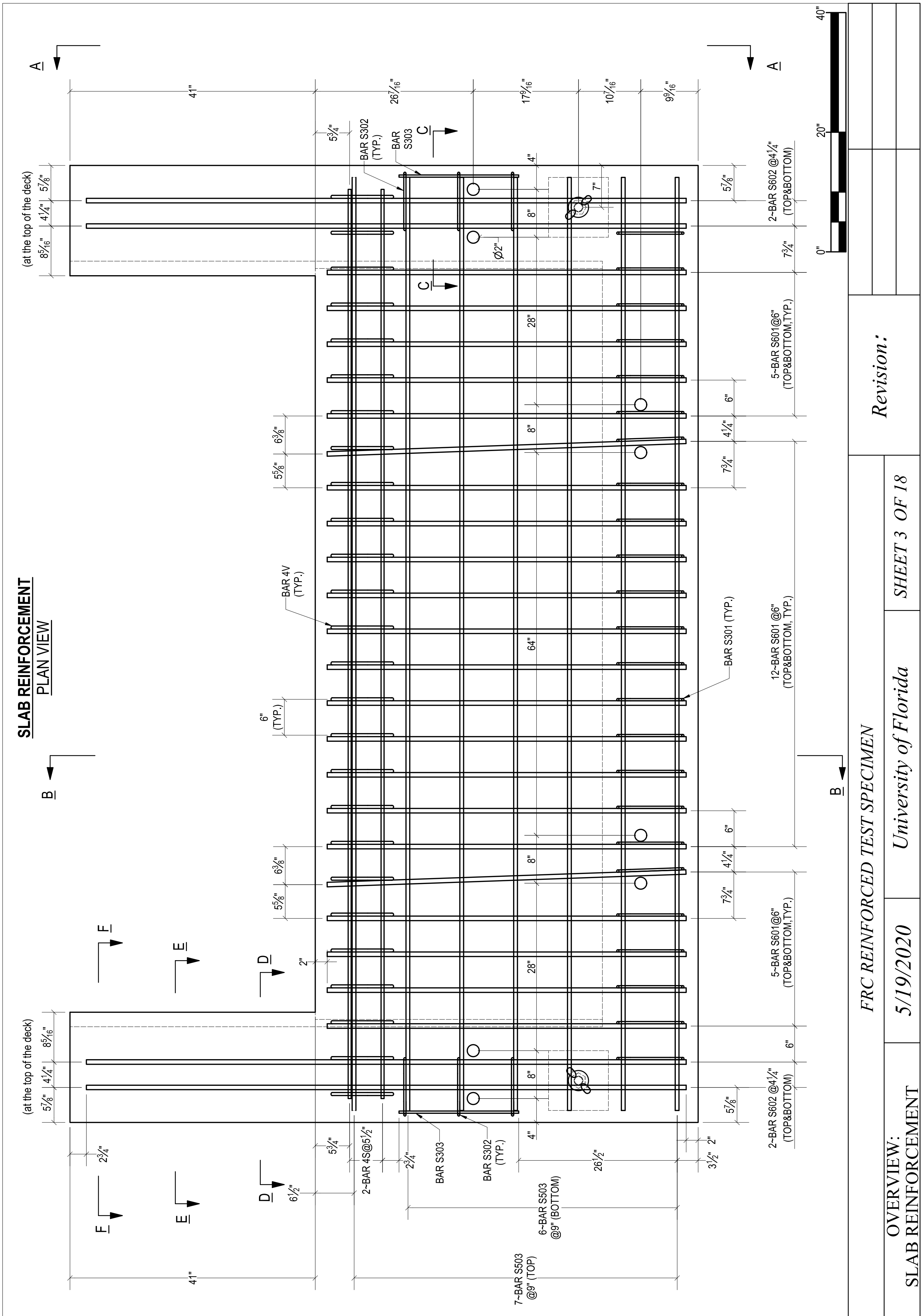

SLAB REINFORCEMENT
PLAN VIEW
(at the top of the deck)
BAR S302 (TYP.)
BAR S303
BAR 4V (TYP.)
BAR S301 (TYP.)
6" (TYP.)
Ø2"
2~BAR S602 @4¼" (TOP&BOTTOM)
5~BAR S601@6" (TOP&BOTTOM,TYP.)
12~BAR S601 @6" (TOP&BOTTOM, TYP.)
2~BAR 4S@5½"
6~BAR S503 @9" (BOTTOM)
7~BAR S503 @9" (TOP)
41"
26½"
28"
64"
FRC REINFORCED TEST SPECIMEN
University of Florida
5/19/2020
SHEET 3 OF 18
Revision:
OVERVIEW:
SLAB REINFORCEMENT

THICKENED DECK AND BUTTRESS REINFORCEMENT
PLAN VIEW

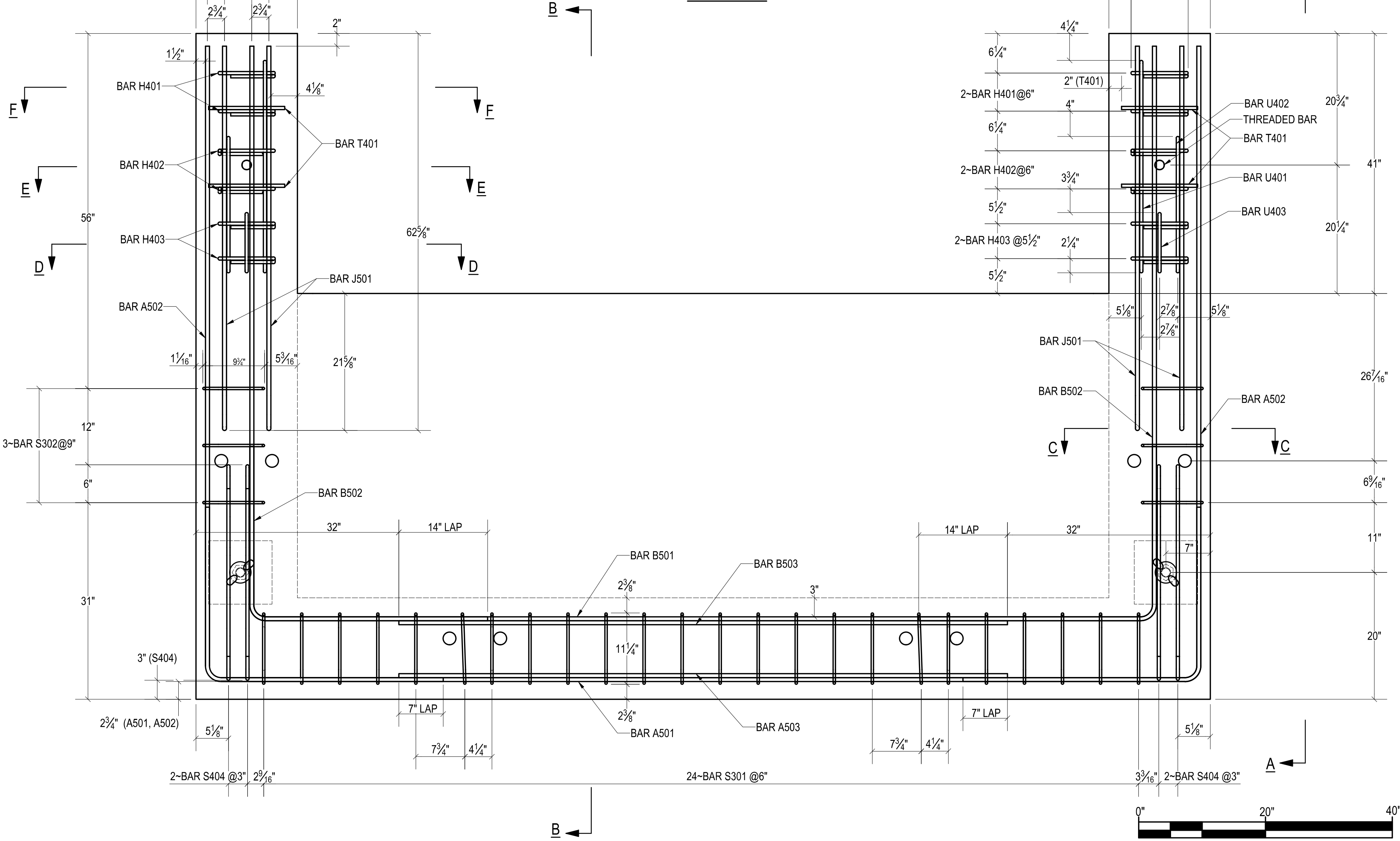

FRC REINFORCED TEST SPECIMEN				Revision:
OVERVIEW: THICKENED DECK REINFORCEMENT	5/19/2020	University of Florida	SHEET 4 OF 18	

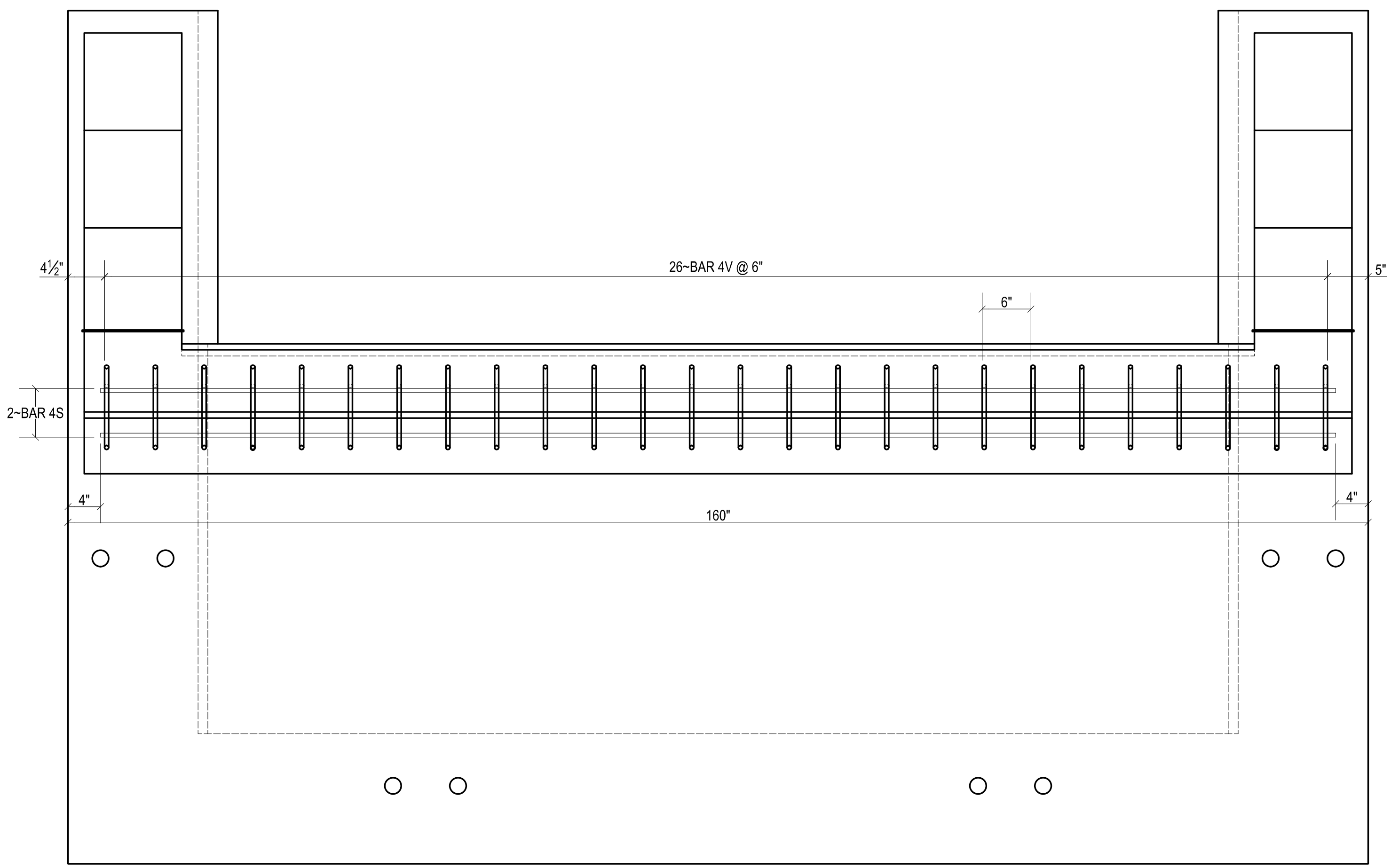

RAIL REINFORCEMENT
(PLAN VIEW)

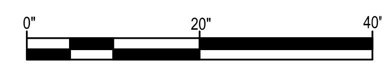

FRC REINFORCED TEST SPECIMEN				*Revision:*
RAILING REINFORCEMENT: OVERVIEW	*5/19/2020*	*University of Florida*	*SHEET 5 OF 18*	

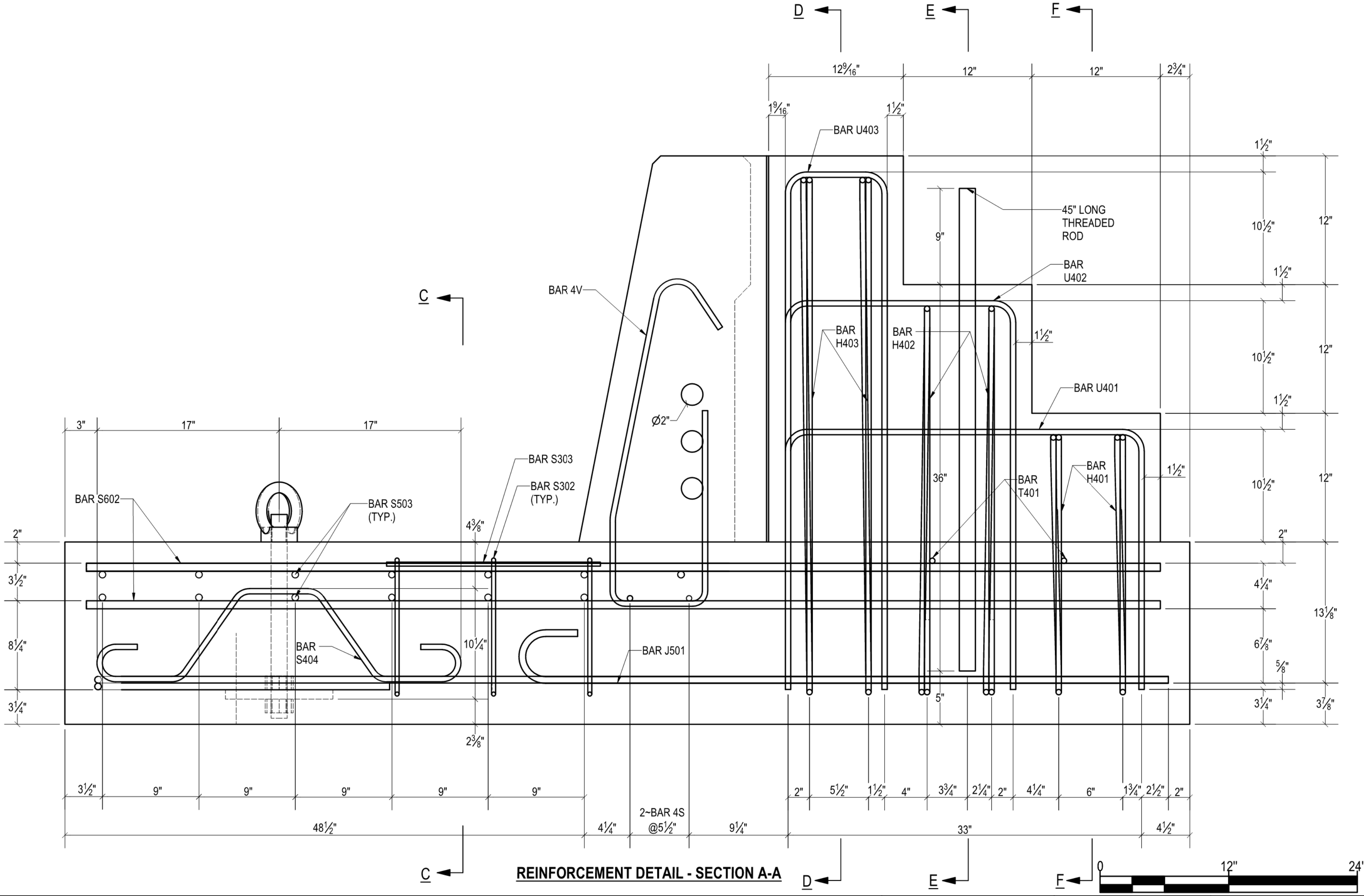

REINFORCEMENT DETAIL - SECTION A-A

FRC REINFORCED TEST SPECIMEN				Revision:
SECTION A-A	5/19/2020	University of Florida	SHEET 6 OF 18	

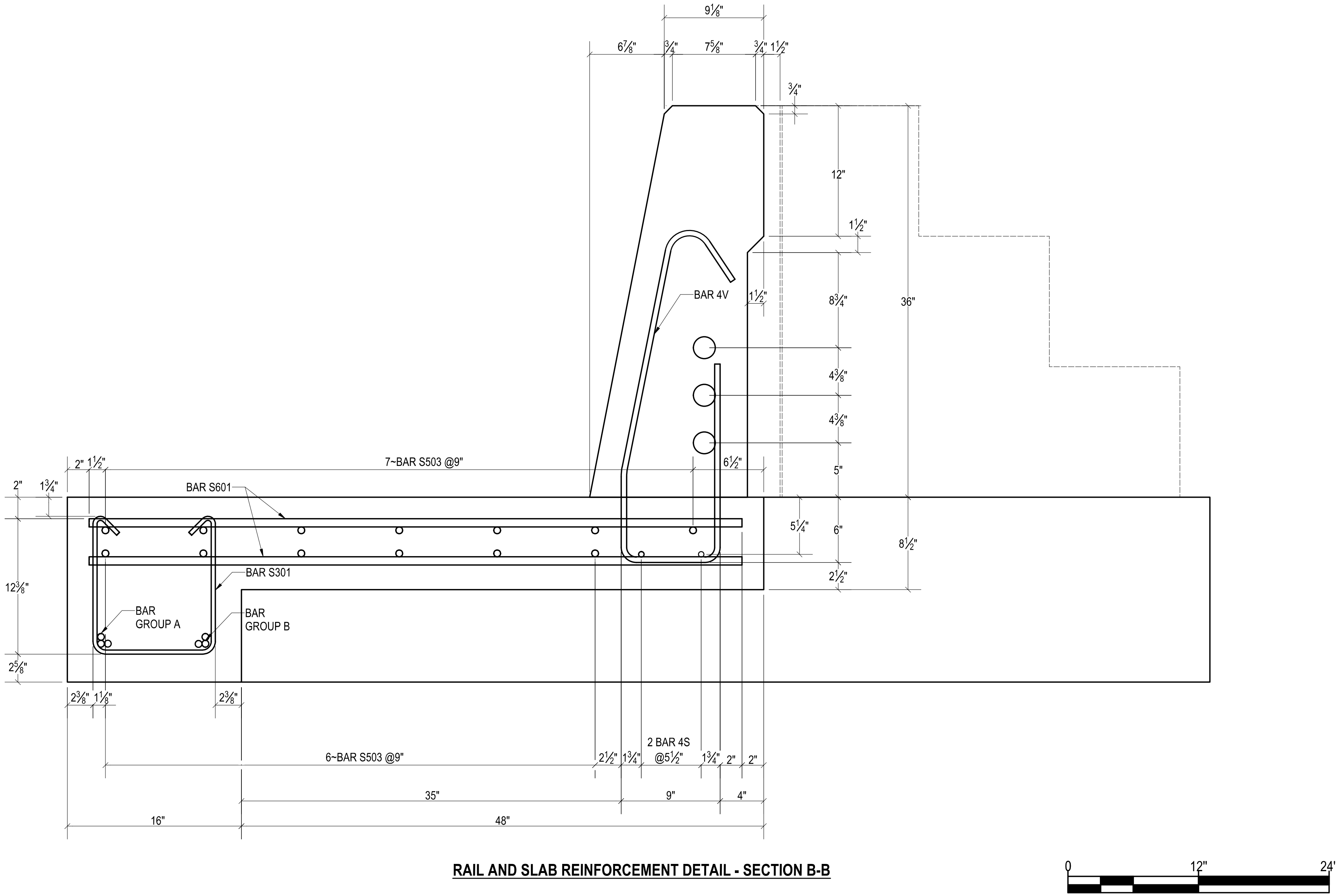

RAIL AND SLAB REINFORCEMENT DETAIL - SECTION B-B

FRC REINFORCED TEST SPECIMEN				Revision:
SECTION B-B	5/19/2020	University of Florida	SHEET 7 OF 18	

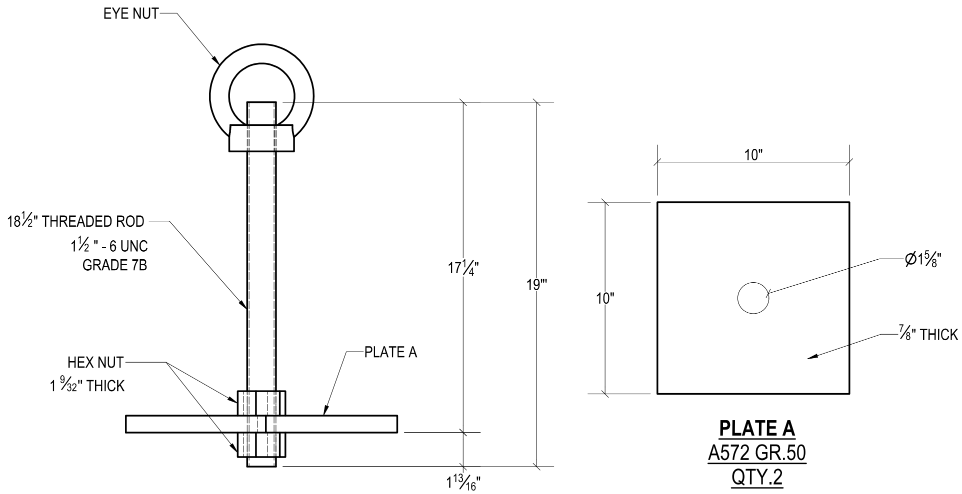

ANCHOR AND PLATE CONNECTION

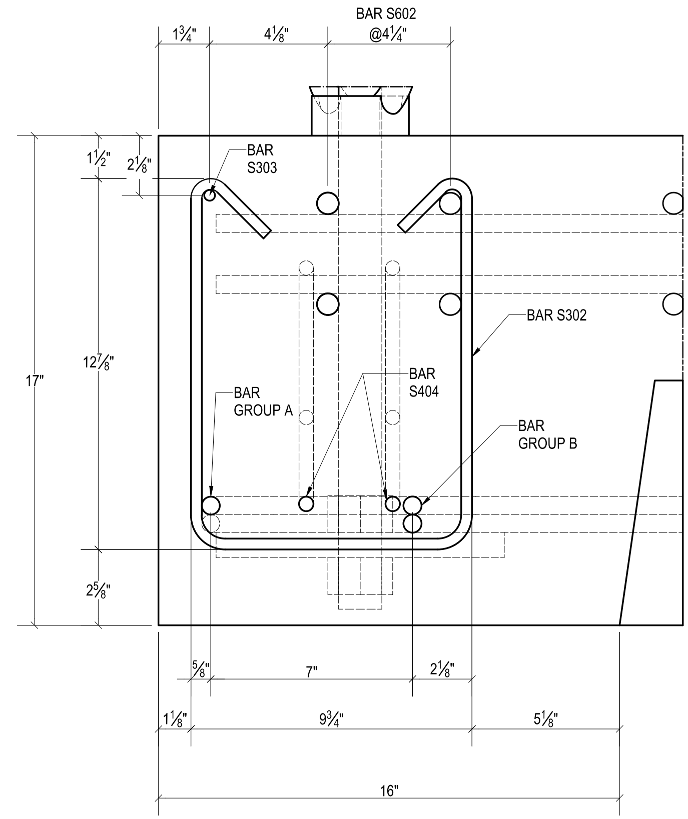

THICKENED EDGE
SECTION C-C

FRC REINFORCED TEST SPECIMEN				*Revision:*
ANCHOR PLATE AND SECTION C-C	*5/19/2020*	*University of Florida*	*SHEET 8 OF 18*	

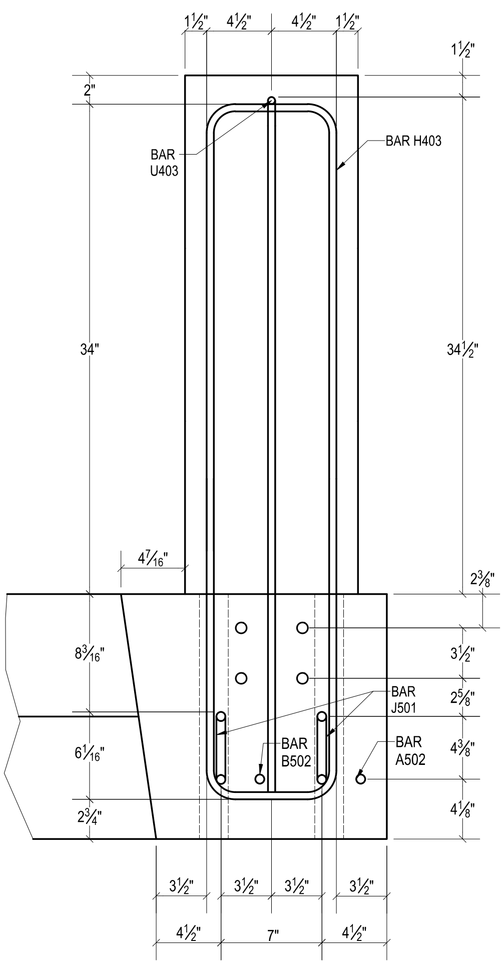

BUTTRESS REINFORCEMENT
SECTION D-D

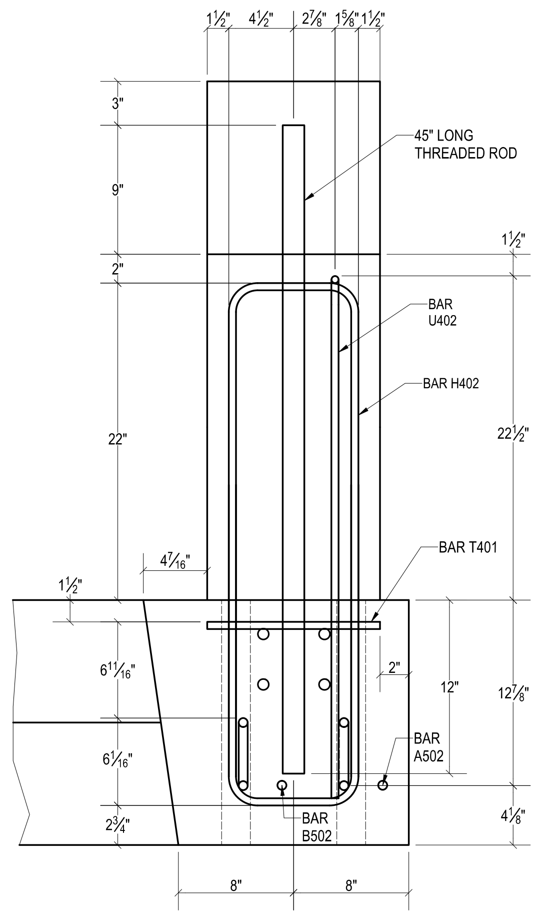

BUTTRESS REINFORCEMENT
SECTION E-E

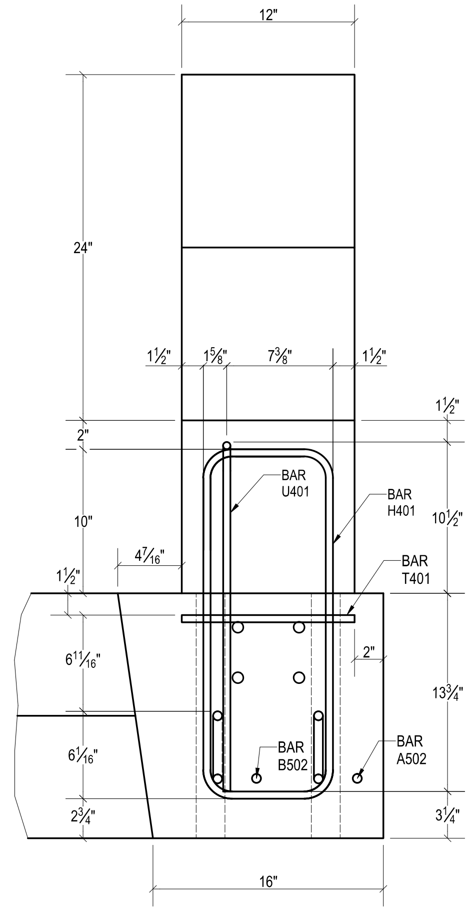

BUTTRESS REINFORCEMENT
SECTION F-F

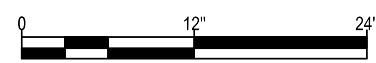

FRC REINFORCED TEST SPECIMEN				Revision:
SECTION D, E, F: BUTTRESS REINFORCEMENT	5/19/2020	University of Florida	SHEET 9 OF 18	

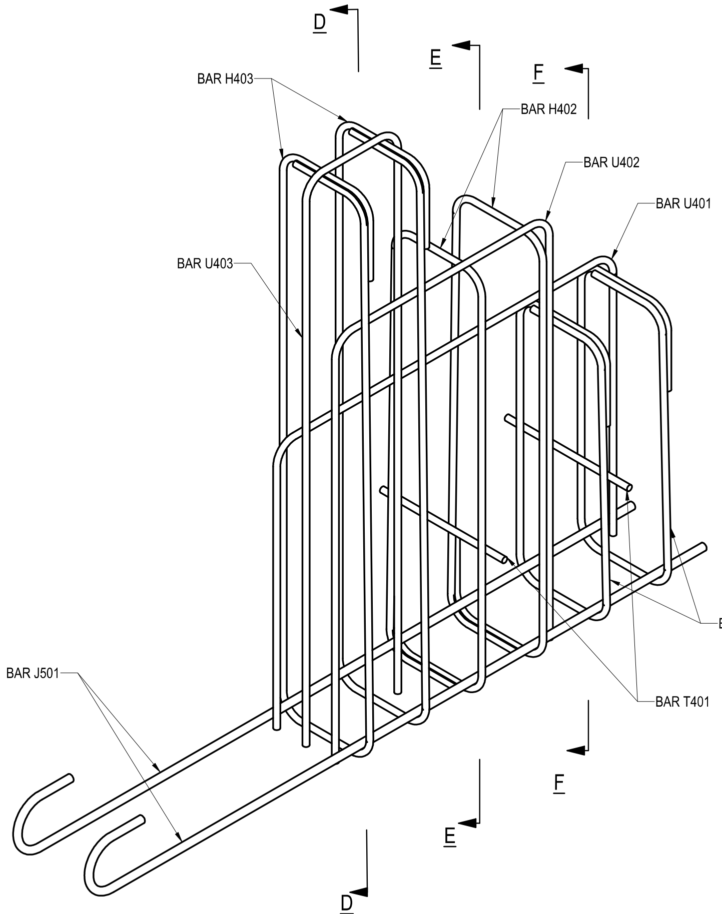

BUTTRESS REINFORCING CAGE
END A: WEST

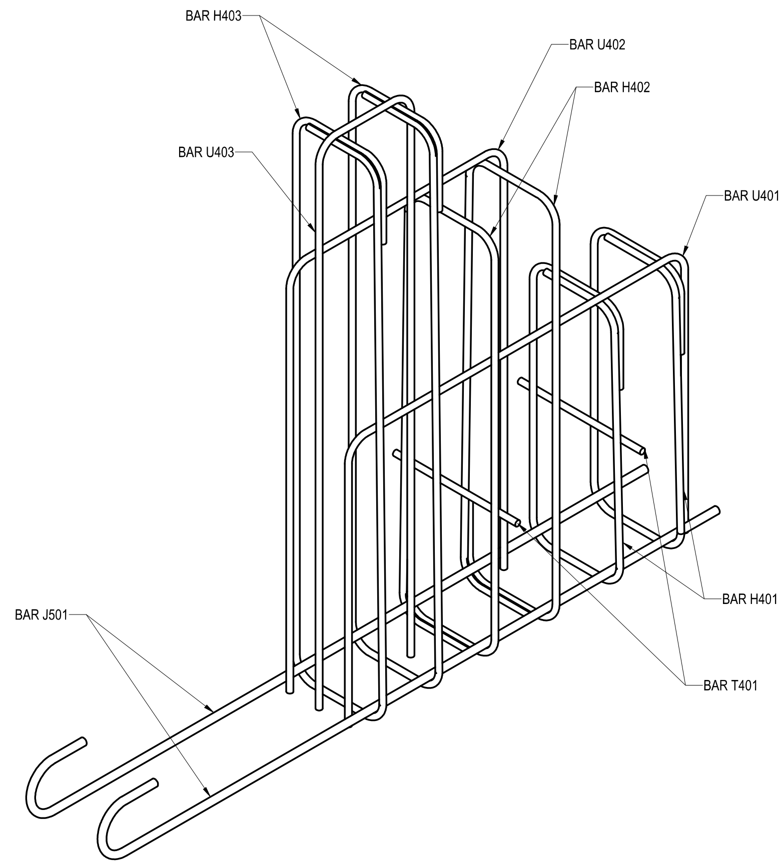

BUTTRESS REINFORCING CAGE
END B: EAST

0 12" 24"

FRC REINFORCED TEST SPECIMEN				*Revision:*
BUTTRESS REINFORCEMENT	*5/19/2020*	*University of Florida*	*SHEET 10 OF 18*	

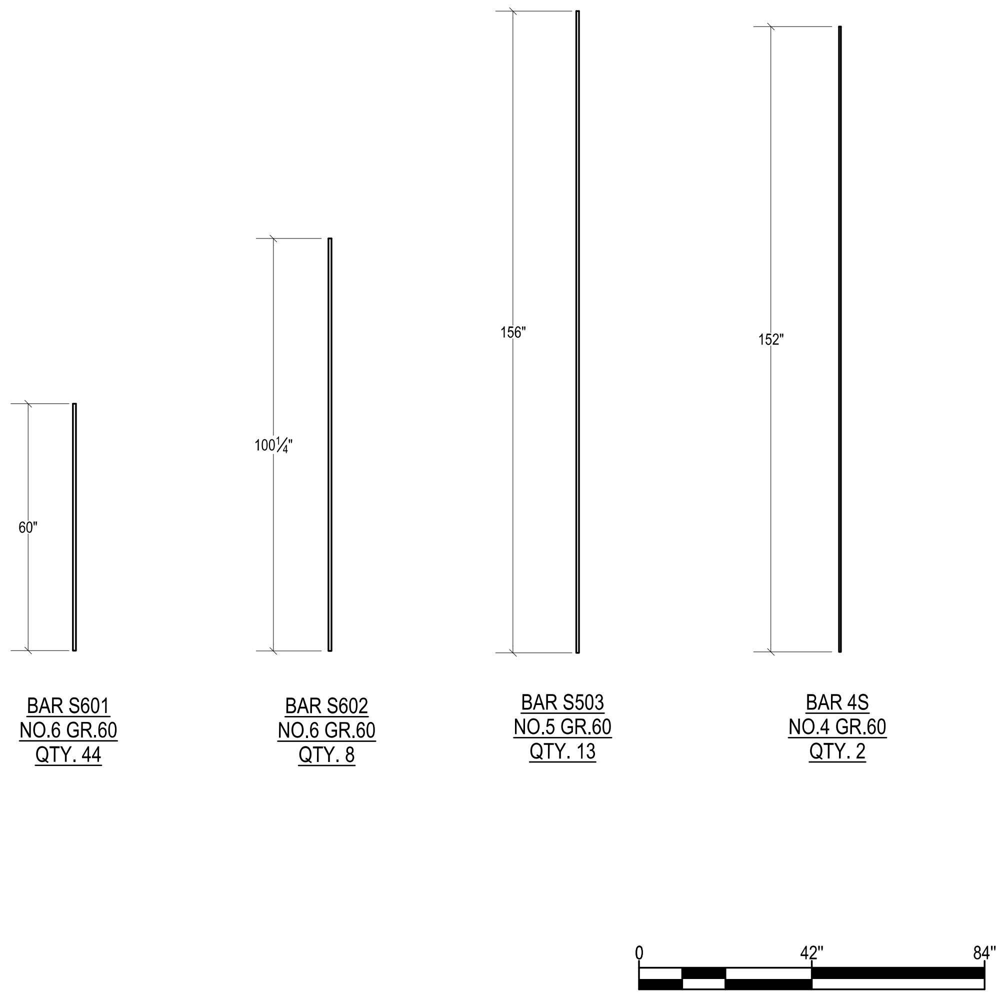

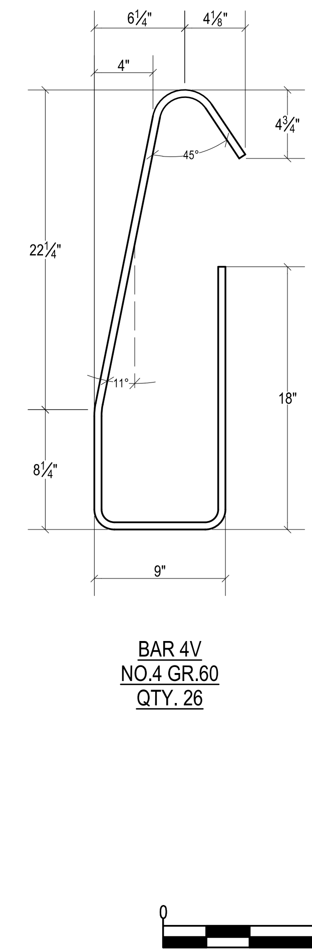

FRC REINFORCED TEST SPECIMEN				*Revision:*	
BAR LIST - SLAB	*5/19/2020*	*University of Florida*	*SHEET 11 OF 18*		

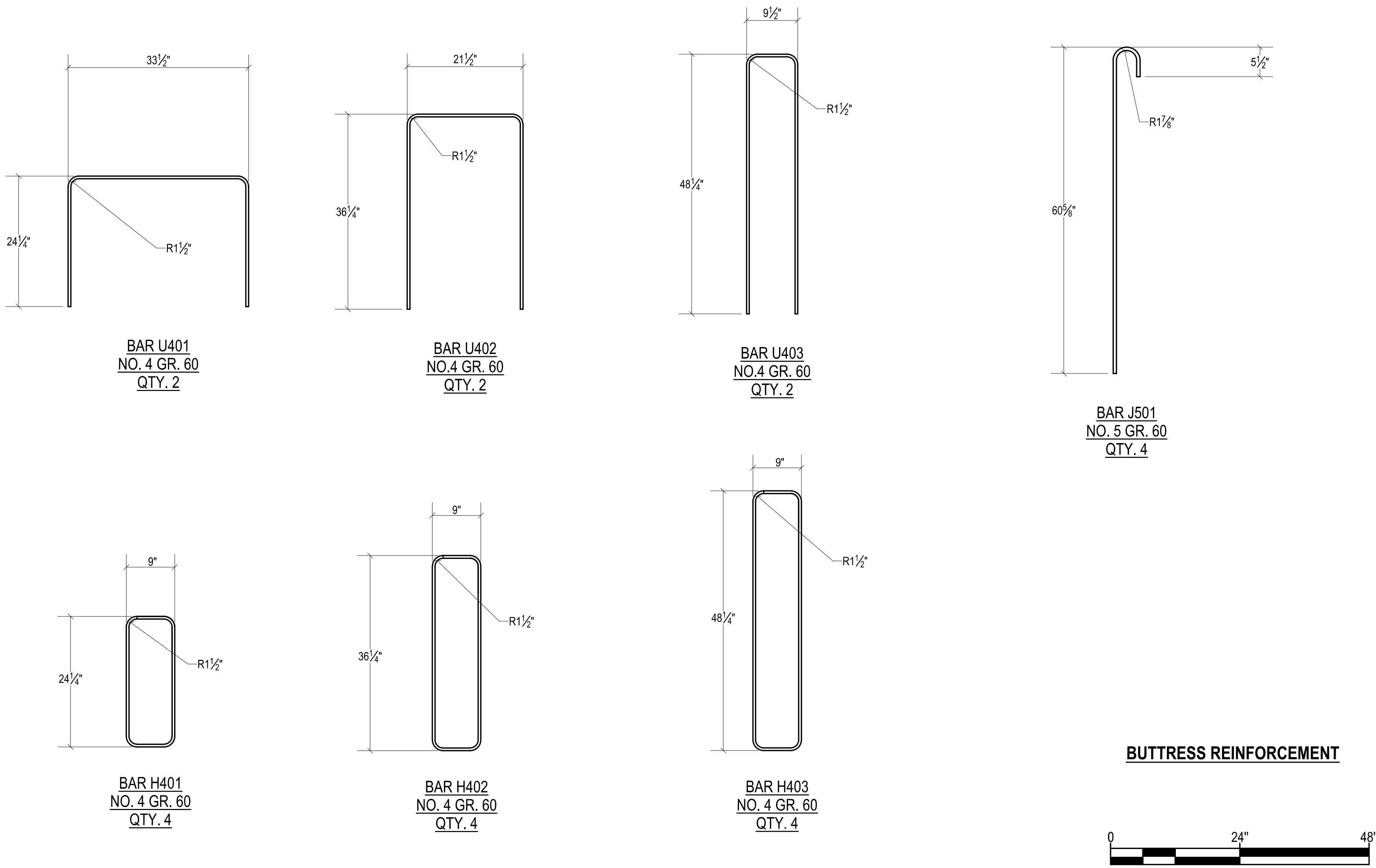

FRC REINFORCED TEST SPECIMEN				*Revision:*
BAR LIST - BUTTRESS	*5/19/2020*	*University of Florida*	*SHEET 12 OF 18*	

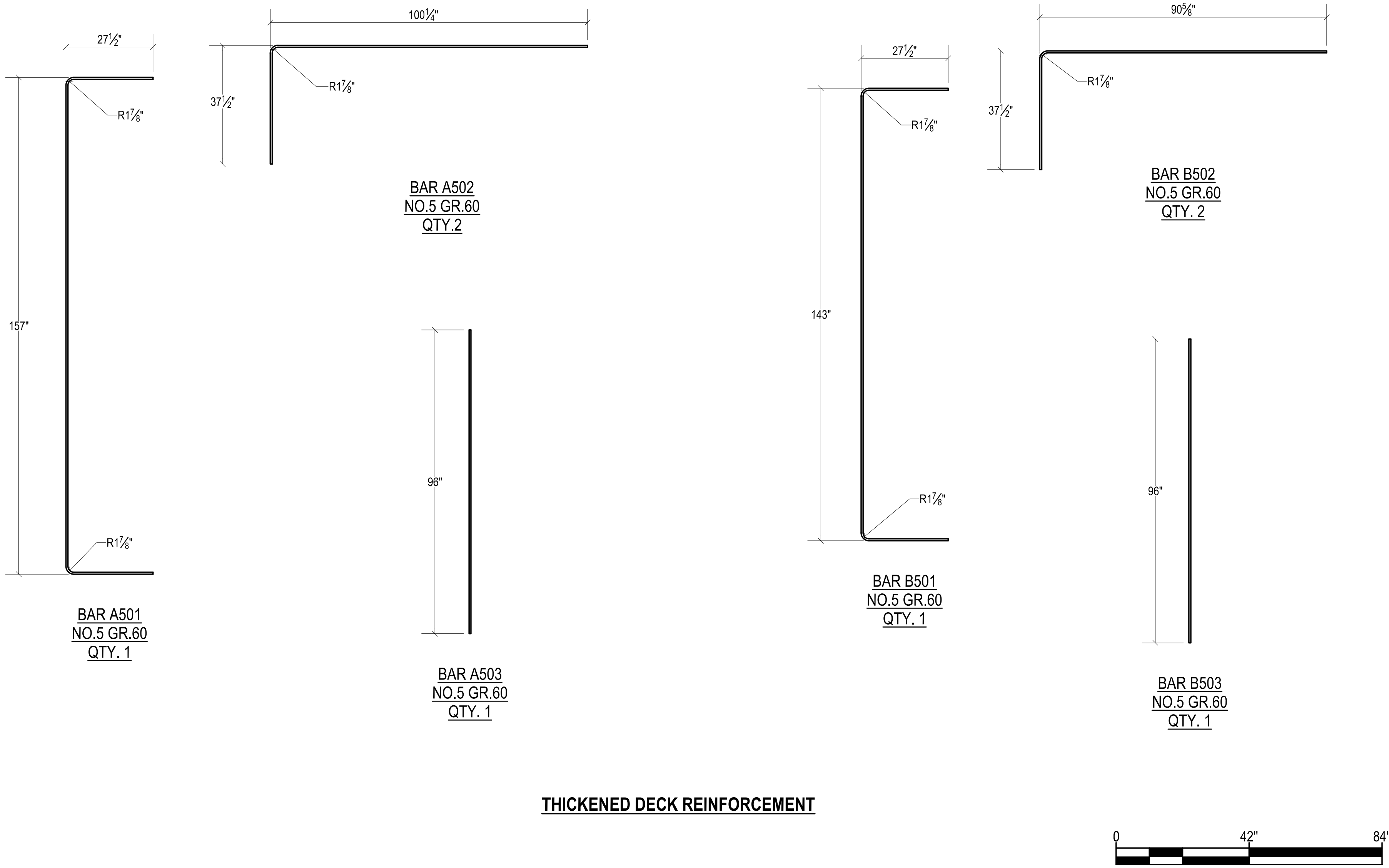

THICKENED DECK REINFORCEMENT

FRC REINFORCED TEST SPECIMEN				*Revision:*
BAR LIST - THICKENED DECK	*5/19/2020*	*University of Florida*	*SHEET 13 OF 18*	

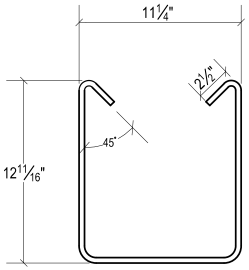

BAR S301
NO.3 GR.60
QTY. 24

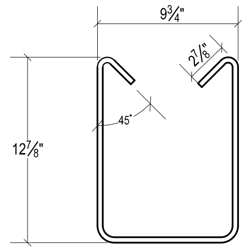

BAR S302
NO.3 GR.60
QTY. 6

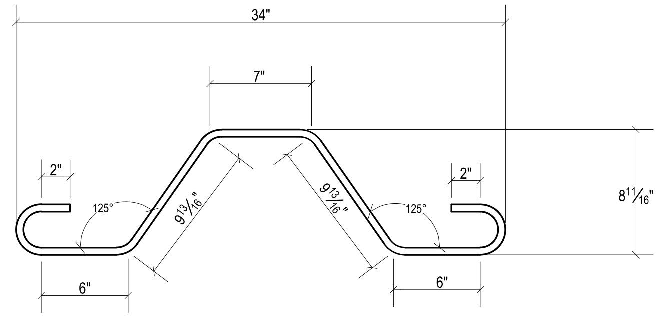

BAR S404
NO.4 GR.60
QTY. 4

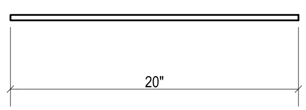

BAR S303
NO.3 GR.60
QTY. 2

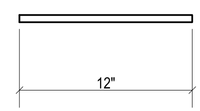

BAR T401
NO.4 GR.60
QTY. 4

THICKENED DECK REINFORCEMENT

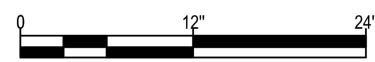

FRC REINFORCED TEST SPECIMEN				*Revision:*
BAR LIST - THICKENED DECK	*5/19/2020*	*University of Florida*	*SHEET 14 OF 18*	

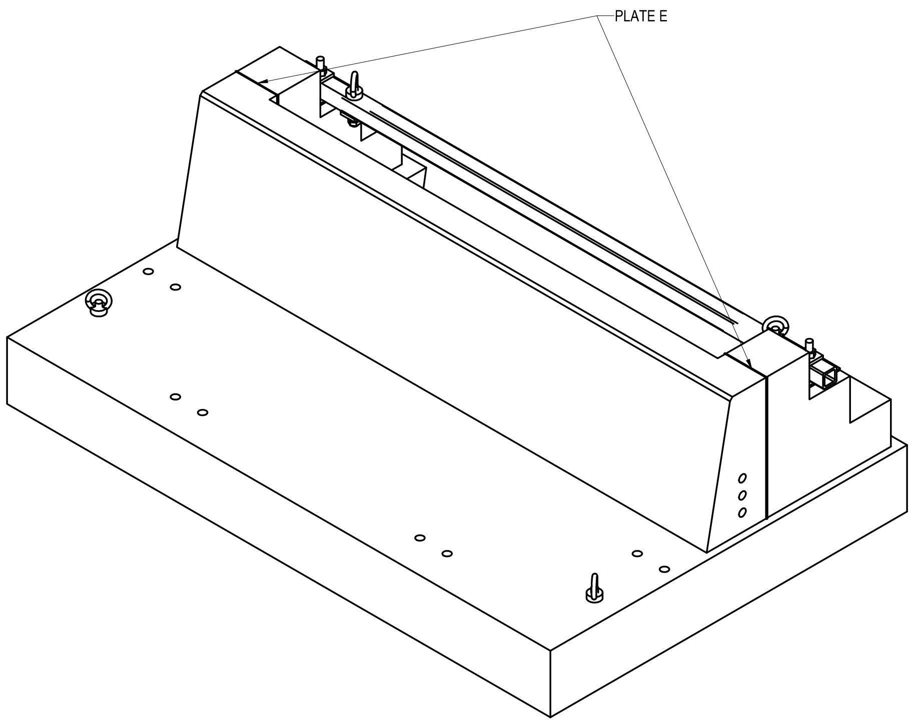

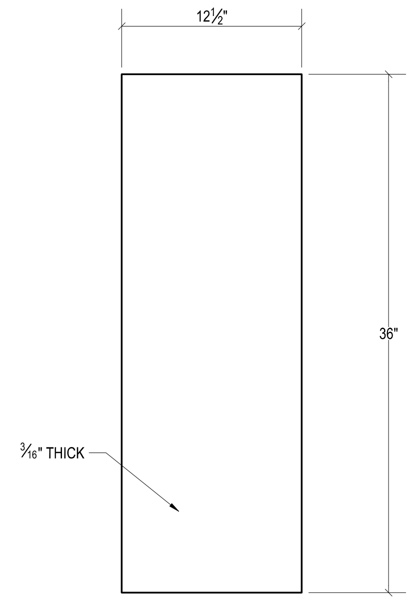

PLATE E
STEEL SEPARATION PLATE
A36
QTY. 2

0 12" 24"

FRC REINFORCED TEST SPECIMEN				Revision:
BUTTRESS-RAIL INTERFACE	*5/19/2020*	*University of Florida*	*SHEET 15 OF 18*	

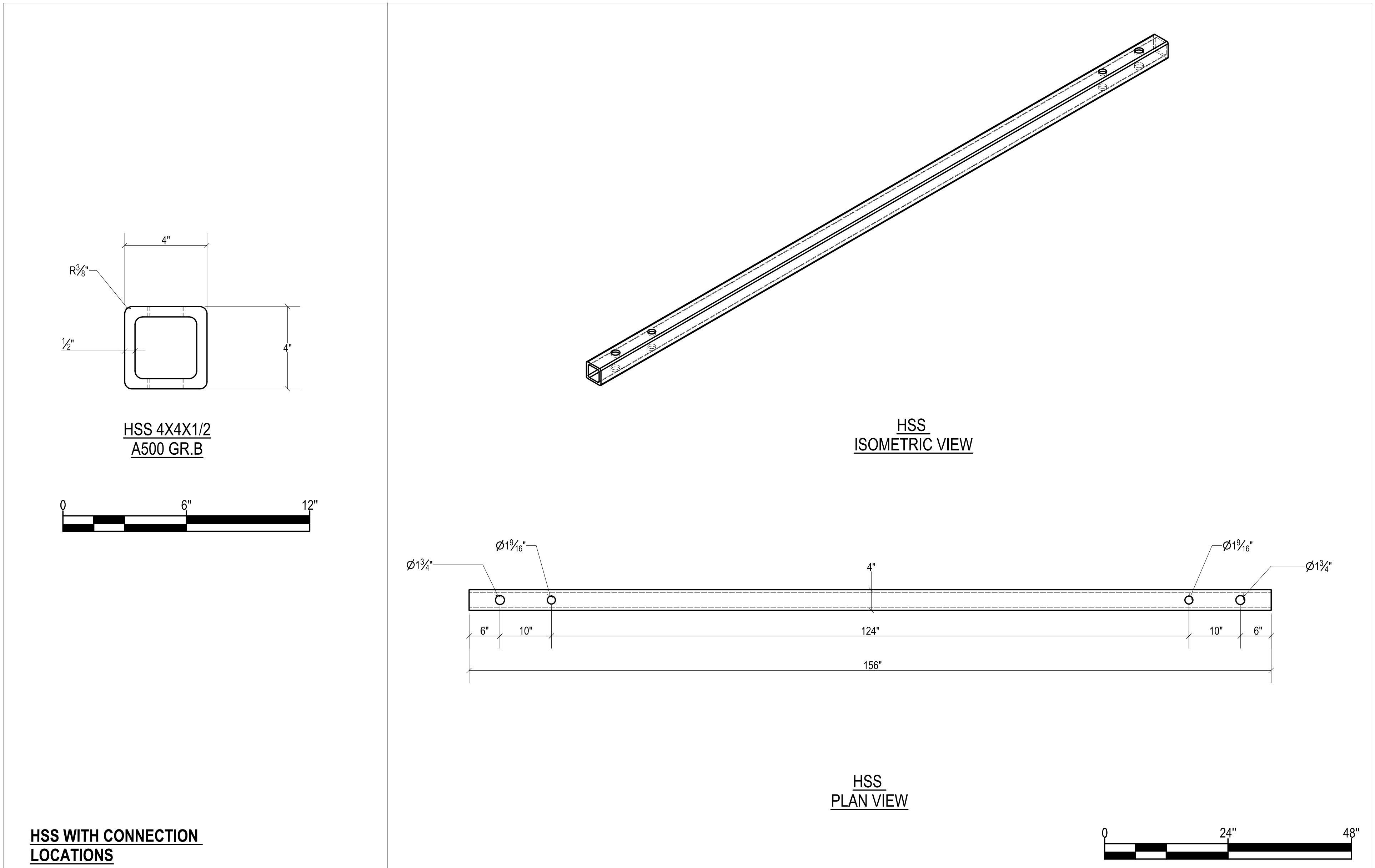

FRC REINFORCED TEST SPECIMEN				*Revision:*	
HSS DETAIL	*5/19/2020*	*University of Florida*	*SHEET 16 OF 18*		

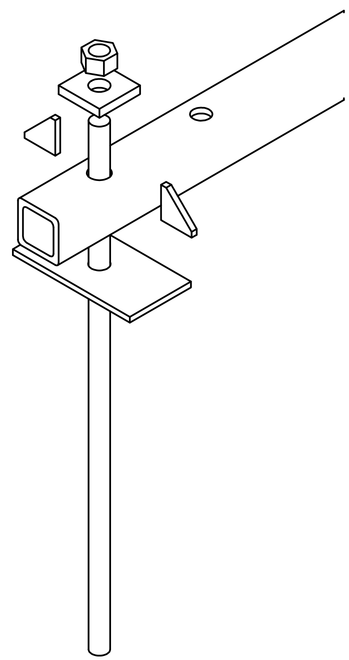

BUTTRESS ANCHOR ASSEMBLY

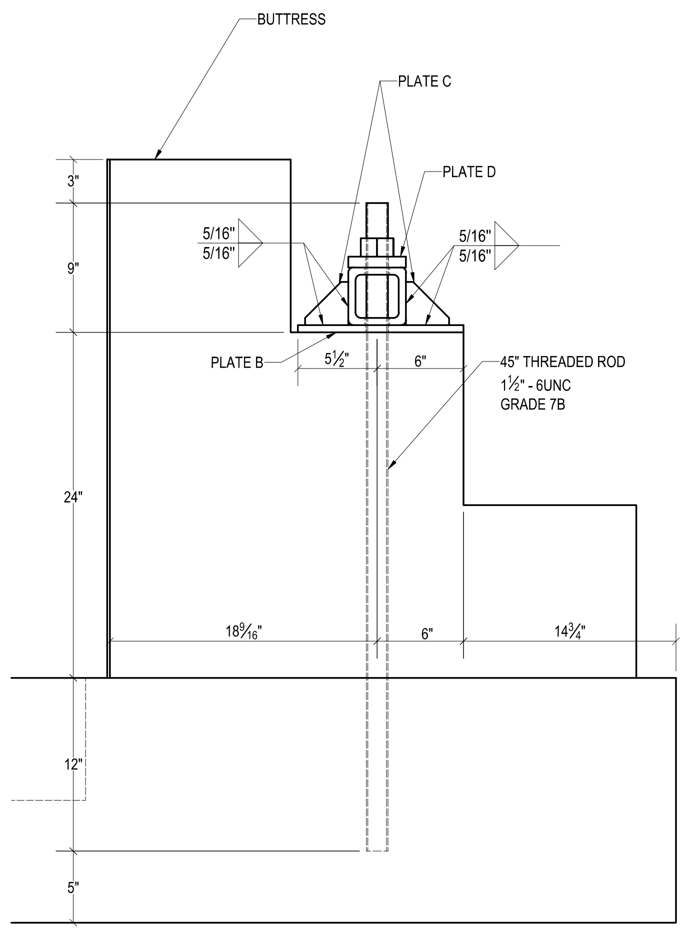

THREADED ROD ANCHOR CONNECTION

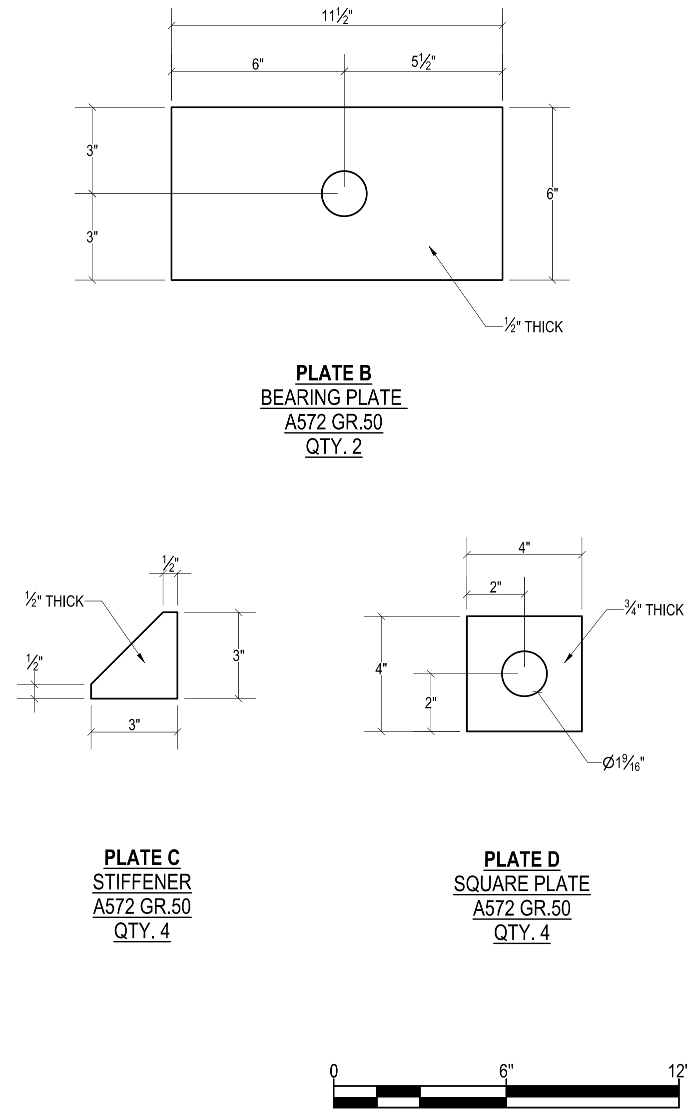

FRC REINFORCED TEST SPECIMEN				*Revision:*	
HSS-BUTTRESS CONNECTION	*5/19/2020*	*University of Florida*	*SHEET 17 OF 18*		

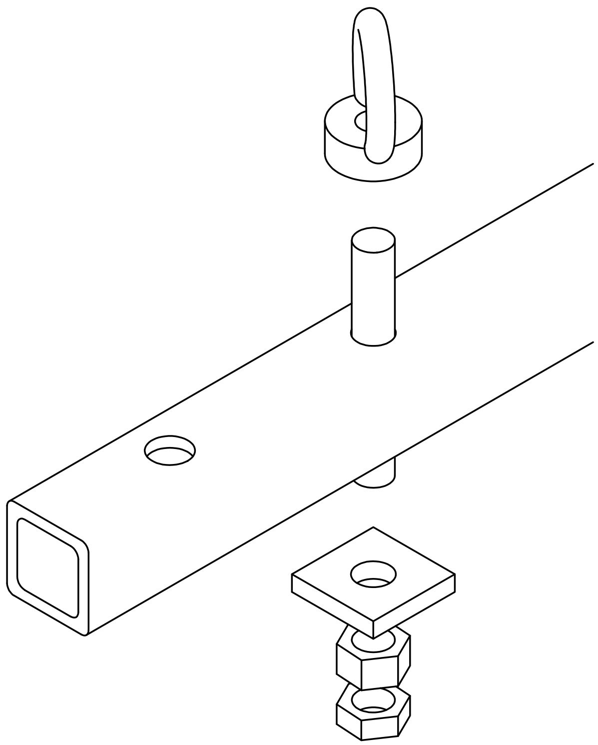

LIFTING EYE NUT ASSEMBLY

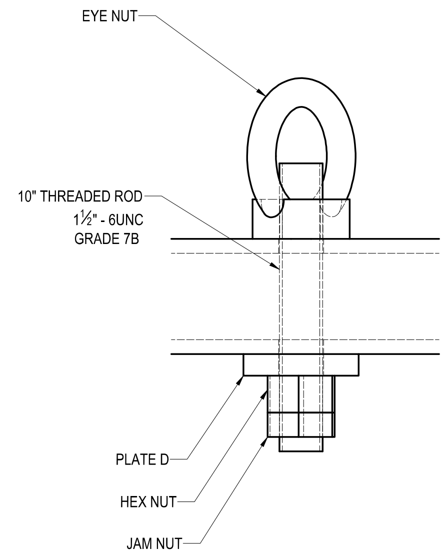

LIFTING EYE NUT CONNECTION

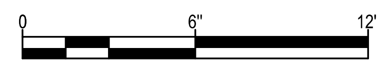

FRC REINFORCED TEST SPECIMEN				*Revision:*
HSS-LIFTING EYE BOLT CONNECTION	*5/19/2020*	*University of Florida*	*SHEET 18 OF 18*	

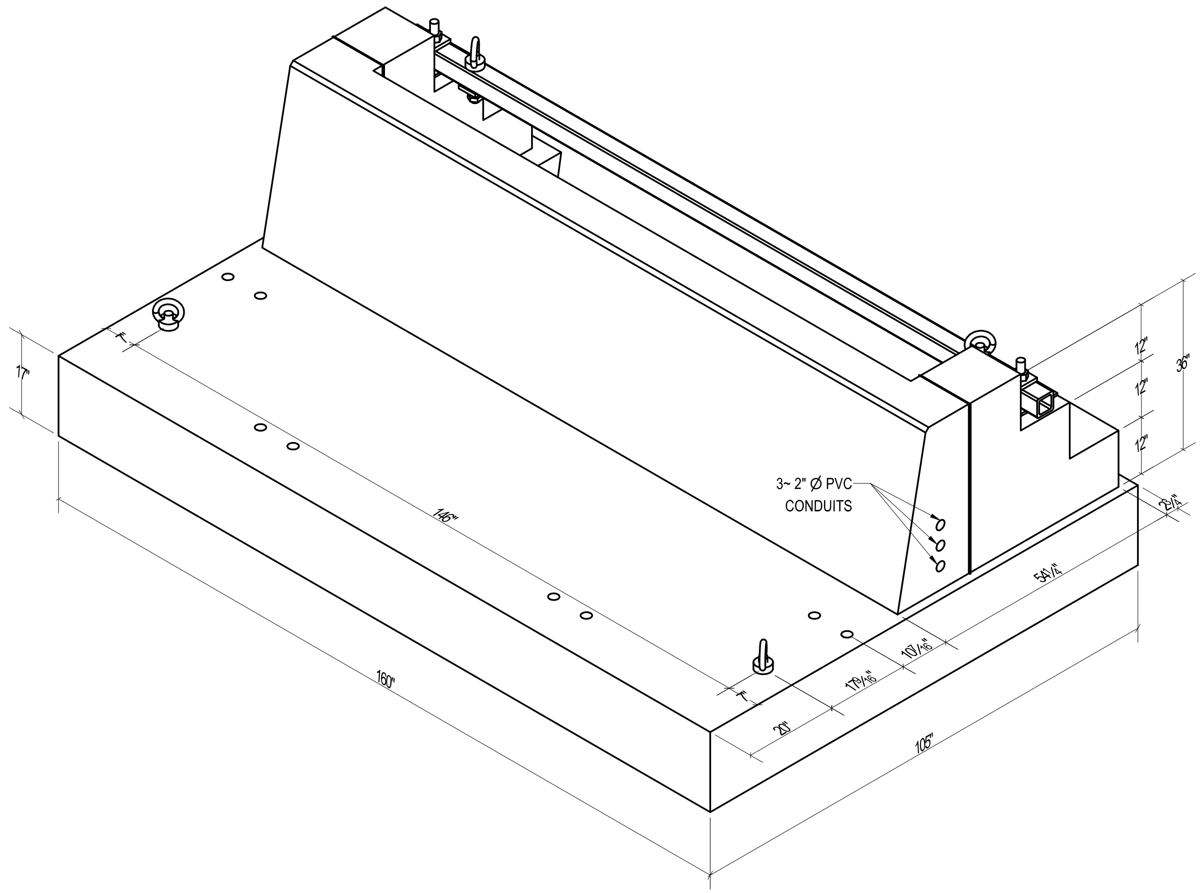

TEST SPECIMEN
FRONT ISOMETRIC VIEW

STEEL REINFORCED TEST SPECIMEN				*Revision:*		
TEST SPECIMEN OVERVIEW	*5/19/2020*	*University of Florida*	*SHEET 1 OF 18*			

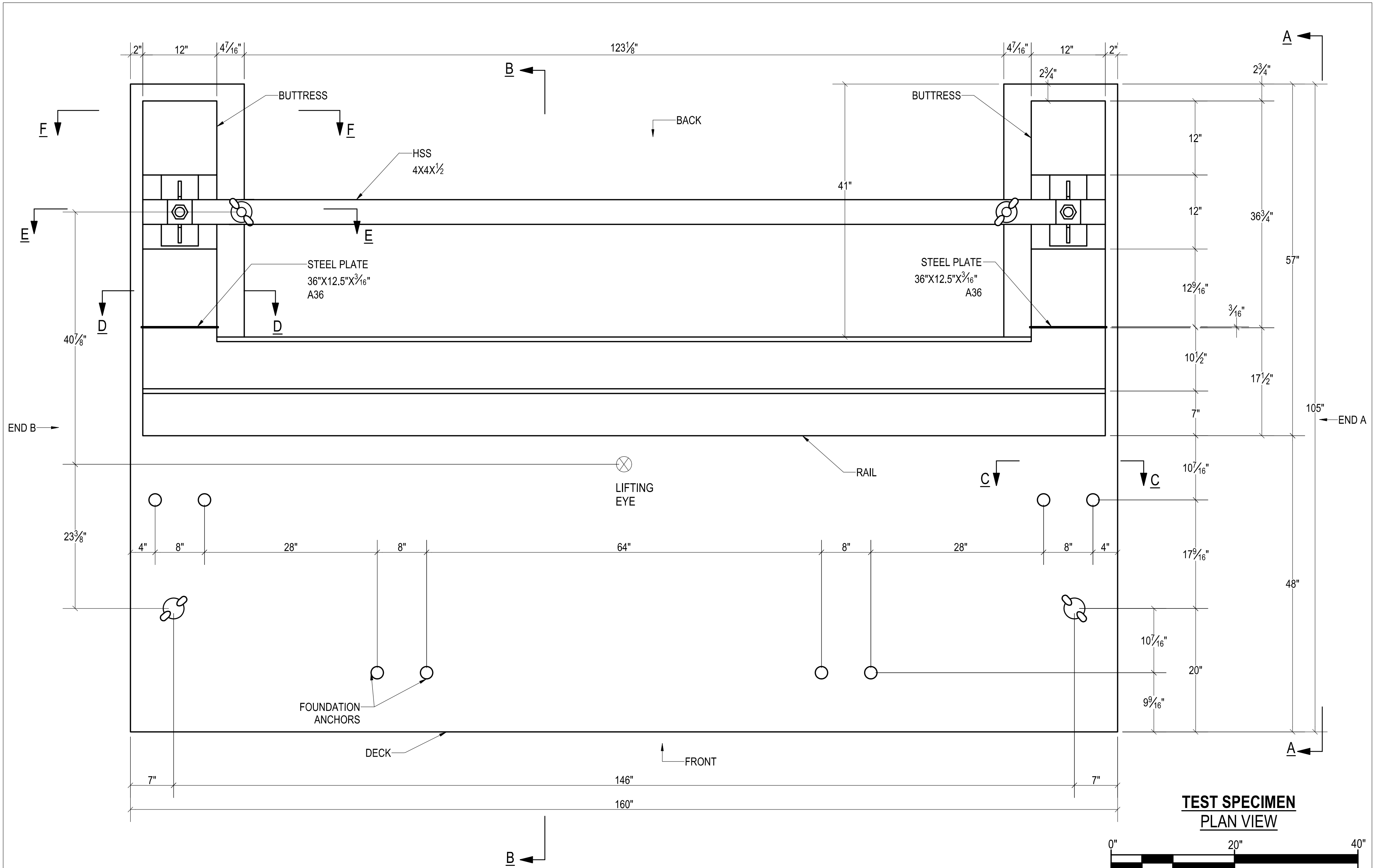

STEEL REINFORCED TEST SPECIMEN				*Revision:*
TEST SPECIMEN OVERVIEW	*5/19/2020*	*University of Florida*	*SHEET 2 OF 18*	

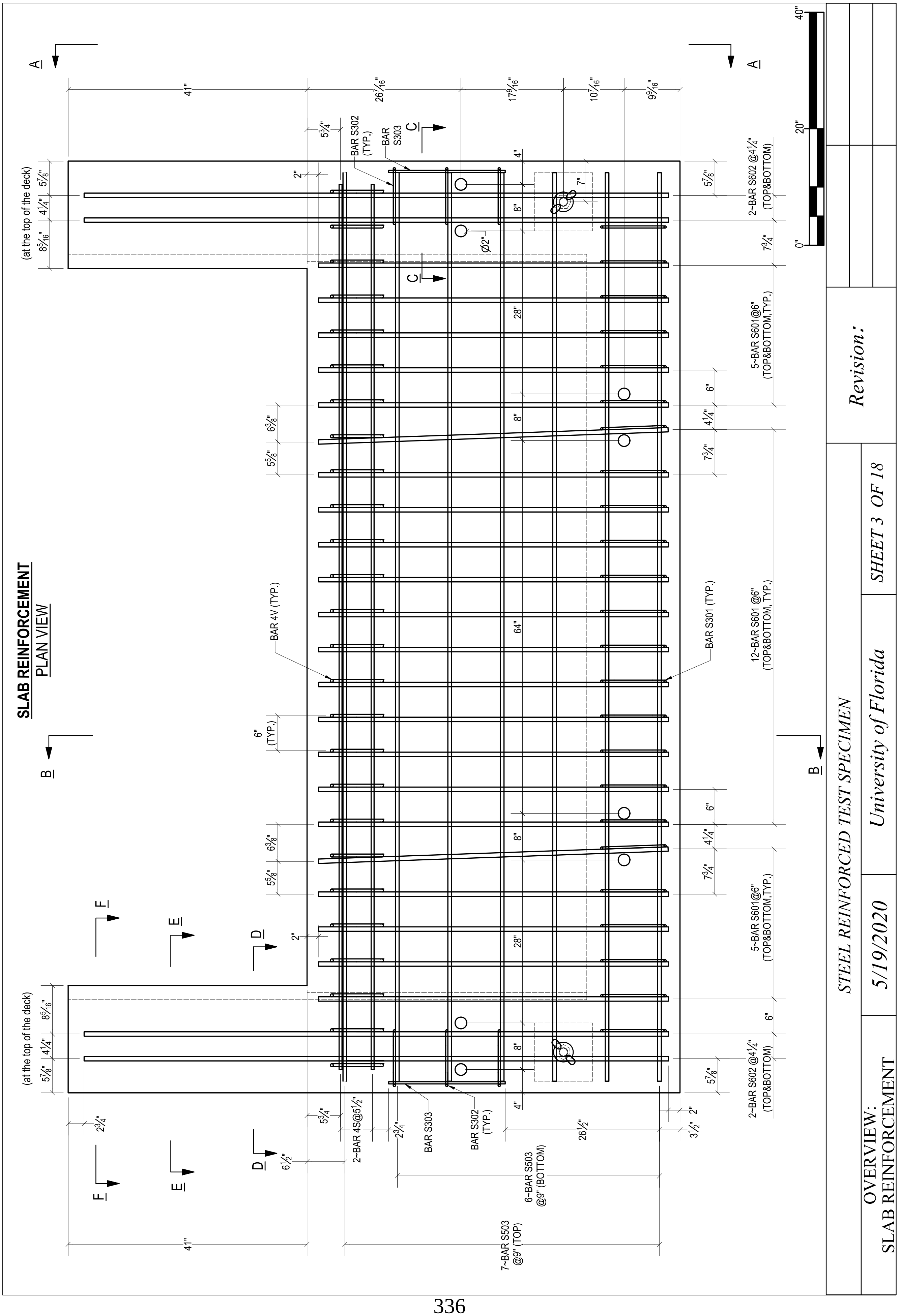
SLAB REINFORCEMENT
PLAN VIEW
(at the top of the deck)
BAR S302 (TYP.)
BAR S303
BAR 4V (TYP.)
BAR S301 (TYP.)
2~BAR S602 @4¼" (TOP&BOTTOM)
5~BAR S601@6" (TOP&BOTTOM,TYP.)
12~BAR S601 @6" (TOP&BOTTOM, TYP.)
2~BAR 4S@5½"
6~BAR S503 @9" (BOTTOM)
7~BAR S503 @9" (TOP)
Ø2"
41"
28"
64"
26½"
STEEL REINFORCED TEST SPECIMEN
University of Florida
5/19/2020
SHEET 3 OF 18
Revision:
OVERVIEW:
SLAB REINFORCEMENT

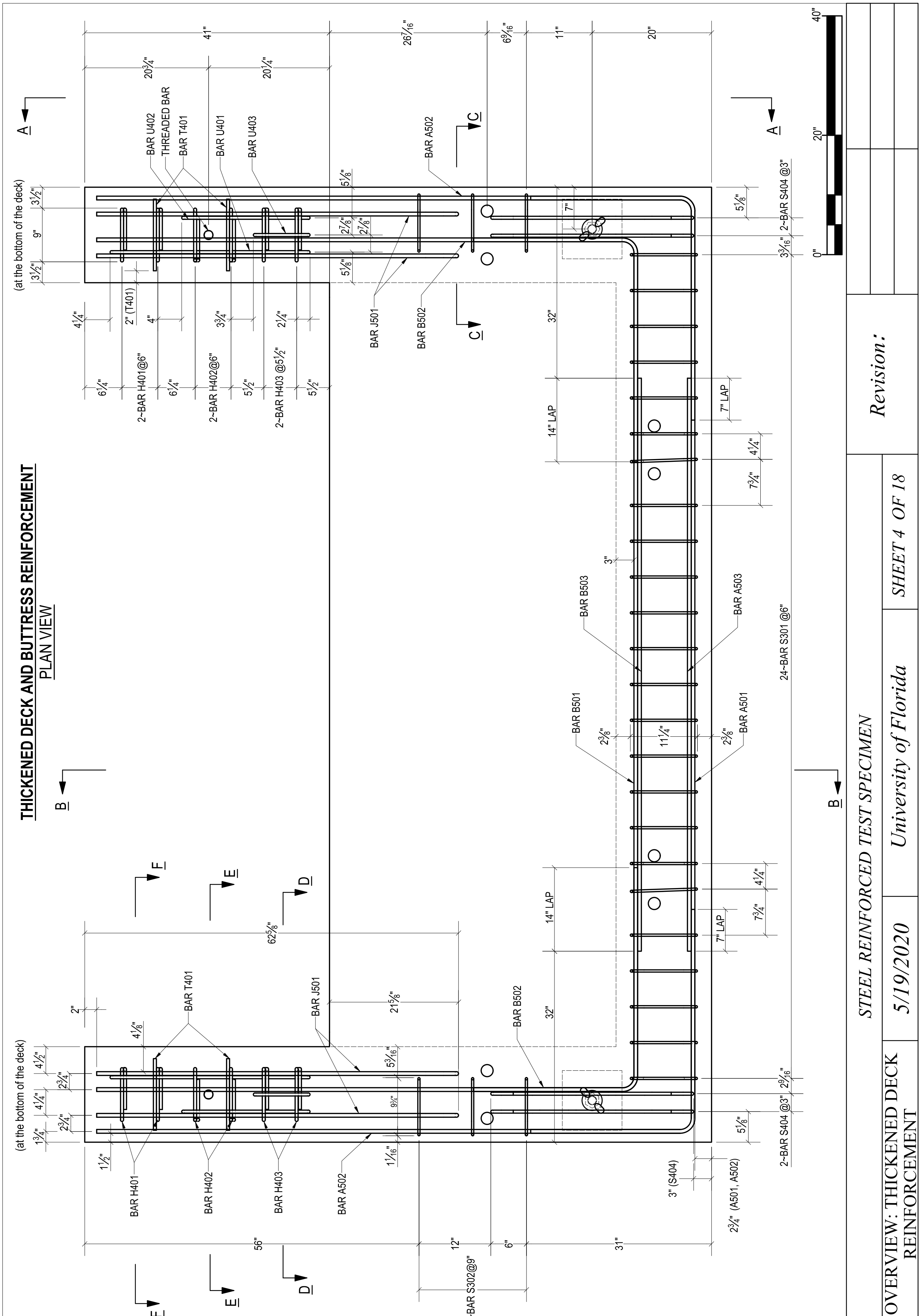
THICKENED DECK AND BUTTRESS REINFORCEMENT
PLAN VIEW
BAR U402
THREADED BAR
BAR T401
BAR U401
BAR U403
BAR A502
BAR J501
BAR B502
BAR B503
BAR A503
BAR B501
BAR A501
BAR H401
BAR H402
BAR H403
2~BAR H401@6"
2~BAR H402@6"
2~BAR H403 @5½"
2~BAR S404 @3"
24~BAR S301 @6"
3~BAR S302@9"
14" LAP
7" LAP
(at the bottom of the deck)
STEEL REINFORCED TEST SPECIMEN
University of Florida
5/19/2020
SHEET 4 OF 18
Revision:
OVERVIEW: THICKENED DECK REINFORCEMENT

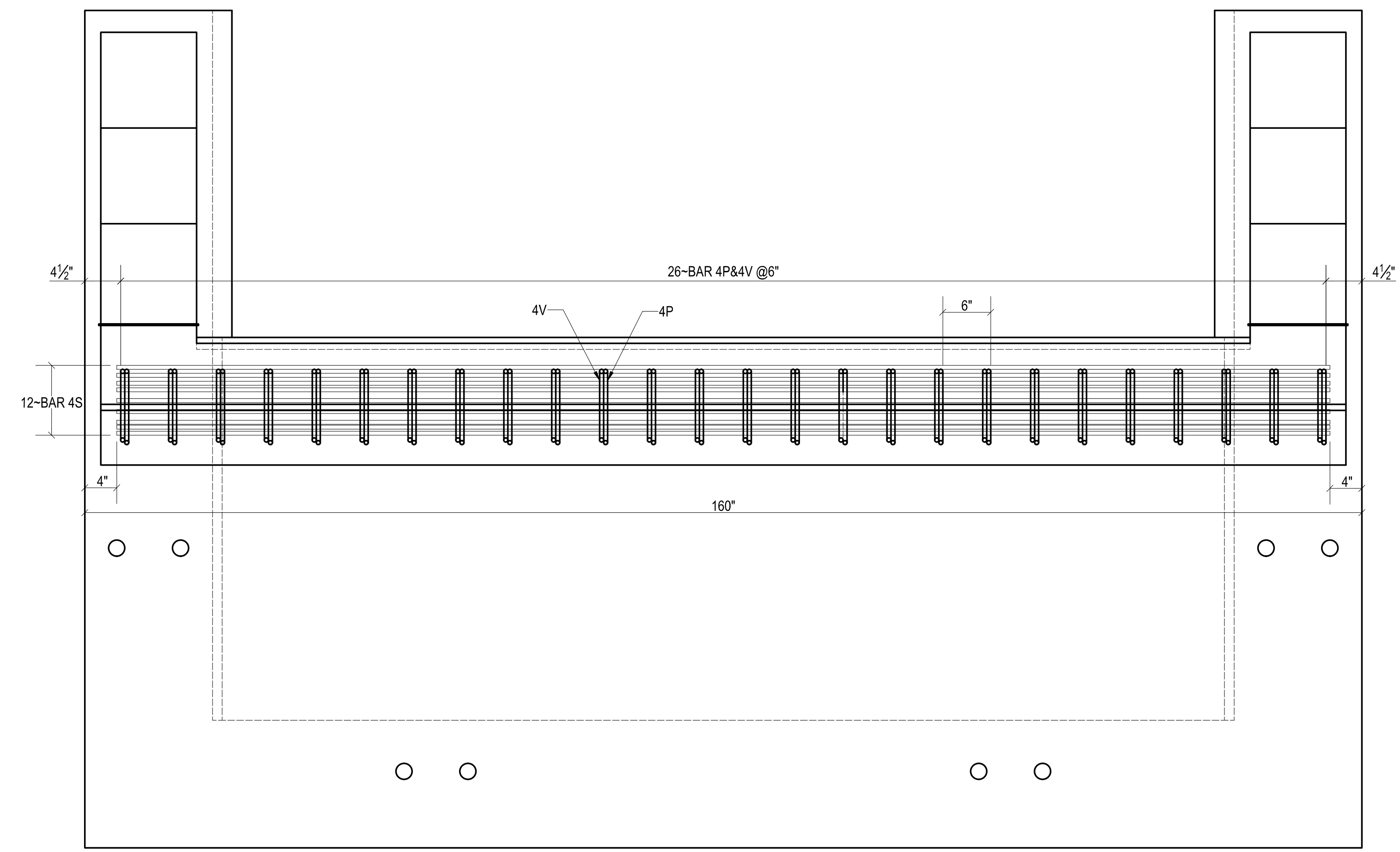

RAIL REINFORCEMENT
(PLAN VIEW)

STEEL REINFORCED TEST SPECIMEN				*Revision:*
RAILING REINFORCEMENT: OVERVIEW	*5/19/2020*	*University of Florida*	*SHEET 5 OF 18*	

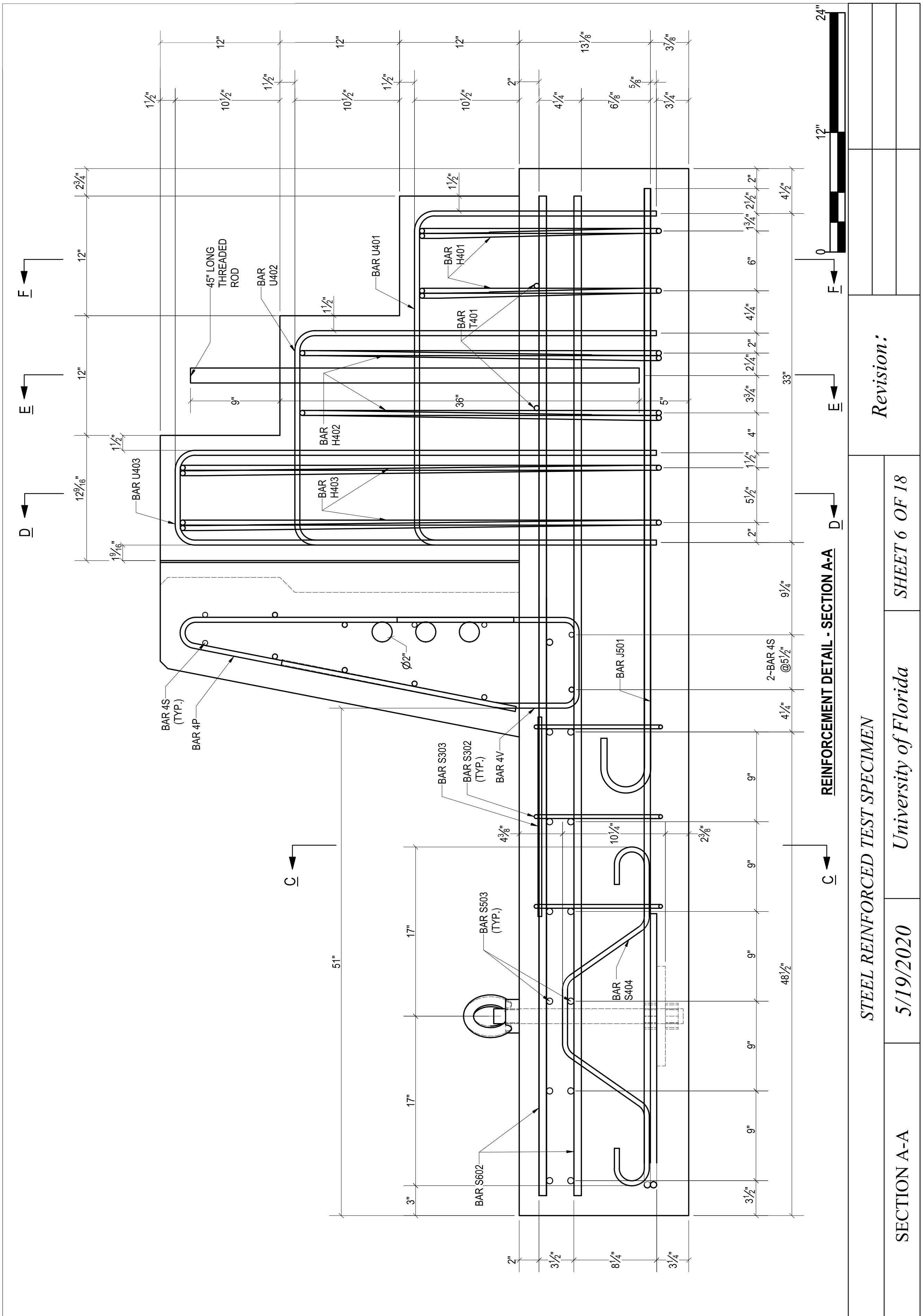
REINFORCEMENT DETAIL - SECTION A-A
45" LONG THREADED ROD
BAR U401
BAR U402
BAR U403
BAR H401
BAR H402
BAR H403
BAR T401
BAR 4S (TYP.)
BAR 4P
BAR 4V
BAR J501
2~BAR 4S @5½"
BAR S302 (TYP.)
BAR S303
BAR S503 (TYP.)
BAR S404
BAR S602
Ø2"
STEEL REINFORCED TEST SPECIMEN
University of Florida
5/19/2020
SECTION A-A
SHEET 6 OF 18
Revision:

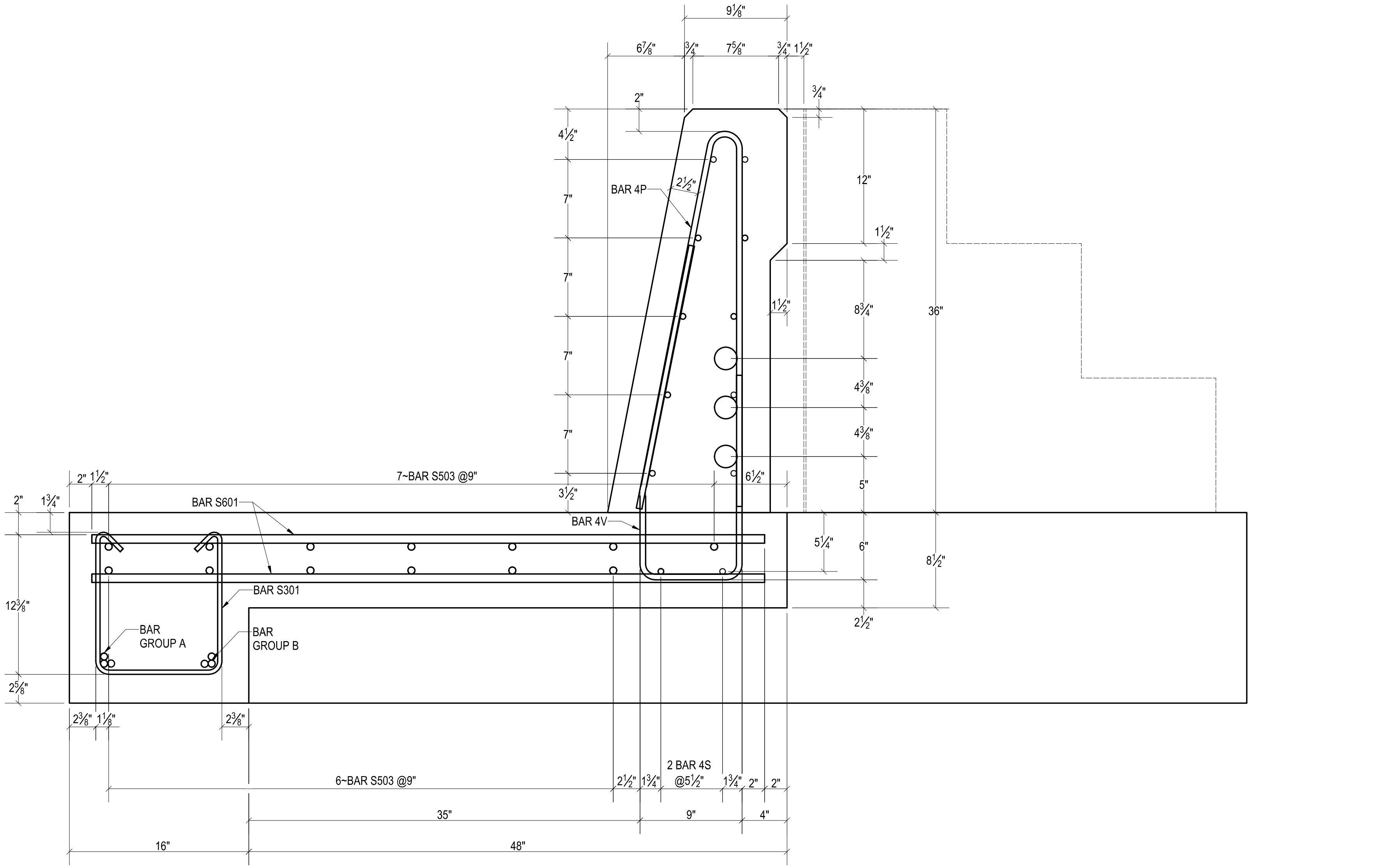

RAIL AND SLAB REINFORCEMENT DETAIL - SECTION B-B

STEEL REINFORCED TEST SPECIMEN				Revision:
SECTION B-B	5/19/2020	University of Florida	SHEET 7 OF 18	

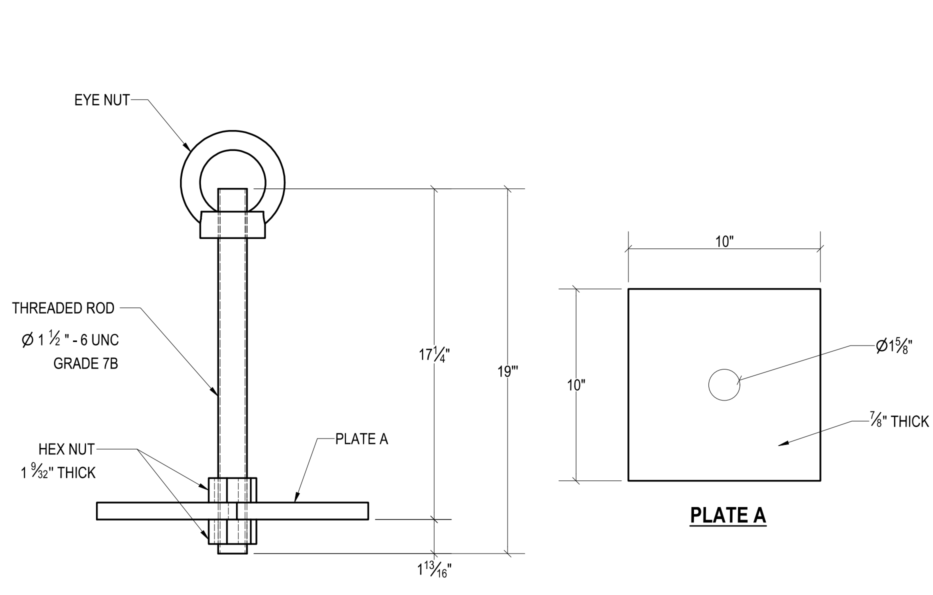

ANCHOR AND PLATE CONNECTION

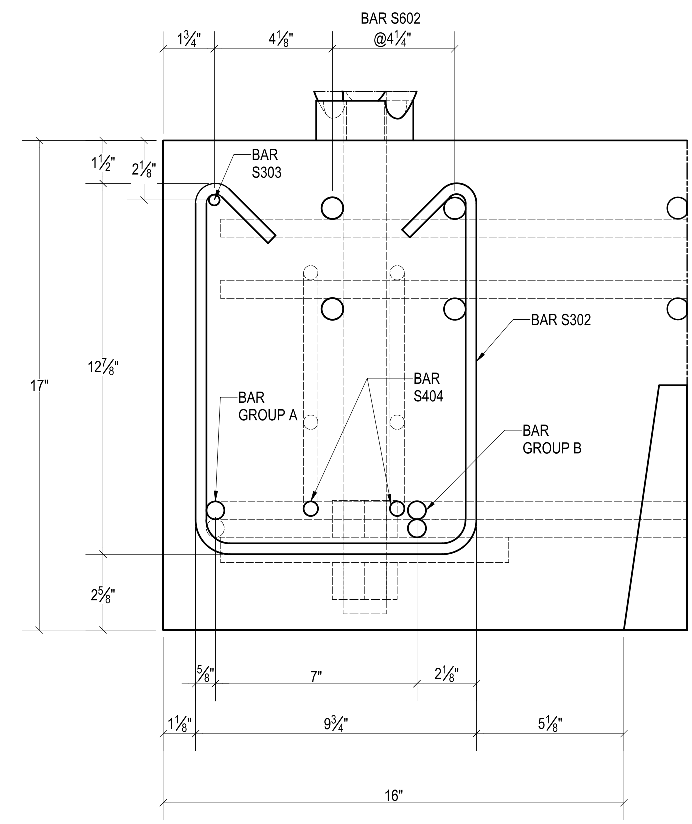

THICKENED EDGE
SECTION C-C

STEEL REINFORCED TEST SPECIMEN				Revision:
ANCHOR PLATE AND SECTION C-C	5/19/2020	University of Florida	SHEET 8 OF 18	

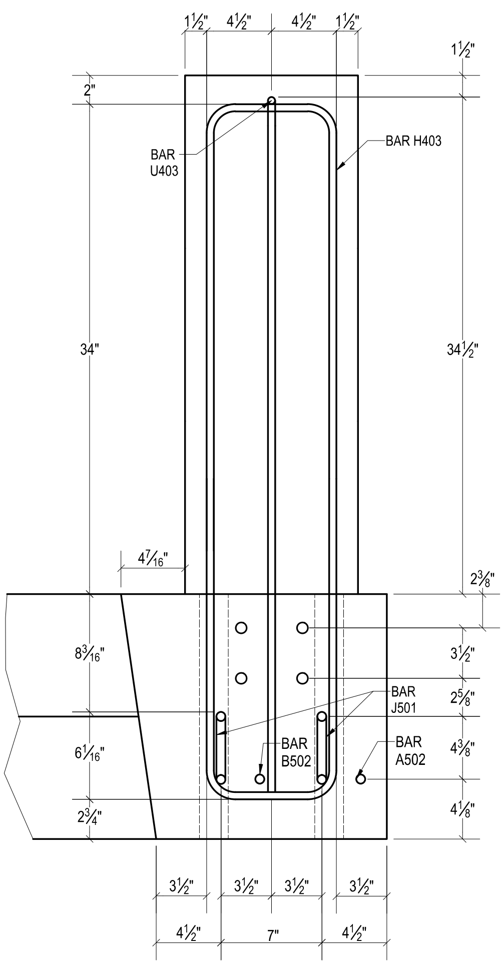

BUTTRESS REINFORCEMENT
SECTION D-D

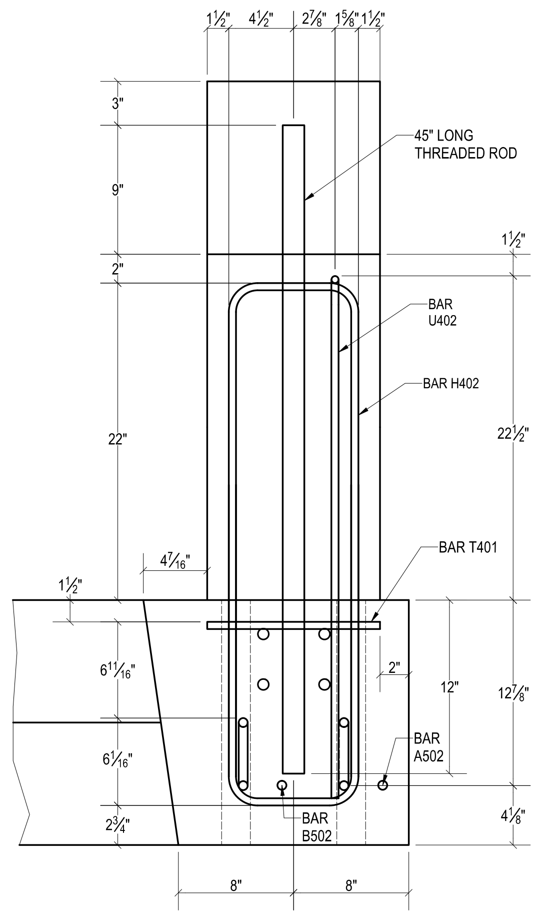

BUTTRESS REINFORCEMENT
SECTION E-E

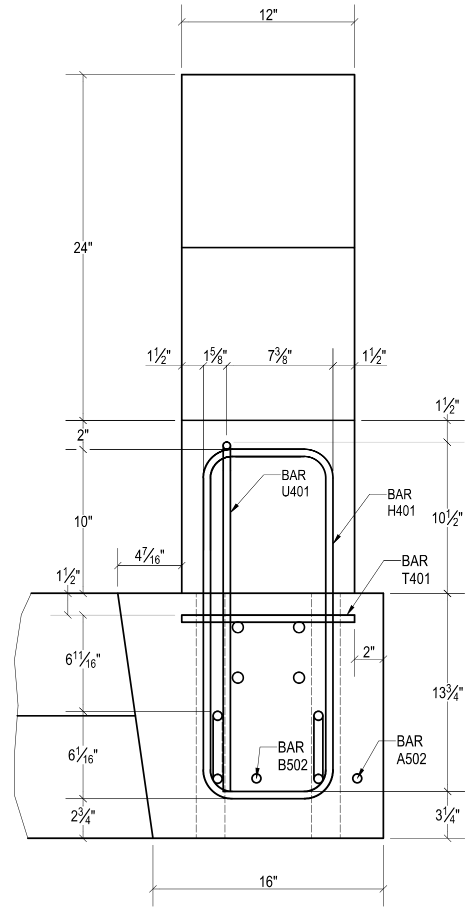

BUTTRESS REINFORCEMENT
SECTION F-F

STEEL REINFORCED TEST SPECIMEN				*Revision:*
SECTION D, E, F: BUTTRESS REINFORCEMENT	*5/19/2020*	*University of Florida*	*SHEET 9 OF 18*	

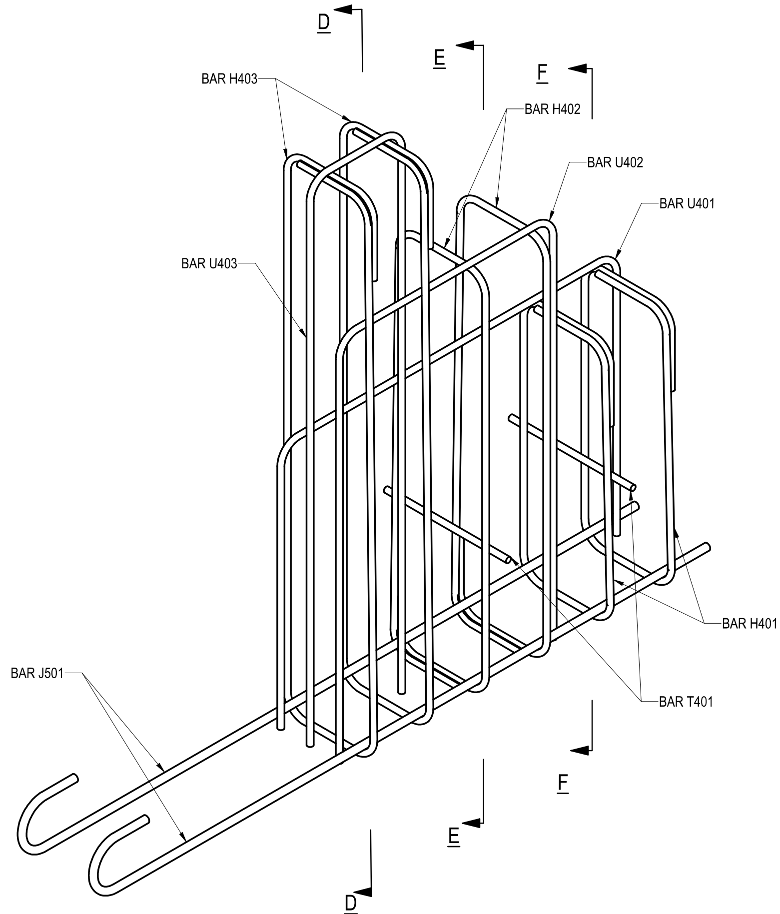

BUTTRESS REINFORCING CAGE
END A: WEST

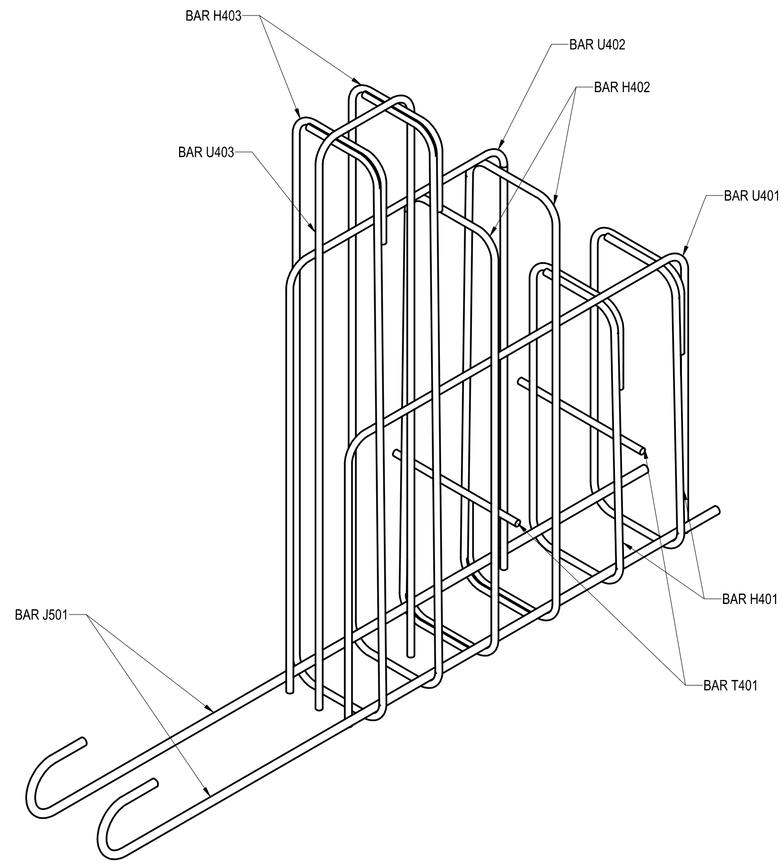

BUTTRESS REINFORCING CAGE
END B: EAST

0 12" 24"

STEEL REINFORCED TEST SPECIMEN				*Revision:*
BUTTRESS REINFORCEMENT	*5/19/2020*	*University of Florida*	*SHEET 10 OF 18*	

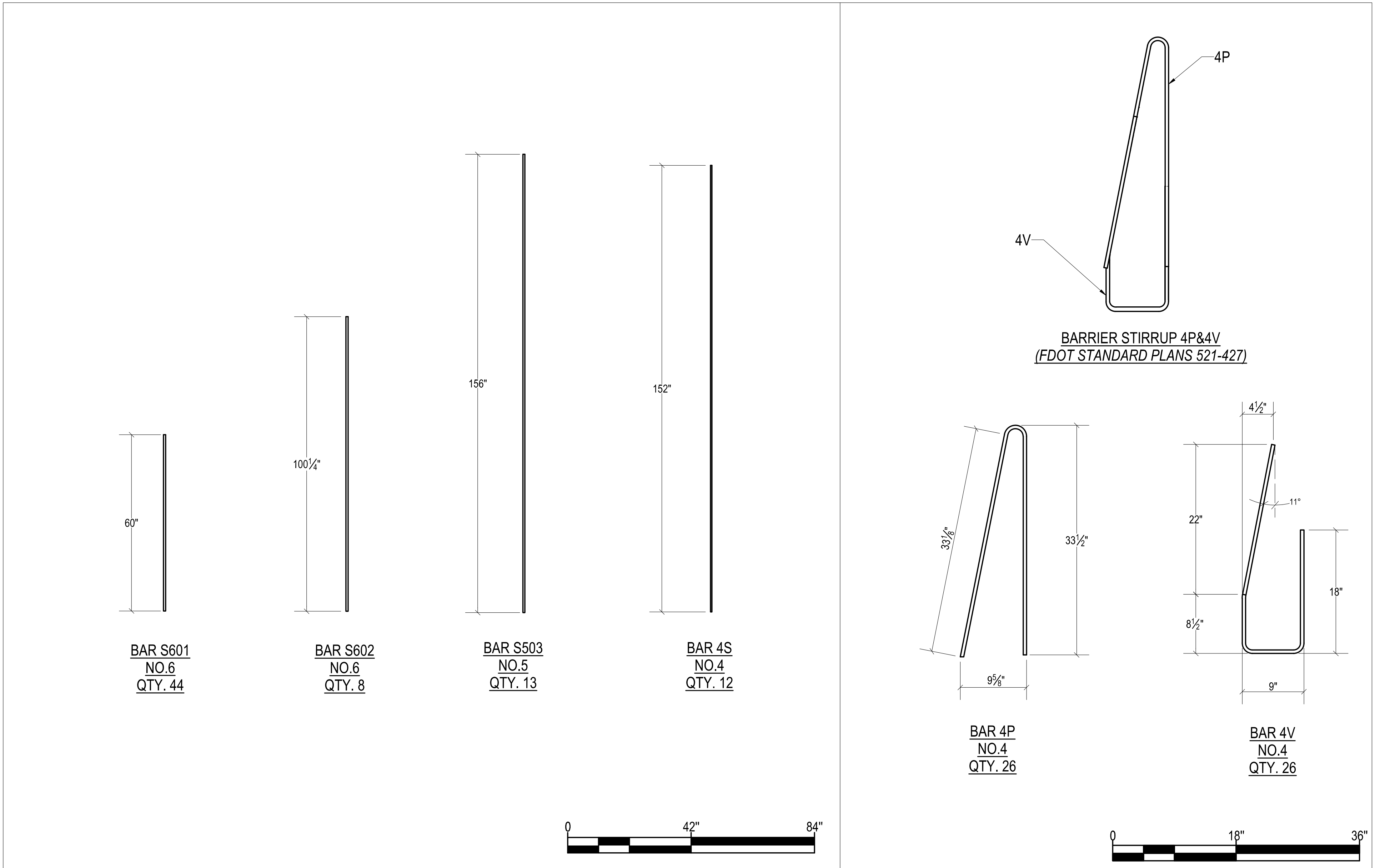

STEEL REINFORCED TEST SPECIMEN				Revision:
BAR LIST - SLAB	5/19/2020	University of Florida	SHEET 11 OF 18	

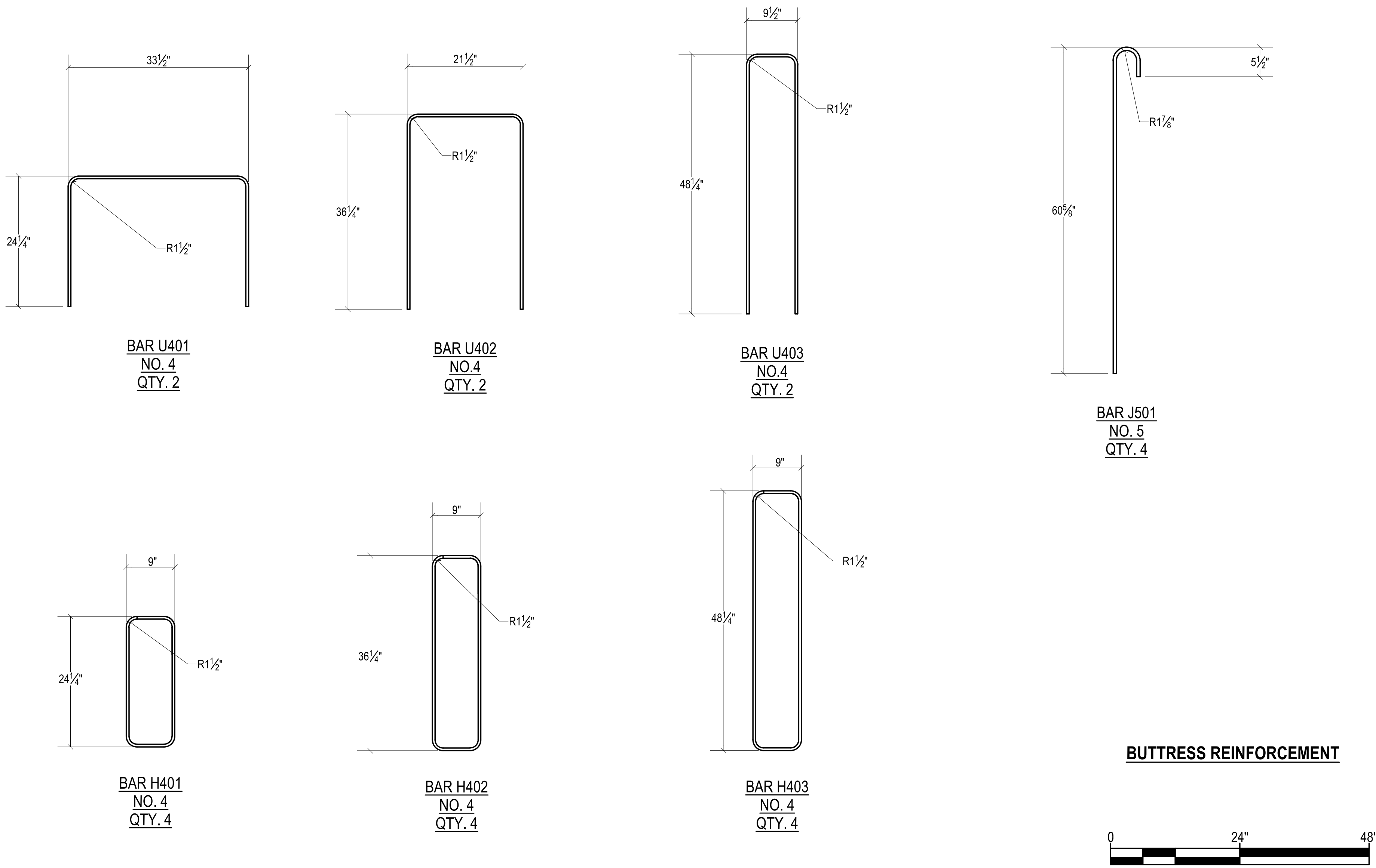

STEEL REINFORCED TEST SPECIMEN				*Revision:*
BAR LIST - BUTTRESS	*5/19/2020*	*University of Florida*	*SHEET 12 OF 18*	

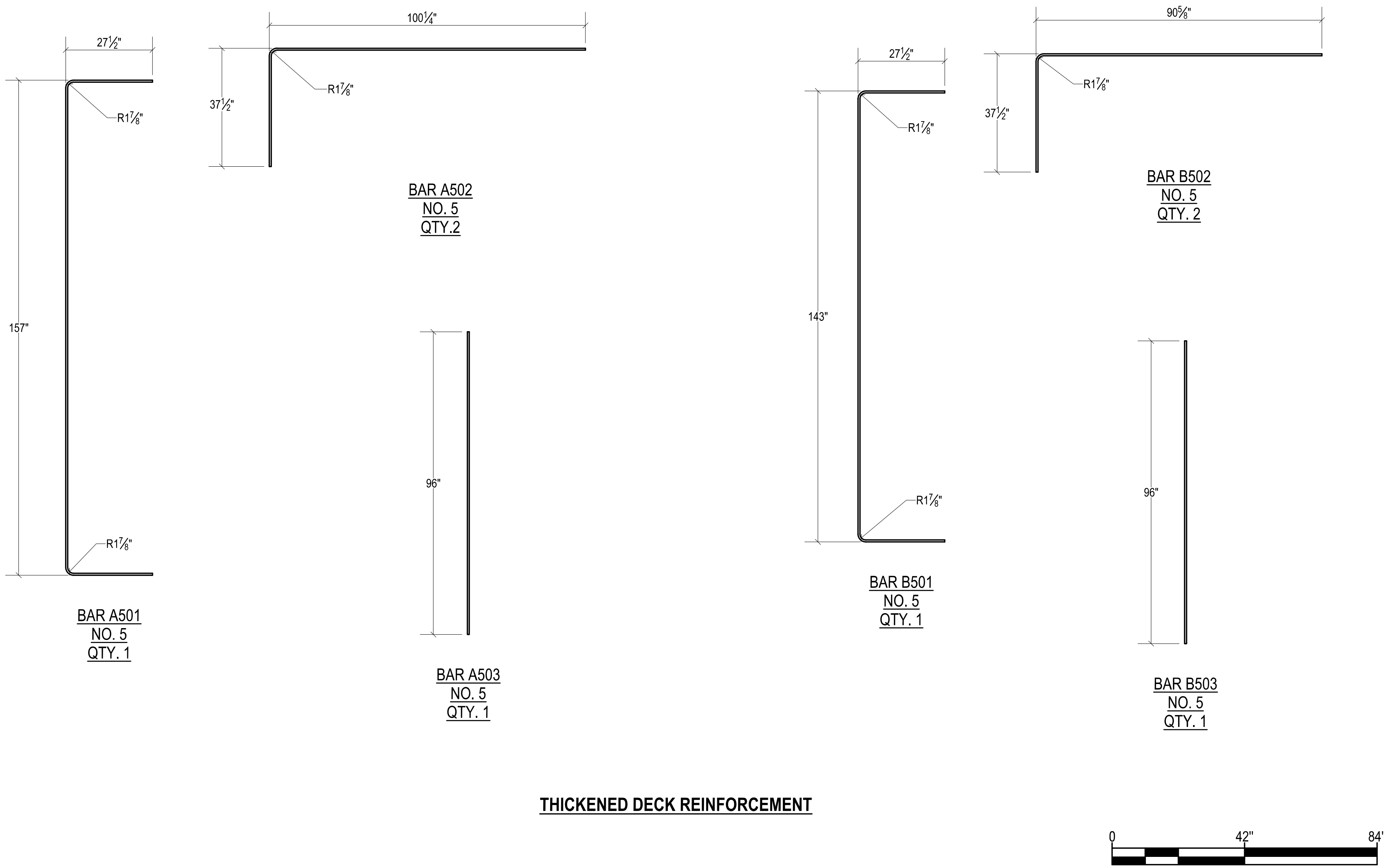

THICKENED DECK REINFORCEMENT

STEEL REINFORCED TEST SPECIMEN				*Revision:*
BAR LIST - THICKENED DECK	*5/19/2020*	*University of Florida*	*SHEET 13 OF 18*	

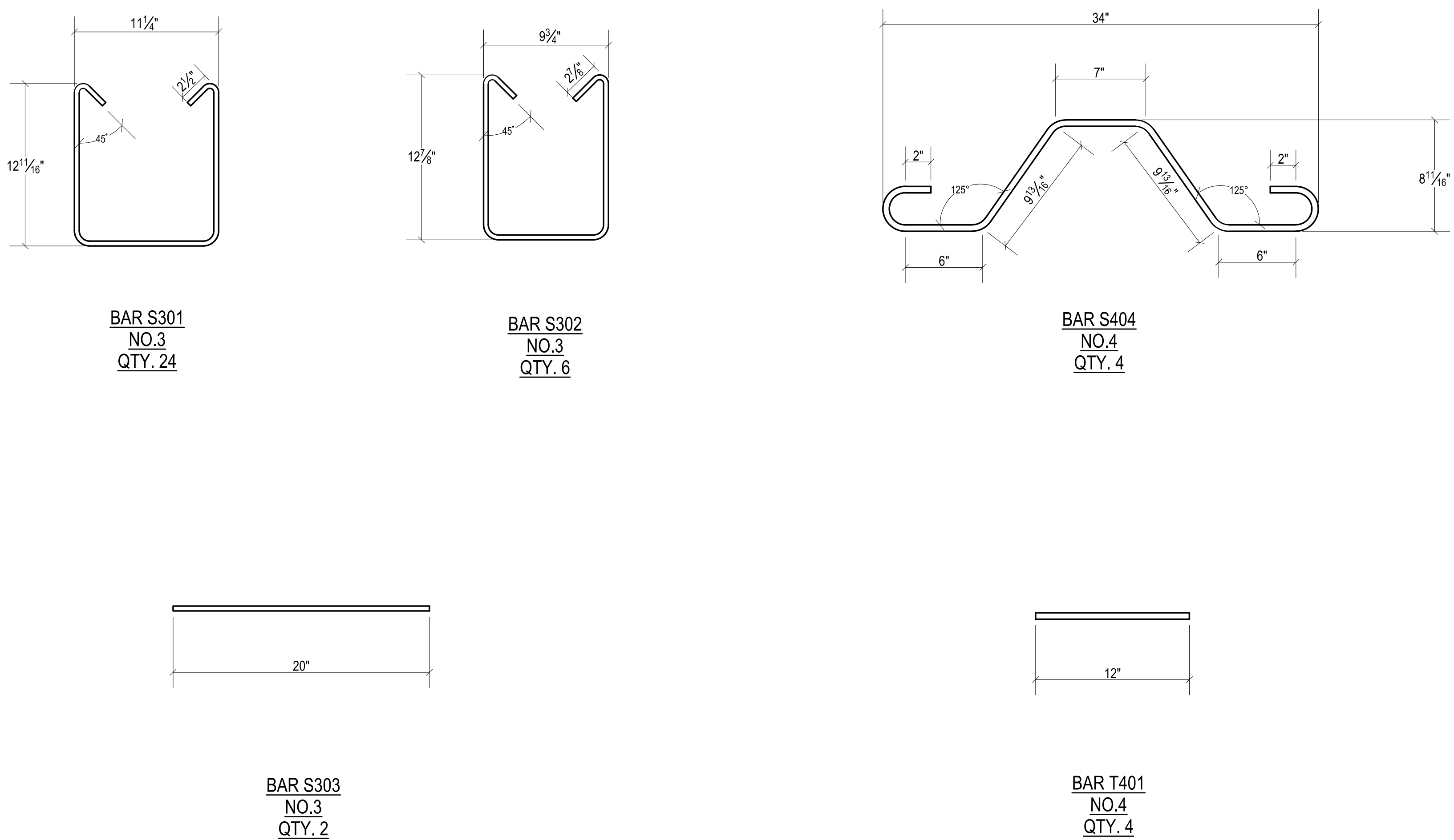

THICKENED DECK REINFORCEMENT

0 12" 24"

STEEL REINFORCED TEST SPECIMEN				*Revision:*		
BAR LIST - THICKENED DECK	*5/19/2020*	*University of Florida*	*SHEET 14 OF 18*			

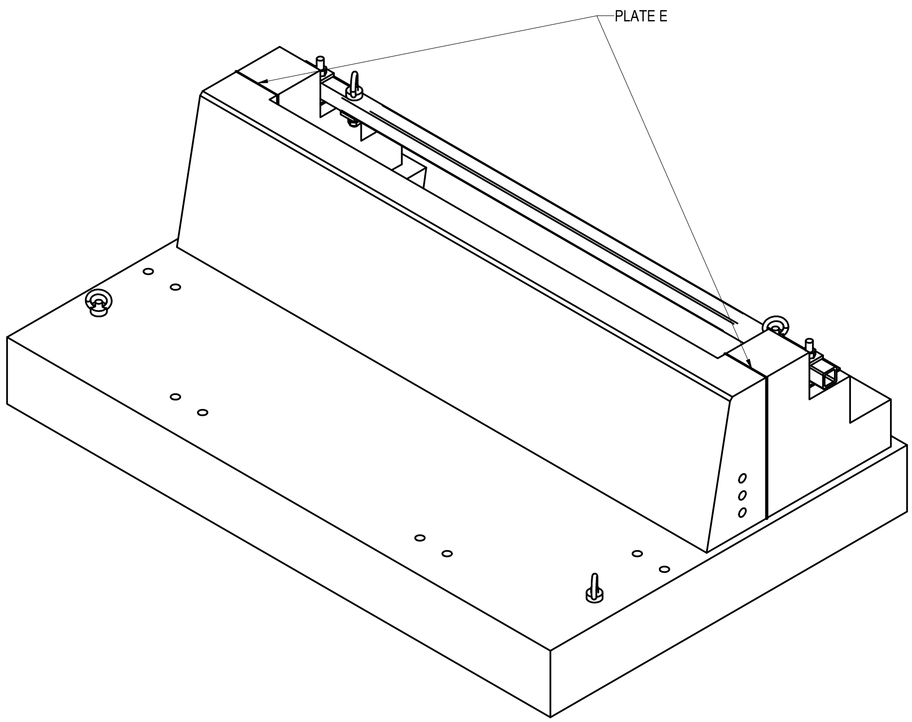

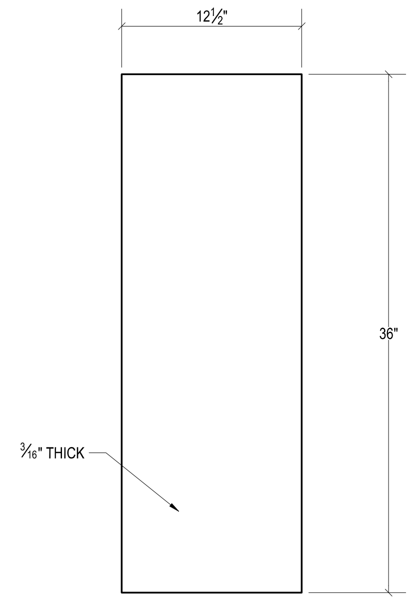

PLATE E
STEEL SEPARATION PLATE
QTY. 2

STEEL REINFORCED TEST SPECIMEN				*Revision:*
BUTTRESS-RAIL INTERFACE	*5/19/2020*	*University of Florida*	*SHEET 15 OF 18*	

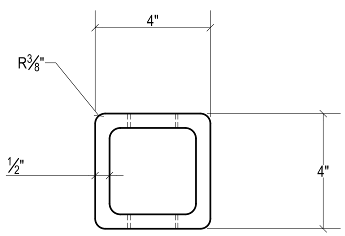

HSS 4X4X1⁄2
A1058

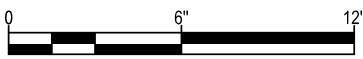

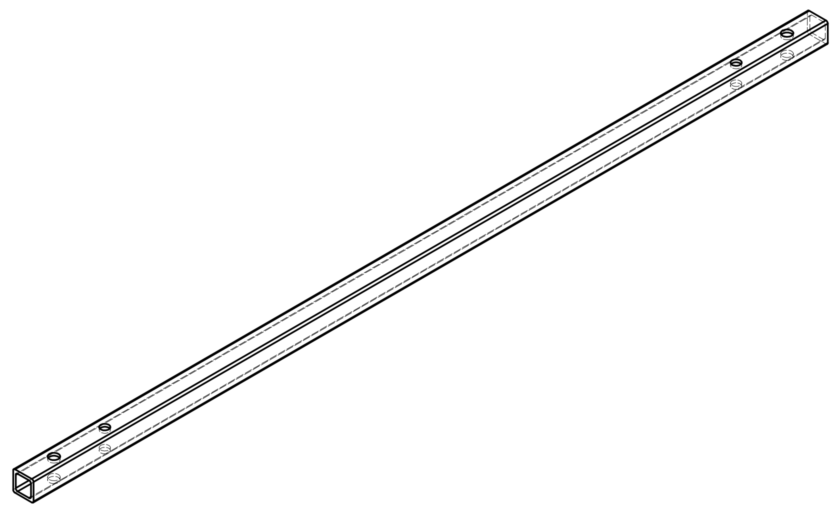

HSS
ISOMETRIC VIEW

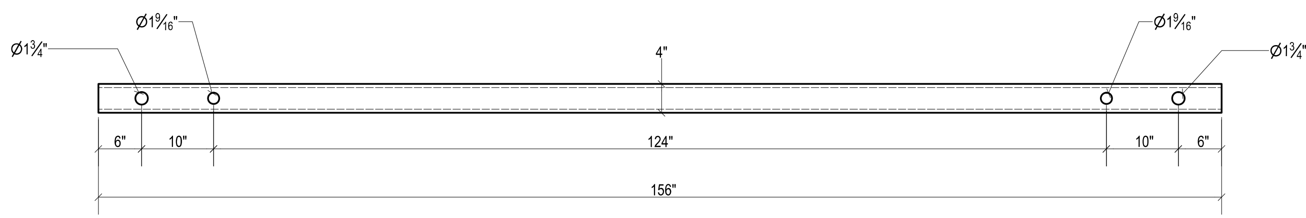

HSS
PLAN VIEW

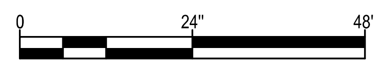

HSS WITH CONNECTION LOCATIONS

STEEL REINFORCED TEST SPECIMEN				Revision:
HSS DETAIL	5/19/2020	University of Florida	SHEET 16 OF 18	

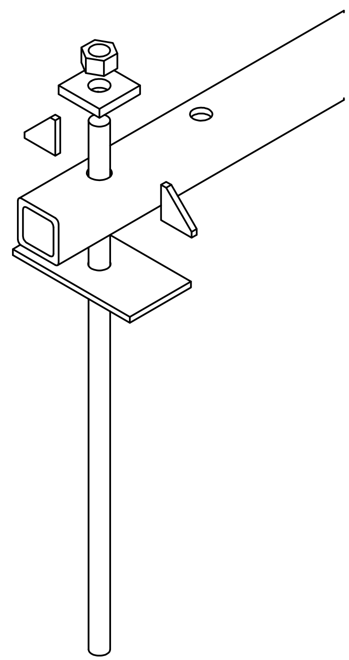

BUTTRESS ANCHOR ASSEMBLY

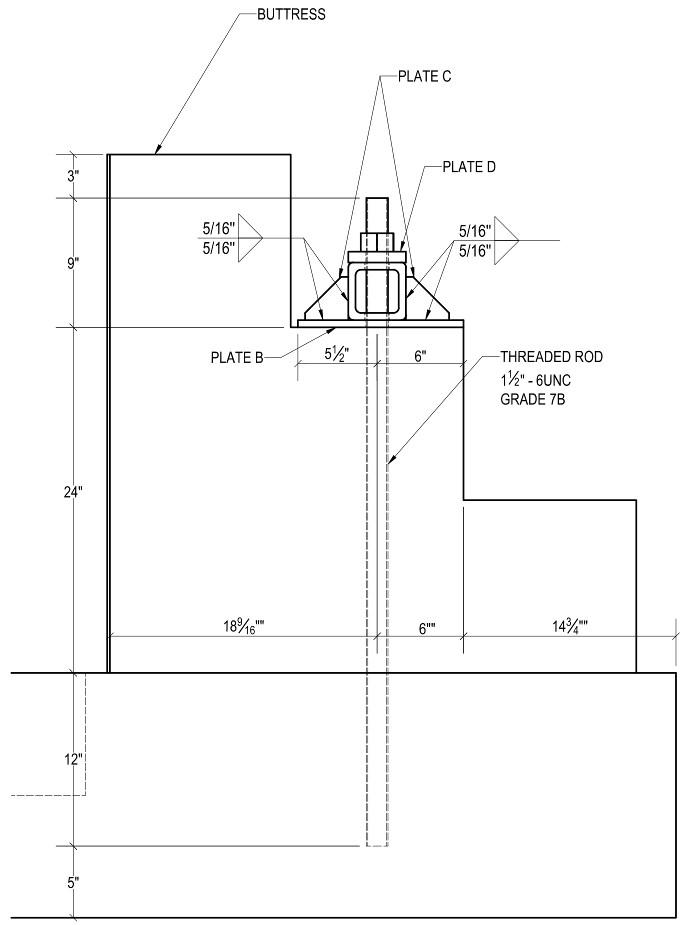

THREADED ROD ANCHOR CONNECTION

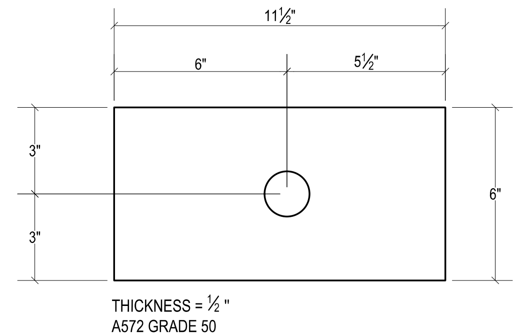

PLATE B
BEARING PLATE
QTY. 2

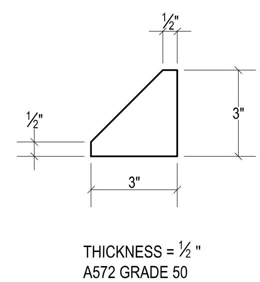

PLATE C
STIFFENER
QTY. 4

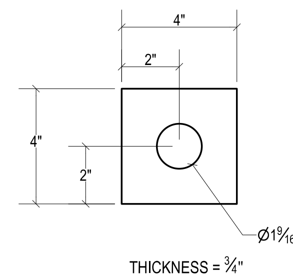

PLATE D
SQUARE PLATE
QTY. 4

STEEL REINFORCED TEST SPECIMEN				*Revision:*
HSS-BUTTRESS CONNECTION	*5/19/2020*	*University of Florida*	*SHEET 17 OF 18*	

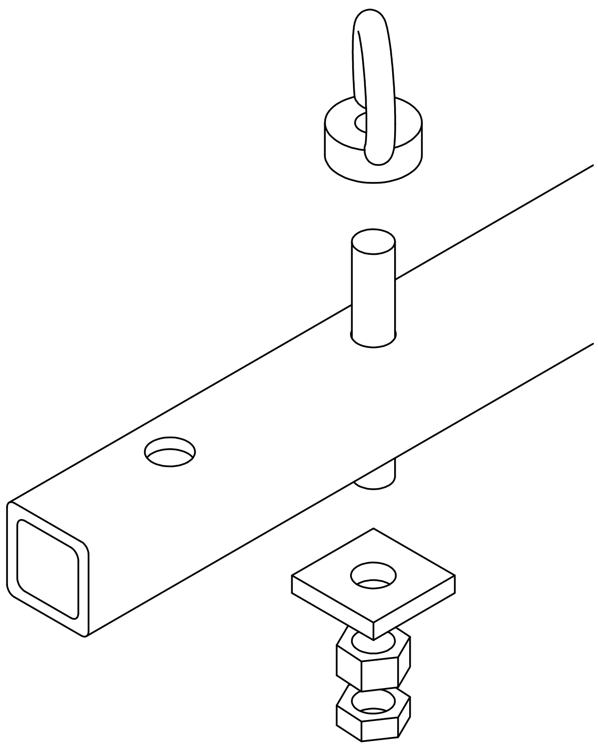

LIFTING EYE NUT ASSEMBLY

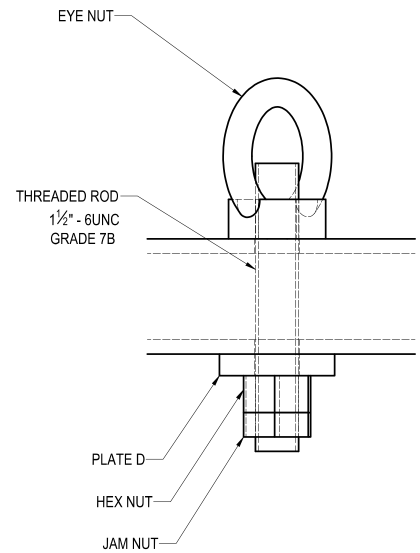

LIFTING EYE NUT CONNECTION

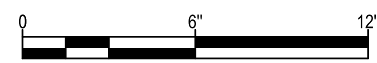

STEEL REINFORCED TEST SPECIMEN				*Revision:*		
HSS-LIFTING EYE BOLT CONNECTION	*5/19/2020*	*University of Florida*	*SHEET 18 OF 18*			

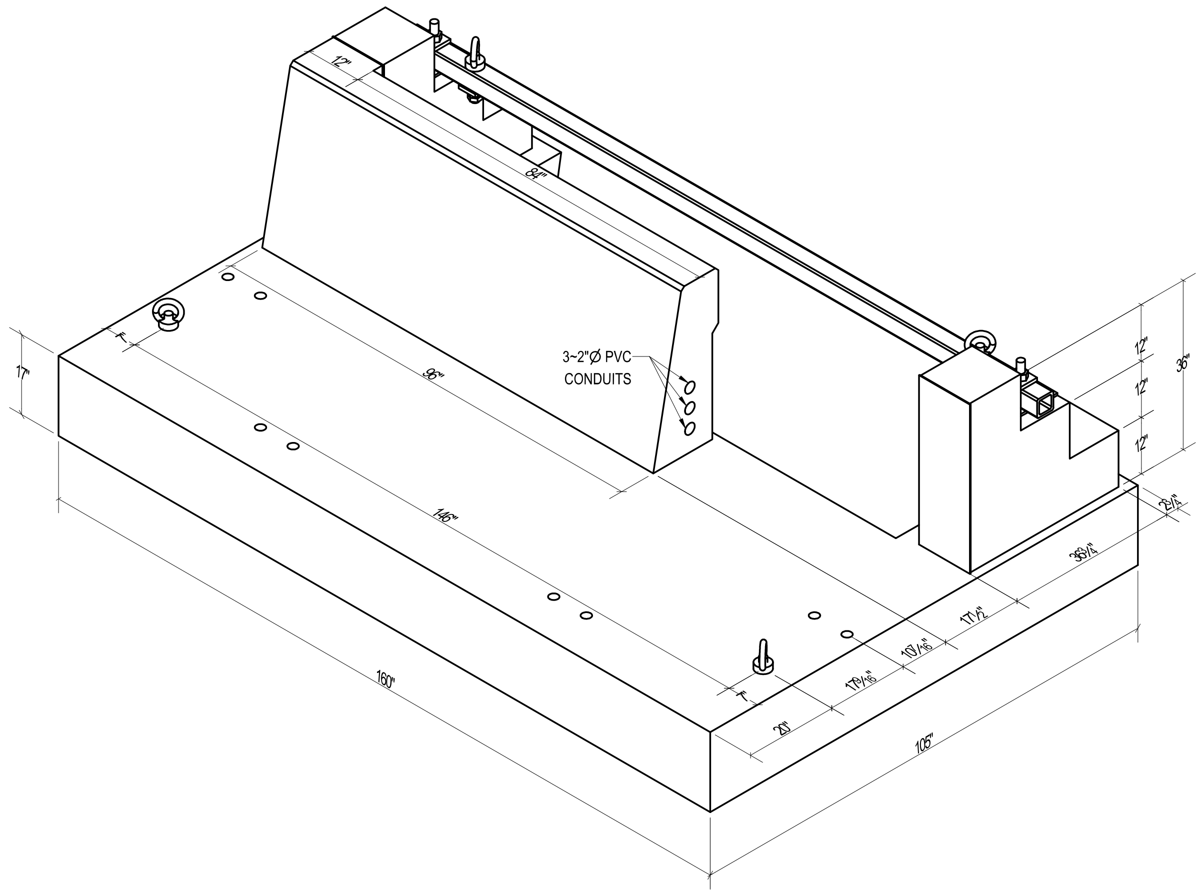

TEST SPECIMEN
FRONT ISOMETRIC VIEW

FRC REINFORCED END-OF-RAIL TEST SPECIMEN				*Revision:*
TEST SPECIMEN OVERVIEW	*11/17/2020*	*University of Florida*	*SHEET 1 OF 18*	

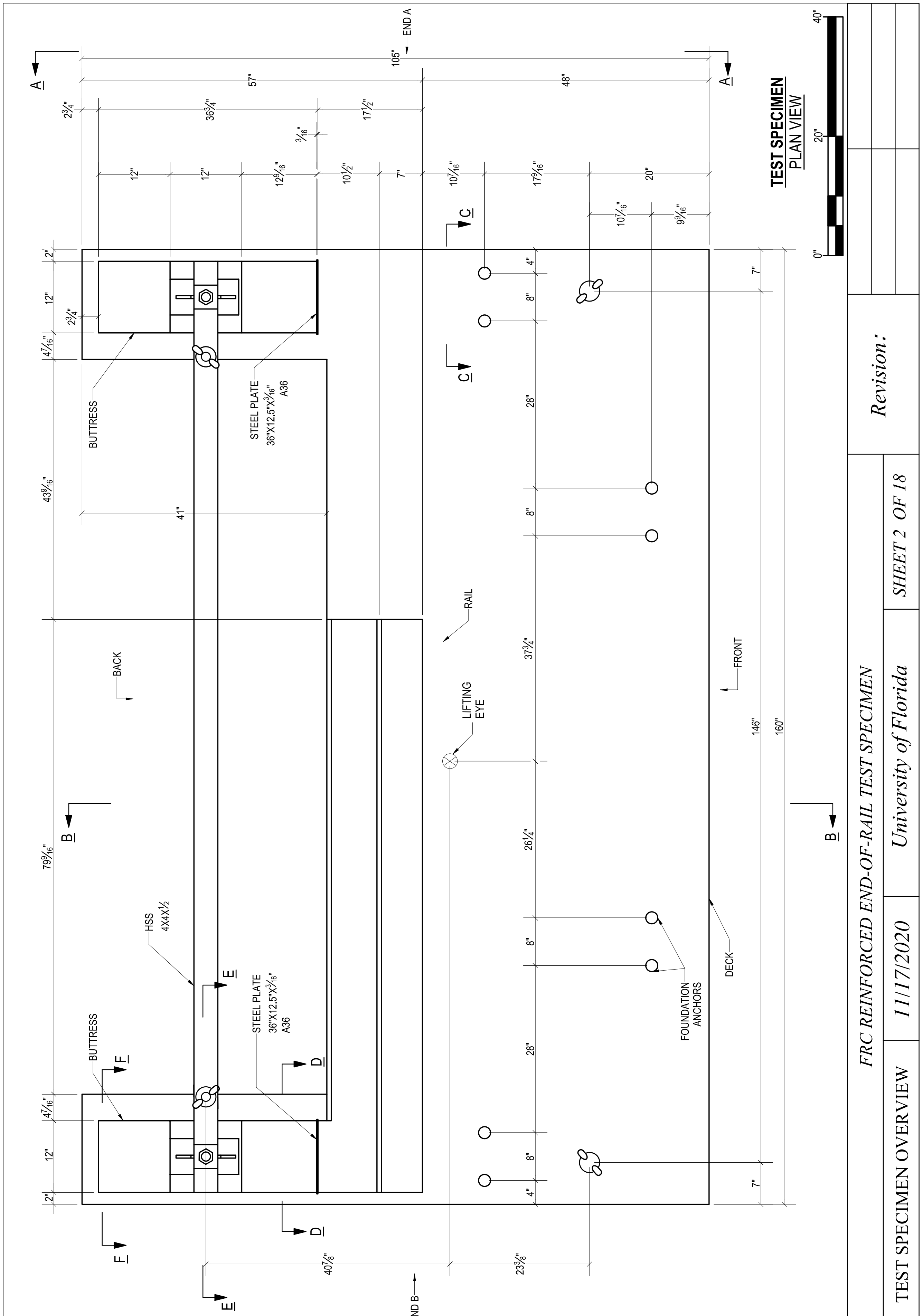
TEST SPECIMEN
PLAN VIEW
TEST SPECIMEN OVERVIEW
FRC REINFORCED END-OF-RAIL TEST SPECIMEN
11/17/2020
University of Florida
SHEET 2 OF 18
Revision:
BUTTRESS
STEEL PLATE
36"X12.5"X3/16"
A36
HSS
4X4X1/2
BACK
FRONT
RAIL
DECK
LIFTING
EYE
FOUNDATION
ANCHORS
END A
END B
105"
57"
48"
160"
146"
0"
20"
40"

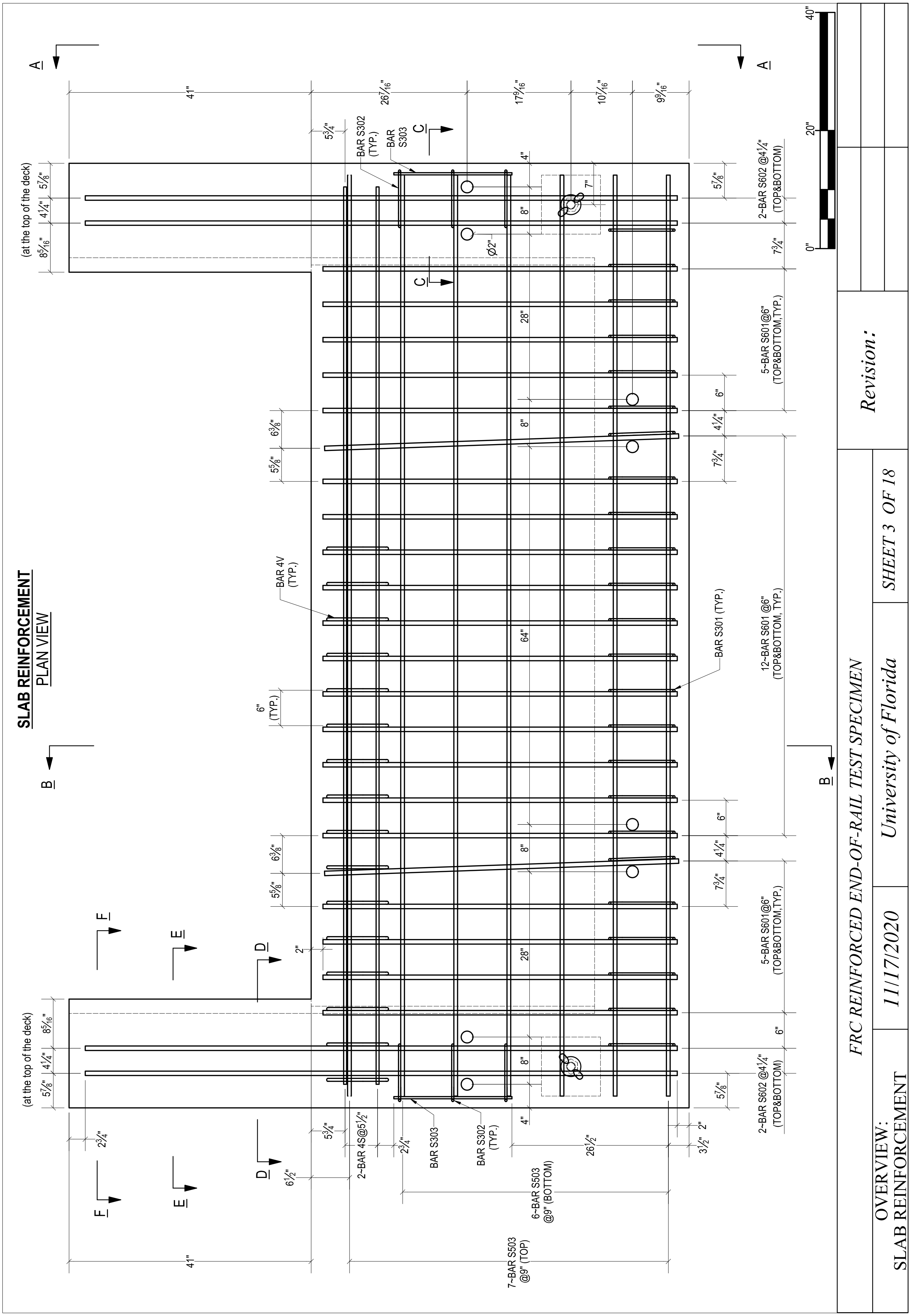

SLAB REINFORCEMENT
PLAN VIEW
(at the top of the deck)
2~BAR S602 @4¼" (TOP&BOTTOM)
5~BAR S601@6" (TOP&BOTTOM,TYP.)
12~BAR S601 @6" (TOP&BOTTOM, TYP.)
BAR S301 (TYP.)
BAR 4V (TYP.)
BAR S302 (TYP.)
BAR S303
2~BAR 4S@5½"
6~BAR S503 @9" (BOTTOM)
7~BAR S503 @9" (TOP)
Ø2"
FRC REINFORCED END-OF-RAIL TEST SPECIMEN
University of Florida
11/17/2020
SHEET 3 OF 18
Revision:
OVERVIEW:
SLAB REINFORCEMENT

THICKENED DECK AND BUTTRESS REINFORCEMENT

PLAN VIEW

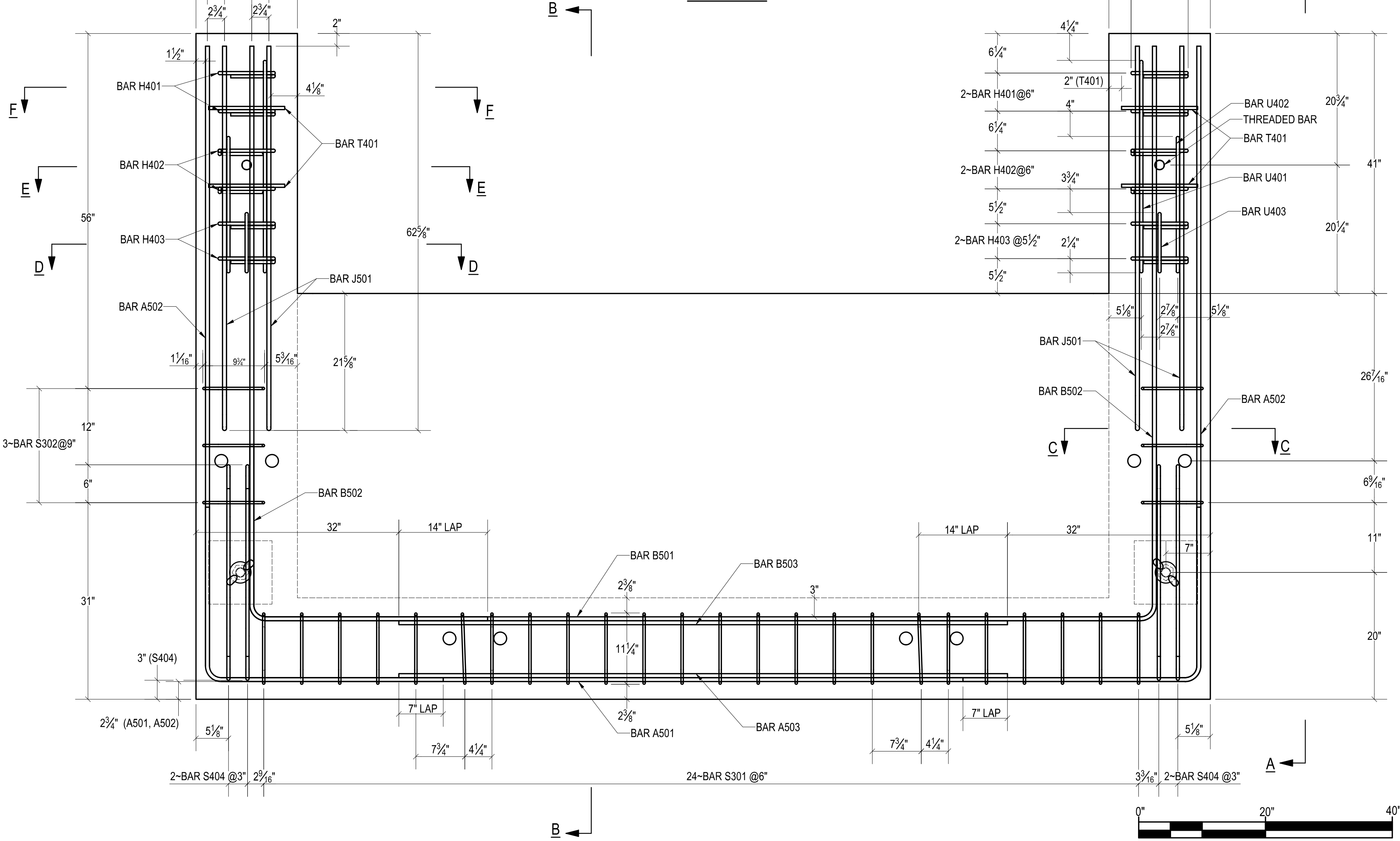

FRC REINFORCED END-OF-RAIL TEST SPECIMEN				Revision:
OVERVIEW: THICKENED DECK REINFORCEMENT	11/17/2020	University of Florida	SHEET 4 OF 18	

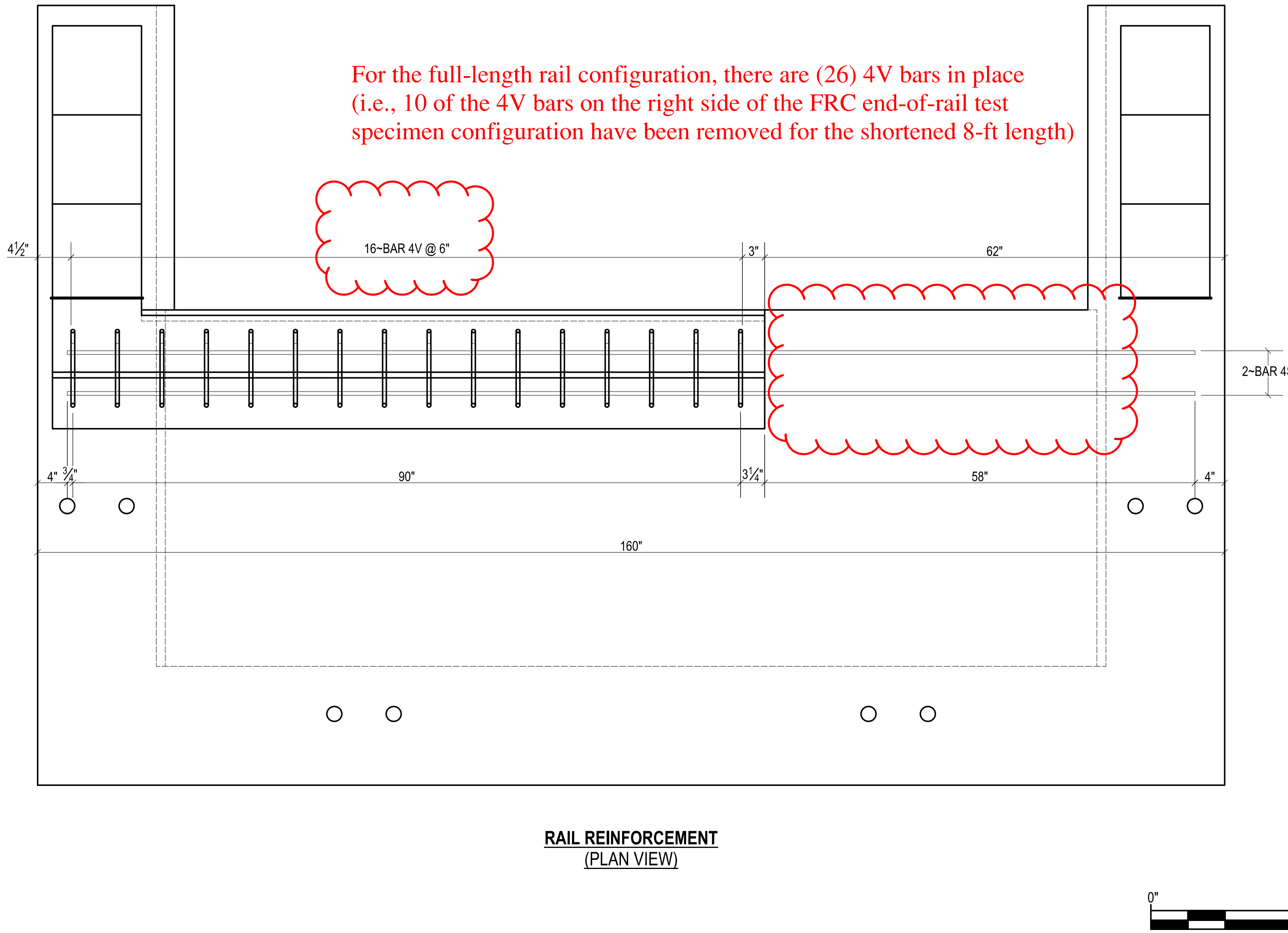

RAIL REINFORCEMENT
(PLAN VIEW)

FRC REINFORCED END-OF-RAIL TEST SPECIMEN				Revision:
RAILING REINFORCEMENT: OVERVIEW	11/17/2020	University of Florida	SHEET 5 OF 18	

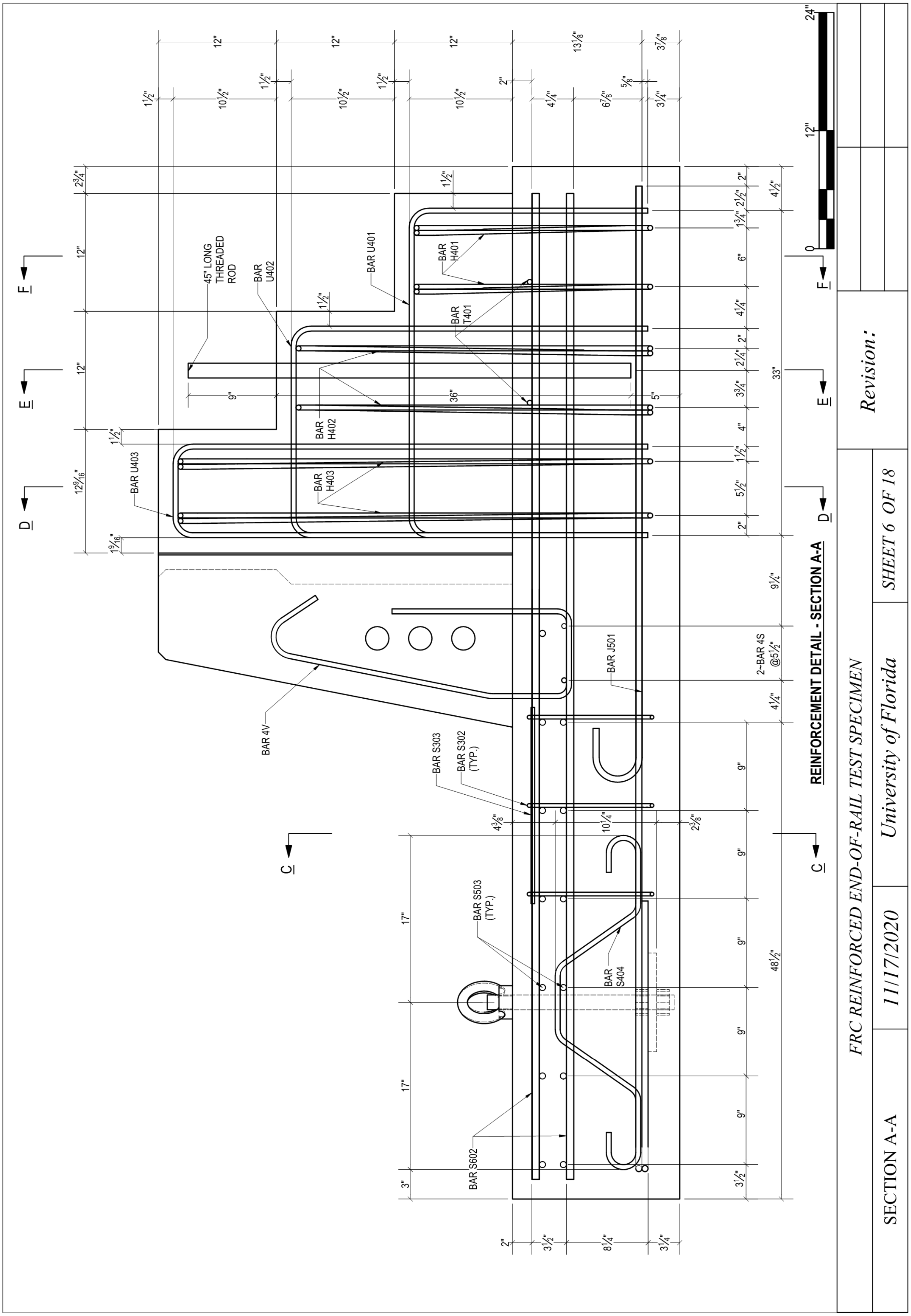
REINFORCEMENT DETAIL - SECTION A-A
45" LONG THREADED ROD
BAR U401
BAR U402
BAR U403
BAR H401
BAR H402
BAR H403
BAR T401
BAR 4V
BAR J501
2~BAR 4S @5½"
BAR S302 (TYP.)
BAR S303
BAR S503 (TYP.)
BAR S404
BAR S602
C
D
E
F
FRC REINFORCED END-OF-RAIL TEST SPECIMEN
University of Florida
11/17/2020
SHEET 6 OF 18
Revision:
SECTION A-A

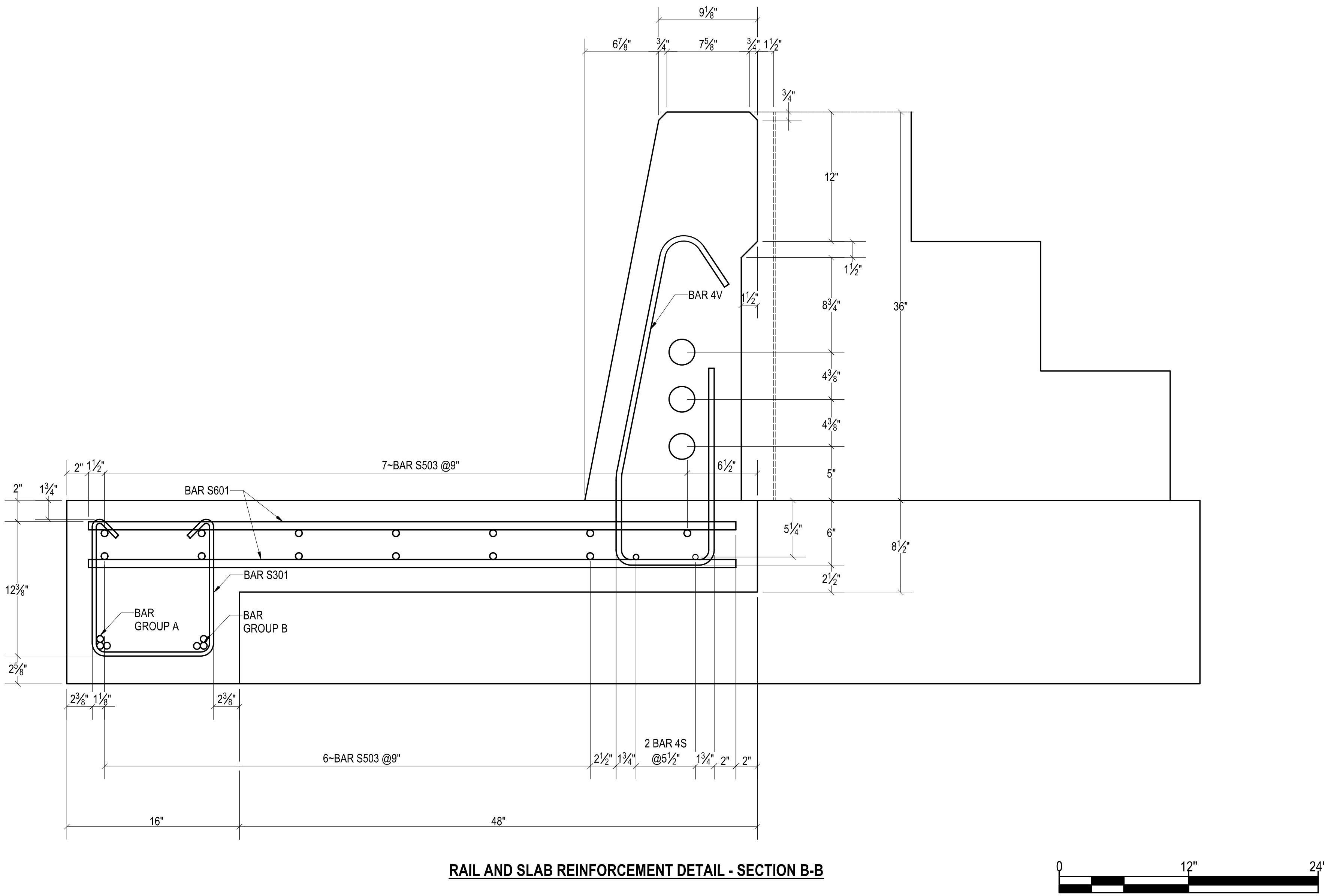

RAIL AND SLAB REINFORCEMENT DETAIL - SECTION B-B

FRC REINFORCED END-OF-RAIL TEST SPECIMEN				*Revision:*
SECTION B-B	*11/17/2020*	*University of Florida*	*SHEET 7 OF 18*	

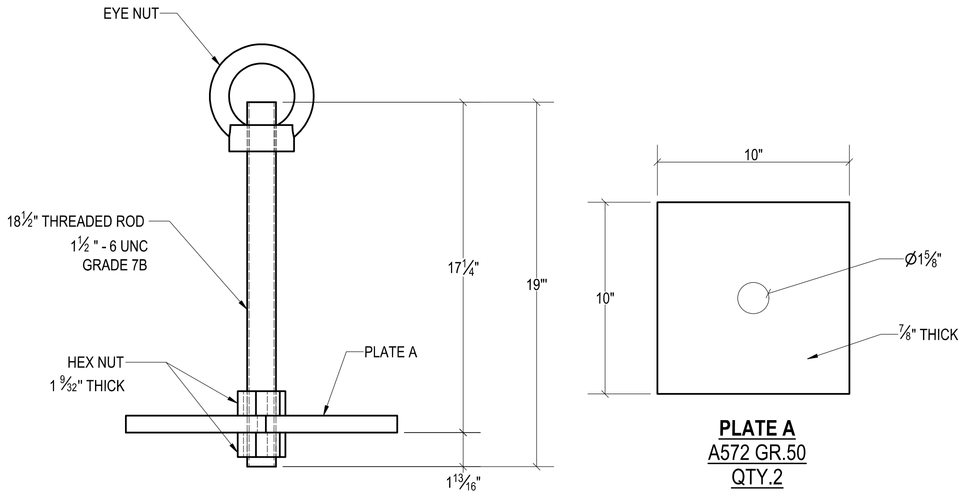

ANCHOR AND PLATE CONNECTION

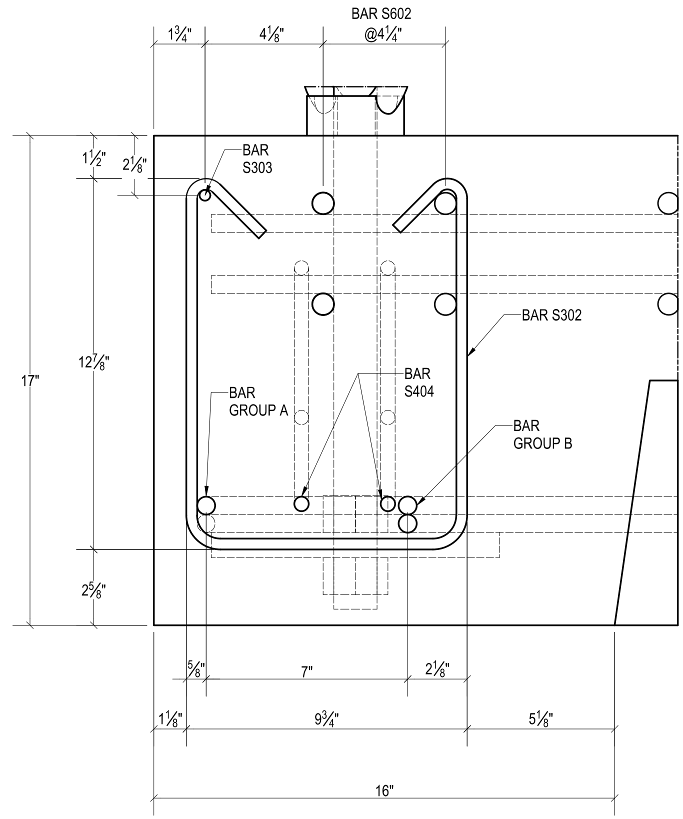

THICKENED EDGE
SECTION C-C

FRC REINFORCED END-OF-RAIL TEST SPECIMEN				Revision:
ANCHOR PLATE AND SECTION C-C	11/17/2020	University of Florida	SHEET 8 OF 18	

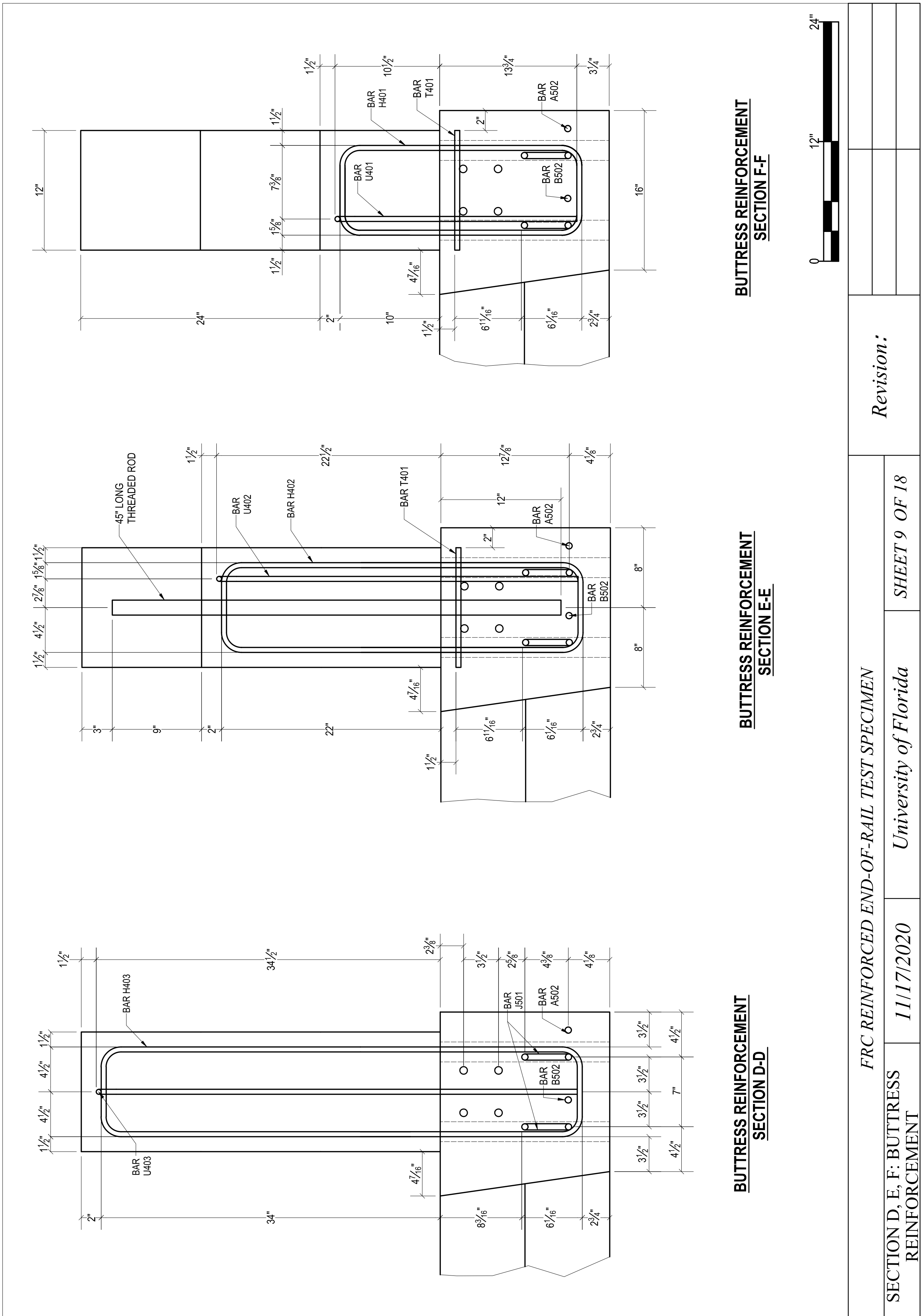
BUTTRESS REINFORCEMENT SECTION D-D
BUTTRESS REINFORCEMENT SECTION E-E
BUTTRESS REINFORCEMENT SECTION F-F
BAR H403
BAR U403
BAR J501
BAR A502
BAR B502
45" LONG THREADED ROD
BAR U402
BAR H402
BAR T401
BAR H401
BAR U401
Revision:
SECTION D, E, F: BUTTRESS REINFORCEMENT
FRC REINFORCED END-OF-RAIL TEST SPECIMEN
11/17/2020
University of Florida
SHEET 9 OF 18

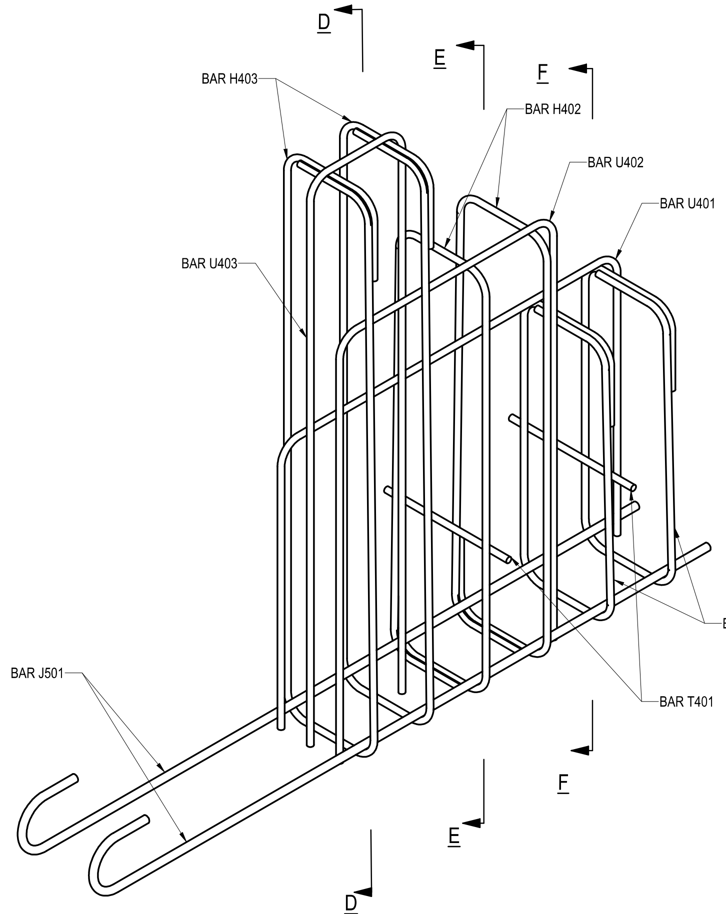

BUTTRESS REINFORCING CAGE
END A: WEST

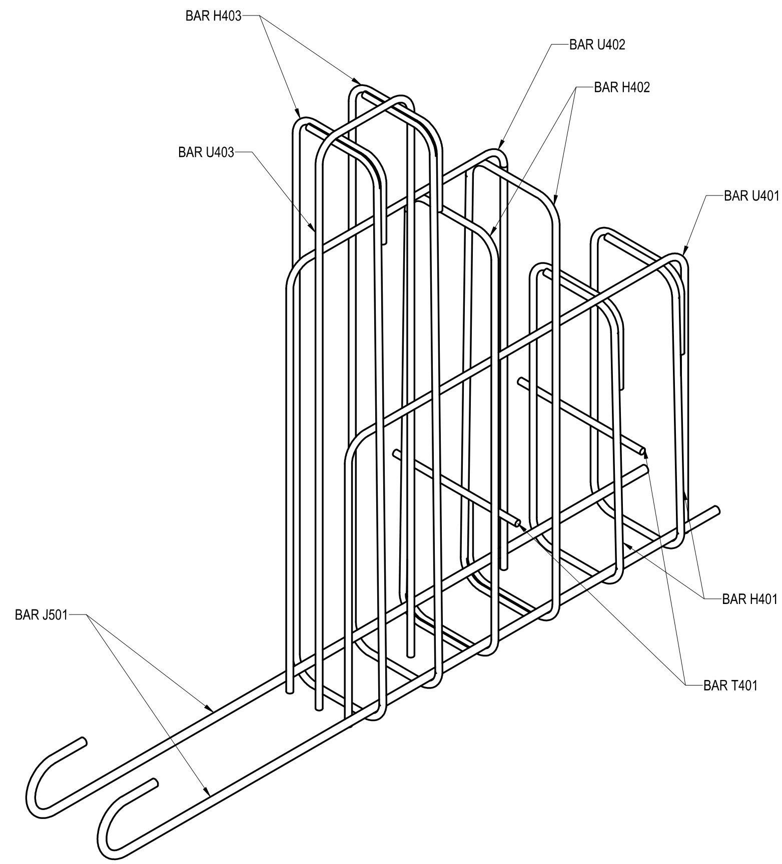

BUTTRESS REINFORCING CAGE
END B: EAST

0 12" 24"

FRC REINFORCED END-OF-RAIL TEST SPECIMEN				Revision:
BUTTRESS REINFORCEMENT	11/17/2020	University of Florida	SHEET 10 OF 18	

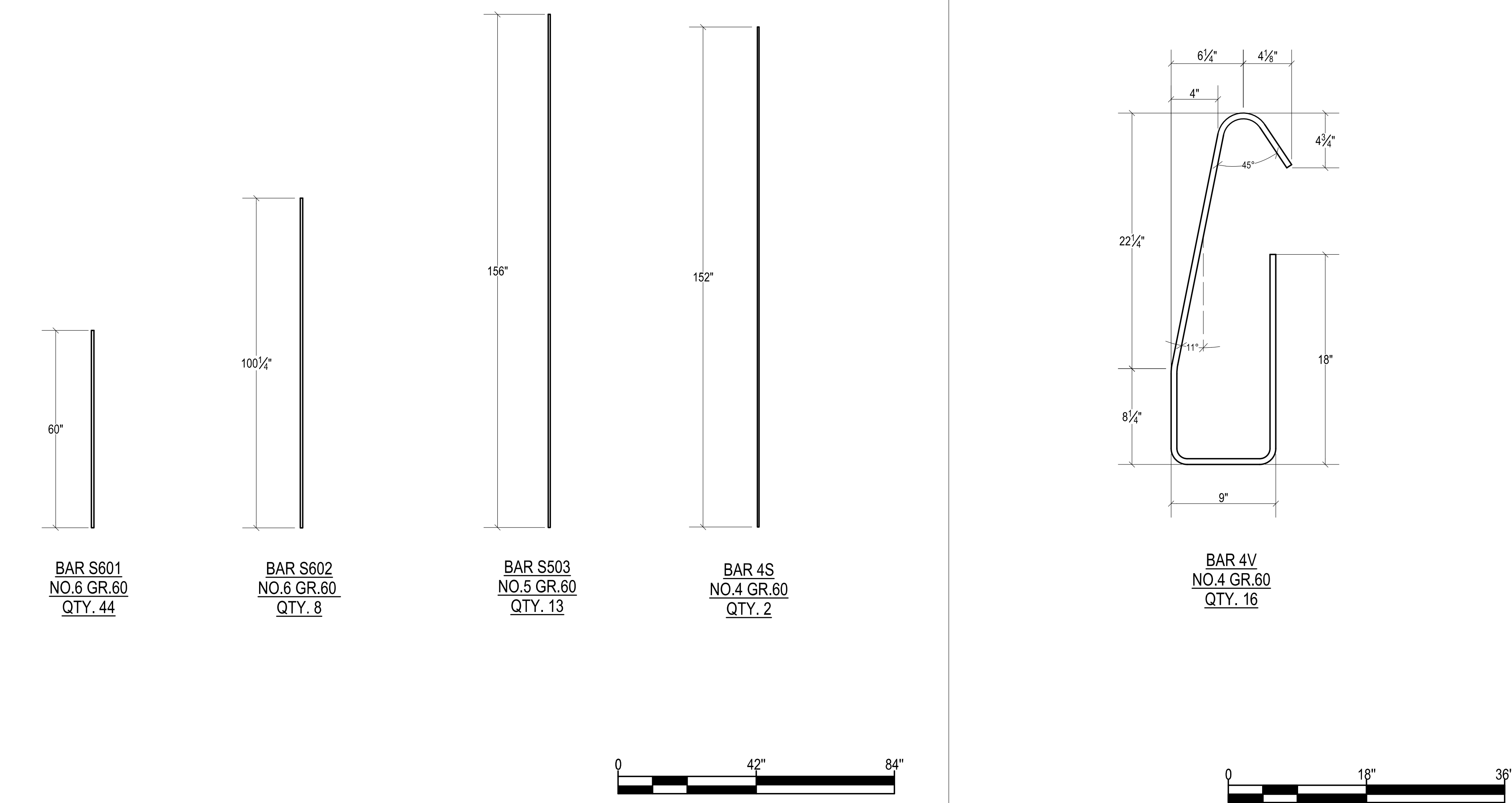

FRC REINFORCED END-OF-RAIL TEST SPECIMEN				*Revision:*		
BAR LIST - SLAB	*11/17/2020*	*University of Florida*	*SHEET 11 OF 18*			

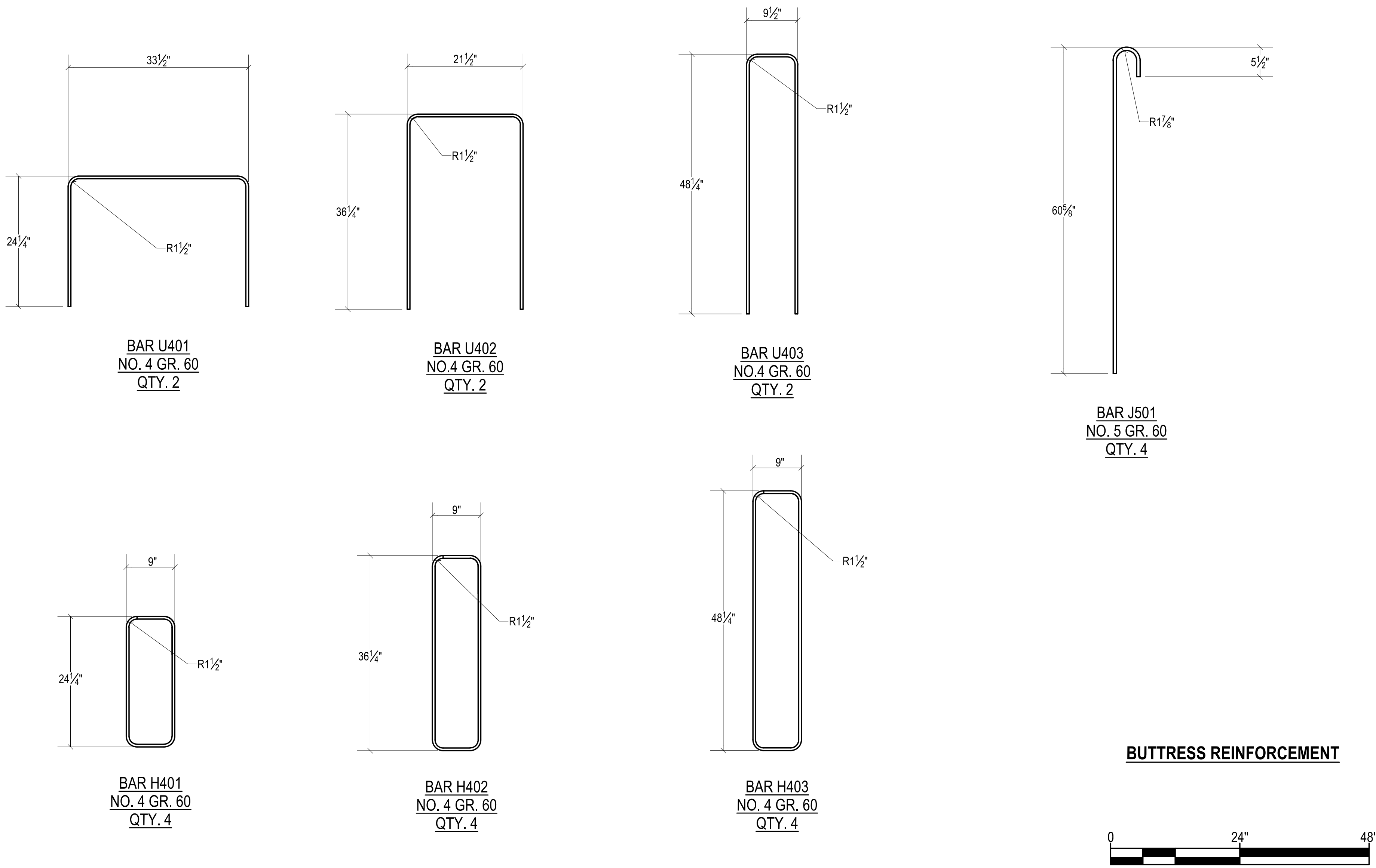

FRC REINFORCED END-OF-RAIL TEST SPECIMEN				*Revision:*
BAR LIST - BUTTRESS	*11/17/2020*	*University of Florida*	*SHEET 12 OF 18*	

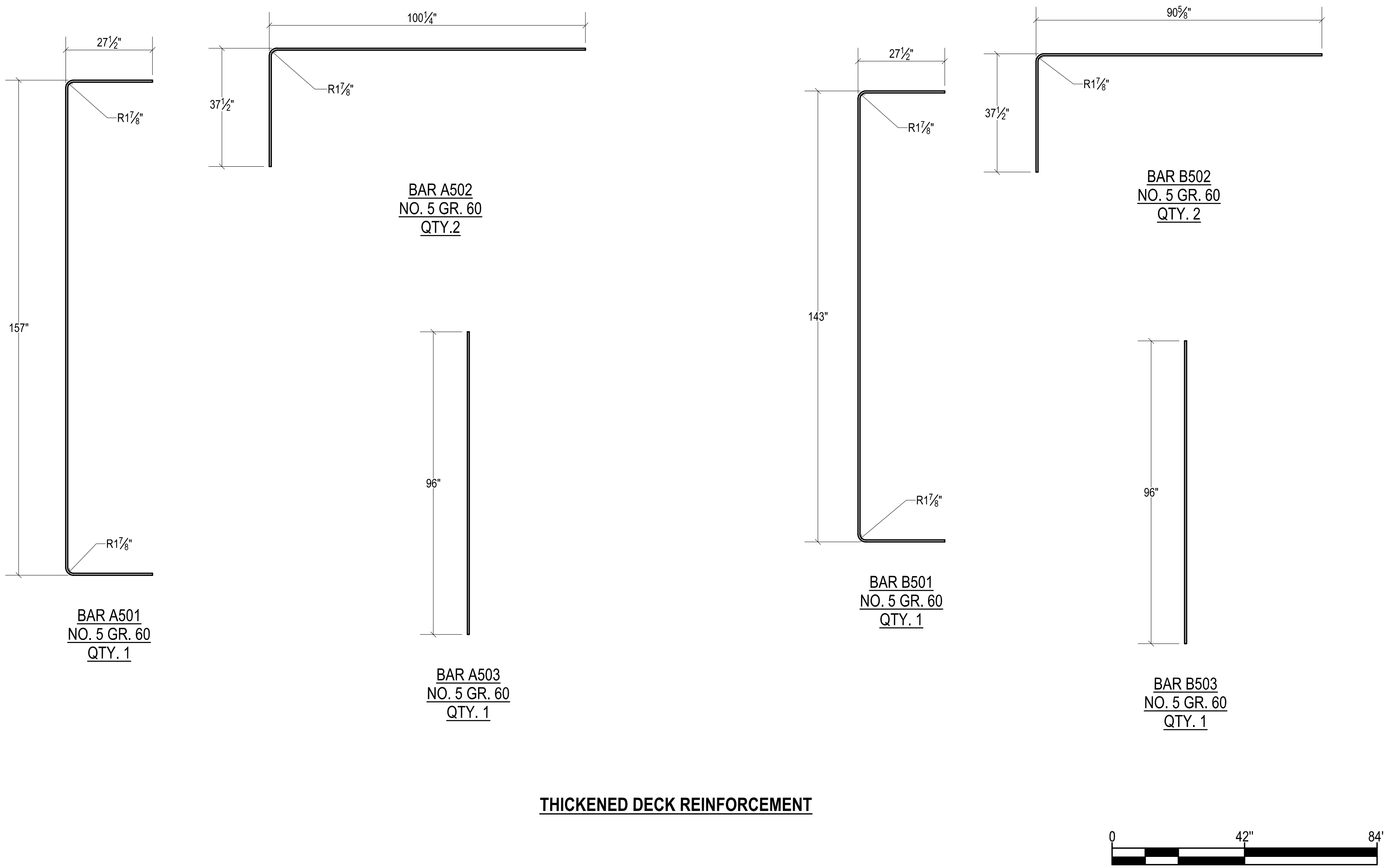

FRC REINFORCED END-OF-RAIL TEST SPECIMEN				*Revision:*		
BAR LIST - THICKENED DECK	*11/17/2020*	*University of Florida*	*SHEET 13 OF 18*			

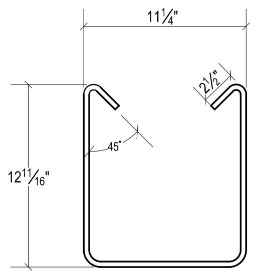

BAR S301
NO.3 GR. 60
QTY. 24

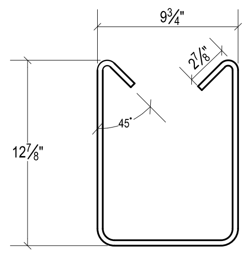

BAR S302
NO.3 GR. 60
QTY. 6

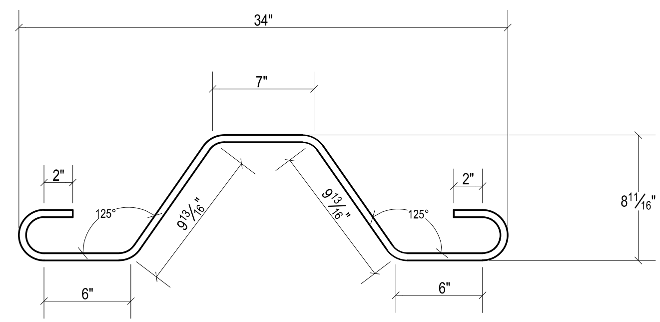

BAR S404
NO.4 GR. 60
QTY. 4

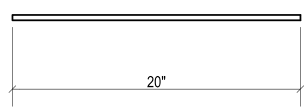

BAR S303
NO.3 GR. 60
QTY. 2

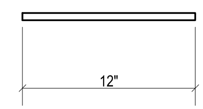

BAR T401
NO.4 GR. 60
QTY. 4

THICKENED DECK REINFORCEMENT

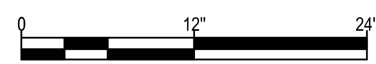

FRC REINFORCED END-OF-RAIL TEST SPECIMEN				Revision:
BAR LIST - THICKENED DECK	11/17/2020	University of Florida	SHEET 14 OF 18	

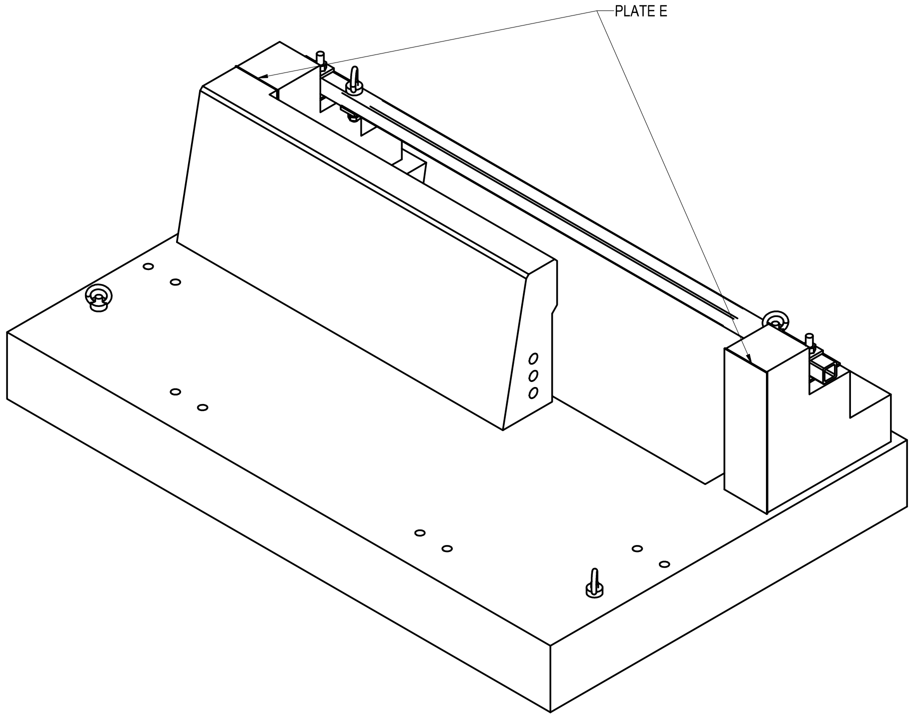

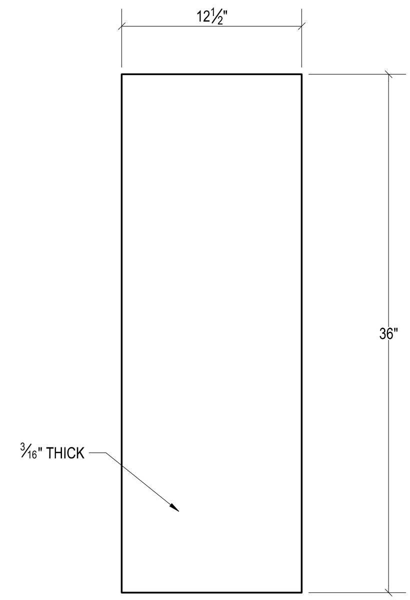

PLATE E
STEEL SEPARATION PLATE
A36
QTY. 2

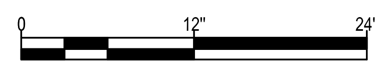

FRC REINFORCED END-OF-RAIL TEST SPECIMEN				Revision:
BUTTRESS-RAIL INTERFACE	11/17/2020	University of Florida	SHEET 15 OF 18	

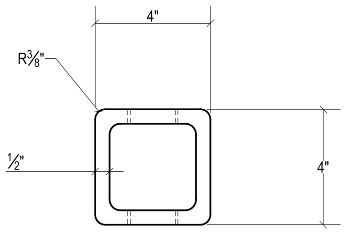

HSS 4X4X1/2
A500 GR.B

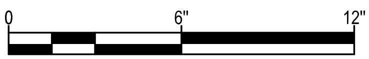

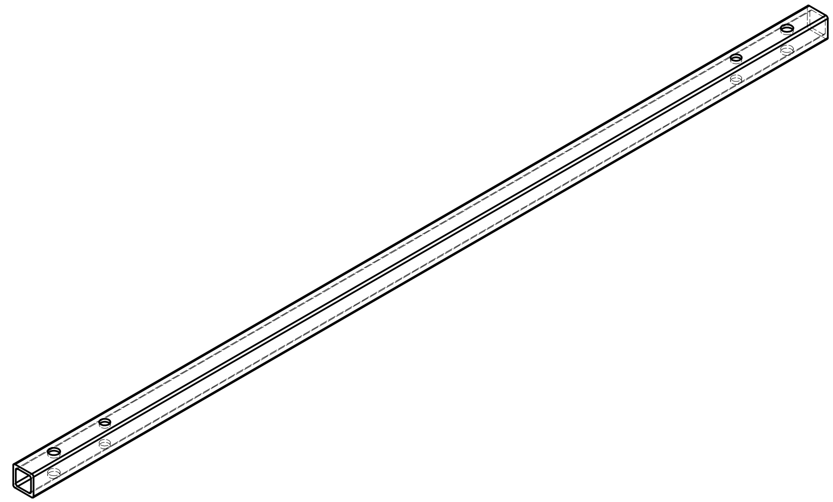

HSS
ISOMETRIC VIEW

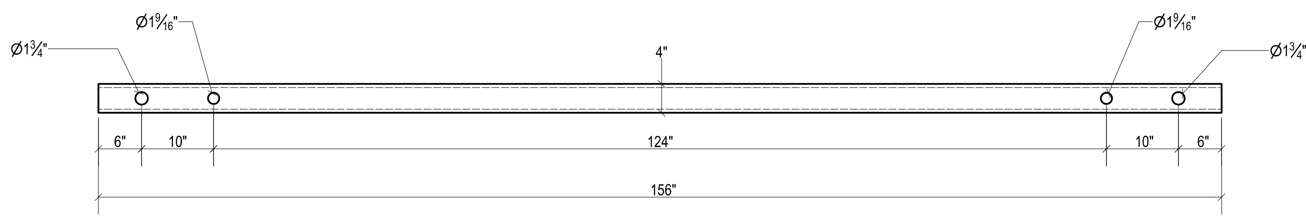

HSS
PLAN VIEW

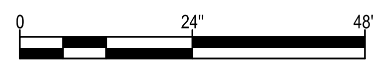

HSS WITH CONNECTION LOCATIONS

FRC REINFORCED END-OF-RAIL TEST SPECIMEN				*Revision:*
HSS DETAIL	*11/17/2020*	*University of Florida*	*SHEET 16 OF 18*	

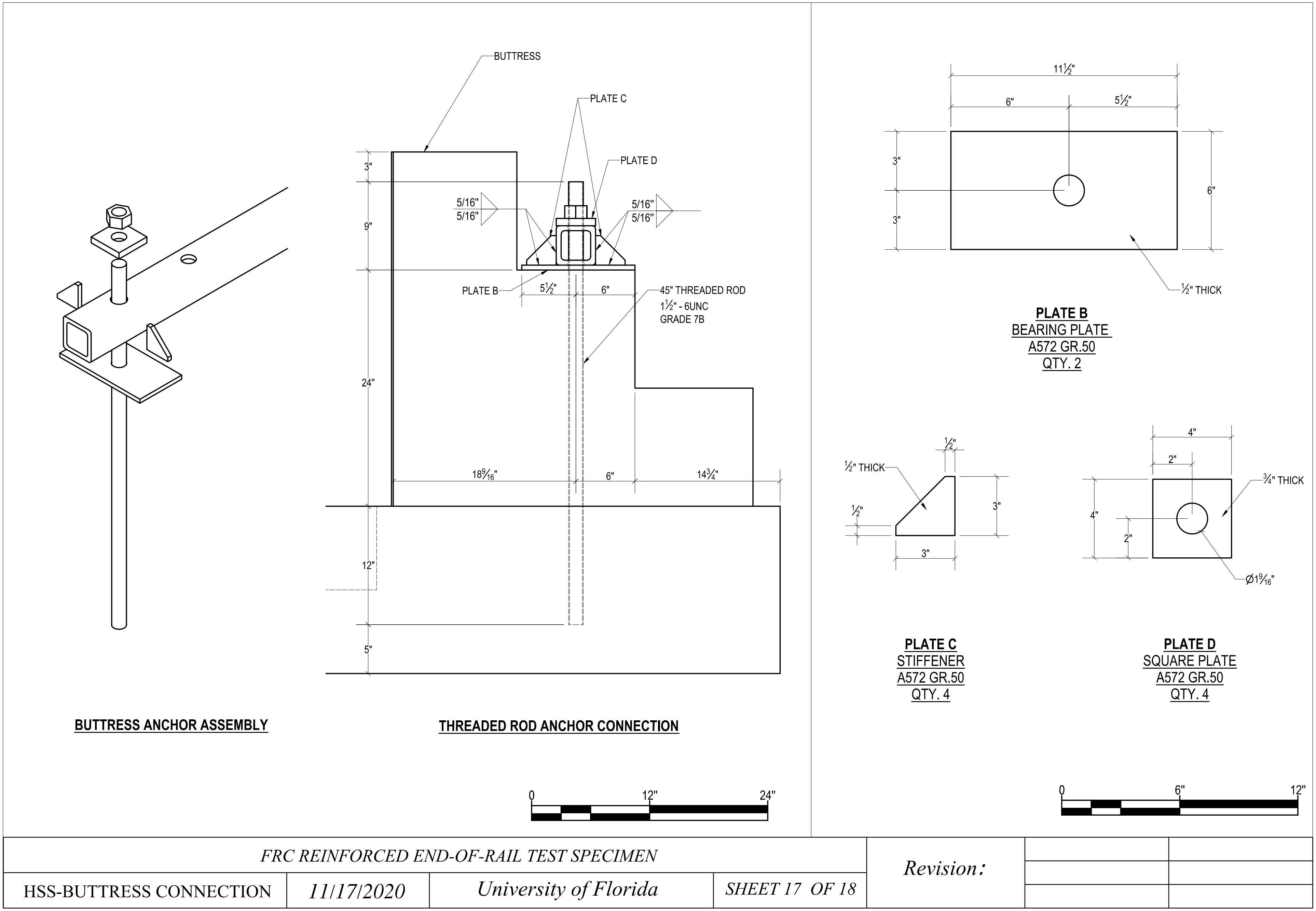

BUTTRESS
PLATE C
PLATE D
5/16"
5/16"
PLATE B
5½"
6"
45" THREADED ROD
1½" - 6UNC
GRADE 7B
3"
9"
24"
12"
5"
18 9/16"
14¾"
BUTTRESS ANCHOR ASSEMBLY
THREADED ROD ANCHOR CONNECTION
11½"
½" THICK
PLATE B
BEARING PLATE
A572 GR.50
QTY. 2
½" THICK
¾" THICK
4"
2"
Ø1 9/16"
PLATE C
STIFFENER
A572 GR.50
QTY. 4
PLATE D
SQUARE PLATE
A572 GR.50
QTY. 4
0
12"
24"
0
6"
12"
FRC REINFORCED END-OF-RAIL TEST SPECIMEN
HSS-BUTTRESS CONNECTION
11/17/2020
University of Florida
SHEET 17 OF 18
Revision:

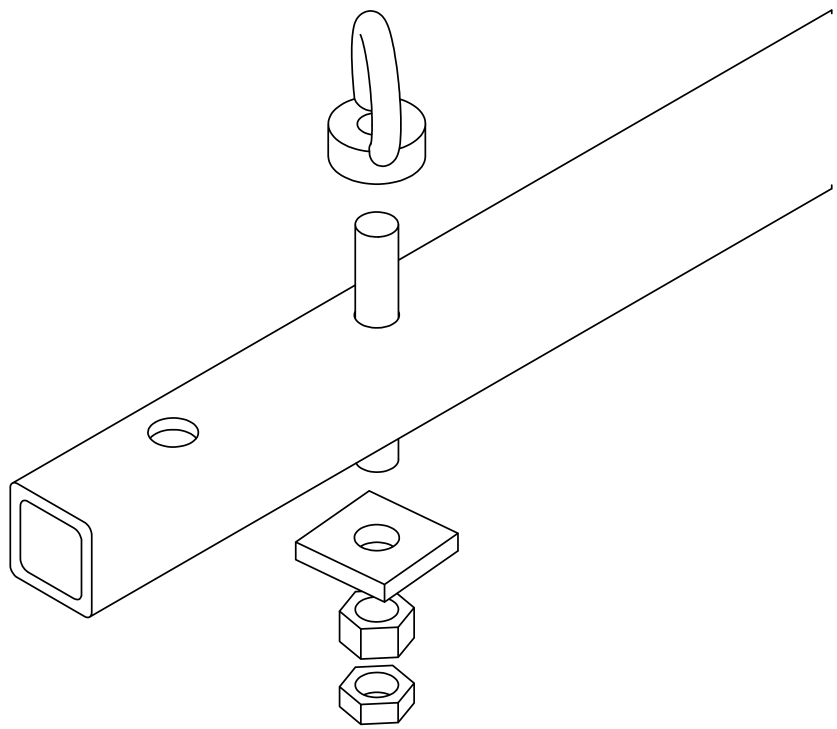

LIFTING EYE NUT ASSEMBLY

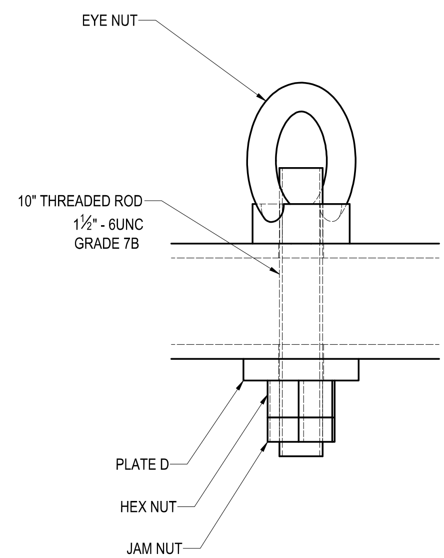

LIFTING EYE NUT CONNECTION

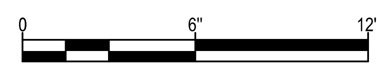

FRC REINFORCED END-OF-RAIL TEST SPECIMEN				*Revision:*	
HSS-LIFTING EYE BOLT CONNECTION	*11/17/2020*	*University of Florida*	*SHEET 18 OF 18*		

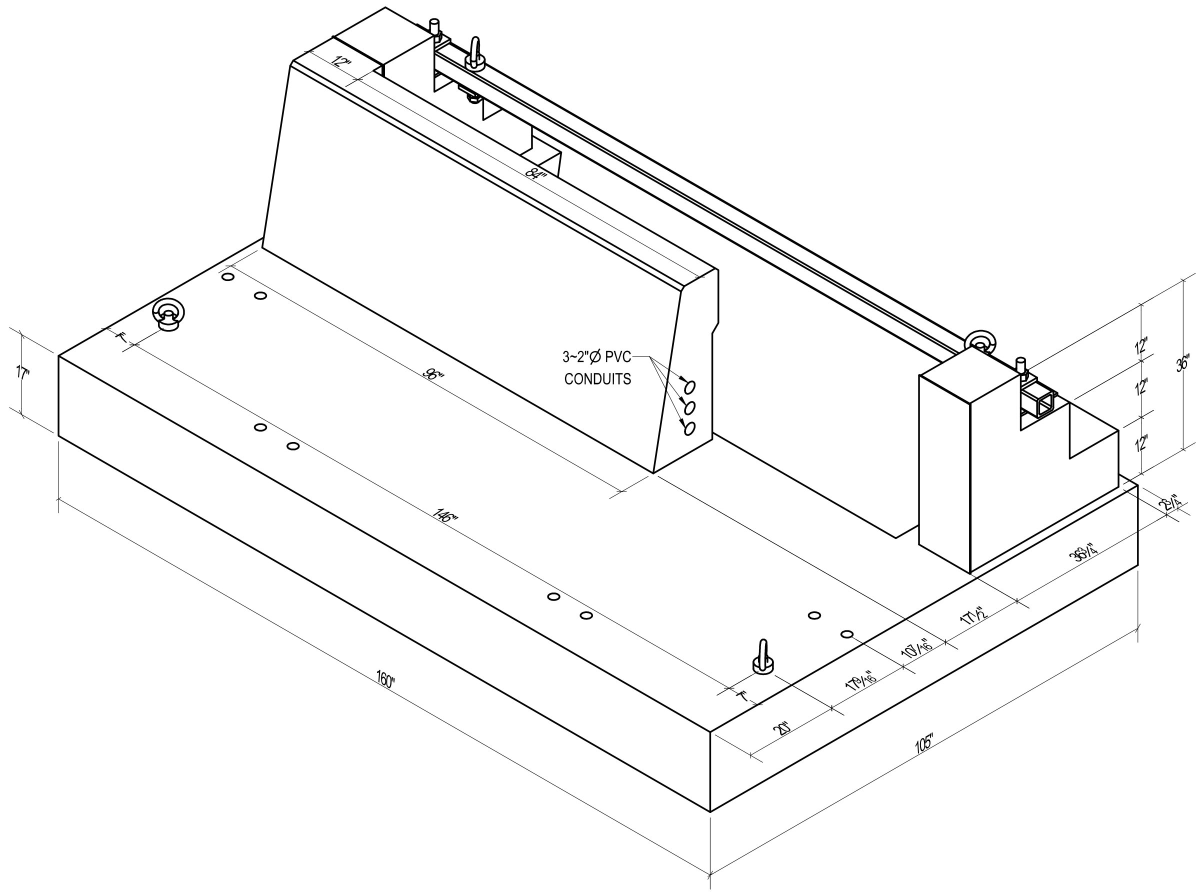

TEST SPECIMEN
FRONT ISOMETRIC VIEW

STEEL REINFORCED END-OF-RAIL TEST SPECIMEN				*Revision:*		
TEST SPECIMEN OVERVIEW	*10/23/2020*	*University of Florida*	*SHEET 1 OF 18*			

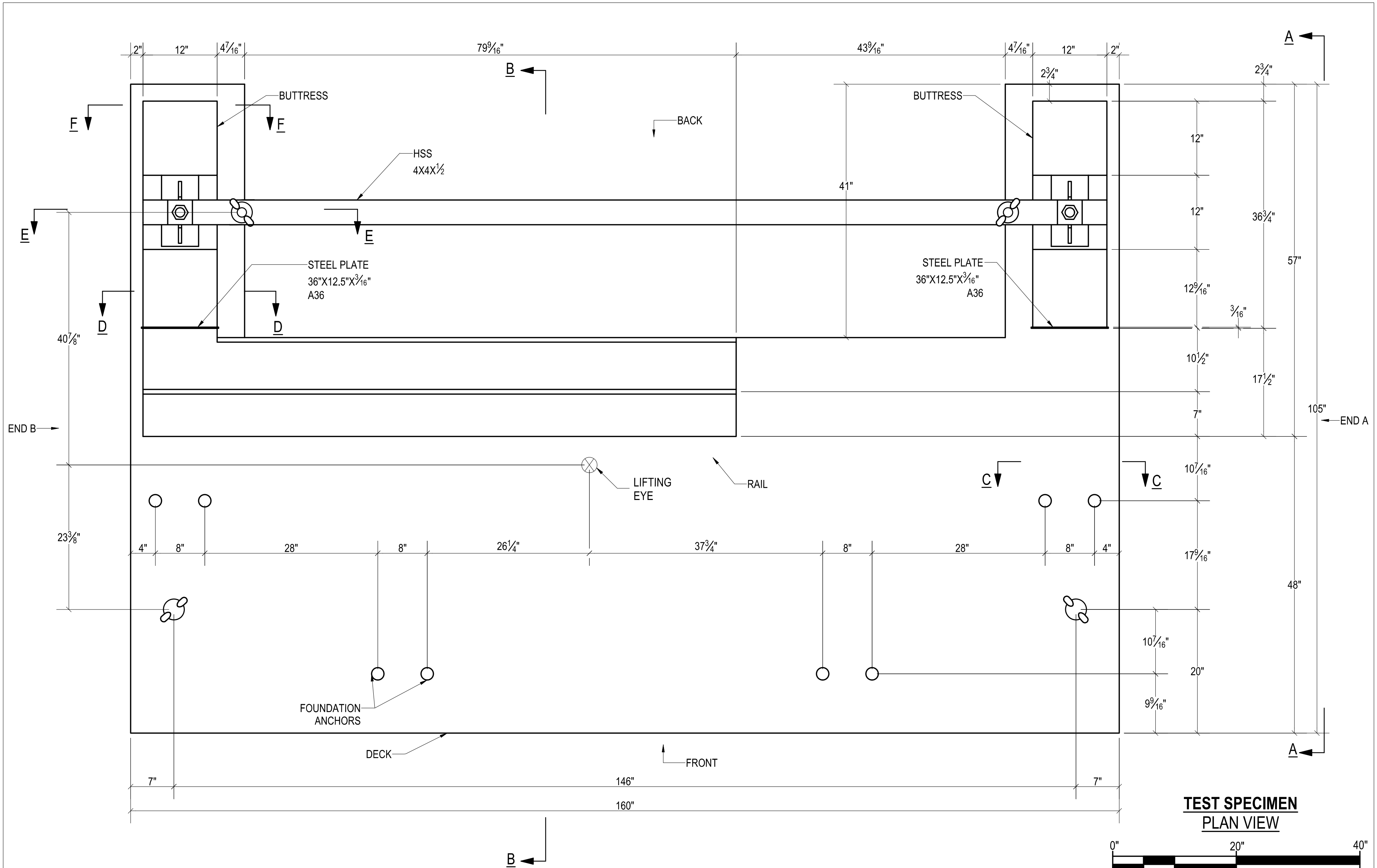

STEEL REINFORCED END-OF-RAIL TEST SPECIMEN				*Revision:*
TEST SPECIMEN OVERVIEW	*10/23/2020*	*University of Florida*	*SHEET 2 OF 18*	

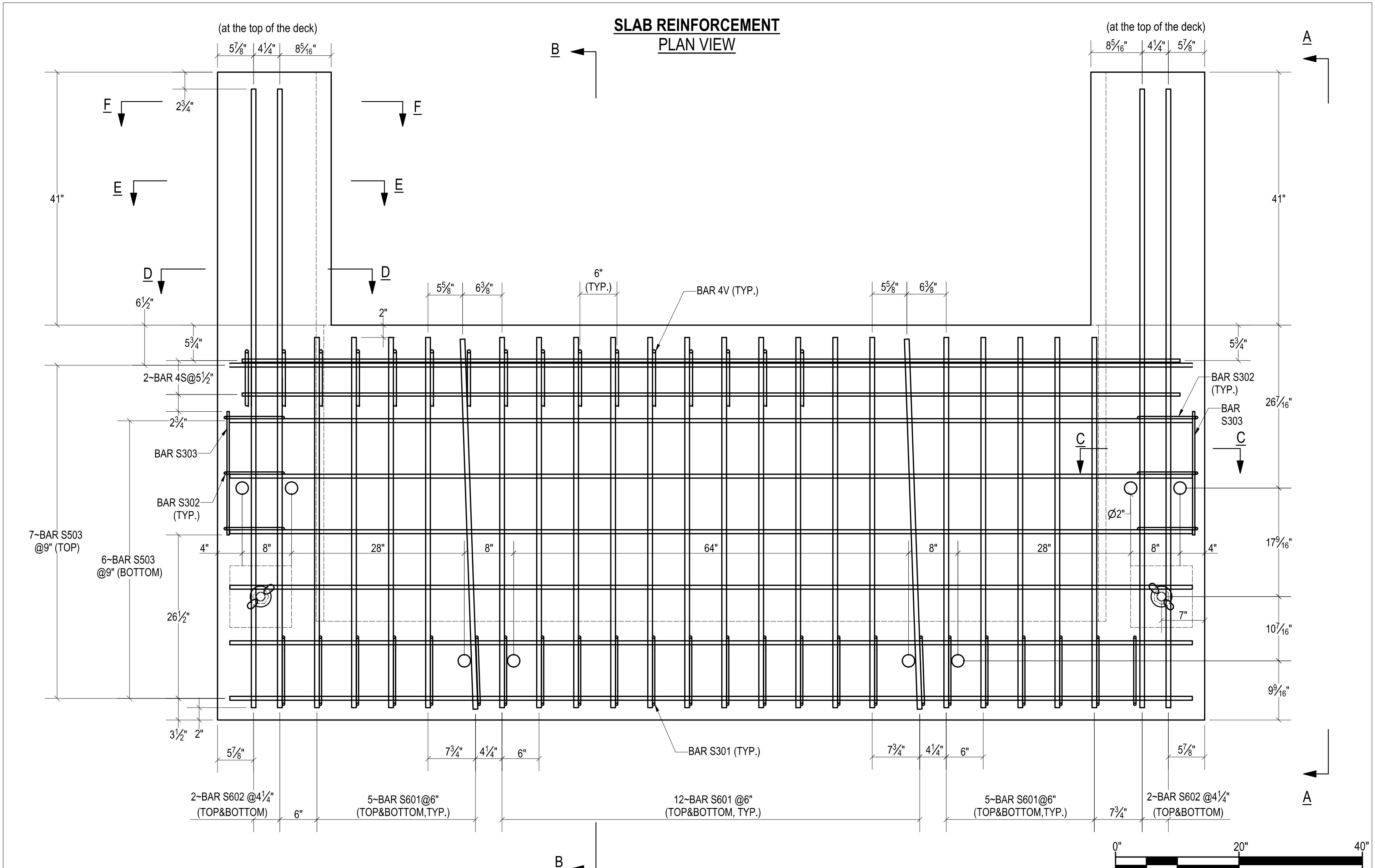

STEEL REINFORCED END-OF-RAIL TEST SPECIMEN

Revision:

OVERVIEW:
SLAB REINFORCEMENT

10/23/2020

University of Florida

SHEET 3 OF 18

THICKENED DECK AND BUTTRESS REINFORCEMENT
PLAN VIEW

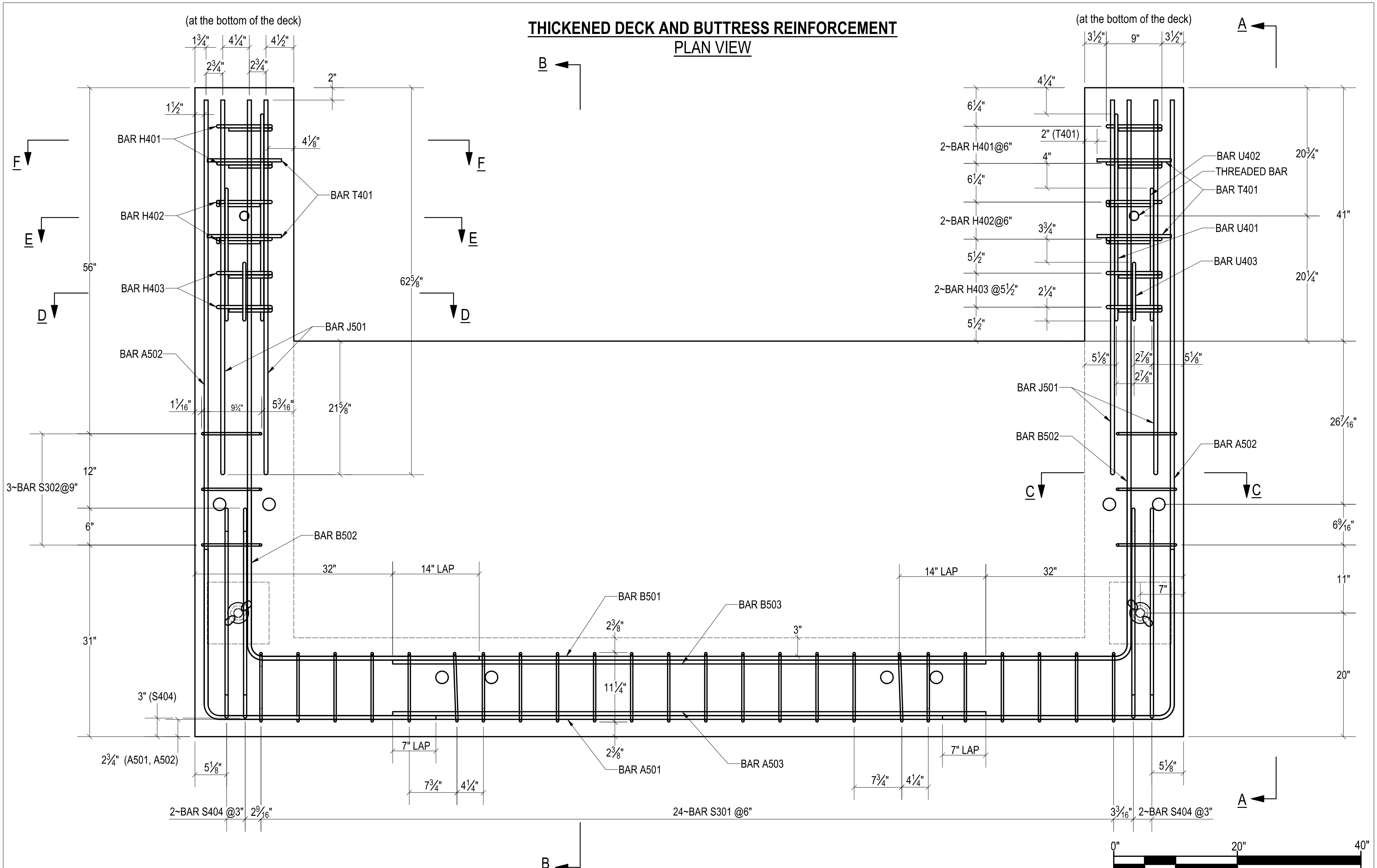

STEEL REINFORCED END-OF-RAIL TEST SPECIMEN			Revision:
OVERVIEW: THICKENED DECK REINFORCEMENT	10/23/2020	University of Florida	SHEET 4 OF 18

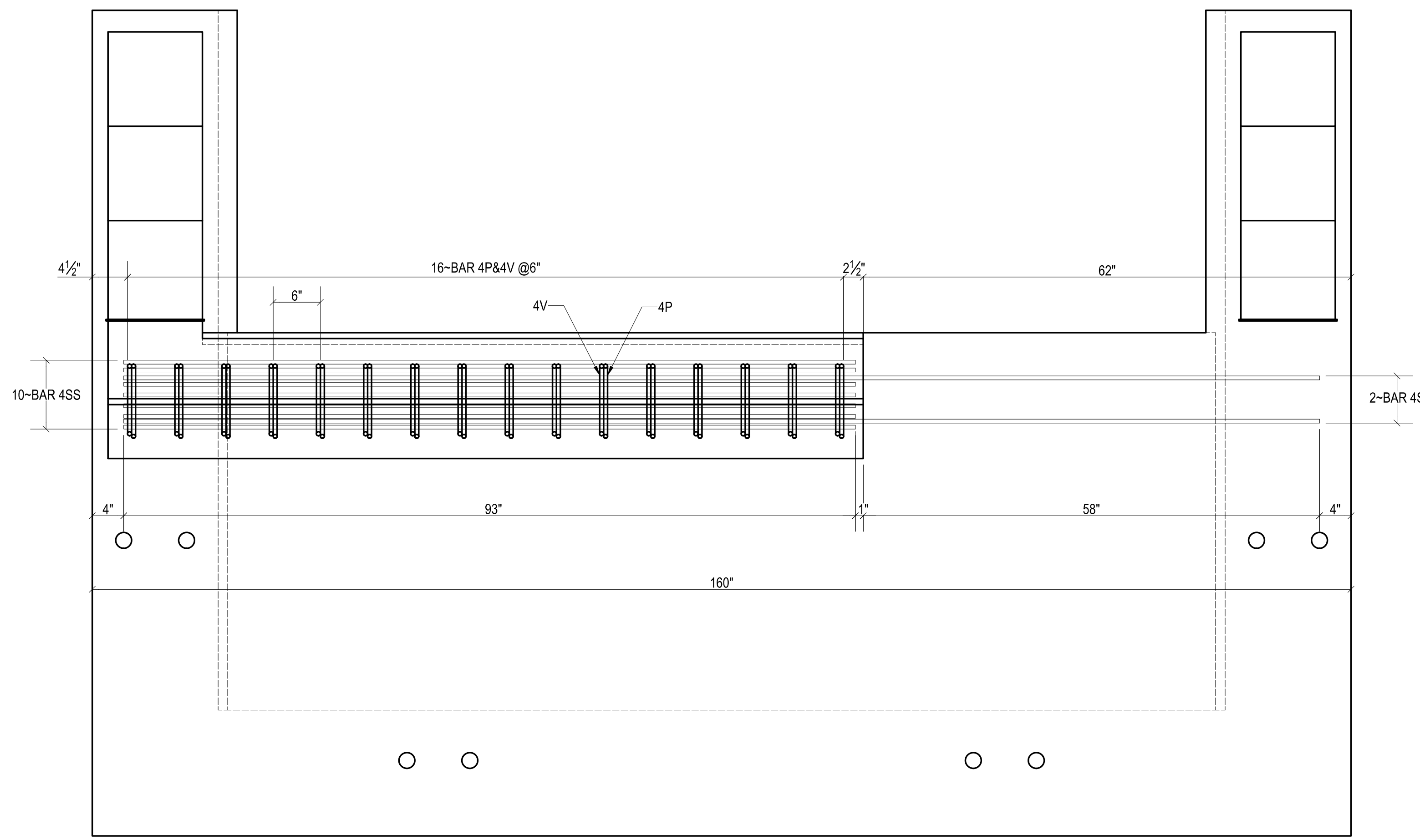

RAIL REINFORCEMENT
(PLAN VIEW)

STEEL REINFORCED END-OF-RAIL TEST SPECIMEN				*Revision:*
RAILING REINFORCEMENT: OVERVIEW	*10/23/2020*	*University of Florida*	*SHEET 5 OF 18*	

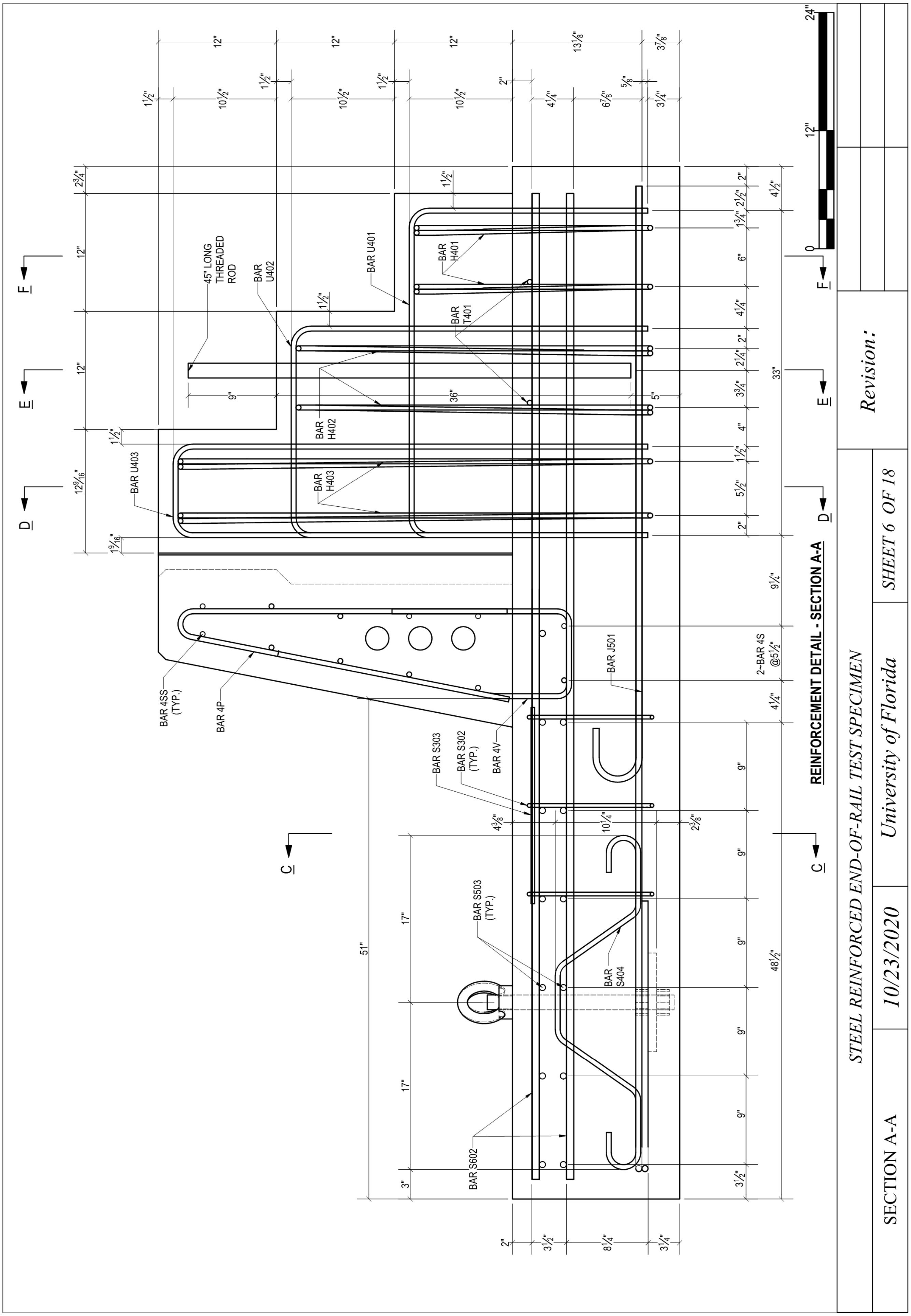
REINFORCEMENT DETAIL - SECTION A-A
STEEL REINFORCED END-OF-RAIL TEST SPECIMEN
University of Florida
10/23/2020
SECTION A-A
SHEET 6 OF 18
Revision:
45" LONG THREADED ROD
BAR U401
BAR U402
BAR U403
BAR H401
BAR H402
BAR H403
BAR T401
BAR 4SS (TYP.)
BAR 4P
BAR 4V
BAR J501
2~BAR 4S @5½"
BAR S302 (TYP.)
BAR S303
BAR S404
BAR S503 (TYP.)
BAR S602
D
E
F
C

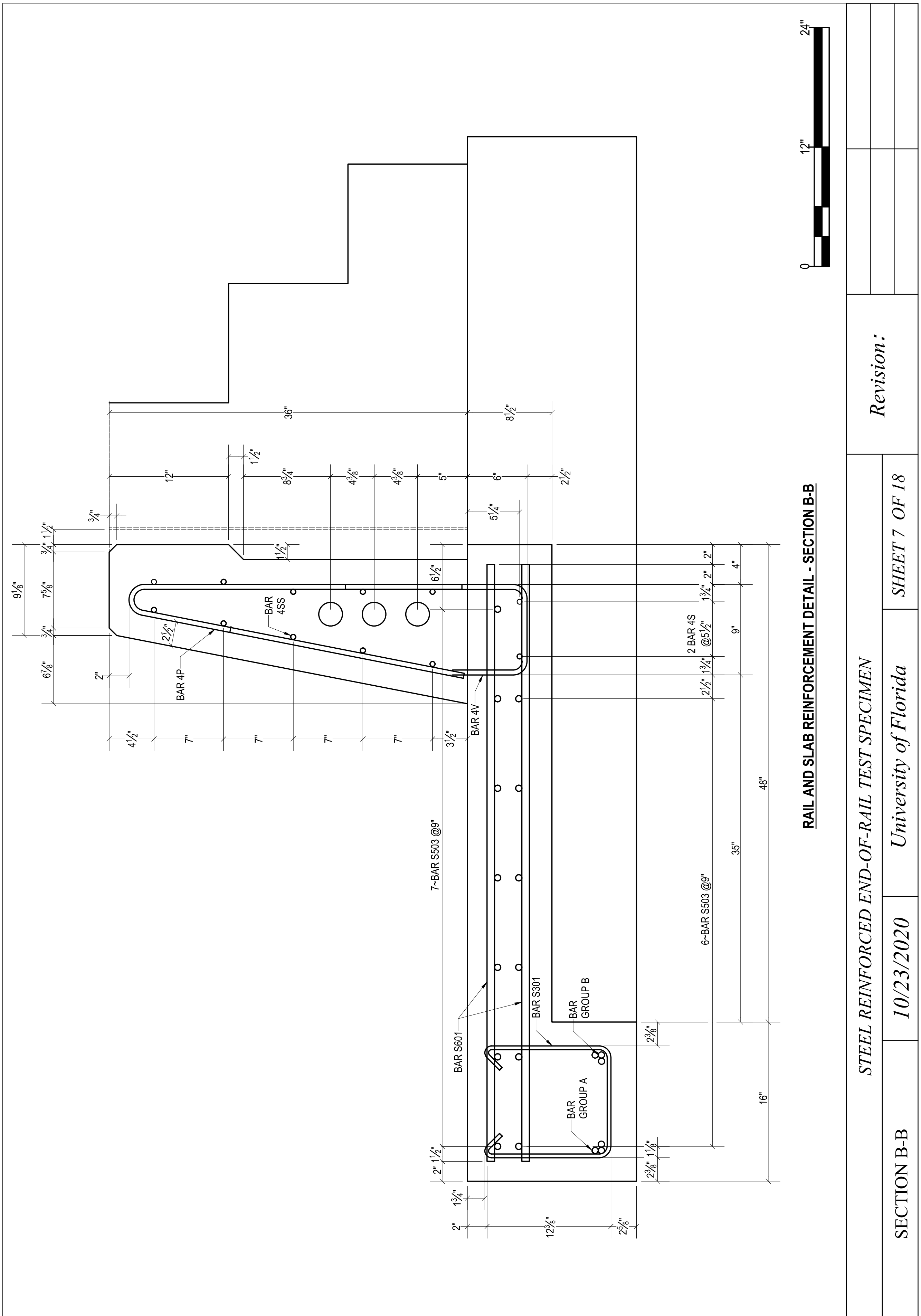
RAIL AND SLAB REINFORCEMENT DETAIL - SECTION B-B
BAR 4SS
BAR 4P
BAR 4V
2 BAR 4S @5½"
7~BAR S503 @9"
6~BAR S503 @9"
BAR S601
BAR S301
BAR GROUP B
BAR GROUP A
STEEL REINFORCED END-OF-RAIL TEST SPECIMEN
University of Florida
SECTION B-B
10/23/2020
SHEET 7 OF 18
Revision:

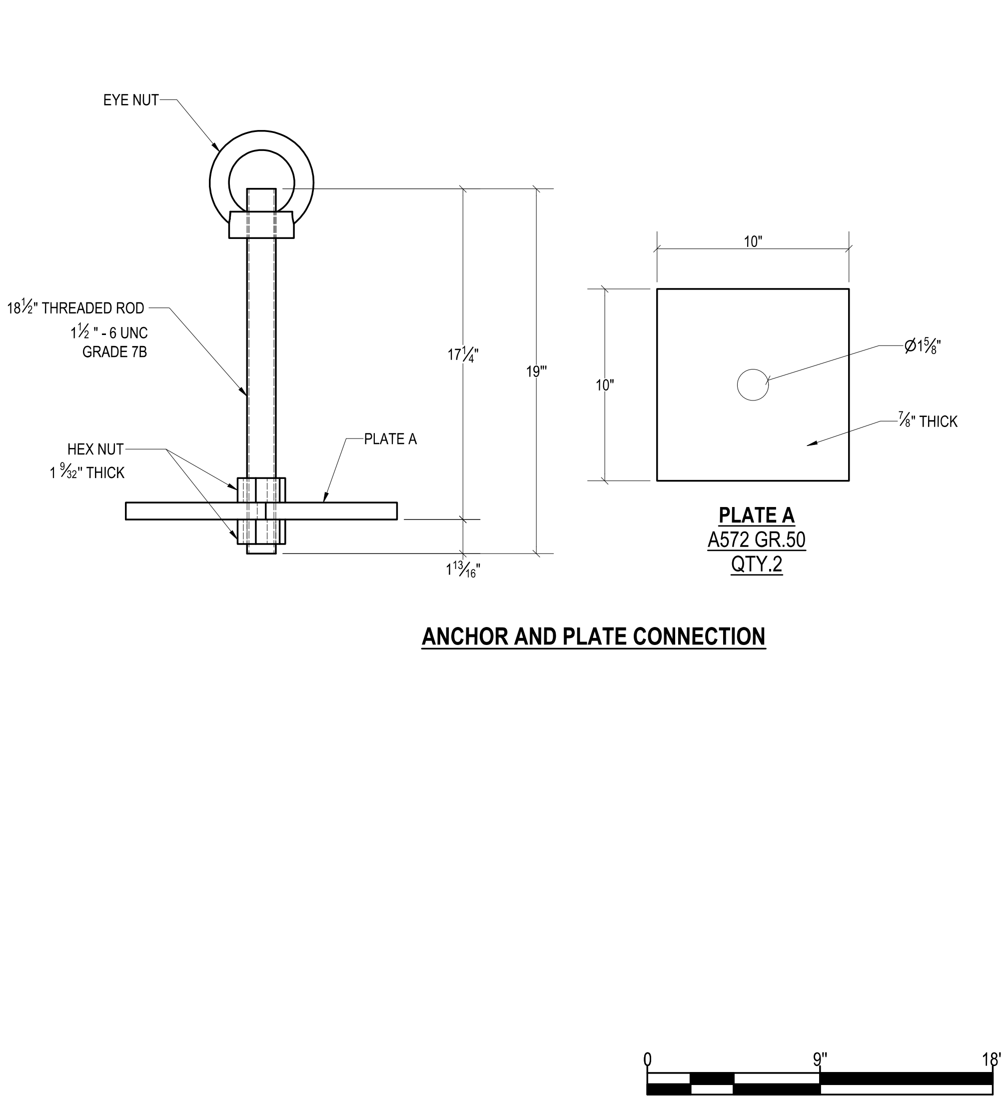

ANCHOR AND PLATE CONNECTION

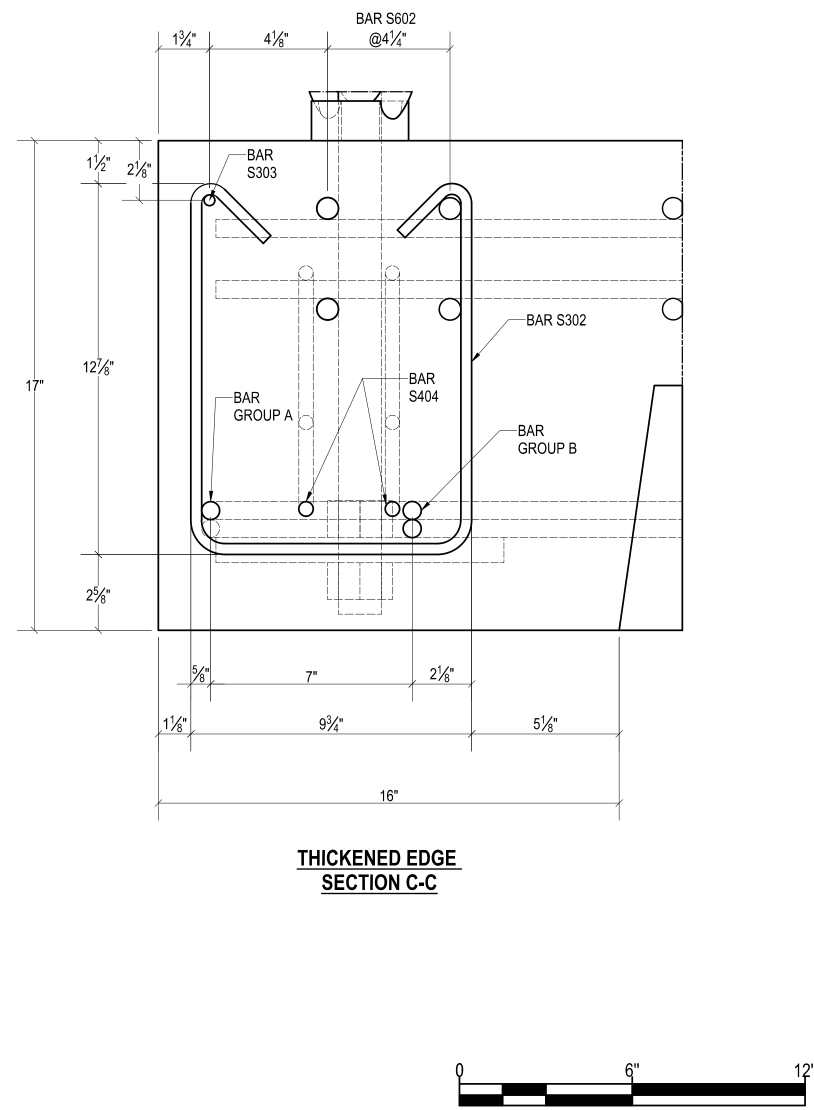

THICKENED EDGE
SECTION C-C

STEEL REINFORCED END-OF-RAIL TEST SPECIMEN

ANCHOR PLATE AND SECTION C-C	10/23/2020	University of Florida	SHEET 8 OF 18	Revision:

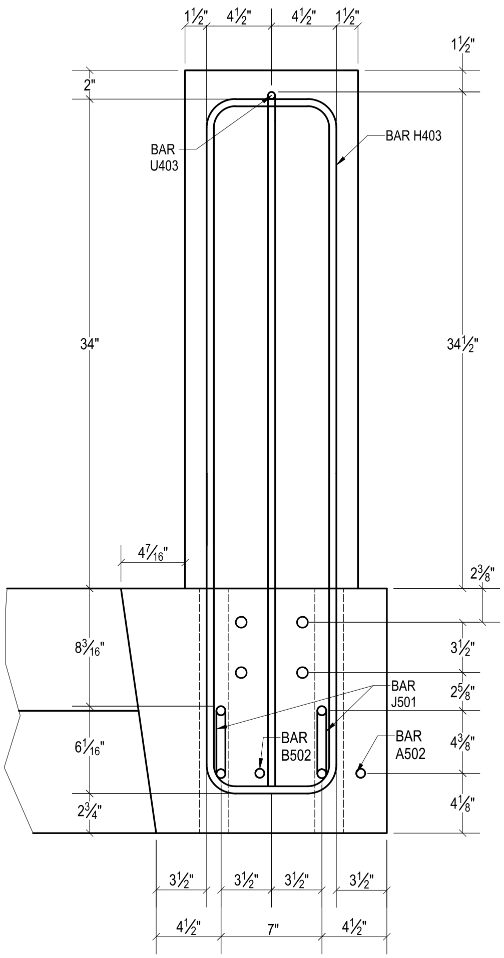

BUTTRESS REINFORCEMENT
SECTION D-D

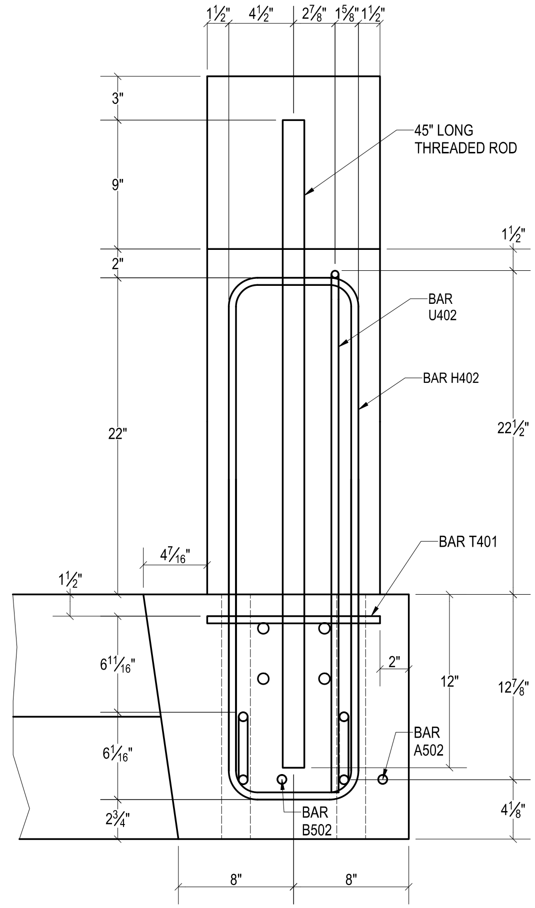

BUTTRESS REINFORCEMENT
SECTION E-E

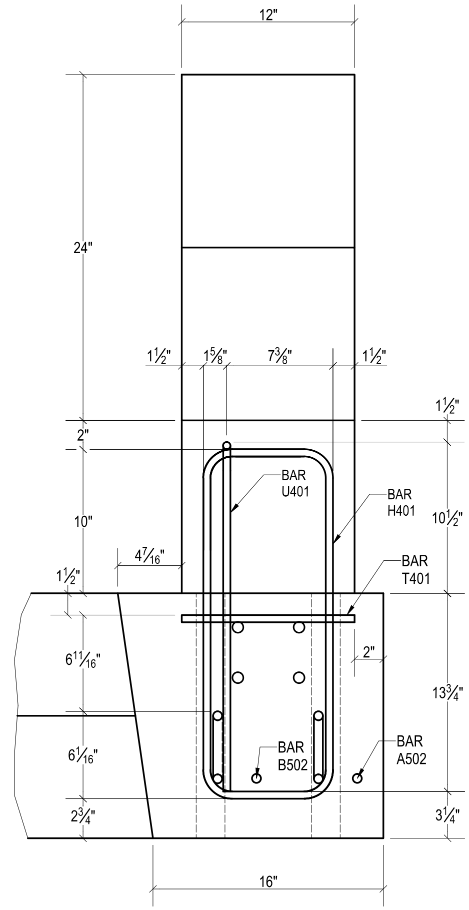

BUTTRESS REINFORCEMENT
SECTION F-F

STEEL REINFORCED END-OF-RAIL TEST SPECIMEN				Revision:
SECTION D, E, F: BUTTRESS REINFORCEMENT	10/23/2020	University of Florida	SHEET 9 OF 18	

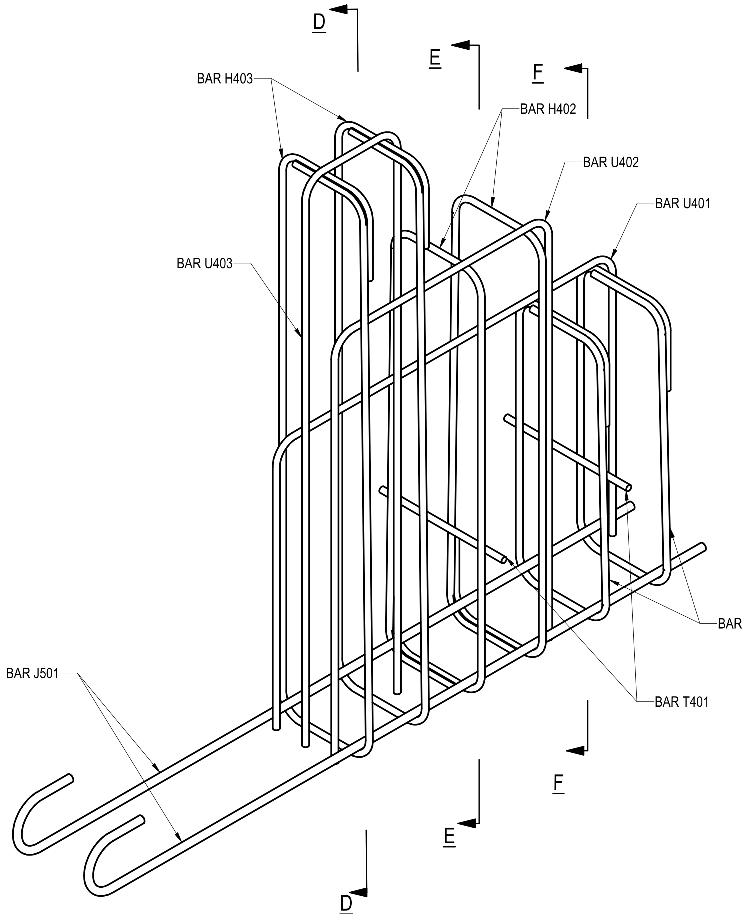

BUTTRESS REINFORCING CAGE
END A: WEST

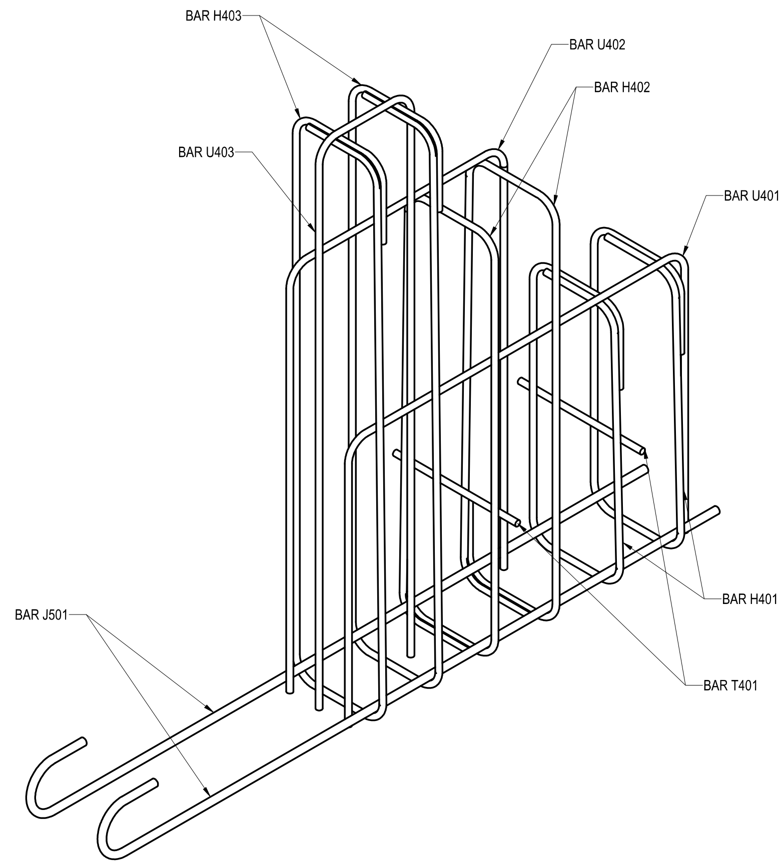

BUTTRESS REINFORCING CAGE
END B: EAST

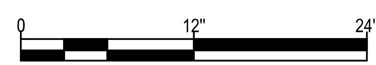

STEEL REINFORCED END-OF-RAIL TEST SPECIMEN				Revision:
BUTTRESS REINFORCEMENT	10/23/2020	University of Florida	SHEET 10 OF 18	

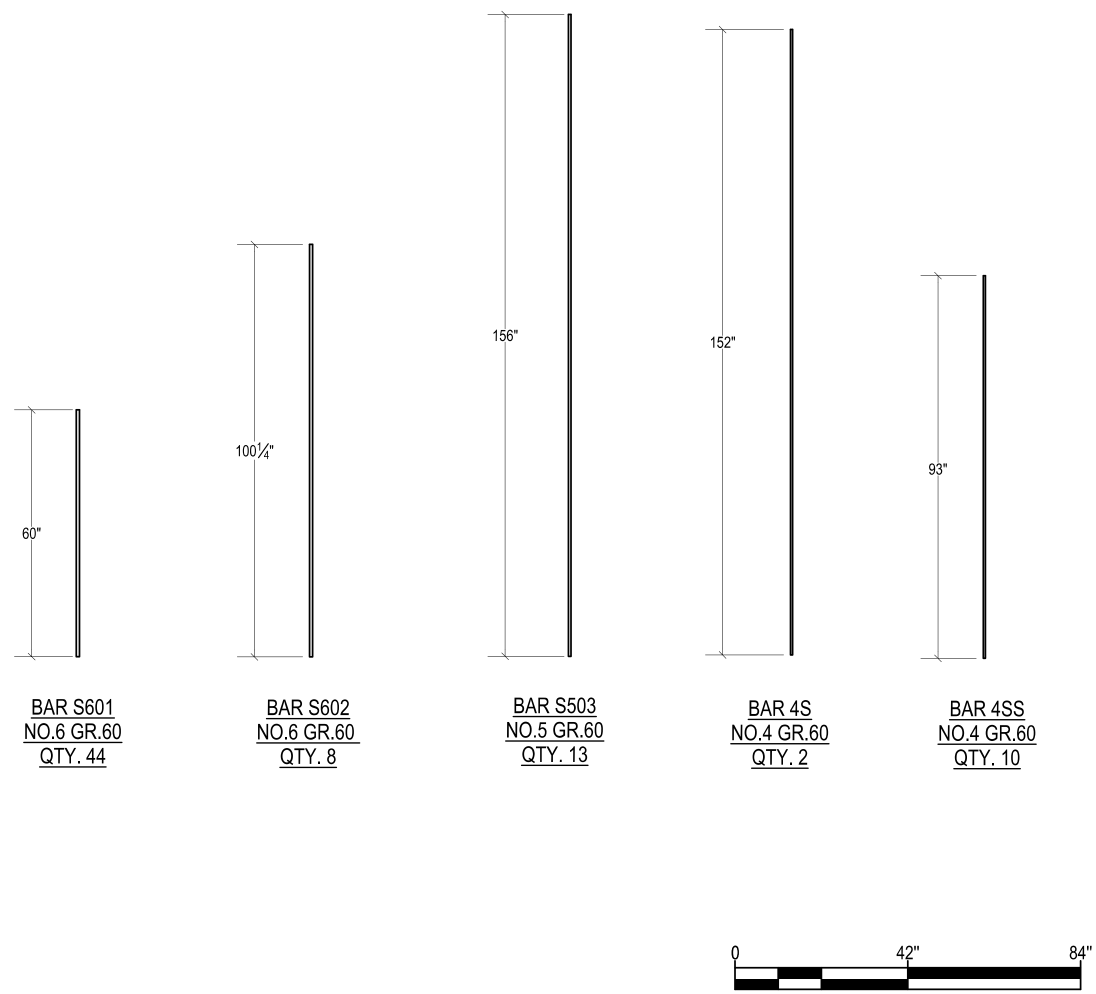

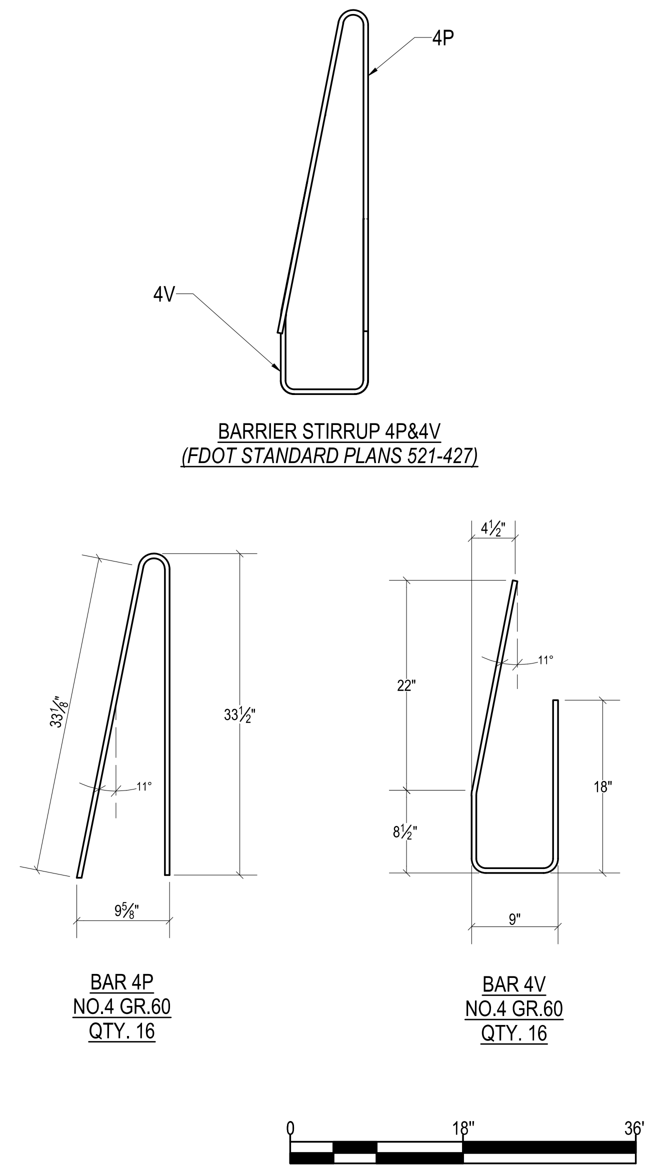

STEEL REINFORCED END-OF-RAIL TEST SPECIMEN				Revision:
BAR LIST - SLAB	10/23/2020	University of Florida	SHEET 11 OF 18	

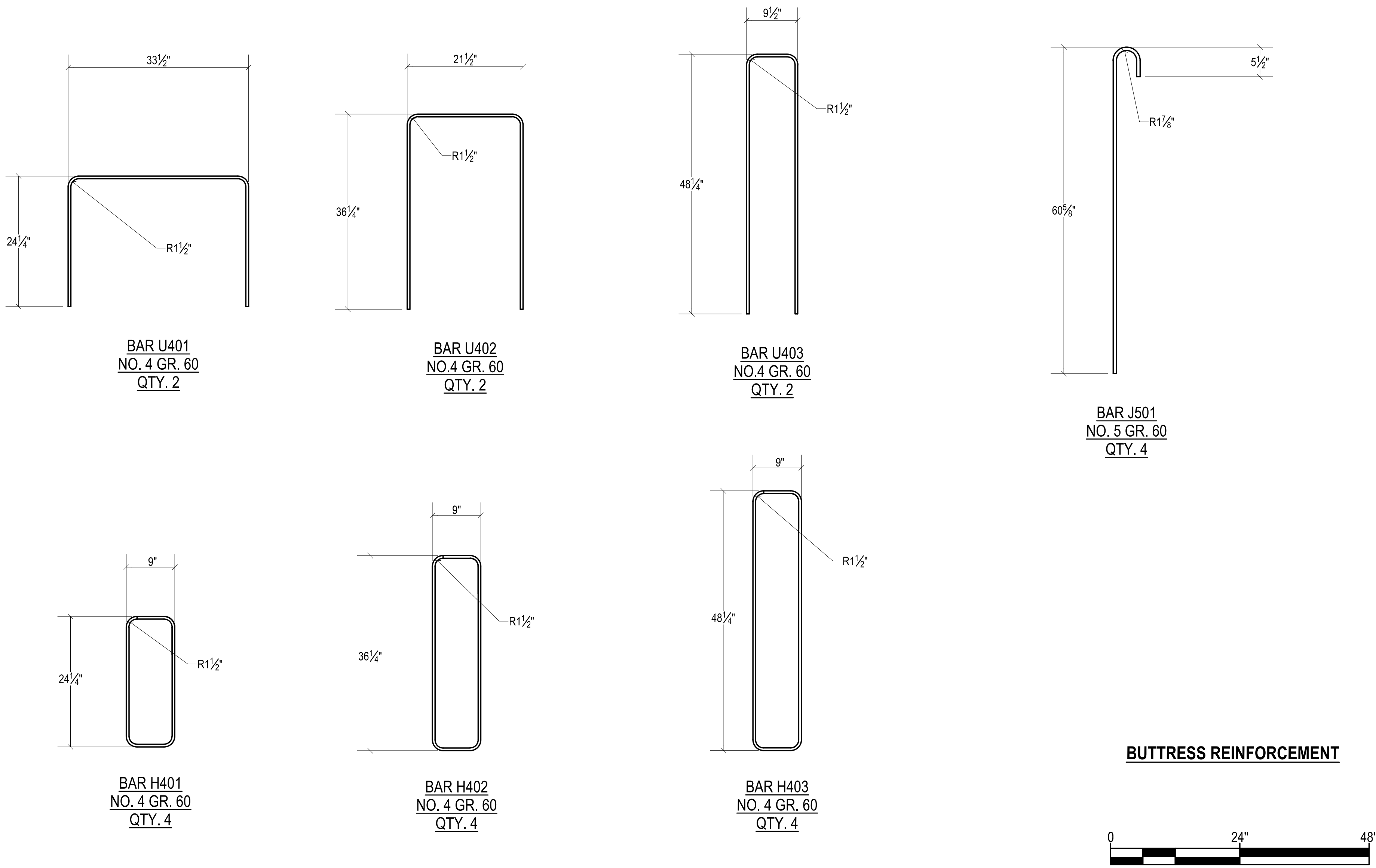

STEEL REINFORCED END-OF-RAIL TEST SPECIMEN				*Revision:*		
BAR LIST - BUTTRESS	*10/23/2020*	*University of Florida*	*SHEET 12 OF 18*			

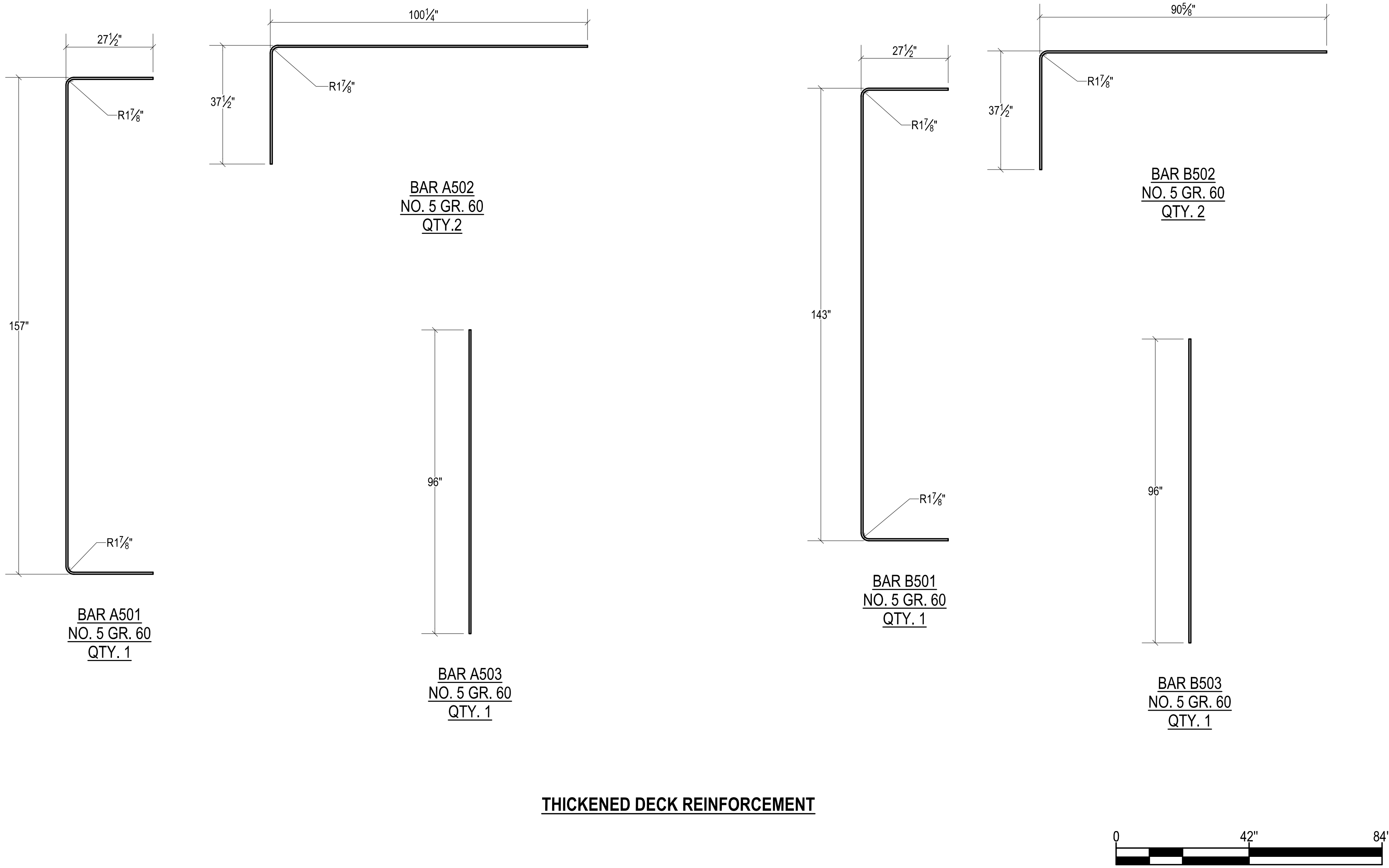

THICKENED DECK REINFORCEMENT

STEEL REINFORCED END-OF-RAIL TEST SPECIMEN				*Revision:*
BAR LIST - THICKENED DECK	*10/23/2020*	*University of Florida*	*SHEET 13 OF 18*	

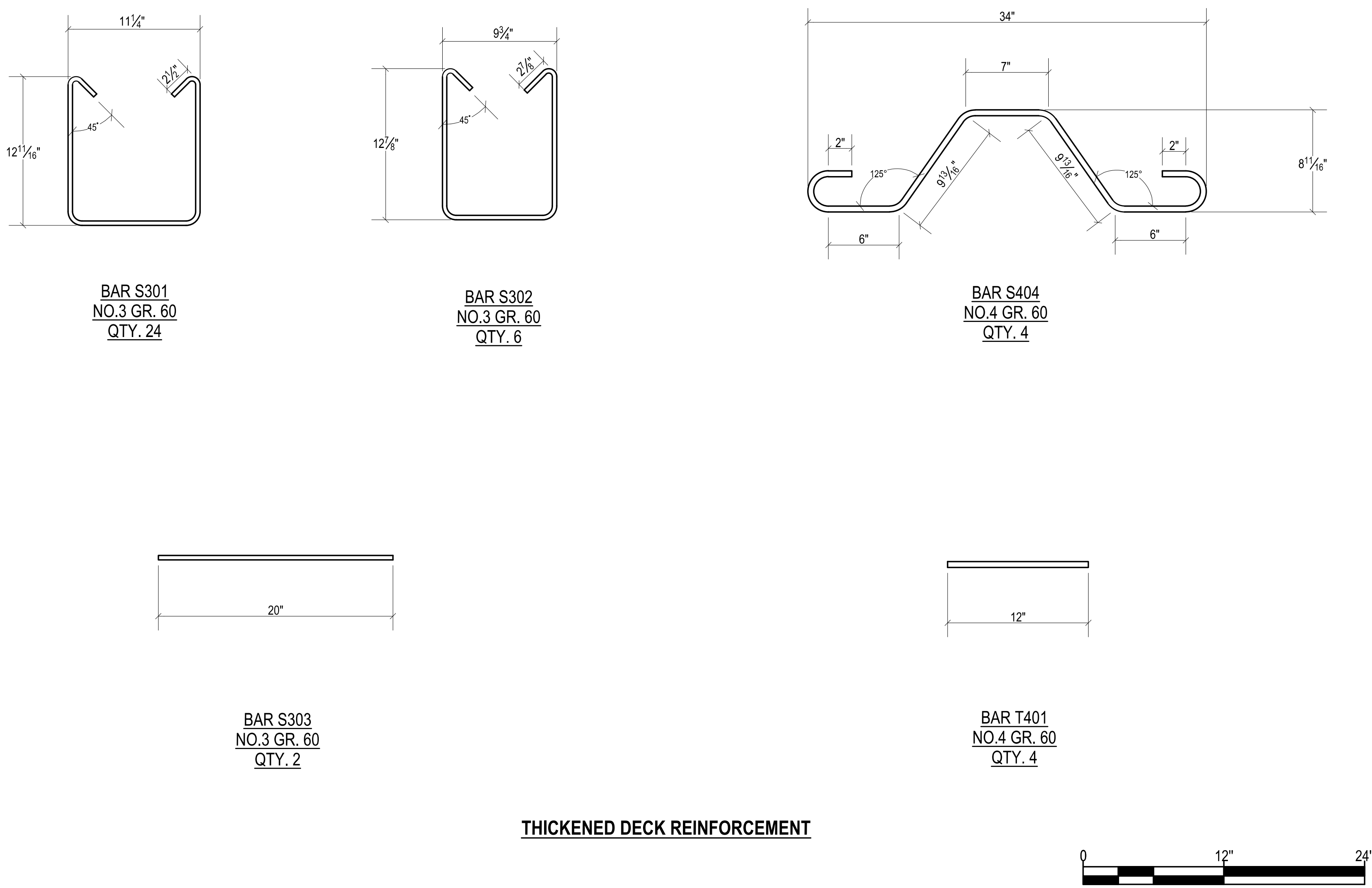

STEEL REINFORCED END-OF-RAIL TEST SPECIMEN				*Revision:*
BAR LIST - THICKENED DECK	*10/23/2020*	*University of Florida*	*SHEET 14 OF 18*	

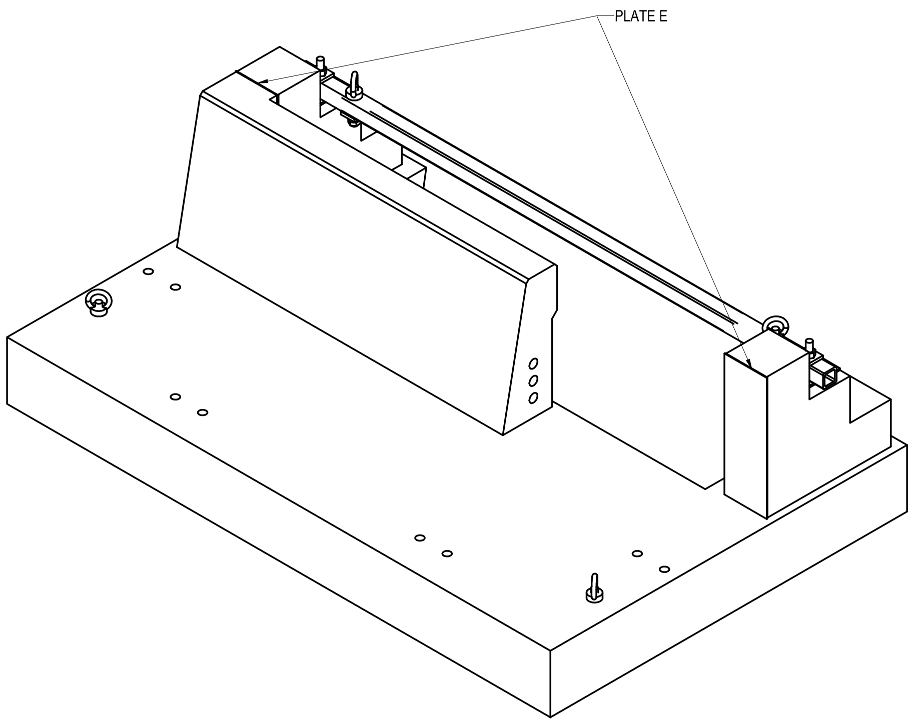

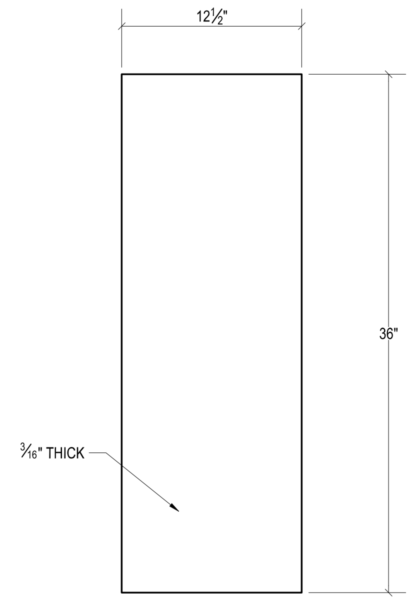

PLATE E
STEEL SEPARATION PLATE
A36
QTY. 2

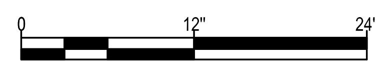

STEEL REINFORCED END-OF-RAIL TEST SPECIMEN				Revision:
BUTTRESS-RAIL INTERFACE	10/23/2020	University of Florida	SHEET 15 OF 18	

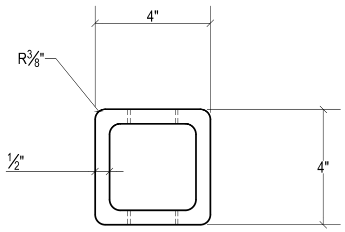

HSS 4X4X1/2
A500 GR.B

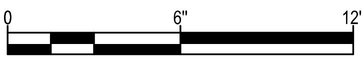

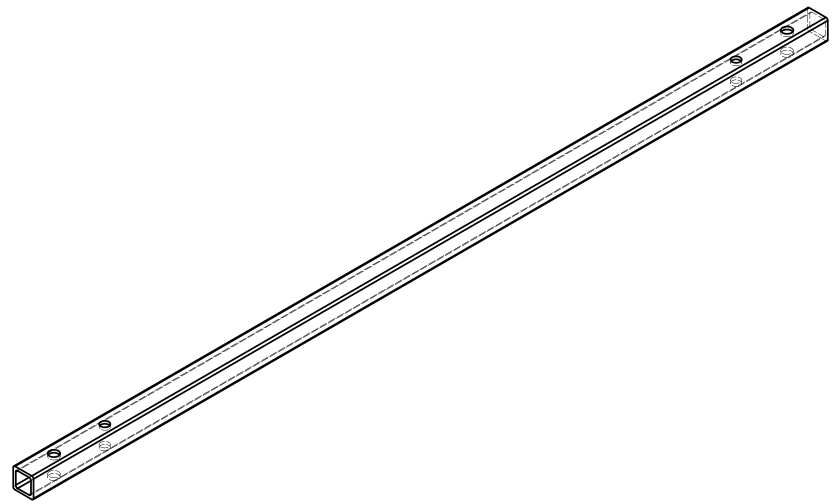

HSS
ISOMETRIC VIEW

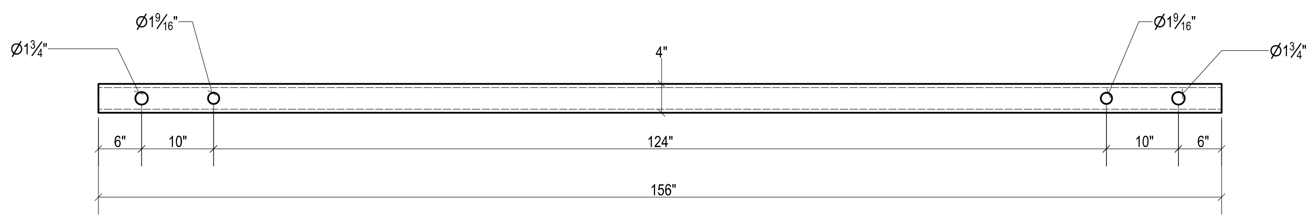

HSS
PLAN VIEW

HSS WITH CONNECTION LOCATIONS

STEEL REINFORCED END-OF-RAIL TEST SPECIMEN				Revision:
HSS DETAIL	10/23/2020	University of Florida	SHEET 16 OF 18	

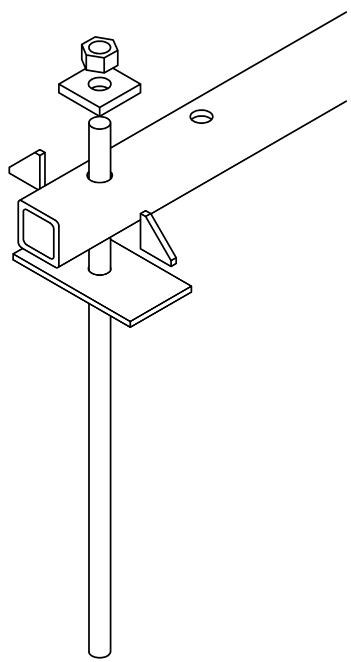

BUTTRESS ANCHOR ASSEMBLY

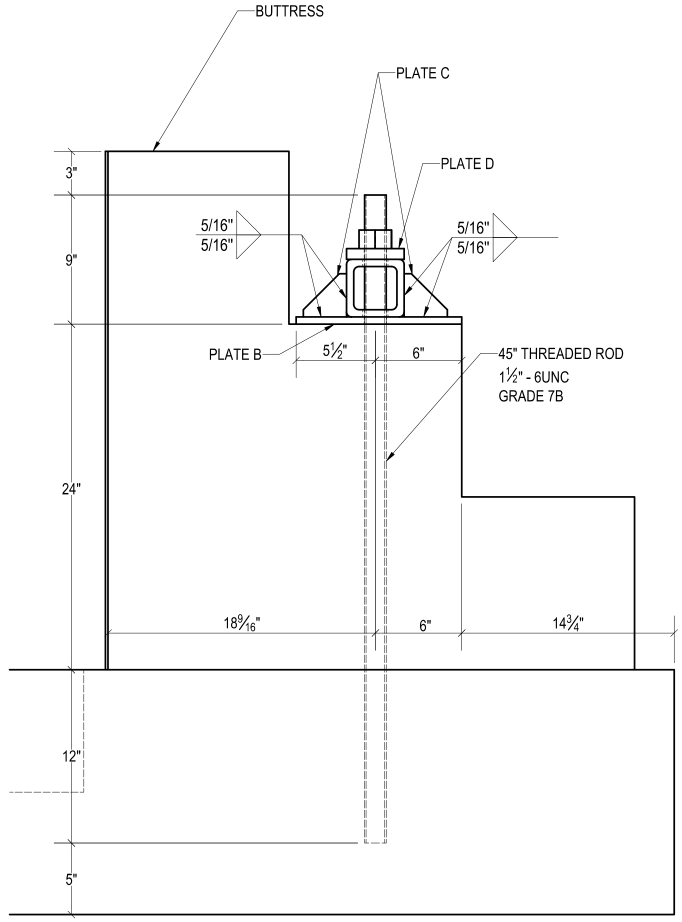

THREADED ROD ANCHOR CONNECTION

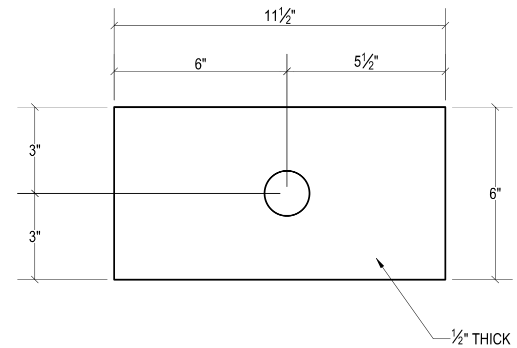

PLATE B
BEARING PLATE
A572 GR.50
QTY. 2

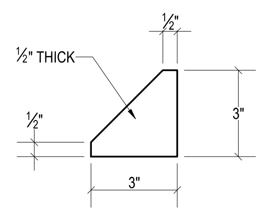

PLATE C
STIFFENER
A572 GR.50
QTY. 4

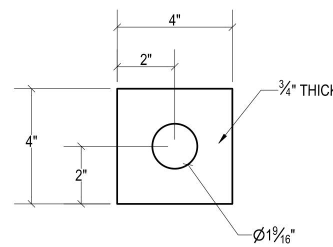

PLATE D
SQUARE PLATE
A572 GR.50
QTY. 4

STEEL REINFORCED END-OF-RAIL TEST SPECIMEN				*Revision:*
HSS-BUTTRESS CONNECTION	*10/23/2020*	*University of Florida*	*SHEET 17 OF 18*	

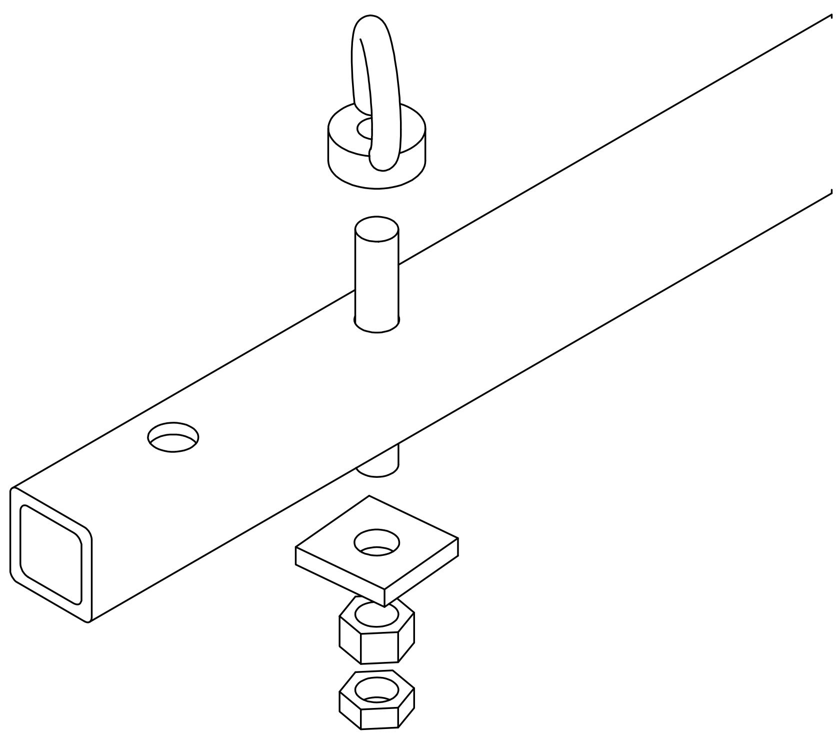

LIFTING EYE NUT ASSEMBLY

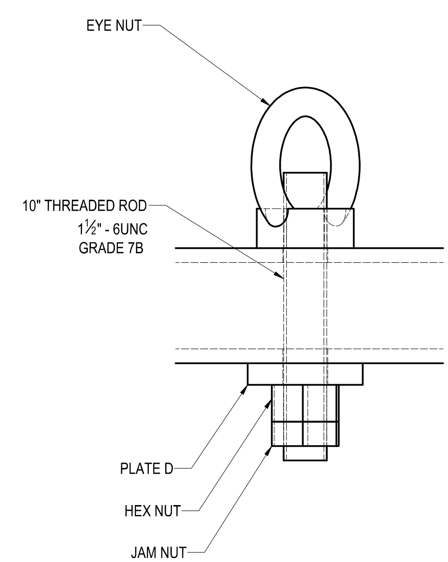

LIFTING EYE NUT CONNECTION

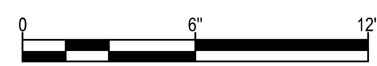

STEEL REINFORCED END-OF-RAIL TEST SPECIMEN				*Revision:*
HSS-LIFTING EYE BOLT CONNECTION	*10/23/2020*	*University of Florida*	*SHEET 18 OF 18*	

APPENDIX H
IMPACT TEST SPECIMEN ANCHORING SEQUENCE DRAWINGS

Presented in this appendix are construction drawings that detail the specimen anchoring sequence, which describe the approach for connecting and anchoring each impact test specimen to the pendulum universal foundation (before impact testing was conducted).

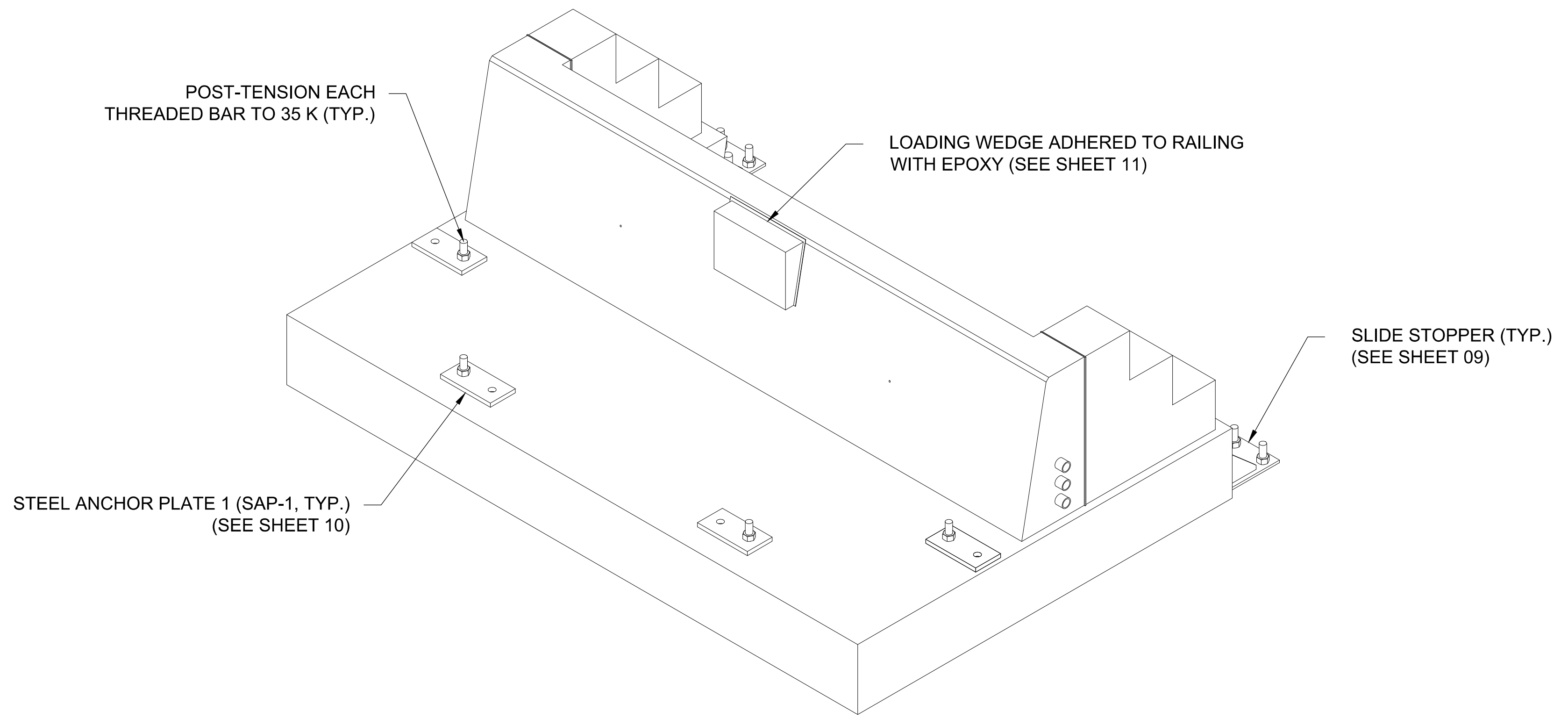

ANCHORED IMPACT SPECIMEN
FRONT ISOMETRIC VIEW

Fiber-Reinforced Concrete Traffic Railings for Impact Loading				*Revisions:*		
Specimen Anchoring Plan	*2020-04-20*	*University of Florida*	*Sheet 01 of 12*			

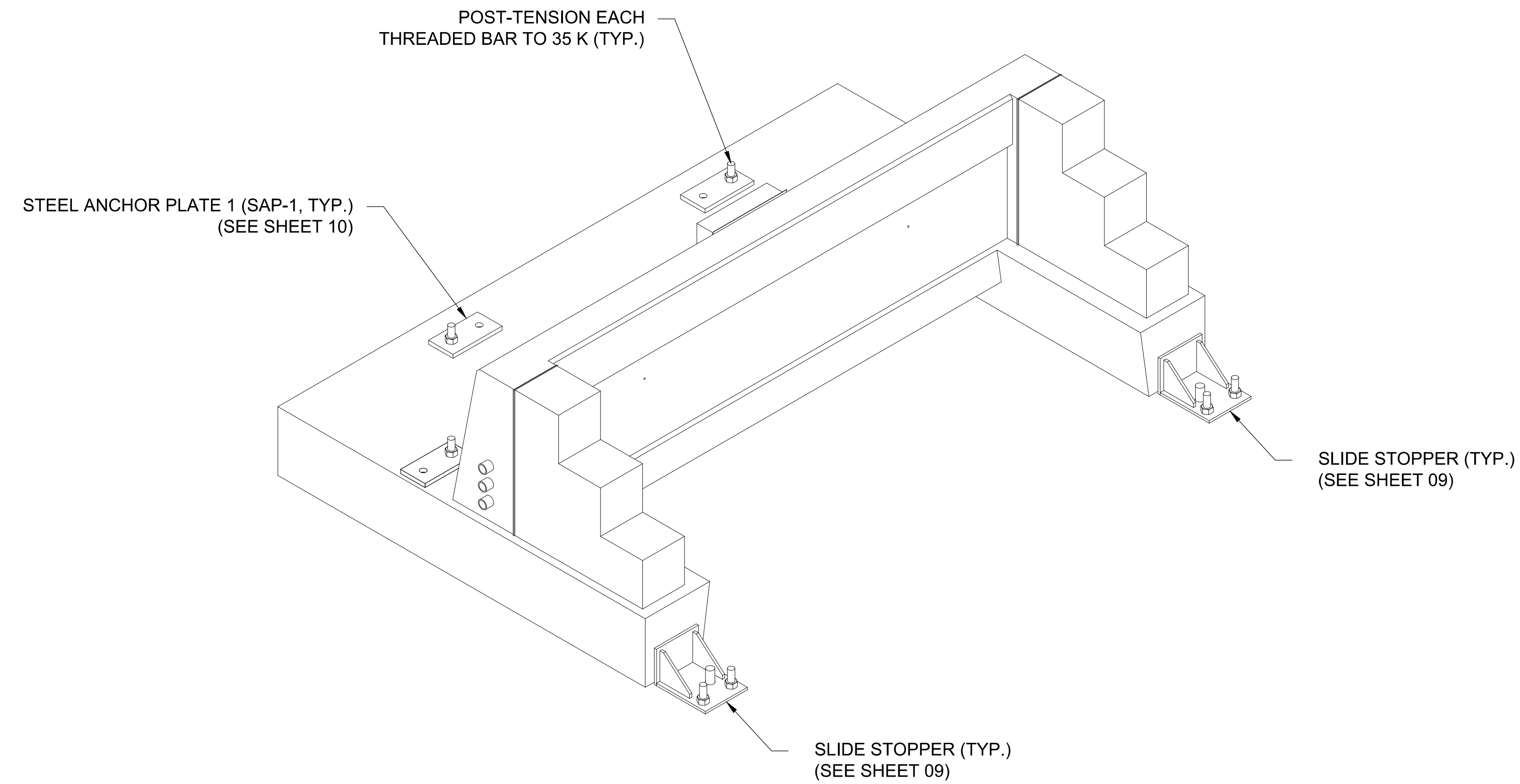

ANCHORED IMPACT SPECIMEN
BACK ISOMETRIC VIEW

Fiber-Reinforced Concrete Traffic Railings for Impact Loading				*Revisions:*
Specimen Anchoring Plan	*2020-04-20*	*University of Florida*	*Sheet 02 of 12*	

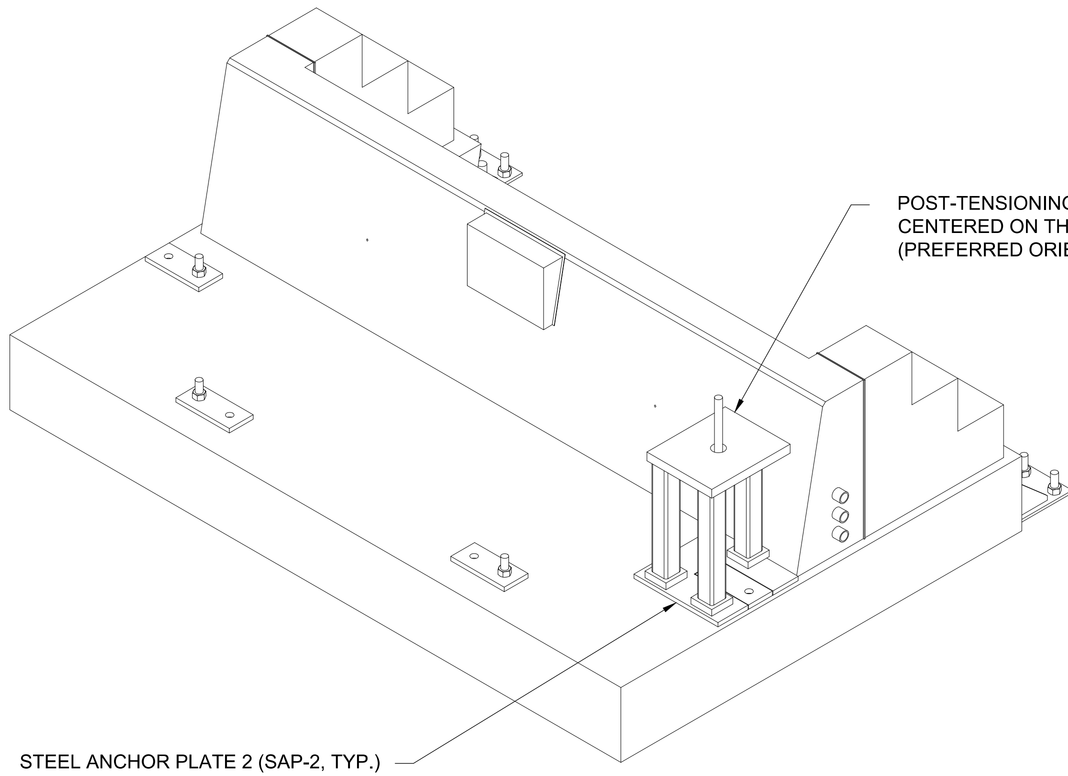

ANCHORED IMPACT SPECIMEN
FRONT ISOMETRIC VIEW

Fiber-Reinforced Concrete Traffic Railings for Impact Loading				*Revisions:*	-Centered loading assembly on bar	
Specimen Anchoring Plan	*2020-04-20*	*University of Florida*	*Sheet 03 of 12*			

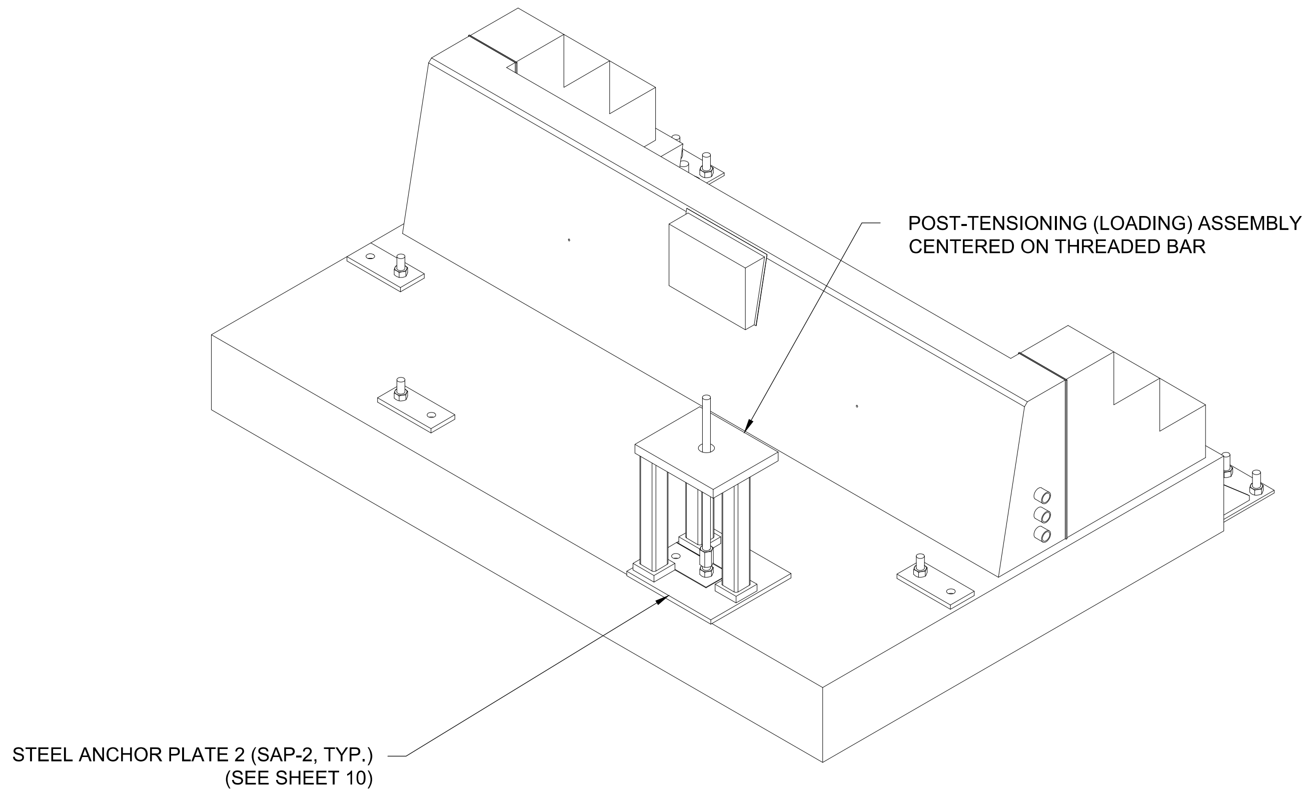

ANCHORED IMPACT SPECIMEN
FRONT ISOMETRIC VIEW

Fiber-Reinforced Concrete Traffic Railings for Impact Loading				*Revisions:*
Specimen Anchoring Plan	*2020-04-20*	*University of Florida*	*Sheet 04 of 12*	

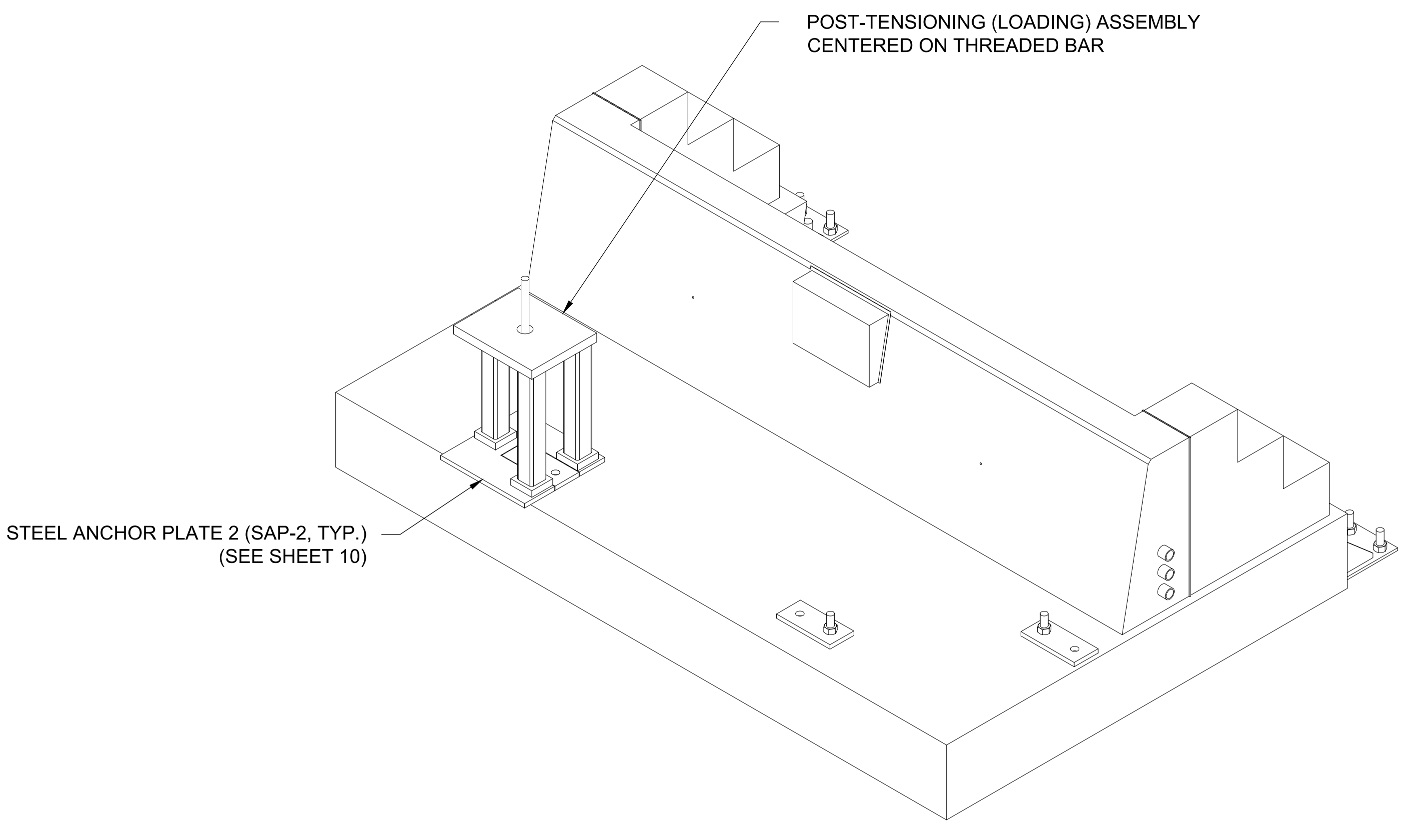

ANCHORED IMPACT SPECIMEN
FRONT ISOMETRIC VIEW

Fiber-Reinforced Concrete Traffic Railings for Impact Loading				*Revisions:*	
Specimen Anchoring Plan	*2020-04-20*	*University of Florida*	*Sheet 05 of 12*		

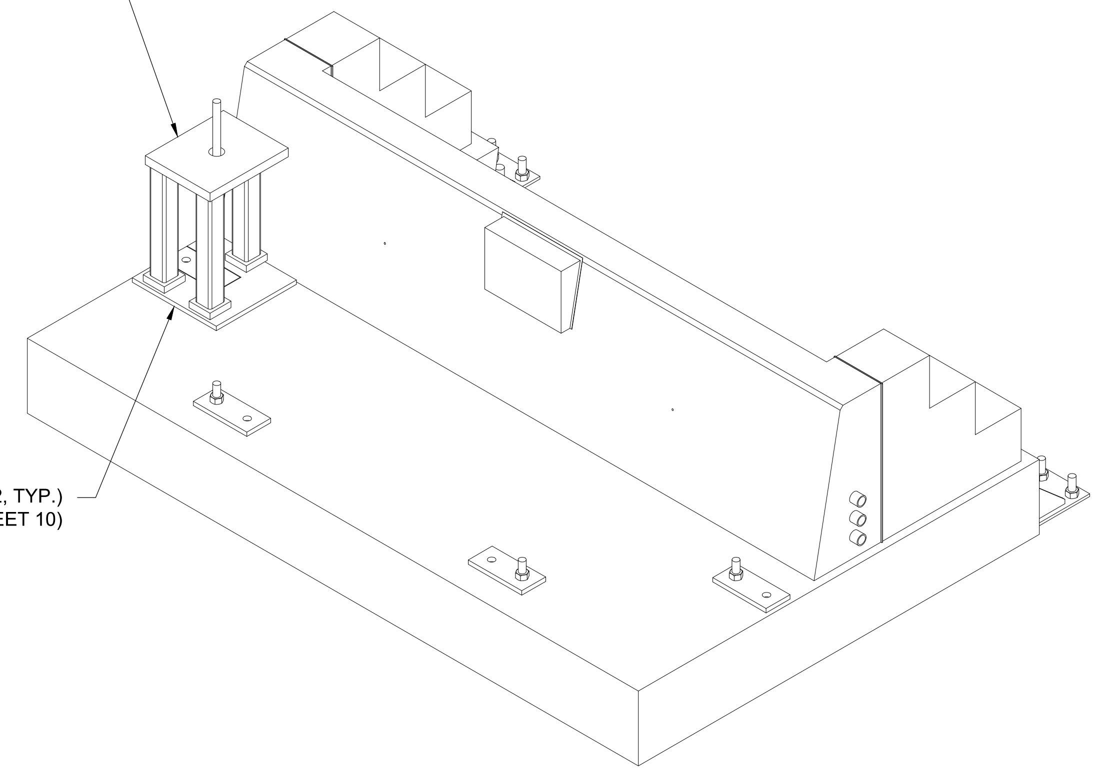

ANCHORED IMPACT SPECIMEN
FRONT ISOMETRIC VIEW

Fiber-Reinforced Concrete Traffic Railings for Impact Loading				*Revisions:*	-Centered loading assembly on bar
Specimen Anchoring Plan	*2020-04-20*	*University of Florida*	*Sheet 06 of 12*		

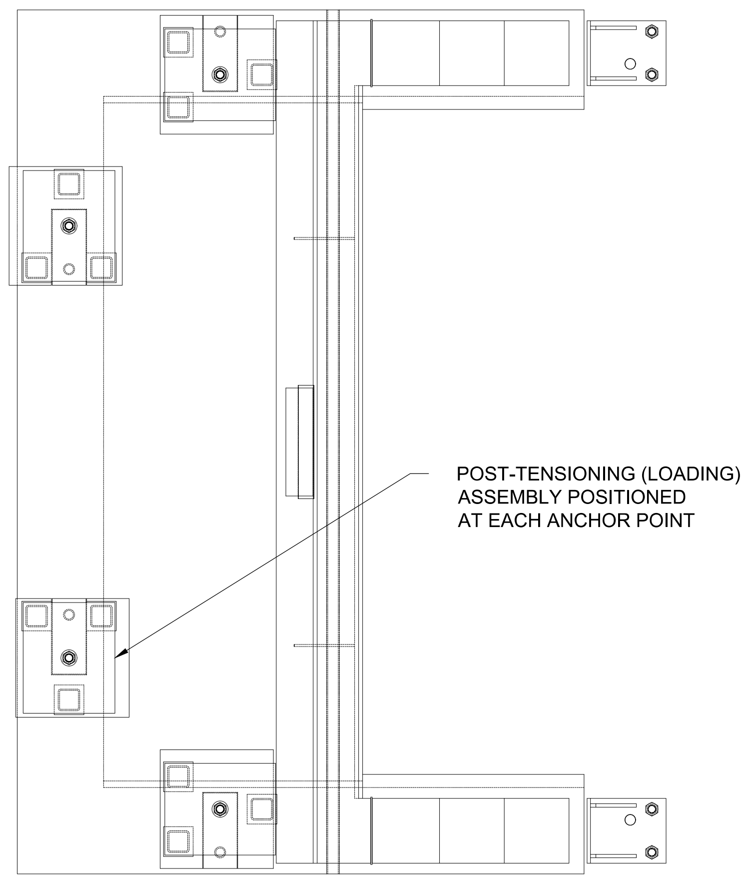

ANCHORED IMPACT SPECIMEN
PLAN VIEW

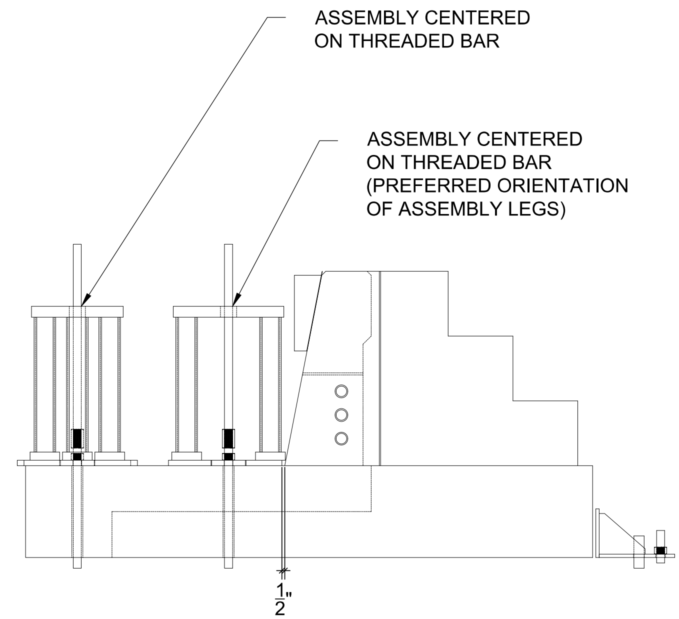

ANCHORED IMPACT SPECIMEN
SIDE ELEVATION VIEW

Fiber-Reinforced Concrete Traffic Railings for Impact Loading				*Revisions:*	-Centered loading assembly on bar
Specimen Anchoring Plan	*2020-04-20*	*University of Florida*	*Sheet 07 of 12*		

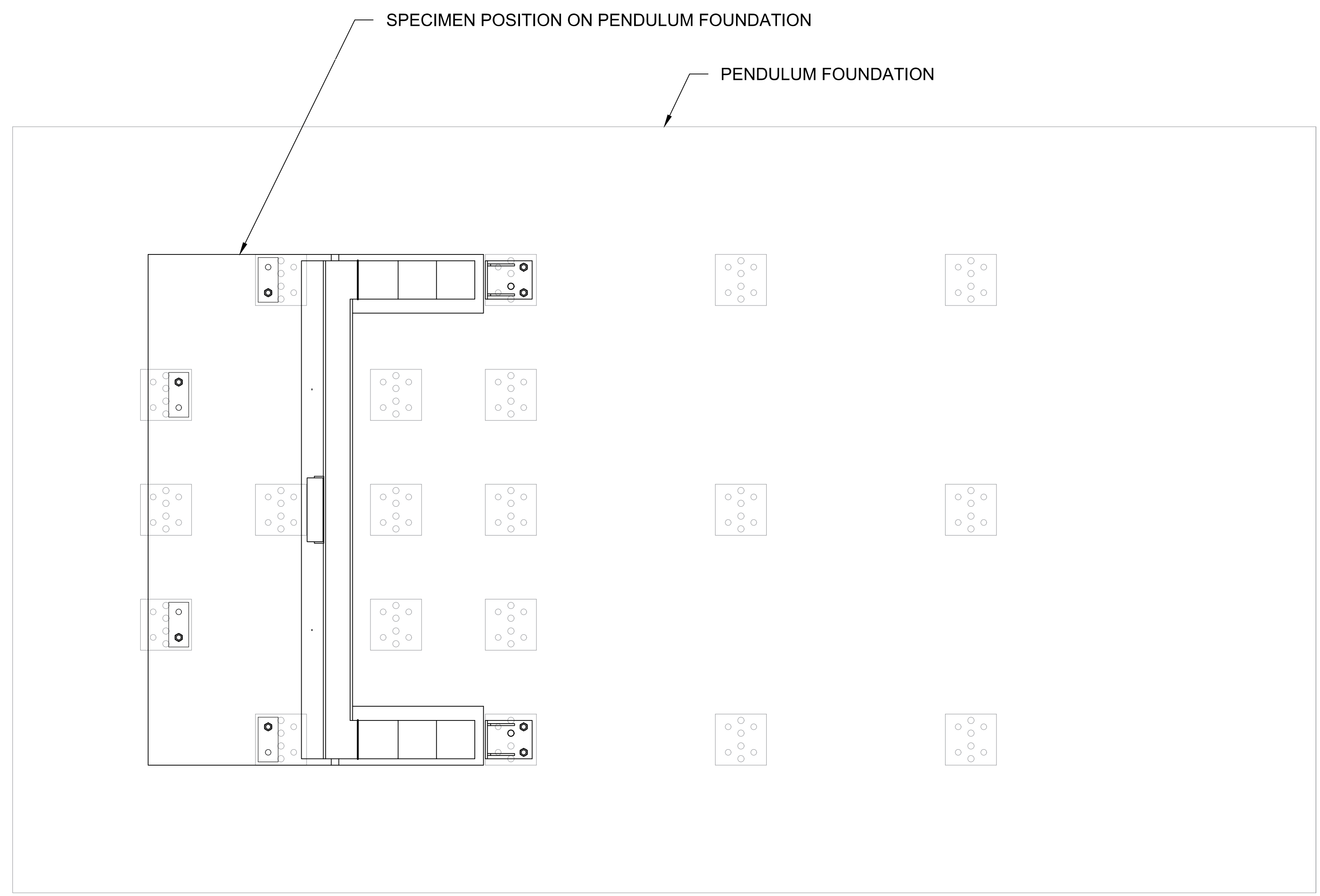

ANCHORED IMPACT SPECIMEN
PLAN VIEW

Fiber-Reinforced Concrete Traffic Railings for Impact Loading				*Revisions:*
Specimen Anchoring Plan	*2020-04-20*	*University of Florida*	*Sheet 08 of 12*	

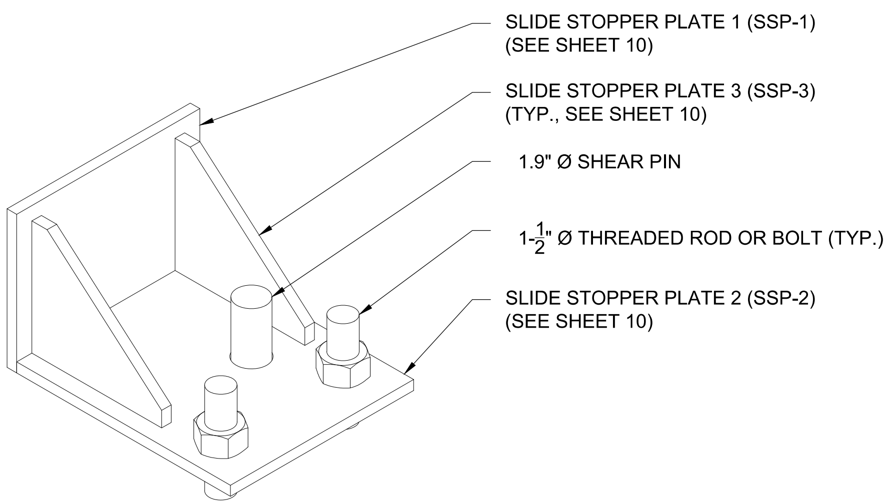

SLIDE STOPPER (QTY: 2)
BACK ISOMETRIC VIEW

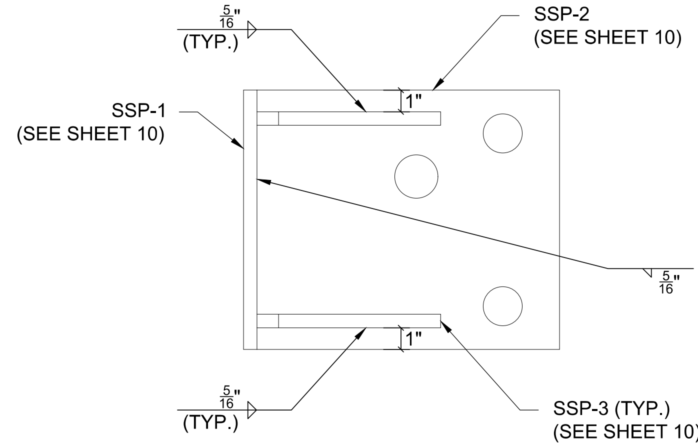

SLIDE STOPPER
PLAN VIEW

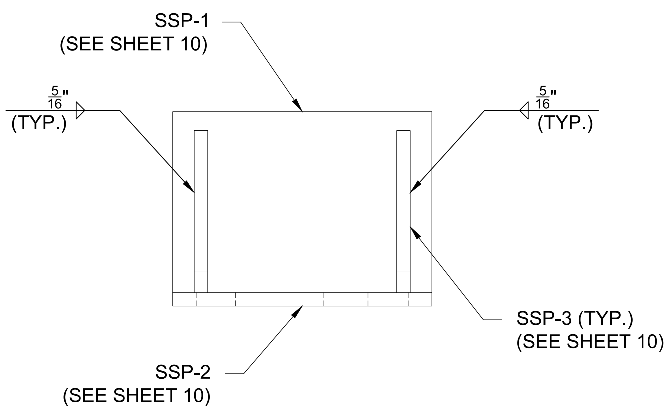

SLIDE STOPPER
BACK ELEVATION VIEW

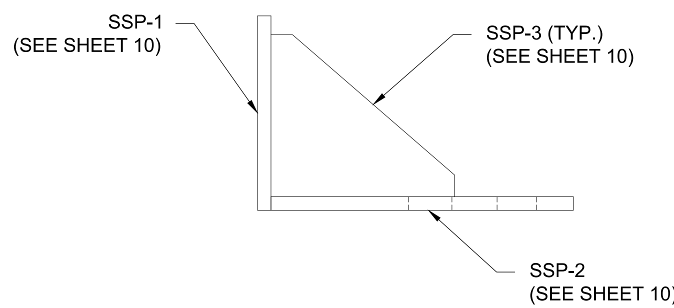

SLIDE STOPPER
SIDE ELEVATION VIEW

Fiber-Reinforced Concrete Traffic Railings for Impact Loading				*Revisions:*	
Specimen Anchoring Plan	*2020-04-20*	*University of Florida*	*Sheet 09 of 12*		

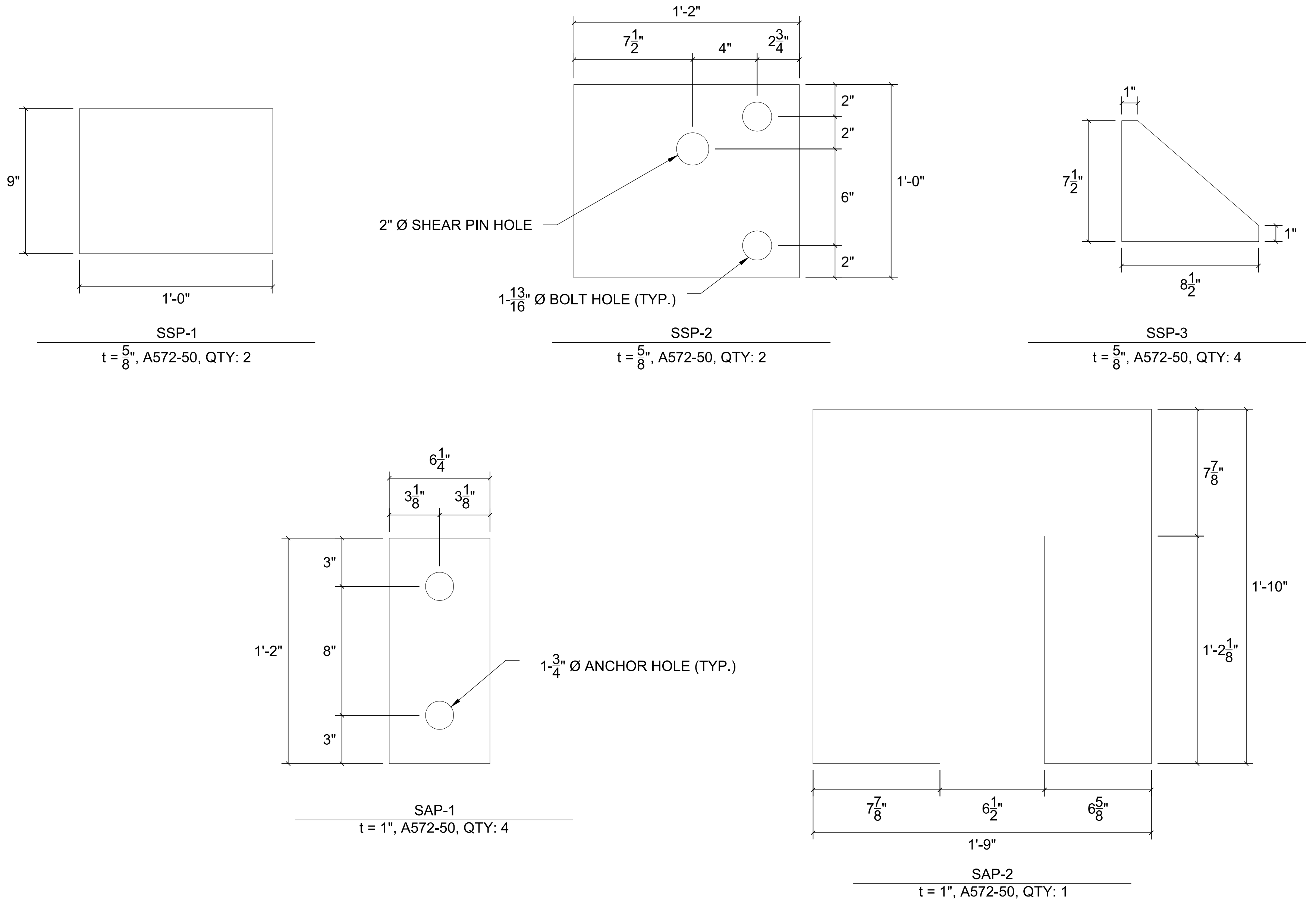

Fiber-Reinforced Concrete Traffic Railings for Impact Loading				*Revisions:*
Specimen Anchoring Plan	*2020-04-20*	*University of Florida*	*Sheet 10 of 12*	

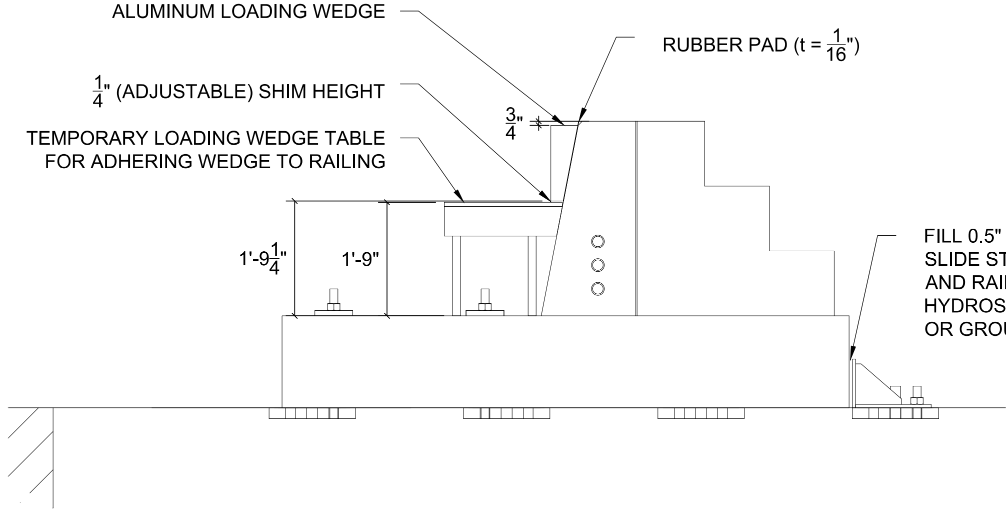

ANCHORED IMPACT SPECIMEN
SIDE ELEVATION VIEW

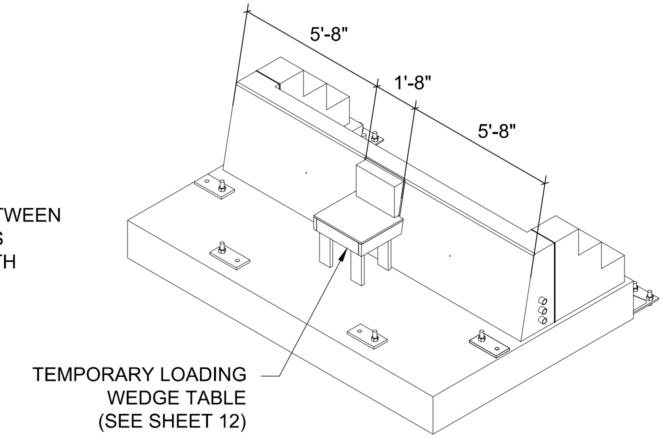

ANCHORED IMPACT SPECIMEN
FRONT ISOMETRIC VIEW

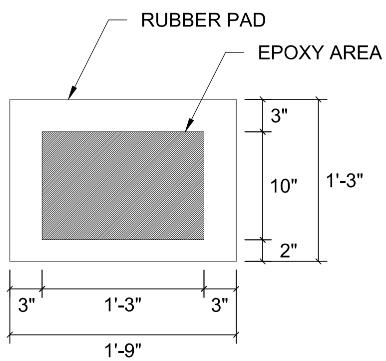

RUBBER TO ALUMINUM SIDE
RUBBER PAD BETWEEN WEDGE AND RAILING

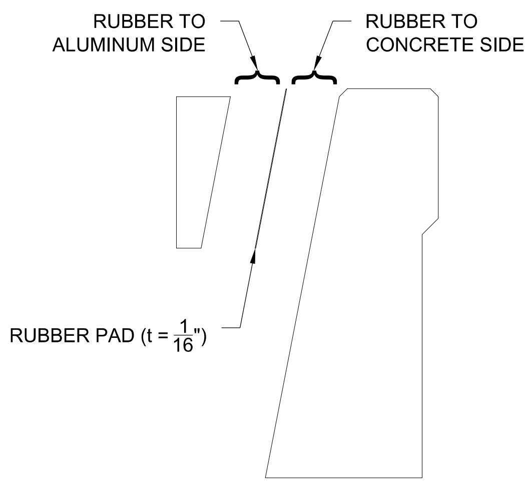

ADHERING LOADING WEDGE TO RAILING
SIDE ELEVATION VIEW

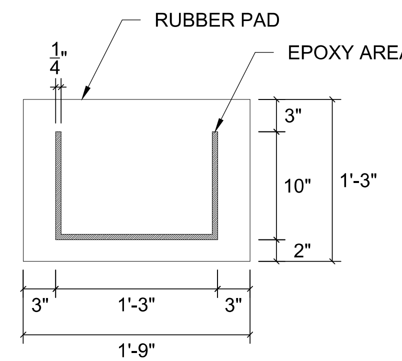

RUBBER TO CONCRETE SIDE
RUBBER PAD BETWEEN WEDGE AND RAILING

Fiber-Reinforced Concrete Traffic Railings for Impact Loading				*Revisions:*
Specimen Anchoring Plan	*2020-04-20*	*University of Florida*	*Sheet 11 of 12*	

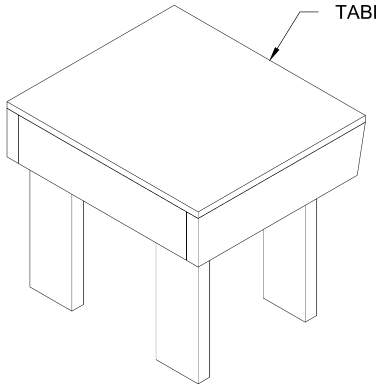

TEMPORARY LOADING WEDGE TABLE
ISOMETRIC VIEW

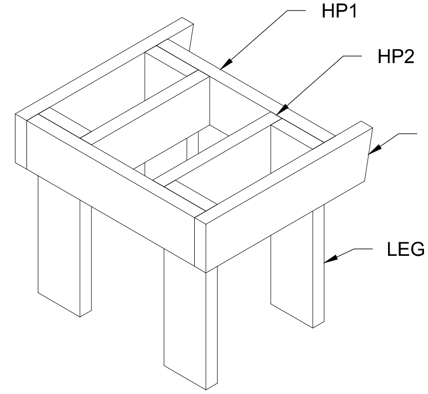

TEMPORARY LOADING WEDGE TABLE
ISOMETRIC VIEW: PLYWOOD REMOVED

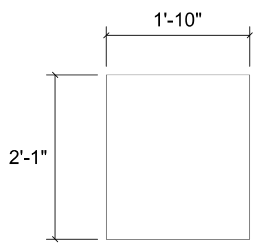

TAPLE TOP PLYWOOD
($\frac{3}{4}$" PLYWOOD)

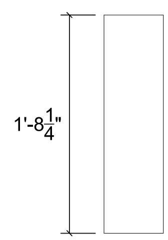

LEG: 2x6
QTY: 4

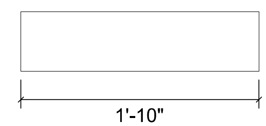

HP1: 2x6
QTY: 2

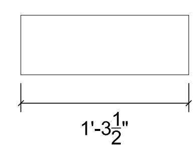

HP2: 2x6
QTY: 2

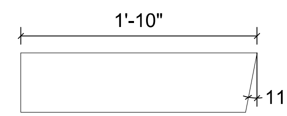

HP3: 2x6
QTY: 2

Fiber-Reinforced Concrete Traffic Railings for Impact Loading				*Revisions:*
Specimen Anchoring Plan	*2020-04-20*	*University of Florida*	*Sheet 12 of 12*	

ANCHORED IMPACT SPECIMEN
FRONT ELEVATION VIEW

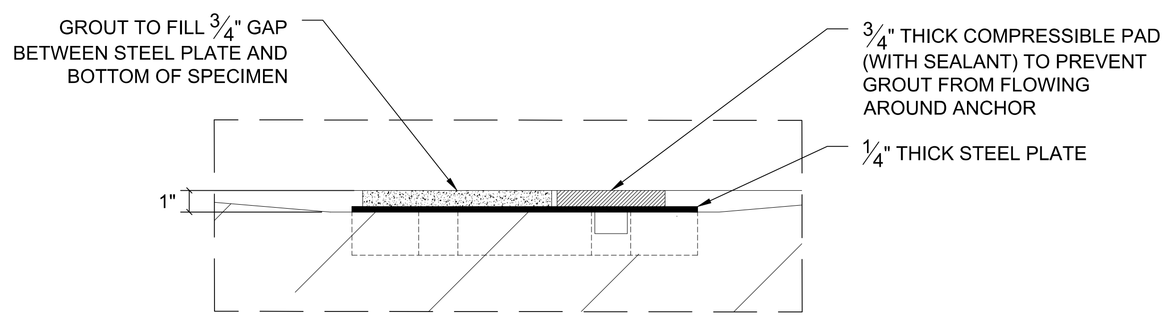

LOW ANCHOR POINT
FRONT ELEVATION VIEW

Fiber-Reinforced Concrete Traffic Railings for Impact Loading				*Revisions:*		
Specimen Anchoring Plan	*2020-05-19*	*University of Florida*	*Sheet 01 of 04*			

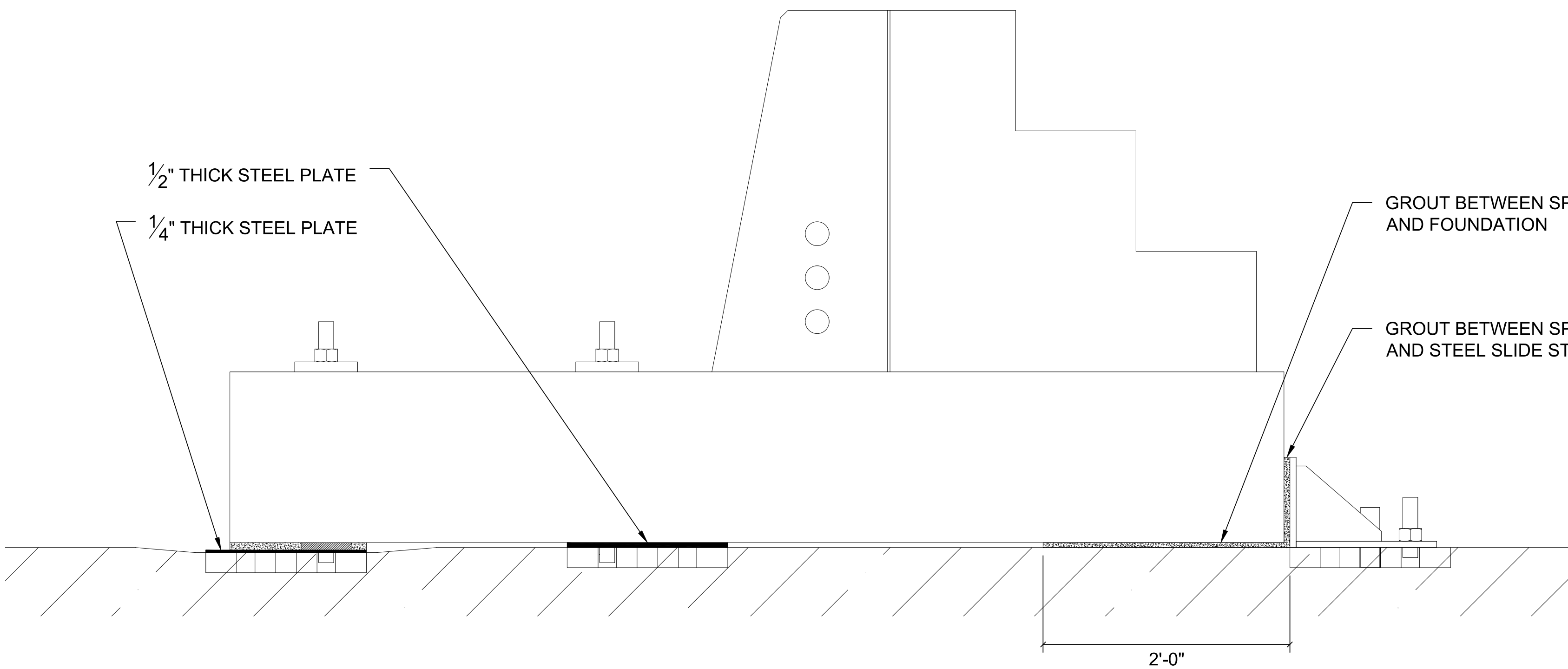

ANCHORED IMPACT SPECIMEN
SIDE ELEVATION VIEW

Fiber-Reinforced Concrete Traffic Railings for Impact Loading				*Revisions:*
Specimen Anchoring Plan	*2020-05-19*	*University of Florida*	*Sheet 02 of 04*	

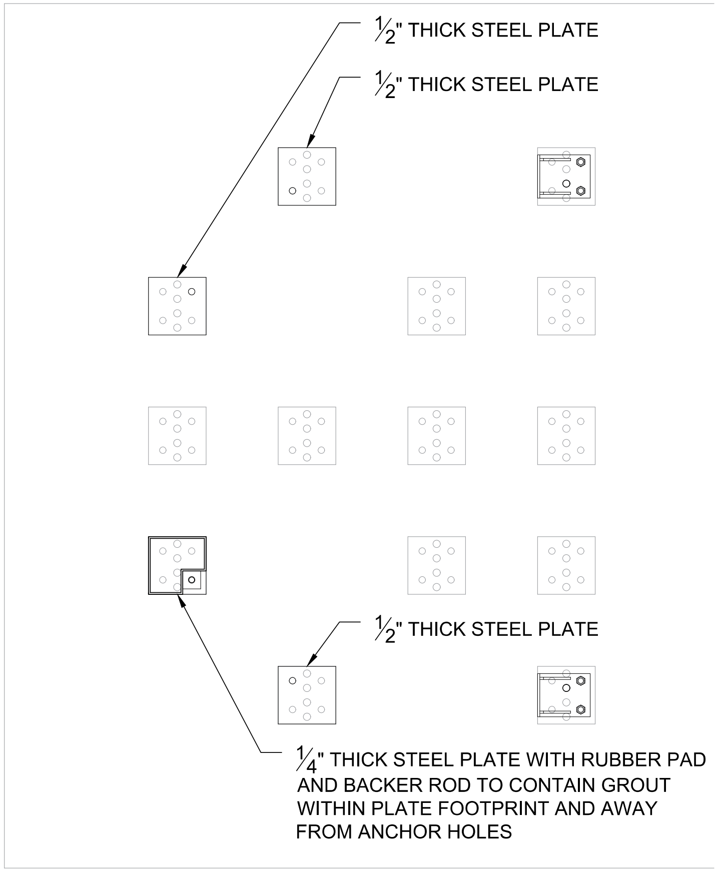

PLATES INSTALLED ONTO FOUNDATION
PLAN VIEW

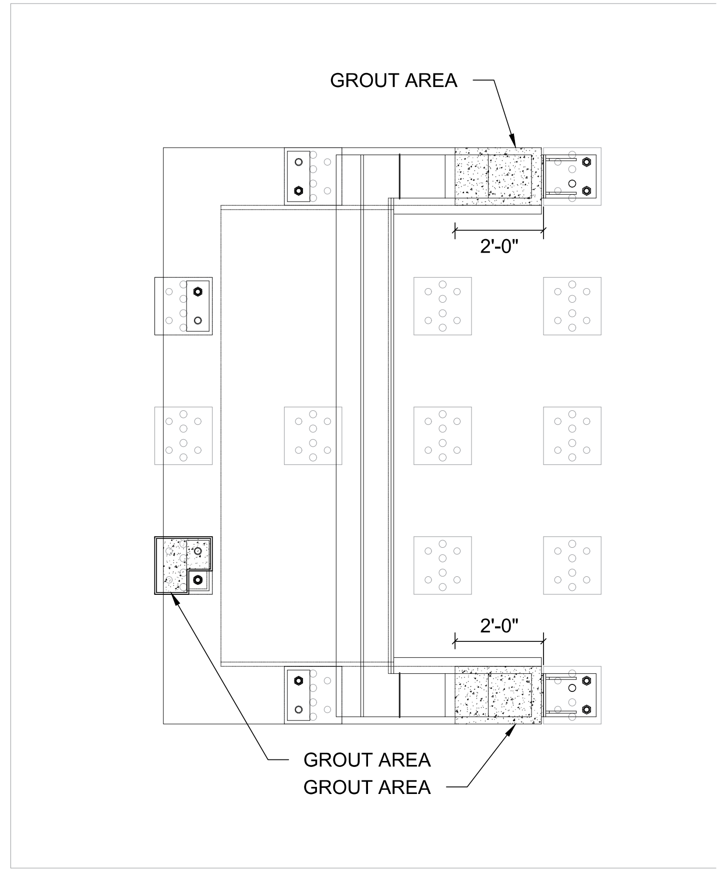

SPECIMEN INSTALLED ONTO FOUNDATION
PLAN VIEW

Sequencing:

(1) Install backer rod and sealant around rubber pad on low anchor point with 1/4" steel plate (see Sheet 04)
(2) With all steel plates installed, place specimen down
(3) Hand tighten nuts on anchor bars to prevent specimen from rocking backward (since the specimen is elevated)
(3) Post-tension the 3 anchor points with 1/2" plates beneath
(4) Grout 4th anchor point (between 1/4" steel plate and specimen)
(5) Let grout set
(6) Post-tension 4th anchor point
(7) Grout buttress regions

Fiber-Reinforced Concrete Traffic Railings for Impact Loading				*Revisions:*
Specimen Anchoring Plan	*2020-05-19*	*University of Florida*	*Sheet 03 of 04*	

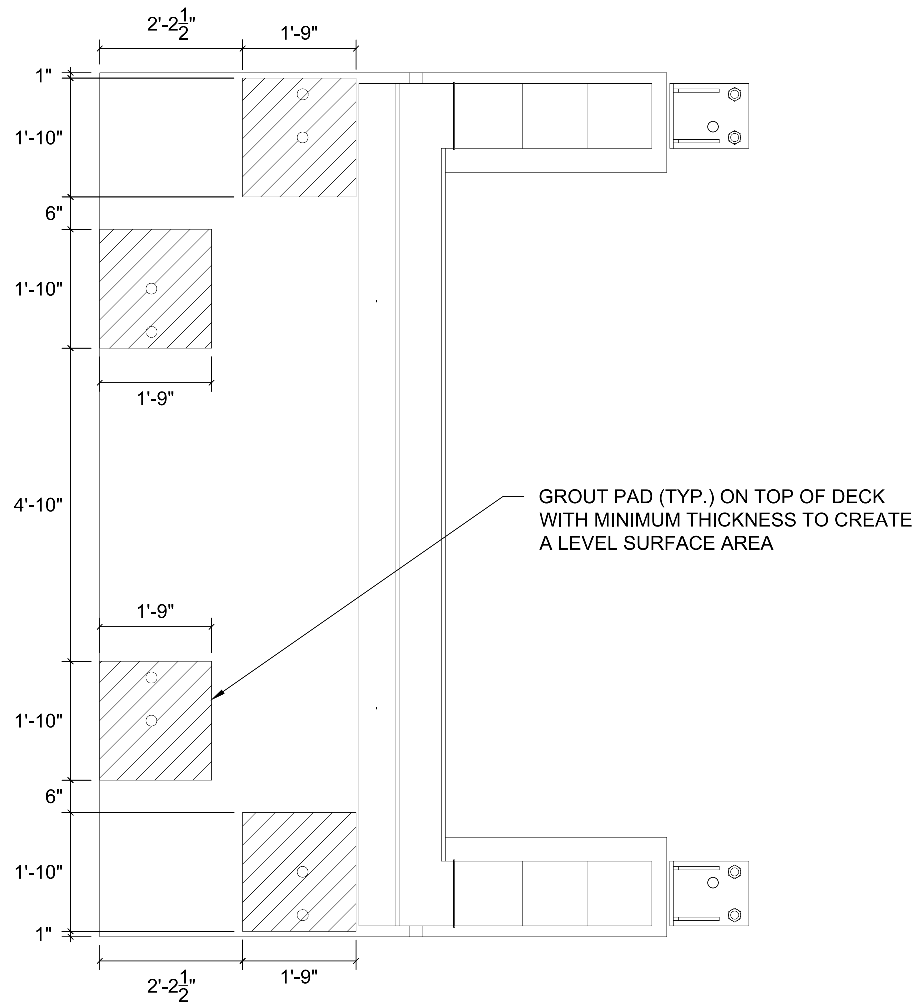

IMPACT SPECIMEN
PLAN VIEW

Fiber-Reinforced Concrete Traffic Railings for Impact Loading				*Revisions:*
Specimen Anchoring Plan	*2020-07-27*	*University of Florida*	*Sheet 03 of 04*	

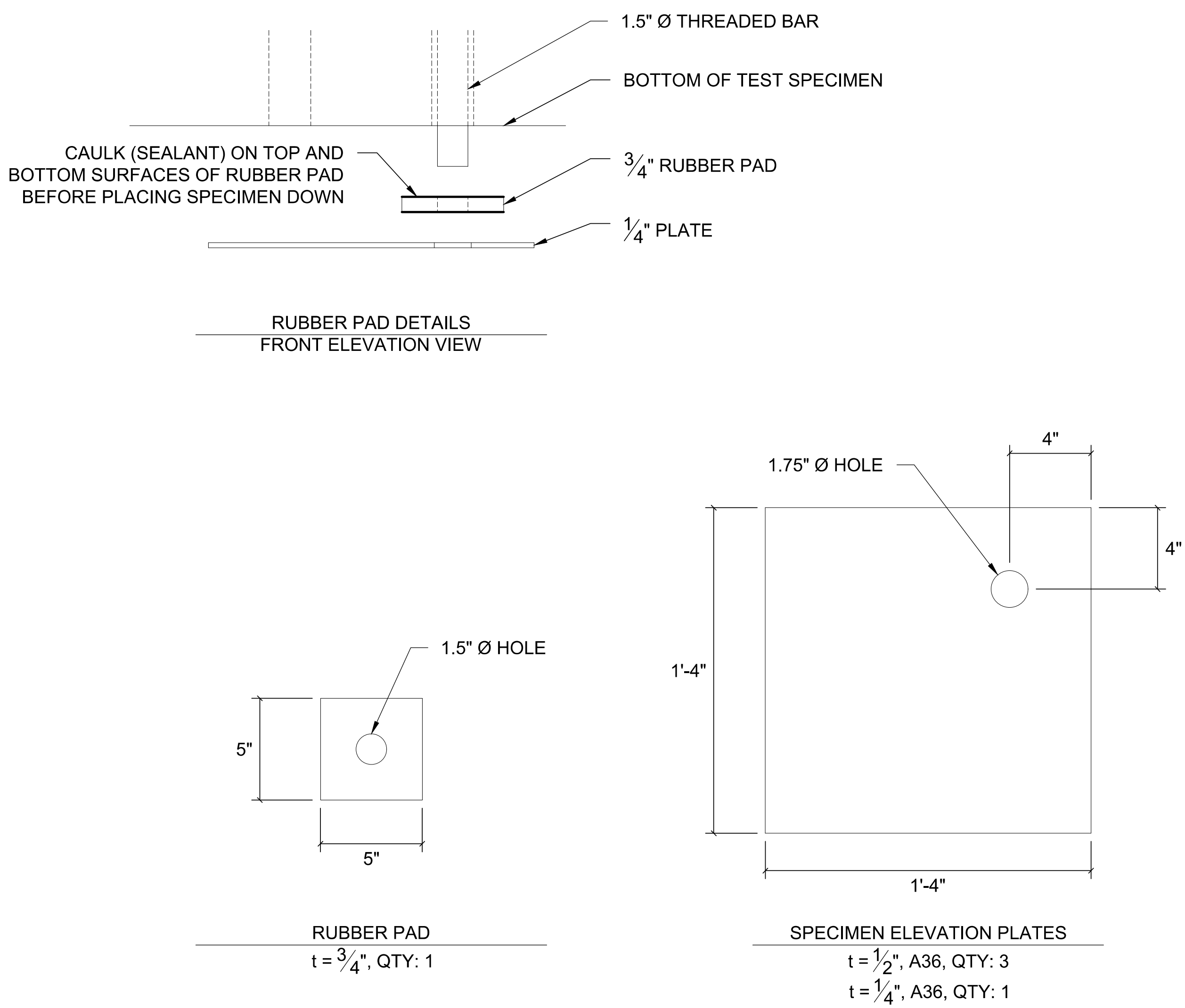

Fiber-Reinforced Concrete Traffic Railings for Impact Loading				*Revisions:*
Specimen Anchoring Plan	*2020-05-19*	*University of Florida*	*Sheet 04 of 04*	

APPENDIX I
IMPACT TEST SPECIMEN INSTRUMENTATION PLANS

Presented in this appendix are the instrumentation plans for each of the pendulum impact tests that were conducted, in the following order:

- Partially-instrumented FRC COR
- Fully-instrumented FRC COR
- Fully-instrumented standard R/C COR
- Fully-instrumented FRC EOR
- Fully-instrumented R/C EOR

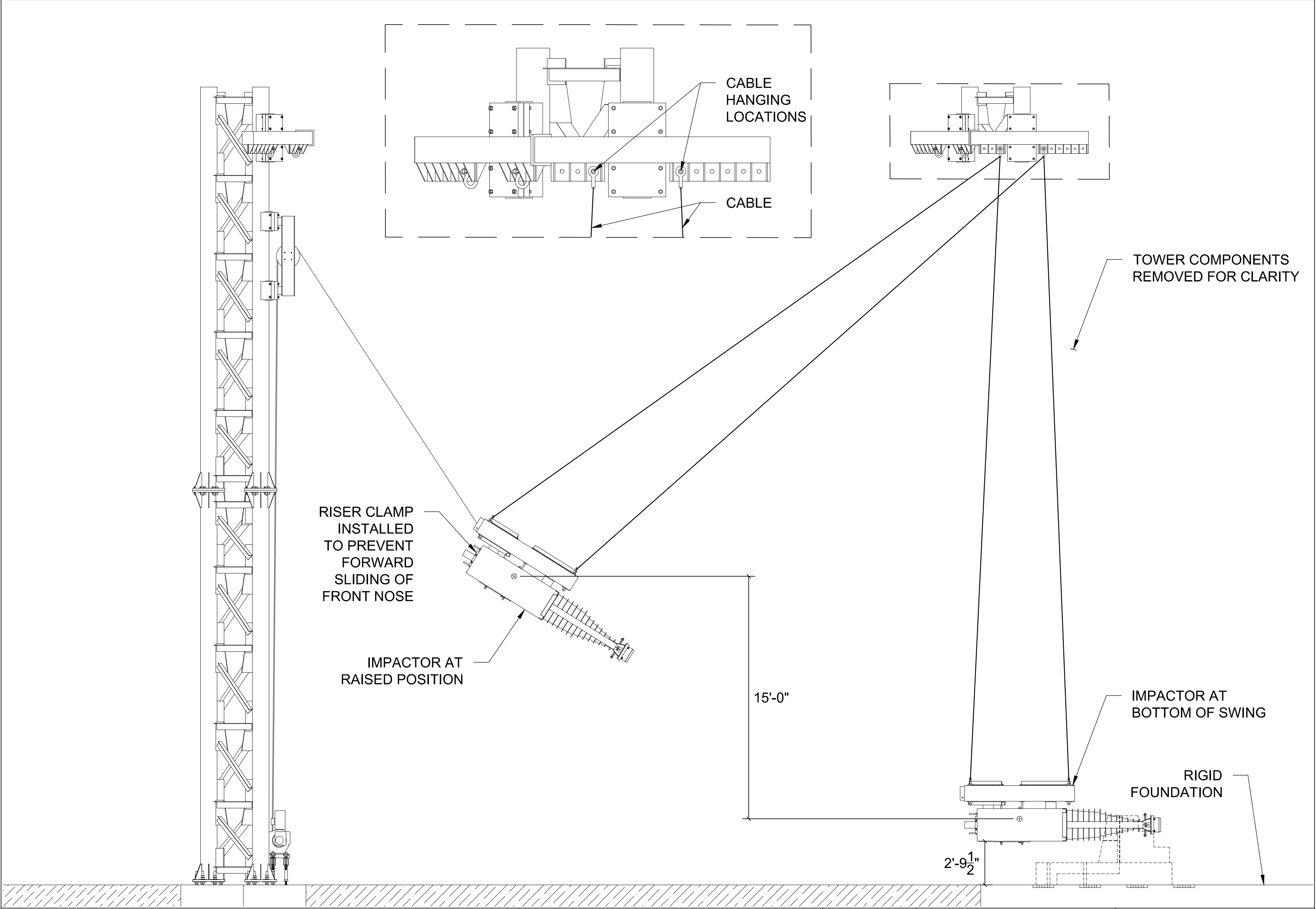

Concrete Traffic Railings for Impact Loading				Revisions:
Hanger cable configuration	2020-05-10	University of Florida	Sheet 01 of 06	

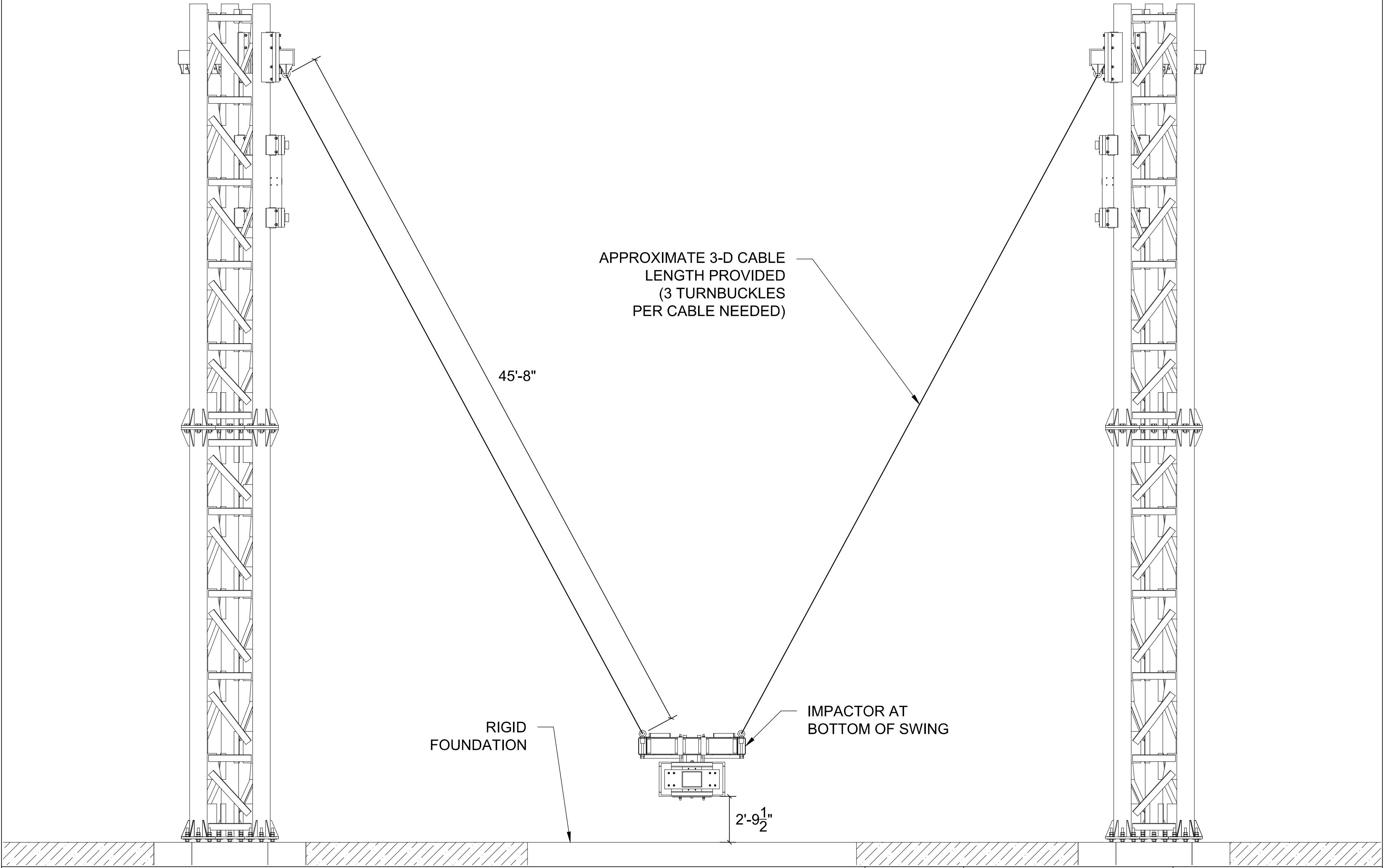

Concrete Traffic Railings for Impact Loading				*Revisions:*	
Hanger cable configuration	*2020-05-10*	*University of Florida*	*Sheet 02 of 06*		

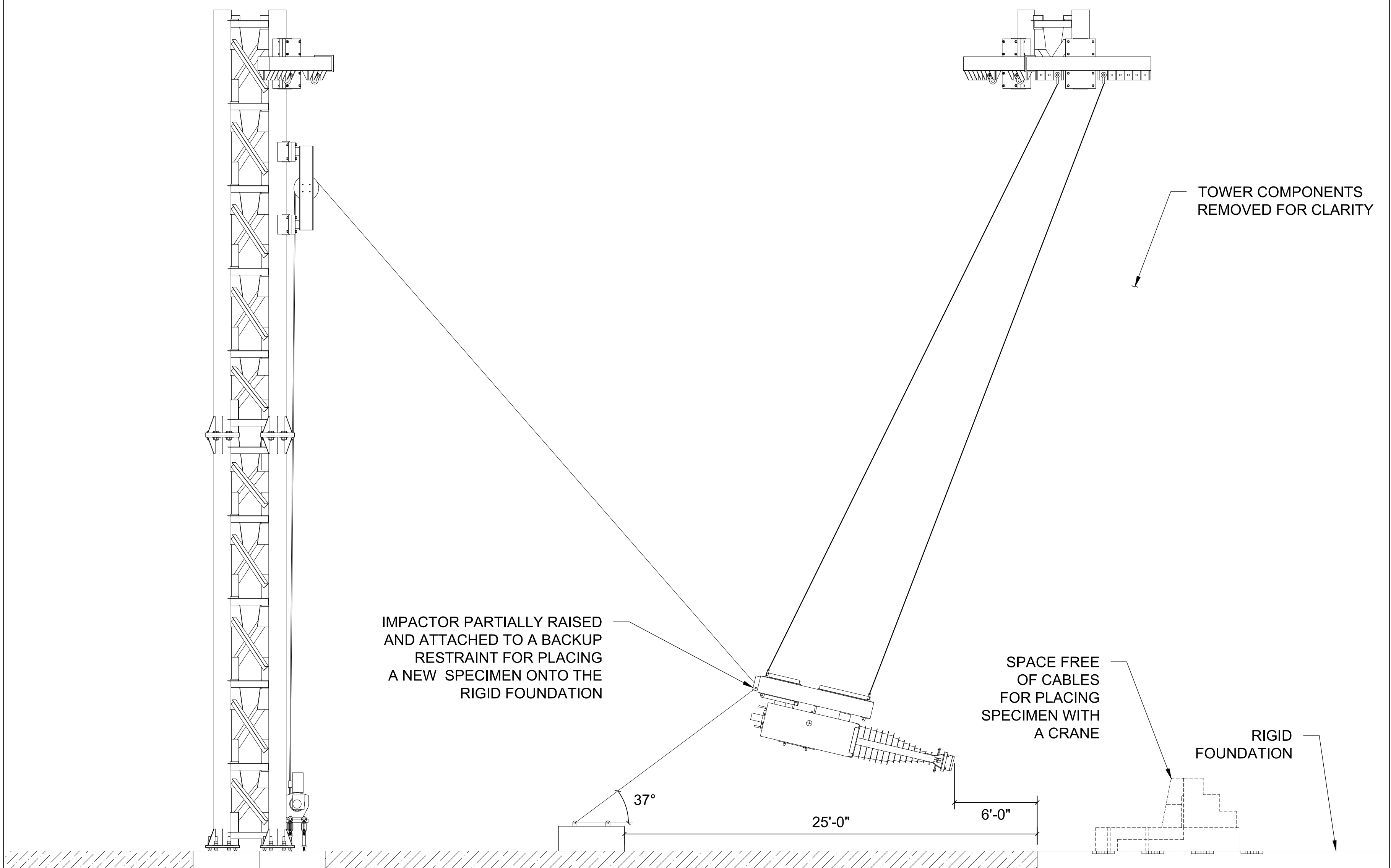

Concrete Traffic Railings for Impact Loading				*Revisions:*
Hanger cable configuration	*2020-05-10*	*University of Florida*	*Sheet 03 of 06*	

Preliminary partially-instrumented impact test - FRC railing

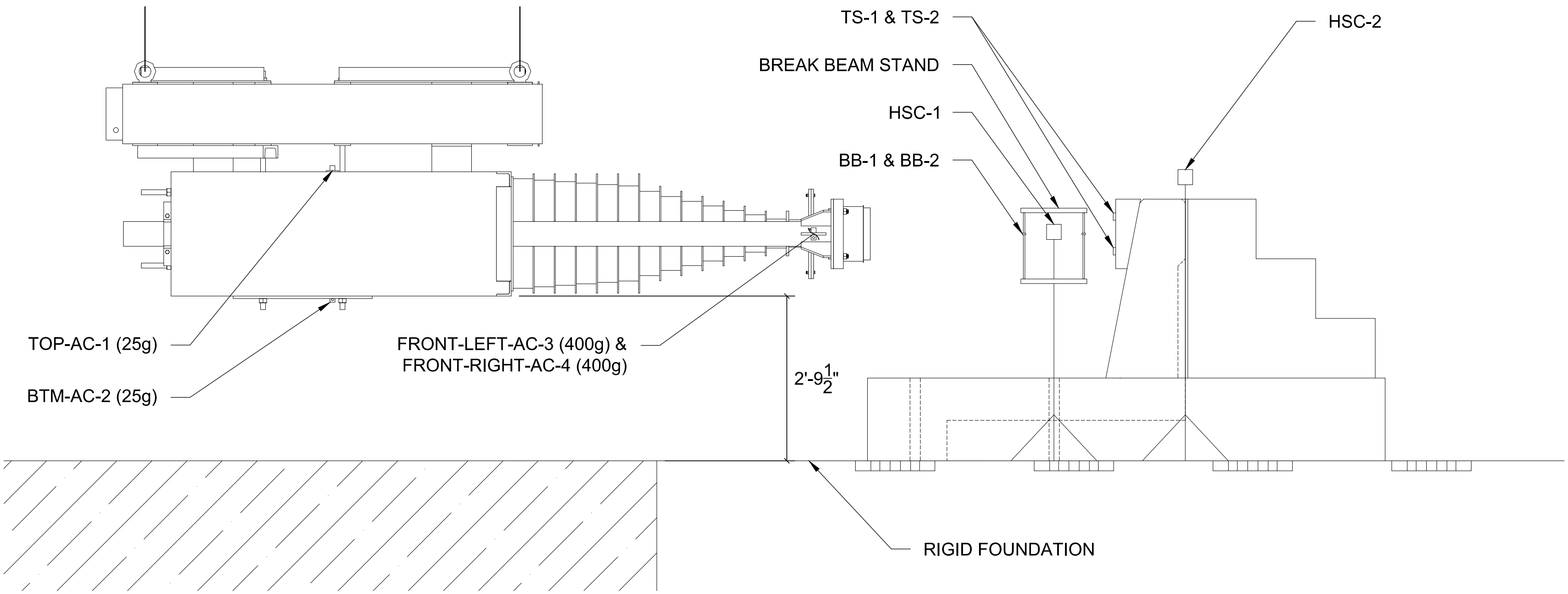

Instrumentation:

-AC: Accelerometer
-BB: Break Beam
-TS: Tape Switch
-HSC: High-Speed Camera

Concrete Traffic Railings for Impact Loading				Revisions:
Instrumentation plan	2020-05-10	University of Florida	Sheet 04 of 06	

Preliminary partially-instrumented impact test - FRC railing

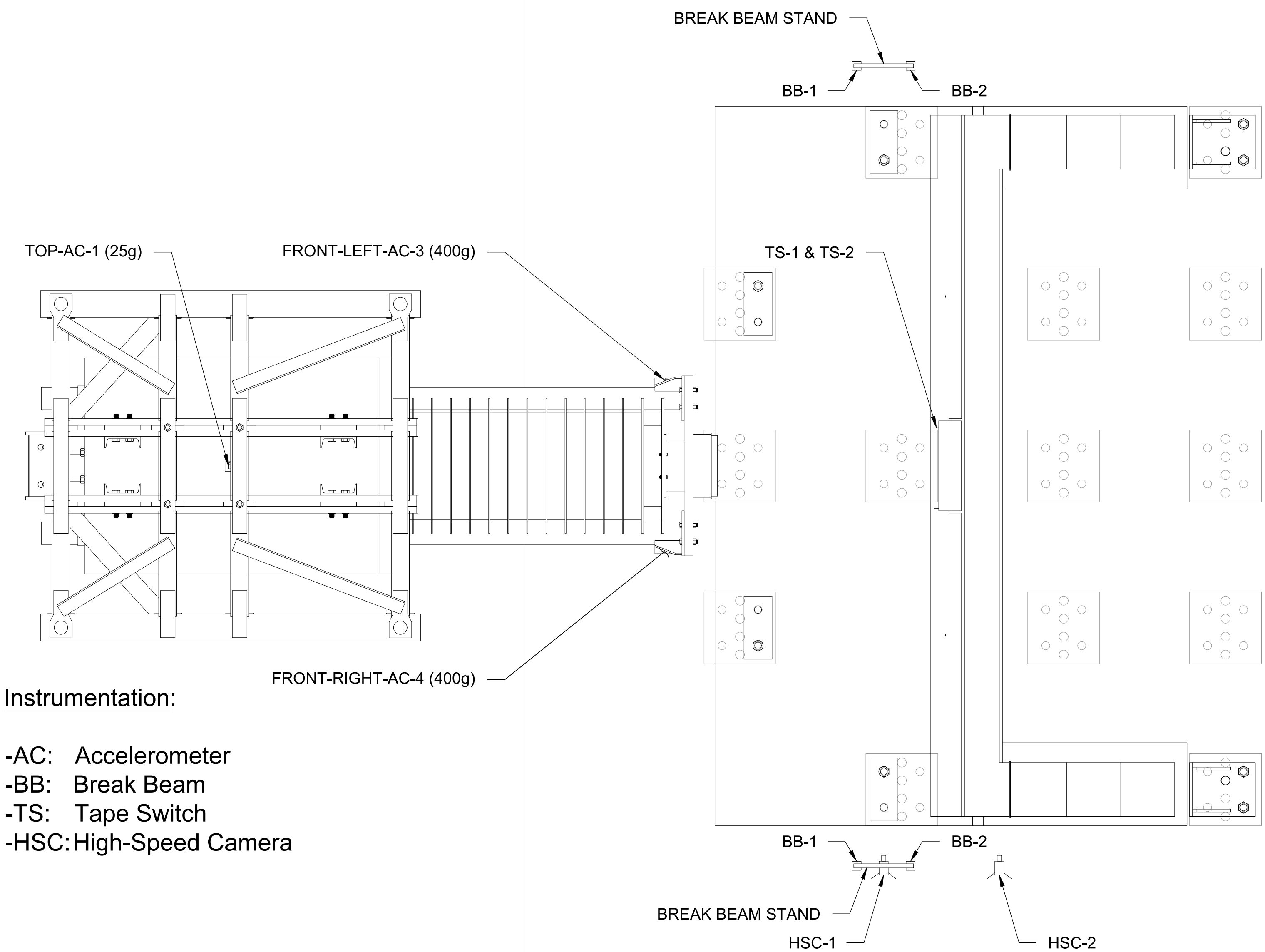

Instrumentation:

-AC: Accelerometer
-BB: Break Beam
-TS: Tape Switch
-HSC: High-Speed Camera

Concrete Traffic Railings for Impact Loading				*Revisions:*
Instrumentation plan	*2020-05-10*	*University of Florida*	*Sheet 05 of 06*	

Preliminary partially-instrumented impact test - FRC railing

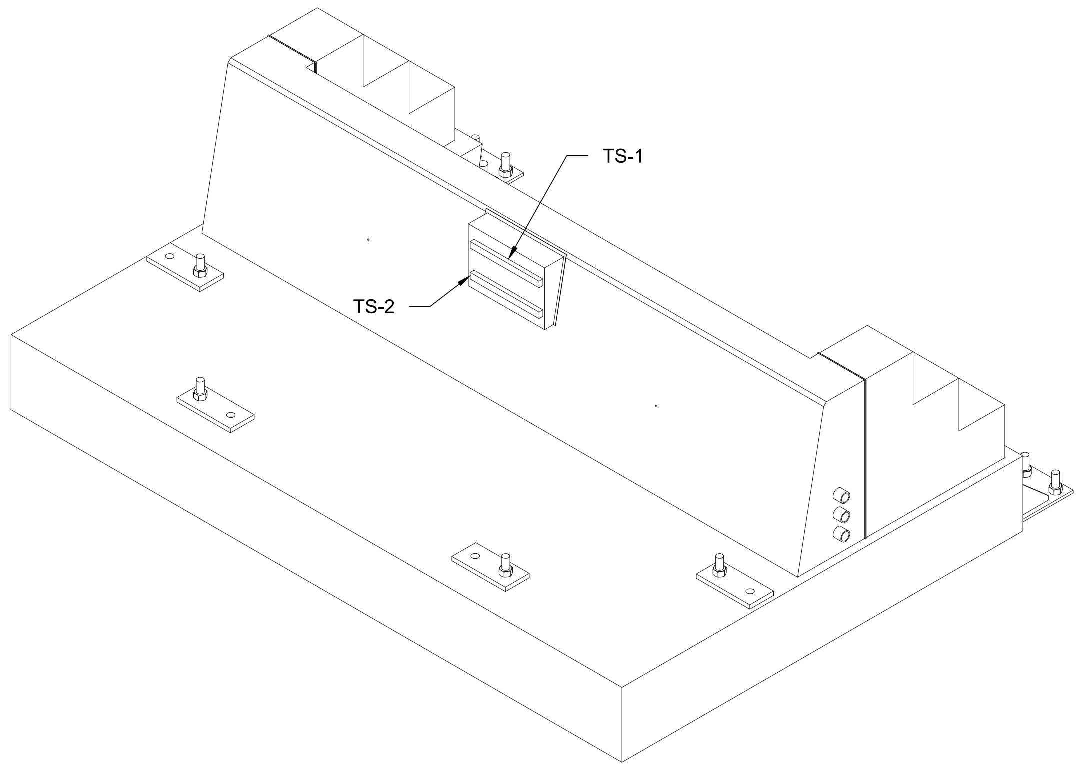

Instrumentation:

- -AC: Accelerometer
- -BB: Break Beam
- -TS: Tape Switch
- -HSC: High-Speed Camera

Concrete Traffic Railings for Impact Loading				*Revisions:*		
Instrumentation plan	*2020-05-10*	*University of Florida*	*Sheet 06 of 06*			

Fully-instrumented impact test - FRC (full-length) center-of-rail (COR) specimen

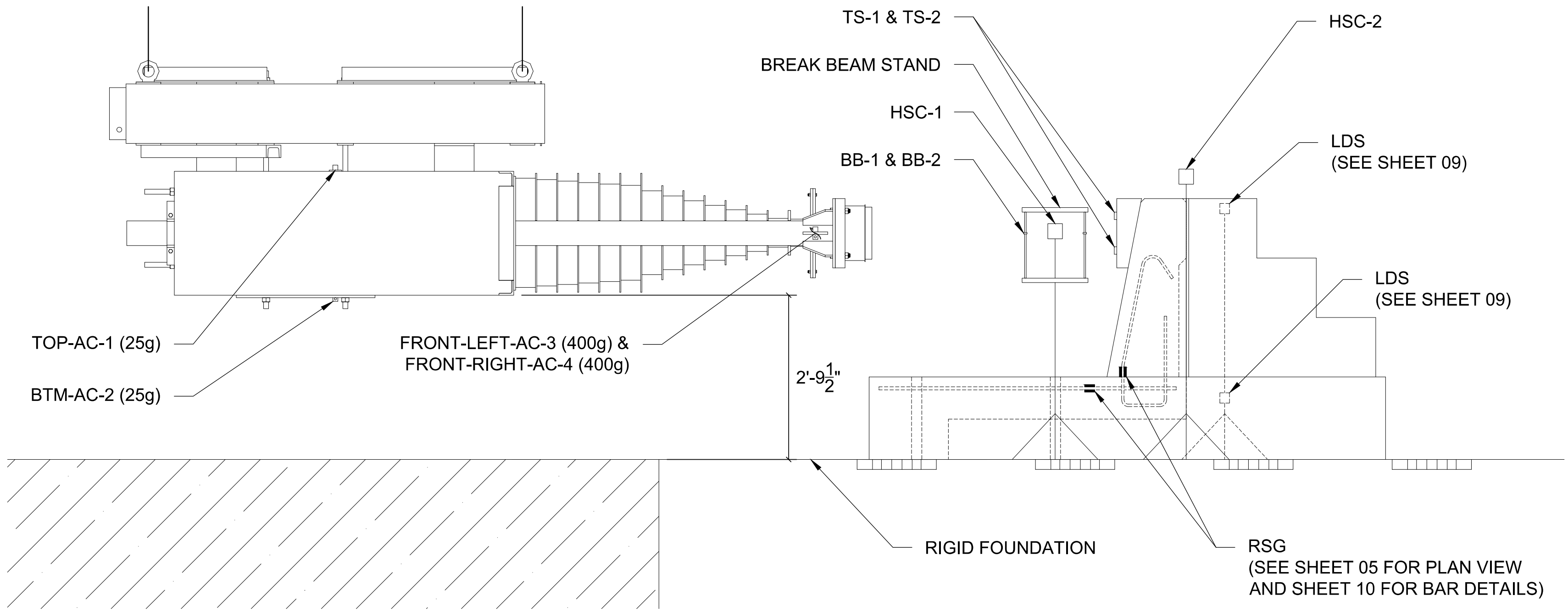

Instrumentation:

-AC: Accelerometer
-BB: Break Beam
-TS: Tape Switch
-HSC: High-Speed Camera
-LDS: Laser Displacement Sensor
-CSG: Concrete Strain Gage
-RSG: Reinforcement Strain Gage

Concrete Traffic Railings for Impact Loading				Revisions:
Instrumentation plan	*2020-09-30*	*University of Florida*	*Sheet 04 of 10*	

Fully-instrumented impact test - FRC (full-length) center-of-rail (COR) specimen

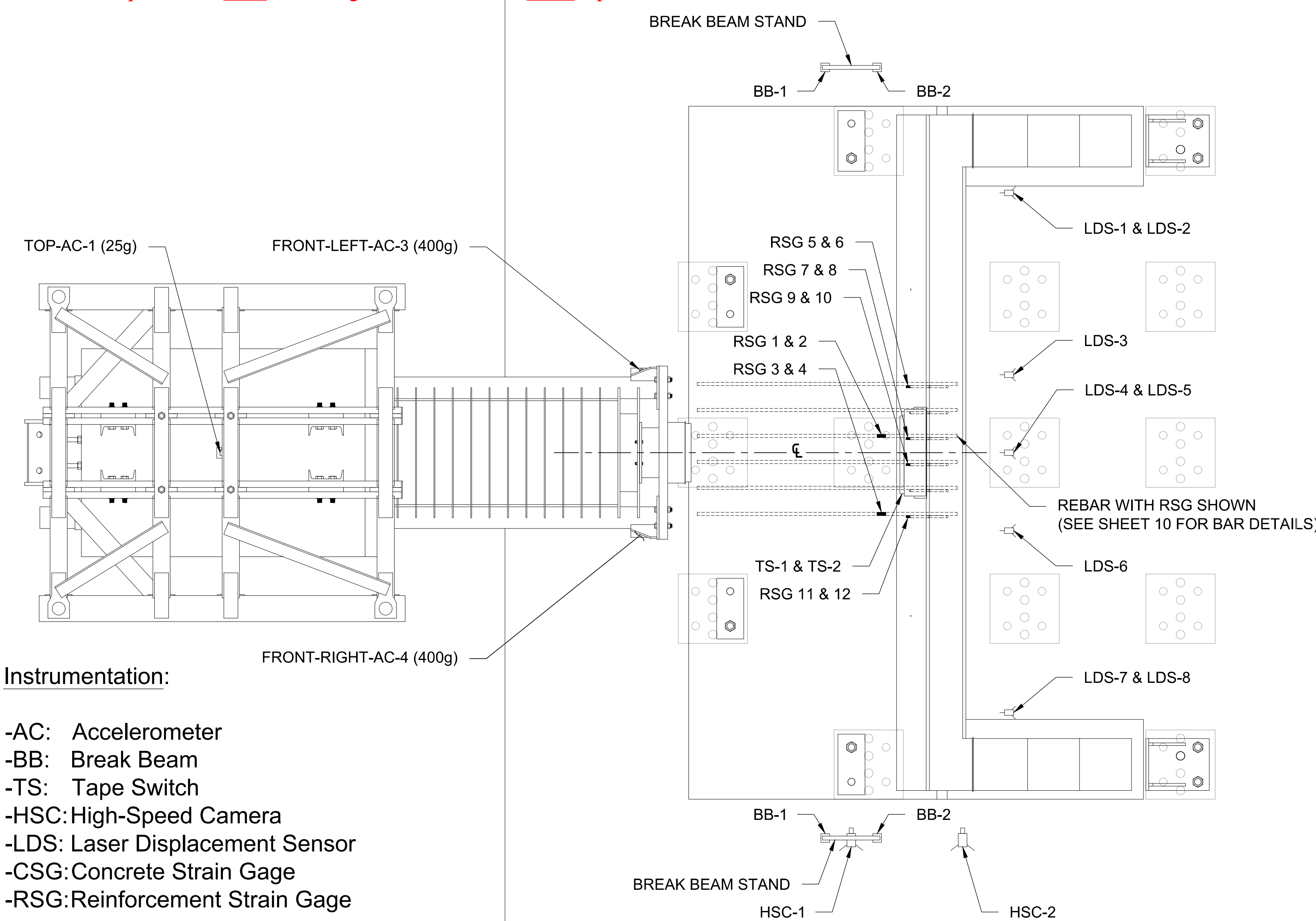

Instrumentation:

-AC: Accelerometer
-BB: Break Beam
-TS: Tape Switch
-HSC: High-Speed Camera
-LDS: Laser Displacement Sensor
-CSG: Concrete Strain Gage
-RSG: Reinforcement Strain Gage

Concrete Traffic Railings for Impact Loading				Revisions:
Instrumentation plan	2020-09-30	University of Florida	Sheet 05 of 10	

Fully-instrumented impact test - FRC (full-length) center-of-rail (COR) specimen

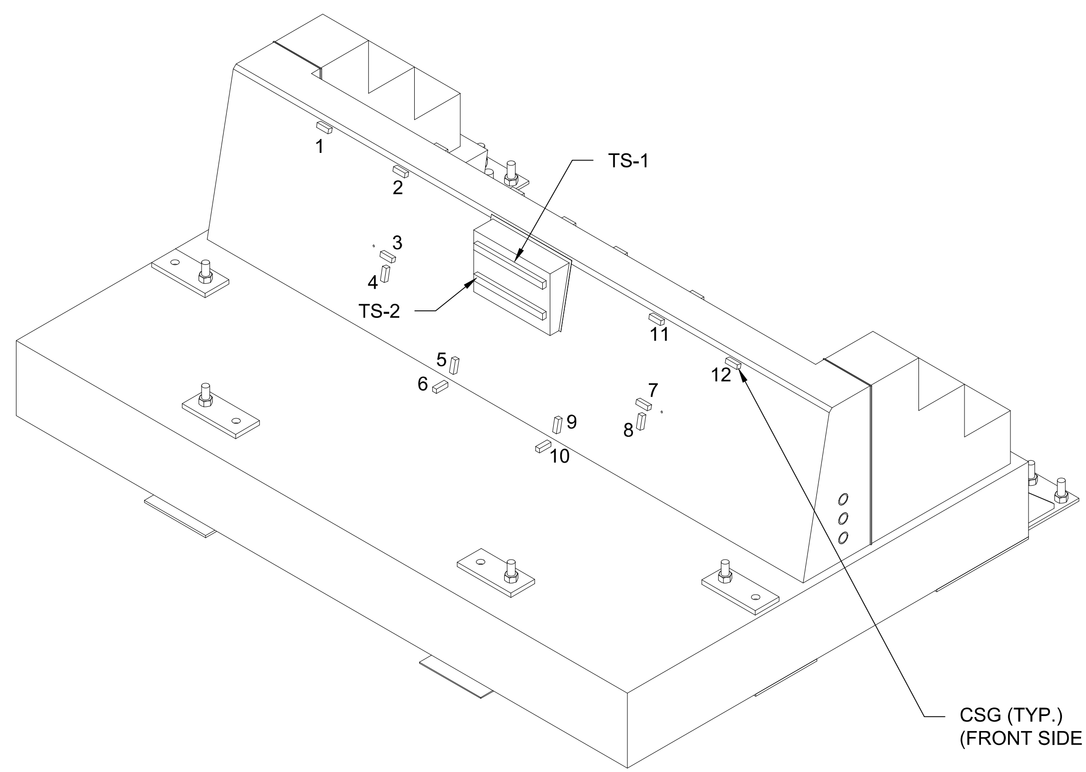

Instrumentation:

-AC: Accelerometer
-BB: Break Beam
-TS: Tape Switch
-HSC: High-Speed Camera
-LDS: Laser Displacement Sensor
-CSG: Concrete Strain Gage
-RSG: Reinforcement Strain Gage

Concrete Traffic Railings for Impact Loading				Revisions:
Instrumentation plan	2020-09-30	University of Florida	Sheet 06 of 10	

Fully-instrumented impact test - FRC (full-length) center-of-rail (COR) specimen

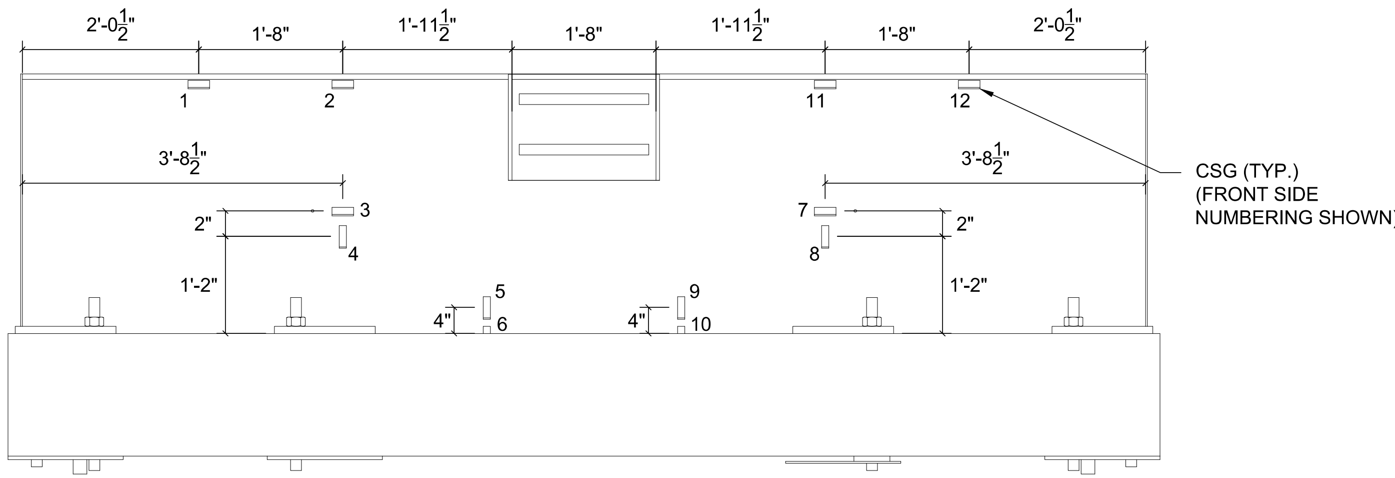

Instrumentation:

-AC: Accelerometer
-BB: Break Beam
-TS: Tape Switch
-HSC: High-Speed Camera
-LDS: Laser Displacement Sensor
-CSG: Concrete Strain Gage
-RSG: Reinforcement Strain Gage

Concrete Traffic Railings for Impact Loading				*Revisions:*	
Instrumentation plan	*2020-09-30*	*University of Florida*	*Sheet 07 of 10*		

Fully-instrumented impact test - FRC (full-length) center-of-rail (COR) specimen

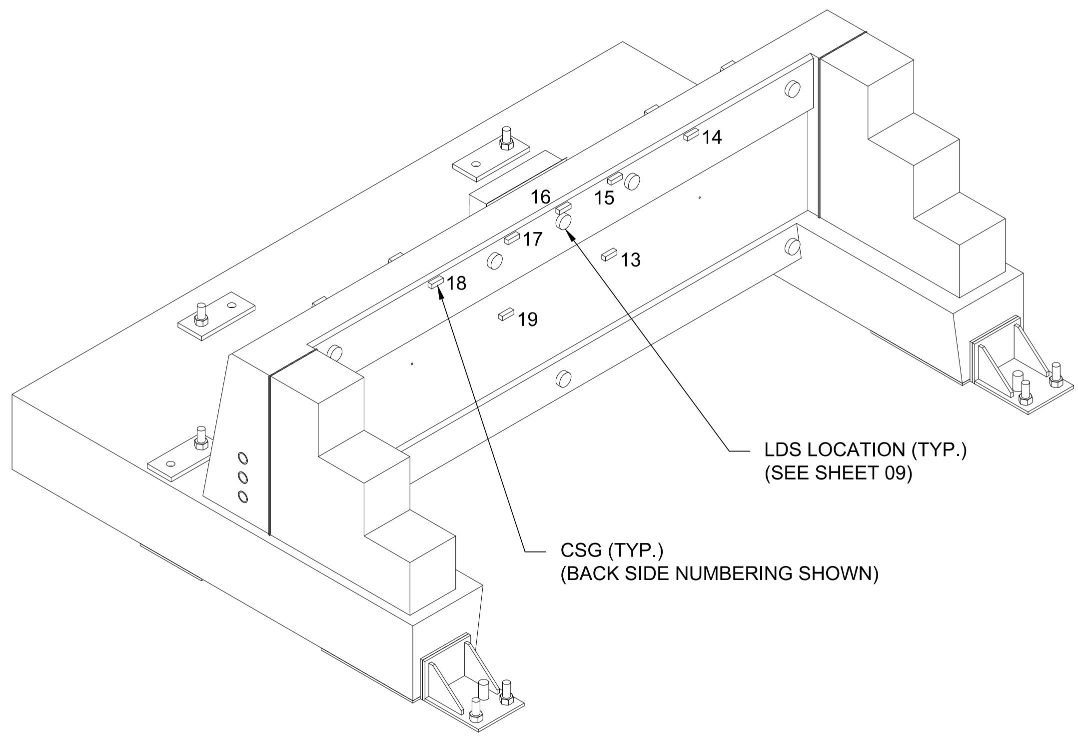

Instrumentation:

- -AC: Accelerometer
- -BB: Break Beam
- -TS: Tape Switch
- -HSC: High-Speed Camera
- -LDS: Laser Displacement Sensor
- -CSG: Concrete Strain Gage
- -RSG: Reinforcement Strain Gage

Concrete Traffic Railings for Impact Loading				*Revisions:*		
Instrumentation plan	*2020-09-30*	*University of Florida*	*Sheet 08 of 10*			

Fully-instrumented impact test - FRC (full-length) center-of-rail (COR) specimen

LDS & SG NUMBERING SHOWN

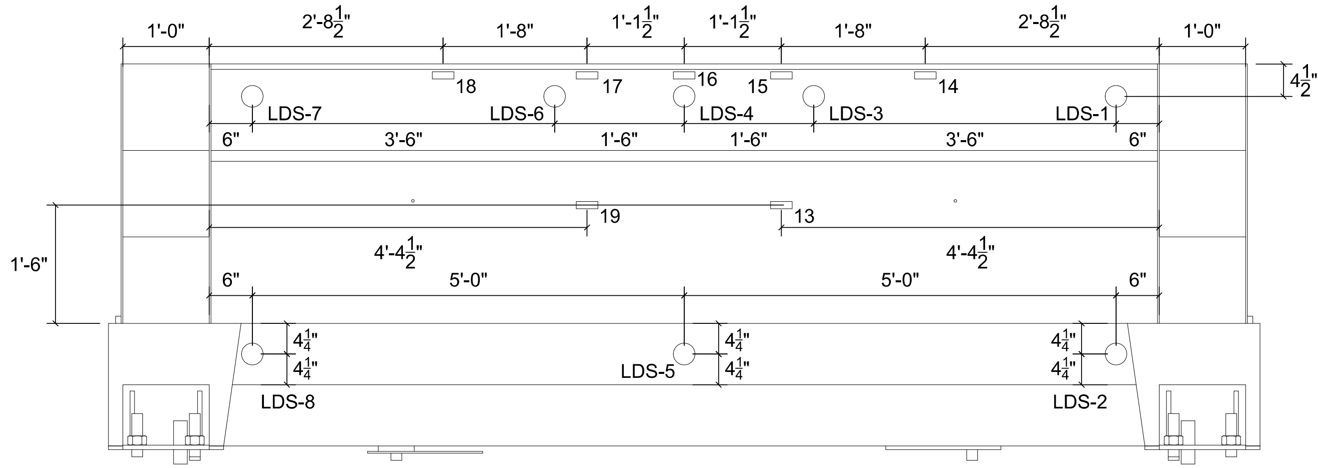

Instrumentation:

-AC: Accelerometer
-BB: Break Beam
-TS: Tape Switch
-HSC: High-Speed Camera
-LDS: Laser Displacement Sensor
-CSG: Concrete Strain Gage
-RSG: Reinforcement Strain Gage

Concrete Traffic Railings for Impact Loading				*Revisions:*
Instrumentation plan	*2020-09-30*	*University of Florida*	*Sheet 09 of 10*	

Fully-instrumented impact test - FRC (full-length) center-of-rail (COR) specimen

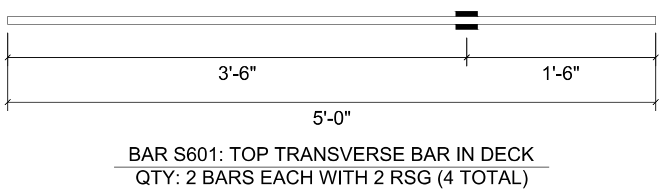

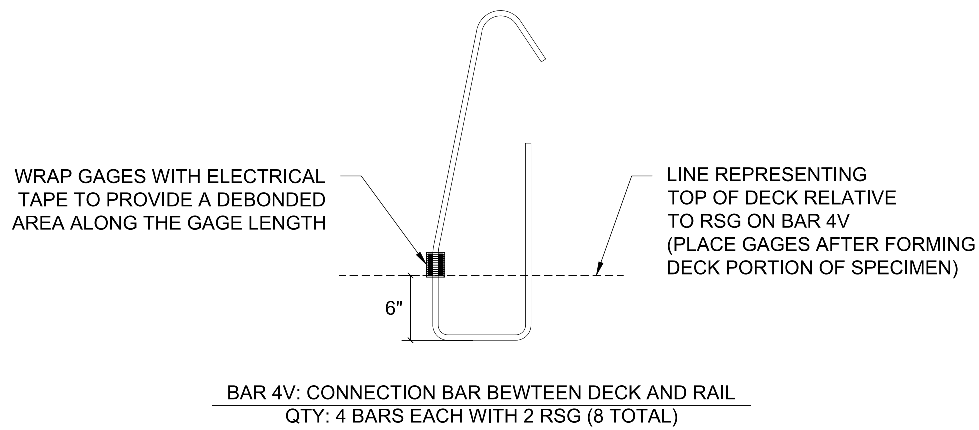

Instrumentation:

-AC: Accelerometer
-BB: Break Beam
-TS: Tape Switch
-HSC: High-Speed Camera
-LDS: Laser Displacement Sensor
-CSG: Concrete Strain Gage
-RSG: Reinforcement Strain Gage

Concrete Traffic Railings for Impact Loading				*Revisions:*
Instrumentation plan	*2020-09-30*	*University of Florida*	*Sheet 10 of 10*	

Fully-instrumented impact test - Standard steel (full-length) center-of-rail (COR) specimen

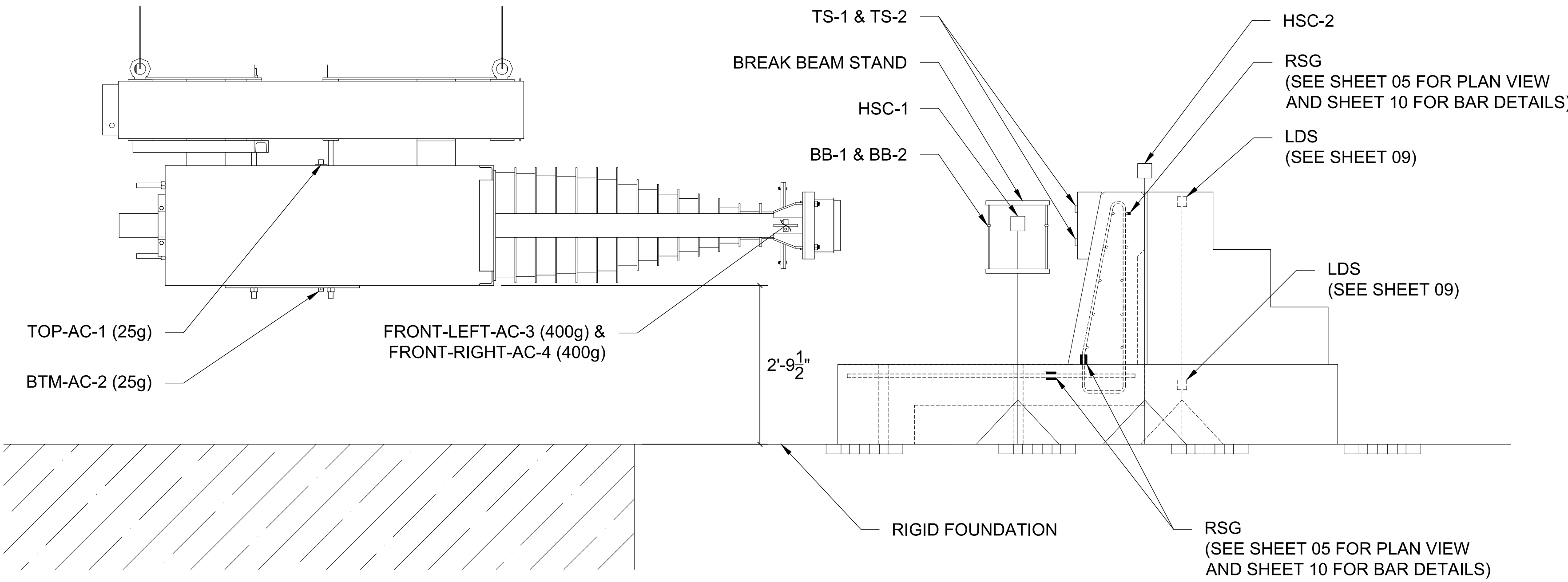

Instrumentation:

-AC: Accelerometer
-BB: Break Beam
-TS: Tape Switch
-HSC: High-Speed Camera
-LDS: Laser Displacement Sensor
-CSG: Concrete Strain Gage
-RSG: Reinforcement Strain Gage

Concrete Traffic Railings for Impact Loading				Revisions:
Instrumentation plan	2020-09-21	University of Florida	Sheet 04 of 10	

Fully-instrumented impact test - Standard steel (full-length) center-of-rail (COR) specimen

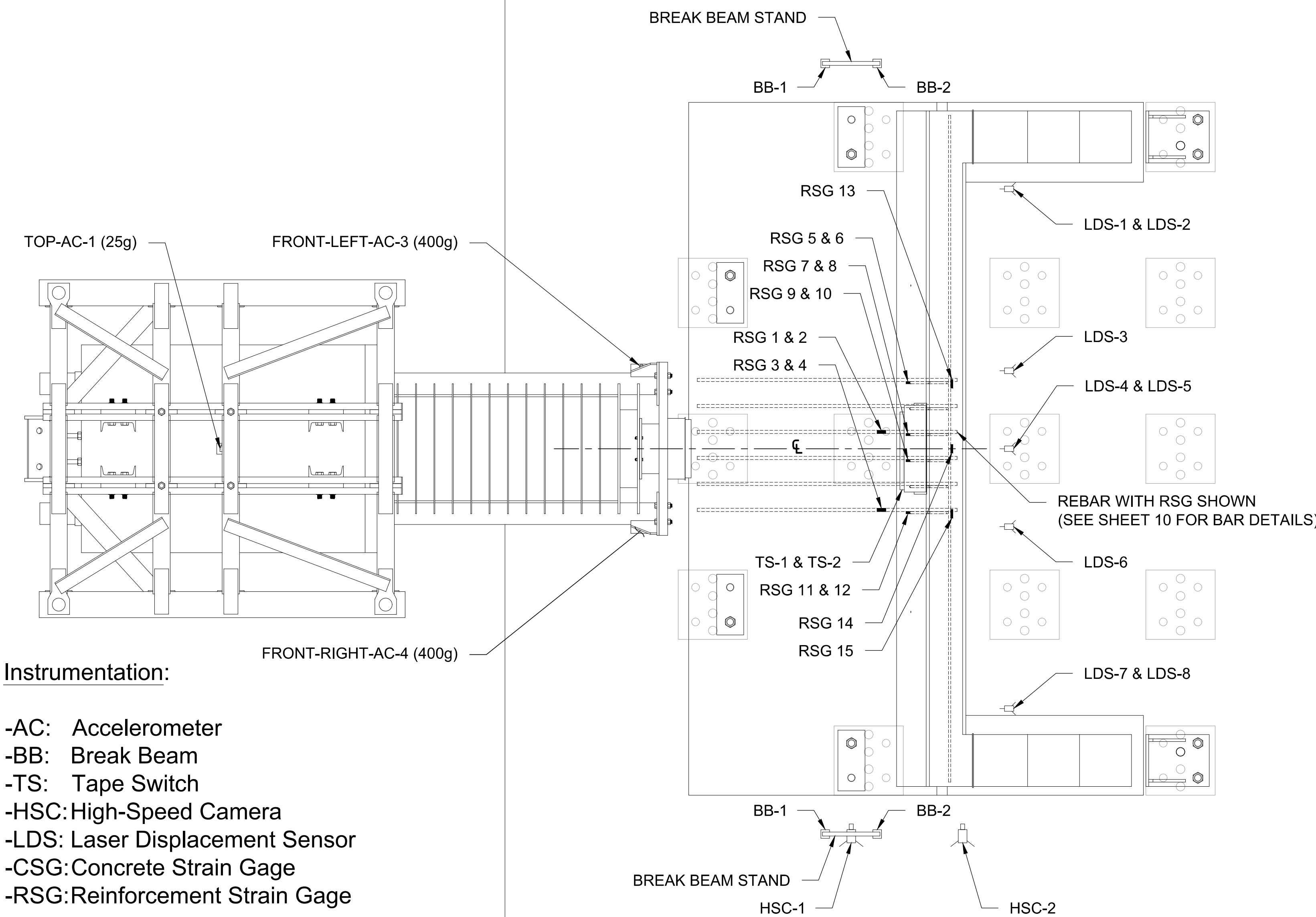

Instrumentation:

-AC: Accelerometer
-BB: Break Beam
-TS: Tape Switch
-HSC: High-Speed Camera
-LDS: Laser Displacement Sensor
-CSG: Concrete Strain Gage
-RSG: Reinforcement Strain Gage

Concrete Traffic Railings for Impact Loading				*Revisions:*
Instrumentation plan	*2020-09-21*	*University of Florida*	*Sheet 05 of 10*	

Fully-instrumented impact test - Standard <u>steel</u> (full-length) center-of-rail (<u>COR</u>) specimen

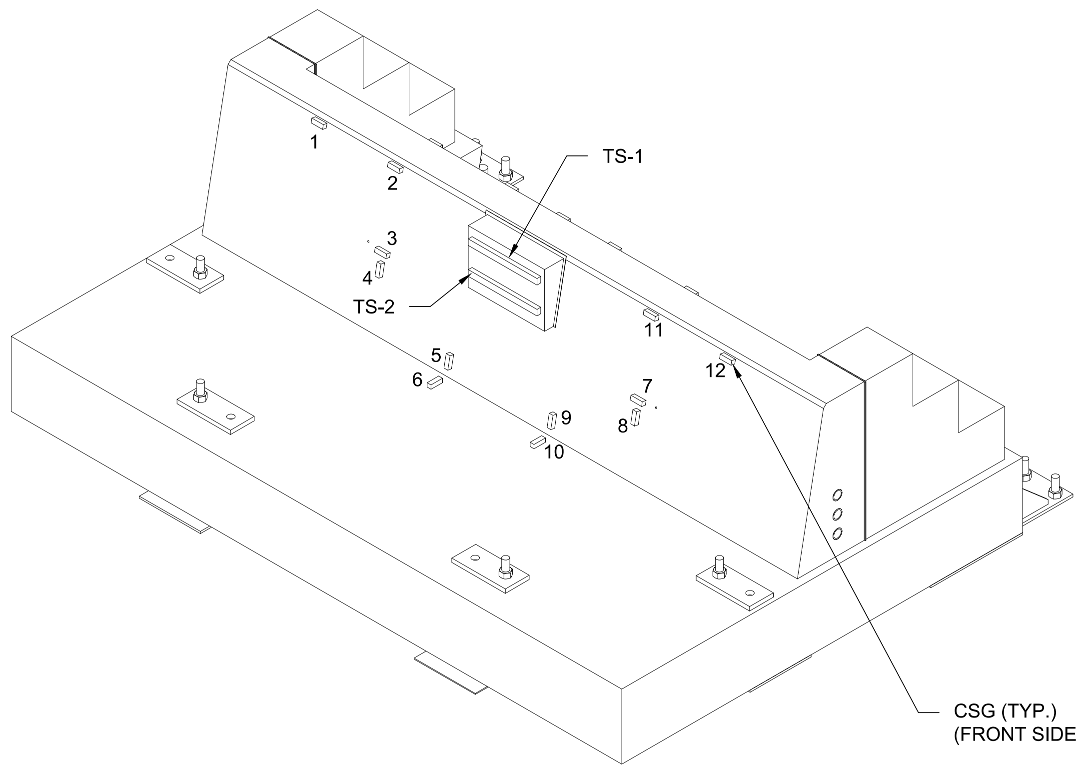

Instrumentation:

-AC: Accelerometer
-BB: Break Beam
-TS: Tape Switch
-HSC: High-Speed Camera
-LDS: Laser Displacement Sensor
-CSG: Concrete Strain Gage
-RSG: Reinforcement Strain Gage

Concrete Traffic Railings for Impact Loading				*Revisions:*
Instrumentation plan	*2020-09-21*	*University of Florida*	*Sheet 06 of 10*	

Fully-instrumented impact test - Standard steel (full-length) center-of-rail (COR) specimen

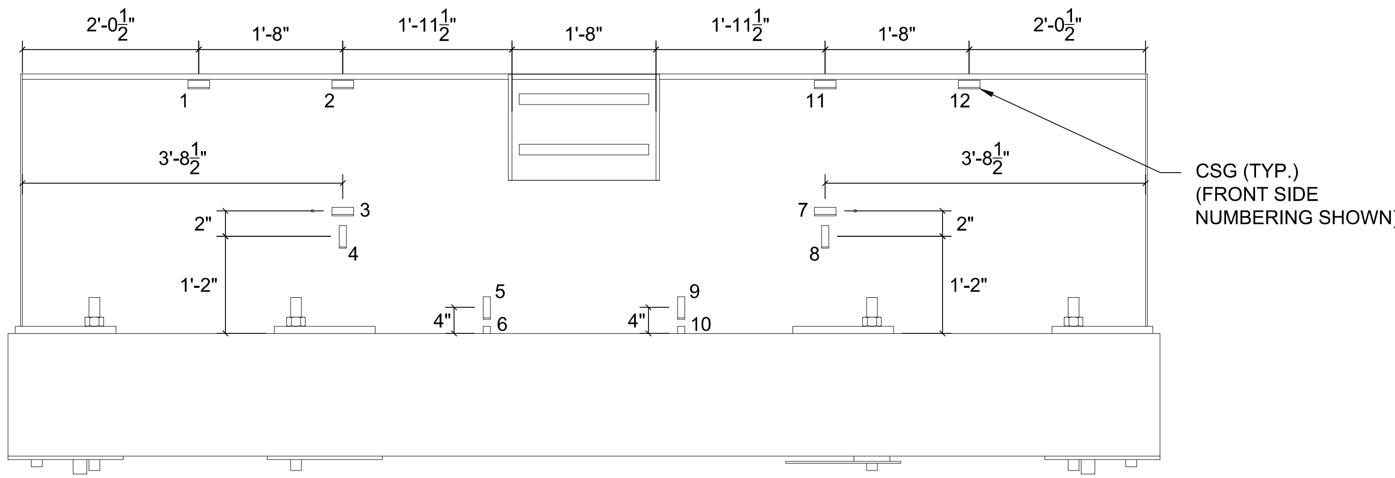

Instrumentation:

- -AC: Accelerometer
- -BB: Break Beam
- -TS: Tape Switch
- -HSC: High-Speed Camera
- -LDS: Laser Displacement Sensor
- -CSG: Concrete Strain Gage
- -RSG: Reinforcement Strain Gage

Concrete Traffic Railings for Impact Loading				Revisions:
Instrumentation plan	2020-09-21	University of Florida	Sheet 07 of 10	

Fully-instrumented impact test - Standard <u>steel</u> (full-length) center-of-rail (<u>COR</u>) specimen

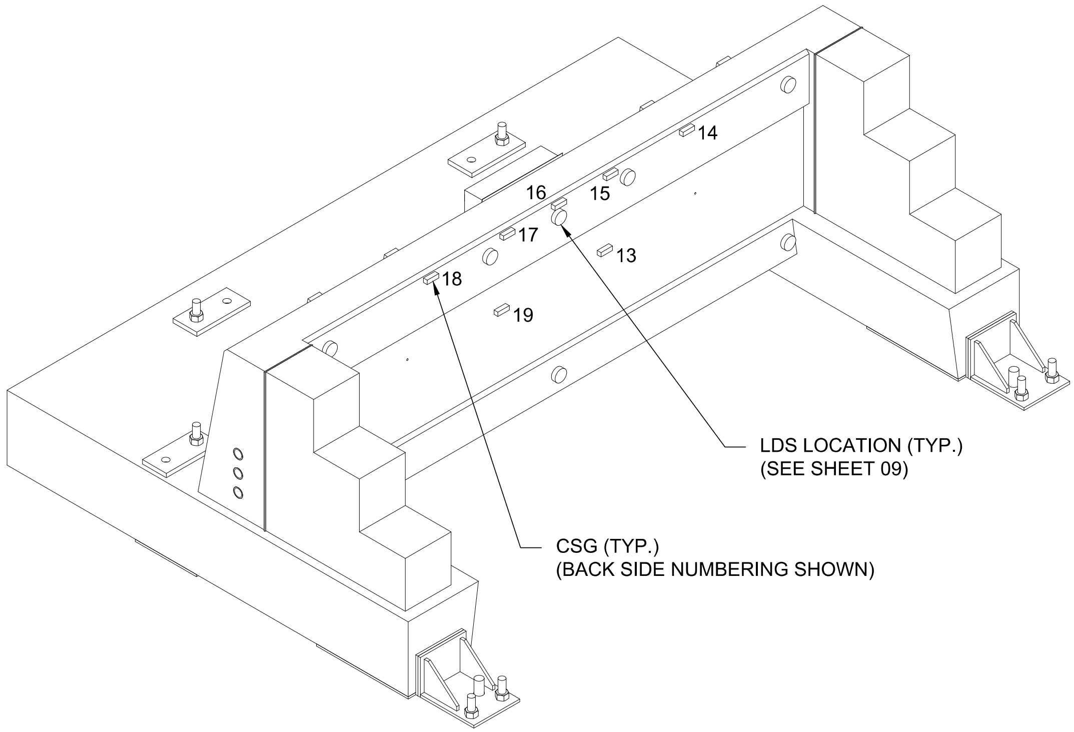

Instrumentation:

- -AC: Accelerometer
- -BB: Break Beam
- -TS: Tape Switch
- -HSC: High-Speed Camera
- -LDS: Laser Displacement Sensor
- -CSG: Concrete Strain Gage
- -RSG: Reinforcement Strain Gage

Concrete Traffic Railings for Impact Loading				Revisions:		
Instrumentation plan	2020-09-21	University of Florida	Sheet 08 of 10			

Fully-instrumented impact test - Standard steel (full-length) center-of-rail (COR) specimen

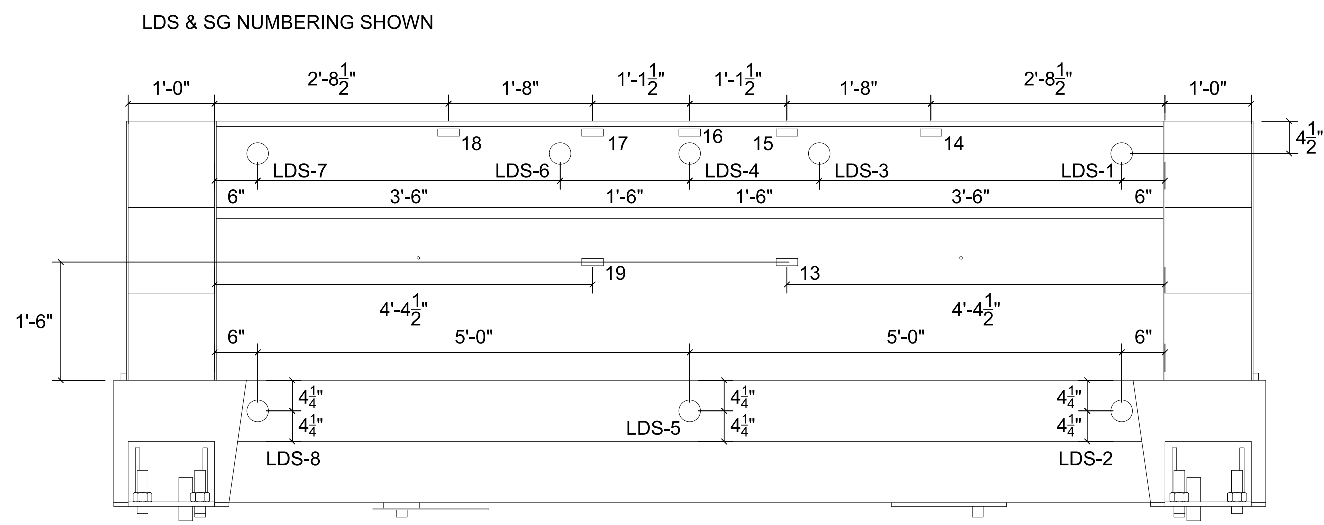

Instrumentation:

- -AC: Accelerometer
- -BB: Break Beam
- -TS: Tape Switch
- -HSC: High-Speed Camera
- -LDS: Laser Displacement Sensor
- -CSG: Concrete Strain Gage
- -RSG: Reinforcement Strain Gage

Concrete Traffic Railings for Impact Loading				Revisions:
Instrumentation plan	*2020-09-21*	*University of Florida*	*Sheet 09 of 10*	

Fully-instrumented impact test - Standard steel (full-length) center-of-rail (COR) specimen

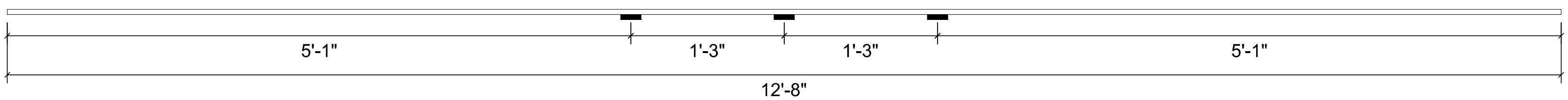

BAR 4S: TOP LONGITUDINAL BAR IN RAILING
QTY: 1 BAR WITH 3 RSG (3 TOTAL)

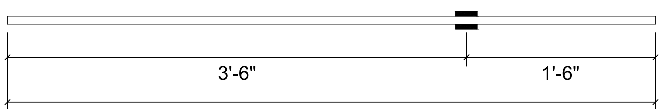

BAR S601: TOP TRANSVERSE BAR IN DECK
QTY: 2 BARS EACH WITH 2 RSG (4 TOTAL)

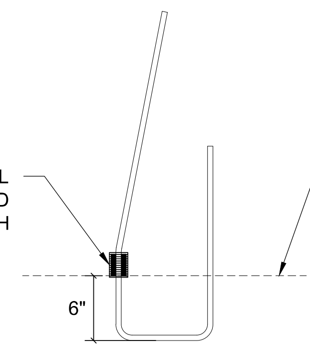

BAR 4V: CONNECTION BAR BEWTEEN DECK AND RAIL
QTY: 4 BARS EACH WITH 2 RSG (8 TOTAL)

Instrumentation:

-AC: Accelerometer
-BB: Break Beam
-TS: Tape Switch
-HSC: High-Speed Camera
-LDS: Laser Displacement Sensor
-CSG: Concrete Strain Gage
-RSG: Reinforcement Strain Gage

Concrete Traffic Railings for Impact Loading				Revisions:		
Instrumentation plan	2020-09-21	University of Florida	Sheet 10 of 10			

Fully-instrumented impact test - FRC (short-length) end-of-rail (EOR) specimen

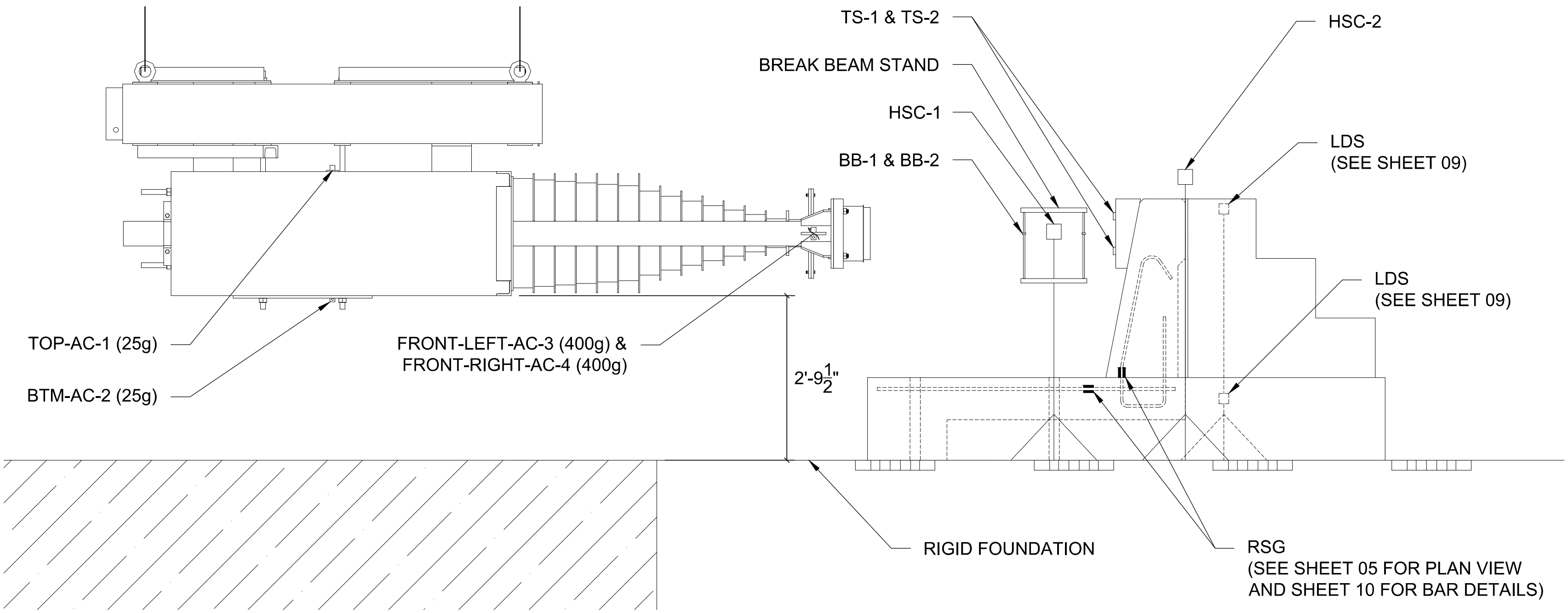

Instrumentation:

- -AC: Accelerometer
- -BB: Break Beam
- -TS: Tape Switch
- -HSC: High-Speed Camera
- -LDS: Laser Displacement Sensor
- -CSG: Concrete Strain Gage
- -RSG: Reinforcement Strain Gage

Concrete Traffic Railings for Impact Loading				Revisions:		
Instrumentation plan	2020-11-18	University of Florida	Sheet 04 of 10			

Fully-instrumented impact test - FRC (short-length) end-of-rail (EOR) specimen

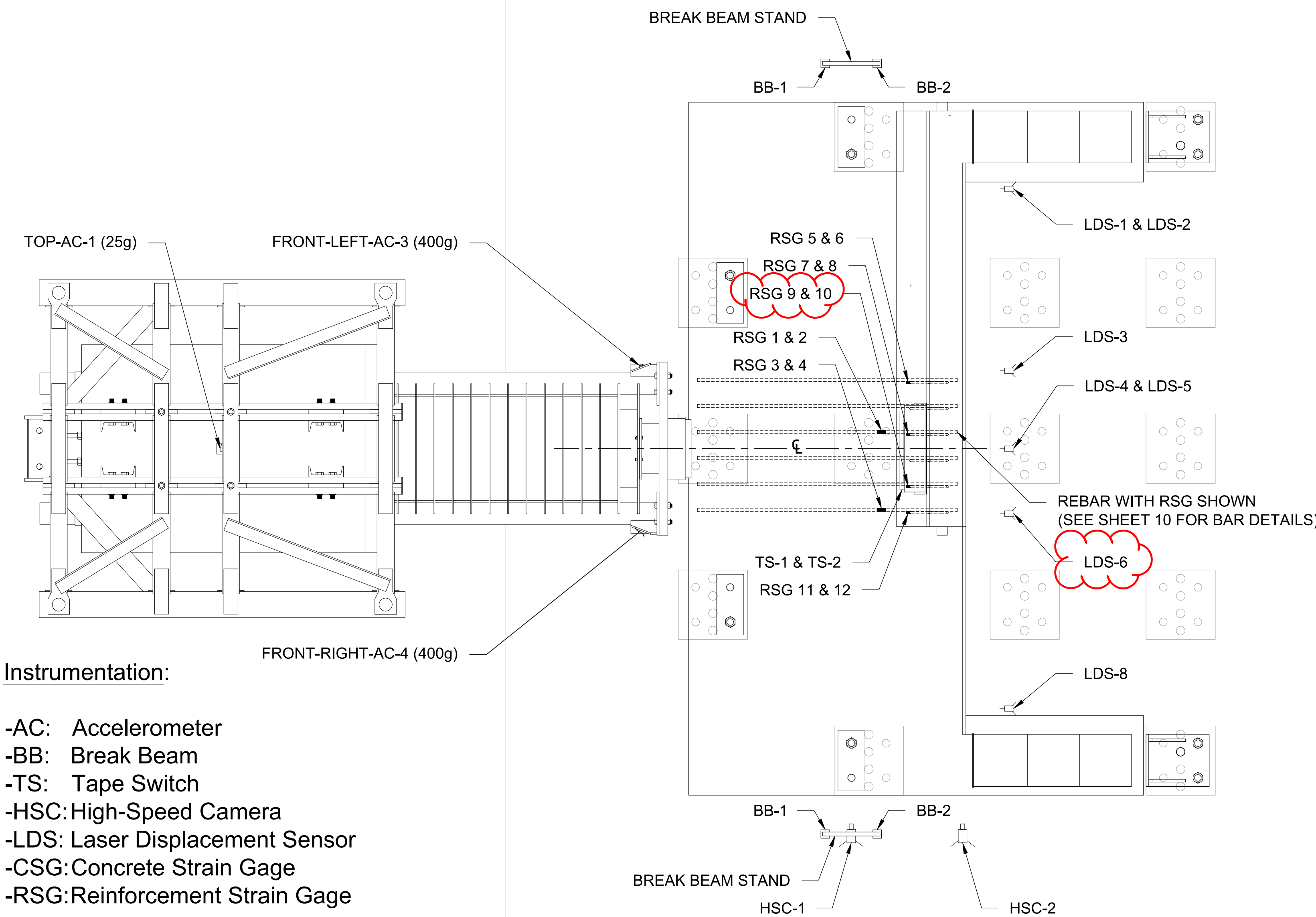

Instrumentation:

-AC: Accelerometer
-BB: Break Beam
-TS: Tape Switch
-HSC: High-Speed Camera
-LDS: Laser Displacement Sensor
-CSG: Concrete Strain Gage
-RSG: Reinforcement Strain Gage

Concrete Traffic Railings for Impact Loading				*Revisions:*	Relocated RSG 9 & 10
Instrumentation plan	*2020-11-18*	*University of Florida*	*Sheet 05 of 10*		Relocated LDS-6; Removed LDS-7 (when compared with center-of-rail specimen)

Fully-instrumented impact test - FRC (short-length) end-of-rail (EOR) specimen

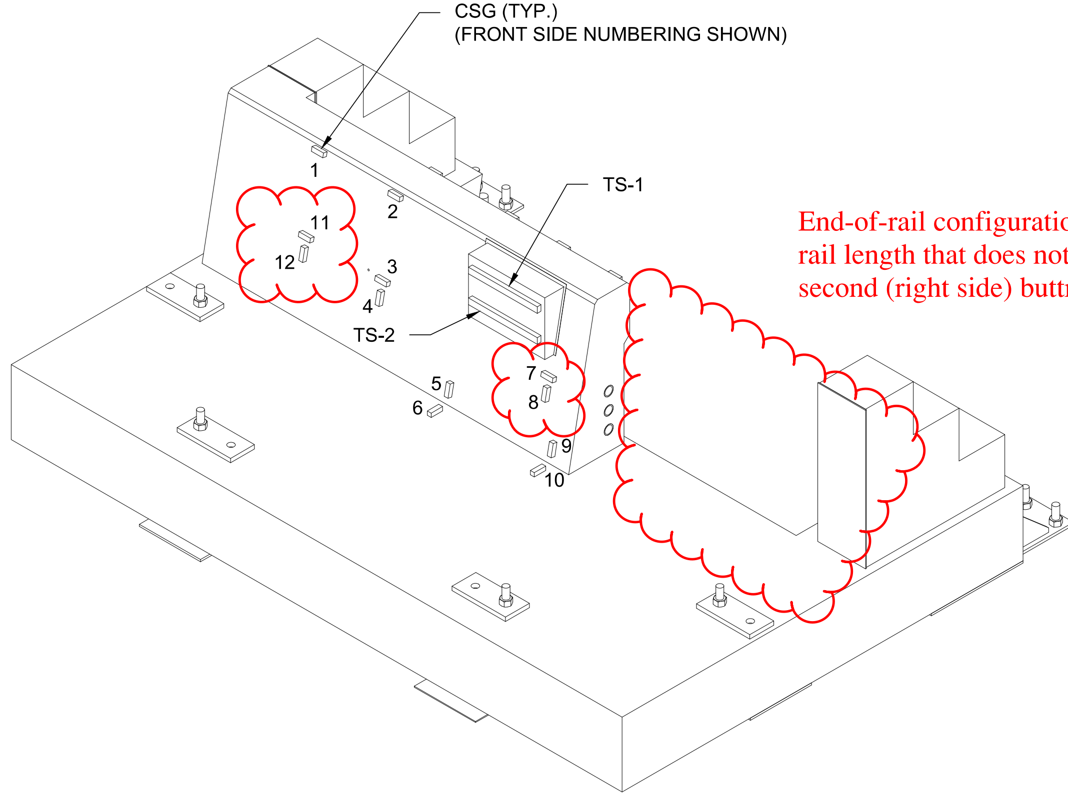

End-of-rail configuration is a shortened 8-ft rail length that does not extend to the second (right side) buttress/end-support

Instrumentation:

- -AC: Accelerometer
- -BB: Break Beam
- -TS: Tape Switch
- -HSC: High-Speed Camera
- -LDS: Laser Displacement Sensor
- -CSG: Concrete Strain Gage
- -RSG: Reinforcement Strain Gage

Concrete Traffic Railings for Impact Loading				Revisions:	Relocated CSG 7, 8 and 11, 12 (when compared with center-of-rail specimen)
Instrumentation plan	2020-11-18	University of Florida	Sheet 06 of 10		

Fully-instrumented impact test - FRC (short-length) end-of-rail (EOR) specimen

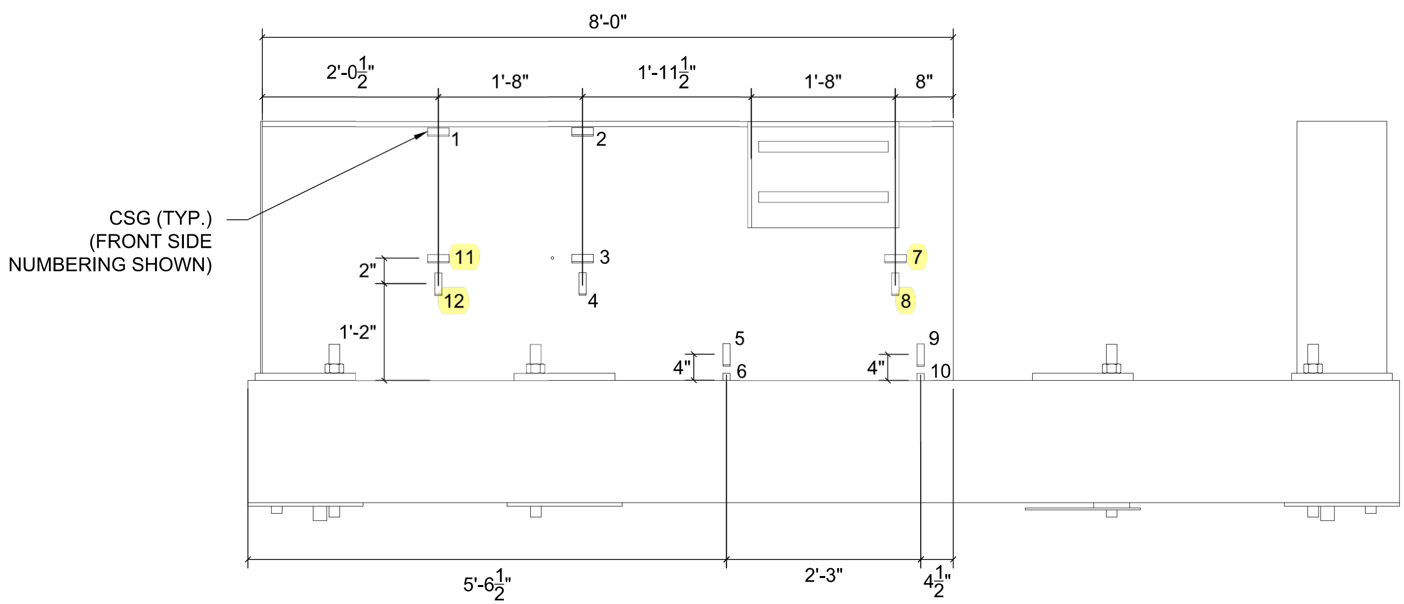

Instrumentation:

-AC: Accelerometer
-BB: Break Beam
-TS: Tape Switch
-HSC: High-Speed Camera
-LDS: Laser Displacement Sensor
-CSG: Concrete Strain Gage
-RSG: Reinforcement Strain Gage

Concrete Traffic Railings for Impact Loading				Revisions:	Relocated CSG 7, 8 and 11, 12 (when compared with center-of-rail specimen)
Instrumentation plan	2020-11-18	University of Florida	Sheet 07 of 10		

Fully-instrumented impact test - FRC (short-length) end-of-rail (EOR) specimen

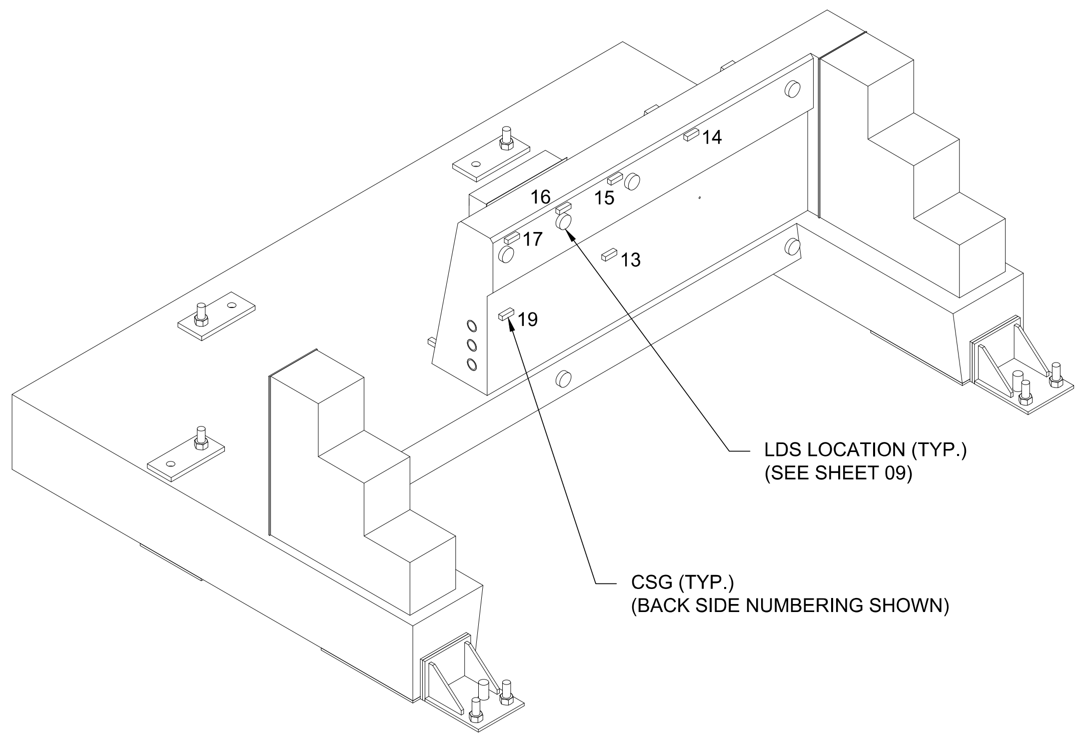

Instrumentation:

-AC: Accelerometer
-BB: Break Beam
-TS: Tape Switch
-HSC: High-Speed Camera
-LDS: Laser Displacement Sensor
-CSG: Concrete Strain Gage
-RSG: Reinforcement Strain Gage

Concrete Traffic Railings for Impact Loading				*Revisions:*	Removed CSG 18
Instrumentation plan	*2020-11-18*	*University of Florida*	*Sheet 08 of 10*		(when compared with center-of-rail specimen)

Fully-instrumented impact test - FRC (short-length) end-of-rail (EOR) specimen

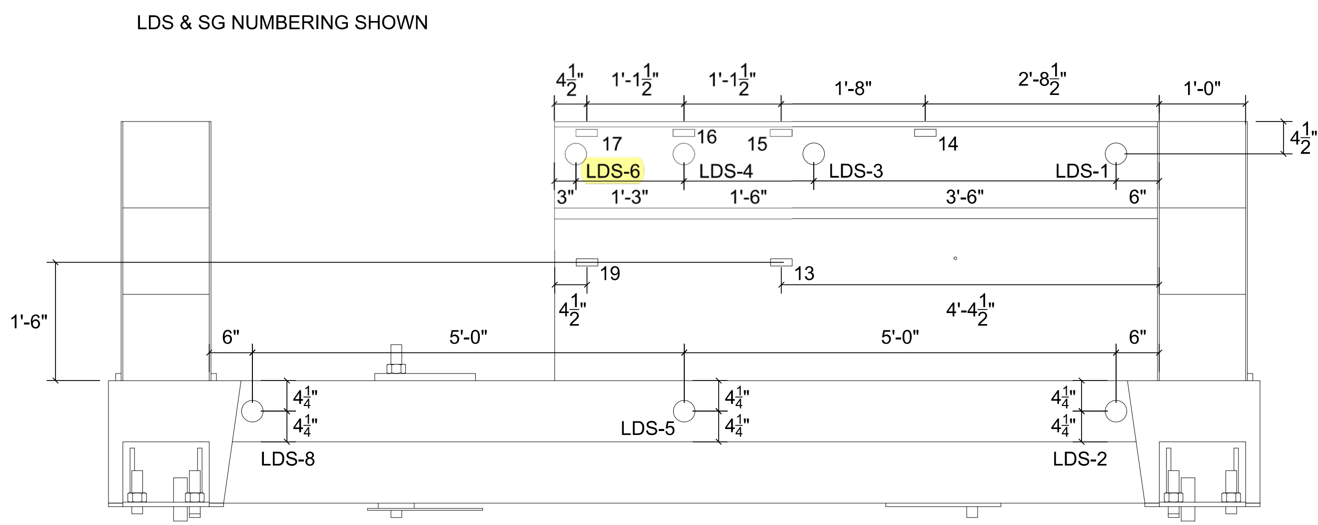

Instrumentation:

-AC: Accelerometer
-BB: Break Beam
-TS: Tape Switch
-HSC: High-Speed Camera
-LDS: Laser Displacement Sensor
-CSG: Concrete Strain Gage
-RSG: Reinforcement Strain Gage

Concrete Traffic Railings for Impact Loading				*Revisions:*	Removed CSG 18	
Instrumentation plan	*2020-11-18*	*University of Florida*	*Sheet 09 of 10*		Relocated LDS 6	Removed LDS 7
					(when compared with center-of-rail specimen)	

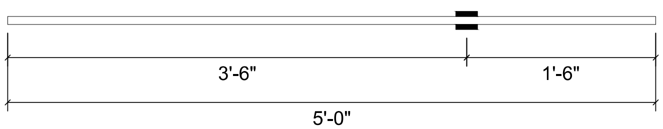

BAR S601: TOP TRANSVERSE BAR IN DECK
QTY: 2 BARS EACH WITH 2 RSG (4 TOTAL)

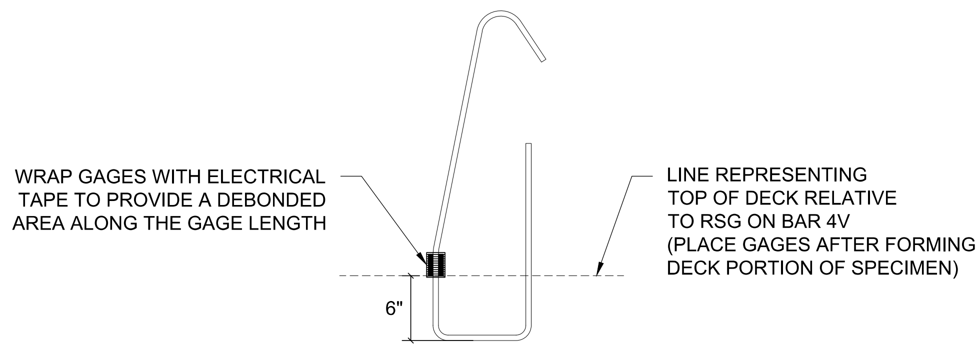

BAR 4V: CONNECTION BAR BEWTEEN DECK AND RAIL
QTY: 4 BARS EACH WITH 2 RSG (8 TOTAL)

Instrumentation:

-AC: Accelerometer
-BB: Break Beam
-TS: Tape Switch
-HSC: High-Speed Camera
-LDS: Laser Displacement Sensor
-CSG: Concrete Strain Gage
-RSG: Reinforcement Strain Gage

Concrete Traffic Railings for Impact Loading				*Revisions:*		
Instrumentation plan	*2020-11-18*	*University of Florida*	*Sheet 10 of 10*			

Fully-instrumented impact test - Standard steel (short-length) end-of-rail (EOR) specimen

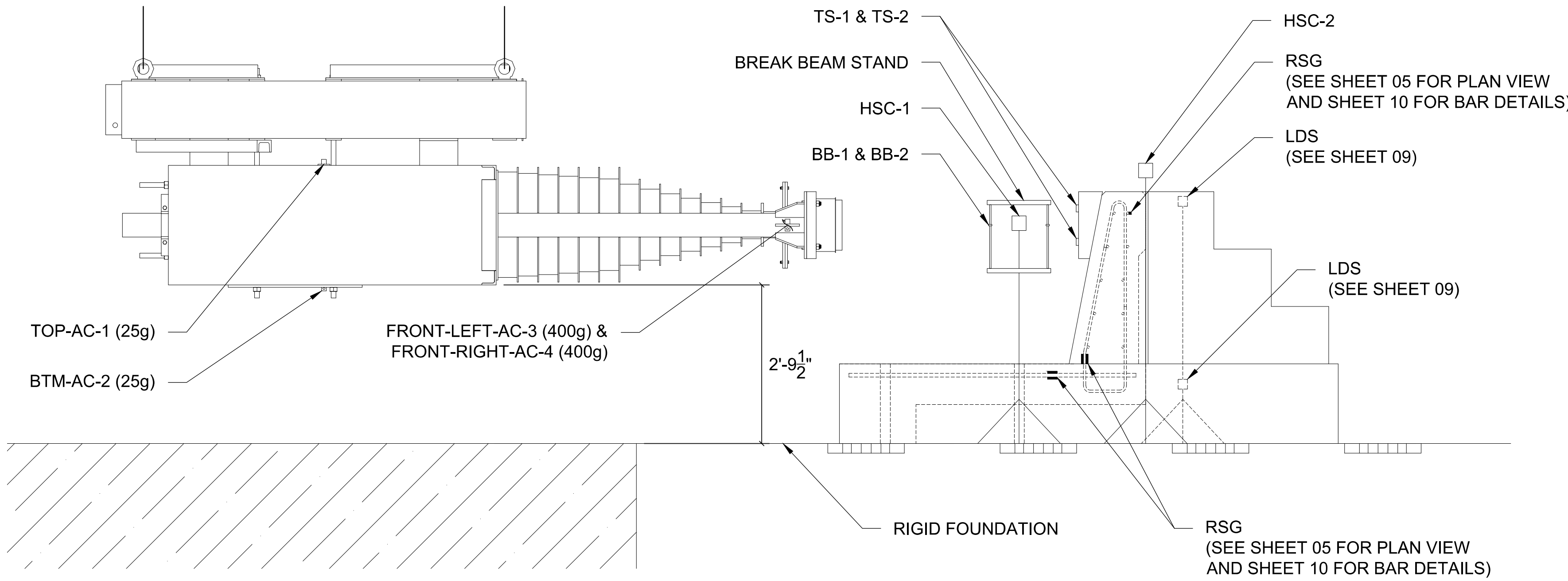

Instrumentation:

-AC: Accelerometer
-BB: Break Beam
-TS: Tape Switch
-HSC: High-Speed Camera
-LDS: Laser Displacement Sensor
-CSG: Concrete Strain Gage
-RSG: Reinforcement Strain Gage

Concrete Traffic Railings for Impact Loading				Revisions:
Instrumentation plan	2020-11-23	University of Florida	Sheet 04 of 10	

Fully-instrumented impact test - Standard steel (short-length) end-of-rail (EOR) specimen

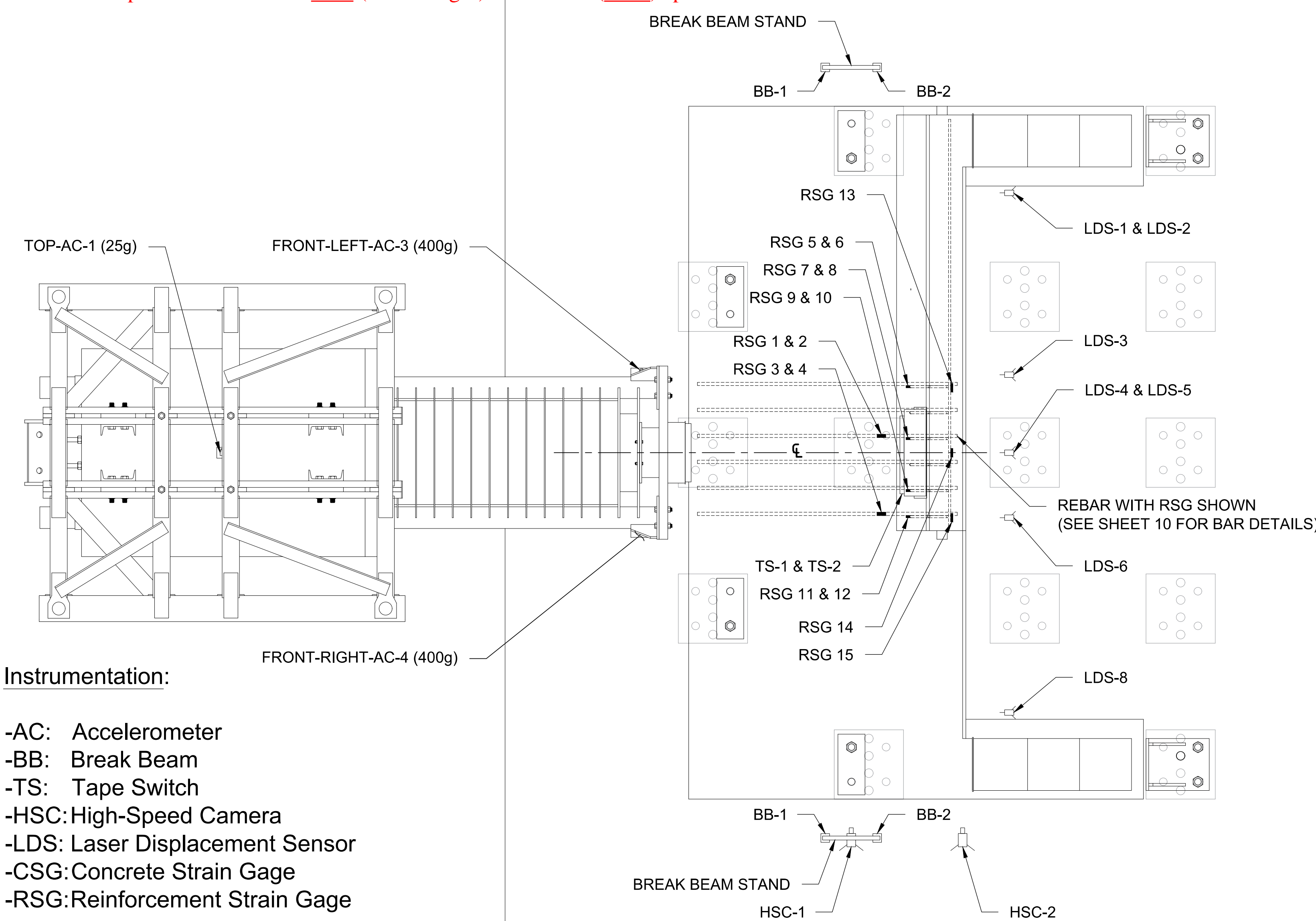

Instrumentation:

-AC: Accelerometer
-BB: Break Beam
-TS: Tape Switch
-HSC: High-Speed Camera
-LDS: Laser Displacement Sensor
-CSG: Concrete Strain Gage
-RSG: Reinforcement Strain Gage

Concrete Traffic Railings for Impact Loading				Revisions:	Relocated RSG 9 & 10	
Instrumentation plan	2020-11-23	University of Florida	Sheet 05 of 10		Relocated LDS-6	Removed LDS-7
					(when compared with center-of-rail specimen)	

Fully-instrumented impact test - Standard steel (short-length) end-of-rail (EOR) specimen

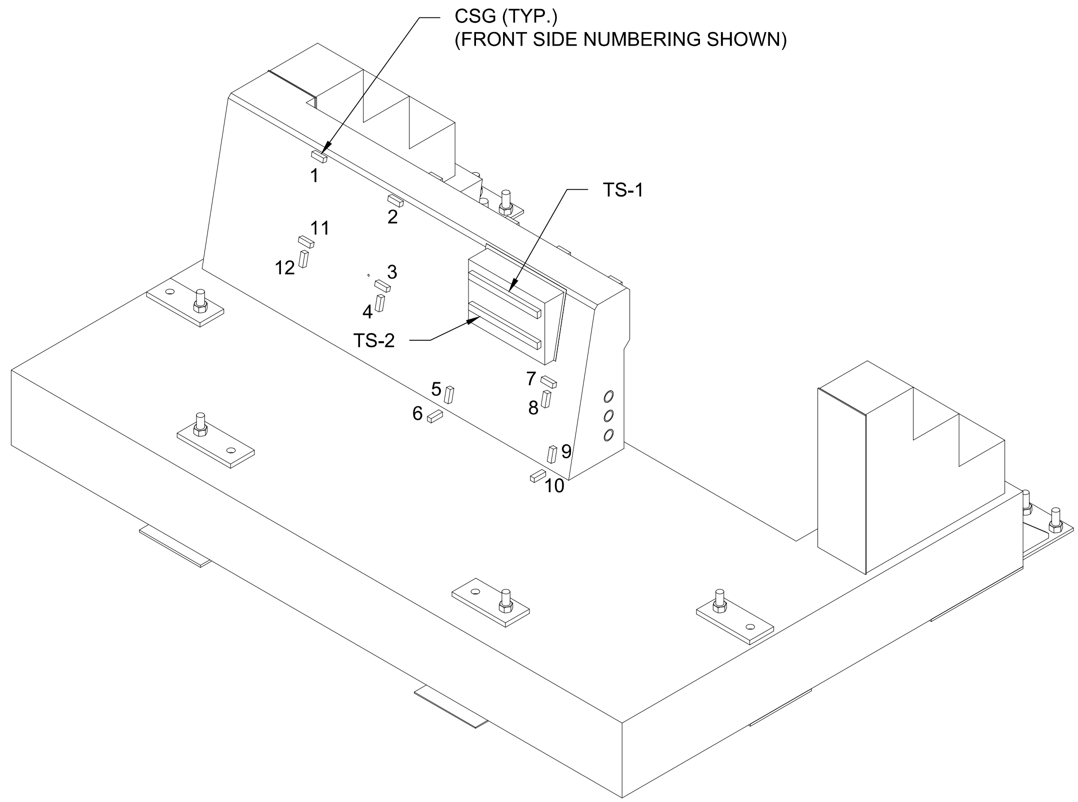

Instrumentation:

-AC: Accelerometer
-BB: Break Beam
-TS: Tape Switch
-HSC: High-Speed Camera
-LDS: Laser Displacement Sensor
-CSG: Concrete Strain Gage
-RSG: Reinforcement Strain Gage

Concrete Traffic Railings for Impact Loading				*Revisions:*	Relocated CSG 7, 8 and 11, 12 (when compared with center-of-rail specimen)
Instrumentation plan	*2020-11-23*	*University of Florida*	*Sheet 06 of 10*		

Fully-instrumented impact test - Standard steel (short-length) end-of-rail (EOR) specimen

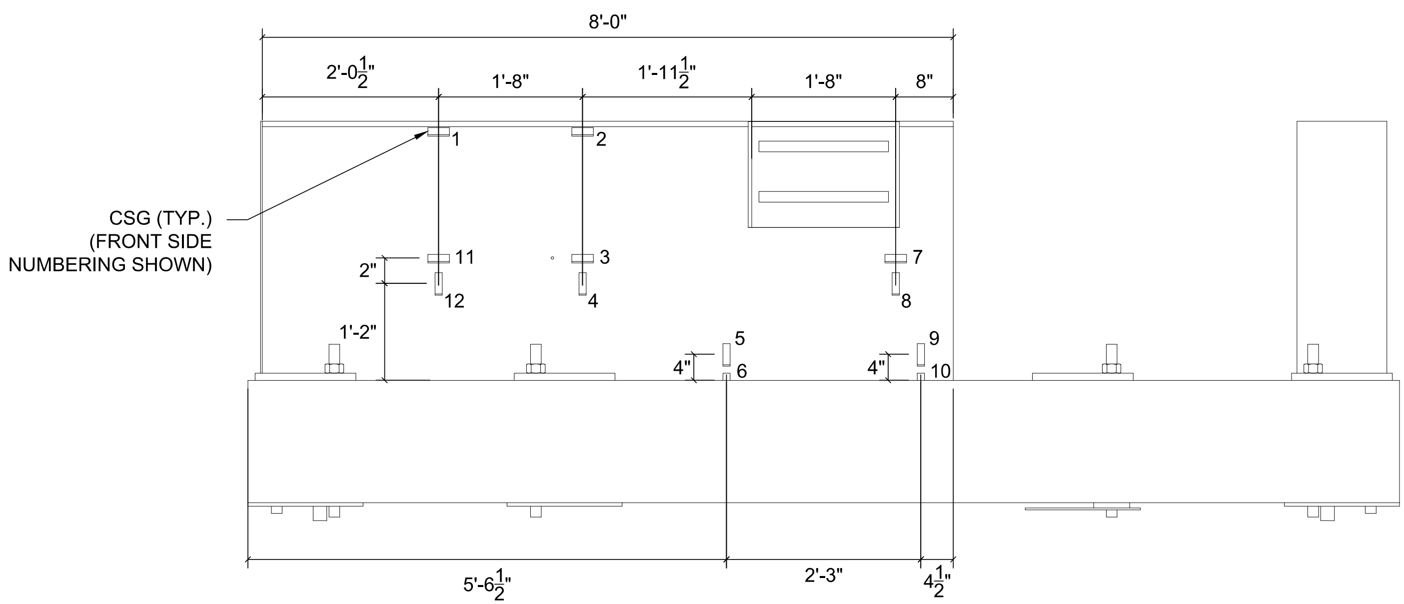

Instrumentation:

-AC: Accelerometer
-BB: Break Beam
-TS: Tape Switch
-HSC: High-Speed Camera
-LDS: Laser Displacement Sensor
-CSG: Concrete Strain Gage
-RSG: Reinforcement Strain Gage

Concrete Traffic Railings for Impact Loading				Revisions:	Relocated CSG 7, 8 and 11, 12 (when compared with center-of-rail specimen)
Instrumentation plan	2020-11-23	University of Florida	Sheet 07 of 10		

Fully-instrumented impact test - Standard <u>steel</u> (short-length) end-of-rail (<u>EOR</u>) specimen

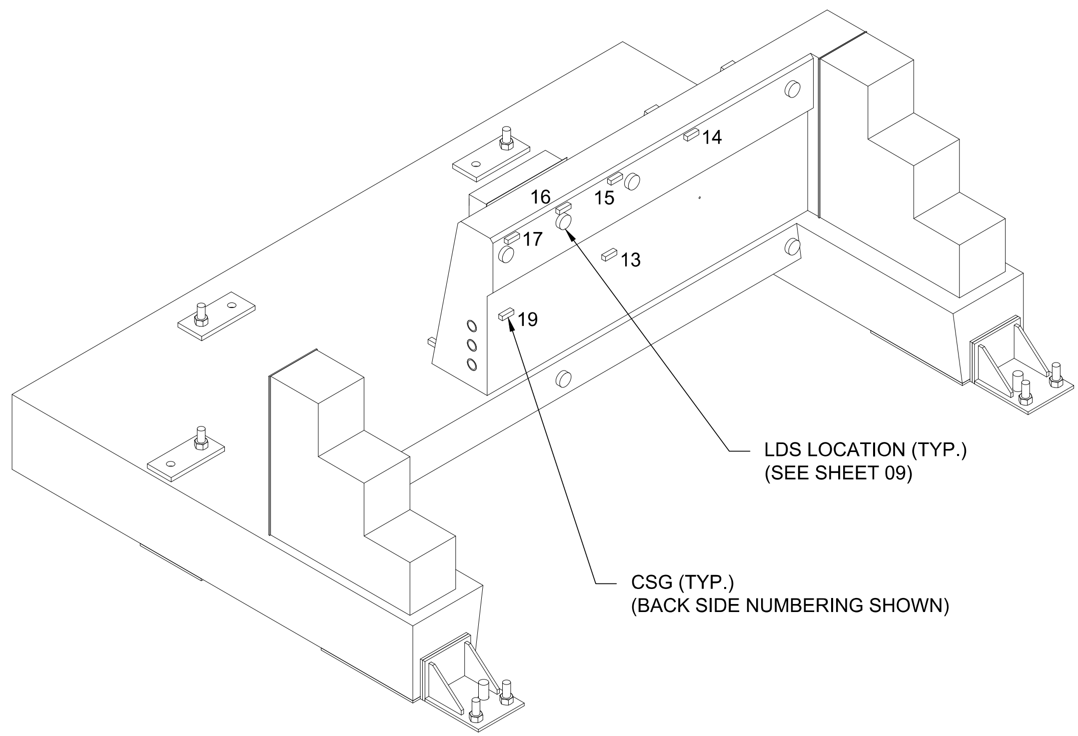

Instrumentation:

-AC: Accelerometer
-BB: Break Beam
-TS: Tape Switch
-HSC: High-Speed Camera
-LDS: Laser Displacement Sensor
-CSG: Concrete Strain Gage
-RSG: Reinforcement Strain Gage

Concrete Traffic Railings for Impact Loading				*Revisions:*	Removed CSG 18
Instrumentation plan	*2020-11-23*	*University of Florida*	*Sheet 08 of 10*		(when compared with center-of-rail specimen)

Fully-instrumented impact test - Standard steel (short-length) end-of-rail (EOR) specimen

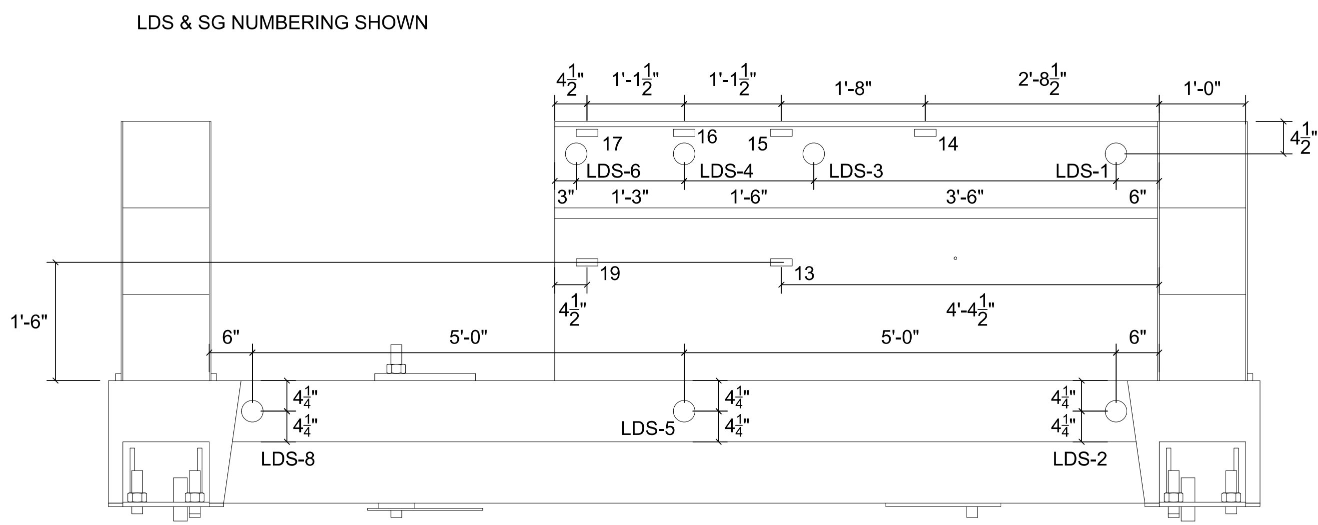

Instrumentation:

-AC: Accelerometer
-BB: Break Beam
-TS: Tape Switch
-HSC: High-Speed Camera
-LDS: Laser Displacement Sensor
-CSG: Concrete Strain Gage
-RSG: Reinforcement Strain Gage

Concrete Traffic Railings for Impact Loading				Revisions:	Removed CSG 18	
Instrumentation plan	2020-11-23	University of Florida	Sheet 09 of 10		Relocated LDS 6	Removed LDS 7
					(when compared with center-of-rail specimen)	

Fully-instrumented impact test - Standard steel (short-length) end-of-rail (EOR) specimen

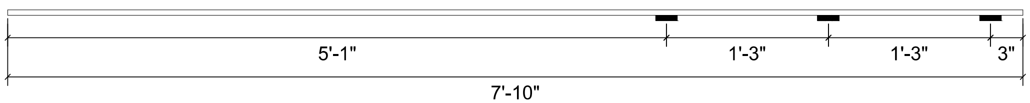

BAR 4SS: TOP LONGITUDINAL BAR IN RAILING
QTY: 1 BAR WITH 3 RSG (3 TOTAL)

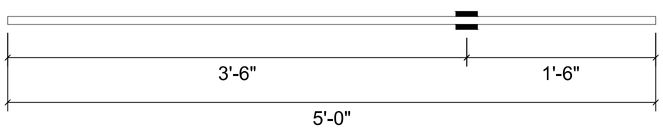

BAR S601: TOP TRANSVERSE BAR IN DECK
QTY: 2 BARS EACH WITH 2 RSG (4 TOTAL)

WRAP GAGES WITH ELECTRICAL TAPE TO PROVIDE A DEBONDED AREA ALONG THE GAGE LENGTH

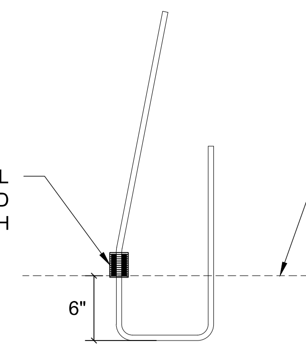

LINE REPRESENTING TOP OF DECK RELATIVE TO RSG ON BAR 4V (PLACE GAGES AFTER FORMING DECK PORTION OF SPECIMEN)

BAR 4V: CONNECTION BAR BEWTEEN DECK AND RAIL
QTY: 4 BARS EACH WITH 2 RSG (8 TOTAL)

Instrumentation:

-AC: Accelerometer
-BB: Break Beam
-TS: Tape Switch
-HSC: High-Speed Camera
-LDS: Laser Displacement Sensor
-CSG: Concrete Strain Gage
-RSG: Reinforcement Strain Gage

Concrete Traffic Railings for Impact Loading				*Revisions:*	Bar 4SS is shorter in length and gages are not centered when compared with Bar 4S in center-of-rail specimen
Instrumentation plan	*2020-11-23*	*University of Florida*	*Sheet 10 of 10*		

Planned railing pendulum impact tests

Material types:
FRC: fiber-reinforced concrete
Steel: standard steel bar reinforced concrete

Specimen configurations:
COR: center-of-rail (full-length) test
EOR: end-of-rail (short-length, one-end support) test

FRC railing project tests:
-One preliminary partially-instrumented FRC (full-length) COR test
-Two standard steel (full-length) COR tests
-One FRC (full-length) COR test
-One FRC (short-length) EOR test

Concrete Traffic Railings for Impact Loading				*Revisions:*	Including end-of-rail (EOR) configurations
Instrumentation plan	*2020-11-23*	*University of Florida*			

FRC railings - Instrumentation Summary:

Notation:
- -AC: Accelerometer
- -BB: Break Beam
- -TS: Tape Switch
- -HSC: High-Speed Camera
- -LDS: Laser Displacement Sensor
- -CSG: Concrete Strain Gage
- -RSG: Reinforcement Strain Gage

☐ One preliminary partially-instrumented FRC (full-length) COR test:

Impactor:	Ground:	Specimen:
-TOP-AC-1 (25g)	-BB-1	-TS-1
-BTM-AC-2 (25g)	-BB-2	-TS-2
-FRONT-LEFT-AC-3 (400g)	-HSC-1	
-FRONT-RIGHT-AC-4 (400g)	-HSC-2	

☐ One fully-instrumented FRC (full-length) COR test:

Impactor:	Ground:	Specimen:
-TOP-AC-1 (25g)	-BB-1	-TS-1 & TS-2
-BTM-AC-2 (25g)	-BB-2	-LDS-1 through LDS-8
-FRONT-LEFT-AC-3 (400g)	-HSC-1	-RSG-1 through RSG-12
-FRONT-RIGHT-AC-4 (400g)	-HSC-2	-CSG-1 through CSG-19

☐ One fully-instrumented FRC (short-length) EOR test:

Impactor:	Ground:	Specimen:
-TOP-AC-1 (25g)	-BB-1	-TS-1 & TS-2
-BTM-AC-2 (25g)	-BB-2	-LDS-1 through LDS-8 (removed LDS-7 for FRC EOR)
-FRONT-LEFT-AC-3 (400g)	-HSC-1	-RSG-1 through RSG-12
-FRONT-RIGHT-AC-4 (400g)	-HSC-2	-CSG-1 through CSG-19 (removed CSG-18 for FRC EOR)

Concrete Traffic Railings for Impact Loading			*Revisions:*	Including end-of-rail (EOR) configurations
Instrumentation plan	*2020-11-23*	*University of Florida*		Including specimens planned for GFRP project